Exploring the Chemistry of Quinones for Accessing Valued Oxygen and Nitrogen Heterocycles

A Thesis Submitted

In Partial Fulfillment of the Requirements

for the Degree of

Doctor of Philosophy

by

"NAVPREET KAUR"

(2018CYZ0008)

DEPARTMENT OF CHEMISTRY

INDIAN INSTITUTE OF TECHNOLOGY ROPAR

APRIL 2023

Copyright © “2023” by Indian Institute of Technology Ropar

All Rights Reserved

DEDICATED

TO

MY FAMILY, FRIENDS & ALMIGHTY

DECLARATION

I declare that this work entitled "Exploring the Chemistry of Quinones for Accessing Valued Oxygen and Nitrogen Heterocycles" has not previously been accepted in substance for any degree and is not being simultaneously submitted in candidature for any other degree. This thesis is being submitted in partial fulfilment of the requirements for the degree of PhD in Chemistry. This thesis is the result of my own independent investigation, except where otherwise stated. I have acknowledged all the other sources by stating the references explicitly. I declare that any idea/data/fact/source stated in my thesis has not been fabricated/falsified/misrepresented. All the principles of academic honesty and integrity have been followed. I understand that any violation of the above will be cause for disciplinary action by the Institute and can also evoke penal action from the sources which have thus not been properly cited or from whom proper permission has not been taken when needed. I hereby give consent for my thesis, if accepted, to be available online in the Institute's Open Access repository and for inter-library loan, and for the title and abstract to be made available to outside organizations.

Navpreet Kaur

Signature

Name: Navpreet Kaur

Entry Number: 2018cyz0008

Date: 24-07-2023

ACKNOWLEDGMENTS

First of all, I am grateful to the Indian Institute of Technology Ropar, Rupnagar, Punjab, India and Department of Chemistry for providing me this opportunity to pursue Ph.D. program. I would like to take this pleasure to thank many individuals for their constant support throughout the journey. Foremost, I would like to express my deep sense of gratitude and profound feeling of admiration to my thesis supervisor **Dr. Prabal Banerjee**, Associate Professor, Department of Chemistry, IIT Ropar for his constant support, motivation and belief in me. He has been my pillar of support since the commencement of this work. During my initial days of research, there were times when the setbacks associated with my research work used to demotivate me. At that time, his constant belief in me and encouragement has kept me going. He has always allowed me to work freely and independently that has strengthened my self-confidence in developing the experimental skills that further led me to execute several independent projects and lead them. While experiencing failures, his valuable inputs and optimistic attitude has helped me advance my scholarly skills with the much-needed scientific temperament to analyze a research problem and look for the solution. Above all, I express my sincere everlasting thankfulness to him. I consider myself very fortunate to have a friendlier supervisor.

I am indebted to Ministry of Human Resource and Development (MHRD), Government of India and IIT Ropar for my doctoral research fellowship. I express my sincere thanks to **Prof. Rajeev Ahuja**, Director, IIT Ropar and **Prof. Sarit K. Das**, Ex-Director, IIT Ropar, **Dr. Navin Kumar** (Dean Research and Development), **Dr. Pushpendra P. Singh** (Associate Dean Research and Development), **Dr. Subhash Chandra Martha** (Associate Dean Student Affairs), **Dr. Dinesh K.S**. (Officiating Registrar) for providing all the required infrastructural facilities for carrying out my research work.

I would also like to thank my doctoral committee members **Dr. Avijit Goswami**, **Dr. Debaprasad Mandal**, **Dr. Anupam Agrawal** and chairperson **Dr. T. J. Dhilip Kumar** for their feedbacks, suggestions and the intellectual inputs during the presentations and other times. My sincere thanks to the present head of the department (HOD) **Dr. Tharamani C.N.** and all the other **faculty members** of Department of Chemistry for their sincere support and invaluable guidance.

I extend my thanks to all the supporting staff of the department of chemistry **Mr. Nagendra ji**, **Mr. Sushil ji**, **Mr. Tanveer**, **Mrs. Samita Saini**, **Ms. Hanspreet Kaur** for helping me out directly or indirectly in my dissertation work. My special thanks to **Mr. Manish Kumar** (for timely processing of NMR data), **Mr. Kamlesh Satpute** (for helping me to analyze single crystal data), **Mr. Nazre Heyat and Dr, Nilotpal** (for recording HRMS data), **Mrs. Poonam Kataria** (for always helping me in the administrative related issues), **Mrs. Gurprakash Kaur** for providing me several informations related to work.

I would like to acknowledge the sincere efforts and constant encouragement by **Dr. Rohit**, my senior labmate who helped me at the beginning of this journey. I thank him for his extensive discussion around my research work that always offered a new interesting challenge and inspired me to try my best.

I feel immensely grateful to all my seniors in the lab **Dr. Priyanka Singh**, **Dr. Asit Ghosh**, **Dr. Kamal Verma**, **Dr. Raghunath Dey**, **Dr. Pankaj Kumar** for exceptional guidance and motivation throughout this journey. All of them were the real motivation and the passion for the research which they carried was very contagious. Also, a special mention to **Priyanka Maam** for being a friend more than a senior and helping me out with the suggestions regarding my research activities.

I am extremely grateful to the other lab members **Dr. Maajid**, **Dr. Debarshi**, **Arijit**, **Rakesh**, **Neeraj**, **Nakshatra**, **Shiv**, **Vikas** and **Rohan** for maintaining a supportive and cheerful nature in the laboratory. A special thanks to **Rakesh**, **Arijit** and **Neeraj** for being a great support and good travel partners. I would like to gratefully acknowledge the M.Sc. students of our lab **Sumitra**, **Shruti**, **Asha**, **Kritika Singh**, **Naveen**, **Manish**, **Tanmay**, **Prince**, **Biswadeep**, **Kritika Verma**, interns **Rashi** and **Sakshi**.

The years of my research were made memorable largely due to my friends who became the part of my life. I cannot forget the blithe company of **Pankaj**, **Debarshi**, **Maajid**, **Diksha**, **Ekta**. The journey of initial years of my research would not have been possible without them. Thank you, guys, for being the fantastic companion. Thanks to my seniors **Dr. Divya Bhatt** and **Dr. Gaje**, and dear friends from other labs **Prasoon**, **Manisha**, **Gulshan**, **Ganga**, **Rajesh**, **Moumita** for their help and assistance.

This acknowledgement would be incomplete without thanking a few special people. Thanks to **Dr. Irshad Maajid Taily** for making my journey of research wonderful by supporting me at every step since we met. Thanks a lot for everything. A special thanks and mention to **Dr. Pankaj** for always being a constant companion and a good friend. Thanks for being there every time with me during all those success and failure with all the guidance and encouragement. Thanks a lot for everything. A special thanks to my friend **Dr. Debarshi** who has always helped me and supported me in every situation. I will miss all the unending laboratory fights/talks and memorable trips with you and thanks a lot for being a such an amazing friend. Words cannot express my feelings, nor my thanks for all your help. Your thoughtfulness will always be remembered. Even the words are not enough to express my gratitude towards you all. Thank you all for giving me these wonderful years. Thanks for the fantastic trips and also for being the fabulous travel buddies. I hope we can have long term association together in the years to come.

At this juncture, I would like to pay my reverence to all the institution where I had my basic education, my school, **Holy Heart Public High School**, Bassi Pathana, my College **AS College** and **MCM DAV College**, Panjab University. I am proud to being a part of them. I would also like express my gratitude to all my teachers. A special thanks to my teacher **Mrs. Madhuri** for motivating me to pursue Ph.D. during my M.Sc.

A special mention to my childhood friends at my home **Ms. Venus, Mr. Akshay, Mr. Amitoj** for their belief in me. Thanks a lot for being a part of my life. Thanks to my graduation and school friends **Ms. Astha**, **Ms. Navdeep**, **Ms. Aanchal**, **Ms. Renu**, and **Ms. Drishti** for always being there and maintaining a cheerful environment in my life.

Words are not enough to express my thanks to my loving family who were there all the time during all the ups and down in this journey. They are the inspiration to reach great heights. Whatever I am today is the result of the sacrifices made by my maternal grandparents **Mr. Swarn Singh** and Late **Mrs. Harbant Kaur**. I love you both from the bottom of my heart. Without their love, affection and moral support, I could not have accomplished this strenuous exercise. My whole hearted thanks to my parents mother **Mrs. Inderpreet Kaur,** father **Mr. Harjeet Singh**, brother **Mr. Gurjot Singh,** aunty **Mrs. Navneet Kaur**, uncle **Mr. Baljodh Singh**, uncle **Mr. Devinder Pal Singh**, aunty **Mrs. Narpinder Kaur**, for their everlasting guidance and support. Thank you, mummy and papa, for all your blessings, tremendous support, and never-ending love for me. I express my sincere regards to my late paternal grandparents Late **Mr. Mewa Singh** and Late **Mrs. Manjeet Kaur** for their love and prayers. Thanks to my brothers and sisters **Balpreet Singh** and **Gurleen Kaur** for their love. At this time, I cannot forget the little champs of the family **Agam**, **Preetkanwal**, **Mankaran**, **Gurkarman (Golu)**, **Sargun**, **Gurseerat**, **Gursimrat**, **Gurvir** and their smiley faces which I missed a lot during these years.

There are many more people to thank but it is not possible to name all of them. But at this moment, I remember each and every person who always stood beside me like a pillar and always supported me in this journey.

Finally, I express my heartfelt thanks to my God, who has made this journey the most exciting by bringing so many people into my life. Thanks a lot for the blessings showered during all the years of my life. The work would not have been possible without these people and their countless blessings.

Thank you all for your blessings and support.

Navpreet Kaur

CERTIFICATE

It is certified that the work contained in the thesis titled "*Exploring the Chemistry of Quinones for Accessing Valued Oxygen and Nitrogen Heterocycles*," by "Navpreet Kaur" has been carried out under my/our supervision and that this work has not been submitted elsewhere for the award of any degree.

Signature of the Supervisor(s)
Dr. Prabal Banerjee
Department of Chemistry
IIT Ropar

LAY SUMMARY

Organic molecules play a very crucial and important role in the development of human society. These molecules are involved in various fields such as agrochemicals, pharmaceuticals, cosmetics, food, detergents etc. Therefore, it has become important to construct these valuable molecules by developing new methodologies in order to meet the demands of the future. From the decades, it has been observed that the synthesis of heterocyclic molecules has always been a very fascinating task. In this direction, large efforts have been contributed for the facile construction of the heterocyclic molecules by employing a variety of precursors. Inspired and motivated by the importance of these molecules, some novel methods have been disclosed that has successfully resulted in the construction of some valuable molecules. The work in this thesis is dedicated towards the synthesis of some new moieties by using simple and straightforward approaches. Chapter 1 describes the importance of various nitrogen- and oxygen-containing heterocycles in our routine life. Further, this chapter also explains the reactivites of quinone and their analogues, urea derivatives, and strained ring systems in order to construct several hererocycles. Chapter 2 highlights the use of quinone methides and urea derivatives towards the synthesis of spirocycles by using hypervalent iodine chemistry. Chapter 3 delineates the construction of two complex molecules under the Lewis acid catalysed conditions by using two different set of precursors. The work in chapter 4 demonstrates the facile construction of two different fused oxacycles by using the same set of precursors just by tuning the Lewis acids. All the works have been published in peer-reviewed international journals.

ABSTRACT

Chapter 1: A Conspectus on the Reactivity of Quinone Derivatives and Strained Rings for Accessing Diverse Nitrogen and Oxygen Heterocycles

Heterocycles are the prevalent structural motifs present in many natural products, enzymes, vitamins, and exhibits a variety of biological properties. In our routine life, we actually deal with so many medicinally and naturally abundant molecules in different ways that shows the importance of various heterocycles. For example, cosmetic products, polymers, and pharmaceuticals constitute a variety of fused oxygen containing compounds. Also, the oxacycles possess many pharmacological properties like anti-tumor, anti-bacterial, anti-fungal and anti-oxidant. In present times, their wide range of application in pharmaceutical and medicinal chemistry has provided an extensive area for research in the synthetic field. Owing to their enormous importance in medicinal, agrochemical and industrial areas, it has become crucial to construct more heterocycles from the different reaction partners to meet the demand of the future. Therefore, an extensive study on the different methods towards the synthesis of an array of heterocyclic compounds is necessary by employing the efficient and straightforward approaches from readily available precursors. In this direction, quinones and their analogues are the prevalent structural motifs that represent an important class in the variety of biological active natural products and pharmaceuticals. Therefore, in order to construct functionalized heterocycles different routes has been showcased in this chapter by using quinones as one of the precursors along with another partner substrate. Also, other than quinones, urea derivatives and strained rings have also proved substantial reacting partners for the synthesis of nitrogen as well as oxygen heterocycles. This chapter describes the use of all these potential precursors to design the diverse methodologies for the development of valued heterocyclic scaffolds. The aim of the thesis and the investigations carried out during the doctoral training are outlined in the form of different chapters as follows.

Chapter 2: Vinylogous Aza-Michael Addition of Urea Derivatives with *p*-Quinone Methides Followed by Oxidative Dearomative Cyclization: Approach to Spiroimidazolidinone Derivatives

Imidazolidin-2-ones and its analogues are ubiquitous structural motifs found in natural products, pharmaceuticals, and other biologically active compounds. They often possess a broad range of biological activities such as antitumor, antibiotic, and anti-hypertonic. These *N*-containing heterocycles show versatile utility as useful structural synthons in organic synthesis. Amid the various spirocyclic scaffolds in drug discovery, spiroimidazolidinone is a promising structural motif. Consequently, continuous efforts have been made towards the synthesis of this type of spirocyclic molecules. On the other hand, it is worth considering that the cyclohexadienones are also the prevalent core structure found in many bioactive natural products and have gained considerable importance due to their abundance in pharmaceuticals. Hence, incorporation of spiroimidazolidinone and cyclohexadienone in one frame can be proved beneficial for medicinal chemists. During the past few years, *p*-quinone methides (*p*-QMs) have emerged as one of the most desirable components to access spiro-cyclohexadienones. In literature, *p*-QMs have been mainly known for their role as vinylogous Michael acceptors in various 1,6- conjugate addition reactions.

Aromatization of the cyclohexadienone moiety is the main driving force for these types of conjugate addition reactions. However, the spirocyclization reactions of *p*-QMs are comparatively less explored due to the requirement of the dearomatization of the reaction intermediate. This chapter demonstrates the reactivities of *p*-QMs and urea derivatives as building blocks towards the construction of spiro-imidazolidinones. The reaction of *p*-quinone methides with urea derivatives in the presence of a base results in the formation of 1,6-conjugate addition product in 90% yield which further on treatment with hypervalent iodine reagent renders the spiro-imidazolidinones in 65% yield. The optimization studies discovered DBU as the base for the conjugate addition product and PIDA as an efficient reagent for the cyclization step in order to construct spiro-imidazolidinones. The transformation exhibited wide substrate scope in terms of both the substrates. In the follow up chemistry, spiro-imidazolidinone were subjected to debenzylation which afforded the *N*-hydroxy urea ring attached cyclohexadienone and corresponding structures are used for metalloenzyme inhibition activities.

Chapter 3: Accessing Complex Tetrahydrofurobenzo-Pyran/Furan Scaffolds via Lewis-Acid Catalyzed Bicyclization of Cyclopropane Carbaldehydes with Quinone Methides/Esters

Benzannulated oxacycles, especially benzannulated [6,5]- and [5,5]- fused oxygen heterocycles, represent a highly privileged class of structural motifs in a variety of bioactive molecules and natural products. Xyloketals, isolated from mangrove fungus, comprising the tetrahydrofurobenzopyran unit, is engaged in the treatment of several neurological disorders like Alzheimer's disease. Alboatrin, a phytotoxic metabolite, is responsible for vascular-wilt disease in alfalfa, whereas aflatoxins bearing the tetrahydrofurobenzofuran units are well-known for their carcinogenicity, toxicity, and antimitoticity. Owing to their unique structure and intriguing activity in biological systems, the construction of such complex structural motifs with multiple stereogenic centers has always been a challenging task for the synthetic fraternity, and consequently, the reports on the synthesis of these frameworks are still rare and underexplored. However, a few methodologies demonstrating the synthesis of benzofused six-five and five-five oxygen tricycles have been reported in recent years. Over time, donor-acceptor cyclopropane carbaldehydes have emerged as versatile synthons for the diverse hetero/carbocyclic synthesis. In this regard, our group has significantly explored the strain-driven reactivity of aryl-substituted cyclopropane carbaldehydes (ACC) towards heterocyclic synthesis via Lewis-acid or metal-free activation of the cyclopropane ring. At the same time, quinone derivatives have also acquired enormous attention for their electrophilic nature towards assembling densely functionalized molecules. Quinone methides and quinone esters are widely known to act as four- and three-atom contributors for accessing intriguing heterocyclic systems. As part of our efforts and inspired by our previous results, we anticipated that the electrophilic dipolar reactivity of quinone derivatives and the *in-situ* ring expansion of ACC could be used in synergy for a possible bicyclization process. In this chapter, we disclosed a straightforward one-pot synthesis of tetrahydrofurobenzopyran and tetrahydrofurobenzofuran systems *via* an *in-situ* ring-expansion of the cyclopropane carbaldehydes followed by a [2+n] cycloaddition with the quinone derivatives. After careful screening of the conditions, we established our standard conditiond where $BF_3.OEt_2$ is an efficient catalyst for the synthesis of benzofused six-five oxacycles and $Sc(OTf)_3$ is an effective catalyst for the synthesis of benzofused five-five oxacycles with good yields. To our delight, the transformation was compatible with variety of cyclopropane carbaldehydes and quinone methides as well as quinone esters and furnished the product in moderate to good yields. Moreover, the tetrahydrofuranobenzopyran derivative was easily transformed to 3,9*a*-dihydro-2*H*-furo[2,3-*b*]chromene, which is also an essential component in many biological scaffolds.

Chapter 4: Switchable Reactivity of Cyclopropane Diesters towards (3+3) and (3+2) Cycloadditions with Benzoquinone Esters

Heterocyclic compounds are privileged structural motifs that have been found as an important core in many natural products. Particularly, oxygen-containing heterocyclic frameworks are widely known for their biological and pharmaceutical activities. However, benzopyran derivatives often possess antitumor, antibiotic and antioxidant properties. Due to their inherent biological properties, chromans have acquired immense attraction in medicinal and organic chemistry. Furthermore, the benzopyran moiety is also a part of PPARγ and PPARα/γ agonists. These PPARs play a very crucial role in the control of different pathological disorders, like hyperlipidaemia, obesity, type 2 diabetes, neurodegenerative and cardiovascular diseases. In addition, bioactive benzopyran scaffolds are used as neuroprotectors in various neurological disorders such as Alzheimer's disease. Over the time, donor-acceptor cyclopropanes (DACs) have appeared as one of the most versatile building blocks for the synthesis of various carbo- and heterocycles. Due to the presence of vicinal donor and acceptor groups and high ring strain in the cyclopropane, the cleavage of the carbon-carbon bond occurs effortlessly. These 1,3 zwitterionic species exhibit several transformations like ring opening, rearrangements, ring expansion, and cycloaddition reactions. Also, these activated cyclopropanes undergo many rearrangement reactions, most commonly the *in-situ* generation of styryl malonates. Interestingly, these styryl malonates can further be a part of cycloaddition reactions by using a suitable reaction partner. Our group has significantly utilized the strain-driven reactivity of DACs for a variety of annulation and cycloaddition reactions to synthesize valuable heterocycles. In this context, we delineate a catalyst-controlled cycloaddition reaction of DACs; a source of 1,3-zwitterionic species as well as 2-styryl malonate by fine-tuning of Lewis acid with the same reaction partner (quinone esters) to furnish densely functionalized five- and six-membered oxacycles. The optimization studies identified that $InCl_3$ (10 mol %) was the most effective Lewis acid for the (3+3) cycloaddition. On the contrary, (3+2) cycloaddition was successfully carried out using $In(OTf)_3$ (20 mol %) in dichloromethane in good yields. The control experiments were also performed in order to prove the mechanism. The desired product was also encountered at the gram scale in moderate yields. Further, in the follow up chemistry, the final product was subjected to the methylation of the phenolic hydroxyl group using methyl iodide and base. Also, the treatment of final product with DIBAL-*H* resulted in the formation of tetrahydro-2*H*-pyrano[3,4,5-*de*]chromene scaffolds.

LIST OF PUBLICATIONS

1. **Navpreet Kaur**, Priyanka Singh, and Prabal Banerjee. Vinylogous Aza-Michael Addition of Urea Derivatives with *p*-Quinone Methides Followed by Oxidative Dearomative Cyclization: Approach to Spiroimidazolidinone Derivatives. *Advanced Synthesis and Catalysis*, **2021**, *363*, 2813-2824.
2. **Navpreet Kaur**, Pankaj Kumar, Shiv Dutt, and Prabal Banerjee. Accessing Complex Tetrahydrofurobenzo-Pyran/Furan Scaffolds via Lewis-Acid Catalyzed Bicyclization of Cyclopropane Carbaldehydes with Quinone Methides/Esters. *The Journal of Organic Chemistry,* **2022**, *87*, 7905-7918.
3. **Navpreet Kaur**, Pankaj Kumar, Arijit Hazra, and Prabal Banerjee. Switchable Reactivity of Cyclopropane Diesters towards (3+3) and (3+2) Cycloadditions with Benzoquinone Esters. *Organic Letters***, 2022,** *24*, 8249-8254.
4. Priyanka Singh, **Navpreet Kaur**, and Prabal Banerjee. Regioselective Brønsted Acid-Catalyzed Annulation of Cyclopropane Aldehydes with *N′*-Aryl Anthranil Hydrazides: Domino Construction of Tetrahydropyrrolo[1,2-*a*]quinazolin-5(1H)ones. *The Journal of Organic Chemistry*, **2020**, *85*, 3393-3406.
5. Rohit Kumar Varshnaya, Priyanka Singh, **Navpreet Kaur**, and Prabal Banerjee. Cascade Intramolecular Rearrangement/ Cycloaddition of Nitrocyclopropane Carboxylate with Alkynes/Alkenes: Access to Uncommon Bi(hetero)cyclic Systems. *Organic Chemistry Frontiers,* **2021,** *8*, 1267-1274.
6. Pankaj Kumar, **Navpreet Kaur**, Rakesh Kumar, and Prabal Banerjee *α*, *β*-Unsaturated Carbonyls for One-Pot Transition-Metal-Free Access to 3,6-Dihydro-2H-pyrans. *The Journal of Organic Chemistry*, **2022**, *87*, 7167-7178.

Conferences

1. Frontiers in Chemical Sciences-2022 (FICS 2022)
Venue: IIT Guwahati, 2-4 December 2022.
Poster Presentation: Accessing Complex Tetrahydrofurobenzo-Pyran/Furan Scaffolds via Lewis-Acid Catalyzed Bicyclization of Cyclopropane Carbaldehydes with Quinone Methides/Esters.

2. Chemical Science Symposium 2022: Sustainable Synthesis and Catalysis
Venue: London, UK. (Attended in online mode), 10-11 November 2022.
Poster Presentation: Accessing Complex Tetrahydrofurobenzo-Pyran/Furan Scaffolds via Lewis-Acid Catalyzed Bicyclization of Cyclopropane Carbaldehydes with Quinone Methides/Esters.

3. CRIKC Symposium: RABMC-2022
Venue: NIPER Mohali, 19 November 2022
Poster Presentation: Switchable Reactivity of Cyclopropane Diesters towards (3+3) and (3+2) Cycloadditions with Benzoquinone Esters.

TABLE OF CONTENTS

LIST OF FIGURES

LIST OF SCHEMES

LIST OF TABLES

NOTATIONS AND ABBREVIATIONS

Acronym	**Name**
A	Acceptor
API	Active pharmaceutical ingredient
APAP	*N*-Acetyl-*para*-aminophenol
Å	Angstrom
ACN (MeCN)	Acetonitrile
NH4OH	Ammonium hydroxide
Ar	Aryl
B. C.	Before Christ

nBu	n-Butyl
$BF_3.OEt_2$	Boron trifluoride dietherate
BINAP	(2,2′-bis(diphenylphosphino)-1,1′-binaphthyl)
Bios	Biology-oriented synthesis
Bn	Benzyl
β	beta
br	Broad
CH_2Cl_2	Dichloromethane
C_6H_5	Phenyl
Cs_2CO_3	Cesium carbonate
$CHCl_3$	Chloroform
CCl_4	Carbon tetrachloride
CF_3	Trifluoro methyl
^{13}C	Carbon NMR
$CDCl_3$	Chloroform-D
COSY	Correlation spectroscopy
°C	Degree Celsius
c.m.	Complex mixture
cm^{-1}	Centimetre
$Cu(OTf)_2$	Copper (II) trifloromethanesulphonate
DAST	Diethylaminosulfur trifluoride
D	Donor
DAC	Donor-acceptor cyclopropane
DABCO	1,4-Diazabicyclo[2.2.2]octane.
DBU	1,8-Diazabicyclo[5.4.0]undec-7-ene
DIPEA	*N*, *N*-Diisopropylethylamine
DMSO	Dimethyl sulphoxide
DMF	Dimethyl formamide
DCB	1,2-Dichlorobenzene
DCM	1,2-Dichloromethane
DCE	1,2-Dichloroethane
d	Doublet
dd	Doublet of doublet
δ	Delta
DEPT	Distortionless enhancement by polarization transfer
E	Electrophile
EDG	Electron donating group
EWG	Electron withdrawing group

ee	Enantiomeric excess
equiv.	Equivalent
Et_2O	Diethyl Ether
EtOAc	Ethyl acetate
ESI	Electronspray ionization
Et	Ethyl
EtOH	Ethanol
FDA	Food and Drug Administration
F	Farad
$FeCl_3$	Iron (III) chloride
g	Gram
gem	*Geminal*
GC	Green Chemistry
GLUT	glucose transporters
h	Hour
H	Hydrogen
^1H	Proton NMR
Hz	Hertz
HRMS	Hexafluoroisopropanol
HFIP	Hydrogen iodide
HI	High Resolution Mass Spectrometry
HPLC	High-Performance Liquid Chromatography
H_2O	Water
I_2	Iodine
$InCl_3$	Indium (III) chloride
FTIR	Fourier Transform Infra-Red
IPA	Isopropyl alcohol
KOH	Potassium hydroxide
L	Ligand
LA	Lewis Acid
LiCl	Lithium Chloride
$LiClO_4$	Lithium perchlorate
m	Multiplet
Me	Methyl
MS	Molecular Sieves
mA	Milliampere
mL	Millilitre
min	Minute

$MgBr_2$	Magnesium (II) bromide
MHz	Mega Hertz
mg	Milligram
MeOH	Methanol
Me_3SiOTf	Trimethylsilyl trifloromethanesulphonate
MgI_2	Magnesium (II) iodide
p-MeC_6H_4	*p*-Tolyl
p-$MeOC_6H_4$	*p*-Methoxy phenyl
mp	Melting point
Nu	Nucleophile
nm	Nanometre
NMR	Nuclear Magnetic Resonance
np	No product
N_2	Nitrogen
Ni	Nickel
OTC	Over-the-counter
SET	Single electron transfer
AgOAc	Silver acetate
Na_2CO_3	Sodium carbonate
NaH	Sodium hydride
Na_2SO_4	Sodium sulphate
NOESY	Nuclear Overhauser effect spectroscopy
HNO_3	Nitric acid
OMe	Methoxy
$Pd(OAc)_2$	palladium(II) acetate
Ph	Phenyl
Pt	Platinum
iPr	Isopropyl
$Pd_2(dba)_3$	Tris(dibenzylideneacetone)dipalladium(0)
PTSA	*p*-Toluene sulphonic acid
ppm	Part per million
KBr	Potassium bromide
KCl	Potassium chloride
q	Quartet
R_f	Retention factor
rac	Recemic
r.t	Room temperature
RSE	Ring stain energy

s	Singlet
SN_1	Unimolecular Nucleophilic Substitution
SN_2	Bimolecular Nucleophilic Substitution
$SOCl_2$	Thionyl chloride
$Sc(OTf)_3$	Scandium (III) trifloromethanesulphonate
$InCl_3$	Indium (III) chloride
$In(OTf)_3$	Indium (III) trifloromethanesulphonate
$[\alpha]D^{T}$	Specific rotation
t	Triplet
TfOH	Triflic acid
TEA	Triethyl amine
PCy_3	tricyclohexylphosphine
$Pd(PPh_3)_2Cl_2$	bis(triphenylphosphine)palladium(II) dichloride
TsCl	Tosyl chloride
THF	Tetrahydrofuran
TsNClNa	Sodium *N*-chloro *p*-Toluenesulfonamide
THP	Tetrahydropyran
$Pd(PPh_3)_4$	tetrakis(triphenylphosphine)palladium
Bu_4NPF_6	Tetrabutylammonium hexafluorophosphate
Bu_4BF_4	Tetrabutylammonium tertafluoroborate
td	Triplet of doublet
TLC	Thin Layer Chromatography
TOF	Time-of-flight
TS	Transition State
US	United States
UV	Ultra Violet
VEC	Vinyl ethylene carbonate
vic	*Vicinal*
V	Volt
v/v	Volume/Volume
XRD	X-Ray Diffraction

Chapter 1

A Conspectus on the reactivity of Quinone Derivatives and Strained Rings for Accessing Diverse Nitrogen and Oxygen Heterocycles

1.1 Heterocyclic Compounds:

In the synthetic organic chemistry, heterocycles are defined as the cyclic compound that involves minimum two different elements as a member of the cyclic ring. The commonly used heteroatoms are nitrogen, oxygen, and sulphur. Based on the electronic arrangement, heterocyclic compounds can be classified into two types: aliphatic heterocyclic compounds and aromatic heterocyclic compounds. A few examples of aliphatic heterocyclic compounds are aziridine, epoxide, oxetane, thietane, tetrahydrofuran, 1,4-dioxane, pyrrolidine, and piperidine etc. On the other hand, aromatic heterocyclic compounds are pyrrole, furan, thiophene, pyridine, imidazole, pyrazole, and pyrimidine etc. Heterocycles are the prevalent structural motifs present in many natural products, enzymes, vitamins, and exhibits a variety of biological properties.[1] After a careful analysis of the database, it has been found that about 70% of the biologically active compounds contain heterocycles as their core moiety and remaining 30% comprises of other systems.[2] Nitrogen heterocycles are majorly used as heterocyclic core in the medicinally important drugs and oxygen heterocycles are the essential component in many pharmaceuticals, agrochemicals and natural products.[3] Among the total heterocyclic drugs in use today, 42% of the drugs incorporates nitrogen heterocycles and 28% of the drugs consists of other heterocycles (Figure 1.1.1).[4] Also, it is quite evident that oxygen and nitrogen heterocyclic compounds are the broadly studied skeletons due to their various biological properties and presence in many natural products. Talking about heterocycles, other than the normal heterocyclic compounds, there are some complex heterocyclic frameworks such as benzo-fused where a heterocyclic ring is fused with the benzene ring and spirocyclic heterocycles where the two different rings are joined together by one atom. This type of heterocycles has gained tremendous attention from the organic chemists by providing them opportunities to synthesize various novel synthetic hybrid molecules with better biological activities. Particularly, in oxacycles the benzo-fused frameworks such as benzofuran and benzopyran (chroman) derivatives have appeared as the unique class of compounds due to their application in numerous biologically important molecules.[5] Apart from these, various spirocyclic scaffolds are also the remarkable core structures in many medicinally important compounds.[6]

Figure 1.1.1. Distribution of heterocycles among total drugs.

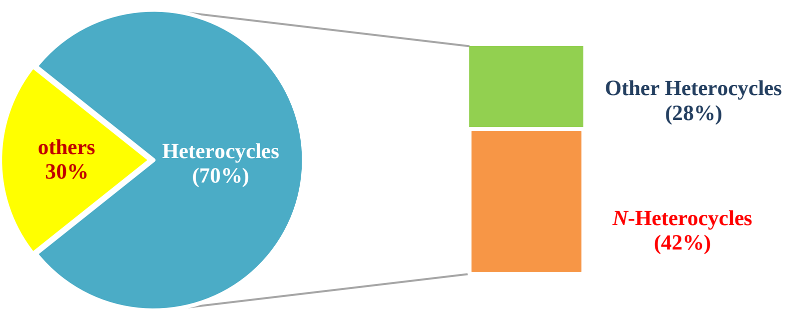

In our routine life, we actually deal with so many medicinally and naturally abundant molecules in different ways that shows the importance of various heterocycles. For example, cosmetic products, polymers, and pharmaceuticals constitute a variety of fused oxygen containing compounds.[7] Also, these oxacycles possess many pharmacological properties like anti-tumor, anti-bacterial, anti-fungal and antioxidant.[8] In present times, their wide range of application in pharmaceutical and medicinal chemistry has provided an extensive area for research in the synthetic field. Further, some of the natural products containing nitrogen and oxygen heterocyclic rings are discussed here. Machicendiol, isolated from the *Machilus glaucescens* is a benzofuran derivative and is a medicine for the treatment of rheumatism, asthma, and ulcers.[9] Next, benzofuran derivative is Liphagal which is isolated from *coralliphaga* collected from Dominica and it shows a significant inhibitory action against P13Kα (phosphatidylinositol-3-kinase).[9] They also exhibit antibiotic properties. Kendomycin is an ansamycin which is isolated from *Streptomyces* species and shows remarkable cytostatic antibacterial activity.[9] This unique metabolite, Xyloketal A is obtained from south china sea and isolated from mangrove fungus *Xylaria*. They are mainly known for their efficient bioactivities such as inhibition of acetylcholine esterase, radical scavenging behavior, antioxidant activity etc.[10] Catechin and epicatechin are the benzopyran derivatives also known as flavanols which provide antioxidant roles in plants. They are the constituents of vascular plants and used in various herbal remedies.[11] Also, they are mostly found as the components of tea and cacao. 5-HT$_{1A}$ agonist is a neurotransmitter and a serotonin receptor. They are basically used as antidepressants, antiemetic and analgesic. Other than this, these 5-HT$_{1A}$ agonist such as lecozotan is mainly used to treat Alzheimer's disease patients.[12] The alkaloid dibromophakellstatin is derived from the marine sponge *Phakellia mauritiana.* The studies show that these imidazolidinones are useful for the inhibition of human tumor growth.[13]

Figure 1.1.2 Representative examples of biologically active scaffolds with oxygen and nitrogen heterocyclic core.

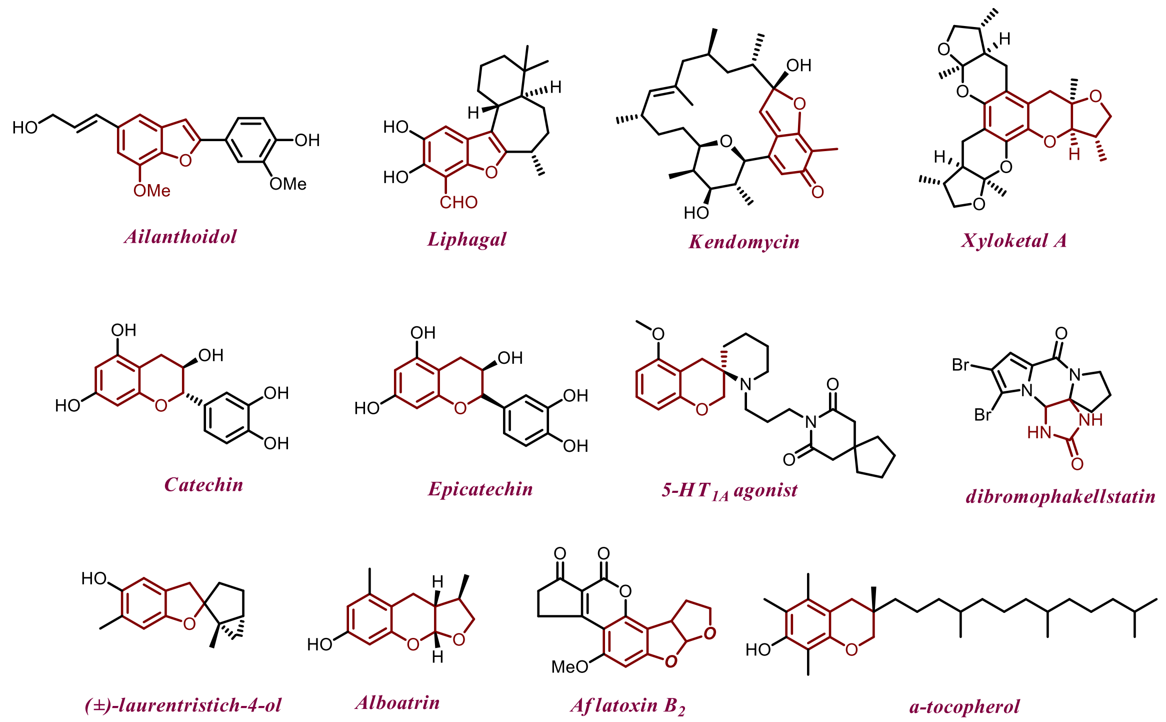

Next, Alboatrin consists of a tetrahydrofurobenzopyran unit and is a phytotoxic metabolite isolated from the filterate of *Verticillium alboatrum.* It is mainly responsible for the inhibition of the root growth of the plant Maris Kabul and causes disease in alfalfa plant.[14] Aflatoxins are the another fused complex skeletons that consists of tetrahydrofurobenzofuran unit and are the toxic secondary metabolites that are derived from *Aspergillus parasiticus*, *Aspergillus flavus.* These fungi are known for their cytotoxic behaviour such as immunotoxicity, antimitoticity etc. α-tocoperol are the chroman derivatives which belong to the vitamin E family therefore it is a natural antioxidant (Figure 1.1.2).[15]

Apart from these, there are plenty of heterocyclic cores that accompany oxygen and nitrogen heterocycles and are known for their intrinsic properties.[16] Nature has provided us with several important natural products with a variety of therapeutic properties that has significantly attracted the synthetic community to design and discover various bioactive molecules in the laboratories. Chemists have gained tremendous interest in building these valuable heterocyclic cores to further get insights of their biological properties. In order to synthesize divergent heterocyclic scaffolds, development of creative and novel methods is highly recommended. Owing to their enormous importance in medicinal, agrochemical and industrial areas, it has become crucial to construct more heterocycles from the different reaction partners and try to study their biological activities in detail to meet the demand of the future. Therefore, an extensive study on the different methods towards the synthesis of an array of heterocyclic compounds is necessary by employing the efficient and straightforward approaches from readily available precursors.

1.2. Quinone and their Analogues in the Construction of Heterocycles

Quinones are the organic compounds which are mainly derived from oxidation of aromatic systems. The basic structure of quinone consists of two carbonyl group with two carbon-carbon double bonds which are in conjugation with each other. Quinones can generally be classified as benzoquinones, naphthoquinones, and anthraquinones which has 1, 2, and 3 rings respectively. There are a few examples of quinones depending upon the position of carbonyls such as 1,2-benzoquinone (*o*-quinone), 1,4-benzoquinone (*p*-quinone), 1,2-Naphthoquinone, 1,4-Naphthoquinone, and 9,10-anthraquinone (Figure 1.2.1). Apart from these, there are structural analogues and derivatives of quinones like quinone methides, quinone dimethanes, and quinone esters. Out of which quinone methides and quinone esters are broadly studied in the synthetic community due to their biological and pharmaceutical importance.[17]

Figure 1.2.1 Types of quinones

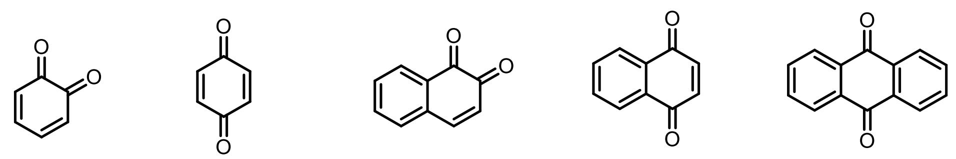

1,2-Benzoquinone *1,4-Benzoquinone* *1,2-Naphthoquinone* *1,4-Naphthoquinone* *9,10-Anthraquinone*

1.2.1 Biological Importance of Quinones

Quinones are the prevalent structural motifs that represent an important class in the variety of biological active natural products and pharmaceuticals.[18] They play a vital role in many biological applications such as oxidative phosphorylation, respiration in plants, and electron transfer in photosynthesis. They are the essential component in some of the naturally occurring substances like vitamin K1 which is mainly responsible for the blood coagulation and bones development. Along with their biological applications, they also possess a wide range of pharmaceutical activities like anticancer, antifungal, antibacterial, antioxidant, and anti-inflammatory.[18] For instance, naphthoquinones such as lapachol (2-hydroxy-3-(3-

methyl-2-butenyl)-1,4-naphthoquinone) and its other cyclic derivative like *α*-lapachone are used in medicines as antimalarial, antiparasitic, and antiseptic agents.[18] Another derivative juglone (5-hydroxy-1,4-naphthoquinone) which is known for its antibacterial and fungicidal properties. A quinone secondary metabolite Shikonin, that is originated by the plant *Lithospermum erythrorhizon* also exhibits antitumor, antimicrobial, and wound healing properties (Figure 1.2.2).[18]

Figure 1.2.2. Representative examples of quinones in pharmaceuticals.

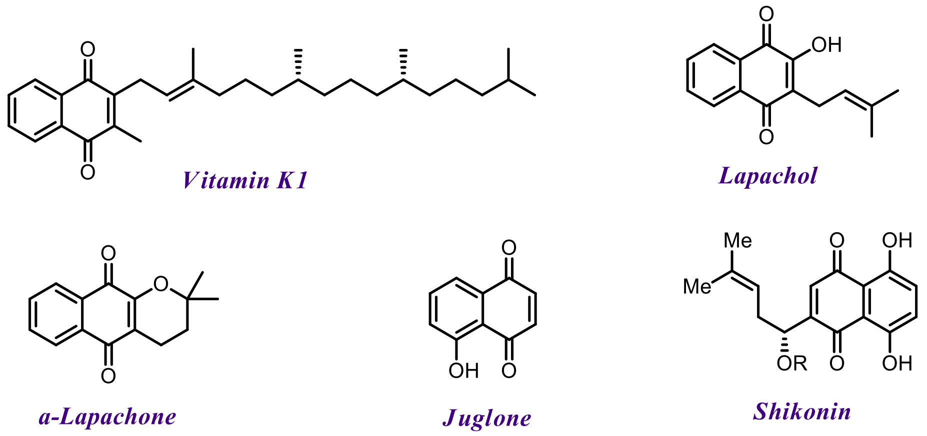

On the other hand, quinones are peculiarly known for their dyeing properties. In ancient times, a derivative of naphthoquinone, Lawsone that is isolated from the *Lawsonia inermis* (henna) is used by women to dye their hair, wool, and silk. Other than naphthoquinones, anthraquinones are also used for dyeing purposes. Alizarin and purpurin are the naturally occurring dyes that are isolated from the roots of the plant *Rubia tinctorum.* Emodin is another important dye from the anthraquinone family that is extracted from the roots and rhizomes of the *Rheum tanguticum* and *Rheum officinale.* It is significantly recognized due to its anticancer, anti-inflammatory, anti-oxidant properties (Figure 1.2.3).[19]

Figure 1.2.3. Representative examples of quinones as dyeing agents.

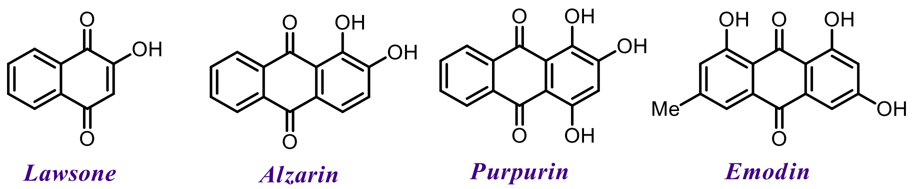

1.2.2. Quinone Methide: A Potential Precursor towards the Synthesis of Heterocycles.

Quinone methide (QM) is a conjugated organic compound in which a carbonyl group of quinone is replaced with an exocyclic methylene group. Unlike benzoquinone, the presence of two different groups on the quinone methides results in the polarization of the molecule and they become very much susceptible to undergo nucleophilic attack at the exocyclic double bond.[20] In that regard, they can behave like very good electrophiles. Also, the formation of the aromatic ring in these quinone methides is the driving force for most of the transformations. They generally exist in three isomeric forms *ortho*-, *meta*-, *para*-quinone methides. From these, *ortho*- and *para*-quinone methides are well-studied in the literature. These two isomers are neutral molecules with an aromatic zwitterionic resonance structure. The meta-quinone methide are the resonance hybrid of the two canonical structures, in which one of them is the zwitterionic form that is stabilized by the aromatization and other is the biradical form which makes this isomer very reactive and unstable. Hence, there are no further studies on the *meta*-quinone methides (Figure 1.2.4).

Figure 1.2.4. Isomeric forms of quinone methides.

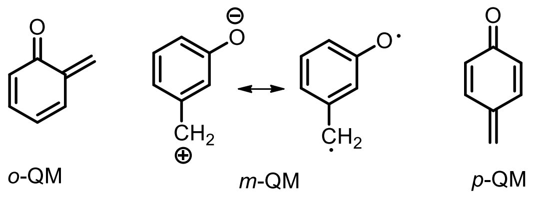

1.2.2.1. *o*-Quinone Methides:

Synthesis and Reactivity: In the past years, *o*-QMs have been the extensively utilized intermediates in the organic chemistry due to their quite high reactivity and applications in the medicinal chemistry. Owing to their great importance, they can be synthesized under various conditions such as thermal, acidic, basic, photochemical and neutral.[21] Typically, *o*-QMs are generated *in situ* by the elimination of a good leaving group at the benzylic position in the thermal conditions. They can also be generated by the condensation or dehydration reactions. In addition to these thermal conditions, these reactive species can also be generated in photochemical conditions by the dehydration of *o*-hydroxy benzyl alcohols or also by excited state intramolecular proton transfer (ESIPT) using *o*-hydroxy styrene (Scheme 1.2.2.1).

Scheme 1.2.2.1. Generation of *o*-quinone methides.

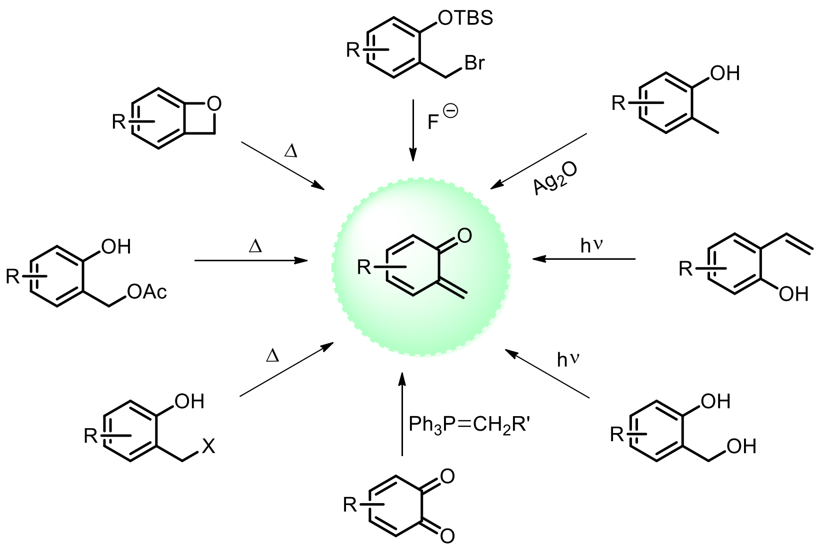

These transient species exist in three reactive forms i.e., neutral, biradical, and zwitterionic which further contributes towards the reactivity of *o*-QMs. These reactive forms of *o*-QMs undergo different type of reactions such as rearrangement, cycloaddition, 1,4-addition, and electrocyclic depending upon the type of reaction partner. Also, due to the high reactivity of these species, there is a high possibility of dimerization and trimerization, which significantly hampers their synthetic development in this area (Figure 1.2.5).[22]

Figure 1.2.5. Different types of reactivities of *o*-quinone methides.

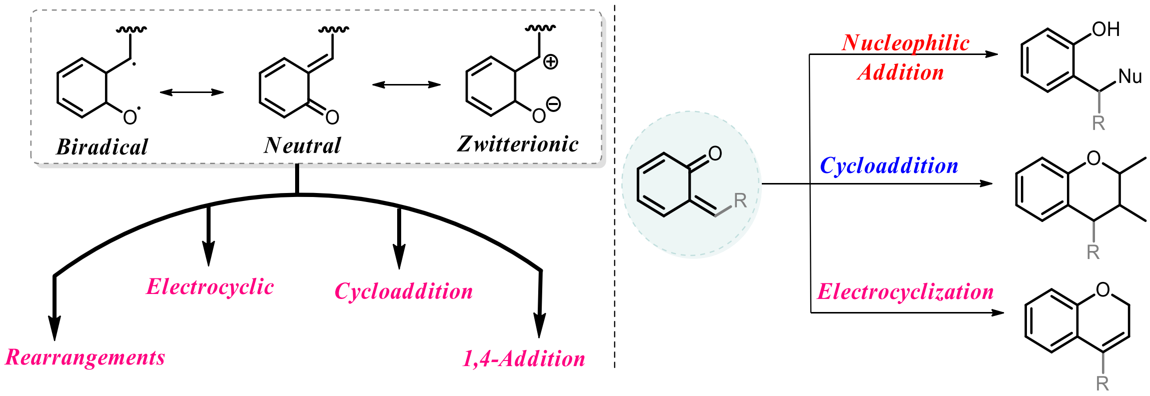

As per literature precedents, these can be stabilized by coordination with metals and their reactivity can be controlled at lower temperatures. These highly reactive intermediates have attained considerable attention due to their tendency to undergo rapid aromatization by reacting with the nucleophiles through Michael addition or by cycloaddition with 2π-reaction partners.[22] Most commonly, these species are known to give cycloaddition reaction with different dienophiles to synthesize valued benzo-fused rings. *o*-QMs are considered as very crucial intermediates in several pharmaceutical drugs.

Cycloadditions: *o*-QMs are the versatile intermediates in the organic chemistry, whose intriguing structural characteristics have attracted many researchers to utilize them in both the aspects of synthetic and medicinal chemistry. They readily give cycloaddition reactions with a variety of reaction partners. They can simply react with alkenes which could be styrene. Also, due to the electrophilic nature of these species, electron-rich alkene is more preferred. Other reaction partners like ethyl vinyl ethers, thiovinyl ethers, benzynes, vinyl ethylene carbonates, dicarbonyl compounds were successful to provide the corresponding cycloaddition products. Moreover, heteroaromatic compounds like oxazoles also proved compatible reaction partners (Scheme 1.2.2.2).[23]

Scheme 1.2.2.2. Cycloaddition reactions of *o*-quinone methides.

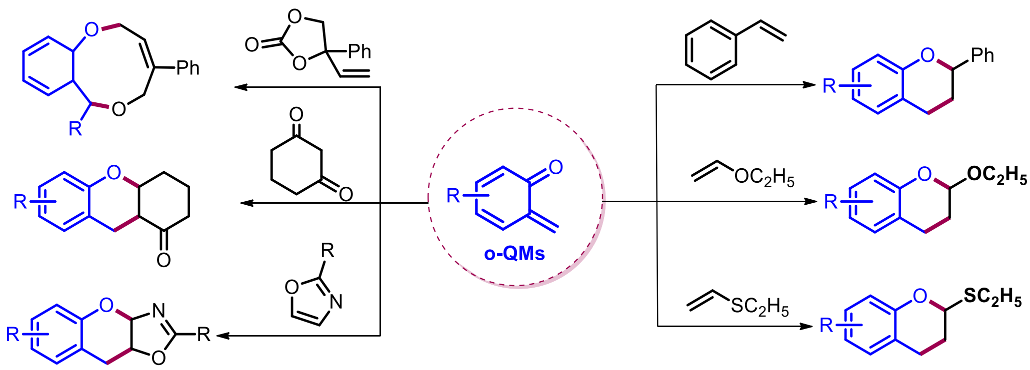

1.2.2.2. Chemistry of *p*-quinone methides (*p*-QMs):

Synthesis and Reactivity: Like *o*-QMs, *p*-QMs are also the prevalent structural motifs present in many natural products and pharmaceutical drugs. They contribute in huge number of biological applications such as adrenergic receptors, enzyme inhibition, lignin biosynthesis, DNA alkylation and cross linking. Over the decades, the inherent reactivity of the *p*-QMs has been thoroughly explored as they are valuable intermediates in natural product synthesis and cycloaddition reactions.[24]

Figure 1.2.6. *p*-Quinone methide and their resonating structures.

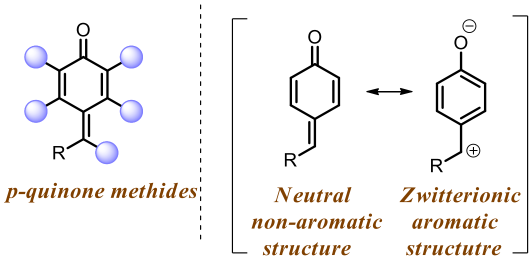

However, in this decade, these new intermediates have proved great boon to the synthetic society. As *o*-QMs, the *p*-QMs also comprises of a carbonyl and an exocyclic double bond, but at the opposite ends which results in the polarization of the molecule (Figure 1.2.6). They can be synthesized *via* condensation of phenol and aldehyde in the presence of base. The *in-situ* generation of these transient species can be carried out by using benzyl alcohol derivatives as starting materials. They can be easily synthesized by placing a good leaving group at the benzylic position (Figure 1.2.7). These species exist as neutral molecules with a zwitterionic resonance structure, which further contributes towards the remarkable reactivity of the *p*-QMs.[24]

Figure 1.2.7. Routes to Synthesize *p*-Quinone Methides (*p*-QMs).

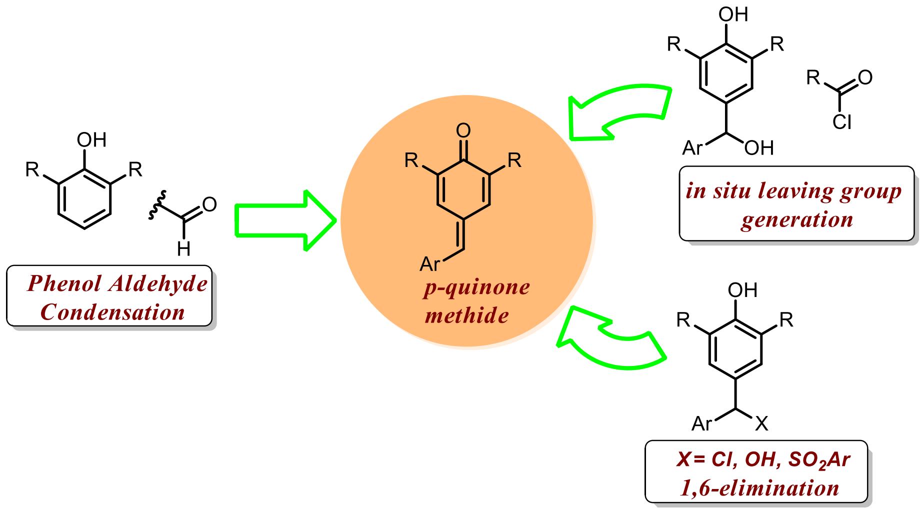

Due to their ability to undergo aromatization, they can easily give 1,6-addition reactions by using various nitrogen-, carbon-, phosphorus-, and sulfur-based nucleophiles under different reaction conditions. Besides, they can also take part in several (2+n) cycloaddition reactions, where these two carbons are of *p*-QMs and n number of carbon comes out from the other substrate. In the recent times, several biologically active scaffolds have been synthesized just by adding various substituents at the *o*-position of the *p*-QMs. These derivatives can be easily used to construct three, five, six-membered cyclic complex structures. A few *p*-QM derivatives are shown here (Figure 1.2.8).[25]

Figure 1.2.8. Different derivatives of *p*-QMs.

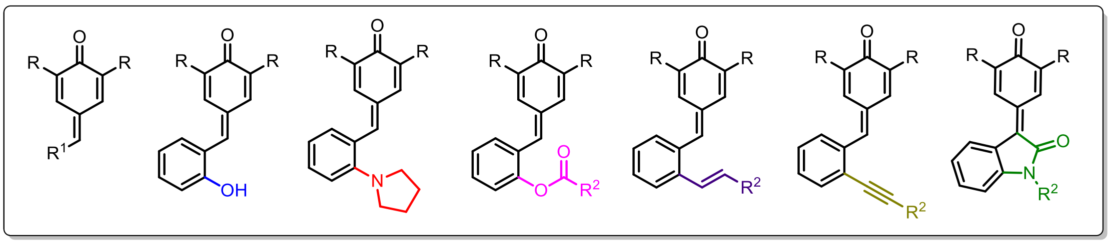

Reactivity: Normally, these species undergo cycloaddition reactions *via* 1,6-conjugate addition followed by dearomatization to give corresponding spirocyclic products. The reactivity of these species has been explored by various groups in the presence of Lewis acids and Bronsted acids by activation of the carbonyl group. Apart from these, taking account of their electrophilic nature, a strong nucleophile with a good leaving group in the presence of a base can be used to build the spirocyclic scaffolds. Also, in some of the cases spiro-cyclization can be achieved by catalyst free conditions. A few examples related to the construction of functionalized spirocyclic compounds under different reaction conditions are described here (Scheme 1.2.2.3).

Keeping in mind the reactivity of quinone methides, the proper choice of partner substrate plays a vital role in the given conditions. In the same line of thought, Lin's and Yao's group in 2015 suggested a methodology for the construction of functionalized spiro-cyclopropanes by employing *p*-quinone methides (*p*-QM) and sulfur ylides.[26] In this particular reaction, there was a nucleophilic attack of ylide at the exocyclic double bond of the QM followed by another nucleophilic attack from the *p*-position of the phenol with a subsequent removal of leaving group to deliver spirocyclopropanes under catalyst free conditions (Scheme 1.2.2.3(a)). In the past years, various transition metals have also been used to activate these reactive species and can further account for their cycloaddition reactions. Some of the examples have been demonstrated to give a glimpse of this type of reactivity. Zhao *et al.* in 2016 presented a palladium catalyzed (3+2) formal cycloaddition of *p*-QMs with vinyl epoxides and cyclopropanes to construct spiro[4.5]decanes under mild reaction conditions. The protocol is highly efficient and suitable for wide range of vinyl epoxides and cyclopropanes.[27] A variety of derivatized products can be obtained from the cycloaddition product under different reaction conditions (Scheme 1.2.2.3 (b)). In addition, Lin *et al.* and Yao *et al.* in 2017 reported a silver catalyzed cascade addition/cyclization reaction of *p*-QMs with propargyl malonates towards the facile synthesis of spirocyclic carbo- and heterocycles. The strategy is highly affordable as it requires inexpensive and easily accessible catalyst silver nitrate for the transformation.[28] Good scalability and various derivatized products are achieved from the given reaction (Scheme 1.2.2.3 (c)). In 2019, Das *et al.* described a formal 1,6-addition/annulation reaction by employing readily available starting materials *p*-QMs and pyrazolones towards the formation of bis-spiro compounds. After performing the control experiments, it was observed that the use of *N*-bromosuccinimide (NBS) is highly crucial for the transformation.[29] The same reaction was also compatible with *p*-QM derivative (*o*-hydroxyphenyl substituted *p*-QM) to construct spiro[pyrazolone-benzofuran] (Scheme 1.2.2.3 (d)).

The chemistry of *p*-QMs with other partners has been well studied under base mediated conditions for the construction of diverse heteroatom bearing spirocyclic scaffolds. From the past several years, chemists have been working on this type of reactivity by using *p*-QMs as model substrates. For example, in 2019, Su *et al.* demonstrated an efficient and straightforward method for the formal (3+2) cycloaddition of *p*-QMs with hydrazonoyl chlorides which *in-situ* generates nitrile imines in the presence of base and provided the corresponding spiro-pyrazoline-cyclohexadienone derivatives.[30] This protocol is scalable and have great functional group tolerance (Scheme 1.2.2.3 (e)). Another example by Zhao *et al.* in 2020 revealed the construction of bis-spiro compounds by the reaction of *p*-QMs and 3-chlorooxindole in the presence of a base.

Scheme 1.2.2.3. Annulation reactions of *p*-QMs.

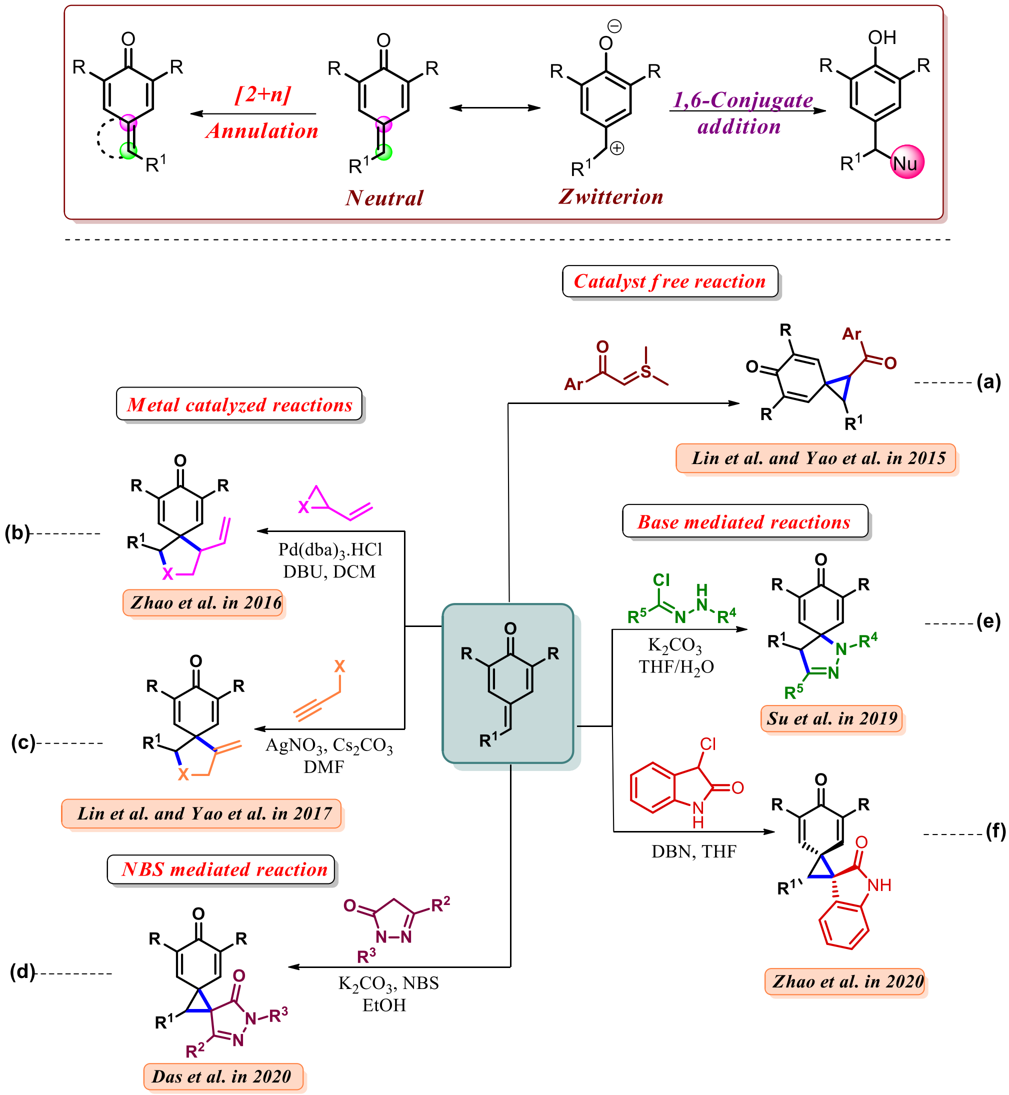

The reaction gave good results at room temperature in a very short interval of time. Initially, base abstracts the proton from the chlorooxiindole and then a nucleophilic attack on the *p*-QM will take place followed by intramolecular nucleophilic substitution to render the bis-spiro[cyclohexadienone-cyclopropane-oxindole] product.[31] Hence, they have showcased a novel scaffold in a concise manner by using a new pair of substrates (Scheme 1.2.2.3 (f)).

Reactivity of *o*-hydroxyphenyl substituted *p*-QMs: Among the different derivatives (Figure 1.2.8), the *o*-hydroxyphenyl substituted *p*-QM derivative has appeared as an amazing tool for the four-atom synthon and provide an efficient method for the construction of fused cyclic rings. This class of quinone methides have remarkably served the synthetic community in terms of variety of functionalized heterocycles. The core structure of the complex fused rings is found to be present in many bioactive molecules and natural products.[32] No doubt the different substitutions on these quinone methide derivatives have made the synthesis of structurally diversified molecules very facile. In the past years, the cycloaddition of these species under different reaction conditions is reported by various groups and are shown here (Scheme 1.2.2.4).

The metal free transformations have been extensively studied in the area of synthetic chemistry. The elegant synthesis of these sophisticated benzo-fused ring systems can be attained by some metal free approaches such as *N*-Heterocyclic carbene (NHC) and proline-based catalysts.[33] Taking into this consideration, Anand *et al.* in 2018 described the construction of benzofuran derivatives through a *N*-heterocyclic carbene catalyzed reaction of aromatic aldehydes and 2-hydroxyphenyl-substituted *p*-quinone methides with a subsequent acid- promoted dehydrative annulation (Scheme 1.2.2.4 (a)). In 2020, Chatterjee *et al.* developed an asymmetric version for the synthesis of chroman skeletons via asymmetric double 1,6-addition reaction.[34] The reaction started with an oxa-Michael reaction selectively to a vinylogous iminium ion followed by the another dienamine based 1,6-addition to *p*-QM derivatives. The persisting *α, β*-unsaturated enal moiety on the obtained chroman scaffolds were successfully modified to other important complex molecules (Scheme 1.2.2.4 (b)). However, base promoted reaction conditions also play a pivotal role in carrying out the reaction of *o*-hydroxyphenyl substituted *p*-QM derivative with different reaction partners for the facile synthesis of functionalized chroman derivatives and variety of fused ring skeletons. Inspired by this reactivity of *p*-QMs, some of the research groups have used these frameworks to construct cores of broad range of natural products. Keeping this in mind, Zhou *et al.* in 2018 demonstrated the construction of 2,3-dihydrobenzofuran derivatives via base promoted 1,6-addition/*O*-alkylation reaction of *p*-QM derivatives and bromomalonates in good to excellent yields under mild reaction conditions (Scheme 1.2.2.4 (c)).[35] Another example by Mei and Shi *et al*. in the subsequent year where they utilized the reactivity of *p*-QM derivative with ynones or benzynes to synthesize functionalized chromene and xanthene derivatives in an efficient manner under basic conditions.[36] The reaction was scalable and the bulky *tert*-butyl groups on the *o*-position were successfully detached by performing the reaction with Lewis acid $AlCl_3$ (Scheme 1.2.2.4 (d)). On the other hand, a series of substituted chroman derivatives can also be synthesized by using *p*-QM derivatives along with allenes under phosphine catalysis.[37] In order to construct chroman derivatives, allenes were activated by using phosphine catalyst and base was used to make the oxygen more nucleophilic by abstracting the proton of the hydroxy group of *p*-QM derivatives. In this direction, in 2019, Wu and Shi *et al.* reported a simple and straightforward approach for the formation of functionalized chromans by employing *p*-QM derivatives and allenes as reacting partners under phosphine catalyzed conditions.[38] This strategy was suitable for the wide range of allenes and *p*-QM derivatives (Scheme 1.2.2.4 (e)). In the same year, another example of these *p*-QMs came up with *β*-acetoxy allenoates by Huang's group. Here they have established a phosphine catalyzed domino 1,6- addition/annulation reaction and generated various chroman derivatives with alkynyl-substituted all-carbon quaternary center in excellent yield. This quaternary carbon center constitutes of an alkyne group which could be both terminal and internal. Further, the functionalized chroman scaffolds derivatized into various valuable products under different reaction conditions (Scheme 1.2.2.4 (f)). In terms of the conventional approaches, metal catalyzed reactions have appeared as one of the powerful approaches for the formation of new bonds. The construction of new bonds is a very crucial part in the synthetic community for the sake of synthesizing new bioactive molecules through different approaches. In this direction, Mei and Shi *et al*. in 2018 used the iridium catalyzed reaction conditions for

Scheme 1.2.2.4. Cycloaddition/Annulation reaction of *o*-hydroxyphenyl substituted *p*-QMs.

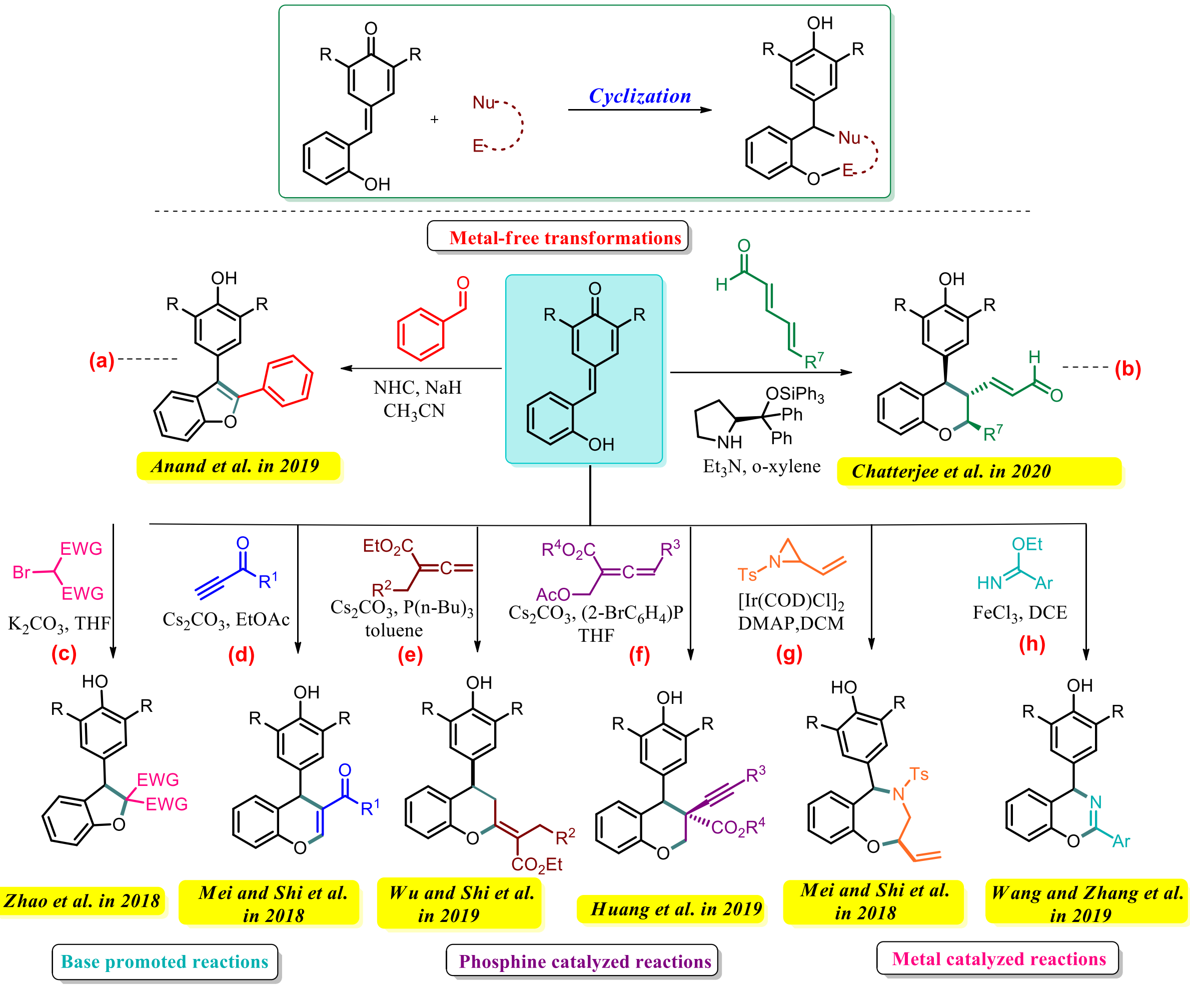

the facile construction of seven-membered benzoxazepine motifs using *p*-QM derivatives and vinyl aziridines.[39] In addition, they have performed the cyclization using palladium catalyst and chiral ligand to afford chiral version of benzoxazepine derivatives with high enantioseletivities. They also carried out the olefin metathesis reaction using Grubbs II catalyst and obtained chiral product with retention of both the diastereo- and enantiomeric ratios (Scheme 1.2.2.4 (g)). Next, a new strategy using *p*-QM derivatives and imidates via $FeCl_3$ catalyzed reaction conditions for the construction of 4-diaryl-1,3-benzoxazines scaffolds was performed by Wang and Zhang *et al.* in 2019.[40] Initially, the Lewis acid will activate the *p*-QM and undergoes a nucleophilic attack by the imidates followed by intramolecular nucleophilic attack of the hydroxy group to carry out the desired cyclization (Scheme 1.2.2.4 (h)).

1.2.3. An another quinone derivative: Benzoquinone Esters

Like quinone methides, this class of quinones is also highly admired by the synthetic community due to its numerous applications in the formation of various cores of many natural products and pharmaceuticals.[41] These quinone derivatives are used as three atom synthons (C-C-O) in several transformations and they have a tendency to undergo aromatization via tautomerization. In the last few years, they have significantly displayed their role in many cycloaddition reactions as a source of π component and appeared as a very convenient reaction partner towards the formation of valuable functionalized aromatic fused products. In order to showcase the reactivity of these prodigious quinone derivatives, some recent examples are shown here (Scheme 1.2.3.1). In 2017, Liu and Feng *et al.* developed a new strategy to synthesize benzofuran derivatives using benzoquinone esters and fulvenes in the presence of chiral Lewis acids.[42] At first, the two substrates were treated with chiral *N, N'*-dioxide-copper(II) complex to afford enantioselective (2+2) cycloaddition product which was further reacted with $In(OTf)_3$ to construct a variety of benzofuran scaffolds in good yields. The transformation was suitable for different quinone and fulvene derivatives with good diastereoselective and enantioselective ratios (Scheme 1.2.3.1 (a)). In 2021, Wang and Luo *et al.* utilized the dipolar reactivity of diaziridines with quinones under Lewis acid catalyzed conditions towards the facile synthesis of oxadiazines in excellent yields.[43] They smartly designed a powerful strategy to construct highly valuable heterocyclic compounds with three heteroatoms. Other than quinone esters, ketones and amides were also giving the final oxadiazines for broadening the scope of the reaction (Scheme 1.2.3.1 (b)).

Scheme 1.2.3.1. Cycloaddition Reactions of Quinone Esters

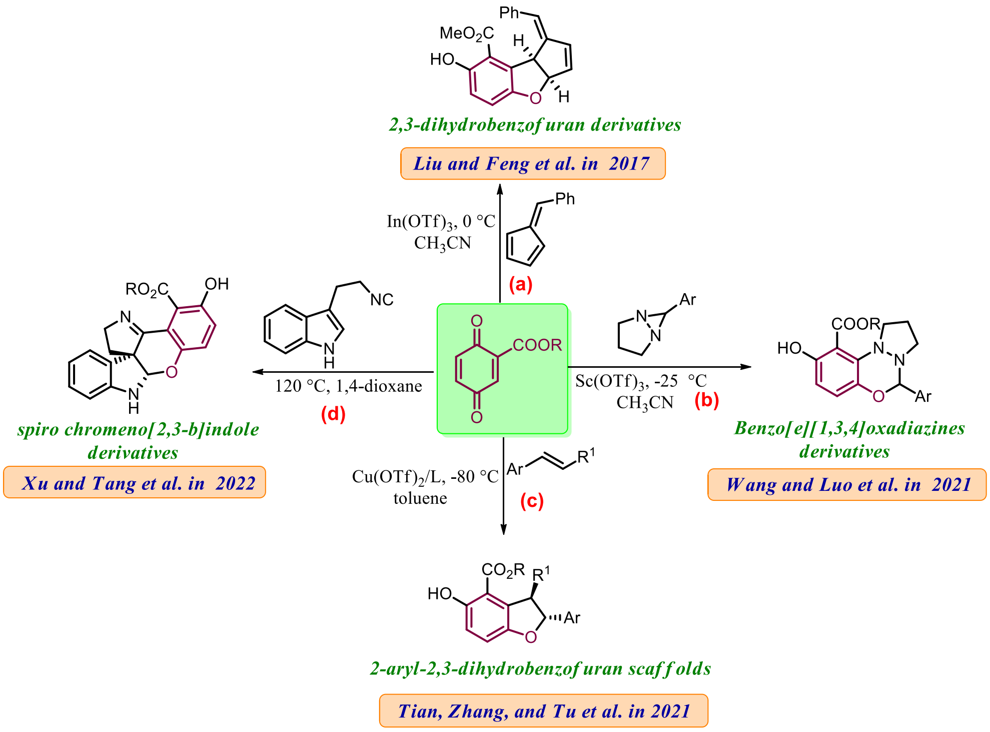

Another method for the synthesis of benzofuran derivatives was reported by Tian, Zhang and Tu *et al.* in 2021 by using styrene derivatives with quinone esters under Cu-SPDO complex catalytic system. This approach provided the variety of chiral benzofuran skeletons in good to excellent yields with good enantioselectivities.[44] They successfully accomplised an efficient strategy for the construction of natural products corsifuran A and B by performing some post-functionalization experiments (Scheme 1.2.3.1 (c)). In the recent year 2022, Xu and Tang *et al.* also described a synthesis of complex chromeno[2,3-*b*]indole and polycyclic spiroindoline scaffolds by employing quinone esters with tryptamine-derived isocyanides under reflux conditions.[45] They discovered a highly simple, catalyst free domino transformation for the effective construction of complex molecules by selecting a suitable pair of substrates. Further, they treated these chromenoindoles with $NaBH_3CN$ and polycyclic spiroindoline derivatives were obtained after three consecutive reactions that are reduction/intramolecular amidation/reductive ring opening of dihydropyran ring (Scheme 1.2.3.1 (d)).

1.3. Urea Derivatives in Heterocyclic Synthesis:

Urea derivatives have emerged as versatile building blocks towards the synthesis of many bioactive molecules, pharmaceuticals, and natural products.[46] The chemistry of urea derivatives has always been a very fascinating area for the construction of complex molecular architectures due to the presence of two nucleophilic centers. They can also be termed as bisnucleophiles and can be further employed to furnish a variety of heterocycles. In the last few years, these urea derivatives have come to light to manifest their utility either by acting as nucleophiles or by generating the diaza-oxyallylic cations which led to the simple and straightforward synthesis of many valuable cyclic compounds. In order to comprehend the reactivity of these elegant urea derivatives, a few examples have been documented by some organic chemists. Like, Jeffrey *et al.* in 2014 described a method for the oxidative 1,4-diamination of alkenes utilizing urea derivatives as a source of diazaoxy-allylic cations in the presence of an oxidant. A variety of diene substrates (cyclic and acyclic) were found to be suitable for the transformation. In this strategy, they had exclusively targeted the 1,4-difunctionalization of alkenes and provided (4+3) cycloaddition products.[47]

Jeffrey et al. in 2014

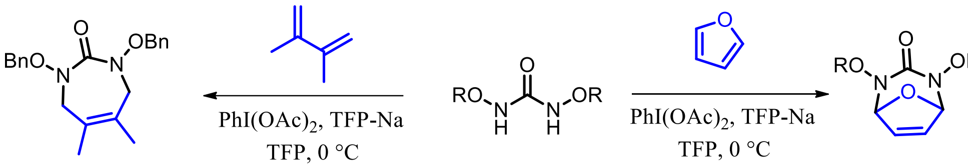

On the other hand, in 2019 Banerjee *et al.* provided an efficient method to render pharmacologically privileged tetrahydropyrimidinones by using readily available starting materials like donor-acceptor cyclopropanes and various dialkyloxy urea derivatives. Firstly, the two starting materials in the reaction provided uriedo-malonates in the presence of Lewis acid which further in the I_2-base mediated conditions furnished the tetrahydropyrimidinones in good yields. In this manner, they have utilized the bis-nucleophilic nature of urea derivatives for the transformation.[48]

Banerjee et al. in 2019

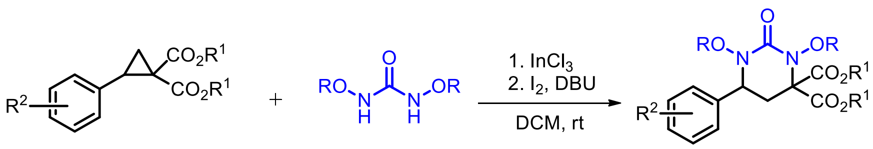

1.4. Strained Ring Systems in Heterocycles:

Over the years, heterocyclic compounds have gained substantial attention from the organic chemists. Heterocycles are the remarkable structural motifs that are present in almost all the natural products, agrochemicals, and exert many physiological and pharmaceutical activities. According to the data, almost 85% of the physiologically active compounds are heterocycles which shows the importance of heterocycles in the modern synthetic world. These valuable motifs can be prepared by various methods such as cycloaddition reactions, ring expansion, and annulation reactions.[49] Cycloaddition and annulation reactions are the conventional approaches for the synthesis of valued heterocycles (Scheme 1.4.1). Also, in the recent times too, there are no signs of abatement in the research activity of this field. Though, these approaches are traditional but still now these are quite alluring and are of paramount interest to the synthetic community for the formation of new carbocycles and heterocycles. In the modern times, cycloaddition reactions using new reaction processes like electrochemical and photochemical have also become more evident for the construction of functionalized heterocycles.

Scheme 1.4.1. The examples for the a). Cycloaddition Reactions b). Annulation reactions.

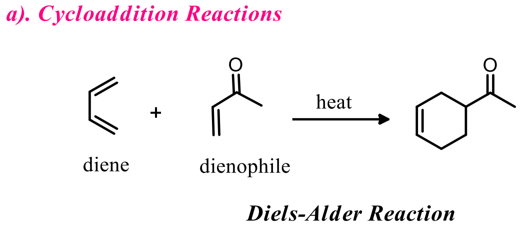

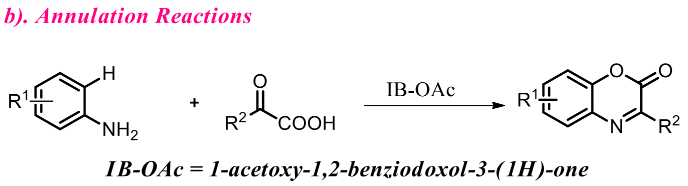

From the decades, small cyclic systems have always appeared as an ideal candidate for the facile construction of many bioactive cyclic frameworks due to their interesting strained reactivity. Some of the common strain ring systems are cyclopropanes, cyclopropenes, epoxides, aziridines, oxaziridines, diaziridines that are widely used as the building blocks towards the synthesis of many heterocyclic scaffolds. In this direction, cyclopropane derivatives have achieved substantial concentration from the synthetic chemists due to their stability at room temperature, easy handling, straightforward synthesis, and tuneable reactivity. Upon activation with Lewis and Bronsted acids, they generate transient species which can further give rise to cycloaddition, annulation reactions by reacting with suitable partner substrates.

Reactivity of Cyclopropane:

In the class of carbocycles, cyclopropane is the smallest cyclic ring which was first discovered by August Freund in 1881.[50] At first sight, cyclopropane seems to be a very unstable molecule due to the presumed strains such as angle strain and torsional strain. The structure of cyclopropane molecule implies a bond angle of 60° which is a huge deviation from the optimum sp^3 bond angle which points toward the large angle strain (or ring strain). Another reason could be the torsional strain due to the eclipsed conformation of the hydrogen atoms (Figure 1.4.1).[50]

Figure 1.4.1. Representation of different angle strain in cyclopropane

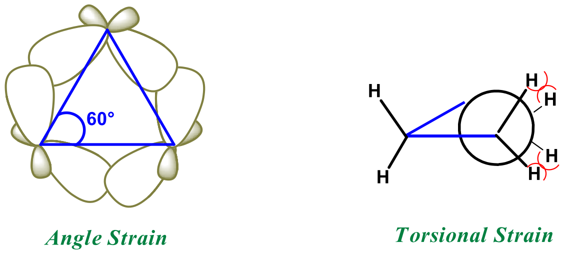

At the same time, the Professor C.A. Coulson and W.E. Moffitt elucidated the stability of the cyclopropane from the famous "Coulson-Moffit model" in the year 1947. This theory demonstrated that the bonds between the carbon atoms of the cyclopropane are bent and therefore, due to the banana bonds the bond angle between the carbon atoms of cyclopropane is 104º which is slightly deviated from the ideal sp^3 bond angle 109.5º. The presence of bent bonds accounts for the stability of the cyclopropane by reducing the ring strain. Hence, this proves that the cyclopropane is a thermodynamically stable molecule and can be further used for the different chemical transformations by using suitable reaction conditions (Figure 1.4.2).[51]

Figure 1.4.2. Coulson-Moffitt Model.

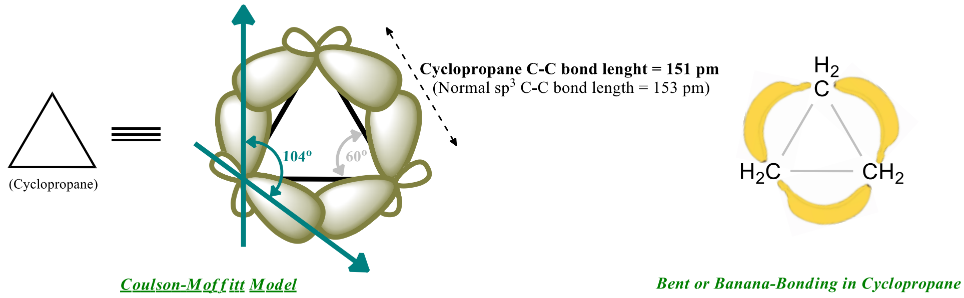

Despite the ring strain, the cyclopropane is kinetically inert and does not intend to relinquish its cyclic structure. To make the cyclopropane reactive or to activate atleast one of the C-C bonds some activating groups must be needed to add on the cyclopropane ring so that it could participate in a reaction. In light of this, the cyclopropanes with different activating groups may involve variety of donor or acceptor groups as substituents. Like, there could be a possibility of cyclopropane with only donor group (electron-donating) at one position, cyclopropane with only acceptor group (electron-withdrawing) at one end, and both a donor and acceptor group at vicinal positions which is called donor-acceptor cyclopropanes (DACs) (Figure 1.4.3).

Figure 1.4.3. Examples of activated cyclopropanes.

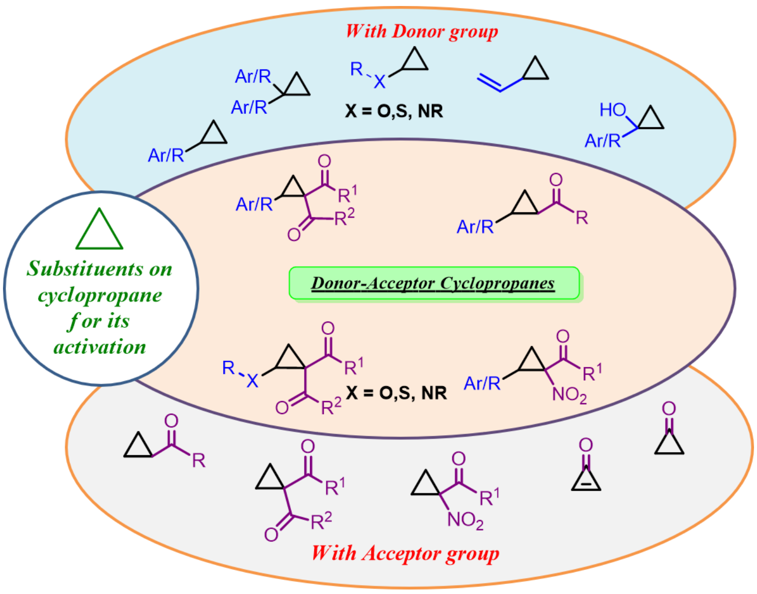

1.4.1. Donor-Acceptor Cyclopropane

Over the years, cyclopropane chemistry has gained enormous attention in the synthetic world due to their involvement in various novel chemical transformations. Among all of the above discussed cyclopropanes, on the basis of their reactivity the donor-acceptor cyclopropanes are the widely used precursors to perform various reactions. Due to the presence of donor and acceptor groups at the vicinal ends of the cyclopropane, the bond between them becomes highly polarized because of the push-pull effect of the substituents on the cyclopropane. The interesting part is even small amount of activation by catalyst, reagent or heat is sufficient to make these species react with a suitable partner or among themselves. Professor Hans-Ulrich Reissig was the one who has introduced the term “donor-acceptor cyclopropane” for the very first time in 1980, but still it took a very long duration to publish early reports on the reactivity of cyclopropanes.[52] Indeed, the presence of these donor and acceptor group on the cyclopropane has proved as an asset for many organic chemists for the development of new methodologies.

Scheme 1.4.2. Examples of different donor and acceptor groups on cyclopropane.

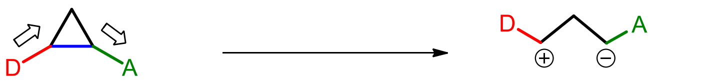

bond activation via push-pull effect of the substituents

1,3-zwitterionic species

D = Aryl, Alkyl, Vinyl, Het-aryl, RO, R_2N, Cyclopropyl.
A = Ester, Aldehyde, Ketone, Amide, Nitrile, Nitro, Sulfonyl, Nitroso

To design a cyclopropane, different donor and acceptor groups that are added on the cyclopropane moiety must have fine tuning with each other. Upon right activation, these groups support the cleavage of the highly polarized C-C bond and generate an intermediate that is 1,3-zwitterionic species in which the positive and negative charges are stabilized by donor and acceptor groups respectively. Some of the donor and acceptor groups that can be incorporated on the cyclopropanes are listed here (Scheme 1.4.2). Like for the donor groups aryl, alkyl, vinyl, heteroaryl, alkyloxy, amino, and cyclopropyl can be used. For acceptor part, groups such as ester, aldehyde, ketone, amide, nitrile, nitro, sulfonyl, nitroso can work as acceptors in DACs to the groups. Keeping in view the stable nature and easy access of these derivatives, this class of cyclopropanes have become the most adored class in the synthetic field for the target synthesis. Out of these DACs, two categories of the cyclopropane will be discussed here which are cyclopropane monocarbonyls and cyclopropane diesters.

1.4.1.1. Donor-Acceptor Cyclopropane Monocarbonyls

From the decades, it is quite evident that cyclopropane diesters are the most extensively used precursors in the synthetic community may be due to their stability at room temperature and easy accessibility. On the other hand, the reactivity of cyclopropane monocarbonyls are comparatively less explored. As the name infers, this class of cyclopropane consists of only one carbonyl group on the acceptor side. Many functional groups like ester, ketone, aldehyde that have been used as substituents on the acceptor side of the cyclopropane involves carbonyls. Although the cyclopropane monocarbonyls also come under the category of DACs. But there are some challenges that also come along with the cyclopropane monocarbonyls. The main challenge is the reduced reactivity of these monocarbonyls. Apparently, due to the presence of two esters groups at the acceptor end, the reactivity of cyclopropane diesters (DACs) is more than the cyclopropane monocarbonyls. However, the reactivity of cyclopropane monocarbonyls can be improved by attaching a more electron withdrawing groups on the acceptor side which can be aldehydes and ketones (Figure 1.4.4).[53] However, as far as our requirement is concerned, on the basis of reactivity donor-acceptor cyclopropane carbaldehydes is an excellent choice.

Figure 1.4.4. General reactivity of cyclopropane monocarbonyls.

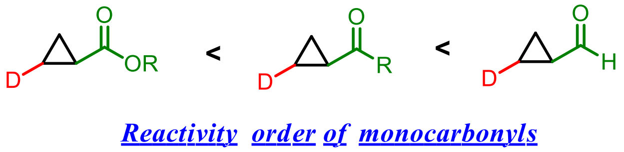

On the other hand, the close inspection of the structure of donor-acceptor cyclopropane carbaldehydes shows that instead of acting like a three-atom synthon, there can be many other possibilities due to the presence of reactive carbonyl group. There are two nucleophilic and electrophilic sites on the cyclopropane carbaldehydes which can give rise to many chemical transformations for the methodology development and target synthesis just by selecting a suitable reaction partner. Consequently, the interesting fact is that the presence of more reactive sites on the cyclopropane carbaldehydes can also result in different type of reactions such as (4+n), (5+n) with partner substrates other than typical (3+n) reactions. Another advantage of these cyclopropane carbaldehydes is that along with this type of reactivity, they can also undergo ring expansion and rearrangement reactions. For example, the well-known rearrangement reaction of cyclopropane monocarbonyls is Cloke-Wilson type rearrangement where the cyclopropane tends to rearrange itself into a five-membered ring (cyclic enol ethers) upon activation with Lewis and Bronsted acids in the presence of nucleophiles or by itself. This type of rearrangement reaction has been used in one of our reports (Scheme 1.4.3).

Scheme 1.4.3. Different type of reactions of cyclopropane monocarbonyls.

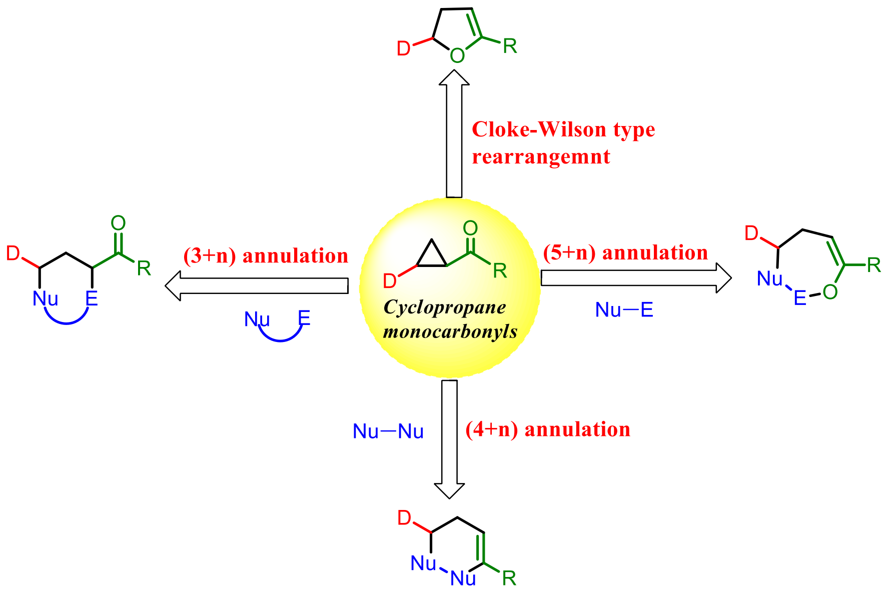

Reactivity of cyclopropane monocarbonyls: Although the cyclopropane monocarbonyls are comparatively less reactive than cyclopropane diesters. In spite of this, they can undergo different type of reactions like cyclopropane diesters. Also, presence of a donor and acceptor group at the vicinal carbon will lead to the polarization of bond by proper activation and form zwitterionic species. This intermediate will give different reactions like ring opening reactions, cycloaddition reactions, ring expansion and rearrangement reactions that can further be used to design various bioactive scaffolds. The existence of more reactive carbonyl group has also unlocked so many opportunities for this cyclopropane to react in different ways that has been shown in the above discussion. Further to examine the reactivity of these strained systems, ring opening reactions are the primary approach that gives assurance to the activation of strained rings by providing open chain products or 1,3-bifunctionalized products. To illuminate the reactivity of cyclopropane monocarbonyls, our group has introduced cyclopropane carbaldehydes and some of the examples of the annulation reactions have also been discussed here.

1.4.1.1.1. Cycloaddition/Annulation Reactions of Cyclopropane Carbaldehydes:

In order to make an effort to exploit the reactivity of cyclopropane carbaldehydes our group has contributed some reports in the presence of Lewis and Bronsted acids for the construction of many valued heterocycles. In 2018, Banerjee and co-workers introduced a report on cyclopropane carbaldehydes to Prins cyclization. In this report, when cyclopropane carbaldehydes were reacted with alkenol like 3-buten-1-ol at lower temperatures by using Lewis acid, the construction of strained (*E*)- hexahydrooxonine was observed.[54]

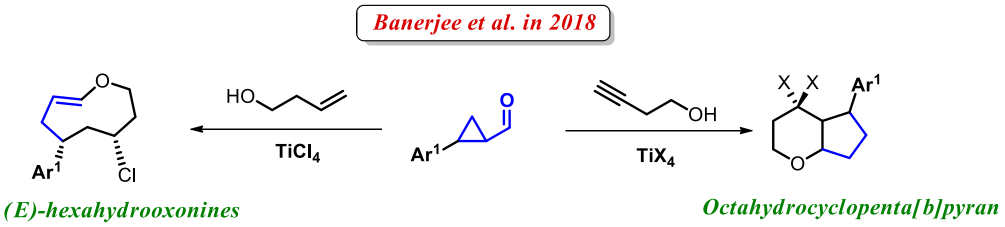

On the other hand, with alkynol such as 3-butyn-1-ol, a bicyclized product was obtained. Therefore, our group has successfully exploited the reactivity of cyclopropane monocarbonyls with two different alcohols under the similar conditions.

In 2019, our group developed a metal free ring opening and cyclization of cyclopropane carbaldehydes with *N*-benzyl amines by simply tuning the amount of the Bronsted acid (PTSA). The reaction begins with the nucleophilic attack of the amines on the cyclopropane carbaldehydes followed by the intramolecular Friedel-Crafts reaction. The presence of electron donating group such as *p*-methoxy is necessary for the cyclization process. The final cyclized product was further reduced to 2,3,4,5-tetrahydro-1*H*-benzo[*b*]azepine derivative using LAH/$FeCl_2$ mixture.

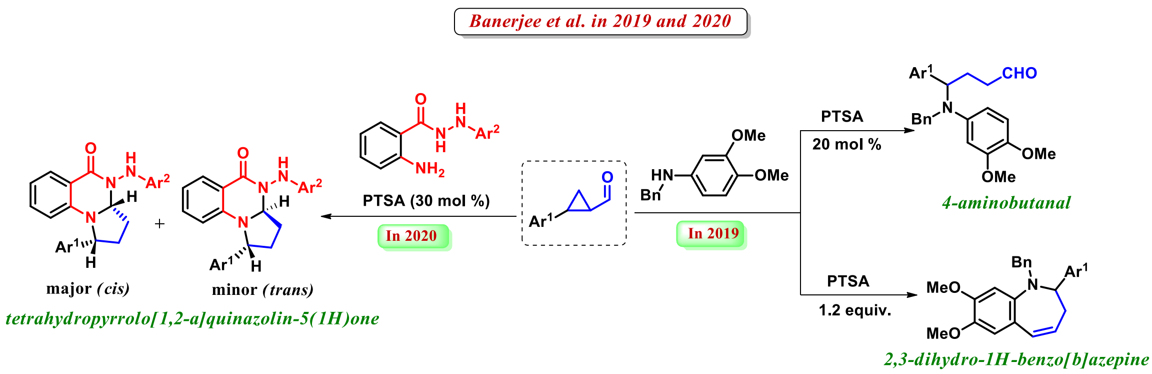

Next, in 2020, our group successfully synthesized tetrahydropyrrolo[1,2-*a*]quinazolin-5(1*H*)one derivatives by using cyclopropane carbaldehydes and anthranil hydrazides in the presence of PTSA. The reaction proceeded via domino imine formation followed by intramolecular cyclization to form 2-

arylcyclopropyl-2,3-dihydroquinolin-4(1*H*)-one and subsequent nucleophilic ring opening of the intact cyclopropane ring to furnish the desired product in good yields.[55]

1.4.1.1.2. Application of Cloke-Wilson type rearrangement towards the construction of heterocyclic scaffolds:

In the construction of structurally diverse heterocycles and carbocycles, the ring enlargemnent feature of cyclopropanes have emerged as a powerful tool to access bioactive molecules. The ring enlargement of cyclopropane imine give 2-pyrrolines and cyclopropane aldehydes and ketones furnish 2,3-dihydrofuran ring after rearrangement. Generally, this transformation of cyclopropane monocarbonyls to dihydrofuran is dependent on substrates and requires high temperature. Many groups have been utilizing the remarkable property of these cyclopropane monocarbonyls in the synthetically important organic reactions. Lewis acids and Bronsted acids under harsh conditions are used for this type of transformations. In the last few years, organocatalytic and photo-redox chemistry has also been introduced to take part in the ring enlargement of cyclopropane ketones. Further, a few examples related to the rearrangement type reactions of cyclopropane monocarbonyls has been discussed below.

In 2017, Silong Xu and co-workers reported an organocatalytic Cloke-Wilson rearrangement of cyclopropane ketones in the presence of DABCO at 120 ºC in DMSO solvent. The transformation took place via nucleophilic attack of the DABCO on cyclopropane and generates an enolate intermediate which subsequently undergoes cyclization and regenerates the catalyst. This transformation is compatible with broad range of substrates and afforded the dihydrofurans in good yields.[56]

Xu et al. in 2017

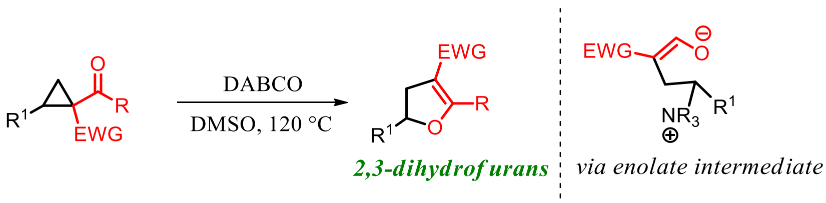

Banerjee and co-workers in 2020 came up with an example where they synthesized the oxybis(2-aryltetrahydrofuran) derivatives by employing metal-free domino Cloke-Wilson rearrangement-hydration-dimerization of cyclopropane carbaldehydes. All the reactions were performed in open flask using Bronsted acid as catalyst. Here the reactivity of cyclopropane carbaldehydes in the absence of another reactive partner has been studied. It was found that under same activation it gives Cloke-Wilson type rearrangement followed by hydration and then undergoes dimerization with another oxocarbenium ion.[57]

Banerjee et al. in 2020

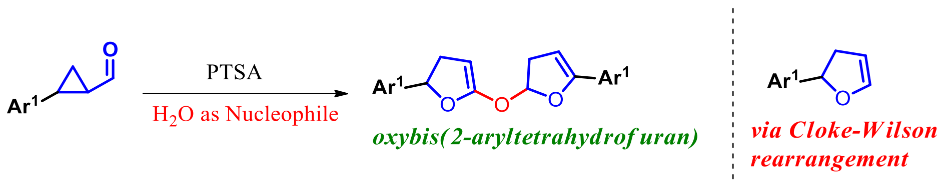

In continuation, our group again utilized this ring expansion feature of cyclopropane carbaldehydes with hydroxylamine salt using additive free technique for the construction of dihydro-4*H*-1,2-oxazine. The same transformation can be achieved with cyclopropane ketones by using catalytic *p*-toluene sulfonic acid monohydrate. Further, the cyclopropane diesters were reacted with dihydro-4*H*-1,2-oxazine to afford valued hexahydro-2*H*-pyrrolo[1,2-*b*][1,2]oxazine derivatives. Most of the cyclopropane derivatives were compatible with the transformation in terms of both cyclopropane monocarbonyls and cyclopropane diesters.[58]

Banerjee et al. in 2020

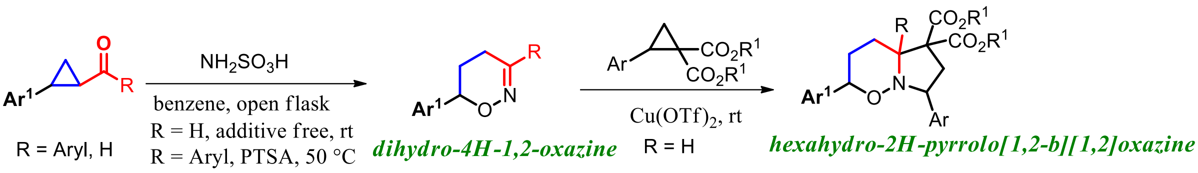

Very recently, Wei and Shi *et al.* used visible light for the construction of oxy-bridged macrocyclic indolinone derivatives by employing Cloke-Wilson type rearrangement of cyclopropyl ketones. The transformation begins with the excitation of the photocatalyst followed by the ring expansion via nucleophilic attack from carbonyl group again followed by intramolecular nucleophilic attack to obtain a bridged macrocyclic framework. The reagent CF_2CO_2Et proved very much crucial for the transformation at different levels. The protocol was scalable and can be used for the synthesis of natural products.[59]

Wei and Shi et al. in 2022

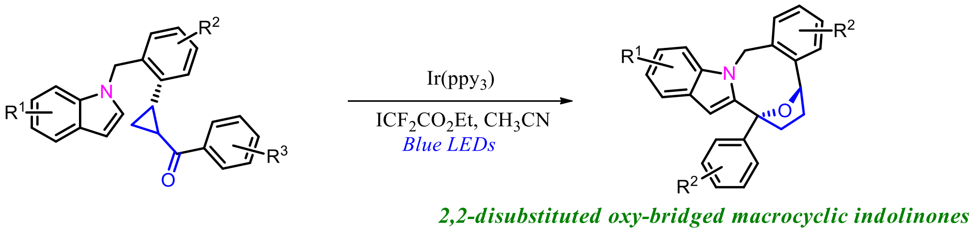

1.4.1.2. Reactivity of Donor-Acceptor Cyclopropane Diesters

One of the widely studied class of strained ring system is the cyclopropane diesters which consists of donor group at one end and two ester groups at the acceptor end. This class is indeed the most favourite among the synthetic chemists from 1980s. Among the DACs, these are commonly used as three atom synthons for the various cycloaddition reactions. The reason for their broad utilization in the synthesis of many biologically active scaffolds is the generation of 1,3-zwitterionic intermediates that can further give rise to many types of reactions like ring opening, cycloaddition, and rearrangement reactions. Instead of cyclopropane monocarbonyls, these cyclopropane diesters are best known for (3+n) type reactions. However, in the past years there have been tremendous advancement in the cyclopropane diester chemistry. Their pairing with a suitable partner substrate can lead to the formation of numerous biologically and structurally valuable frameworks. Enlightened by the reactivity of cyclopropane diesters, many research groups has used their predictable nature in the total synthesis to develop natural products. From the decades, transition metals, Lewis acids, and Bronsted acids has been used for the activation of these strained ring system. Now, in the modern times, the new research fields like photo-redox and electro-organic have also appeared as prominent areas to play with reactivity of the strained rings and came up with many interesting molecules. Some of the reports on the diverse reactivity of cyclopropane diesters has been shown here.

1.4.1.2.1. Lewis acid catalyzed reactions:

In the history of cyclopropane diesters, various Lewis acids has always been used for proper activation of these species. The choice of Lewis acid also plays a very vital role in the reaction depending upon the partner substrate. Many research groups have documented numerous reports on the reactivity of cyclopropane diesters using different Lewis acids. Like, if we look into the literature, there are a lot of (3+2) cycloaddition reaction of the DACs with a variety of 2π systems using catalytic amount of Lewis acids. For instance, Johnson and co-workers in the year 2005 disclosed the single step highly distereoselective synthesis of 2,5-disubstituted tetrahydrofurans from donor-acceptor cyclopropanes and aldehydes in the presence of $Sn(OTf)_2$. Cyclopropane diesters with electron-rich, slightly electron poor substituents were tolerating the reaction conditions and various aldehyde were also compatible to the reaction.[60]

Johnson et al. in 2005

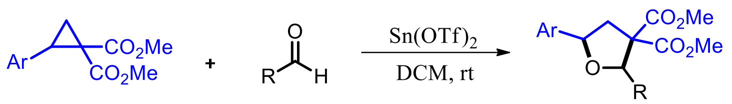

dihydrosubstituted tetrahydrofuran

In the year 2009, Tang and co-workers used the donor-acceptor cyclopropane diesters with enol silyl ethers under a suitable set of ligand/Lewis acid system and successfully furnished the controllable synthesis of cyclopentanes and 1,6-dicarbonyl compounds. In the presence of copper catalyst and ligand, they got a cyclized product with good diastereoselectivity. On the other hand, without ligand ring opening product was obtained through a cycloaddition-ring opening reaction. Reaction times played a very important role in bringing out this transformation.[61]

Tang et al. in 2009

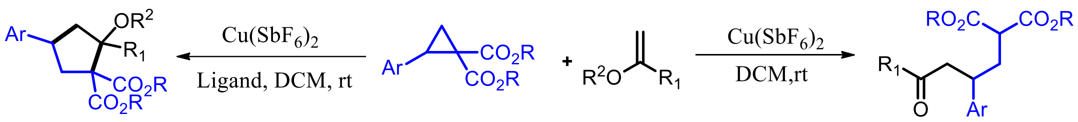

substituted cyclopentane derivatives *acyclic 1,6-dicarbonyl products*

Another new reactivity of these DACs showed by Melnikov and co-workers in 2013, where they discovered the synthesis of various hetero(arene)-annulated frameworks by using $SnCl_4$ and $BF_3{\cdot}Et_2O$ Lewis acids. In this report, the electrophilic centre of the cyclopropane is the same but the nucleophilic centre is shifted toward the ortho- position of the aromatic ring because of which it behaves as a different three-carbon synthon. Here, they have smartly used the new reactivity of these highly reactive DACs with alkenes for the construction of polyfunctionalized indanes via a (3+2) annulation reaction. Cyclopropanes with the highly

Melnikov et al in 2013

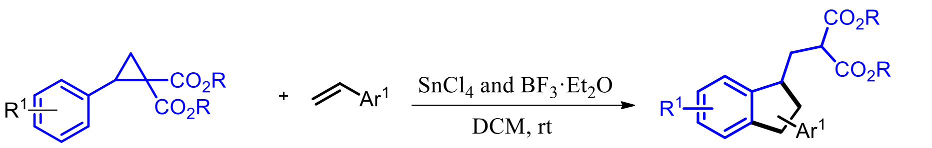

polyfunctionalized indanes

electron-rich and heteroaryl substituents were successful for the reaction.[62]

In 2016, Biju and co-workers described the tunable reactivity of donor-acceptor cyclopropane diesters with two different Lewis acids which further resulted in the formation of two interesting scaffolds. In this particular reaction, when cyclopropane diester reacts with 2-naphthols in the presence of catalytic amount of $Bi(OTf)_3$, they observed a selective (3+2) annulation reaction with an elimination of water molecule to construct naphthalene-fused cyclopentane systems. Alternatively, in the presence of $Sc(OTf)_3$, a Friedal Crafts type addition took place to furnish 1-functionalized-2-naphthols.[63]

Biju et al. in 2016

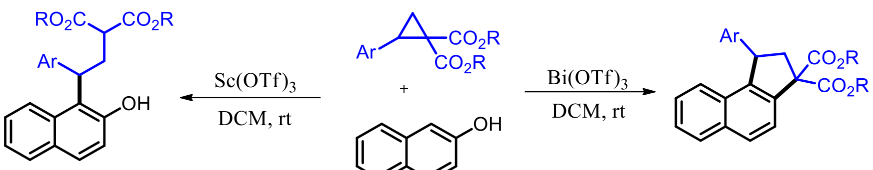

functionalized 2-naphthols *naphthalene-fuzed cyclopentane*

Further, an interesting example was disclosed in 2019 by Werz and co-workers where they illustrated the (3+3) annulation reaction of DACs with carbonyl ylides via synergistic catalysis. At first, diazo carbonyl compounds generate *in-situ* carbonyl ylides in the presence of $Rh_2(OAc)_4$ while Lewis acid $Sc(OTf)_3$ activates the strained ring and resulted in the formation of 9-oxabicyclo-[3.3.1]nonan-2-one. With a slight modification in the diazo compound, nine-membered oxygen-bridged products can be obtained.[64]

Werz et al. in 2019

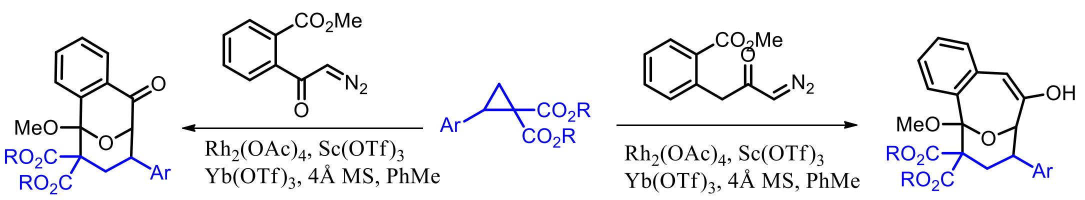

9-oxabicyclo-[3.3.1]nonan-2-one derivatives *10-oxabicyclo[4.3.1]decen-2-ol derivatives*

1.4.1.2.2. Bronsted acid catalyzed reactions:

In modern organic synthesis, Bronsted acid catalysis is the new growing area in the research field. In the past decades, many organic chemists have started working under metal-free conditions. However, many groups have also utilized the Bronsted acids to activate the DACs. From the above reports, it is quite clear that in the presence of Lewis acids cyclopropane diesters generate reactive dipolar species that are used for the synthesis of variety of structurally significant molecular architectures. Inspite of the inherent advantages of the Lewis acids, they suffer from serious limitations like high cost and toxicity etc.

Therefore, these issues could be addressed by taking advantage of these Bronsted acids instead of Lewis acids. Last few decades have experienced a huge utilization of these Bronsted acids for the generation of several reactive species. A few groups have also exploited the reactivity of cyclopropane diesters by using Bronsted acids.

In 2014, Wang and co-workers documented that trifluoromethanesulfonic acid (TfOH) could catalyze the reaction of DACs and nitriles to afford substituted pyrrolines. A variety of DACs and nitriles were suitable for the transformation and the reaction took place in 5 minutes which accounts for the simple and straightforward approach for the synthesis of diverse pyrrolines.[65]

Wang et al. in 2014

pyrrolines derivatives

In 2018, Moran and co-workers delineated nucleophilic ring opening of DACs under the Bronsted acid catalyzed conditions using fluorinated solvent hexafluoroisopropanol (HFIP). Here, the catalytic amount of TfOH in hexafluoroisopropanol worked as a highly reactive system for the ring opening process. This method worked well for various nucleophiles such as indoles, azides, arenes, dicarbonyls, and alcohols to access a variety of acyclic frameworks.[66]

Moran et al. in 2018

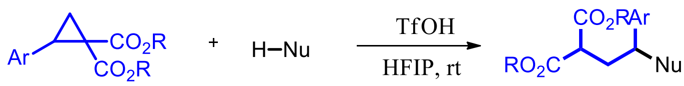

Nu = Arenes, azides, alcohols, indoles

1,3-bifunctionalized derivatives

Recently, in 2021, Zhao and Zhai *et al.* revealed a new Bronsted acid catalyzed (3+2) dehydration cycloaddition reaction of DACs and 2-Naphthols to access naphthalene-fused ring systems. The same fused products have also been synthesized by Biju *et al.* in the presence of Lewis acid but in that case yield of the product with respect to the vinyl group at the donor end was comparatively less.[67]

Zhao and Zhai et al. in 2021

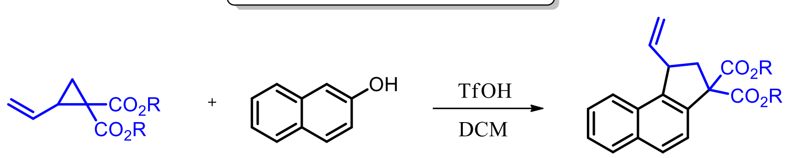

naphthalene-fuzed cyclopentane derivatives

In this particular method they have specifically standardized the reactions with vinyl group at the donor end and replaced Lewis acid with Bronsted acid, a significant improvement in the yields have been observed. Several derivatives have been synthesized by taking advantage of the vinylic group present in the naphthalene-fused cyclopentane rings.

1.4.1.2.3. Transition metal catalyzed reactions:

Transition metal catalysts are the powerful tool for the construction of variety of hetero- and carbocycles. Taking into consideration the reactivity of DACs, it has been observed that cyclopropane diesters form 1,3-dipolar species under Lewis or Bronsted acid catalysis. However, Vinyl cyclopropane (VCP) diesters can also perform transition metal catalyzed reaction by forming an acyclic zwitterionic π-allylpalladium complex via ring-opening of the VCP by oxidative addition to Pd(0). Some of the examples related to the transition metal catalyzed reactions of DACs are shown here.

In 2011, Trost and co-workers utilized the transition metal catalyzed approach for the (3+2) cycloaddition of vinyl cyclopropanes and alkylidene azalactone to render substituted vinyl cyclopentane derivatives. Here, they have used bis(2,2,2-trifluoroethyl)malonate vinyl cyclopropane for the sake of high yields and selectivities. The final product was further modified to a bicyclic system by treating it with dicyclohexyl borane in THF, followed by oxidation to alcohols and then cyclization to give fused lactone.[68]

Trost et al. in 2011

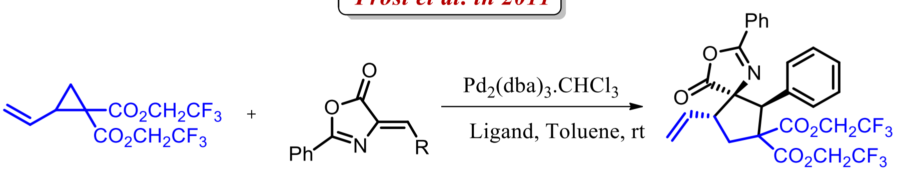

substituted vinyl cyclopentane derivatives

In the year 2018, Huang and Guo *et al.* came up with another palladium catalyzed (3+2) cycloaddition of vinyl cyclopropane with 1-azadienes to construct cyclopentane derivatives with good to excellent yields and diastereoselectivities. The protocol was scalable and an efficient method for construction of biologically valued scaffolds.[69]

Huang and Guo et al. in 2018

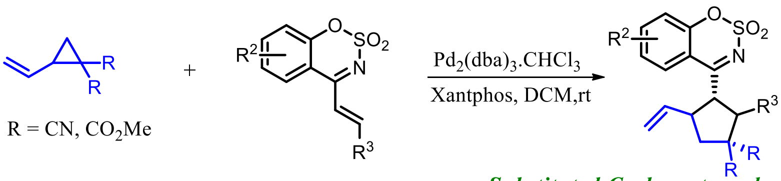

Substituted Cyclopentane derivatives

Another example in 2019 in which Chu, He, and Liu *et al.* described the palladium catalyzed cycloaddition reaction of vinyl cycloropanes and aldimines or isatin-derived ketimines by using chiral phosphoramidite ligands to synthesize pyrrolidine or spiro-[pyrrolidin-3,2′-oxindole] derivatives. The obtained final products were subjected to many post-fuctionalization reactions and the process was scalable too.[70]

Chu et al., He et al., and Liu et al. in 2019

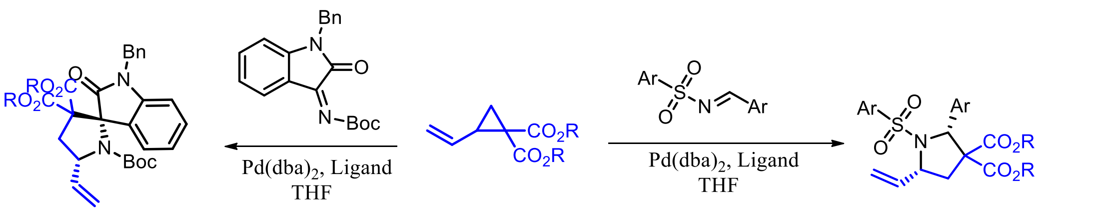

spiro-[pyrrolidin-3,2'-oxindole] derivatives ***Substituted pyrrolidine derivatives***

1.4.1.2.4. Photo- and Electro-catalyzed reactions:

In the modern world, photocatalysis and electrocatalysis has displayed an amazing progress in the field of synthetic organic chemistry. DACs has always been a wonderful molecule to work on under different catalysis. Undoubtedly, this remarkable molecule has also gained considerable attention in this modern field due to its numerous applications in the synthetic community. They are used as the building blocks of many natural products and bioactive molecules.

In 2021, Werz and Jacob *et al.* demonstrated the electrochemical ring opening of DACs via insertion of an oxygen molecule and successfully provided a new route for the 1,3-bifunctionalization process. This protocol was compatible with another strained ring like donor-acceptor cyclobutanes. This methodology can be utilized for the construction of *β*- and *γ*-hydroxy ketones. Several mechanistic studies and DFT experiments were conducted to prove the mechanism. In the same year, Banerjee *et al.* also revealed the same type of 1,3-bifunctionalization under different electrochemical conditions to afford substituted *β*-hydroxy ketones. The protocol involves the cleavage of C-C bond via activation of aryl ring and insertion of molecular oxygen under comparatively milder conditions. The strategy was scalable and further derivatized to various functionalized scaffolds.[71]

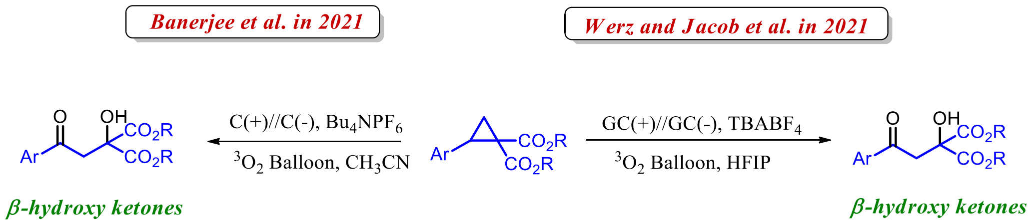

In the year 2022, Wei and Shi *et al.* reported a visible light induced ring opening hydrogenolysis of DACs towards the synthesis of alkylated aryl ketones in good to excellent yields. This method has many advantages over the previously used methods like mild reaction condition, conversion rates are high, straightforward approach for the variety of alkylated aryl ketones. They have also performed various experiments like deuterium labelling, ^{1}H NMR tracing etc. to prove the mechanism.[72]

1.4.1.3. Isomerisation of Cyclopropane diesters to Styryl malonates:

All the above examples have vividly showcased the reactivity of DACs as three-atom synthon in the organic chemistry. DACs are the perfect example for the (3+n) type formal cycloaddition reactions. Also, this strained carbocycle can be used as two atom synthons for the (2+n) type cycloaddition reactions by generating *in-situ* styryl malonates.[73] This process takes place by the isomerization of 1,3-zwitterionic species into the parallel styrene in the presence of a Lewis acid via a positive charge shift. This type of reactivity of DACs have also been well explored. Following are some of the literature reports on another type of reactivity of DACs.

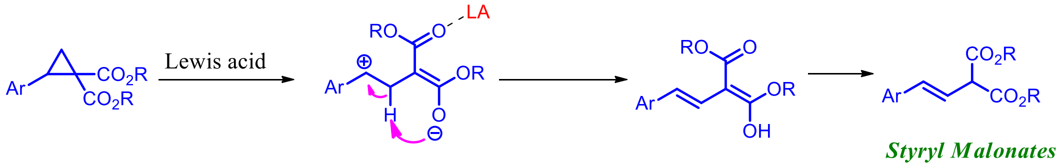

Wang and co-workers in the year 2014 delineated a new strategy for (2+3) cycloaddition where they have used the isomeric styryl malonates with *N*-benzylic sulfonamides in the presence of $AlCl_3$ to construct substituted indane skeletons. Here, the role of DACs is to serve the source of styryl malonates and sulfonamides generates a benzylic carbocation by cleaving C-N bond to form benzo-fused rings via intramolecular Friedal-Crafts cyclization.[74]

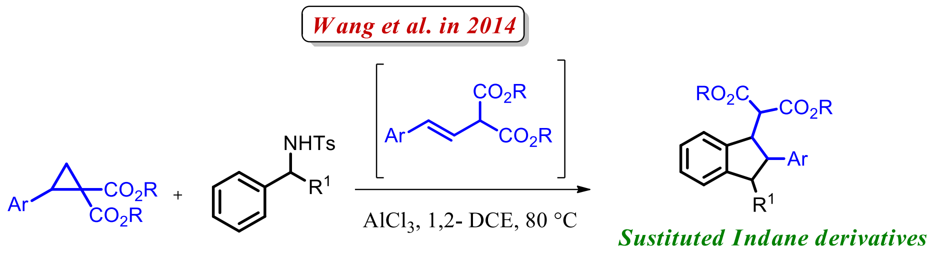

In 2018, Banerjee and co-workers disclosed a Lewis acid catalyzed (2+4) cycloaddition of styryl malonates generated from DACs with chalconimines to synthesize substituted indenopyridine frameworks under mild conditions. For the sake of the mechanism the styryl malonate was especially prepared and then the reaction was performed with the isolated styrene. Further, a nine membered lactam was also synthesized from the indenopyridine derivative.[75]

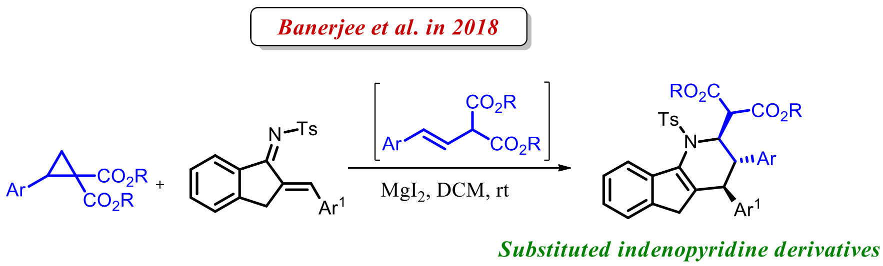

In conclusion, this chapter highlights the importance of valued heterocycles in a wide range of biologically relevant compounds and their significant role in the synthesis of many natural products as well as pharmaceuticals. Hence, in order to construct various structurally and biologically important heterocycles, the significance of different quinone derivatives, urea derivatives, and strained ring systems has been disclosed. This chapter majorly discusses the potential and intriguing reactivity of quinones derivatives such as quinone methide and quinone esters in terms of the synthesis of functionalized oxacycles due to their numerous applications. On the other hand, the utilization of reactivity of strained ring systems like donor-acceptor cyclopropane aldehydes and cyclopropane diesters with different reaction partners for the construction of diverse heterocyclic scaffolds has also been described. With the available information in hand, it is quite evident that all these reactive species under suitable conditions can be effectively used as potential precursors for the development of new methodologies as well as construction of synthetically valuable molecular architectures.

1.5 Aim of the thesis

This doctoral thesis is aimed to reveal new methodologies for the construction of heterocycles by coordinating the inherent reactivity of quinone derivatives with bis-nucleophiles (Ureas) and strained ring systems (Donor-Acceptor cyclopropanes). The thesis also revealed the facile construction of the diverse heterocyclic architectures such as spirocyclic and benzo-fused systems by employing the set of potential precursors. The other studies for the objective of thesis are detailed in the coming chapters.

Chapter 2 illustrates the efficient and straightforward approach for the spiro-imidazolidinone-cyclohexadie- nones from *p*-quinone methides (*p*-QMs) and dialkyloxy ureas under mild conditions.

Chapter 3 displays the Lewis acid catalyzed bicyclization of cyclopropane carbaldehydes with quinone methide and quinone esters to access benzo-fused oxygen tricycles that can be further dehydrogenated to access the valued dihydro-2*H*-furo[2,3-*b*]chromene frameworks.

Chapter 4 describes the reactivity of donor-acceptor cyclopropanes in the presence of two different Lewis acids with quinone esters toward the facile synthesis of chroman and benzofuran skeletons.

1.6 References

1. a) Taylor, R. D.; MacCoss, M. A.; Lawson, D. G. Rings in Drugs. *J. Med. Chem.* **2014**, *57*, 5845−5859. b) Simone, R. W.; Currie, K. S.; Mitchell, S. A.; Darrow, J. W.; Pippin, D. A. *Comb. Chem*. *High Throughput Screening*, **2004**, *7*, 473−493.
2. Vitaku, E.; Smith, D. T.; Njardarson, J. T. *J. Med. Chem.* **2014**, *57*, 10257-10274.
3. Gichinga, M. G.; Olson, J. P.; Butala, E.; Navarro, H. A.; Gilmour, B. P.; Mascarella, S. W.; Carroll, F. I. *ACS Med. Chem. Lett*. **2011**, *2*, 882–884.
4. Zadsirjan, V.; Heravi, M. M. *RSC Adv.*, **2020**, *10*, 44247-44311.
5. Martins, P.; Jesus, J.; Santos, S.; Raposo, L. R.; Roma-Rodrigues, C.; Baptista, P. V.; Fernandes A. R. *Molecules* **2015**, *20*, 16852-16891.
6. a) Hoffmann, H.; Lindel, T. *Synthesis* **2003**, 1753-1783. b) Weinreb, S. M. *Nat. Prod. Rep.* **2007**, *24*, 931-948.
7. Kushwaha, R. K. Singh, K. Kumar, P. Chandra, D. Research, J. *Pharm. and Tech.*, **2019**, *12*, 5566-5574.
8. Szumilak, M.; Stanczak, A. *Molecules*, **2019**, *24*, 2271.
9. Zadsirjan, V.; Hamidi, H.; Amiri, P.H.T.; Heravi, M.M, *RSC Adv.*, **2017**, *7*, 24470–24521.
10. Panda, B.; and Sarkar, T. K.; *J. Org. Chem*., **2013,** *78*, 2413–2421.
11. Singh, B.N.; Shankar, S.; Srivastava, R.K. *Biochemical Pharmacology***,** **2011**, 82, 1807-1821.
12. Garcia-Garcia, A. L.; Newman-Tancredi, A.; Leonardo, E. D. *Psychopharmacology*, **2014,** *231*, 623-636.
13. Poullennec, K. G.; Romo, D. *J. Am. Chem. Soc.* **2003,** *125*, 6344-6345.
14. Ichihara, A.; Nonaka, M.; Sakamura, S.; Sato, R.; Tajimi, A. *Chem. Lett.* **1988**, *17*, 27-30.
15. Trost, B. M.; Toste,F. D. *J. Am. Chem. Soc.* **2003**, *125*, 3090–3100.
16. Chupakhin, E.; Babich, O.; Prosekov, A.; Asyakina, L.; Krasavin, M. *Molecules*, **2019**, *24*, 4165.

17. Aminin, D.; Polonik, S. *Chem. Pharm. Bull.* **2020**, *68*, 46-57.
18. Abraham, I.; Joshi, R.; Pardasani, P.; Pardasani, R.T. *J. Braz. Chem. Soc.* **2011**, *22*, 385-421.
19. Bolhaar, S. T.; Mulder, M.; Van Ginkel, C. J. *Allergy*, **2001**, *56*, 248.
20. a) Van de Water, R. W. & Pettus, T. R. R. *Tetrahedron,* **2002**, *58*, 5367–5405. b) Jaworski, A. A. Scheidt, K. A. *J. Org. Chem.* **2016**, *81*, 10145-10153.
21. Chowdhury, S.; Anand, N.; Nagaraju, A.; Singh, M. S. *RSC Adv.*, **2014**, *4*, 55924-55959.
22. Wang, J.-Y.; Hao, W.-J.; Tu, S.-J.; Jiang, B. *Org. Chem. Front*., **2020**, *7*, 1743–1778.
23. Willis, N. J.; Bray, C. D. *Chem. Eur. J.* **2012**, *18*, 9160 -9173.
24. a) Caruana, L.; Kniep, F.; Johansen, T. K.; Poulsen, P. H.; Jørgensen, K. A. *J. Am. Chem. Soc*. **2014**, *136*, 15929-15932. b) Chu, W.-D.; Zhang, L.-F.; Bao, X.; Zhao, X.-H.; Zeng, C.; Du, J.-Y.; Zhang, G.; Wang, F.-X.; Ma, X.-Y.; Fan, C.-A. *Angew. Chem. Int. Ed.* **2013**,*52*, 9229 – 9233.
25. a) Zhao, K.; Zhi, Y.; Shu, T.; Valkonen, A.; Rissanen, K.; Enders, D. *Angew. Chem., Int. Ed.* **2016**, *55*, 12104−12108. b) Zhang, Z.-P.; Xie, K.-X.; Yang, C.; Li, M.; Li, X. *J. Org. Chem.* **2018**, *83*, 364-373. c) Lima, C. G. S.; Pauli, F. P. Costa, D. C. S.; De Souza, A. S. Forezi, L. S. M.; Ferreira, V. F. Da silva, F. C. *Eur. J. Org. Chem*. **2020**, 2650–2692.
26. Yuan, Z.; Fang, X.; Li, X.; Wu, J.; Yao, H.; Lin, A. *J. Org. Chem.* **2015**, *80*, 11123-11130.
27. Ma, C.; Huang, Y.; Zhao, Y. *ACS Catal*. **2016**, *6*, 6408-6412.
28. Yuan, Z.; Liu, L.; Pan, R.; Yao, H.; Lin, A. *J. Org. Chem*. **2017**, *82*, 8743-8751.
29. Kale, S. B.; Jori, P. K.; Thatikonda, T.; Gonnade, R. G.; Das, U. *Org. Lett*. **2019**, *21*, 7736-7740.
30. Zhao, Y.; Chang, B.; Zhao, X.; Zhang, R.; Liu, X.; Huang, D.; Wang, K.-H.; Huo, C.; Hu, Y.; Su, Y. *J. Org. Chem*. **2019**, *84*, 6719-6728.
31. Zhang, J.-R.; Jin, H.-S.; Sun, J.; Wang, J.; Zhao, L.-M. *Eur. J. Org. Chem.* **2020**, 4988–4994.
32. a) Hart, D. J.; Cain, P. A.; Evans, D. A.; *J. Am. Chem. Soc.* **1978**, *100*, 1548–1557. b) Zhang, X.-F.; Xie, L.; Liu, Y.; Xiang, J.-F.; Li, L.; Tang, Y.-L. *J. Mol. Struct.* **2008**, *888*, 145−151.
33. Singh, G.; Goswami, P.; Sharma, S.; Anand, R. V. *J. Org. Chem.* **2018**, *83,* 10546-10554.
34. Roy, S.; Pradhan, S.; Kumar, K.; Chatterjee, I. *Org. Chem. Front*., **2020**, *7*, 1388–1394.
35. Zhou, J.; Liang, G.; Hu, X.; Zhou, L.; Zhou, H. *Tetrahedron* **2018**, *74*, 1492-1496.
36. Xu, S.-L.; Zheng, W.-Q.; Bian, C.-Y.; Mei, G.-J.; Shi, F. *J. Org. Chem*. **2018**, *83*, 1414-1421.
37. Yuan, F.-R.; Jiang, F.; Chen, K.-W.; Mei, G.-J.; Wu, Q.; Shi, F. *Org. Biomol. Chem*. **2019**, *17,* 2361-2369.
38. Zhu, Y.; Wang, D.; Huang, Y. *Org. Lett*. **2019**, *21*, 908-912.
39. Jiang, F.; Yuan, F.-R.; Jin, L.-W.; Mei, G.-J.; Shi, F. *ACS Catal.* **2018,** *8*, 10234-10240.
40. Zhang, J.-R.; Jin, H.-S.; Wang, R.-B.; Zhao, L.-M. *Adv. Synth. Catal*. **2019**, *361*, 4811-4816.
41. Saepua, S.; Kornsakulkarn, J.; Choowong, W.; Suriyachadkun, C.; Boonlappradab, C.; Thongpanchang, C. J. *Nat. Prod.* **2021**, *84*, 2775−2785.
42. Zheng, H.; Xu, C.; Wang, Y.; Kang, T.; Liu, X.; Lin, L.; Feng, X. *Chem. Commun*. **2017**, *53*, 6585-6588.

43. Vazquez, J. C.; Davis, J.; Nestrov, V. N.; Wang, H.; Luo, W. *Org. Lett*. **2021**, *23*, 3136-3140.
44. Jing, Z. -R.; Liang, D. D.; Tian, J, -M.; Zhang, F.-M.; Tu, Y.-Q. *Org. Lett*. **2021**, *23*, 1258−1262.
45. Wang, X.; Dong, J.; Wu, T.; Xu, X.; Tang, B. *Org. Lett.* **2022**, *24*, 6700-6704.
46. Das, P.; Delost, M. D.; Qureshi, M. H.; Smith, D. T.; Njardarson, J. T. *J. Med.Chem.* **2019**, *62*, 4265–4311.
47. Anumandla, D.; Littlefield, R.; Jeffrey, C. S. *Org. Lett*. **2014**, *16*, 5112–5115.
48. Taily, I. M.; Saha, D.; Banerjee, P. *Eur. J. Org. Chem*. **2019**, 7804-7813.
49. a) Wang, J.; Gu, L.; Yang, S.; Qiao, L.; Luo, G.; Long, L.; Chen, G.; *J. Org. Chem.* **2021**, *86*, 12084-12092. b) Ylijoki, K. E. O.; Stryker, J. M. Chem Rev. 2013, 113, 2244-2266.
50. a) Freund, A. Journal fur *Praktische Chemie* **1881**, *26*, 367-377. b) Freund. A *Monatshefte fur Chemie,* **1882**, *3*, 625.
51. Coulson, C. A.; Moffit, W. E. *J. Chem. Phys*. **1947**, *15*, 151.
52. Reissig, H. -U.; Hirsch, E. *Angew. Chem. Int. Ed. Engl*. **1980**, *19*, 813.
53. Kharasch, M. S.; Cooper, J. H. *J. Org. Chem*. **1945**, *10*, 46.
54. Kumar, P.; Dey, R.; Banerjee, P. *Org. Lett*. **2018**, *20*, 5163-5166.
55. a) Dey, R.; Banerjee, P. *Adv. Synth. Catal.* **2019**, *361*, 2849–2854. b) Singh, P.; Kaur, N. Banerjee, P. *J. Org. Chem*. **2020**, *85*, 3393-3406.
56. Zhang, J.; Tang, Y.; Wei, W.; Wu, Y.; Li, Y.; Zhang, J.; Zheng, Y.; Xu, S. *Org. Lett.* **2017**, *19*, 3043–3046
57. Dey, R.; Rajput, S.; Banerjee, P. *Tetrahedron,* **2020**, *76*, 131080.
58. Kumar, P.; Kumar, R.; Banerjee, P. *J. Org. Chem.* **2020**, *85*, 6535–6550.
59. Liu, Z.; Wei, Y.; Shi, M. *Tetrahedron Chem,* **2022**, *1*, 100001.
60. Pohlhaus, P. D.; Johnson, J. S. *J. Org. Chem*. **2005**, *70*, 1057 – 1059.
61. Qu, J.-P.; Deng, C.; Zhou, J.; Sun, X. -L.; Tang, Y. *J. Org. Chem*. **2009**, *74*, 7684–7689.
62. Volkova, Y. A.; Kaplun, A. E.; Ivanova, O. A.; Chagarovskiy, A. O.; Skvortsov, D. A.; Rybakov, V. B.; Trushkov, I. V.; Melnikov, M. Y.; Budynina, E. M. *Chem. Eur. J.* **2013**, *19*, 6586-6590.
63. Kaicharla, T.; Roy, T.; Thangaraj, M.; Gonnade, R. G.; Biju, A. T. *Angew. Chem. Int. Ed.* **2016**, *55*, 10061-10064.
64. Petzold, M.; Jones, P. G.; Werz, D. B. *Angew. Chem. Int. Ed.* **2019**, *58*, 6225 –6229.
65. Cui, B.; Ren, J.; Wang, Z. *J. Org. Chem*. **2014**, *79*, 790-796.
66. Richmond, E.; Vukovic, V. D.; Moran, J. *Org. Lett*. **2018**, *20*, 574-577.
67. Shen, P.; Sun, D.; Zhao, Y.; Zhai, H.; Zhao, H. *Front Chem*. **2021**, *9*, 711257.
68. Morris, P. J.; Trost, B. M. *Angew. Chem. Int. Ed.* **2011**, *50,* 6167-6170.
69. Lin, Y.; Wang, Q.; Wu, Y.; Wang, C.; Jia, H.; Zhang, C.; Huang, J.; Guo, H. *RSC Adv*., **2018**, *8*, 40798–40803.
70. Huang, X. -B.; Li, X. -J.; Li, T. -T.; Chen, B.; Chu, W. -D.; He, L.; Liu, Q. -Z. *Org. Lett*. **2019**, *21*, 1713-1716.

71. a) Kolb, S.; Petzold, M.; Brandt, F.; Jones, P. G.; Jacob, C. R.; Werz, D. B. Angew.Chem.Int.Ed.2021,60,15928-15934. b) Saha, D.; Taily, I. M.; Banerjee, P. *Eur. J. Org. Chem.* **2021**, 5053-5057.
72. Liu, Z.; Wei. Y.; Shi, M. *Org. Chem. Front.*, **2022**, *9*, 1960–1966.
73. Chagarovskiy, A. O.; Ivanova, O. A.; Rakhmankulov, E. R. Budynina, E. M.; Trushkov, I. V.; Melnikov, M. Y. *Adv. Synth. Catal.* **2010**, *352*, 3179-3184.
74. Zhu, M.; Liu, J.; Chen, L.; Zhang, C.; Yu, J.; Wang, L. *Org. Lett*. **2014**, *16*, 1856-1859.
75. Verma, K.; Banerjee, P. *Adv. Synth. Catal*. **2018**, *360*, 3687-3692.

Chapter 2

Vinylogous Aza-Michael Addition of Urea Derivatives with p-Quinone Methides Followed by Oxidative Dearomative Cyclization: Approach to Spiroimidazolidinone Derivatives

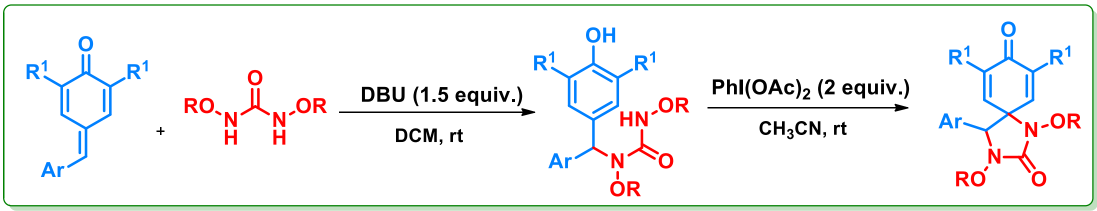

- *Metal free*
- *Moderate to good yields*
- *Mild reaction conditions*
- *Broad substrate scope*

This work was published in *Advanced Synthesis and Catalysis* (A journal of *Wiley-VCH*). Please see citation "Kaur, N.; Singh, P.; Banerjee, P. *Adv. Synth. Catal.* **2021**, *363*, 2813– 2824."

2.1 Introduction

Imidazolidin-2-ones and its analogues are ubiquitous structural motifs found in natural products, pharmaceuticals, and other biologically active compounds.[1] They often possess a broad range of biological activities such as antitumor, antibiotic, and anti-hypertonic.[2] These *N*-containing heterocycles show versatile utility as useful structural synthons in organic synthesis.[3] Amid the various spirocyclic scaffolds in drug discovery, spiroimidazolidinone is a promising structural motif.[4] Consequently, continuous efforts have been made towards the synthesis of this type of spirocyclic molecules.[5] On the other hand, it is worth considering that the cyclohexadienones are also the prevalent core structure found in many bioactive natural products and have gained considerable importance due to their abundance in pharmaceuticals.[6,7] Hence, incorporation of spiroimidazolidinone and cyclohexadienone in one frame can be proved beneficial for medicinal chemists.
During the past few years, *p*-quinone methides (*p*-QMs) have emerged as one of the most desirable components to access spiro-cyclohexadienones. In literature, *p*-QMs have been mainly known for their role as vinylogous Michael acceptors in various 1,6-conjugate addition reactions.[8,9] Aromatization of the cyclohexadienone moiety is the main driving force for these types of conjugate addition reactions. However, the spirocyclization reactions of *p*-QMs are comparatively less explored due to the requirement of the dearomatization of the reaction intermediate. In the past few years, many significant annulations have been developed using *p*-QMs like base-catalyzed [2 + 1] spiro-cyclization reactions of *p*-QMs with prefunctionalized nucleophiles such as 2-bromo malonate, sulfonium salts, sulfur, and ammonium ylides.[10] In 2016, the Lin and Yao group and the Zhao group separately demonstrated the palladium-catalyzed [3 + 2] cyclo- addition reaction of *p*-QMs with vinyl epoxides/cyclopropanes.[11] Recently, Su and co-workers disclosed a base-catalyzed [3 + 2] cycloaddition of *p*-QMs with *in situ* generated nitrile imines from hydrazonyl chlorides towards the construction of spiro-pyrazoline-cyclohexadienones (Scheme 2.1.1a).[12]

Scheme 2.1.1 Outline of *p*-QMs involved Spiro Cyclization Reactions.

a). Su et al.

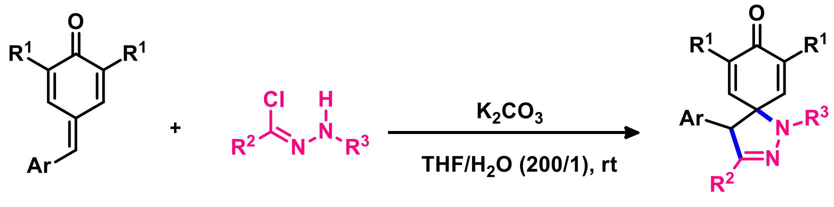

In addition, Das and co-workers also reported a base-catalyzed 1,6-conjugate addition mediated [2 + 1] annulation of *p*- QMs and pyrazolones to form bis-spiro compounds (Scheme 2.1.1b).[13]

b). Das et al.

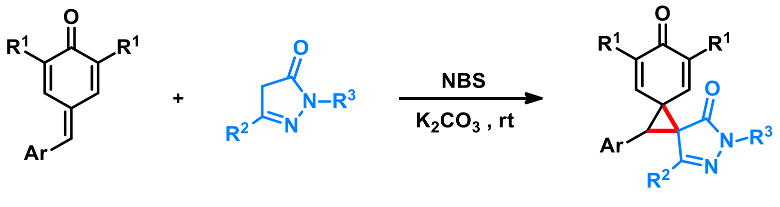

Urea and its derivatives are recognized as crucial functionalities in the medicinal chemistry discipline and constitute a key structural component of many FDA approved drugs.[14] The *N*-alkyloxy ureas have attracted researchers' considerable attention due to their involvement in a number of remarkable transformations.[15] In

2019, our group has reported the synthesis of tetrahydropyrimidinones via ring-opening/cyclization of donor-acceptor cyclopropanes with (un) symmetrical ureas.[16a] Also, in 2020, we have documented the palladium catalyzed regio- and stereo- selective access to allylic urea/carbamate derivatives from readily available vinyl ethylene carbonates and substituted urea derivatives.[16b] Encouraged by these results and studies, we tried to exploit the reactivities of *p*-QMs and urea derivatives as building blocks towards the construction of spiro-imidazolidinones. To the best of our knowledge, there have been no previous reports so far for the synthesis of spiro-imidizolidinone-cyclohexadienones using *p*-QMs and dialkyloxy/diaryloxy ureas. Herein, an efficient method for the cyclization of urea derivatives with *p*-QMs has been delineated to construct functionalized spiroimidazolidinones (Scheme 2.1.1c).

c). Our Idea

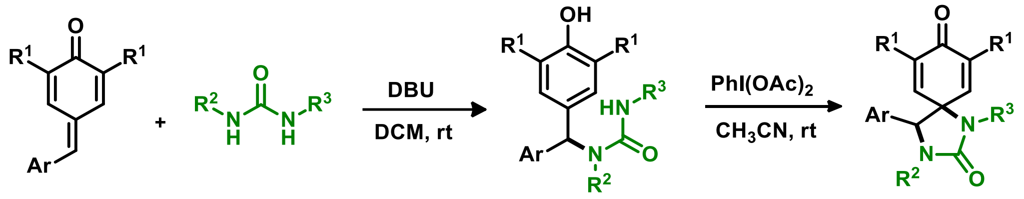

2.2 Results and Discussion

We commenced the present investigation by employing 2,6-di-*tert*-butyl *p*-QM **1a** and dibenzyloxyurea **2a** as model substrates in the presence of different bases. Initially, DBU (1 equiv.) was used as a base in DCM (solvent), and fortunately, desired 1,6-conjugate addition product was obtained with 70% yield.

Table 2.2.1. Optimization of reaction conditions for 1,6-conjugate addition.[a]

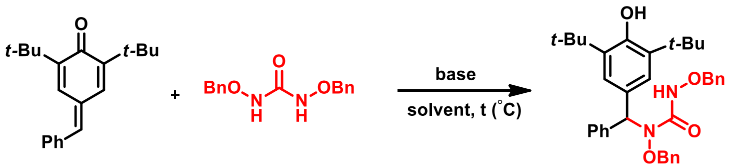

1a 2a 3aa

Entry	Base [b]	Loading (equiv.)	Time (h)	Solvent[c]	Yield (%)[d]
1.	DBU	1	3	DCM	70
2.	DBU	1.5	1	DCM	90
3.	DIPEA	1.5	16	DCM	50
4.	Et_3N	1.5	17	DCM	70
5.	DABCO	1.5	18	DCM	20
6.	DMAP	1.5	18	DCM	10
7.	Piperidine	1.5	18	DCM	n.r.[e]
8.	Pyridine	1.5	18	DCM	n.r.
9.	DBU	1.5	1	CH_3CN	85
10.	DBU	1.5	1	THF	78
11.	DBU	1.5	1	toluene	70

[a]Unless otherwise stated, Reactions were carried out with 1 equiv. of **1a**, 1 equiv. of **2a**. [b]DBU = 1,8-Diazabicyclo[5.4.0]undec-7-ene, DIPEA = *N*,*N*-Diisopropylethylamine, Et_3N = Triethylamine, DABCO = 1,4-diazabicyclo[2.2.2]octane, DMAP = 4-Dimethylaminopyridine. [c]DCM = dichloromethane, CH_3CN = acetonitrile, THF = tetrahydrofuran, [d]isolated yields. [e]n.r. = no reaction.

A subsequent increase in the yield to 90% was also observed when loading of DBU was increased to 1.5 equivalents (Table 2.2.1, entries 1 and 2). Other organic bases such as DIPEA, Et_3N, DABCO, DMAP proved less efficient for this transformation (Table 2.2.1, entries 3-6). In the case of piperidine and pyridine, both the starting materials remain unconsumed (Table 2.2.1, entries 7 and 8). Further, to improve the product yield, solvents like CH_3CN, THF, and toluene were also screened using DBU (1.5 equiv.) as base. In all the cases, conjugate addition product was obtained with compromised yield (70-85%) as compared to reaction in DCM (Table 2.2.1, entries 2 and 9-11).

With the optimized conditions in hand (Table 2.2.1, entry 2), initially, substrate scope with reference to *p*-QMs was investigated (Scheme 2.2.1). A series of *p*-QMs bearing electron-rich and electron-deficient substituents at the aromatic ring (Ar) **1a-1j** were examined, affording the 1,6-conjugate addition products **3aa–3ja** in moderate to good yields. *p*-QMs bearing electron- rich groups such as methoxy **1b**, methyl **1c**, benzyloxy **1d** at the *p*-position of the aryl ring (Ar) offered conjugate addition products **3ba-3da** in good yields.

Scheme 2.2.1. Scope of investigation with regard to *p*-QMs.[a,b]

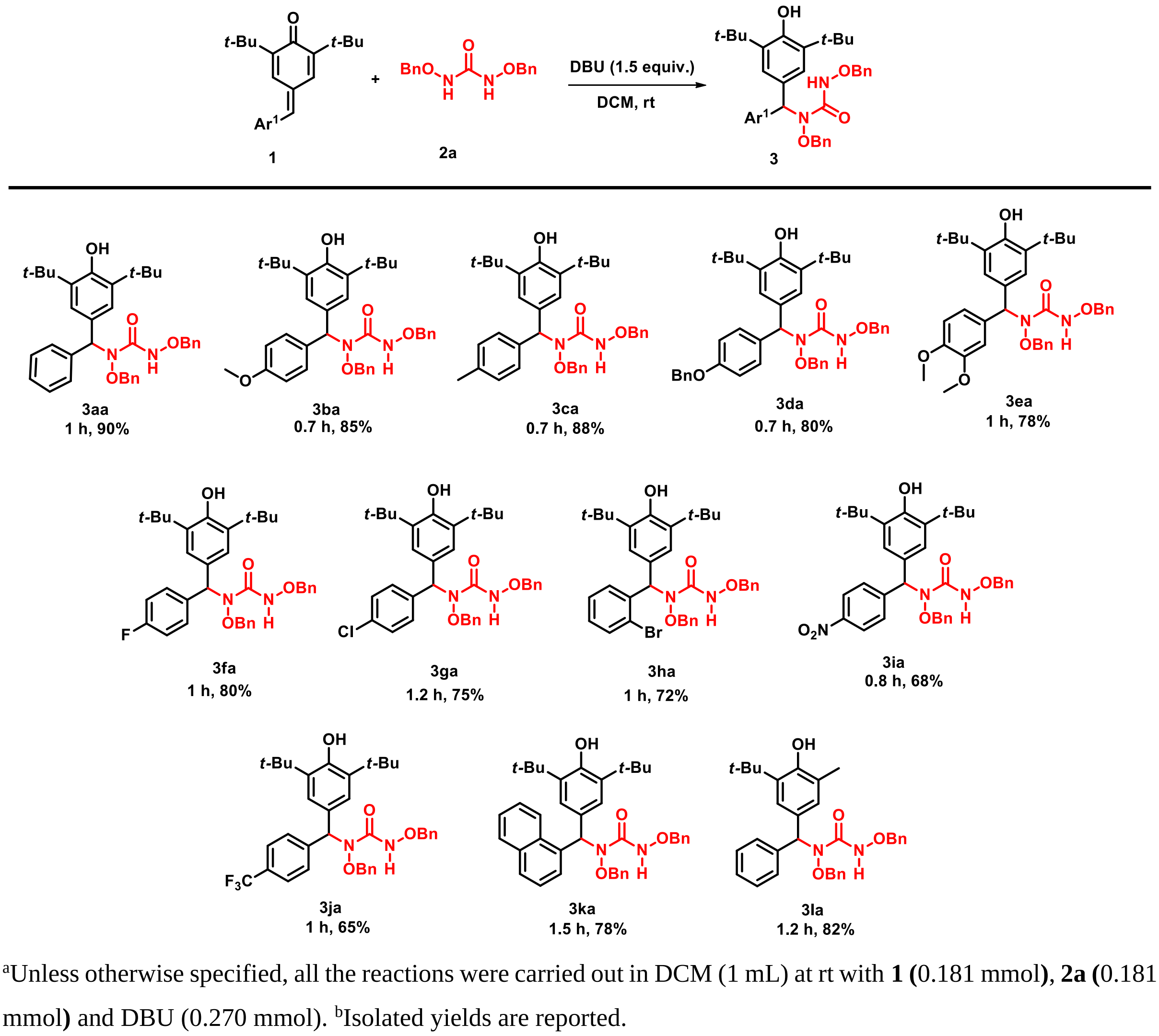

[a]Unless otherwise specified, all the reactions were carried out in DCM (1 mL) at rt with **1 (**0.181 mmol**)**, **2a (**0.181 mmol**)** and DBU (0.270 mmol). [b]Isolated yields are reported.

Compound **3ea** having 3,4-dimethoxy group as substituent was obtained from *p*-QM **1e** with 78% yield. Also, this transformation demonstrated consistency with *p*-QMs **1f-1h** bearing halogen group at aryl ring. Compounds **3fa-3ha** were obtained in good to moderate yields. Substrates enduring electron-withdrawing group (-NO_2, -CF_3) **1i-1j** at the *p*-position of the aryl ring offered the addition products **3ia** and **3ja** in 65–68% yield. Further, *p*-QM **1k** bearing naphthyl group delivered the addition product **3ka** in 78% yield. Besides this, unsymmetrical *p*-QM **1l** also afforded the conjugate addition product **3la** in good yield.

Later on, the generality and viability of the reaction was tested for dibenzyloxy ureas **2a-2e** by reacting them with *p*-QMs **1a** (Scheme 2.2.2). Fortunately, benzyloxy ureas with 4-Cl, 4-F, 4-Br, 4-Me substitution **2b-2e** afforded the conjugate addition products **3ab-3ae** in appreciable yields. Further, on using the dimethoxy urea **2f**, no profound effect on yield was observed. Compound **3af** was obtained with 80% yield. To evaluate the viability of the protocol with unsymmetrical urea, we attempted the synthesis of **3ag** using *N*-benzyloxy *N'*-methoxy urea **2g** as substrate**.** As expected, NMR data unveiled the formation of two regioisomers **3ag** and **3ag'** which were separated by column chromatography. Afterward, we also analyzed *N*-benzyloxy *N*-aryl unsymmetrical ureas **2h-2i** and found that the reaction went smoothly affording product **3ah** and **3ai** in good yields.

Scheme 2.2.2. Scope of investigation with regard to urea[a, b]

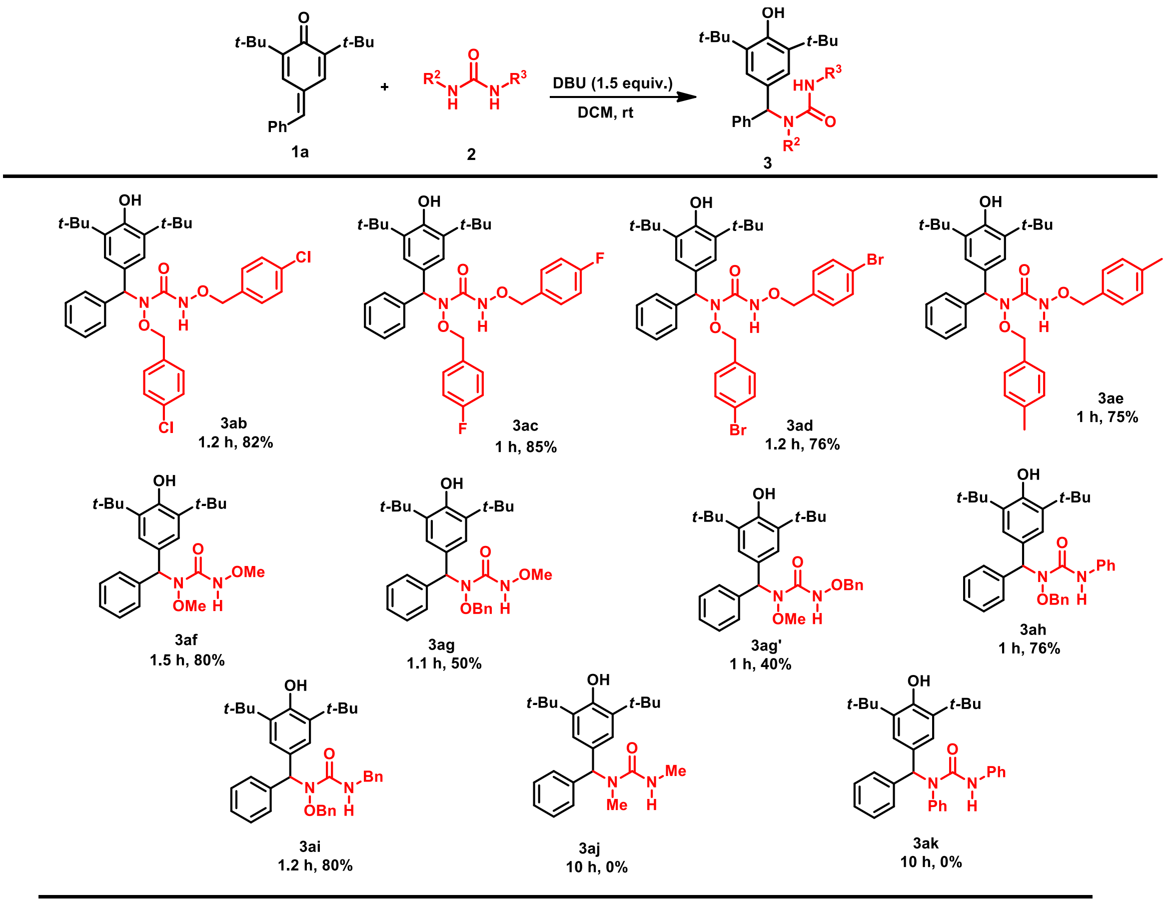

[a]Unless otherwise specified, all the reactions were carried out in DCM (1 mL) at rt with **1a** (0.181 mmol), **2** (0.181mmol) and DBU (0.270 mmol). [b]Isolated yields are reported.

The regioselective attack of *N*-benzyloxy nitrogen of unsymmetrical urea at the double bond of *p*-QM is due to the higher nucleophilicity of *N*-atom.[15] The ^{1}H-NMR spectrum evinced the formation of **3ai**. The participation of *N*-benzyloxy group in **3ai** was confirmed by a triplet of characteristic N-H at 6.1 ppm. In contrast, *N*,*N*-dialkyl urea **2j** and biaryl urea **2k** proved incompatible, presumably due to the poor nucleophilicity of the *N*-atom.[15]

Having synthesized a range of conjugate addition products, we subjected **3aa** to undergo an intramolecular dearomative ring closure to get the desired spirocyclic product. Initially, different oxidizing agents were screened. Oxidizing agents, such as DDQ, CAN were unable to catalyze the reaction (Table 2.2.2, entries 1-5). Whereas hypervalent iodine reagents proved compatible for the transformation, PIDA was found to catalyze the reaction, albeit in low yield (25%) as most of the conjugate addition product **3aa** remain unconsumed (Table 2.2.2, entry 6). Further, on increasing the loading of PIDA the yield of the final product was improved to 65% (Table 2.2.2, entry 7). Further, screening of different solvents using PIDA (2 equiv.) as oxidant was carried out. There was a significant decrease in the yield when CH_3CN was replaced with other solvents like DCM, THF, toluene, and DCE (Table 2.2.2, entries 8-11). On the other hand, various fluorinated solvents like HFIP, TFA, TFE proved fatal for the reaction (Table 2.2.2, entries 12-15).

Table 2.2.2. Optimization of reaction conditions[a]

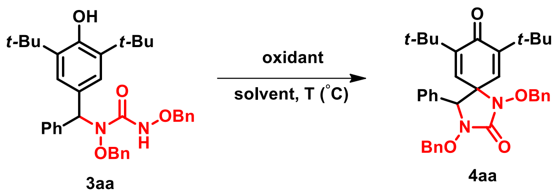

Entry no.	Catalyst [b]	Loading (equiv.)	Solvent [c,g]	T(°C)	Yield [d]
1.	DDQ	1	DCM	0-rt	n.r.[e]
2.	DDQ	2	MeOH	0-rt	n.r.
3.	DDQ	2	CH_3CN	0-rt	n.r.
4.	CAN	2	CH_3CN	rt	n.r.
5.	CAN	2	DCM	rt	n.r.
6.	PIDA	1	CH_3CN	0-rt	25
7.	PIDA	2	CH_3CN	rt	65
8.	PIDA	2	DCM	rt	40
9.	PIDA	2	THF	rt	45
10.	PIDA	2	toluene	rt	40
11.	PIDA	2	DCE	rt	34
12.	PIDA	1	HFIP	0-rt	c.m.[f]
13.	PIDA	2	HFIP	rt	c.m.
14.	PIDA	2	TFA	0-rt	c.m.
15.	PIDA	2	TFE	0-rt	c.m.
16.	PIFA	2	CH_3CN	rt	40

[a]Reactions were carried out with 1 equiv. of **3aa**. [b]DDQ = 2,3-dichloro-5,6-dicyano-1,4-benzoquinone, CAN = cerium ammonium nitrate, PIDA = diacetoxy iodobenzene, PIFA= (bis(trifluoroacetoxy)iodo)benzene. [c]DCM = dichloromethane, MeOH = methanol, CH_3CN= acetonitrile, THF= tetrahydrofuran, DCE = dichloroethane, HFIP = hexafluoroisopropanol, TFA = trifluoroaceticacid, TFE = 2,2,2-trifluoroethanol. [d]isolated yield. [e]n.r. = no reaction. [f]c.m. = complex mixture. [g]anhydrous solvents.

Hence, CH_3CN was adopted as the solvent of choice due to the better yield. Another hypervalent iodine oxidant PIFA was also screened, but a comparatively lower yield (40%) was obtained for the product **4aa** (Table 2.2.2, entry 16**)**. Therefore, on the basis of above optimization studies, 2 equiv. of PIDA in CH_3CN at room temperature was used as an optimal reaction condition for the final spirocyclization.

With the optimized conditions in hand (Table 2.2.2, entry 7), further cyclization of the conjugate addition products was performed (Scheme 2.2.3). It was found that conjugate addition products possessing moderately electron-releasing groups like *p*-methyl, *p*-methoxy, *p*-benzyloxy on the phenyl ring furnished the final cyclized product **4ba-4da** in 48-65% yield.

Scheme 2.2.3. Scope investigation with regard to 1,6- conjugate addition products[a,b]

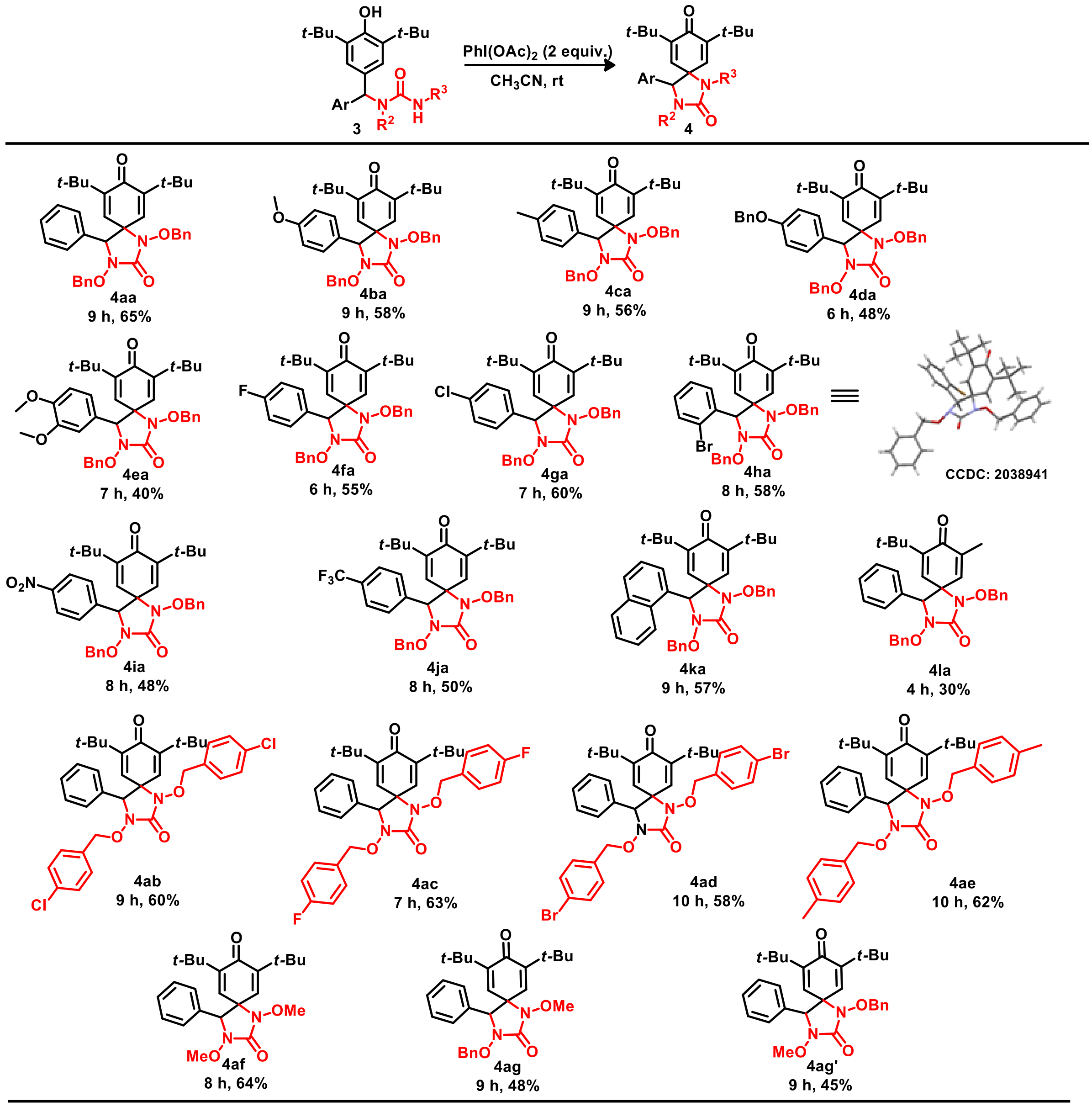

[a]Unless otherwise stated, all the reactions were carried out in anhydrous CH_3CN (1 mL) at rt with **3** (0.171 mmol) and PIDA (0.352 mmol). [b]Isolated yields

In contrast, the conjugate addition product with 3,4-dimethoxy group on the phenyl ring showed compromised yield for the cyclized product **4ea**. Substrates with F and Cl at the *p*-position of the phenyl ring gave the desired product **4fa**, **4ga** in 55% and 60% yields, respectively. The substrate with Br at the *o*-position offered the final cyclized product **4ha** with 58% yield. The structure of **4ha** was also ascertained by single crystal X-ray analysis. The substrate with other electron-withdrawing groups on the phenyl ring such as --NO_2, -CF_3 were also well tolerated with the reaction conditions, affording **4ia**, **4ja** in moderate yields. Naphthyl substituted conjugate addition product also participated in the cyclization reaction and offered **4ka** in 57% yield. The conjugate addition product of unsymmetrical *p*-QM **3la** gave the desired product **4la** in 30% yield. The low yield of product **4la** may be due to the formation of other unidentified side products in the reaction. Conjugate addition products **3ab-3af** with a range of *N,N'*-dialkyloxy ureas afforded their respective product **4ab-4af** in satisfactory yields. Spirocyclized product **4ag**, **4ag**' from the regioisomers **3ag**, **3ag'** were also obtained in 45-48% yield. Further, conjugate addition products **3ah**, **3ai** were also tested for spirocyclization, but the formation of the desired cyclized product was not observed, possibly due to the lower nucleophilicity of the *N*-atom or lack of the alkyloxy group giving the nitrenium ion.

Based on literature reports[17] and our observations, a plausible mechanism is disclosed for the proposed gradual transformation. Initial nucleophilic attack of urea **2a** on *p*-QMs **1a** under basic conditions resulted in the formation of fully aromatized open-chain product **3aa** through vinylogous aza-Michael addition. As per literature reports, it is well established that in the presence of hypervalent iodine reagents, *N*-alkyloxyamides generates nitrenium ion.[17] Hence, it was anticipated that oxidizing agent (PIDA) might have generated the nitrenium ion intermediate **B** from conjugate addition product **3aa**. As nitrenium ions are highly susceptible to nucleophilic attack due to their electrophilic nature, intermediate **B** could have undergone an intramolecular dearomative cyclization to afford 1,3-diazaspiro[4.5]deca-6,9-diene-2,8-dione **4aa** (Scheme 2.2.4).

Scheme 2.2.4 Plausible mechanism

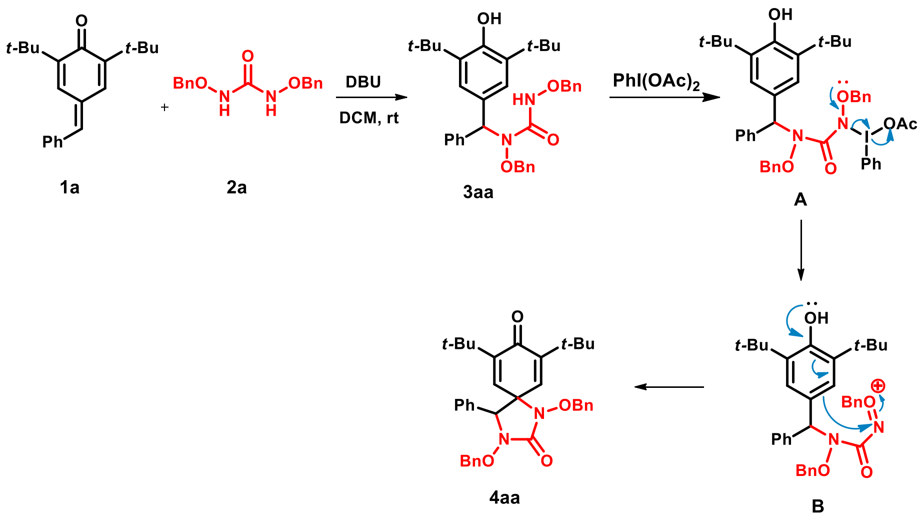

Having sufficient spirocycles in hand, the following transformation was carried out in sequential one pot fashion. The conjugate addition product **3aa** was *in situ* generated in the reaction mixture starting from *p*-QM **1a** and urea derivative **2a** in the presence of DBU at rt in anhydrous CH_3CN. After the complete consumption of both the starting materials in the reaction mixture as observed from thin layer chromatography, PIDA (2 equiv.) was then added, and the reaction mixture was further stirred at rt for 8 h. The desired cyclized product **4aa** was obtained in 35% overall yield (Scheme 2.2.5).

Scheme 2.2.5. One-pot sequential synthesis of 4

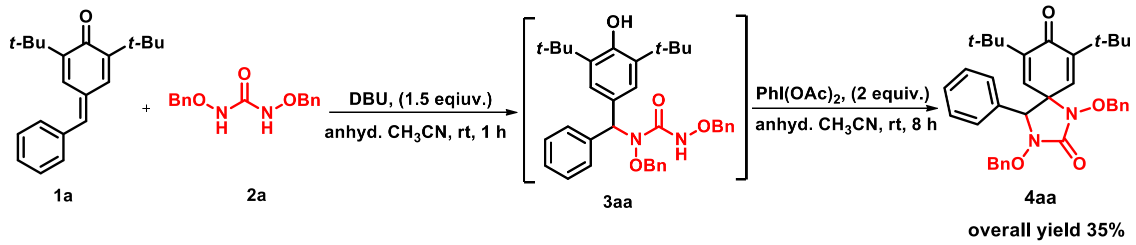

Further, to investigate the synthetic potential of the synthesized spiroimidazolidinones, the debenzylation of the compound **4aa** was executed using H_2/Pd-C conditions. Product **5aa** having *N*-hydroxy urea ring attached cyclohexadienone was obtained with 80% yield (Scheme 2.2.6).

Scheme 2.2.6. Debenzylation of 4

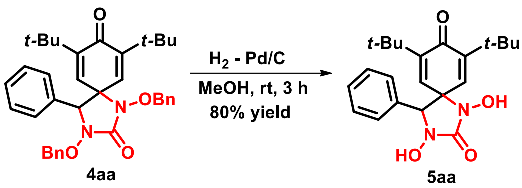

These *N*-hydroxy cyclic ureas can act as crucial structural elements in various metalloenzyme inhibitors.[18] In order to check the applicability of the proposed protocol, a gram-scale synthesis for the stepwise spirocyclization of *p*-QMs and dialkyloxy urea was also carried out under the optimized reaction conditions. The final spirocyclized product was obtained in 48% overall yield (Scheme 2.2.7).

Scheme 2.2.7. Stepwise Spiro-cyclization in gram scale

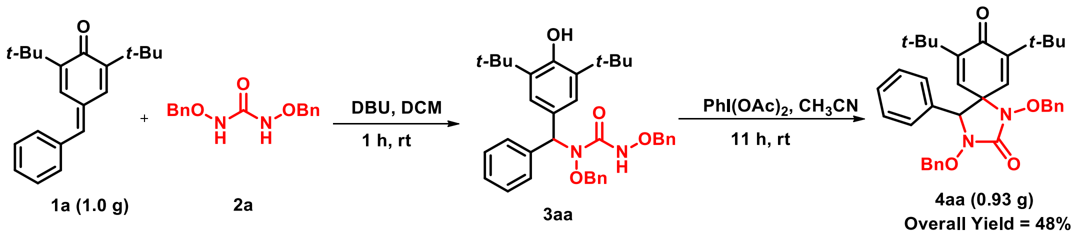

2.3 Conclusion

In conclusion, an efficient method for the formation of spiro-imidazolidinone-cyclohexadienones via vinylogous aza-Michael addition of urea derivatives (dialkyloxy/diaryloxy ureas) with *p*-QMs followed by cyclization under mild conditions has been demonstrated. This protocol has a wide substrate scope in terms of both of the reactants and also demonstrates a sequential one-pot approach. These scaffolds may seek attention in pharmaceutical industries and organic synthesis due to the diverse activities of imidazolidinones and cyclo-hexadienones. Also, debenzylation of spiroimidazolidinones gave biologically important *N*-hydroxy cyclic ureas.

2.4 Experimental Section

2.4.1 General information

All solvents and reagents were obtained from commercial sources and were purified following the standard procedure prior to use. The developed chromatogram was analyzed by UV lamp (254 nm) or *p*-anisaldehyde solution. Products were purified by flash chromatography on silica gel (mesh size 230–400). Unless otherwise specified, all the ^{1}H NMR and ^{13}C NMR spectra were recorded in $CDCl_3$. Chemical shifts of ^{1}H NMR and ^{13}C NMR spectra are expressed in parts per million (ppm). All coupling constants are absolute values and are expressed in Hertz. The description of the signals includes the following: s = singlet, d = doublet, dd = doublet of doublet, t = triplet, dt = doublet of triplet, q = quartet, br = broad, and m = multiplet. All ^{13}C spectra were recorded with broadband proton decoupling.

2.4.2 General Procedure for the preparation of *p*-quinone methides (1a-l)[9]

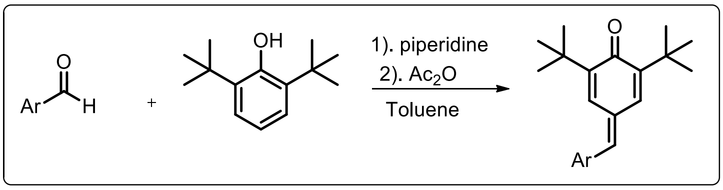

In a Dean-Stark apparatus, a solution of phenols (1 equiv., 9.69 mmol) and the corresponding aldehydes (1 equiv., 9.69 mmol) in toluene (100 mL) was heated to reflux. Piperidine (2 equiv., 2 mL) was dropwise added within 1 h. The reaction mixture was continued to reflux for 12 h. After cooling just below the boiling point of the reaction mixture, acetic anhydride (2 equiv., 2 mL) was added and stirring was continued for 15 min. Then the reaction mixture was poured on ice-water (500 mL) and extracted with CH_2Cl_2 (4 × 200 mL). The combined organic phases were dried over anhydrous Na_2SO_4, and the solvent of the filtrate was removed under reduced pressure. The crude products were purified by flash column chromatography and further recrystallized from *n*-hexane, affording the desired *p*-QMs.

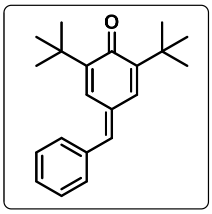

4-benzylidene-2,6-di-*tert*-butylcyclohexa-2,5-dienone (1a): ^{1}H NMR (400 MHz, $CDCl_3$): δ 7.54-7.34 (m, 5H), 7.26 (s, 1H), 7.19 (s, 1H), 7.02 (s, 1H), 1.34 (s, 9H), 1.30 (s, 9H).

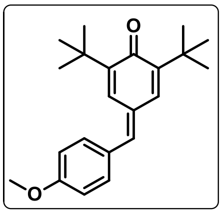

2,6-di-*tert*-butyl-4-(4-methoxybenzylidene)cyclohexa-2,5-dienone (1b): ^{1}H NMR (400 MHz, $CDCl_3$): δ 7.55 (d, J = 2.3 Hz, 1H), 7.45 (d, J = 8.7 Hz, 2H), 7.14 (s, 1H), 7.02-6.96 (m, 3H), 3.87 (s, 3H), 1.33 (s, 9H), 1.31 (s, 9H).

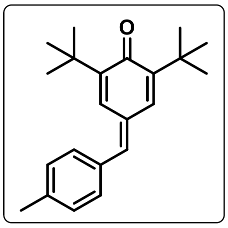

2,6-di-*tert*-butyl-4-(4-methylbenzylidene)cyclohexa-2,5-dienone (1c): ^{1}H NMR (400 MHz, $CDCl_3$): δ 7.54 (d, J = 2.1 Hz, 1H), 7.35 (d, J =8.1 Hz, 2H), 7.25 (d, J =7.9 Hz, 2H), 7.15 (s, 1H), 6.99 (d, J = 2.3 Hz, 1H), 2.39 (s, 3H), 1.31 (s, 9H), 1.29 (s, 9H).

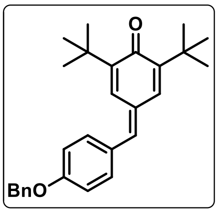

4-(4-(benzyloxy)benzylidene)-2,6-di-*tert*-butylcyclohexa-2,5-dienone (1d): ^{1}H NMR (400 MHz, $CDCl_3$): δ 7.56 (s, 1H), 7.47-7.33 (m, 7H), 7.13 (s, 1H), 7.05 (d, J = 8.4 Hz, 2H), 7.00 (d, J = 2.5 Hz, 1H), 5.13 (s, 2H), 1.33 (s, 9H), 1.31 (s, 9H).

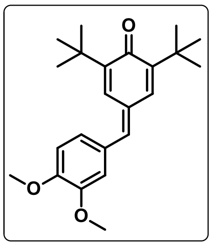

2,6-di-*tert*-butyl-4-(3,4-dimethoxybenzylidene)cyclohexa-2,5-dienone (1e): ^{1}H NMR (400 MHz, $CDCl_3$): δ 7.59 (d, J = 7.7 Hz, 1H), 7.12 (s, 1H), 7.06 (d, J = 8.5 Hz, 1H), 7.01 (d, J = 1.6 Hz, 1H), 6.98 (d, J = 2.2 Hz, 1H), 6.93 (d, J = 8.2 Hz, 1H), 3.93 (s, 3H), 3.90 (s, 3H), 1.31 (s, 9H), 1.30 (s, 9H).

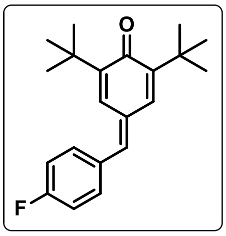

2,6-di-*tert*-butyl-4-(4-fluorobenzylid ene)cyclohexa-2,5-dienone (1f): ^{1}H NMR (400 MHz, $CDCl_3$): δ 7.46-7.40 (m, 3H), 7.18-7.11 (m, 3H), 6.99 (d, J = 2.3 Hz, 1H), 1.32 (s, 9H), 1.29 (s, 9H).

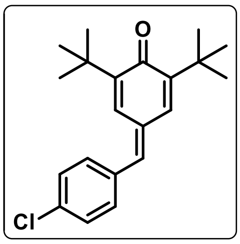

2,6-di-*tert*-butyl-4-(4-chlorobenzylidene)cyclohexa-2,5-dienone (1g): ^{1}H NMR (400 MHz, $CDCl_3$): δ 7.43-7.33 (m, 5H), 7.09 (s, 1H), 6.98 (d, J = 2.3 Hz, 1H), 1.31 (s, 9H), 1.27 (s, 9H).

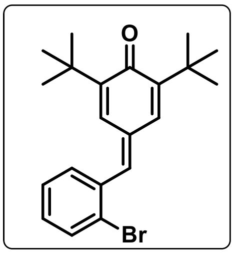

4-(2-bromobenzylidene)-2,6-di-*tert*-butylcyclohexa-2,5-dienone (1h): ^{1}H NMR (400 MHz, $CDCl_3$): δ 7.68 (d, J = 7.7 Hz, 1H), 7.39 (d, J = 4.2 Hz, 2H), 7.30-7.21 (m, 3H), 7.07 (d, J = 2.7 Hz, 1H), 1.34 (s, 9H), 1.26 (s, 9H)

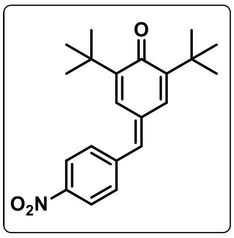

2,6-di-*tert*-butyl-4-(4-nitrobenzylidene)cyclohexa-2,5-dienone (1i): ^{1}H NMR (400 MHz, $CDCl_3$): δ 8.31 (d, J = 8.6 Hz, 2H), 7.58 (d, J = 8.3 Hz, 2H), 7.36 (d, J =2.3 Hz, 1H), 7.15 (s, 1H), 7.01 (d, J = 2.3 Hz, 1H), 1.32 (s, 9H), 1.28 (s, 9H).

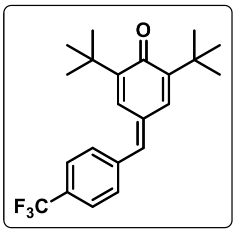

2,6-di-*tert*-butyl-4-(4-(trifluoromethyl)benzylidene)cyclohexa-2,5-dienone (1j): ^{1}H NMR (400 MHz, $CDCl_3$): δ 7.70 (d, J = 8.3 Hz, 2H), 7.54 (d, J = 8.2 Hz, 2H), 7.41 (d, J = 2.3 Hz, 1H), 7.16 (s, 1H), 7.01 (d, J = 2.4 Hz, 1H), 1.34 (s, 9H), 1.26 (s, 9H).

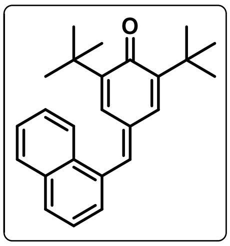

2,6-di-*tert*-butyl-4-(naphthalen-1-ylmethylene)cyclohexa-2,5-dienone (1k): ^{1}H NMR (400 MHz, $CDCl_3$): δ 8.05-8.00 (m, 1H), 7.94-7.89 (m, 2H), 7.77 (s, 1H), 7.60-7.51 (m, 3H), 7.48 (d, *J* = 7.5 Hz, 1H), 7.38 (d, *J* = 2.1 Hz, 1H), 7.19 (d, *J* = 2.2 Hz, 1H), 1.38 (s, 9H), 1.24 (s, 9H).

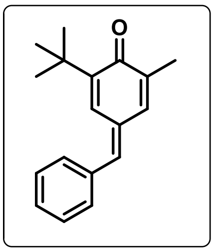

(Z)-4-benzylidene-2-(*tert*-butyl)-6-methylcyclohexa-2,5-dienone (1l): ^{1}H NMR (400 MHz, $CDCl_3$): 7.59 (d, *J* =2.4 Hz, 1H), 7.48-7.44 (m, 5H), 7.17 (s, 1H), 7.03 (s, 1H), 2.04 (s, 3H), 1.30 (s, 9H).

2.4.3 General Procedure for the Synthesis of Symmetrical Urea:

To a mixed solution of 2-hydroxyisoindoline-1,3-dione (10 mmol,1.63 g) in DMSO (15 mL) and anhydrous potassium carbonate (8 mmol, 1.2 g), benzylbromide (20 mmol, 3.42 g) was added and the resulting mixture was stirred for 24 h at room temperature. After that, 30 mL of cool water was added and the resulting mixture was allowed to stand for 30 minutes. The obtained precipitate was filtered and washed with water (3 × 5 mL). Then the precipitate was recrystallized from ethanol and give the product *N*-benzyloxyphthalimide as white needle like crystals.

A mixture of *N*-benzyloxyphthalimide (4 mmol, 1.0 g), acetic acid (4 mL) and hydrochloric acid (aq. 37 %) (1.5 mL) was refluxed for 1.5 hours. The reaction mixture was cooled to room temperature and concentrated. Then cold water (10 mL) was added to the solid residue, and the suspension was adjusted to alkaline by addition of 10 % sodium hydroxide solution. The obtained solution was subsequently extracted with CH_2Cl_2 (3 × 15 mL), and the combined organic phases were dried with anhydrous Na_2SO_4 and concentrated to a final volume of 10mL.

To the final concentrate obtained above 6M HCl (5 mL) was added to it whilst stirring at 0-5 °C. After further stirring for another 1 hour at room temperature, the solid was filtered, washed with CH_2Cl_2 (10 mL) and dried extensively in vacuo at 45 °C. The product was obtained as a white solid.

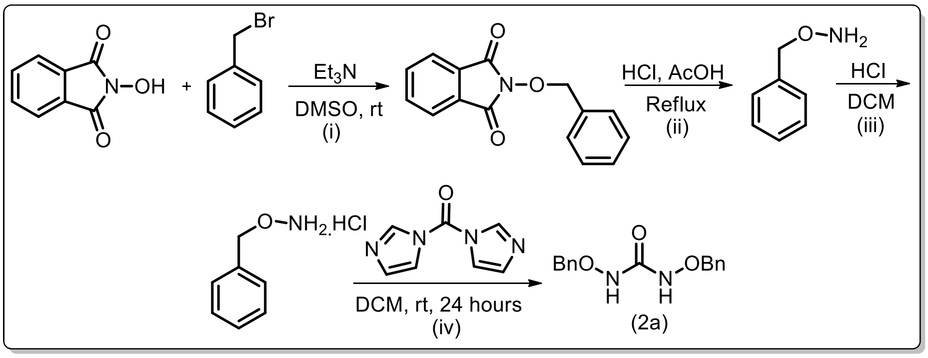

To a solution of *O*-Benzylhydroxylamine hydrochloride (20.0 g, 125.30 mmol) in dichloromethane (313 mL) was added triethylamine (17.264 mL, 125.30 mmol) at 0 °C and stirred for 10 minutes before the addition of 1,1′-Carbonyldiimidazole (10.16 g, 62.65 mmol) over a period of 15 minutes in 3 portions. The reaction mixture was stirred at room temperature for 24 hours. The reaction was quenched with water (100 mL) and extracted with dichloromethane (3 × 400 mL). The combined organic phases were dried with anhydrous Na_2SO_4 and concentrated under reduced pressure. The crude product was purified via column chromatography (4:1 to 3:2, hexanes/ethyl acetate) to provide the white solid product (12.1 g, 51.78 mmol, 70 %). R_f = 0.25 (3:2, hexanes/ethyl acetate).

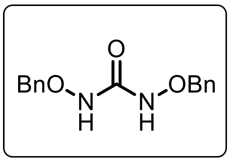

1,3-Bis(benzyloxy)urea (2a): ^{1}H NMR (400 MHz, $CDCl_3$): δ 7.59 (brs, 2H), 7.41–7.27 (m, 10H), 4.78 (s, 4H).

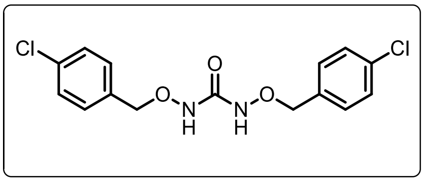

1,3-bis((4-chlorobenzyl)oxy)urea (2b): ^{1}H NMR (400 MHz, $CDCl_3$): *δ* 7.59 (brs, 2H), 7.31-7.24 (m, 4H), 7.23-7.13 (m, 4H), 4.68 (s, 4H).

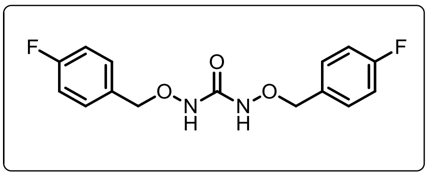

1,3-bis((4-fluorobenzyl)oxy)urea (2c): ^{1}H NMR (400 MHz, $CDCl_3$): δ 7.59 (brs, 2H), 7.35-7.27 (m, 4H), 7.10-6.98 (m, 4H), 4.75 (s, 4H).

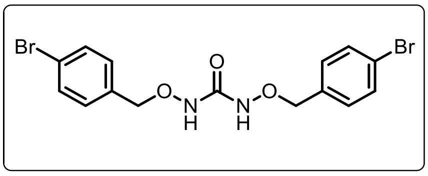

1,3-bis((4-bromobenzyl)oxy)urea (2d): ^{1}H NMR (400 MHz, $CDCl_3$): δ 7.55 (brs, 2H), 7.50 (d, J = 8.1 Hz, 4H), 7.19 (d, J = 8.1 Hz, 4H), 4.73 (s, 4H).

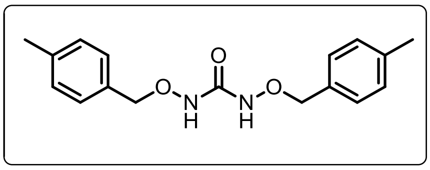

1,3-bis((4-methylbenzyl)oxy)urea (2e): ^{1}H NMR (400 MHz, $CDCl_3$): *δ* 7.48 (brs, 2H), 7.22–7.14 (m, 8H), 4.74 (s, 4H), 2.37 (s, 6H).

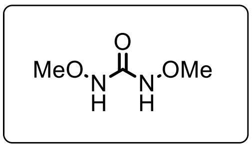

1,3-dimethoxy urea (2f): ^{1}H NMR (400 MHz, $CDCl_3$): *δ* 7.80 (brs, 2H), 3.74 (s, 6H).

2.4.3 General Procedure for the Synthesis of Unsymmetrical Urea: [16b]

(i) Amine hydrochloride was suspended in dry dichloromethane (DCM) (200 mL) and pyridine (7.9 g, 10 mmol). 4-Nitrophenylchloroformate (20.16 g, 10 mmol) dissolved in DCM (100 mL) was added dropwise while stirring at room temperature for 45 min. After the addition was completed, the reaction mixture was refluxed for 6 h and then cooled to r.t., diluted with DCM (200 mL), washed sequentially with 1N HCl, H_2O, 1M sodium bicarbonate solution, water, and brine. The DCM layer was dried with sodium sulfate and the solvents evaporated under vacuum. The crude product was purified by flash chromatography using a mixture of ethyl acetate/hexane.

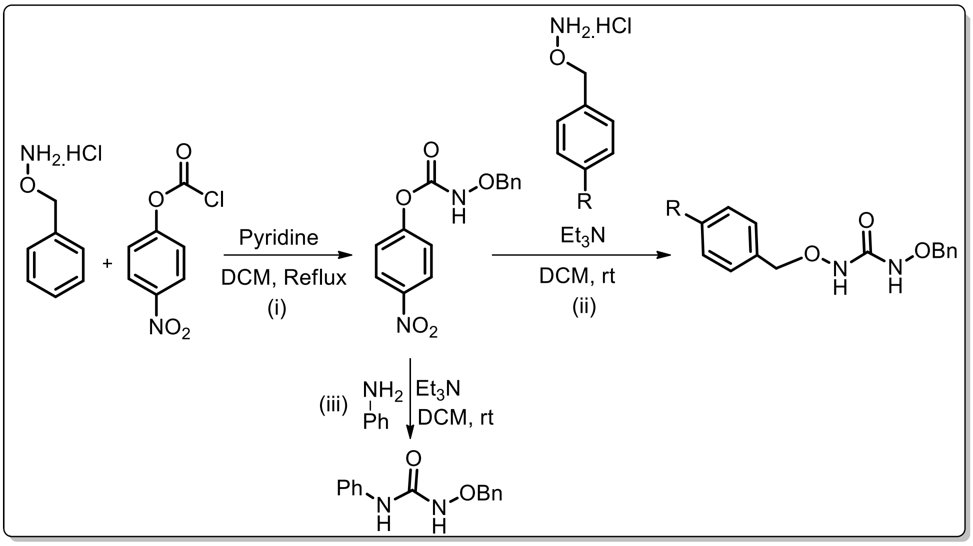

(ii) To a solution of *O*-Benzylhydroxylamine hydrochloride (20.0 g, 125.30 mmol) in dichloromethane (313 mL) was added triethylamine (17.264 mL, 125.30 mmol) at 0 °C and stirred for 10 minutes before the addition of 4-nitrophenyl(benzyloxy)carbamate over a period of 15 minutes in 3 portions. The reaction mixture was stirred at room temperature for 24 hours. The reaction mixture was extracted with dichloromethane (3 × 400 mL). The combined organic phase was dried with anhydrous Na_2SO_4 and concentrated under reduced pressure. The crude product was purified via column chromatography (4:1 to 3:2, hexanes/ethyl acetate) to provide the colourless solid product.

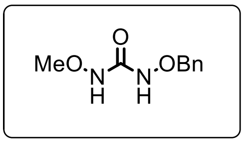

1-(Benzyloxy)-3-methoxyurea (2g): ^{1}H NMR (400 MHz, $CDCl_3$): δ 8.27 (s, 1H), 8.14 (s, 1H), 7.42-7.31 (m, 4H), 4.83 (s, 2H), and 3.62 (s, 3H).

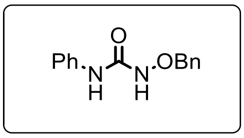

1-(Benzyloxy)-3-phenylurea (2h): ^{1}H NMR (400 MHz, $CDCl_3$): *δ* 7.38–7.36 (m, 5H), 7.26–7.12 (m, 5H), 7.04 (dt, *J* = 8.4 Hz, 1.2 Hz, 2H), 4.90 (s, 2H).

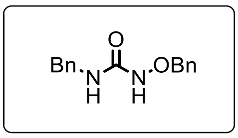

1-Benzyl-3-(benzyloxy)urea (2i): ^{1}H NMR (400 MHz, $CDCl_3$): *δ* 7.37–7.23 (m, 8H), 7.20–7.18 (m, 2H), 6.98 (s, 1H), 5.89 (brs, 1H), 4.78 (s, 2H), and 4.39 (d, *J* = 6.0 Hz, 2H).

2.4.4 Representative procedure for conjugate addition reaction of *p*- quinone methide (1) and urea (2): A round-bottom flask equipped with a magnetic stir bar was charged with *p*-quinone methide **1** (0.181 mmol, 1 equiv.), urea derivative **2** (0.181 mmol, 1 equiv.) and DBU (0.270 mmol, 1.5 equiv.). DCM (1 mL) was added as a solvent and the reaction mixture was stirred at room temperature until completion of the reaction (as monitored by TLC). The solvent was evaporated on a rotary evaporator and further purified by silica gel column chromatography taking ethyl acetate/hexanes as eluent to afford **3**.

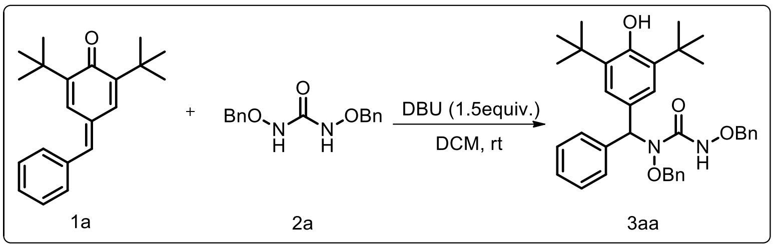

(+/-)1,3-bis(benzyloxy)-1-((3,5-di-*tert*-butyl-4-hydroxy phenyl)(phenyl)methyl) urea(3aa): Yield = 92 mg

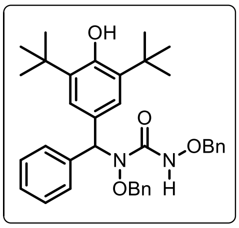

(90%); R_f = 0.60 (EtOAc: Hexanes = 2.0:8.0); White solid; Melting Point: 162–164 °C; ^{1}H NMR (400 MHz, $CDCl_3$): δ 8.14 (s, 1H), 7.40– 7.17 (m, 15H), 6.78 (d, *J* = 7.6 Hz, 2H), 6.48 (s, 1H), 5.20 (s, 1H), 4.83 (d, *J* = 2.7 Hz, 2H), 4.15 (d, *J* = 9.5 Hz, 1H), 4.02 (d, *J* = 9.5 Hz, 1H), 1.37 (s, 18H); ^{13}C-NMR (100 MHz, $CDCl_3$): δ 160.1, 153.4, 139.3, 135.8, 135.6, 134.4, 129.3, 129.1, 128.8, 128.6, 128.6, 128.5, 128.2, 127.3, 126.7, 78.7, 78.3, 66.4, 55.3, 34.4, 30.3; IR (neat): 3380, 2949, 1697, 1446, 1362, 1232, 1106, 945, 743, 646, 478 cm^{-1}; HRMS (ESI, Q-TOF) m/z: $[M + H]^+$ Calculated for $C_{36}H_{43}N_2O_4$ 567.3223, found 567.3214.

(+/-)1,3-bis(benzyloxy)-1-((3,5-di-*tert*-butyl-4-hydroxyphenyl)(4-methoxyphenyl)methyl)urea(3ba):

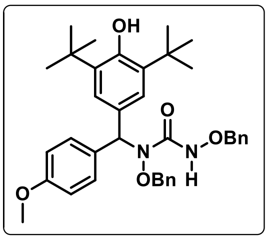

Yield = 75 mg (85%); R_f = 0.60 (EtOAc: Hexanes = 2.0:8.0); White solid; Melting Point: 179–181 °C; ^{1}H NMR (400 MHz, $CDCl_3$): δ 8.12 (s, 1H), 7.37-7.18 (m, 12H), 6.84 (d, *J* = 8.2 Hz, 2H), 6.79 (d, *J* = 7.7 Hz, 2H), 6.43 (s, 1H), 5.19 (s, 1H), 4.82 (s, 2H), 4.16 (d, *J* = 9.4 Hz, 1H), 4.05 (d, *J* = 9.3 Hz, 1H), 3.79 (s, 3H), 1.37 (s, 18H); ^{13}C-NMR (100 MHz, $CDCl_3$): δ 160.2, 158.8, 153.3, 135.8, 135.6, 131.2, 129.3, 129.1, 128.8, 128.6, 128.6, 128.6, 113.6, 78.7, 78.3, 65.9, 55.3, 34.3, 30.4; IR (neat): 2960, 1679, 1511, 1452, 1356, 1236, 1178, 1116, 971, 895, 827, 697, 607 cm^{-1}; HRMS (ESI, Q-TOF) m/z: $[M + H]^+$ Calculated for $C_{37}H_{45}N_2O_5$ 597.3328, found 597.3269.

(+/-)1,3-bis(benzyloxy)-1-((3,5-di-*tert*-butyl-4-hydroxyphenyl)(*p*-tolyl)methyl)urea (3ca): Yield =

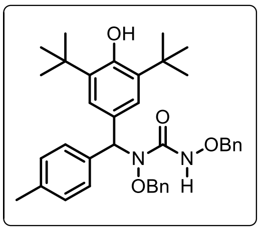

82 mg, (88%); R_f = 0.60 (EtOAc: Hexanes = 2.0:8.0); White solid; Melting Point: 185–187 °C; ^{1}H NMR (400 MHz, $CDCl_3$): δ 8.13 (s, 1H), 7.35 (s, 4H), 7.29-7.17 (m, 8H), 7.10 (d, *J* = 7.8 Hz, 2H), 6.80 (d, *J* = 7.5 Hz, 2H), 6.44 (s, 1H), 5.19 (s, 1H), 4.82 (s, 2H), 4.16 (d, *J* = 9.6 Hz, 1H), 4.04 (d, *J* = 9.5 Hz, 1H), 2.32 (s, 3H), 1.37 (s, 18H); ^{13}C-NMR (100 MHz, $CDCl_3$): δ 160.1, 153.3, 136.9, 136.1, 135.8, 135.6, 134.5, 129.3, 129.1, 128.9, 128.8, 128.6, 128.5, 126.6, 78.6, 78.3, 66.2, 34.4, 30.4, 21.2; IR (neat): 3634, 2954, 1689, 1435, 1365, 1235, 1120, 739, 698 cm^{-1}; HRMS (ESI, Q-TOF) m/z: $[M + Na]^+$ Calculated for $C_{37}H_{44}N_2O_4Na$ 603.3186, found 603.3199

(+/-)1,3-bis(benzyloxy)-1-((4-(Benzyloxy)phenyl)(3,5-di-*tert*-butyl-4-hydroxyphenyl)methyl)urea

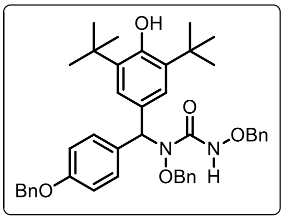

(3da): Yield = 65 mg (80%); R_f = 0.60 (EtOAc:Hexanes = 2.0:8.0); White solid; Melting Point: 145–147 °C; ^{1}H NMR (400 MHz, $CDCl_3$): δ 8.13 (s, 1H), 7.43-7.16 (m, 17H), 6.91 (d, *J* = 8.4 Hz, 2H), 6.79 (d, *J* = 7.6 Hz, 2H), 6.43 (s, 1H), 5.18 (s, 1H), 5.04 (s, 2H), 4.82 (s, 2H), 4.16 (d, *J* = 9.9 Hz, 1H), 4.05 (d, *J* = 9.8 Hz, 1H), 1.37 (s, 18H); ^{13}C-NMR (100 MHz, $CDCl_3$): δ 160.1, 158.1, 153.3, 137.0, 135.8, 135.6, 134.5, 131.6, 130.2, 129.3, 129.2, 128.8, 128.6, 128.6, 128.0, 127.6, 126.5, 114.6, 78.7, 78.3, 70.1, 66.0, 34.4, 30.4; IR (neat): 2951, 1696, 1610, 1581, 1510, 1436, 1363, 1300, 1111, 1025, 894, 696, 535 cm^{-1}; HRMS (ESI, Q-TOF) m/z: [M + Na]$^+$ Calculated for $C_{43}H_{48}N_2O_5Na$ 695.3441, found 695.3461.

(+/-)1,3-bis(benzyloxy)-1-((3,5-di-tert-butyl-4-hydroxyphenyl)(3,4-dimethoxyphenyl)methyl)urea

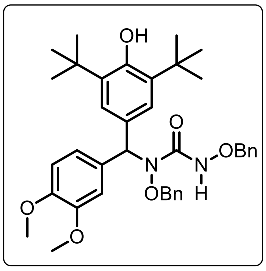

(3ea): Yield = 68 mg (78%); R_f = 0.60 (EtOAc:Hexanes = 2.0:8.0); White solid; Melting Point: 152–154 °C; ^{1}H NMR (400 MHz, $CDCl_3$): δ 8.14 (s, 1H), 7.36-7.32 (m, 5H), 7.28-7.17 (m, 5H), 6.96 (d, *J* = 9.0 Hz, 2H), 6.80 (d, *J* = 7.8 Hz, 3H), 6.42 (s, 1H), 5.21 (s, 1H), 4.83 (s, 2H), 4.19 (d, *J* = 9.5 Hz, 1H), 4.09 (d, *J* = 9.6 Hz, 1H), 3.85 (s, 3H), 3.75 (s, 3H), 1.35 (s, 18H); ^{13}C-NMR (100 MHz, $CDCl_3$): δ 160.2, 153.3, 148.5, 148.3, 135.8, 135.6, 134.5, 131.5, 129.3, 129.0, 128.8, 128.6, 128.6, 126.5, 121.4, 112.4, 110.7, 78.6, 78.3, 66.2, 55.9, 55.8, 34.4, 30.4; IR (neat): 2960, 1691, 1509, 1451, 1266, 1232, 1108, 947, 890, 669, 542 cm^{-1}; HRMS (ESI, Q-TOF) m/z: [M + Na]$^+$ Calculated for $C_{38}H_{46}N_2O_6Na$ 649.3250, found 649.3254.

(+/-) 1,3-bis(benzyloxy)-1-((3,5-di-*tert*-butyl-4-hydroxyphenyl)(4-fluorophenyl)methyl)urea (3fa):

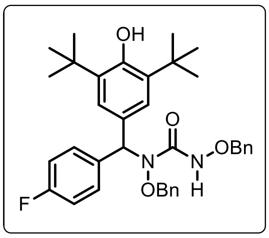

Yield = 75 mg (80%); R_f = 0.60 (EtOAc:Hexanes = 2.0:8.0); White solid; Melting Point: 195–197 °C; ^{1}H NMR (400 MHz, $CDCl_3$): δ 8.13 (s, 1H), 7.39- 7.32 (m, 7H), 7.28-7.16 (m, 5H), 6.99 (t, *J* = 8.8 Hz, 2H), 6.77 (d, *J* = 7.2 Hz, 2H), 6.46 (s, 1H), 5.23 (s, 1H), 4.83 (d, *J* = 5.4 Hz, 2H), 4.16 (d, *J* = 9.6 Hz, 1H), 4.02 (d, *J* = 9.3 Hz, 1H), 1.37 (s, 18H); ^{13}C-NMR (100 MHz, $CDCl_3$): δ 162.1 (d, *J* = 245.5 Hz), 160.0, 153.5, 135.7, 135.1, 134.3, 130.4, 129.2 (d, *J* = 12.1 Hz), 128.9, 128.6, 128.3, 126.6, 115.1 (d, *J* = 21.3 Hz), 78.8, 78.3, 65.8, 34.4, 30.3; ^{19}F (376 MHz, $CDCl_3$): δ = -115.2 ppm IR (neat): 2958, 1688, 1508, 1452, 1369, 1212, 1120, 976, 849, 747, 605, 530 cm^{-1}; HRMS (ESI, Q-TOF) m/z: [M + H]$^+$ Calculated for $C_{36}H_{42}N_2O_4F$ 607.2948, found 607.292.

(+/-)1,3-bis(benzyloxy)-1-((4-Chlorophenyl)(3,5-di-*tert*-butyl-4-hydroxyphenyl)methyl)urea (3ga):

Yield = 68 mg (75%); R_f = 0.60 (EtOAc: Hexanes = 2.0:8.0); White solid; Melting Point: 190–192 °C; ^{1}H NMR (400 MHz, $CDCl_3$): δ 8.10 (s, 1H), 7.38-7.31 (m, 5H), 7.30-7.12 (m, 9H), 6.75 (d, *J* = 7.5 Hz, 2H), 6.41(s, 1H), 5.21 (s, 1H), 4.83 (d, *J* = 11.3 Hz, 1H), 4.78 (d, *J* = 11.4 Hz, 1H), 4.14 (d, *J* = 9.8 Hz, 1H), 3.90 (d, *J* = 9.6 Hz, 1H), 1.35 (s, 18H); ^{13}C-

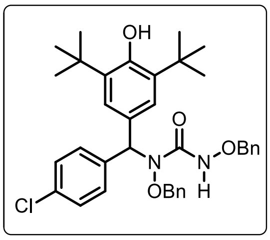

NMR (100 MHz, $CDCl_3$): δ 159.9, 153.6, 137.9, 135.8, 135.7, 134.2, 133.1, 130.0, 129.3, 129.1, 128.9, 128.6, 128.4, 127.9, 126.7, 78.8, 78.3, 65.8, 34.4, 30.3; IR (neat): 3396, 3024, 2958, 1689, 1451, 1361, 1258, 1014, 978, 800, 606, 519 cm^{-1}; HRMS (ESI, Q-TOF) m/z: $[M + H]^+$ Calculated for $C_{36}H_{42}N_2O_4Cl$ 601.2833, found 601.2838.

(+/-) 1,3-bis(benzyloxy)-1-((2-Bromophenyl)(3,5-di-*tert*-butyl-4-hydroxyphenyl)methyl)urea (3ha):

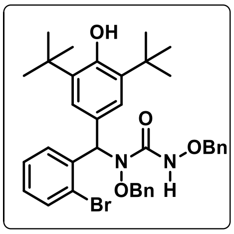

Yield = 62 mg (72%); R_f = 0.60 (EtOAc: Hexanes = 2.0:8.0); White solid; Melting Point: 152–154 °C; ^{1}H NMR (400 MHz, $CDCl_3$): δ 8.13 (s, 1H), 7.57-7.19 (m, 10H), 7.15-7.10 (m, 3H), 6.80-6.76 (m, 3H), 5.19 (s, 1H), 4.83 (d, *J* = 4.0 Hz, 2H), 4.04 (d, *J* = 9.2 Hz, 1H), 3.95 (d, *J* = 9.1 Hz, 1H), 1.37 (s, 18H); ^{13}C-NMR (100 MHz, $CDCl_3$): δ 159.5, 153.4, 139.3, 135.8, 135.7, 134.2, 133.1, 129.3, 129.3, 129.0, 128.9, 128.6, 127.3, 126.4, 124.5, 78.8, 78.3, 65.9, 34.4, 30.4; IR (neat): 2957, 2880, 1696, 1585, 1433, 1399, 1235, 1024, 893, 698, 616 cm^{-1}; HRMS (ESI, Q-TOF) m/z: $[M + H]^+$ Calculated for $C_{36}H_{42}N_2O_4Br$ 645.2328, found 645.2300.

(+/-) 1,3-bis(benzyloxy)-1-((3,5-di-*tert*-butyl-4-hydroxyphenyl)(4-nitrophenyl)methyl)urea (3ia):

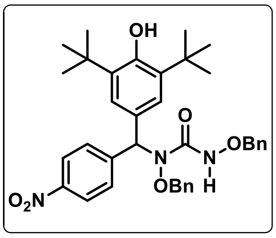

Yield = 59 mg (68%); R_f = 0.60 (EtOAc: Hexanes = 2.0:8.0); White solid; Melting Point: 155–157 °C; ^{1}H NMR (400 MHz, $CDCl_3$): δ 8.16 (d, *J* = 8.6 Hz, 3H), 7.52 (d, *J* = 8.5 Hz, 2H), 7.40-7.35 (m, 4H), 7.33-7.18 (m, 6H), 7.12 (s, 1H), 6.77 (d, *J* = 7.5 Hz, 2H), 6.54 (s, 1H), 4.86 (d, *J* = 11.5 Hz, 1H), 4.80 (d, *J* = 11.3 Hz, 1H), 4.04 (d, *J* = 9.2 Hz, 1H), 3.95 (d, *J* = 9.1 Hz, 1H), 1.37 (s, 18H); ^{13}C-NMR (100 MHz, $CDCl_3$): δ 159.6, 154.0, 147.4, 147.1, 136.1, 135.6, 133.9, 129.2, 129.2, 129.1, 128.7, 128.7 127.0, 126.9, 123.5, 79.0, 78.4, 65.9, 34.4, 30.3; IR (neat): 3627, 2956, 1691, 1520, 1435, 1346, 1236, 1120, 744, 699 cm^{-1}; HRMS (ESI, Q-TOF) m/z: $[M + H]^+$ Calculated for $C_{36}H_{42}N_3O_6$ 612.3074, found 612.3075.

(+/-)1,3-bis(benzyloxy)-1-((3,5-di-*tert*-butyl-4-hydroxyphenyl)(4-(trifluoromethyl)phenyl)methyl) urea (3ja):

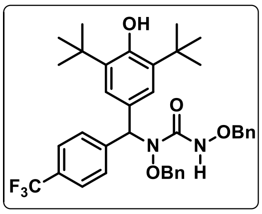

Yield = 54 mg (65%); R_f = 0.60 (EtOAc: Hexanes = 2.0:8.0); White solid; Melting Point: 166–168 °C; ^{1}H NMR (400 MHz, $CDCl_3$): δ 8.25 (s, 1H), 7.66 (d, *J* = 8.2 Hz, 2H), 7.58 (d, *J* = 8.0 Hz, 2H), 7.50-7.44 (m, 6H), 7.40- 7.28 (m, 4H), 6.87 (d, *J* = 7.6 Hz, 2H), 6.62 (d, *J* = 7.6 Hz, 2H), 5.36 (s, 1H), 4.96 (d, *J* = 11.4 Hz, 2H), 4.91 (d, *J* = 11.3 Hz, 1H), 4.27 (d, *J* = 9.5 Hz, 1H), 4.11 (d, *J* = 9.2 Hz, 1H), 1.48 (s, 18H); ^{13}C-NMR (100 MHz, $CDCl_3$): δ 159.8, 153.7, 143.6, 135.9, 135.7, 134.1, 129.5 (*J* = 32.5 Hz), 129.2, 129.1, 129.0, 128.7, 127.5, 126.9, 125.2 (q, *J* = 3.8 Hz), 124.2 (*J* = 272.5 Hz), 78.9, 78.4, 66.1, 34.4, 30.3; ^{19}F (376 MHz, $CDCl_3$): δ = -62.3 ppm; IR (neat): 2947, 2922, 2887, 2865, 1693, 1435, 1324, 1170, 1114, 1017, 895, 749 cm^{-1}; HRMS (ESI, Q-TOF) m/z: $[M + H]^+$ Calculated for $C_{37}H_{42}N_2O_4F_3$ 635.3082, found 635.3097.

(+/-) 1,3-bis(benzyloxy)-1-((3,5-di-*tert*-butyl-4-hydroxyphenyl)(naphthalen-1-yl)methyl)urea (3ka):

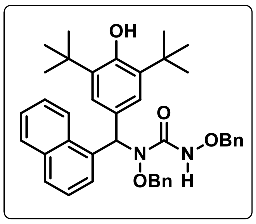

Yield = 68 mg (78%); R_f = 0.60 (EtOAc:Hexanes = 2.0:8.0); White solid; Melting Point: 209-211 °C; ^{1}H NMR (400 MHz, $CDCl_3$): δ 8.15 (s, 1H), 7.88-7.77 (m, 2H), 7.54-7.31 (m, 8H), 7.27-7.15 (m, 7H), 6.73 (d, *J* = 7.5 Hz, 2H), 5.16 (s, 1H), 4.84 (s, 2H), 3.77 (d, *J* = 9.6 Hz, 2H), 1.35 (s, 18H); ^{13}C-NMR (100 MHz, $CDCl_3$): δ 159.6, 153.2, 135.8, 135.7, 135.2, 134.4, 133.7, 131.8, 129.3, 129.0, 128.8, 128.7, 128.6, 128.5, 126.6, 125.8, 125.1, 124.1, 78.5, 78.4, 62.6, 34.4, 30.4; IR (neat): 3408, 2954, 1676, 1432, 1363, 1232, 1116, 909, 857, 792, 740, 609 cm^{-1}; HRMS (ESI, Q-TOF) m/z: $[M + Na]^+$ Calculated for $C_{40}H_{44}N_2O_4Na$ 639.3199, found 639.3189.

(+/-) 1,3-bis(benzyloxy)-1-((3-(*tert*-butyl)-4-hydroxy-5-methylphenyl)(phenyl)methyl)urea (3la):

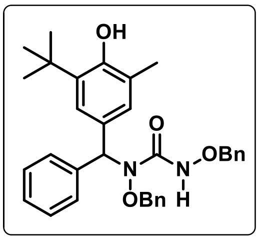

Yield = 85 mg (82%); R_f = 0.60 (EtOAc:Hexanes = 2.0:8.0); White solid; Melting Point: 150–152 °C; ^{1}H NMR (400 MHz, $CDCl_3$): δ 8.15 (s, 1H), 7.40-7.34 (m, 7H), 7.33-7.17 (m, 7H), 6.97 (s, 1H), 6.81 (d, *J* = 7.7 Hz, 2H), 6.46 (s, 1H), 4.83 (d, *J* = 2.3 Hz, 3H), 4.14 (d, *J* = 9.6 Hz, 1H), 4.03 (d, *J* = 9.4 Hz, 1H), 2.18 (s, 3H), 1.35 (s, 9H); ^{13}C-NMR (100 MHz, $CDCl_3$): δ 160.0, 152.3, 139.3, 135.8, 135.5, 134.4, 129.3, 129.2, 128.9, 128.6, 128.6, 128.3, 127.4, 126.8, 122.8, 78.8, 78.3, 66.0, 34.6, 29.8, 16.2; IR (neat): 3369, 2952, 1684, 1452, 1170, 911, 747, 698 cm^{-1}; HRMS (ESI, Q-TOF) m/z: $[M + H]^+$ Calculated for $C_{33}H_{37}N_2O_4$ 525.2759, found 525.2753.

(+/-)1,3-bis((4-chlorobenzyl)oxy)-1-((3,5-di-*tert*-butyl-4-hydroxyphenyl)(phenyl)methyl)urea (3ab):

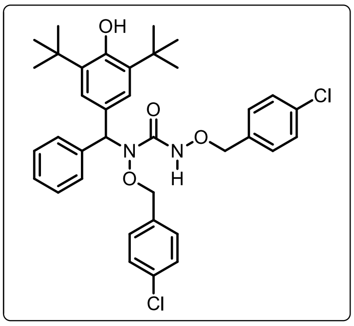

Yield = 91 mg (82%); R_f = 0.60 (EtOAc:Hexanes = 2.0:8.0); White solid; Melting Point: 90–92 °C; ^{1}H NMR (400 MHz, $CDCl_3$): δ 7.98 (s, 1H), 7.31-7.18 (m, 9H), 7.15-7.08 (m, 4H), 6.64 (d, *J* = 8.1 Hz, 2H), 6.39 (s, 1H), 5.14 (s, 1H), 4.71 (s, 2H), 4.05 (d, *J* = 10.1 Hz, 1H), 3.94 (d, *J* = 9.9 Hz, 1H), 1.29 (s, 18H); ^{13}C- NMR (100 MHz, $CDCl_3$): δ 160.0, 153.4, 139.0, 135.7, 134.9, 134.5, 134.3, 132.8, 130.6, 130.4, 128.8, 128.8, 128.2, 77.8, 77.5, 66.6, 34.4, 30.3; IR (neat): 2955, 1676, 1434, 1364, 1235, 1088, 1015, 847, 808, 732, 614, 542 cm^{-1}; HRMS (ESI, Q- TOF) m/z: $[M + Na]^+$ Calculated for $C_{36}H_{40}N_2O_4NaCl_2$ 657.2255, found 657.2263.

(+/-)1-((3,5-di-*tert*-butyl-4-hydroxyphenyl)(phenyl)methyl)-1,3-bis((4-fluorobenzyl)oxy)urea(3ac):

Yield = 88 mg (85%); R_f = 0.60 (EtOAc:Hexanes = 2.0:8.0); White solid; Melting Point: 126–128 °C; ^{1}H NMR (400 MHz, $CDCl_3$): δ 8.16 (s, 1H), 7.47-7.32 (m, 9H), 7.11 (t, *J* = 8.5 Hz, 2H), 6.99 (t, *J* =

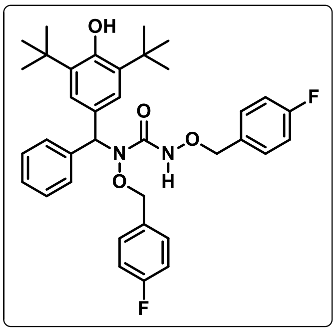

8.1 Hz, 2H), 6.89-6.83 (m, 2H), 6.55 (s, 1H), 5.29 (s, 1H), 4.87 (s, 2H), 4.23 (d, *J* = 10.1 Hz, 1H), 4.12 (d, *J* = 9.9 Hz, 1H), 1.45 (s, 18H); ^{13}C-NMR (100 MHz, $CDCl_3$): δ 163.0 (d, *J* = 248.3 Hz), 162.9 (d, *J* = 246.6 Hz), 160.2, 153.4, 139.1, 135.7, 131.2 (d, *J* = 8.5 Hz), 131.0 (d, *J* = 8.5 Hz), 130.3, 128.7, 128.4, 128.3, 127.5, 126.7, 115.6 (d, *J* = 21.5 Hz), 115.5 (d, *J* = 21.3 Hz), 77.9, 77.5, 66.5, 34.4, 30.3; ^{19}F (376 MHz, $CDCl_3$): δ = -112.1 ppm, -113.0 ppm; IR (neat): 3380, 2949, 1703, 1602, 1510, 1448, 1365, 1226, 833, 698, 614 cm^{-1}; HRMS (ESI, Q-TOF) m/z: $[M + H]^+$ Calculated for $C_{36}H_{41}N_2O_4F_2$ 603.3013, found 603.3034.

(+/-) 1-((3,5-di-*tert*-butyl-4-hydroxyphenyl)(phenyl)methyl)-1,3-bis((4-bromobenzyl)oxy)urea

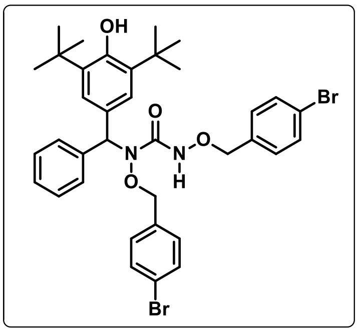

(3ad): Yield = 93 mg (76%); R_f = 0.60 (EtOAc:Hexanes = 2.0:8.0); White solid; Melting Point: 130–132 °C; ^{1}H NMR (400 MHz, $CDCl_3$): δ 8.13 (s, 1H), 7.58 (d, *J* = 8.3 Hz, 2H), 7.47-7.28 (m, 11H), 6.75 (d, *J* = 8.3 Hz, 2H), 6.55 (s, 1H), 5.30 (s, 1H), 4.86 (d, *J* = 1.8 Hz, 2H), 4.20 (d, *J* = 9.9 Hz, 1H), 4.09 (d, *J* = 9.8 Hz, 1H), 1.46 (s, 18H); ^{13}C-NMR (100 MHz, $CDCl_3$): δ 160.0, 153.4, 139.0, 135.7, 134.8, 133.2, 131.8, 131.8, 130.9, 130.6, 128.7, 128.3, 127.5, 126.6, 123.1, 122.7, 77.9, 77.5, 66.6, 34.4, 30.3; IR (neat): 3632, 2955, 1676, 1434, 1364, 1235, 1121, 1070, 846, 737, 701 cm^{-1}; HRMS (ESI, Q-TOF) m/z: $[M + Na]^+$ Calculated for $C_{36}H_{40}N_2O_4NaBr_2$ 745.1251, found 745.1253.

(+/-)1-((3,5-di-*tert*-butyl-4-hydroxyphenyl)(phenyl)methyl)-1,3-bis((4-methylbenzyl)oxy)urea(3ae):

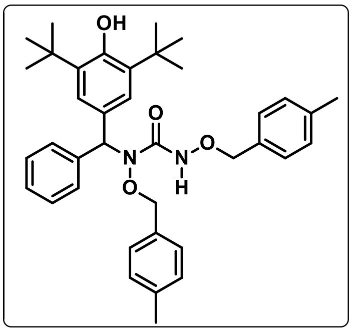

Yield = 76 mg (75%); R_f = 0.60 (EtOAc:Hexanes = 2.0:8.0); White solid; Melting Point: 162–164 °C; ^{1}H NMR (400 MHz, $CDCl_3$): δ 8.04 (s, 1H), 7.31-7.08 (m, 11H), 6.93 (d, *J* = 7.8 Hz, 2H), 6.59 (d, *J* = 7.8 Hz, 2H), 6.40 (s, 1H), 5.12 (s, 1H), 4.71 (s, 2H), 4.03 (d, *J* = 9.3 Hz, 1H), 3.89 (d, *J* = 9.2 Hz, 1H), 2.29 (s, 3H), 2.23 (s, 3H), 1.30 (s, 18H); ^{13}C-NMR (100 MHz, $CDCl_3$): δ 160.0, 153.3, 139.3, 138.8, 138.4, 135.5, 132.8, 131.4, 129.4, 129.3, 129.2, 128.6, 128.2, 127.3, 78.5, 78.1, 66.3, 34.4, 30.3, 21.3, 21.3; IR (neat): 3633, 2954, 1690, 1435, 1363, 1235, 1120, 804, 738, 616 cm^{-1}; HRMS (ESI, Q-TOF) m/z: $[M + H]^+$ Calculated for $C_{38}H_{47}N_2O_4$ 595.3536, found 595.3539.

(+/-) 1-((3,5-di-*tert*-butyl-4-hydroxyphenyl)(phenyl)methyl)-1,3-dimethoxyurea (3af): Yield = 56 mg

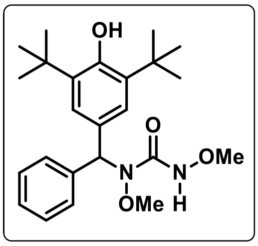

(80%); R_f = 0.60 (EtOAc:Hexanes = 2.0:8.0); White solid; Melting Point: 151-153 °C; ^{1}H NMR (400 MHz, $CDCl_3$): δ 8.44 (s, 1H), 7.39-7.21 (m, 5H), 7.13 (s, 2H), 6.41 (s, 1H), 5.19 (s, 1H), 3.72 (s, 3H), 3.20 (s, 3H), 1.38 (s, 18H);^{13}C-NMR (100 MHz, $CDCl_3$): δ 160.3, 153.2, 139.2, 135.6, 128.9, 128.7, 128.1, 127.3, 126.0,66.0, 64.7, 64.1, 34.4, 30.4; IR (neat): 3626, 3236, 2952, 1663, 1478, 1232, 1141, 1111, 1003, 932, 769, 696 cm^{-1}; HRMS (ESI, Q-TOF) m/z: [M + H]$^+$ Calculated for $C_{24}H_{35}N_2O_4$ 415.2597, found 415.2586.

(+/-) 1-(benzyloxy)-1-((3,5-di-*tert*-butyl-4-hydroxy phenyl)(phenyl)methyl)-3-methoxyurea (3ag):

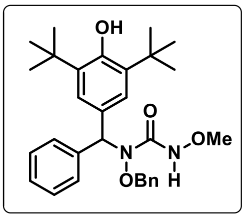

Yield = 34 mg (40%); R_f = 0.50 (EtOAc: Hexanes = 2.0:8.0); White solid; Melting Point: 108–110 °C; ^{1}H NMR (400 MHz, $CDCl_3$): δ 8.22 (s, 1H), 7.36-7.23 (m, 10H), 7.13 (s, 2H), 6.42 (s, 1H), 5.18 (s, 1H), 4.88 (s, 2H), 3.12 (s, 3H), 1.38 (s, 18H); ^{13}C-NMR (100 MHz, $CDCl_3$): δ 159.9, 153.2, 139.2, 135.6, 129.5, 128.9, 128.6, 128.6, 128.2, 127.3, 126.2, 78.5, 66.1, 64.0, 34.4, 30.4; IR (neat): 3635, 2954, 1675, 1434, 1235, 1120, 996, 736, 698, 616 cm^{-1}; HRMS (ESI, Q-TOF) m/z: [M + Na]$^+$ Calculated for $C_{30}H_{38}N_2O_4Na$ 513.2717, found 513.2729.

(+/-) 3-(benzyloxy)-1-((3,5-di-tert-butyl-4-hydroxy phenyl)(phenyl)methyl)-1-methoxyurea (3ag'):

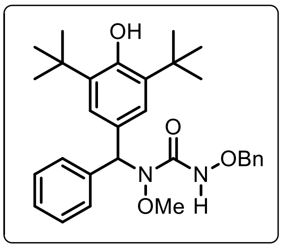

Yield = 42 mg (50%); R_f = 0.60 (EtOAc:Hexanes = 2.0:8.0); White solid; Melting Point: 98–100 °C; ^{1}H NMR (400 MHz, $CDCl_3$): δ 8.29 (s, 1H), 7.46 (d, *J* = 7.6 Hz, 2H), 7.39-7.28 (m, 6H), 7.25 (s, 2H), 7.13-7.08 (m, 2H), 6.54 (s, 1H), 5.25 (s, 1H), 4.31 (d, *J* = 9.9 Hz, 1H), 4.31 (d, *J* = 9.8 Hz, 1H), 3.67 (s, 3H), 1.42 (s, 18H); ^{13}C-NMR (100 MHz, $CDCl_3$): δ 160.5, 153.4, 139.3, 135.6, 134.7, 129.1, 128.9, 128.7, 128.5, 128.2, 127.4, 126.6, 78.6, 66.5, 64.5, 34.4, 30.3; IR (neat): 3635, 2954, 1675, 1434, 1235, 1120, 996, 736, 698, 616 cm^{-1}; HRMS (ESI, Q-TOF) m/z: [M + Na]$^+$ Calculated for $C_{30}H_{38}N_2O_4Na$ 513.2717, found 513.2729.

(+/-) 1-(benzyloxy)-1-((3,5-di-*tert*-butyl-4-hydroxy phenyl)(phenyl)methyl)-3-phenylurea (3ah):

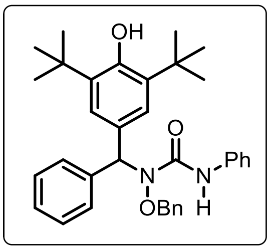

Yield = 70 mg (76%); R_f = 0.60 (EtOAc:Hexanes = 2.0:8.0); White solid; Melting Point: 134–136 °C; ^{1}H NMR (400 MHz, $CDCl_3$): δ 7.71 (s, 1H), 7.44 (d, *J* = 7.6 Hz, 2H), 7.35-7.20 (m, 12H), 7.15-7.11 (m, 2H), 7.03-6.98 (m, 1H), 6.63 (s, 1H), 5.20 (s, 1H), 4.30 (d, *J* = 10.3 Hz, 1H), 4.23 (d, *J* = 10.4 Hz, 1H), 1.38 (s, 18H); ^{13}C- NMR (100 MHz, $CDCl_3$): δ 157.0, 153.3, 139.7, 138.0, 135.7, 134.9, 129.2, 129.1, 128.9, 128.9, 128.3, 127.3, 126.7, 123.5, 119.1, 79.3, 66.2, 34.4, 30.3; IR (neat): 2963, 1670, 1595, 1520, 1441, 1220, 1119, 915, 695, 583 cm^{-1}; HRMS (ESI, Q-TOF) m/z: $[M + H]^+$ Calculated for $C_{35}H_{41}N_2O_3$ 537.3102, found 537.311.

(+/-) 3-benzyl-1-(benzyloxy)-1-((3,5-di-tert-butyl-4-hydroxyphenyl)(phenyl)methyl)urea (3ai):

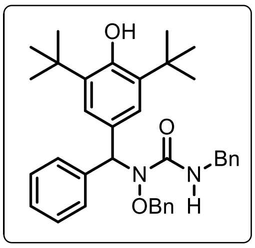

Yield = 75 mg (80%); R_f = 0.60 (EtOAc: Hexanes = 2.0:8.0); White solid; Melting Point: 136–138 °C; ^{1}H NMR(400 MHz, $CDCl_3$): δ 7.47 (d, J = 7.5 Hz, 2H), 7.36-7.19 (m, 11H), 7.03 (d, J = 7.2 Hz, 2H), 6.99 (d, J = 7.1 Hz, 2H), 6.56 (s, 1H), 6.16 (t, J = 6.0 Hz, 1H), 5.21 (s, 1H), 4.34 (brs, 2H), 4.28 (d, J = 10.4 Hz, 1H), 4.19 (d, J = 10.1 Hz, 1H), 1.39 (s, 18H); ^{13}C-NMR (100 MHz, $CDCl_3$): δ 160.3, 153.2, 139.8, 138.8, 135.5, 135.1, 129.2, 129.0, 128.7, 128.6, 128.2, 127.2, 127.2, 126.7, 78.6, 67.0, 44.0, 34.4, 30.3; IR (neat): 3635, 3363, 2958, 1655, 1520, 1433, 1263, 994, 739, 697, 600 cm^{-1}; HRMS (ESI, Q-TOF) m/z: $[M + H]^+$ Calculated for $C_{36}H_{43}N_2O_3$ 551.3260, found 551.3274.

2.4.5 Representative procedure for spirocyclization of conjugate addition product 3:

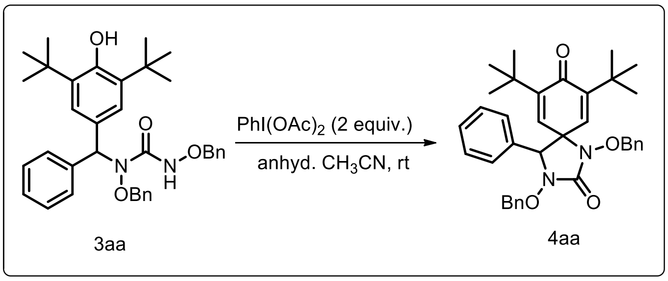

A round-bottom flask equipped with a magnetic stir bar was charged with **3** (0.171 mmol, 1 equiv.) and diacetoxy iodobenzene (0.352 mmol, 2 equiv.) under inert atmosphere. Anhydrous acetonitrile (1 mL) was added as a solvent to the reaction mixture and stirred at room temperature until completion of the reaction (as monitored by TLC). The solvent was evaporated on a rotary evaporator and further purified by silica gel column chromatography taking ethyl acetate/hexanes as eluent to afford **4.**

(+/-) 1,3-bis(benzyloxy)-7,9-di-*tert*-butyl-4-phenyl-1,3-diazaspiro[4.5]deca-6,9-diene-2,8-dione

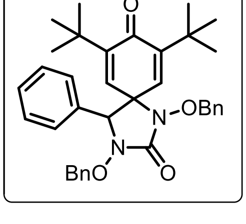

(4aa): Yield = 65%; R_f: 0.50 (EtOAc:Hexanes = 1.5:8.5); white solid; Melting point: 120-122 °C; ^{1}H NMR (400 MHz, $CDCl_3$): δ 7.34-7.19 (m, 13H), 7.05 (d, J = 7.5 Hz, 2H), 6.32 (d, J = 2.8 Hz, 1H), 6.28 (d, J = 2.8 Hz, 1H), 5.31 (d, J = 9.8 Hz, 1H), 5.08-4.95 (m, 3H), 4.36 (s, 1H), 1.13 (s, 9H), 0.92 (s, 9H); ^{13}C-NMR (100 MHz, $CDCl_3$): δ 185.0, 162.0, 151.7, 151.0, 136.4, 135.3, 135.3, 135.2, 131.7, 129.5, 129.3, 129.0, 128.8, 128.7, 128.5, 128.4, 128.1, 127.8, 79.5, 79.0, 68.9, 64.6, 35.0, 29.2, 28.8; IR (neat): 2955, 17159, 1646, 1455, 1365, 1296, 1009, 883, 745, 698 cm^-

^{1}; HRMS (ESI, Q-TOF) m/z: $[M + H]^+$ Calculated for $C_{36}H_{41}N_2O_4$ 565.3054, found 564.3066.

(+/-)1,3-bis(benzyloxy)-7,9-di-*tert*-butyl-4-(4-methoxyphenyl)-1,3-diazaspiro[4.5]deca-6,9-diene-2,8-dione (4ba): Yield= 58 mg (58%); R_f = 0.50 (EtOAc: Hexanes = 1.5:8.5); White solid; Melting Point: 115-117 °C; ^{1}H NMR (400 MHz, $CDCl_3$): δ 7.27-7.17 (m, 10H), 6.89 (d, J = 8.7 Hz, 2H), 6.68 (d, J = 8.8 Hz, 2H), 6.27 (d, J = 2.9 Hz, 1H), 6.17 (d, J = 2.6 Hz, 1H), 5.19 (d, J = 10.0 Hz, 1H), 4.98 (d, J = 10.6 Hz, 1H), 4.89 (dd, J = 10.3, 3.5 Hz, 2H), 4.23 (s, 1H), 3.68 (s, 3H), 1.04 (s, 9H), 0.89 (s, 9H); ^{13}C-NMR (100 MHz, $CDCl_3$): δ 185.0, 162.0, 160.1, 151.6, 150.9, 136.6, 135.4, 135.4, 129.4, 129.3, 129.2, 128.7, 128.7, 128.5, 128.4, 113.5, 79.4, 78.9, 68.6, 64.9, 55.4, 35.1, 35.0, 29.2, 28.8; IR (neat): 2956, 1756, 1642, 1513, 1454, 1365, 1248, 1173, 1011, 885, 808, 697, 530 cm^{-1}; HRMS (ESI, Q-TOF) m/z: $[M + H]^+$ Calculated for $C_{37}H_{43}N_2O_5$ 595.3172, found 595.3167.

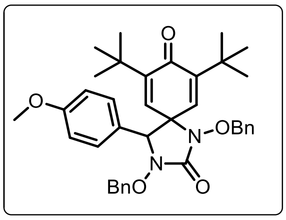

(+/-)1,3-bis(benzyloxy)-7,9-di-*tert*-butyl-4-(*p*–tolyl)-1,3-di-azaspiro[4.5]deca-6,9-diene-2,8-dione (4ca): Yield = 56 mg (56%); R_f = 0.50 (EtOAc:Hexanes = 1.5:8.5); Orange solid; Melting Point: 131–133 °C; ^{1}H NMR (400 MHz, $CDCl_3$): δ 7.33-725 (m, 10H), 7.04 (d, J = 8.1 Hz, 2H), 6.94 (d, J = 8.0 Hz, 2H), 6.32 (d, J = 2.8 Hz, 1H), 6.26 (d, J = 2.7 Hz, 1H), 5.29 (d, J = 10.0 Hz, 1H), 5.05 (d, J = 10.7 Hz, 1H), 4.97 (dd, J = 10.7, 4.9 Hz, 2H), 4.33 (s, 1H), 2.29 (s, 3H), 1.12 (s, 9H), 0.92 (s, 9H); ^{13}C-NMR (100 MHz, $CDCl_3$): δ 185.1, 162.0,151.5, 150.8, 138.9, 136.6, 135.5, 135.4, 135.3, 129.4, 129.3, 128.8, 128.7, 128.7, 128.5, 128.4, 127.7, 79.5, 79.0, 68.7, 64.7, 35.0, 29.2, 28.8, 21.2; IR (neat): 2953, 1760, 1642, 1453, 1304, 1248, 1078, 882, 806, 696, 504 cm^{-1}; HRMS (ESI, Q-TOF) m/z: $[M + H]^+$ Calculated for $C_{37}H_{43}N_2O_4$ 579.3231, found 579.3223.

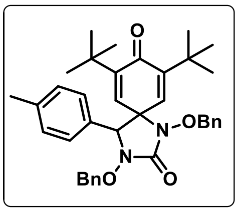

(+/-)1,3-bis(benzyloxy)-4-(4-(Benzyloxy)phenyl)-7,9-di-*tert*-butyl-1,3-diazaspiro[4.5]deca-6,9-diene-2,8-dione (4da): Yield= 50 mg (48%); R_f = 0.50 (EtOAc: Hexanes = 1.5:8.5); White solid; Melting Point: 94–96 °C; ^{1}H NMR (400 MHz, $CDCl_3$): δ 7.33-7.29 (m, 3H), 7.27-7.15 (m, 12H), 6.88 (d, J = 8.6 Hz, 2H) 6.75 (d, J = 8.6 Hz, 2H), 6.25 (d, J = 2.6 Hz, 1H), 6.17 (d, J = 2.6 Hz, 1H), 5.19 (d, J = 9.9 Hz, 1H), 5.01-4.93 (m, 3H), 4.90 (d, J = 10.5 Hz, 2H), 4.22 (s, 1H), 1.04 (s, 9H), 0.88 (s, 9H); ^{13}C-NMR (100 MHz, $CDCl_3$): δ 185.0, 162.0, 159.2, 151.6, 151.0, 136.6, 136.6, 135.4, 135.3, 129.5, 129.3, 129.2, 128.8, 128.7, 128.6, 128.5, 128.4, 128.1, 127.4, 123.8, 114.5, 79.4, 78.9, 70.1, 68.6, 64.9, 35.1, 35.0, 29.2, 28.9; HRMS

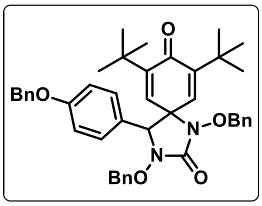

(ESI, Q-TOF) m/z: $[M + H]^+$ Calculated for $C_{43}H_{47}N_2O_5$ 671.3485, found 671.3472.

(+/-) 1,3-bis(benzyloxy)-7,9-di-*tert*-butyl-4-(3,4-dimethoxyphenyl)-1,3-diazaspiro[4.5]deca-6,9-diene-2,8-dione (4ea): Yield= 39 mg (40%); R_f = 0.50 (EtOAc: Hexanes = 1.5:8.5); Yellow solid; Melting Point: 125–127 °C; ^{1}H NMR (400 MHz, $CDCl_3$): δ 7.26-7.17 (m, 10H), 6.66 (d, *J* = 7.9 Hz, 2H), 6.58-6.53 (m, 2H), 6.26 (d, *J* = 2.8 Hz, 1H), 6.23 (d, *J* = 2.7 Hz, 1H), 5.24 (d, *J* = 9.9 Hz, 1H), 4.99 (d, *J* = 10.7 Hz, 1H), 4.90 (dd, *J* = 10.5, 3.9 Hz, 2H), 4.24 (s, 1H), 3.77 (s, 3H), 3.72 (s, 3H), 1.07 (s, 9H), 0.88 (s, 9H); ^{13}C-NMR (100 MHz, $CDCl_3$): δ 185.1, 161.7, 151.5, 150.8, 149.5, 148.7, 136.7, 135.4, 135.3, 135.2, 129.3, 129.2, 128.8, 128.5, 128.5, 124.3, 120.6, 110.7, 110.7, 79.5, 79.0, 68.7, 64.7, 56.0, 55.9 35.0, 29.3, 28.9; IR (neat): 2924, 1759, 1644, 1514, 1454, 1364, 1298, 1144, 1010, 883, 745, 589 cm^{-1}; HRMS (ESI, Q-TOF) m/z: $[M + H]^+$ Calculated for $C_{38}H_{45}N_2O_6$ 625.3278, found 625.3281.

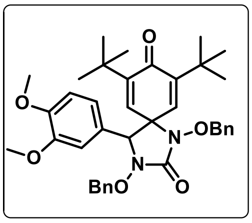

(+/-) 1,3-bis(benzyloxy)-7,9-di-*tert*-butyl-4-(4-fluorophenyl)-1,3-diazaspiro[4.5]deca-6,9-diene-2,8-dione (4fa): Yield= 55 mg (55%); R_f = 0.50 (EtOAc:Hexanes = 1.5:8.5); White solid; Melting Point: 180–182 °C; ^{1}H NMR (400 MHz, $CDCl_3$): δ 7.35-7.23 (m, 10H), 7.01-6.89 (m, 4H), 6.30 (d, *J* = 2.7 Hz, 1H), 6.24 (d, *J* = 2.6 Hz, 1H), 5.27 (d, *J* = 10.1 Hz, 1H), 5.06 (d, *J* = 10.7 Hz, 1H), 4.98 (dd, *J* = 10.3, 4.8 Hz, 2H), 4.32 (s, 1H), 1.18 (s, 9H), 0.95 (s, 9H); ^{13}C-NMR (100 MHz, $CDCl_3$): δ 184.9, 163.0 (d, *J* = 248.0 Hz), 161.9, 151.9, 151.3, 134.9, 129.6 (d, *J* = 8.2 Hz), 129.5 129.3, 128.8, 128.5, 115.2 (d, *J* = 21.8 Hz), 79.5, 78.9, 68.3, 64.6, 35.1, 35.1, 29.2, 28.8; ^{19}F (376 MHz, $CDCl_3$): δ = -112.1 ppm; IR (neat): 2955, 1759, 1644, 1508, 1364, 1285, 1218, 1000, 843, 550 cm^{-1}; HRMS (ESI, Q-TOF) m/z: $[M + H]^+$ Calculated for $C_{36}H_{40}N_2O_4F$ 583.2972, found 583.2950.

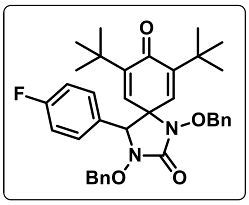

(+/-) 1,3-bis(benzyloxy)-7,9-di-*tert*-butyl-4-(4-chlorophenyl)-1,3-diazaspiro[4.5]deca-6,9-diene-2,8-dione (4ga): Yield= 60 mg (60%); R_f = 0.50 (EtOAc: Hexanes = 1.5:8.5); White solid; Melting Point: 159–161 °C; ^{1}H NMR (400 MHz, $CDCl_3$): δ 7.37-7.23 (m, 10H), 7.20 (d, *J* = 8.3 Hz, 2H), 6.94 (d, *J* = 8.5 Hz, 2H), 6.27 (d, *J* = 2.7 Hz, 1H), 6.25 (d, *J* = 2.8 Hz, 1H), 5.27 (d, *J* = 10.1 Hz, 1H), 5.08-4.95 (m, 3H), 4.31 (s, 1H), 1.12 (s, 9H), 0.94 (s, 9H); ^{13}C-NMR (100 MHz, $CDCl_3$): δ 184.8, 161.8, 152.0, 151.4, 136.1, 135.2, 135.1, 134.9, 134.8, 130.4, 129.5, 129.3, 129.1, 128.8, 128.5, 128.3, 79.5, 78.9, 68.3, 64.4, 35.1, 35.1, 29.2, 28.8; IR (neat): 2955, 1762, 1668, 1647,

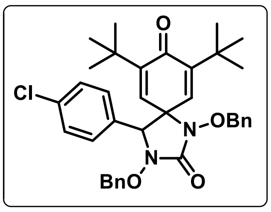

1491, 1364, 1298, 1087, 1011, 884, 740, 507 cm^{-1}; HRMS (ESI, Q-TOF) m/z: [M + H]$^+$ Calculated for $C_{36}H_{40}N_2O_4Cl$ 599.2671, found 599.2677.

(+/-) 1,3-bis(benzyloxy)-4-(2-Bromophenyl)-7,9-di-*tert*-butyl-1,3-diazaspiro[4.5]deca-6,9-diene-2,8-dione (4ha): Yield = 58 mg (58%); R_f = 0.50 (EtOAc:Hexanes = 1.5:8.5); White solid; Melting Point: 178–180 °C; ^{1}H NMR (400 MHz, $CDCl_3$): δ 7.46 (d, 1H), 7.32-7.21 (m, 12H), 7.17-7.12 (m, 1H), 6.52 (d, *J* = 2.7 Hz 1H), 6.18 (d, J = 2.6 Hz, 1H), 5.19 (d, *J* = 10.1 Hz, 1H), 5.04-4.90 (m, 4H), 1.15 (s, 9H), 0.97 (s, 9H); ^{13}C-NMR (100 MHz, $CDCl_3$): δ 185.0, 161.3, 151.0, 150.3, 136.8, 133.4, 130.4, 129.4, 128.8, 128.5, 128.5, 128.5, 79.9, 78.7, 67.1, 64.3, 35.1, 35.1, 28.9, 28.9; IR (neat): 2957, 1758, 1644, 1454, 1366, 1298, 996, 881, 743, 697, 494 cm^{-1}; HRMS (ESI, Q-TOF) m/z: [M + H]$^+$ Calculated for $C_{36}H_{40}N_2O_4Br$ 643.2171, found 643.214.

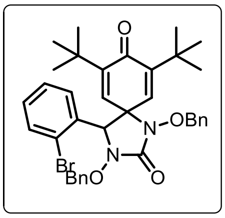

(+/-) 1,3-bis(benzyloxy)-7,9-di-*tert*-butyl-4-(4-nitrophenyl)-1,3-diazaspiro[4.5]deca-6,9-diene-2,8-dione (4ia): Yield= 48 mg (48%); R_f = 0.50 (EtOAc: Hexanes = 1.5:8.5); White solid; Melting Point: 152–154 °C; ^{1}H NMR (400 MHz, $CDCl_3$): δ 8.04 (d, *J* = 8.6 Hz, 2H), 7.37-7.22 (m, 10H), 7.10 (d, *J* = 8.6 Hz, 2H), 6.28 (d, *J* = 2.7 Hz, 1H), 6.24 (d, *J* = 2.7 Hz, 1H), 5.28 (d, *J* = 10.3 Hz, 1H), 5.06 (dd, *J* = 10.9, 5.6 Hz, 2H), 4.99 (d, *J* = 10.7 Hz, 1H), 4.40 (s, 1H), 1.12 (s, 9H), 0.90 (s, 9H); ^{13}C-NMR (100 MHz, $CDCl_3$): δ 184.6, 161.7, 151.9, 148.0, 139.2, 135.1, 135.0, 134.2, 129.6, 129.3, 129.0 129.0, 128.7, 128.6, 128.6, 123.2, 79.6, 78.7, 68.2, 64.1, 35.2, 29.2, 28.8; IR (neat): 2958, 1689, 1648, 1522, 1346, 1203, 976, 881, 852, 699 cm^{-1}; HRMS (ESI, Q-TOF) m/z: [M + H]$^+$ Calculated for $C_{36}H_{40}N_3O_6$ 610.2917, found 610.2926.

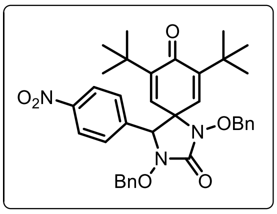

(+/-)1,3-bis(benzyloxy)-7,9-di-*tert*-butyl-4-(4-(trifluoromethyl)phenyl)-1,3-diazaspiro[4.5]deca-6,9-diene-2,8-dione (4ja): Yield = 50 mg (50%); R_f = 0.50 (EtOAc: Hexanes = 1.5:8.5); White solid; Melting Point: 161–163 °C; ^{1}H NMR (400 MHz, $CDCl_3$): δ 7.39 (d, *J* = 8.1 Hz, 2H), 7.27-7.16 (m, 10H), 7.04 (d, *J* = 8.0 Hz, 2H), 6.21 (d, *J* = 2.7 Hz, 1H), 6.17 (d, *J* = 2.7 Hz 1H), 5.23 (d, *J* = 10.1 Hz, 1H), 5.02-4.89 (m, 3H), 4.32 (s, 1H), 1.06 (s, 9H), 0.82 (s, 9H); ^{13}C-NMR (100 MHz, $CDCl_3$): δ 184.7, 161.8, 152.1, 151.5, 136.1, 136.0, 135.1, 134.6, 131.2 (*J* = 32.2 Hz), 129.5, 129.3, 128.9, 128.6, 128.5, 128.3, 128.0, 125.1 (q, *J* = 3.8 Hz), 123.7 (*J* = 270.3 Hz) 79.6, 78.8, 68.3, 64.2, 35.1, 35.1, 29.2, 28.7; ^{19}F (376 MHz, $CDCl_3$): δ =

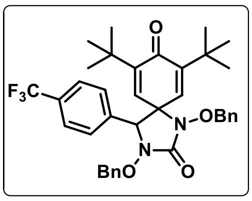

-62.6 ppm; IR (neat): 2922, 1761, 1646, 1454, 1367, 1320, 1164, 1066, 859, 735, 594 cm^{-1}; HRMS (ESI, Q-TOF) m/z: [M + H]$^+$ Calculated for $C_{37}H_{40}N_2O_4F_3$ 633.2940, found 633.2943.

(+/-) 1,3-bis(benzyloxy)-7,9-di-*tert*-butyl-4-(naphthalen-1- yl)-1,3-diazaspiro [4.5]deca-6,9-diene-2,8-dione (4ka): Yield = 57 mg (57%); R_f = 0.50 (EtOAc: Hexanes = 1.5:8.5); White solid; Melting Point: 158- 160 °C; ^{1}H NMR (400 MHz, $CDCl_3$): δ 7.81 (t, J = 8.2 Hz, 2H), 7.54 (t, J = 8.2 Hz, 2H), 7.47-7.16 (m, 13H), 6.53 (d, J = 2.4 Hz, 1H), 6.15 (d, J = 2.4 Hz, 1H), 5.33-5.27 (m, 2H), 5.05-4.95 (m, 3H), 1.02 (s, 9H), 0.76 (s, 9H); ^{13}C-NMR (100 MHz, $CDCl_3$): δ 184.7, 161.7, 150.6, 150.3, 136.8, 136.1, 135.4, 135.2, 133.8, 131.6, 129.5, 129.4, 129.3, 129.1, 128.7, 128.5, 127.8, 126.3, 126.2, 125.7, 124.6, 122.9, 79.8, 79.0, 64.3, 64.2 34.9, 34.9, 28.8, 28.7; IR (neat): 2922, 1763, 1649, 1455, 1365, 1289, 1016, 882, 777, 494 cm^{-1}; HRMS (ESI, Q-TOF) m/z: [M + H]$^+$ Calculated for $C_{40}H_{43}N_2O_4$ 615.3223, found 615.3208.

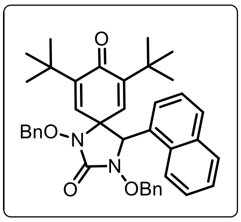

(+/-) 1,3-bis(benzyloxy)-7-(*tert*-butyl)-9-methyl-4-phenyl-1,3-diazaspiro[4.5]deca-6,9-diene-2,8-dione (4la): Yield = 30 mg (30%); R_f = 0.50 (EtOAc: Hexanes = 1.5:8.5); White solid; Melting Point: 145–147 °C; ^{1}H NMR (400 MHz, $CDCl_3$): δ 7.35-7.31 (m, 5H), 7.29-7.20 (m, 8H), 7.06 (d, *J* = 7.9 Hz, 2H), 6.28 (s, 2H), 5.26 (d, *J* = 10.0 Hz, 1H), 5.06-4.93 (m, 3H), 4.32 (s, 1H), 1.56 (s, 3H), 1.11 (s, 9H); ^{13}C-NMR (100 MHz, $CDCl_3$): δ 185.0, 162.0, 150.4, 140.6, 138.2, 137.0, 135.2, 131.6, 129.8, 129.4, 129.1, 128.9, 128.7, 128.5, 128.4, 128.1, 127.9, 79.4, 79.0, 69.1, 64.7, 34.9, 34.9, 16.1; HRMS (ESI, Q- TOF) m/z: [M + H]$^+$ Calculated for $C_{33}H_{35}N_2O_4$ 523.2590, found 523.2597.

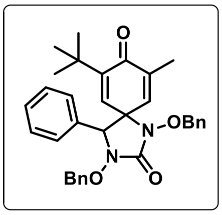

(+/-) 7,9-di-*tert*-butyl-1,3-bis((4-chlorobenzyl)oxy)-4-phenyl-1,3-diazaspiro[4.5]deca-6,9-diene-2,8-dione (4ab): Yield= 59 mg (60%); R_f = 0.50 (EtOAc: Hexanes = 1.5:8.5); White solid; Melting Point: 171–173 °C; ^{1}H NMR (400 MHz, $CDCl_3$): δ 7.26-7.10 (m, 11H), 6.97 (d, *J* = 7.5 Hz, 2H), 6.24 (d, *J* = 2.8 Hz, 1H), 6.18 (d, *J* = 2.7 Hz, 1H), 5.18 (d, *J* = 10.3 Hz, 1H), 4.96 (m, 3H), 4.31 (s, 1H), 1.06 (s, 9H), 0.85 (s, 9H); ^{13}C- NMR (100 MHz, $CDCl_3$): δ 184.8, 162.0, 152.0, 151.2, 136.1, 134.8, 134.8, 134.6, 133.8, 133.7, 131.5, 130.7, 130.6, 129.2, 128.7, 128.6, 128.2, 127.8, 78.6, 78.2, 68.9, 64.7, 35.1, 29.2, 28.8; IR (neat): 2953, 1762, 1644, 1492, 1459, 1364, 1249, 1091, 952, 811, 701, 495 cm^{-1}; HRMS (ESI, Q-TOF) m/z: [M + H]$^+$ Calculated for $C_{36}H_{39}N_2O_4Cl_2$ 633.2287, found 633.2278.

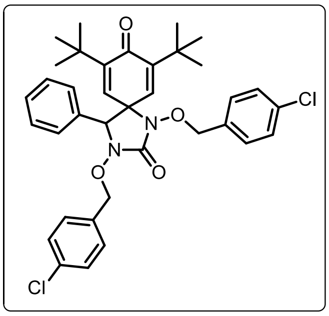

(+/-) 7,9-di-*tert*-butyl-1,3-bis((4-fluorobenzyl)oxy)-4-phenyl-1,3-diazaspiro[4.5]deca-6,9-diene-2,8-dione (4ac): Yield = 62 mg (63%); R_f = 0.50 (EtOAc:Hexanes = 1.5:8.5); White solid; Melting Point: 120–122 °C; ^{1}H NMR (400 MHz, $CDCl_3$): δ 7.34-7.18 (m, 6H), 7.10-6.90 (m, 7H), 6.32 (d, *J* =2.8 Hz, 1H), 6.28 (d, *J* = 2.7Hz, 1H), 5.26 (d, *J* = 10.0 Hz, 1H), 5.04-4.86 (m, 3H), 4.39 (s, 1H), 1.14 (s, 9H), 0.92 (s, 9H); ^{13}C-NMR (100 MHz, $CDCl_3$): δ 184.9, 163.0 (d, *J* = 247.0 Hz), 162.9 (d, *J* = 247.0 Hz), 162.0, 152.0, 151.1, 136.1, 135.0, 131.6, 31.3 (d, *J* = 8.3 Hz), 131.2 (d, *J* = 8.1 Hz), 129.1, 128.2, 127.8, 115.5 (d, *J* = 21.3 Hz), 115.4 (d, *J* = 122.0 Hz) 78.7, 78.2, 68.9, 64.6, 35.0, 29.2, 28.8; ^{19}F (376 MHz, $CDCl_3$): δ = -112.7 ppm, 112.8 ppm; IR (neat): 2955, 1761, 1643, 1510, 1364, 1299, 1224, 1157, 1015, 824, 747, 508 cm^{-1}; HRMS (ESI, Q-TOF) m/z: [M + H]$^+$ Calculated for $C_{36}H_{39}N_2O_4F_2$ 601.2868, found 601.2878.

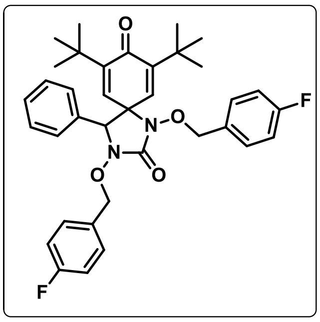

(+/-) 1,3-bis((4-bromobenzyl)oxy)-7,9-di-*tert*-butyl-4-phenyl-1,3-diazaspiro[4.5]deca-6,9-diene-2,8-dione (4ad): Yield= 58 mg (58%); R_f = 0.50 (EtOAc: Hexanes = 1.5:8.5); White solid; Melting Point: 188–190 °C; ^{1}H NMR (400 MHz, $CDCl_3$): δ 7.46 (d, *J* = 8.3 Hz, 2H), 7.37 (d, *J* = 8.1 Hz, 2H), 7.28-7.19 (m, 3H), 7.16 (d, *J* = 8.3 Hz, 2H), 7.11 (d, *J* = 8.1 Hz, 2H), 7.01 (d, *J* = 7.2 Hz, 2H), 6.28 (d, *J* = 2.8 Hz, 1H), 6.22 (d, *J* = 2.8 Hz, 1H), 5.21 (d, *J* = 10.3 Hz, 1H), 5.00 (m, 3H), 4.35 (s, 1H), 1.11 (s, 9H), 0.90 (s, 9H); ^{13}C-NMR (100 MHz, $CDCl_3$): δ 184.8, 162.0, 152.0, 151.2, 136.0, 134.8, 134.3, 134.2, 131.7, 131.6, 131.5, 130.9, 130.9, 129.2, 128.2, 127.8, 123.0, 122.9, 78.6, 78.2, 69.0, 64.7, 35.1, 29.2, 28.8; IR (neat): 2995, 2951, 2864, 1765, 1644, 1487, 1364, 1302, 1249, 1071, 1013, 884, 748, 503 cm^{-1}; HRMS (ESI, Q-TOF) m/z: [M + H]$^+$ Calculated for $C_{36}H_{39}N_2O_4Br_2$ 721.1260, found 721.1277.

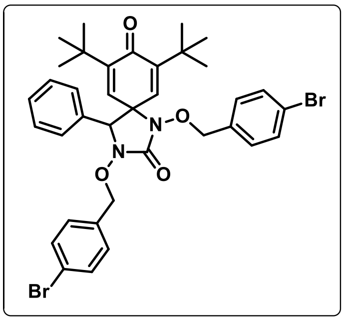

(+/-) 7,9-di-*tert*-butyl-1,3-bis((4-methylbenzyl)oxy)-4-phenyl-1,3-diazaspiro[4.5]deca-6,9-diene-2,8-dione (4ae): Yield= 62 mg (62%); R_f = 0.50 (EtOAc: Hexanes = 1.5:8.5); White solid; Melting Point: 200–202 °C; ^{1}H NMR (400 MHz, $CDCl_3$): δ 7.24-6.94 (m, 13H), 6.23 (d, *J* = 2.7 Hz, 1H), 6.14 (d, *J* = 2.7 Hz, 1H), 5.20 (d, *J* = 9.9 Hz, 1H), 4.93 (d, *J* = 10.8 Hz, 1H), 4.87 (dd, *J* = 10.6, 4.3 Hz, 2H), 4.26 (s, 1H), 2.25 (s, 3H), 2.24 (s, 3H), 1.04 (s, 9H), 0.84 (s, 9H); ^{13}C-NMR (100 MHz, $CDCl_3$): δ 185.0, 162.1, 151.5, 150.8, 138.6, 136.6, 135.4, 132.4, 132.2, 131.8, 129.5, 129.5, 129.2, 129.1, 128.9, 128.1, 127.8, 79.2, 78.8, 68.9, 64.6, 35.0, 29.1, 28.8, 21.3; IR (neat): 2995, 2953, 2865, 1760, 1642, 1458, 1364, 1250, 1076, 884, 799, 622,

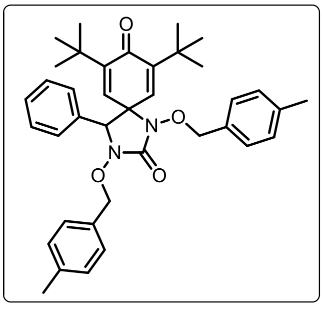

499 cm^{-1}; HRMS (ESI, Q-TOF) m/z: $[M + H]^+$ Calculated for $C_{38}H_{45}N_2O_4$ 593.3379, found 593.3381.

(+/-) 7,9-di-*tert*-butyl-1,3-dimethoxy-4-phenyl-1,3-diaza spiro[4.5]deca-6,9-diene-2,8-dione (4af):

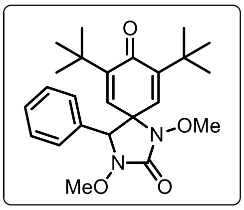

Yield =64 mg (64%); R_f = 0.50 (EtOAc:Hexanes = 1.5:8.5); White solid; Melting Point: 180–182 °C; ^{1}H NMR (400 MHz, $CDCl_3$): δ 7.31-7.25 (m, 3H), 7.19-7.12 (m, 2H), 6.59 (d, *J* = 2.8 Hz, 1H), 6.33 (d, *J* = 2.8 Hz, 1H), 4.45 (s, 1H), 3.91 (s, 3H), 3.83 (s, 3H), 1.24 (s, 9H), 0.92 (s, 9H); ^{13}C-NMR (100 MHz, $CDCl_3$): δ 184.9, 161.4, 152.2, 151.3, 136.0, 134.8, 131.8, 129.1, 128.2, 127.6, 124.3, 120.6, 68.6, 65.9, 64.6, 64.5, 35.2, 35.0, 29.4, 28.8; IR (neat): 2950, 2865, 2819, 1750, 1645, 1457, 1365, 1299, 1078, 883, 622cm^{-1}. HRMS (ESI,Q-TOF) m/z: $[M + H]^+$ Calculated for $C_{24}H_{33}N_2O_4$ 413.2440, found 413.2463.

(+/-)3-(benzyloxy)-7,9-di-*tert*-butyl-1-methoxy-4-phenyl-1,3-diazaspiro[4.5]deca-6,9-diene-2,8-dione (4ag): Yield = 24 mg (48%); R_f = 0.50 (EtOAc: Hexanes = 1.5:8.5); White solid; Melting Point: 148–150 °C; ^{1}H NMR (400 MHz, $CDCl_3$): δ 7.30-7.20 (m, 8H), 7.09-7.05 (m, 2H), 6.54 (d, *J* = 2.8 Hz, 1H), 6.28 (d, *J* = 2.9 Hz, 1H), 5.29 (d, *J* = 9.9 Hz, 1H), 4.99 (d, *J* = 9.9 Hz, 1H), 4.39 (s, 1H), 3.81 (s, 3H), 1.21 (s, 9H), 0.91 (s, 9H); ^{13}C-NMR (100 MHz, $CDCl_3$): δ 185.0, 161.5, 152.1, 151.2, 136.2, 135.3, 135.0, 131.7, 129.4, 129.0, 128.7, 128.4, 128.2, 127.7, 78.9, 69.0, 65.9, 64.5, 35.1, 35.0, 29.4, 28.8; IR (neat): 2958, 1759, 1646, 1456, 1364, 1265, 1031, 882, 735, 699 cm^{-1}; HRMS (ESI, Q-TOF) m/z: $[M + H]^+$ Calculated for $C_{30}H_{37}N_2O_4$ 489.2751, found 489.2753.

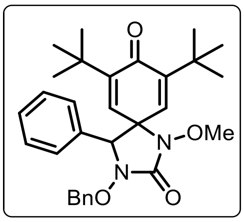

(+/-) 1-(benzyloxy)-7,9-di-tert-butyl-3-methoxy-4-phenyl-1,3-diazaspiro[4.5]deca-6,9-diene-2,8-dione (4ag'): Yield = 22 mg (45%); R_f = 0.50 (EtOAc: Hexanes = 1.5:8.5); White solid; Melting Point: 162–164 °C; ^{1}H NMR (400 MHz, $CDCl_3$): δ 7.38-7.22 (m, 8H), 7.17-7.09 (m, 2H), 6.38 (d, *J* = 2.8 Hz, 1H), 6.30 (d, *J* = 2.9 Hz, 1H), 5.07 (d, *J* = 11.0 Hz, 1H), 4.97 (d, *J* = 11.1 Hz, 1H), 4.42 (s, 1H), 3.92 (s, 3H), 1.14 (s, 9H), 0.92 (s, 9H); ^{13}C-NMR (100 MHz, $CDCl_3$): δ 185.0, 161.5, 152.1, 151.2, 136.2, 135.3, 135.0, 131.7, 129.4, 129.0, 128.7, 128.4, 128.2, 127.7, 78.9, 69.0, 65.9, 64.5, 35.1, 35.0, 29.4, 28.8; IR (neat): 2955, 1759, 1645, 1455, 1364, 1295, 1030, 882, 847, 698 cm^{-1}; HRMS (ESI, Q-TOF) m/z: $[M + H]^+$ Calculated for $C_{30}H_{37}N_2O_4$ 489.2751, found 489.2753.

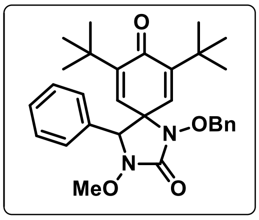

2.4.6 Representative procedure for the sequential one pot synthesis of 4aa

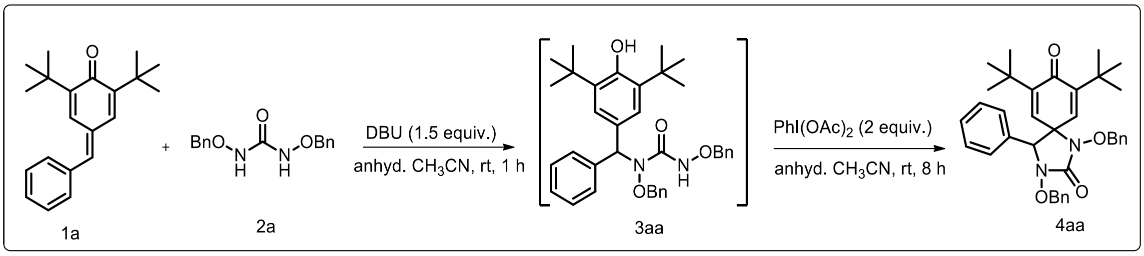

A round-bottom flask equipped with a magnetic stir bar was charged with *p*-QM **1a** (0.170 mmol, 1 equiv.) and dibenzyloxy urea **2**a (0.170 mmol, 1 equiv.) under nitrogen atmosphere and anhydrous CH_3CN (2 mL) was added to it. The reaction was stirred for 1 h until the formation of conjugate addition product **3aa**. After full consumption of the starting materials (as monitored by TLC), PIDA (0.340 mmol, 2 equiv.) was added, and the mixture was stirred for the next 8 h. The excess of solvent was evaporated on a rotary evaporator. The crude mixture obtained was further purified by column chromatography on silica gel using ethyl acetate/hexanes as eluent to afford the required compound **4aa** in 35% yield.

2.4.7 Representative scheme for the debenzylation of 4aa

To the solution of **4aa** (50 mg, 0.12 mmol) in methanol (3 mL) was added 10% Pd/C and then hydrogenated at 45 psi. The reaction was monitored by TLC. After completion of reaction, the mixture was filtered over a bed of celite, washed with methanol (5 mL), and concentrated in vacuo. The crude product was further purified by column chromatography on silica gel (230-400 mesh) using 30% ethyl acetate/hexanes (3:7 v/v) as an eluent to afford **5aa**.

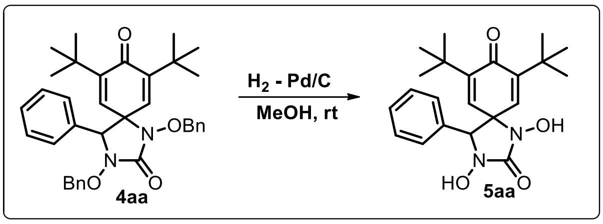

(+/-) 7,9-di-*tert*-butyl-1,3-dihydroxy-4-phenyl-1,3-diazaspiro[4.5]deca-6,9-diene-2,8-dione (5aa):

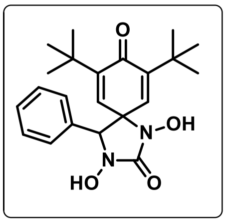

Yield = 27 mg (80%); R_f: 0.50 (EtOAc:Hexane = 5.0:5.0); white solid; ^{1}H NMR (400 MHz, $CDCl_3$): δ 7.25-7.18 (m, 3H), 7.13-7.06 (m, 2H), 6.60 (d, J = 2.5 Hz, 1H), 6.32 (d, J = 2.5 Hz, 1H), 4.62 (s, 1H), 1.21 (s, 9H), 0.88 (s, 9H); ^{13}C-NMR (100 MHz, $CDCl_3$): δ 184.8, 164.3, 152.9, 151.7, 136.0, 134.4, 131.4, 129.0, 128.5, 126.8, 69.2, 65.2, 35.3, 35.0, 29.4, 28.8; HRMS (ESI, Q-TOF) *m/z*: [M + H]$^+$ Calculated for $C_{24}H_{33}N_2O_4$ 385.2111, found 385.2127.

2.5 References

1. a) Pettit, G. R.; McNulty, J.; Herald, D.L.; Doubek, D. L.; Chapuis, J.-C.; Schmidt J. M., Tackett, L. P.; Boyd, M. R. *J. Nat. Prod.* **1997**, *60*, 180–183; b) Chang, C.-S.; Lin, Y.-T.; Shih, S.-R.; Lee, C.-C.; Lee, Y.-C.; Tai, C.-L.; Tseng, S.-N.; Chern, J.-H. *J. Med. Chem.* **2005**, *48*, 3522–3535; c) Lee, K.-C.; Venkateswararao, E.; Sharma, V. K.; Jung, S.-H. *Eur. J. Med. Chem*. **2014**, *80*, 439–446.
2. a) Chern, J.; Chang, C.; Tai, C.; Lee, Y.; Lee, C.; Kang, I.; Lee, C.; Shih, S. *Bioorg. Med. Chem. Lett*. **2005**, *15*, 4206-4211; b) Blass, B. E.; Fensome, A.; Trybulski, E.; Magolda, R.; Gardell, S. J. Liu, K.; Samuel, M.; Feingold, I.; Huselton, C.; Jackson, C. M.; Djandjighian, L.; Ho, D.; Hennan, J.; Janusz, J. M. *J. Med. Chem*. **2009**, *52*, 6531-6534; c) Leslie, C. P.; Biagetti, M. S.; Bison, S; Bromidge, M.; Di Fabio, R.; Donati, D.; Falchi, A.; Garnier, M. J.; Jaxa-Chamiec, A.; Manchee, G.; Merlo, G.; Pizzi, D. A.; Stasi, L. P.; Tibasco, J.; Vong, A.; Ward, S. E.; Zonzini, L. *J. Med. Chem*. **2010**, *53*, 8228-8240; d) Moussa, Z.; El-Sharief, M. A. M. Sh.; Sh. El-Sharief, A. M. *Eur. J. Med. Chem*. **2011,** *46*, 2280-2289.
3. a) Xiao, L.-F.; Xu, L.-W.; Xia, C.-G. *Green Chem*., **2007**, *9*, 369-372; b) Lakhdar, S.; Maji, B.; Mayr, H. *Angew. Chem.* **2012,** *124*, 5837-5840; *Angew. Chem. Int. Ed.* **2012**, *51*, 5739-5742.
4. a) Jung, S.; Lee, H.; Song, J.; Kim, H.; Han, S.; Lee, C.; Lee, M.; Choi, D.; Lee, J.; Chung, Y.; Yoon, S.; Moon, E.; Hwang, H.; Seong, S.; Lee, D. *Bioorg. Med. Chem. Lett.* **1998**, *8*, 1547-1550; b) Zollinger, M.; Mayer, P.; Lindel, T. *J. Org. Chem.* **2006**, *71*, 9431-9439; c) Yoshimitsu, T.; Ino, T.; Tanaka, T. *Org. Lett.* **2008**, *10*, 5457-5460; d) Calvo, M. G.; Meurer, R. D.; Lisnock, J.; Bull, H. G.; McMasters, D. R.; McCann, M. E.; Mills, S. G.; DeVita, R. J.; Howell, K. L. *Bioorg. Med. Chem. Lett.* **2010**, *20*, 6929-6932.
5. a) Ramirez, T. A.; Wang, Q.; Zhu, Y.; Zheng, H.; Peng, X.; Cornwall, R. G.; Shi, Y. *Org. Lett.* **2013**, *15*, 4210–4213; b) Xiao, J.-A.; Wang, C.-M.; Ou, G.-U.; Zhangf, X.-Y.; Yang, H. *Tetrahedron*, **2015**, *71*, 805-812.
6. a) Antunes, E. M.; Copp, B. R.; Samaai, T.; Davies-Coleman, M. T. *Nat. Prod. Rep.* **2005**, *22*, 62−72; b) Liimatainen, J.; Karonen, M.; Wiinamaki, K.; Eklund, P.; Sjoholm, R.; Pihlaja, K. A.; Sinkkonen, J. *Angew. Chem.,* **2007,** 119, 4226-4228; *Angew. Chem., Int. Ed*. **2007**, *46*, 4148−4150; c) Chin, Y.-W.; Salim, A. A.; Su, B.-N.; Mi, Q.; Chai, H.-B.; Riswan, S.; Kardono, L. B. S.; Ruskandi, A.; Farnsworth, N. R.; Swanson, S. M.; Kinghorn, A. D. *J. Nat. Prod.* **2008**, *71*, 390−395; d) MacMillan, K. S.; Boger, D. L. *J. Med. Chem.* **2009**, *52*, 5771−5780; e) Fan, H.; Xiong, J.; Wu, S.-B.; Hu, J.-F. *Chem. Rev.* **2011**, *111*, 5465−5491; f) Kaysser, L.; Bernhardt, P.; Nam, S.-J.; Loesgen, S.; Ruby, J. G.; Skewes-Cox, P.; Jensen, P. R.; Fenical, W.; Moore, B. S. *J. Am. Chem. Soc*. **2012**, *134*, 11988−11991; g) Ma, S. -G.; Gao, R.-M.; Li, Y.-H.; Jiang, J.-D.; Gong, N.-B.; Li, L.; Lü, Y.; Tang, W.-Z.; Liu, Y.-B.; Qu, J.; Lü, H.-N.; Li, Y.; Yu, S.-S. *Org. Lett*. **2013**, *15*, 4450-4453.
7. a). Lee, C.-S.; McGovren, J. P.; Warpehoski, M. A.; Mitchell, M. A.; Kelly, R. C.; Aristoff, P. A.; Hurley, L. H. *Biochemistry* **1988**, *27*, 3886-3892; b) Parrish, J. P.; Kastrinsky, D. B.; Wolkenberg, S. E.; Igarashi, Y.; Boger, D. L. *J. Am. Chem. Soc.* **2003**, *125*, 10971-10976; c) Canesi, S.; Bouchu,

D.; Ciufolini, M. A. *Angew. Chem.,* **2004**, *116,* 4436-4438; *Angew. Chem., Int. Ed.* **2004**, *43,* 4336−4338; d) Burge, M. S.; Wardrop, D. J. *Chem. Commun*. **2004**, 1230−1231; e) Jin, Z. *Nat. Prod. Rep.* **2005**, *22*, 111−126; f) Ciufolini, M.; Braun, N.; Canesi, S.; Ousmer, M.; Chang, J.; Chai, D. *Synthesis,* **2007**, 3759−3772; g) Pouysegu, L.; Deffieux, D.; Quideau, S. *Tetrahedron.* **2010**, *66*, 2235−2261; h) Bauer, R. A.; Wenderski, T. A.; Tan, D. S. *Nat. Chem. Biol.* **2013**, *9*, 21−29.

8. For selected examples see: a) Chu, W.-D.; Zhang, L.-F.; Bao, X.; Zhao, X.-H.; Zeng, C.; Du, J.-Y. Zhang, G.-B.; Wang, F.-X.; Ma, X.-Y.; Fan, C.-A. *Angew. Chem., Int. Ed.* **2013**, *52*, 9229-9233; b) Caruana, L. Kniep, F. Johansen, T. K. Poulsen, P. H. Jørgensen, K. A. *J. Am. Chem. Soc.* **2014**, *136*, 15929-15932; c) Lou, Y. Cao, P. Jia, T. Zhang, Y. Wang, M. Liao, J. *Angew. Chem.* **2015**, 127, 12302-12306; *Angew. Chem. Int. Ed.* **2015**, *54*, 12302-12306; d) Deng, Y.-H. Zhang, X.-Z Yu, K.-Y. Yan, X. Du, J.-Y. Huang, H. Fan, C.-A. *Chem. Commun.* **2016**, *52*, 4183-4186; e) Dong, N. Zhang, Z.-P. Xue, X.-S. Li, X. Cheng, J.-P. *Angew. Chem.* **2016**, 128, 1482-1486; *Angew. Chem. Int. Ed.* **2016**, *55*, 1460-1464; f) He, F.-S. Jin, J.-H. Yang, Z.-T. Yu, X. Fossey, J. S. Deng, W. -P *ACS Catal.* **2016**, *6*, 652-656; g) Zhang, X.-Z. Deng, Y.-H. Yan, X. Yu, K.-Y. Wang, F.-X. Ma, X.-Y. Fan, C.-A. *J. Org. Chem.* **2016**, *81*, 5655-5662; h) Li, X. Xu, X. Wei, W. Lin, A. Yao, H.*Org. Lett.* **2016**, *18*, 428-431; i) Yang, C. Gao, S. Yao, H. Lin, A. *J. Org. Chem.* **2016**, *81*, 11956-11964; j) Gao, S. Xu, X.-Y. Yuan, Z.-B. Zhou, H.-P. Yao, H. Lin, A. *Eur. J. Org. Chem.* **2016**, 3006-3012; k) Harish, B. Subbireddy, M. Obulesu, O. Suresh, S. *Org. lett.* **2019**, *21*, 1823-1827; l) Curti, C. Battistini, L. Sartori, A. Zanardi, F. *Chem. Rev*. **2020**, *120*, 2448-2612; m) Li, D. Yang, Y. Zhang, M. Wang, L. Xu, Y. Yang, D. Wang, R. *Nat. Commun.* **2020**, *11*, 2559.
9. For selected examples, see: a) Parra, A. Tortosa, M. *ChemCatChem*, **2015**, 1524-1526; b) Huang, B. Shen, Y.-Y. Mao, Z.-J. Liu, Y. Cui, S.-L. *Org. Lett.* **2016**, *18*, 4888-4891; c) Jarava-Barrera, C. Parra, A. Lopez, A. Cruz-Acosta, F. Collado-Sanz, D. Cardenas, D. J. Tortosa, M. *ACS Catal.* **2016**, *6*, 442-446; d) Shen, Y. Qi, J. Mao, Z. Cui, S. *Org. Lett.* **2016**, *18*, 2722-2725; e) Zhao, K. Zhi, Y.. Wang, A. Enders, D. *ACS Catal.* **2016**, *6*, 657-660; f) Li, S. Liu, Y. Huang, B. Zhou, T. Tao, H. Xiao, Y. Liu, L. Zhang, J. *ACS Catal.* **2017**, *7*, 2805-2809; g) Zhuge, R. Wu, L. Quan, M. Butt, N. Yang, G. Zhang, W.*Adv. Synth. Catal.* **2017**, *359*, 1028-1036; h) Molleti, N. Kang, J.-Y.*Org. Lett.* **2017**, *19*, 958-961; i) Pauli, F. P. Costa, D. C. S. Souza, A. S. Forezi, L. S. M. Ferreira, V. F. Lima, C.G.S Silva, F. C. *Eur. J. Org. Chem.* **2020**, 2650–2692. 1
10. a) Yuan, Z. Fang, X. Li, X. Wu, J. Yao, H. Lin, A. *J. Org. Chem.* **2015,** *80*, 11123-11130; b) Gai, K. Fang, X. Li, X. Xu, J. Wu, X. Lin, A. Yao, H. *Chem. Commun.* **2015**, *51*, 15831-15834; c) Zhang, X.-Z..Du, J.-Y. Deng, Y.-H. Chu, W.-D. Yan, X. Yu, K.-Y. Fan, C.-A. *J. Org. Chem.* **2016**, *81*, 2598-2606; d) Zhang, X.-Z. Deng, Y.-H. Gan, K.-J. Yan, X. Yu, K.-Y. Wang, F.-X. Fan, C.-A. *Org. Lett.* **2017**, *19*, 1752-1755; e) Roiser, L. Waser, M. *Org. Lett*. **2017**, *19*, 2338-2341; f) Yuan, Z. Gai, K. Wu, Y. Wu, J. Lin, A. Yao, H. *Chem. Commun.* **2017**, *53*, 3485-3488; g) Pan, R. Hu, L. Han, C. Lin, A. Yao, H. *Org. Lett.* **2018**, *20*, 1974-1977.
11. a) Yuan, Z. Wei, W. Lin, A. Yao, H. *Org. Lett.* **2016**, *18*, 3370-3373; b) Ma, C. Huang, Y. Zhao, Y. *ACS Catal.* **2016**, *6*, 6408-6412; c) Yuan, Z. Liu, L. Pan, R. Yao, H. Lin, A. *J. Org. Chem.* **2017**, *82*, 8743-8751.

12. a) Zhao, Y. Chang, B. Zhao, X. Zhang, R. Liu, X. Huang, D. Wang, K.-H Huo, C. Hu, Y. Su, Y. *J. Org. Chem.* **2019**, *84*, 6719-6728.
13. Kale, S. B. Jori, P. K. Thatikonda, T. Gonnade, R. G. Das, U. *Org. Lett.*, **2019**, *21*, 7736-7740.
14. a) Gallou, I. *Org. Prep. Proced. Int*. **2007**, *39*, 355- 383; b) Brindisi, M. Ghosh, A. *J. Med. Chem.*, **2020**, *63*, 2751–2788.
15. a) Acharya, A. Anumandla, D. Jeffrey, C. S. *Org. Lett.*, **2014**, *16*, 5112-5115; b) Anumandla, D. Littlefield, R. Jeffrey, C. S. *J. Am. Chem. Soc*, **2015**, *137*, 14858-14860. c) Rosser, A. A. Taherpour, A. A. Greatrex, B. W. Glover, S. A. *Aust. J. Chem*. **2014**, *67*, 507-520;
16. a) Taily, I. M. Saha, D. Banerjee, P. *Eur. J. Org. Chem*, **2019**, 7804-7813; b) Taily, I. M. Saha, D. Banerjee, P. *Org. Biomol. Chem.*, **2020**, 6564-6570
17. Burge, M. S. Zhang, W. Ortiz, J. A. Wardrop, D. J. *Tetrahedron Letters*, **2003**, *44*, 2587-2591. For reviews, see: Maiti, S. Alam, M. T. Bal, A. Mal, P. *Adv. Synth Catal*. **2019**, *361*, 4401-4425.
18. a) Follows, B. C. Hergenrother, P. J. Franklin, C. L. Martin, S. F. *J. Org. Chem*., **2000**, *65*, 4509-4514; b) Day, J. A. Cohen, S. M. *J. Med. Chem.,* **2013**, *56*, 7997-8007.

2.6 NMR Spectra (^{1}H, ^{13}C, DEPT) of compounds:

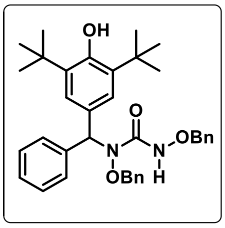

^{1}H NMR ($CDCl_3$, 400 MHz) of 3aa

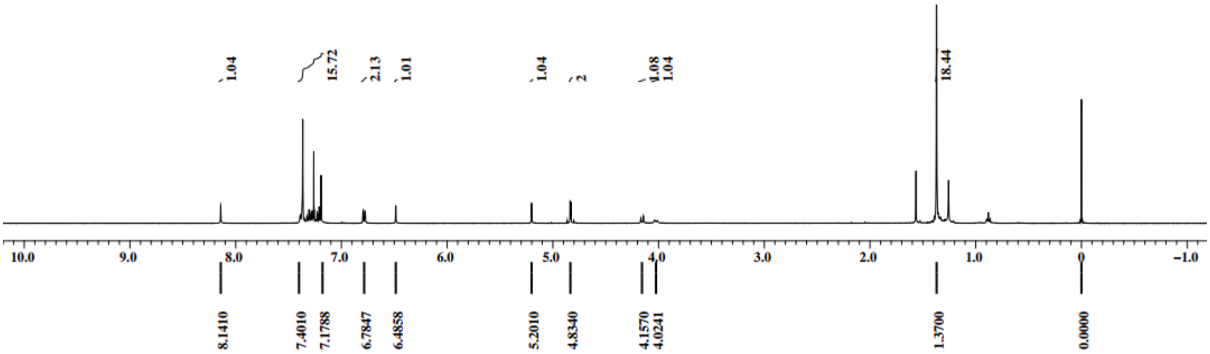

^{13}C NMR ($CDCl_3$, 400 MHz) of 3aa

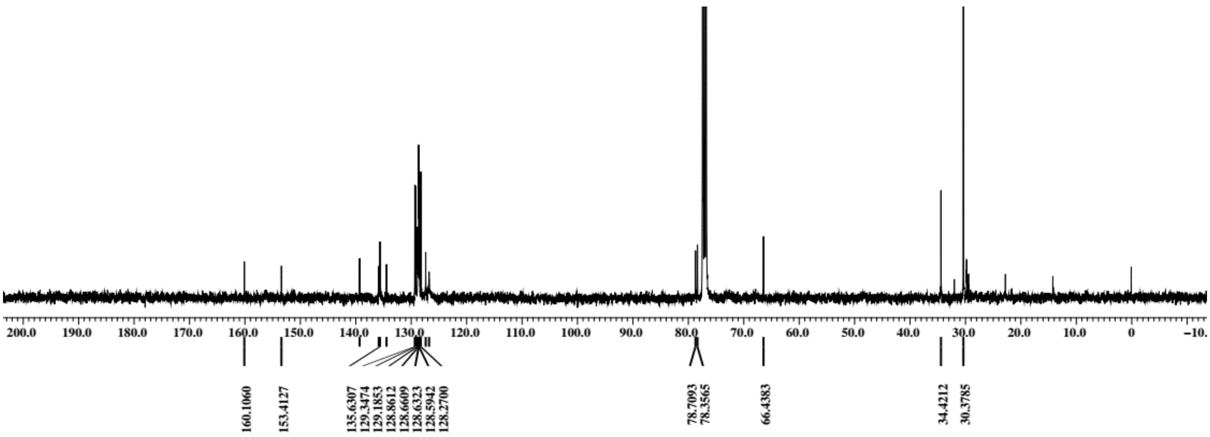

^{13}C DEPT NMR ($CDCl_3$, 400 MHz) of 3aa

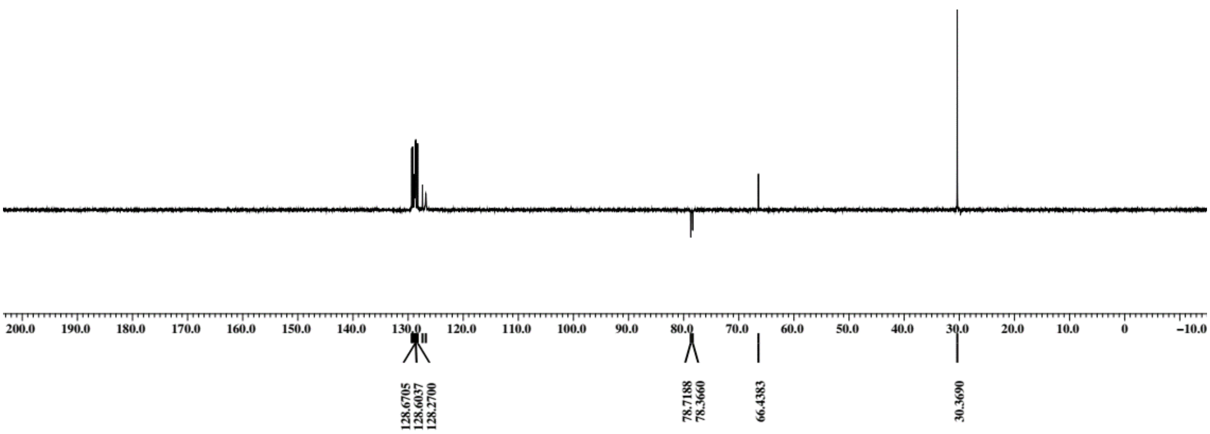

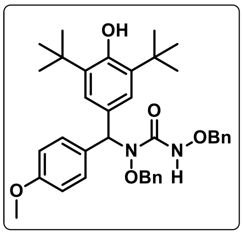

[1]H NMR ($CDCl_3$, 400 MHz) of 3ba

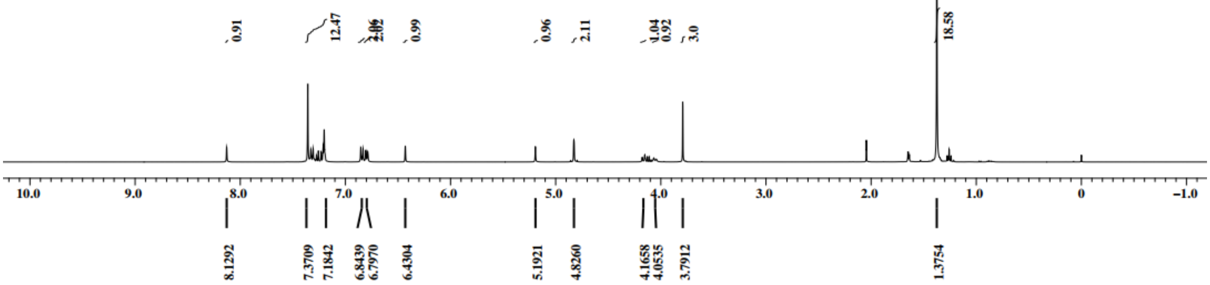

[13]C NMR ($CDCl_3$, 100 MHz) of 3ba

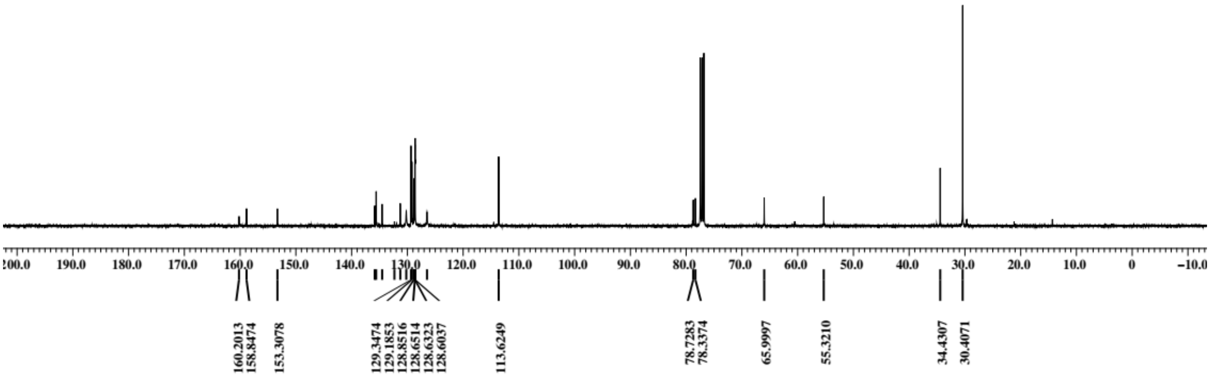

[13]C DEPT NMR ($CDCl_3$, 100 MHz) of 3ba

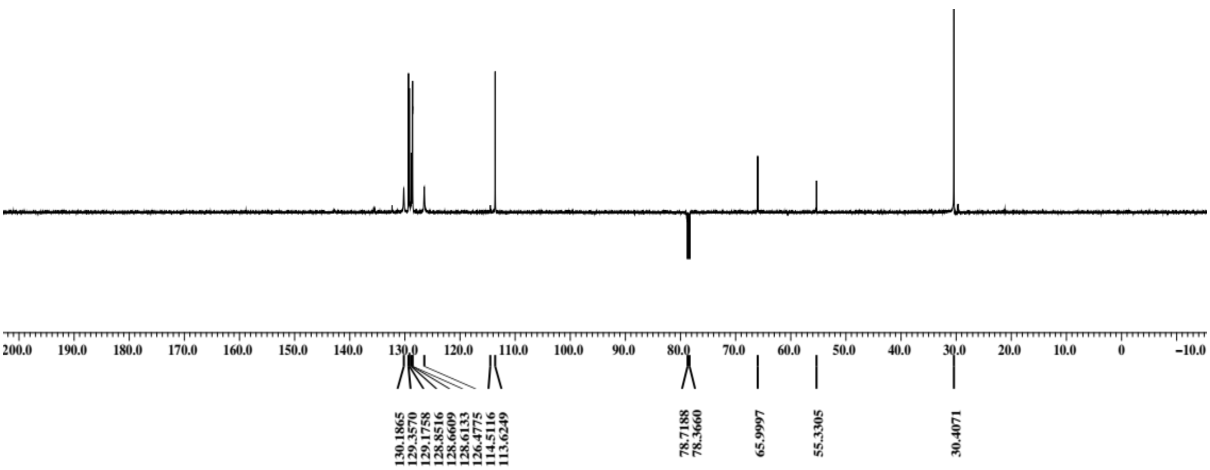

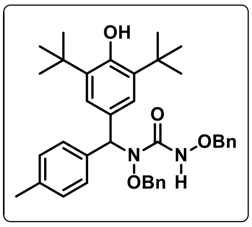

^1H NMR ($CDCl_3$, 400 MHz) of 3ca

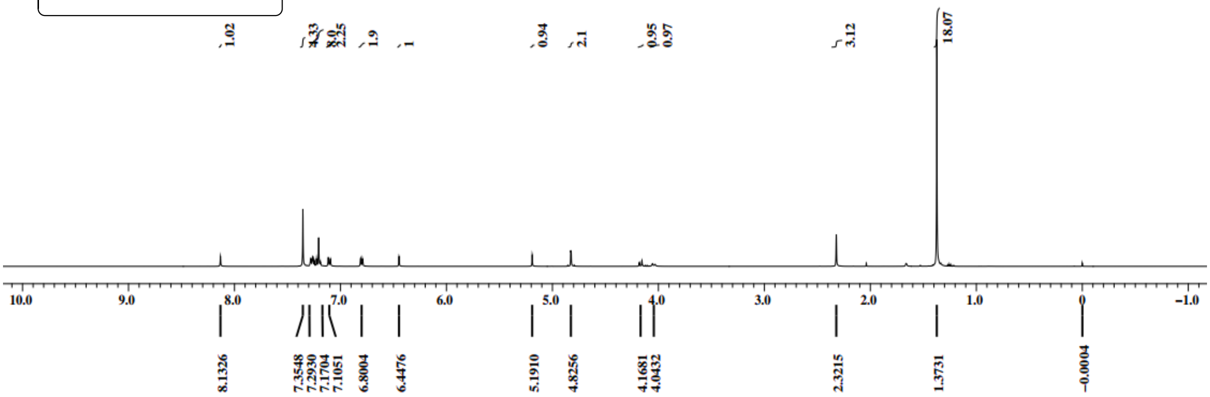

^{13}C NMR ($CDCl_3$, 100 MHz) of 3ca

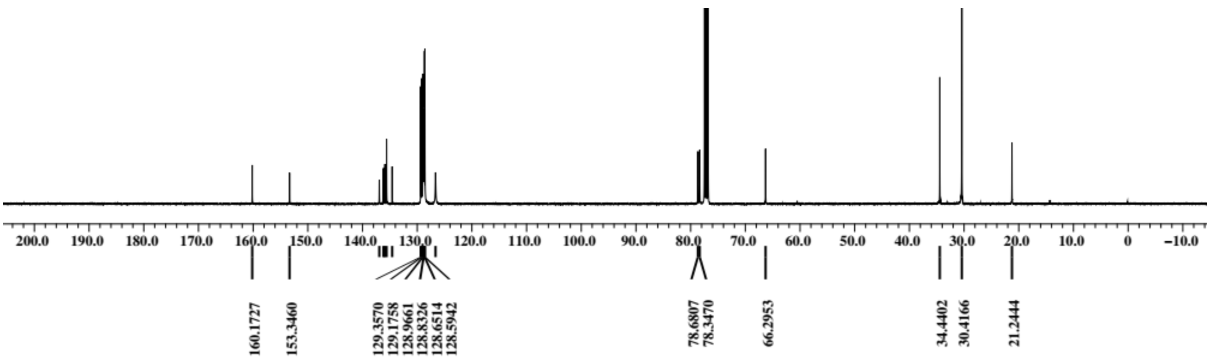

^{13}C DEPT NMR ($CDCl_3$, 100 MHz) of 3ca

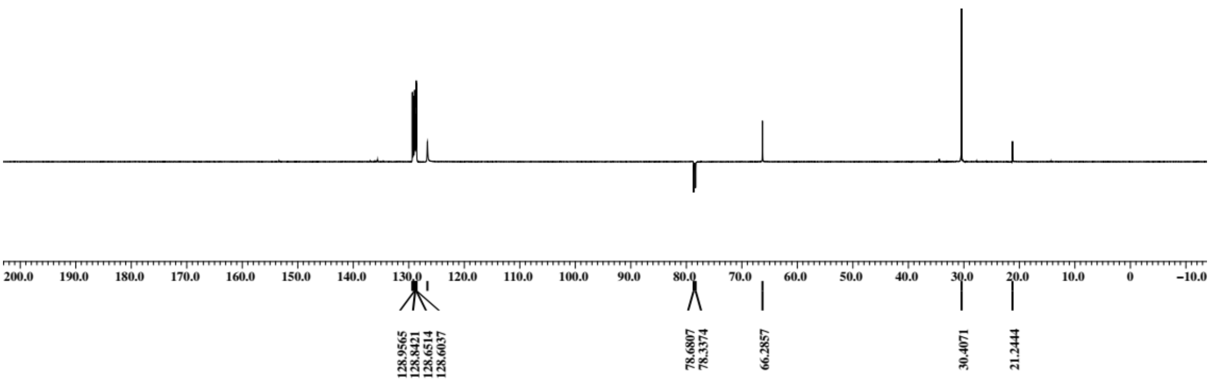

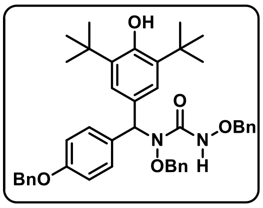

^{1}H NMR ($CDCl_3$, 400MHz) of 3da

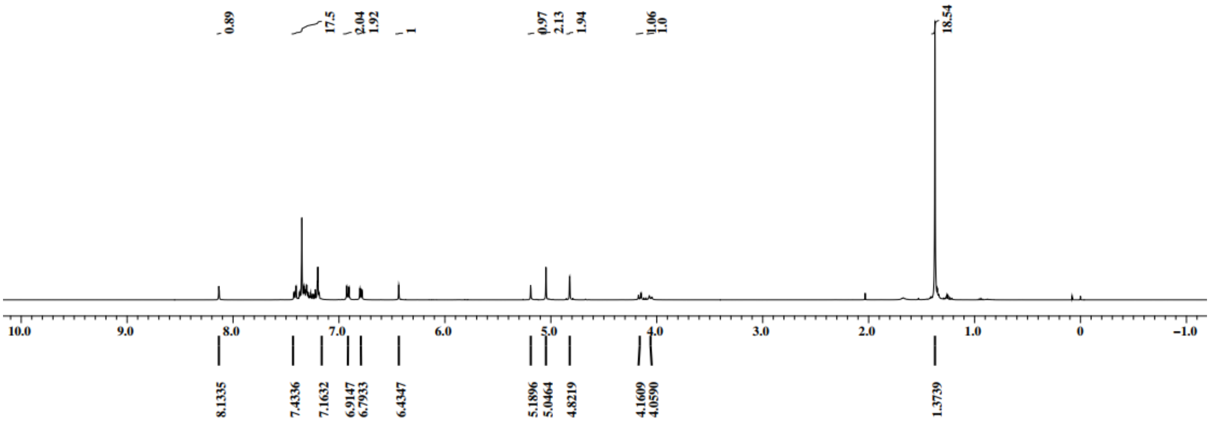

^{13}C NMR ($CDCl_3$, 100 MHz) of 3da

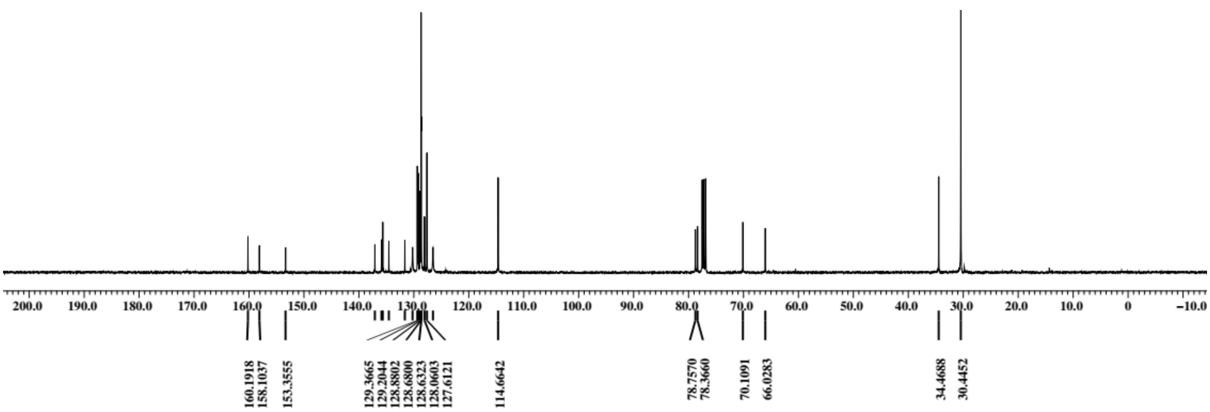

^{13}C DEPT NMR ($CDCl_3$, 100 MHz) of 3da

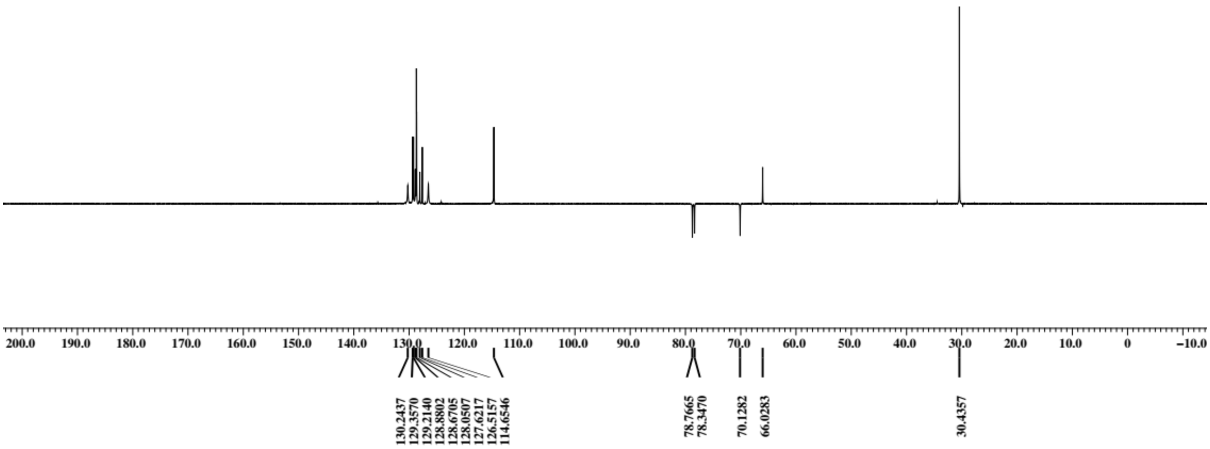

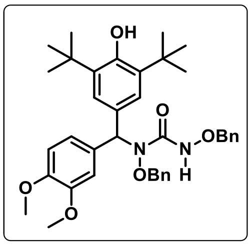

[1]H NMR (CDCl₃, 400 MHz) of 3ea

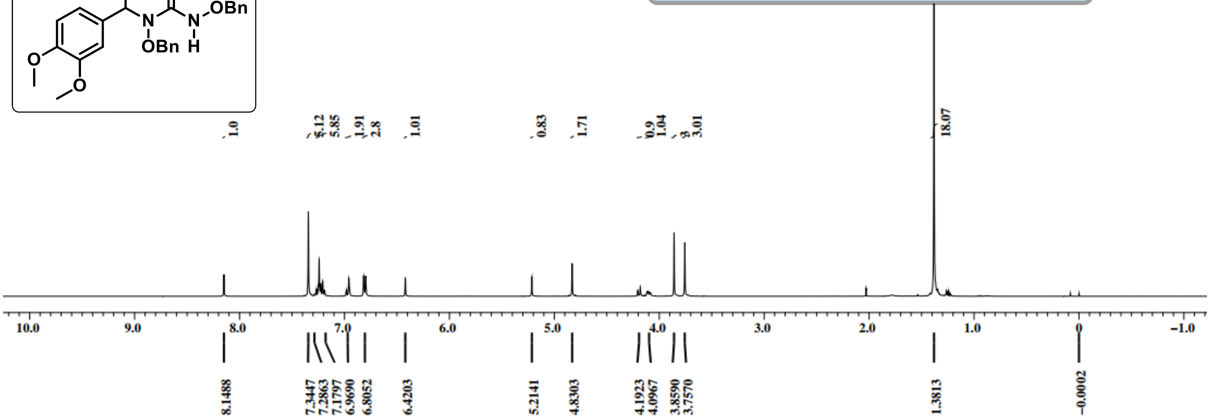

[13]C NMR (CDCl₃, 100 MHz) of 3ea

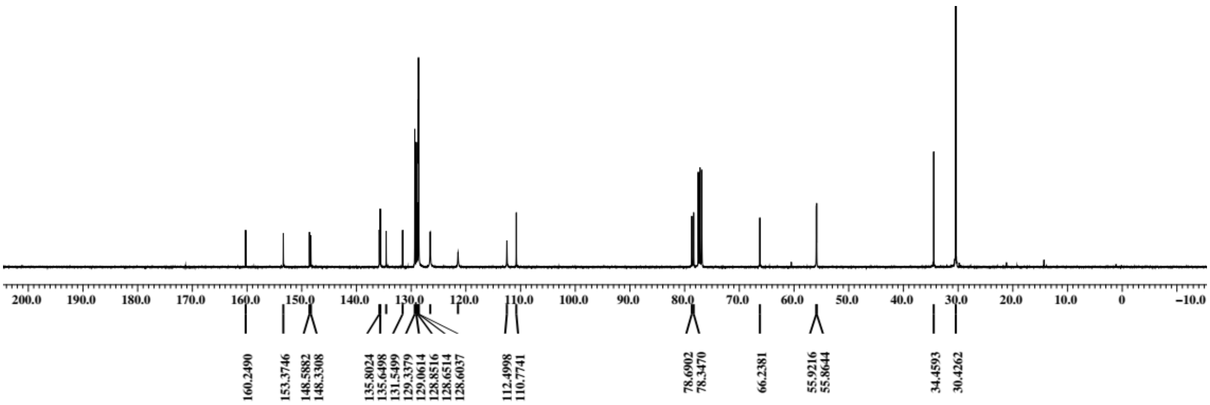

[13]C DEPT NMR (CDCl₃, 100 MHz) of 3ea

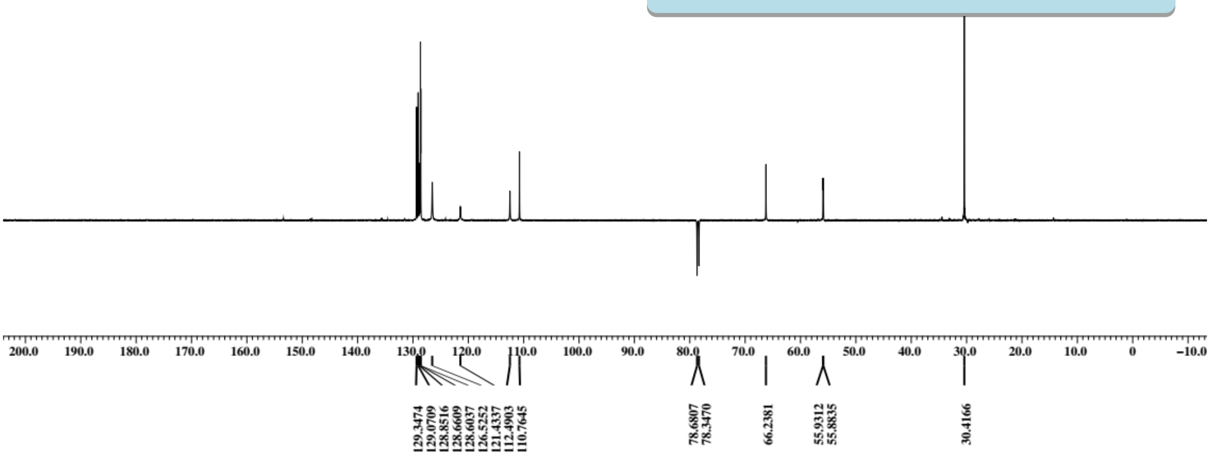

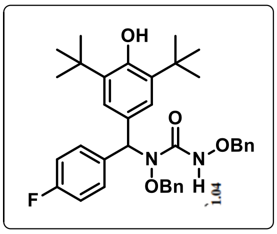
OH
O
N
OBn
OBn
H
F

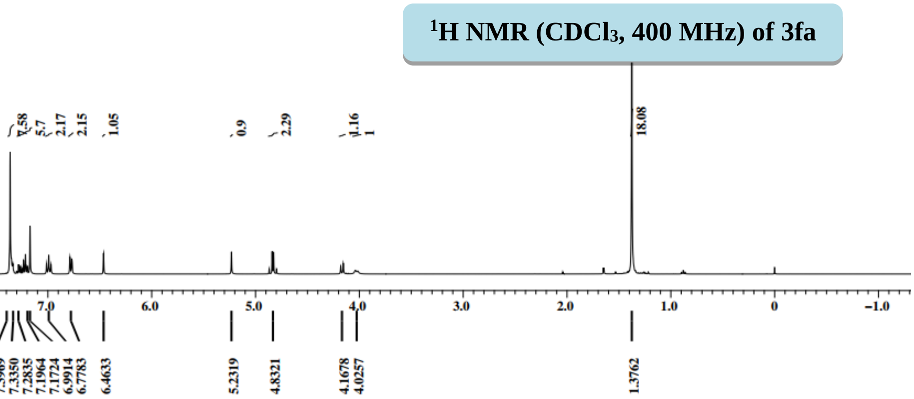
^{1}H NMR (CDCl$_3$, 400 MHz) of 3fa
8.1369
7.3969
7.3350
7.2835
7.1964
7.1724
6.9914
6.7783
6.4633
5.2319
4.8321
4.1678
4.0257
1.3762
18.08

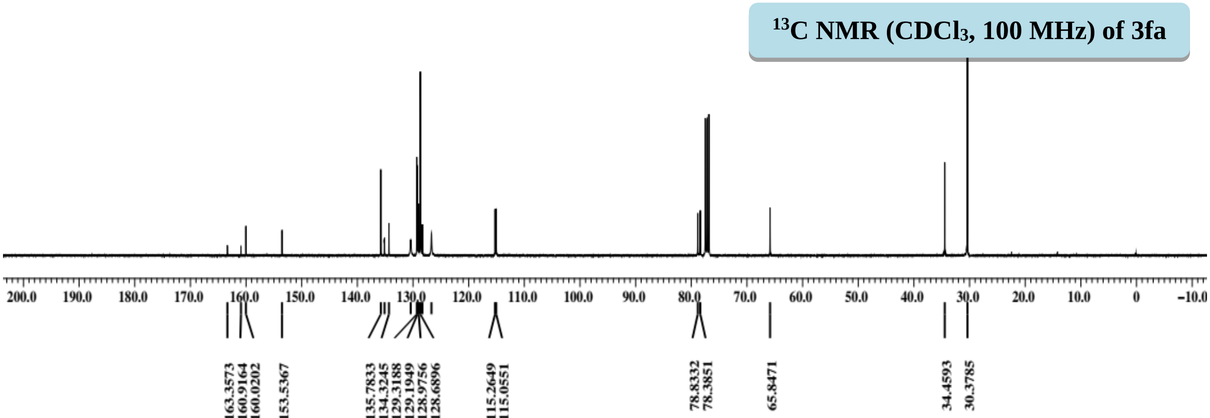
^{13}C NMR (CDCl$_3$, 100 MHz) of 3fa
163.3573
160.9164
160.0202
153.5367
135.7833
134.3245
129.3188
129.1949
128.9756
128.6896
115.2649
115.0551
78.8332
78.3851
65.8471
34.4593
30.3785

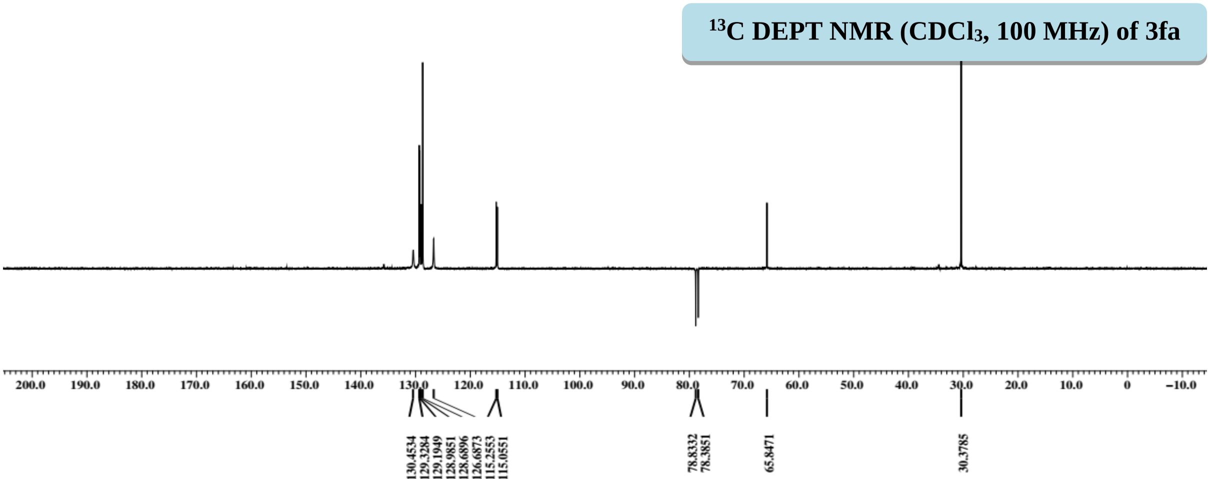
^{13}C DEPT NMR (CDCl$_3$, 100 MHz) of 3fa
130.4534
129.3284
129.1949
128.9851
128.6896
126.6873
115.2553
115.0551
78.8332
78.3851
65.8471
30.3785

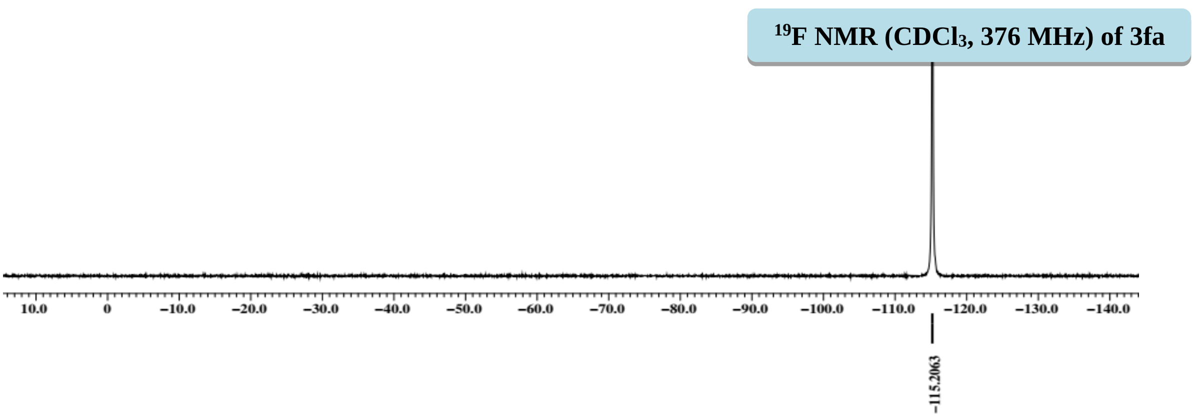
^{19}F NMR (CDCl$_3$, 376 MHz) of 3fa
−115.2063

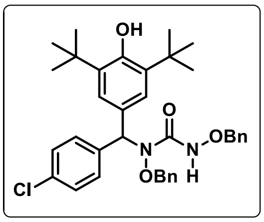

^{1}H NMR ($CDCl_3$, 400 MHz) of 3ga

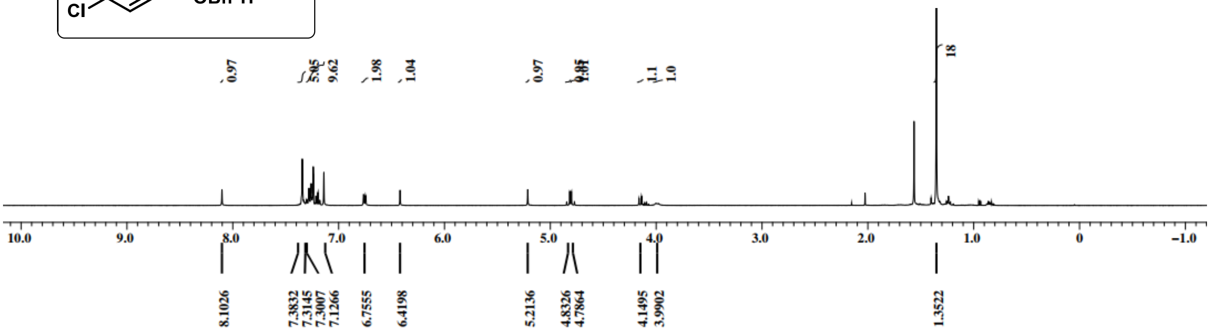

^{13}C NMR ($CDCl_3$, 100 MHz) of 3ga

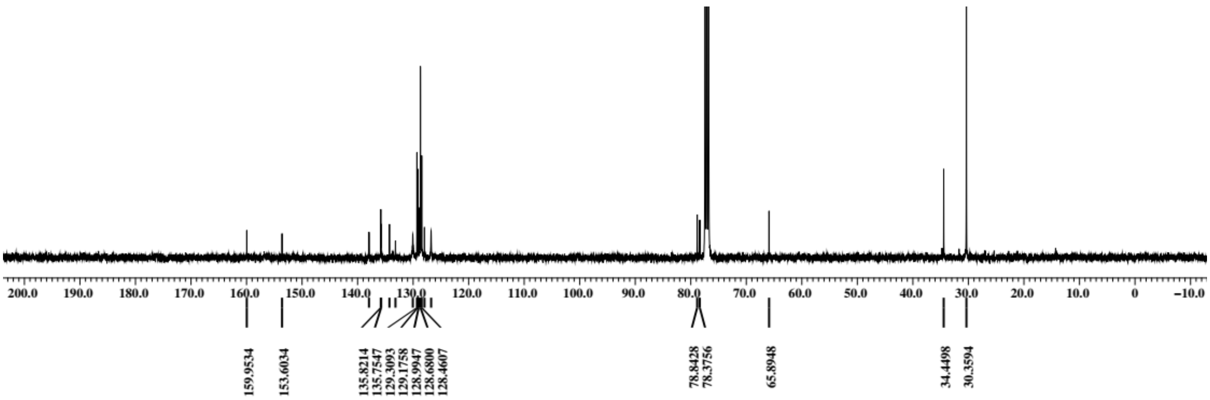

^{13}C DEPT NMR ($CDCl_3$, 100 MHz) of 3ga

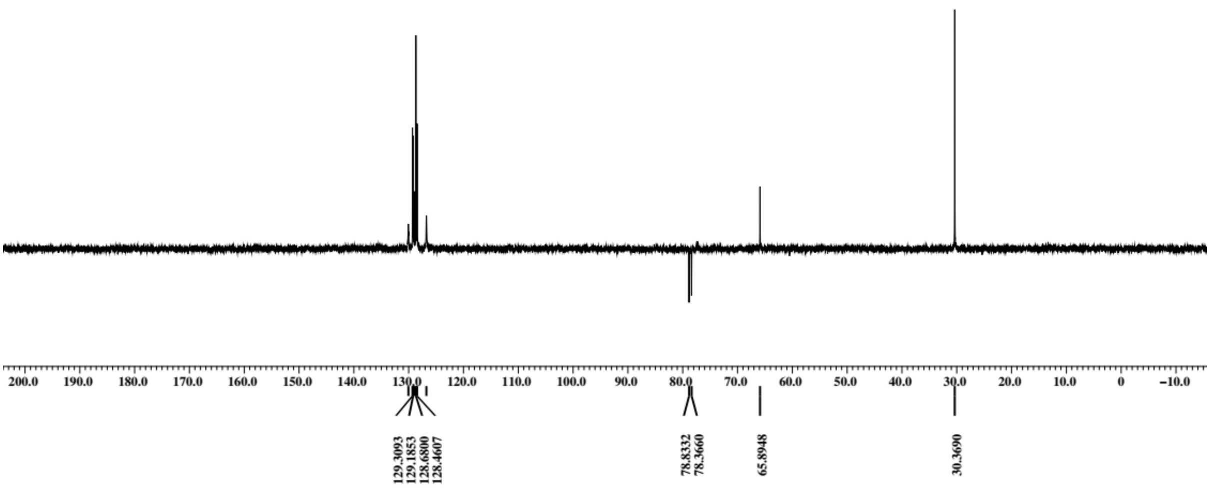

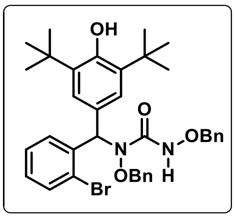

[1]H NMR ($CDCl_3$, 400 MHz) of 3ha

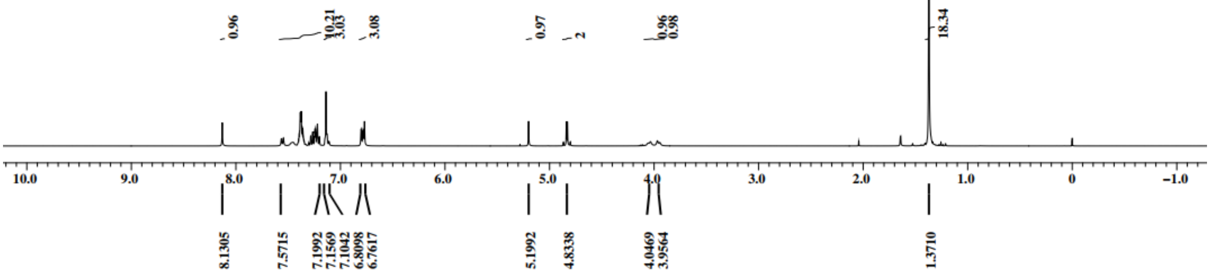

[13]C NMR ($CDCl_3$, 100 MHz) of 3ha

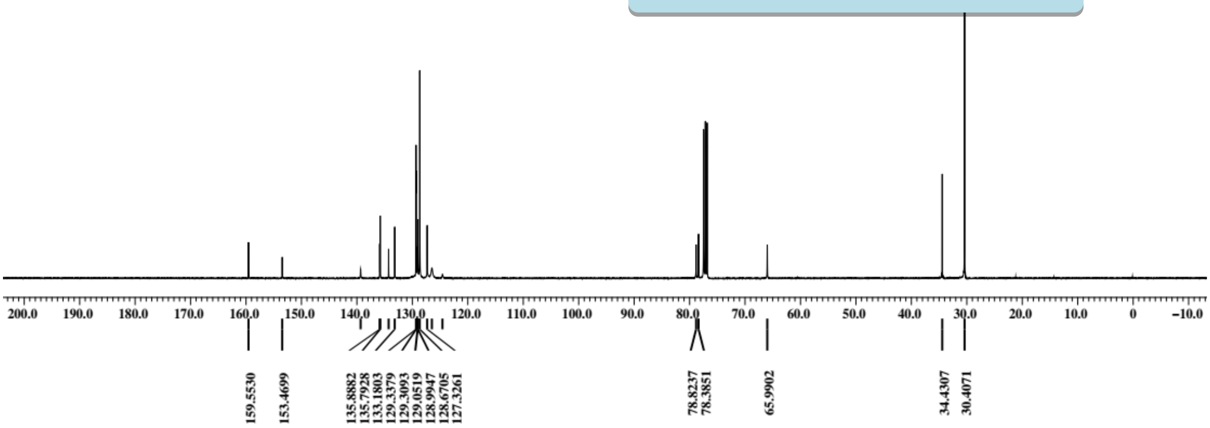

[13]C DEPT NMR ($CDCl_3$, 100 MHz) of 3ha

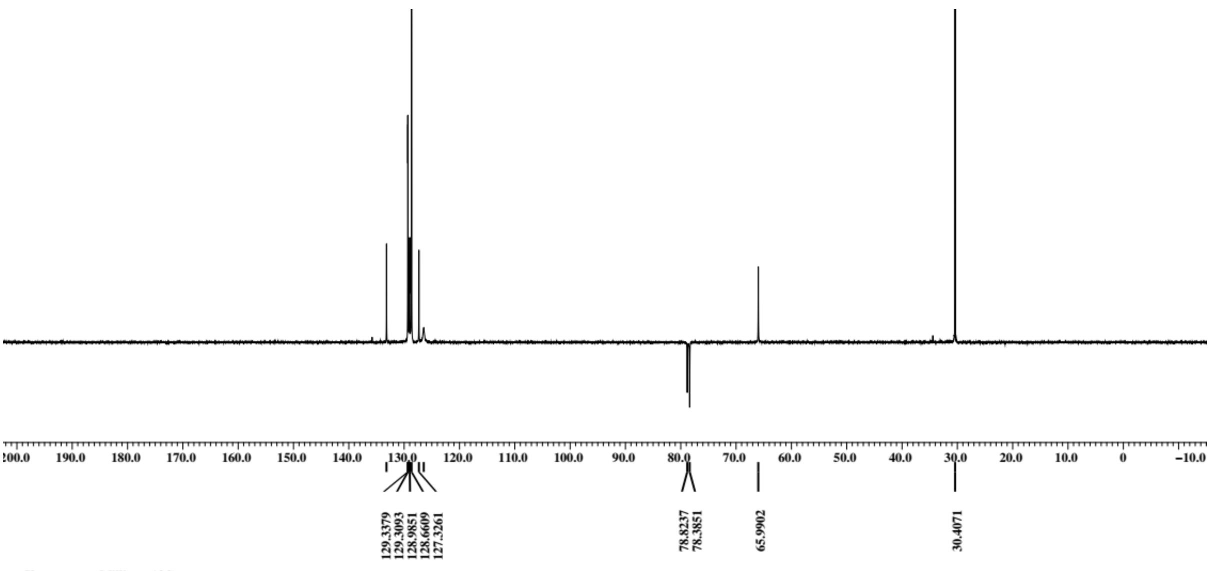

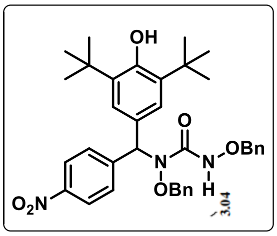

¹H NMR (CDCl₃, 400 MHz) of 3ia

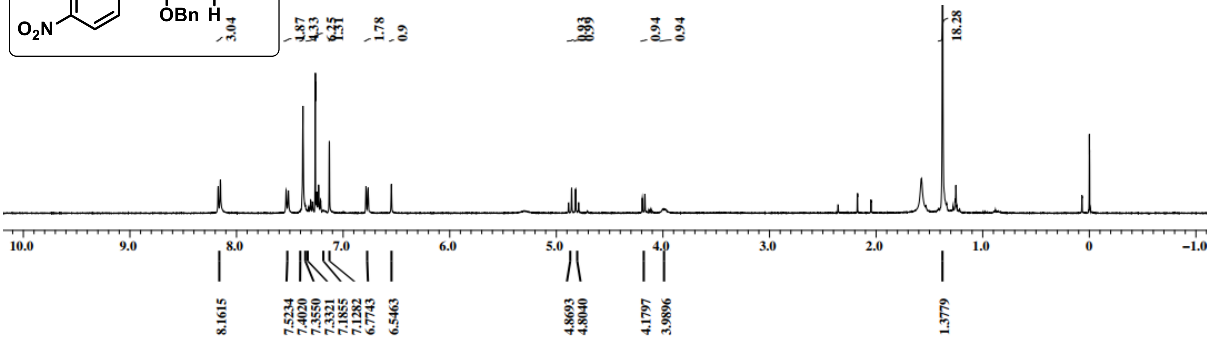

¹³C NMR (CDCl₃, 100 MHz) of 3ia

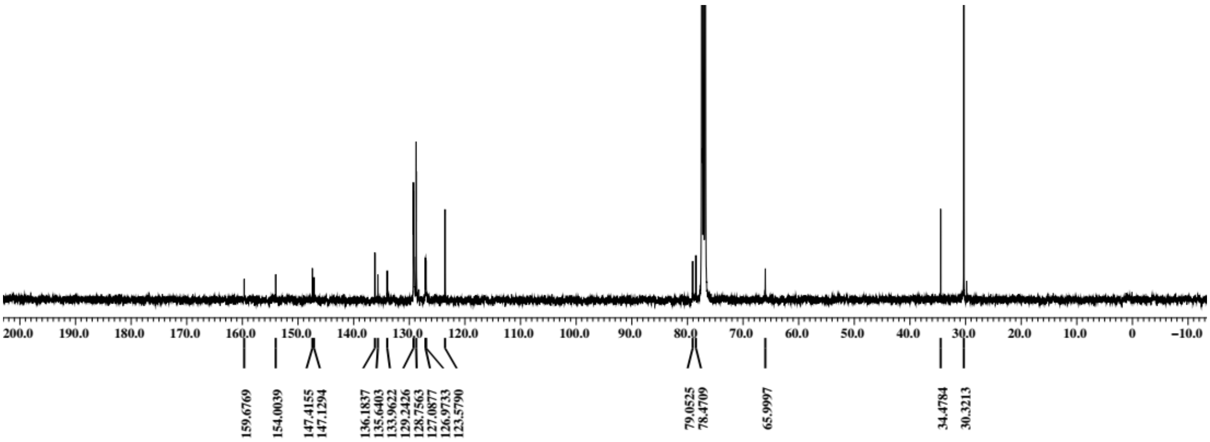

¹³C DEPT NMR (CDCl₃, 100 MHz) of 3ia

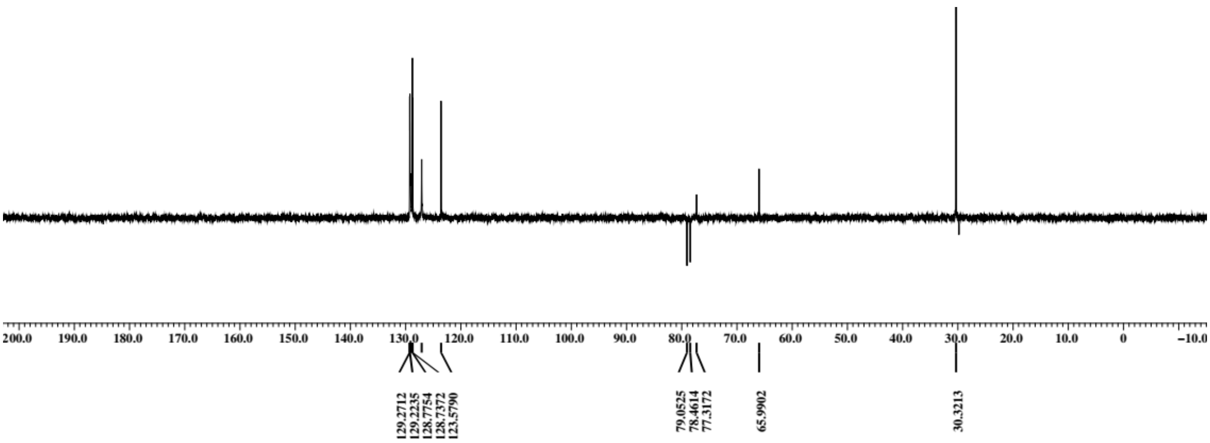

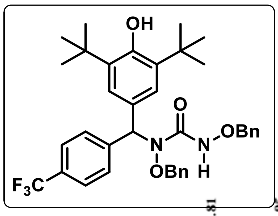

^{1}H NMR ($CDCl_3$, 400 MHz) of 3ja

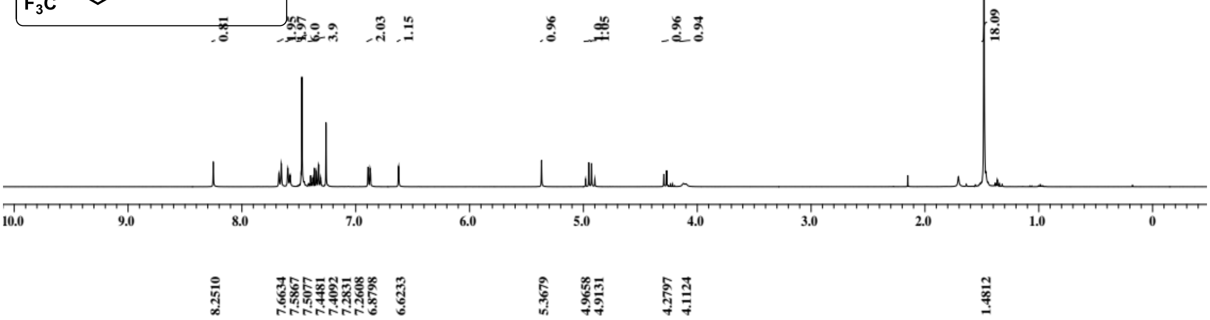

^{13}C NMR ($CDCl_3$, 100 MHz) of 3ja

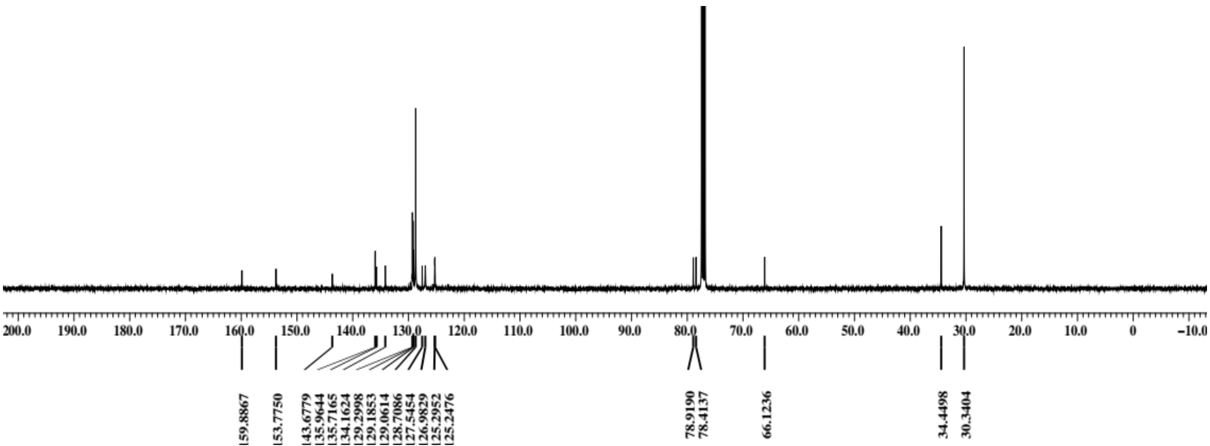

^{13}C DEPT NMR ($CDCl_3$, 100 MHz) of 3ja

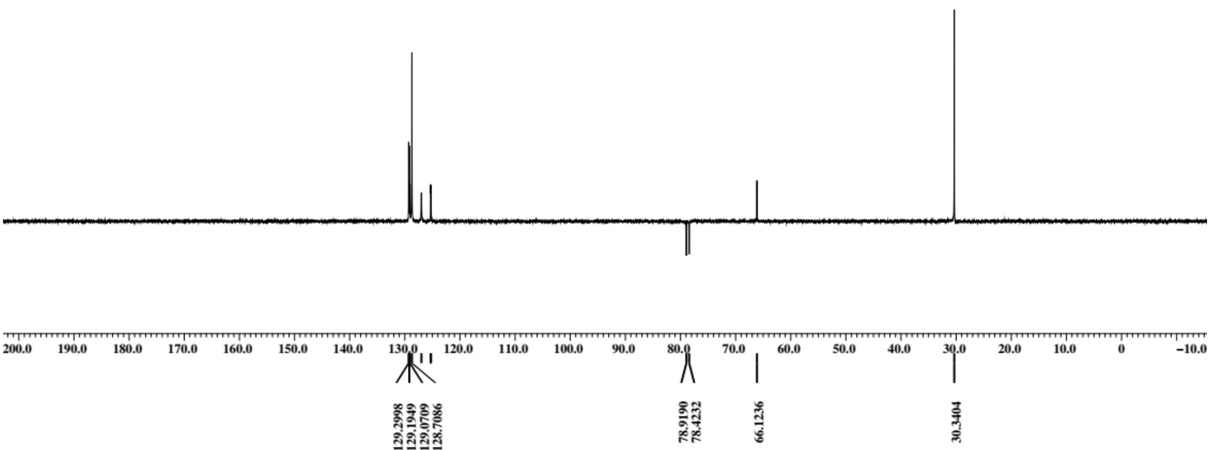

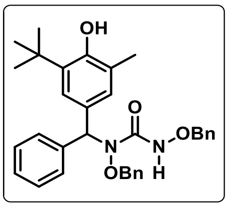

^{1}H NMR ($CDCl_3$, 400 MHz) of 3ka

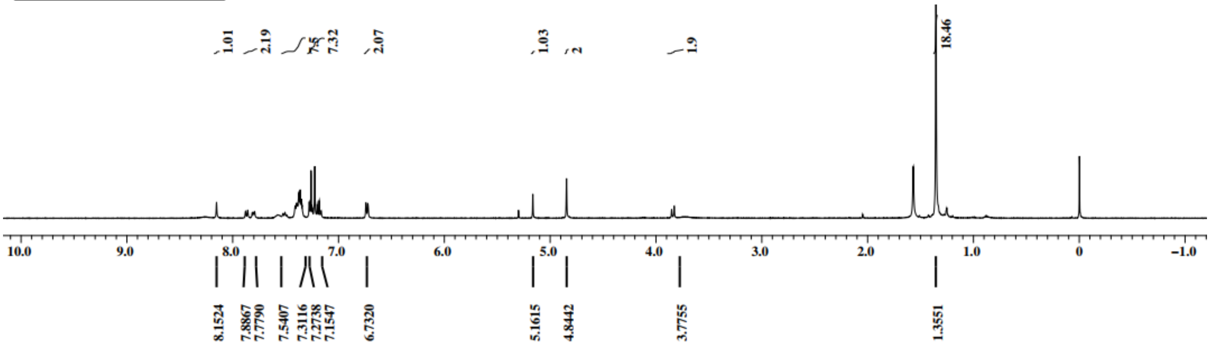

^{13}C NMR ($CDCl_3$, 100 MHz) of 3ka

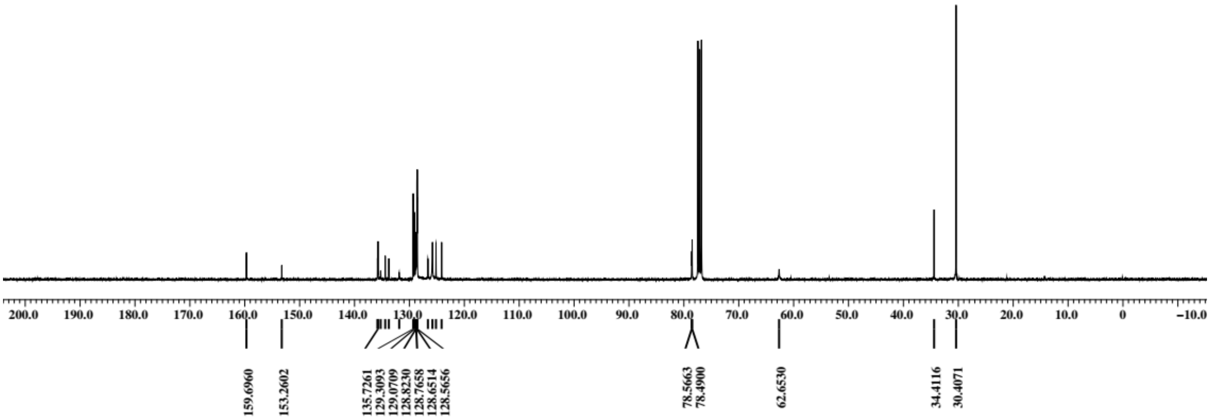

^{13}C DEPT NMR ($CDCl_3$, 100 MHz) of 3ka

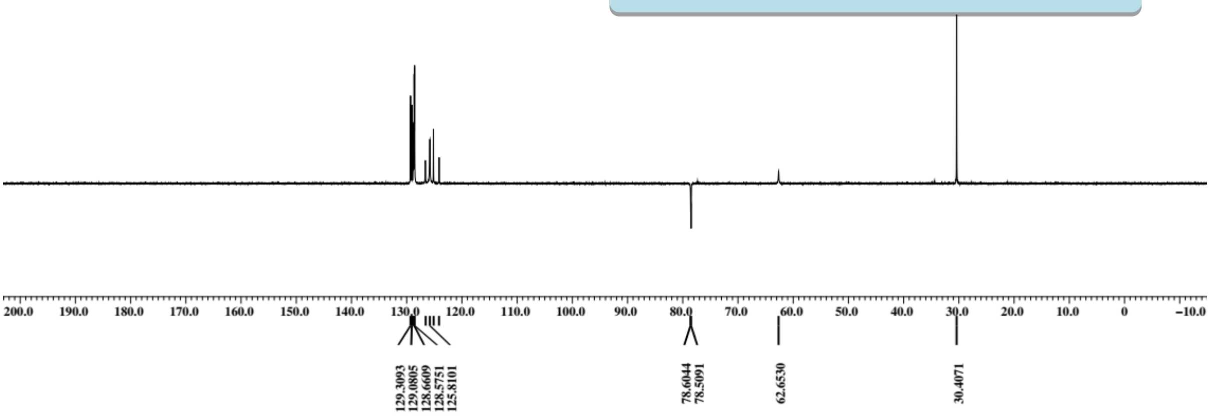

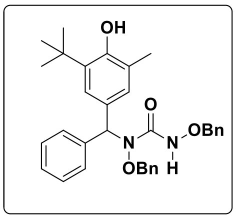

^{1}H NMR ($CDCl_3$, 400 MHz) of 3la

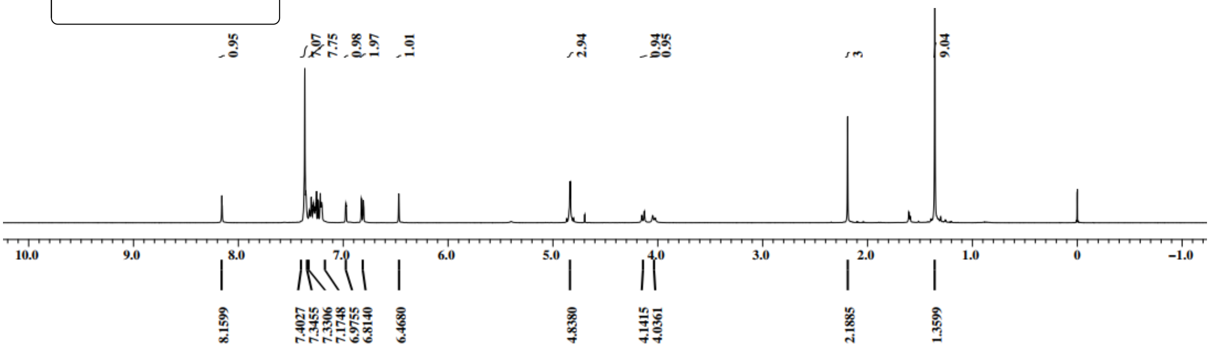

^{13}C NMR ($CDCl_3$, 100 MHz) of 3la

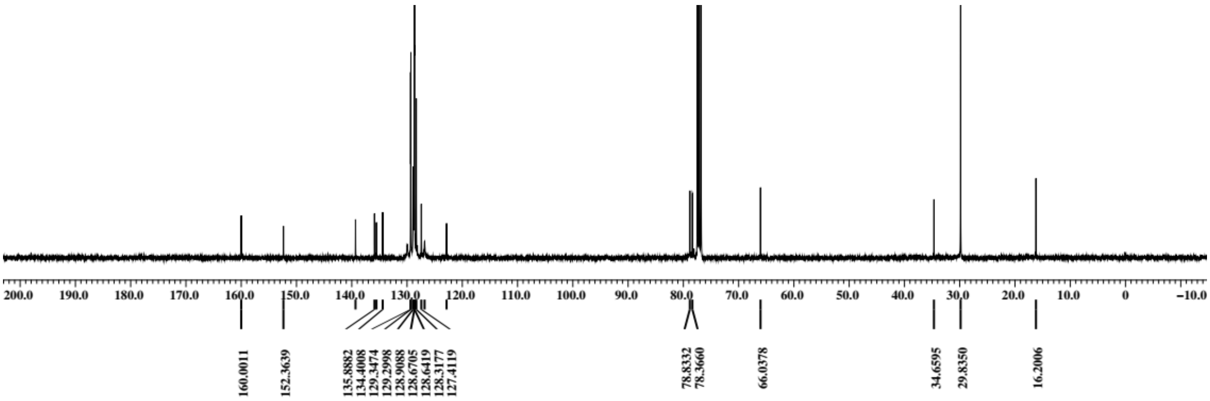

^{13}C DEPT NMR ($CDCl_3$, 100 MHz) of 3la

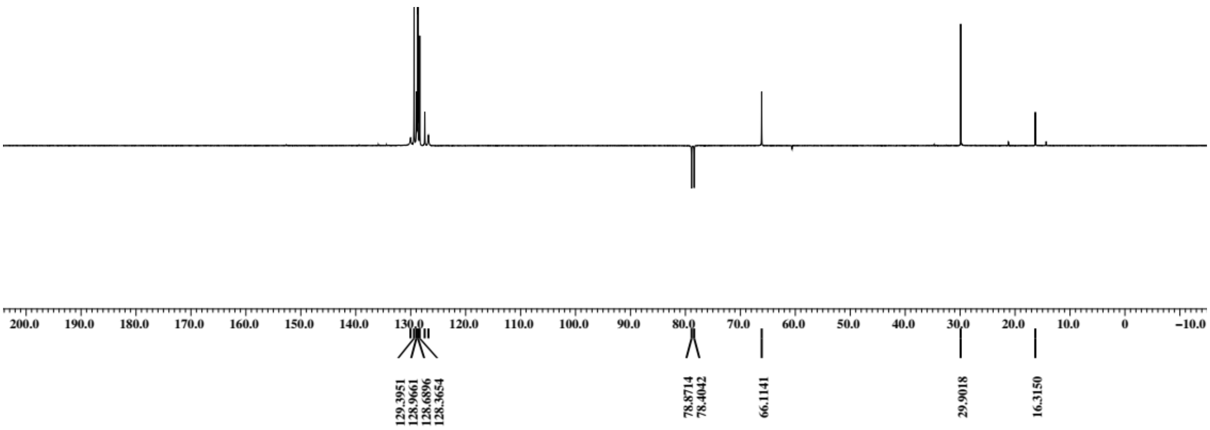

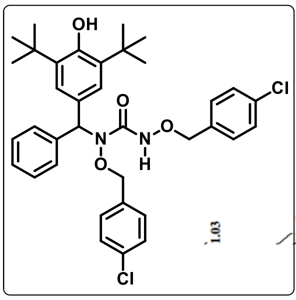

^{1}H NMR ($CDCl_3$, 400 MHz) of 3ab

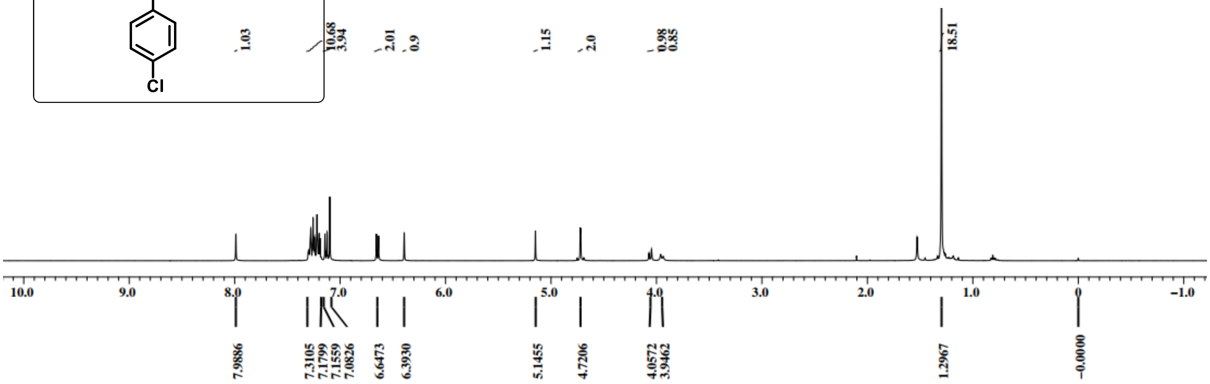

^{13}C NMR ($CDCl_3$, 100 MHz) of 3ab

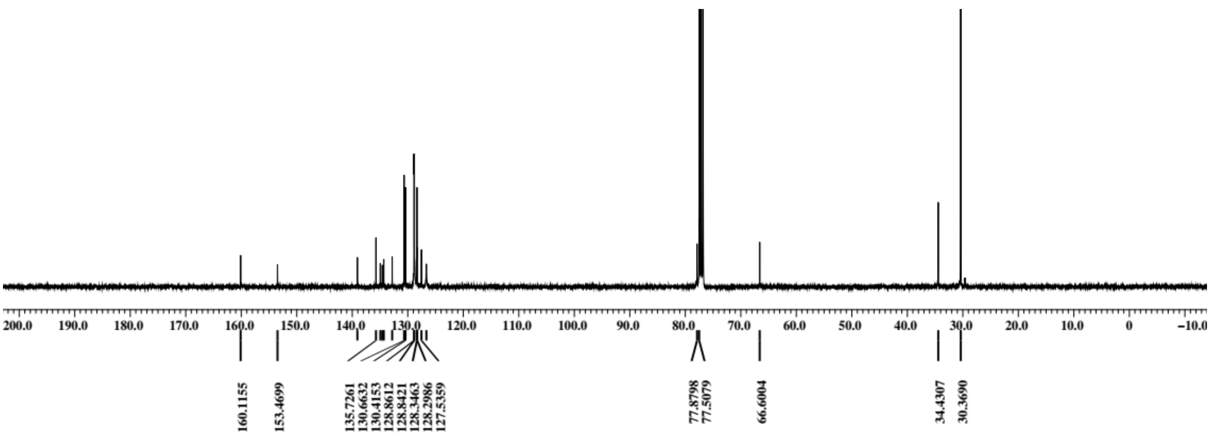

^{13}C DEPT NMR ($CDCl_3$, 100 MHz) of 3ab

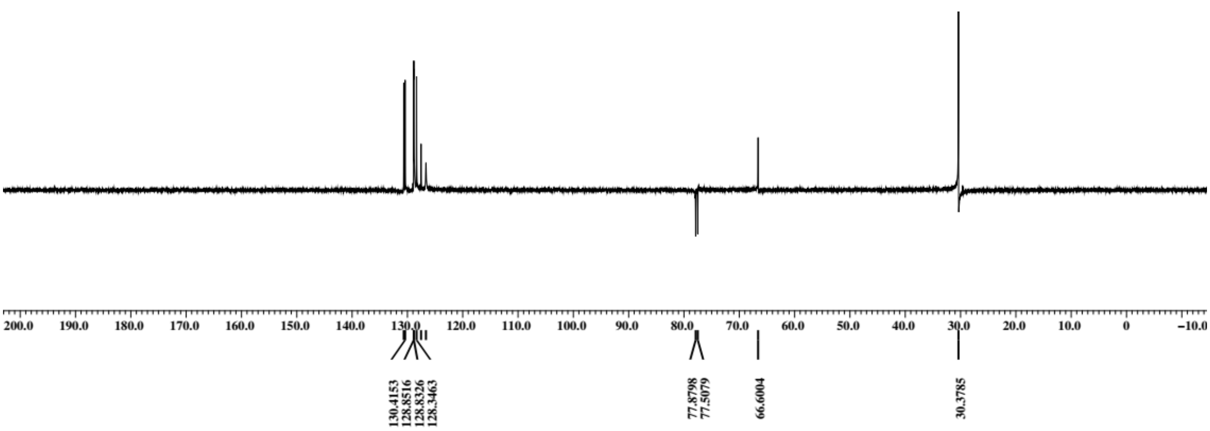

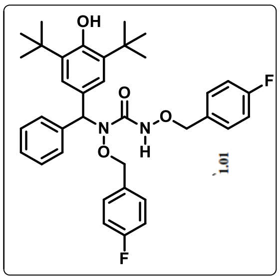

^{1}H NMR (CDCl$_3$, 400 MHz) of 3ac

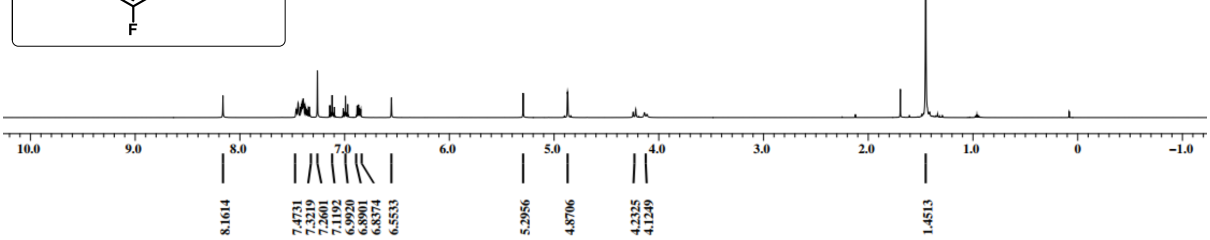

^{13}C NMR (CDCl$_3$, 100 MHz) of 3ac

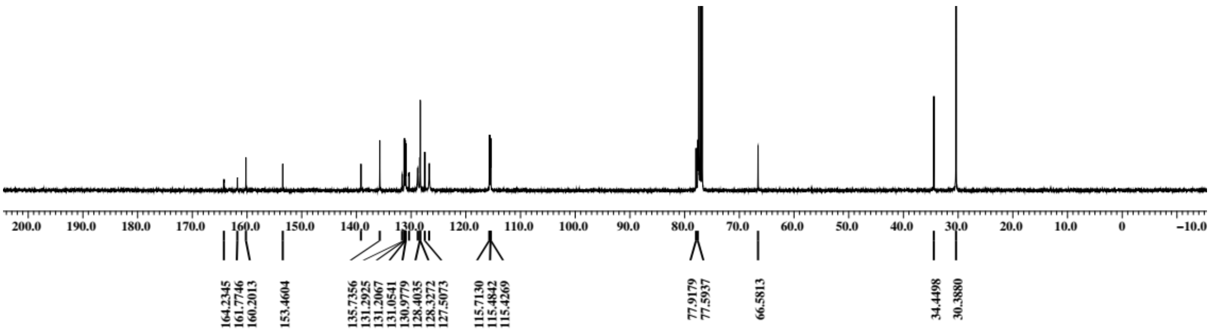

^{13}C DEPT NMR (CDCl$_3$, 100 MHz) of 3ac

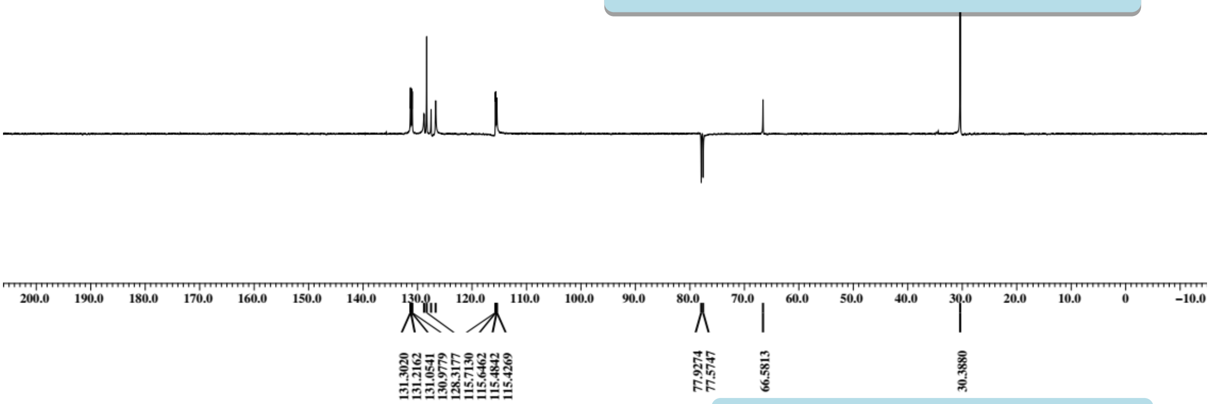

^{19}F NMR (CDCl$_3$, 376 MHz) of 3ac

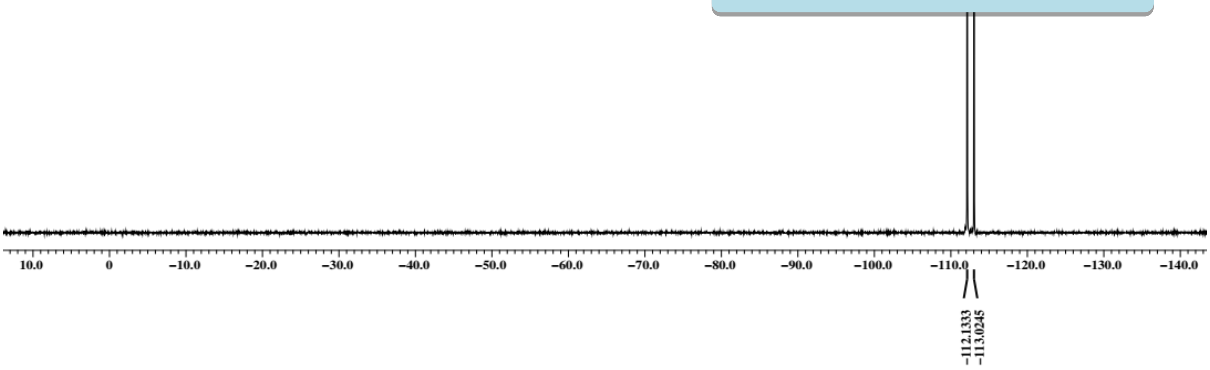

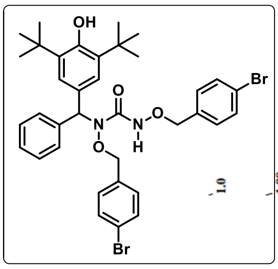

[1]H NMR ($CDCl_3$, 400 MHz) of 3ad

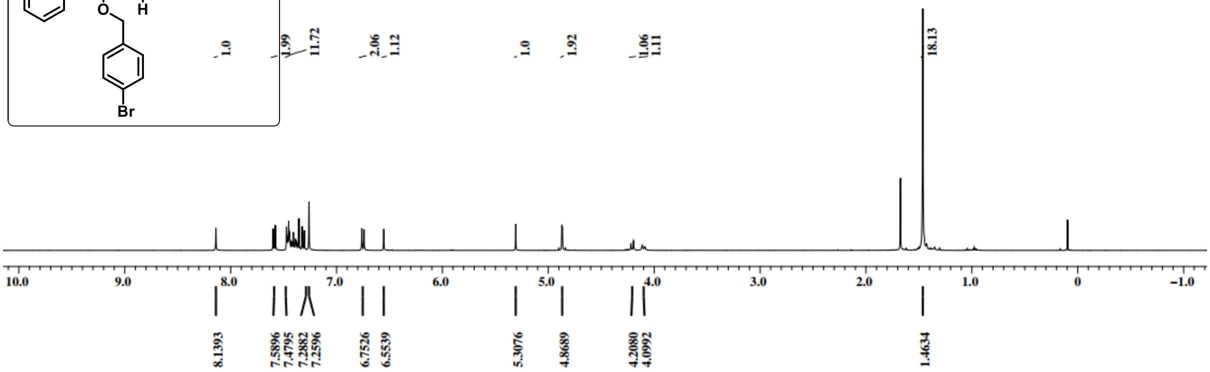

[13]C NMR ($CDCl_3$, 100 MHz) of 3ad

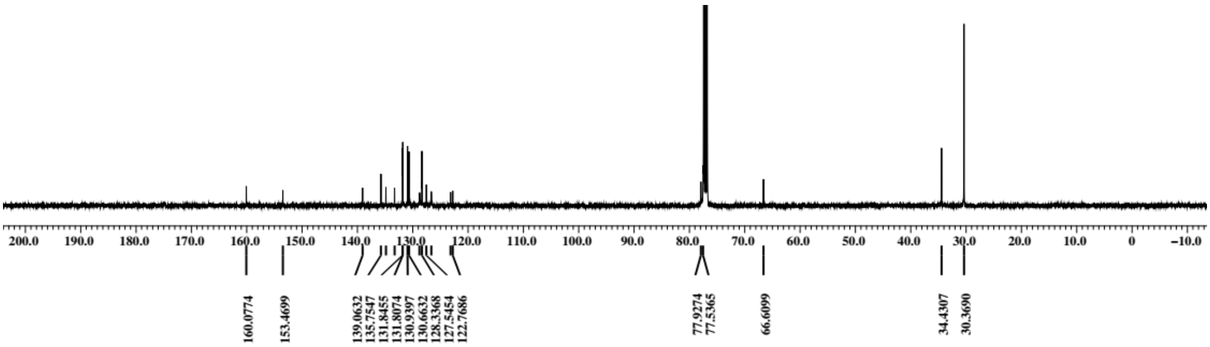

[13]C DEPT NMR ($CDCl_3$, 100 MHz) of 3ad

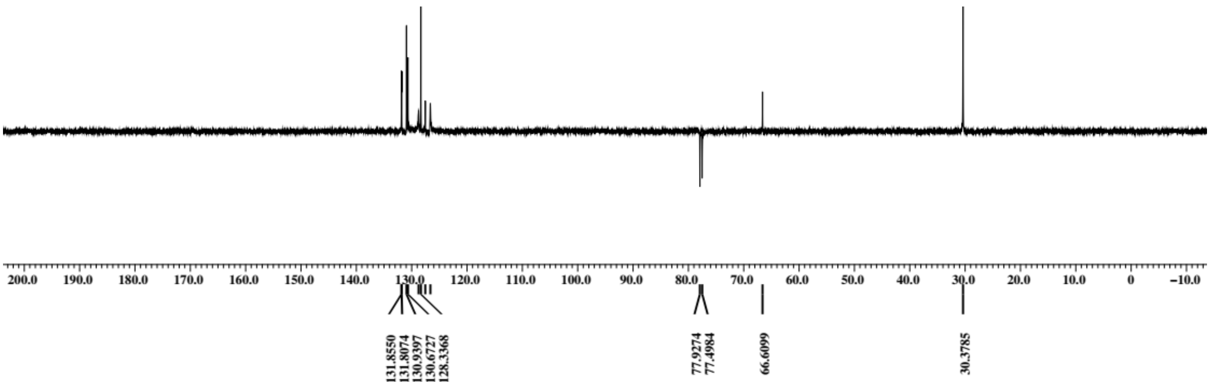

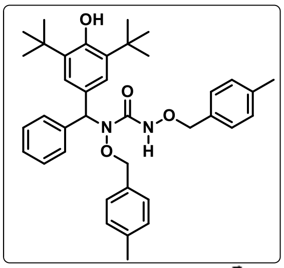

¹H NMR ($CDCl_3$, 400 MHz) of 3ae

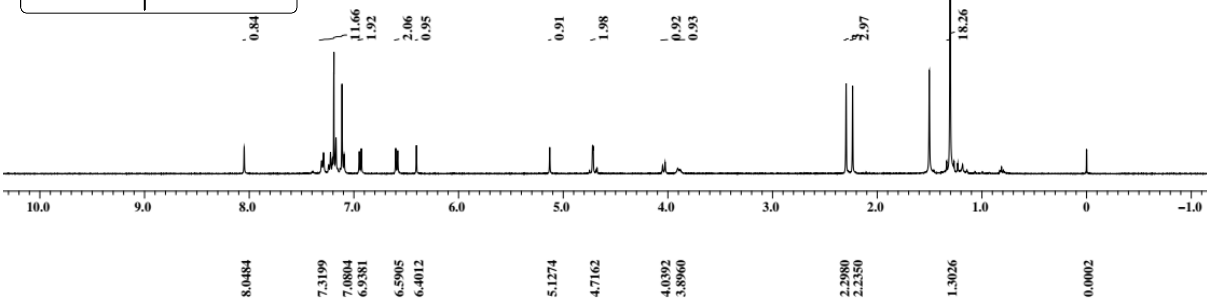

¹³C NMR ($CDCl_3$, 100 MHz) of 3ae

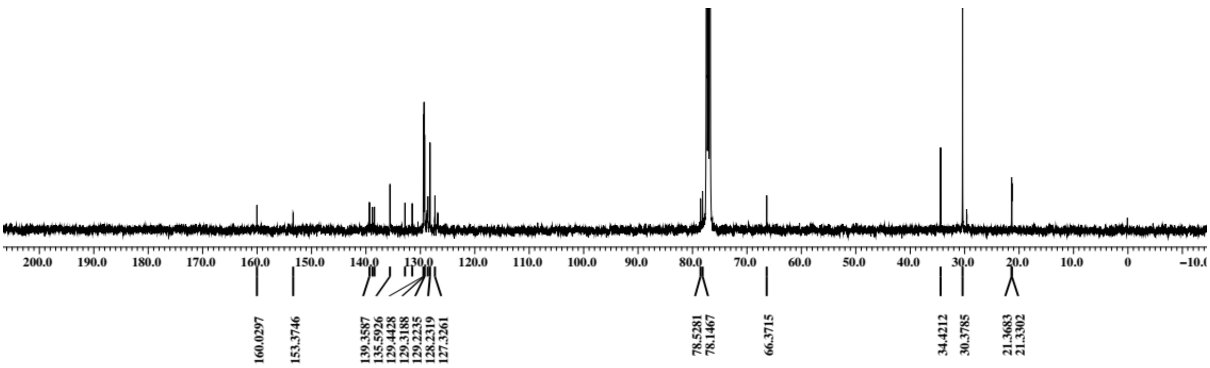

¹³C DEPT NMR ($CDCl_3$, 100 MHz) of 3ae

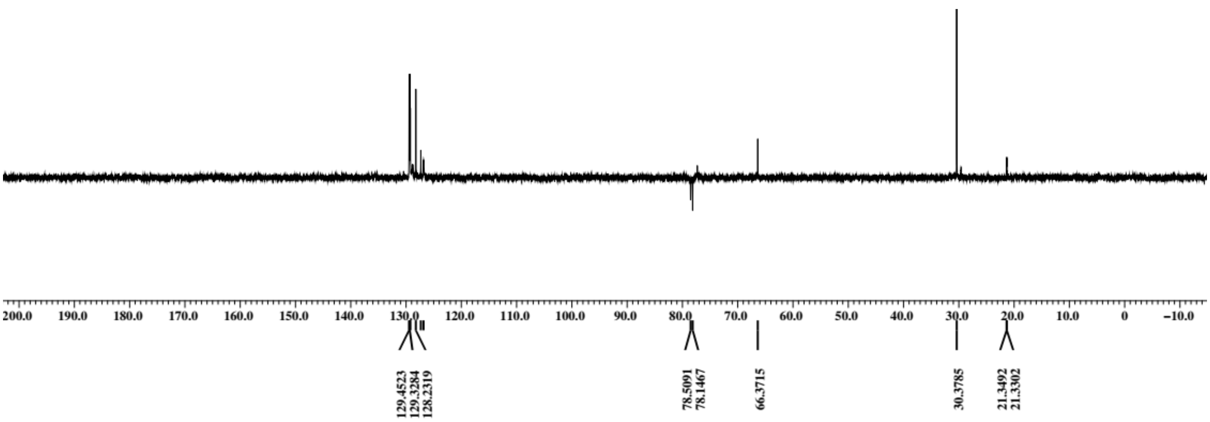

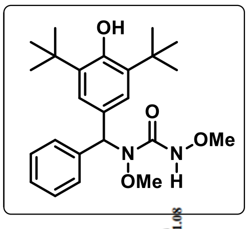

^{1}H NMR ($CDCl_3$, 400 MHz) of 3af

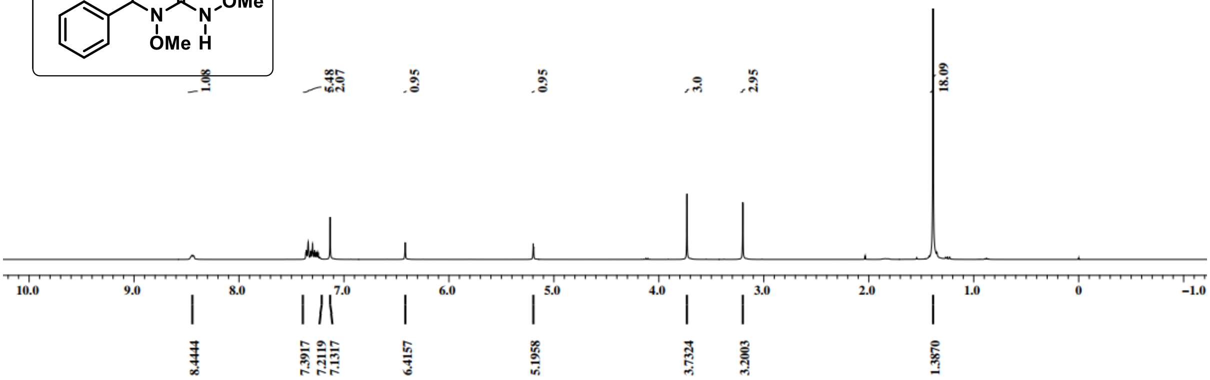

^{13}C NMR ($CDCl_3$, 100 MHz) of 3af

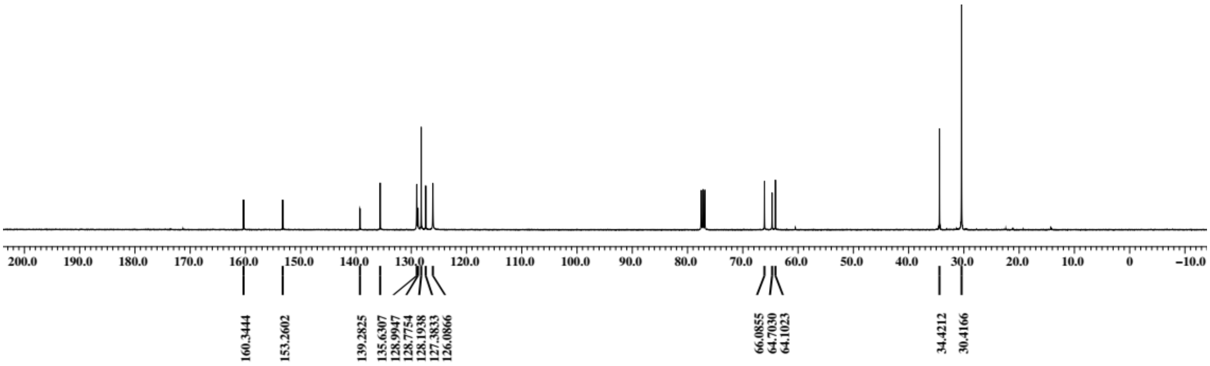

^{13}C DEPT NMR ($CDCl_3$, 100 MHz) of 3af

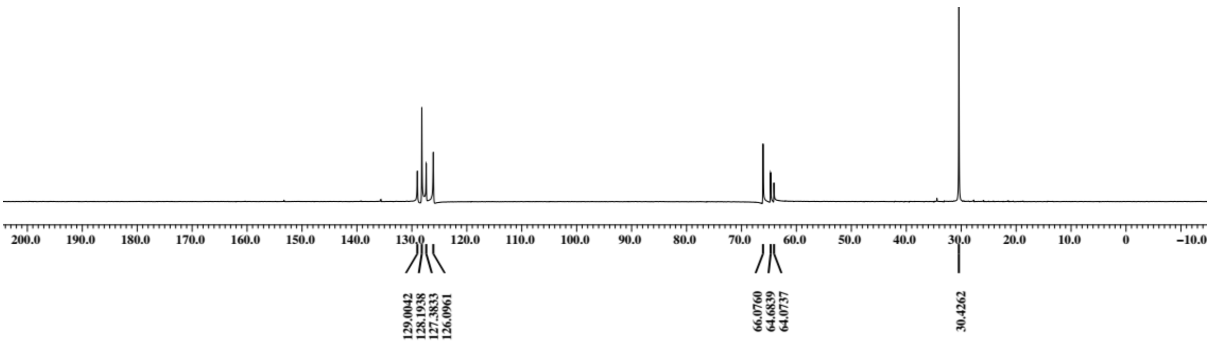

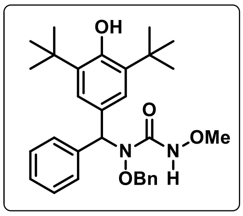

^{1}H NMR ($CDCl_3$, 400MHz) of 3ag

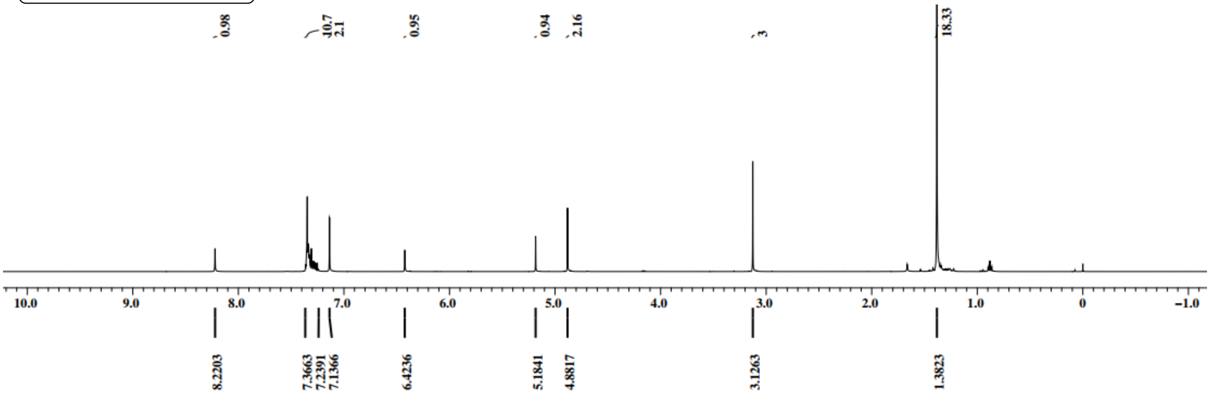

^{13}C NMR ($CDCl_3$, 100MHz) of 3ag

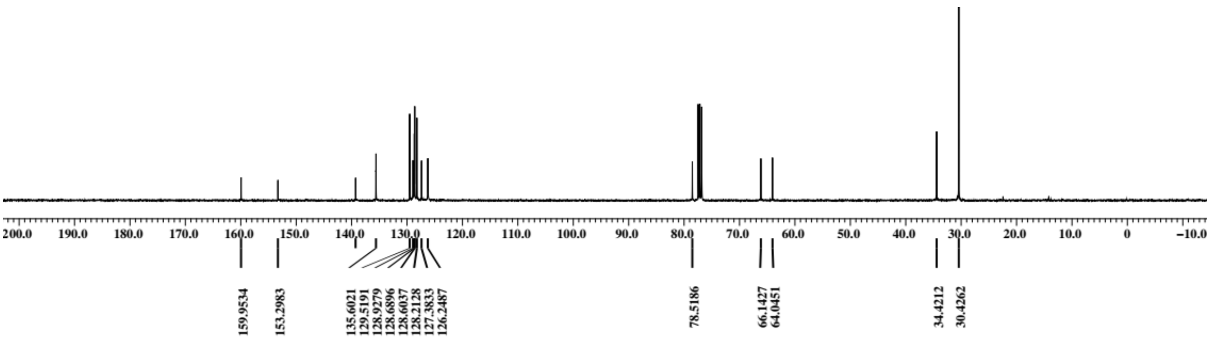

^{13}C DEPT NMR ($CDCl_3$, 100 MHz) of 3ag

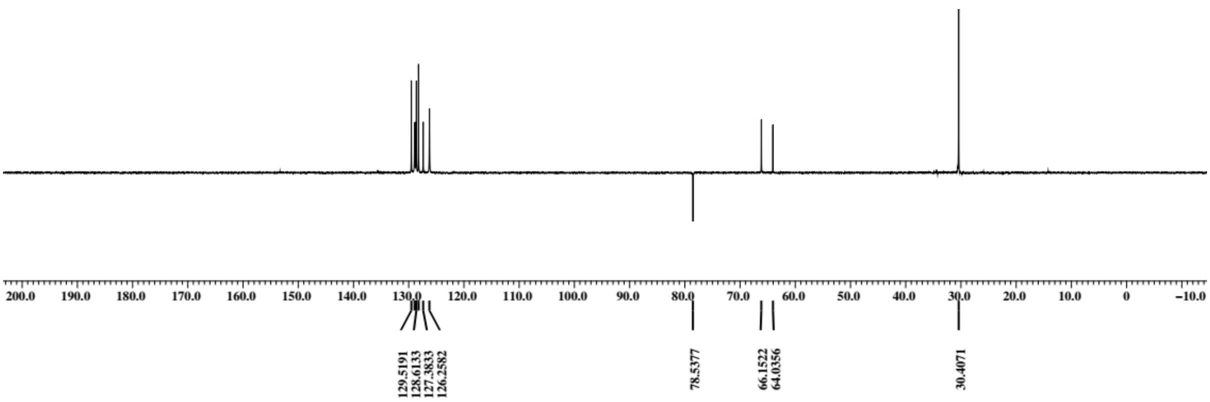

^{1}H NOE-NMR ($CDCl_3$, 400MHz) of 3ag

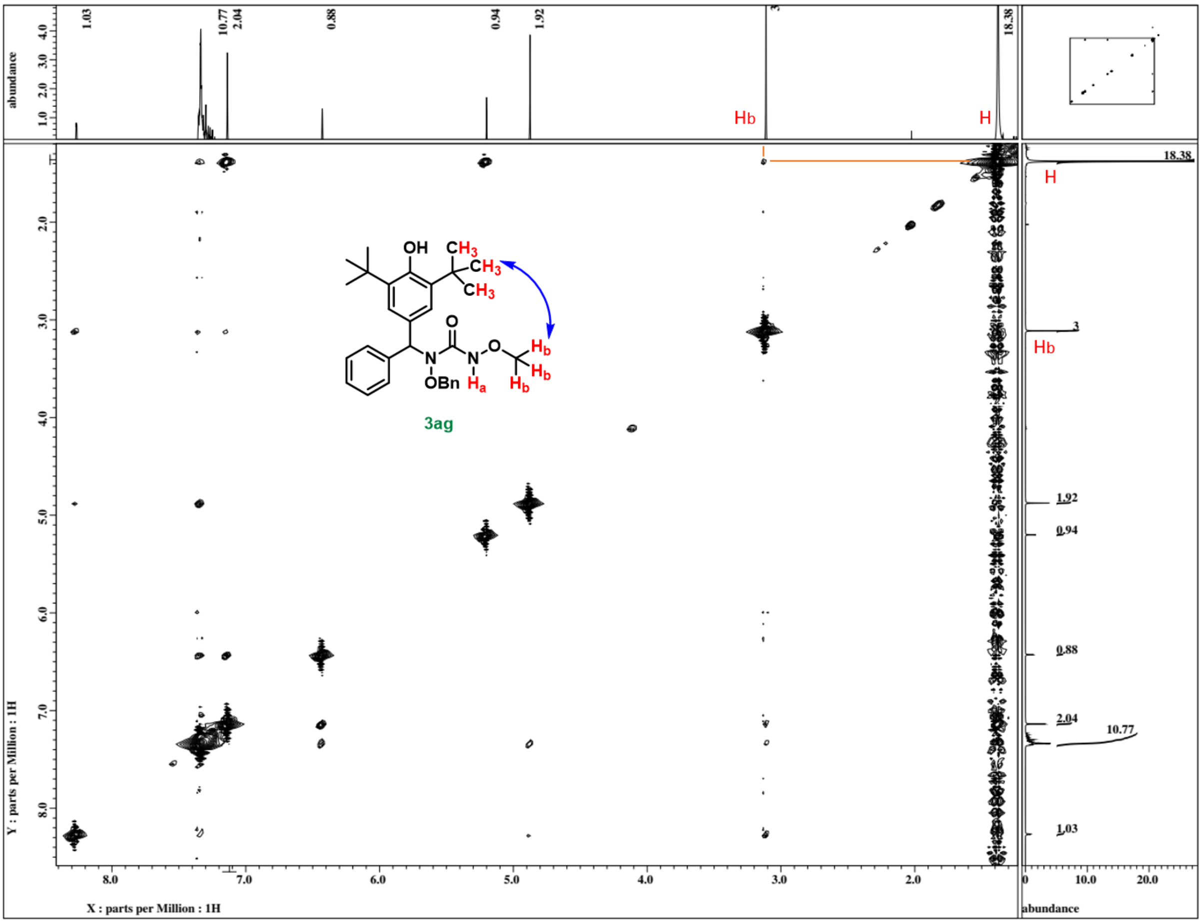

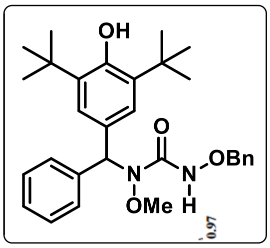

[1]H NMR ($CDCl_3$, 400 MHz) of 3ag'

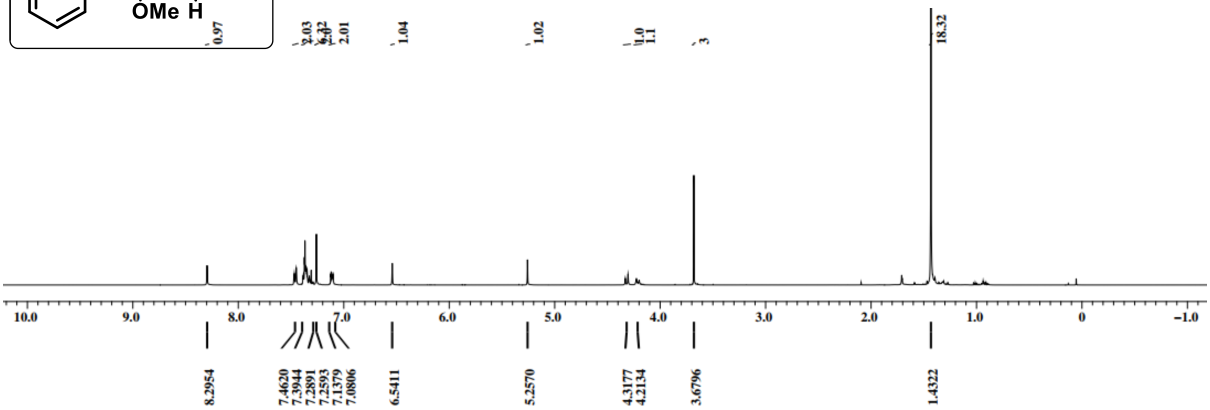

[13]C NMR ($CDCl_3$, 100 MHz) of 3ag'

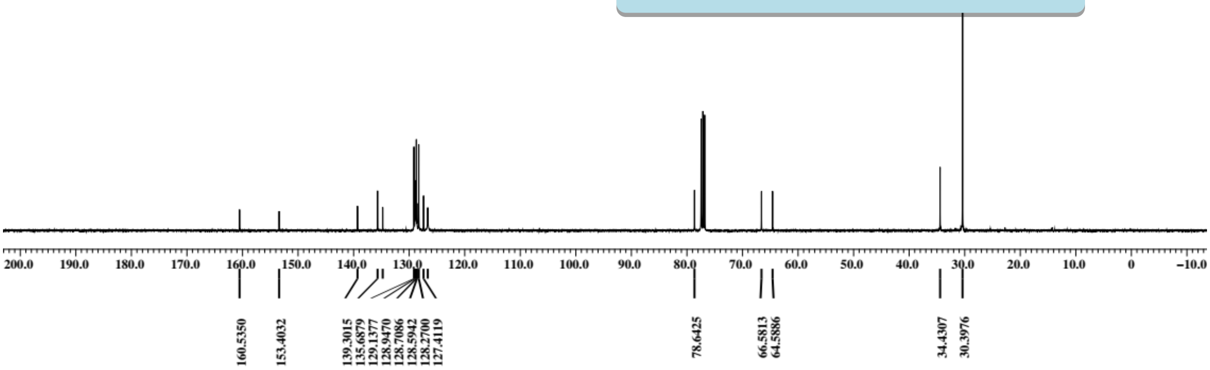

[13]C DEPT NMR ($CDCl_3$, 100 MHz) of 3ag'

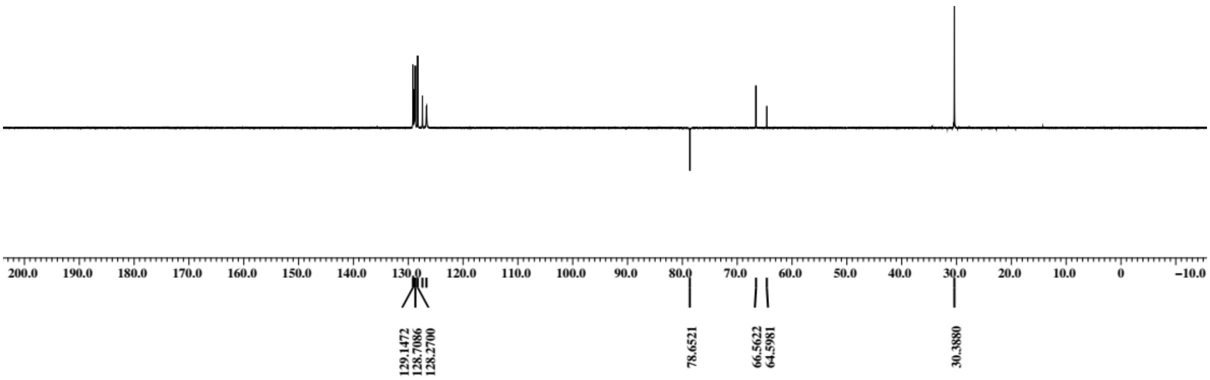

[1]H NOE-NMR ($CDCl_3$, 400 MHz) of 3ag'

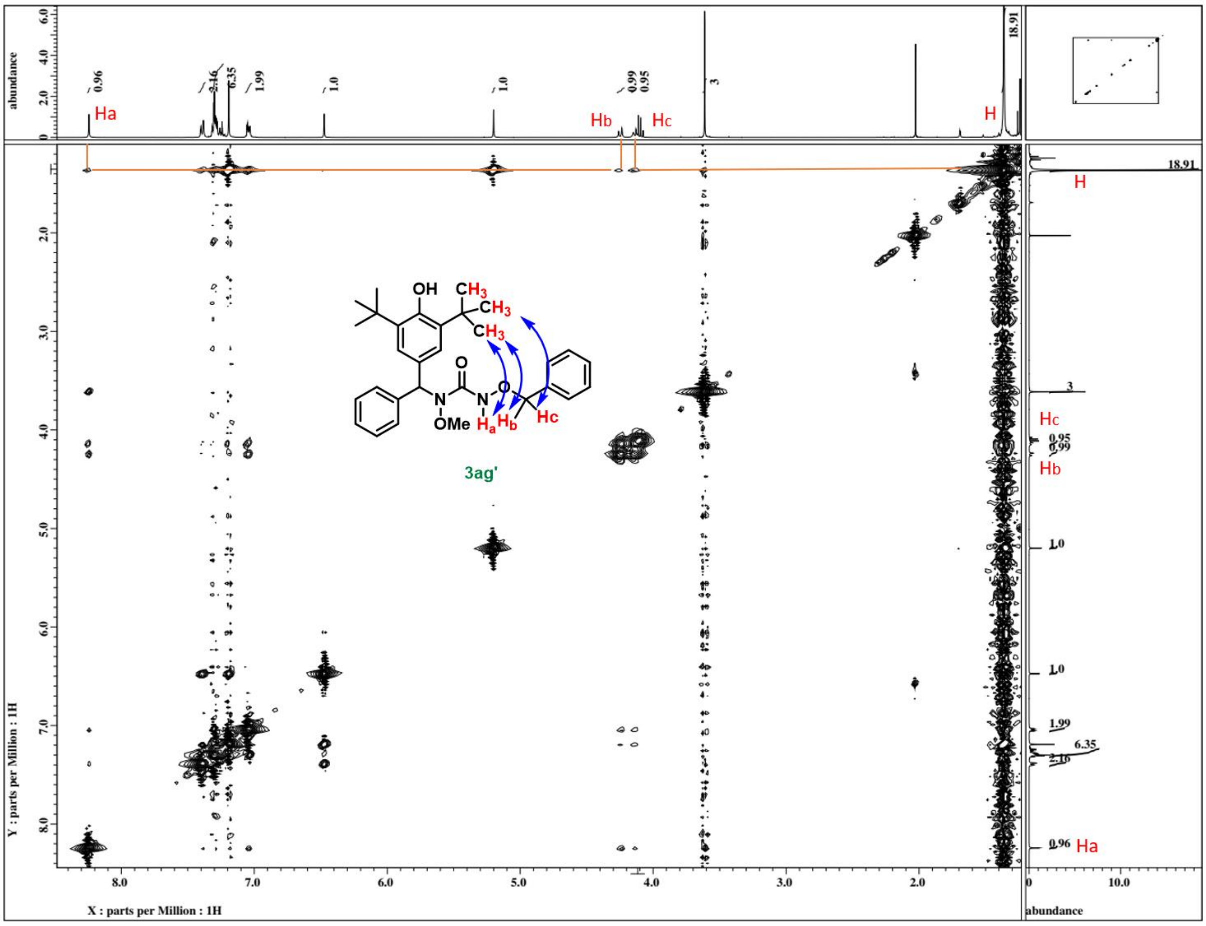

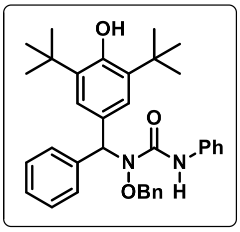

[1]H NMR ($CDCl_3$, 400MHz) of 3ah

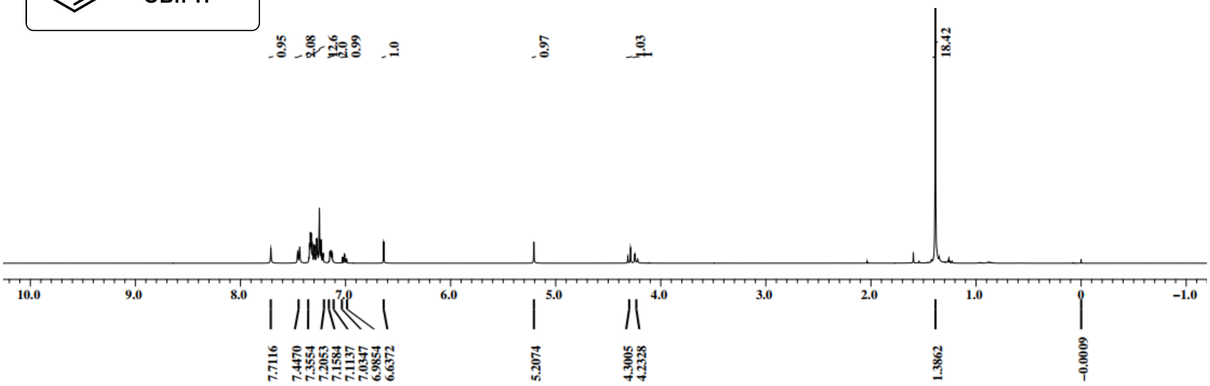

[13]C NMR ($CDCl_3$, 100MHz) of 3ah

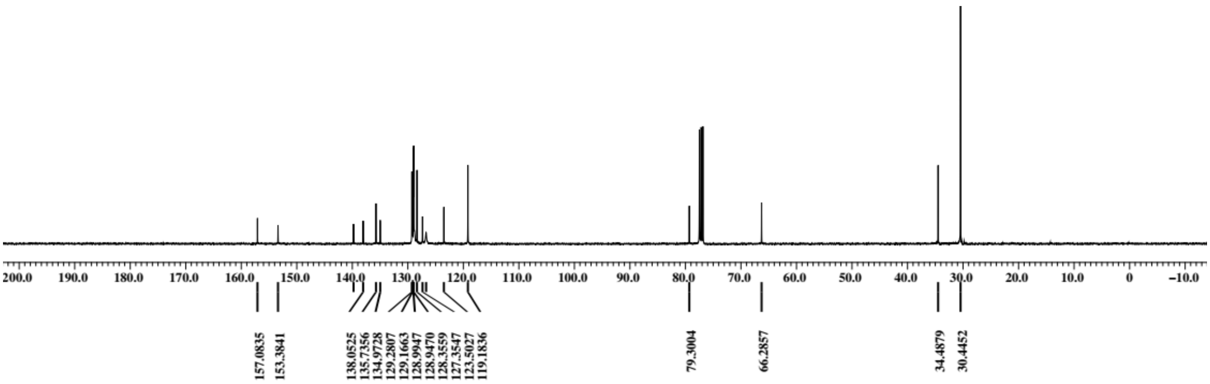

[13]C DEPT NMR ($CDCl_3$, 100 MHz) of 3ah

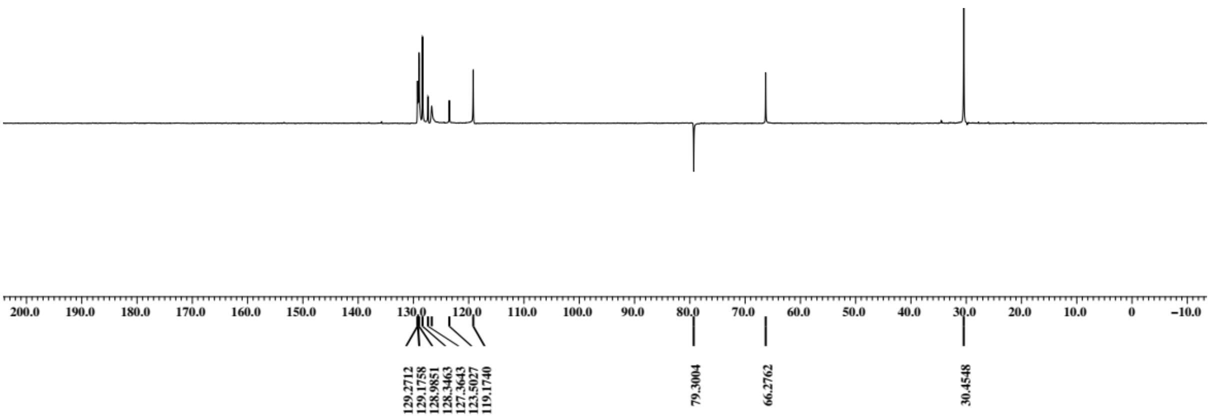

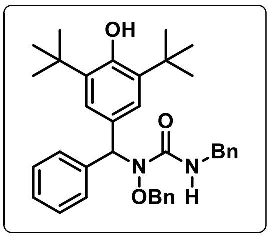

^{1}H NMR ($CDCl_3$, 400 MHz) of 3ai

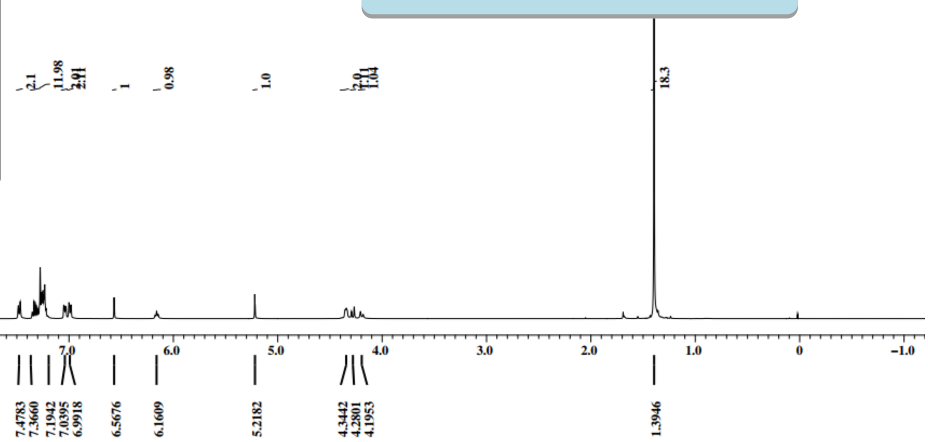

^{13}C NMR ($CDCl_3$, 100 MHz) of 3ai

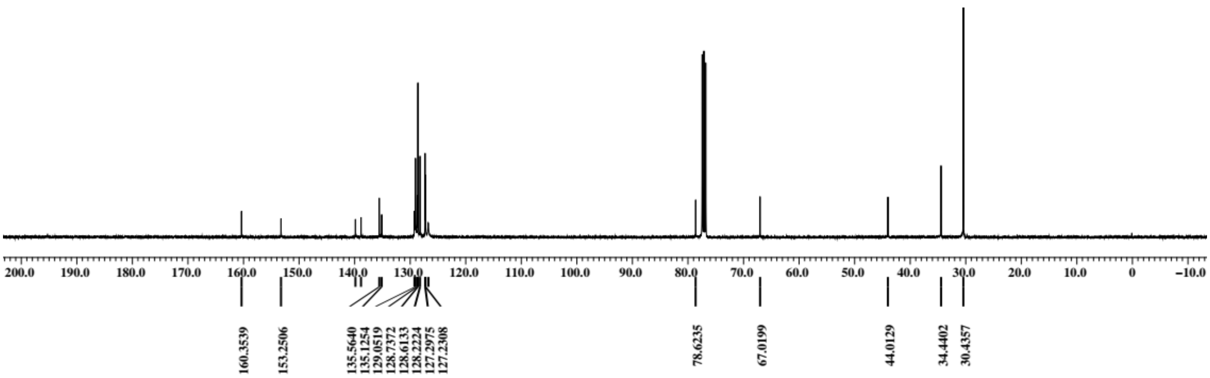

^{13}C DEPT NMR ($CDCl_3$, 100 MHz) of 3ai

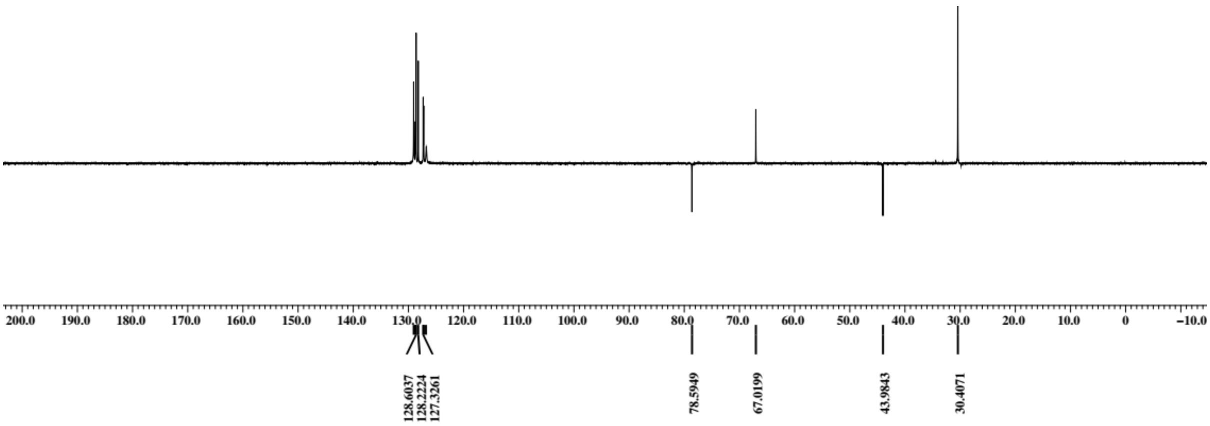

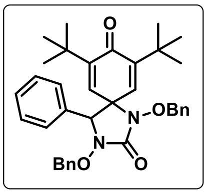

^{1}H NMR ($CDCl_3$, 400 MHz) of 4aa

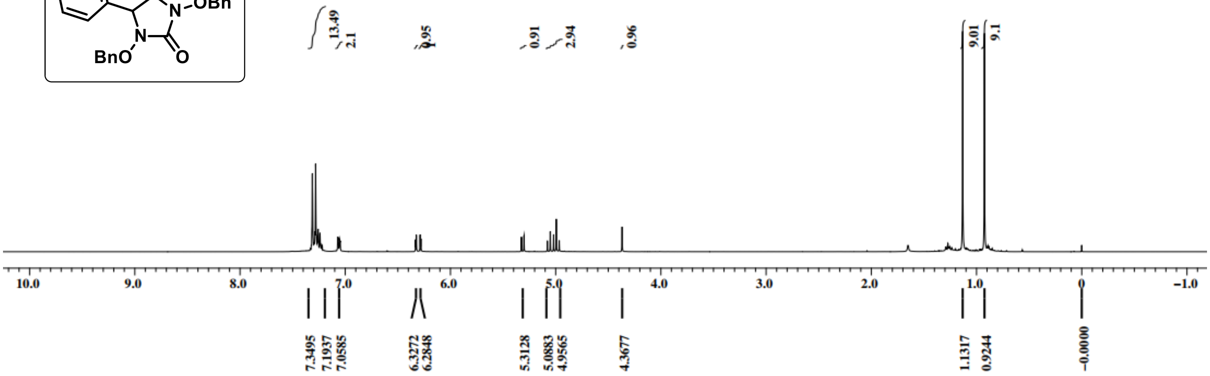

^{13}C NMR ($CDCl_3$, 100 MHz) of 4aa

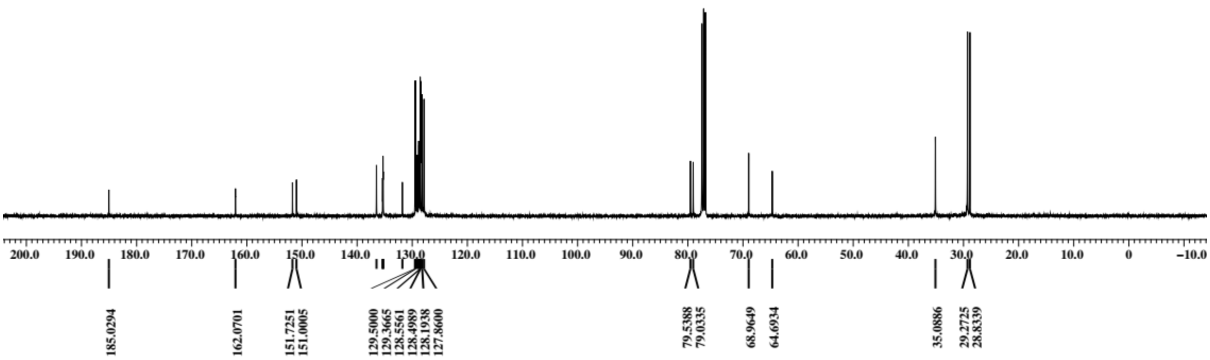

^{13}C DEPT NMR ($CDCl_3$, 100 MHz) of 4aa

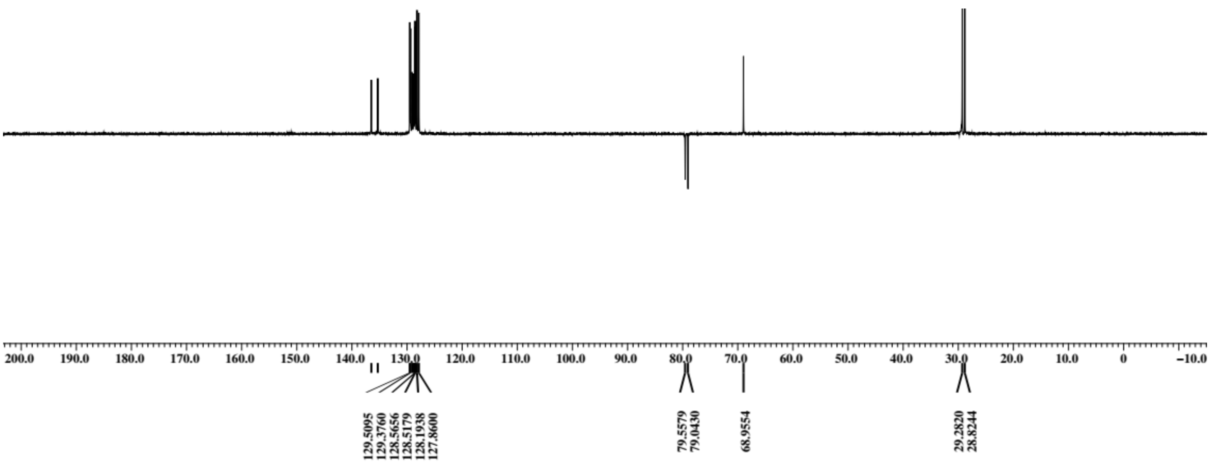

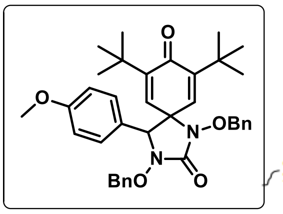

^{1}H NMR ($CDCl_3$, 400 MHz) of 4ba

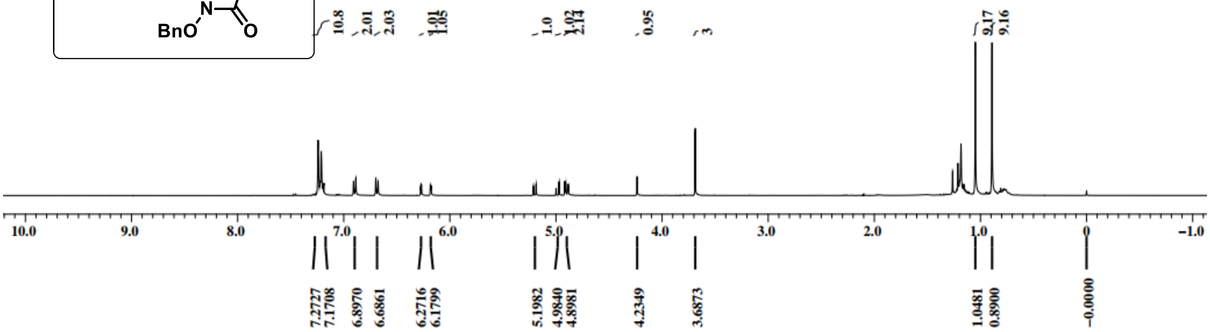

^{13}C NMR ($CDCl_3$, 100 MHz) of 4ba

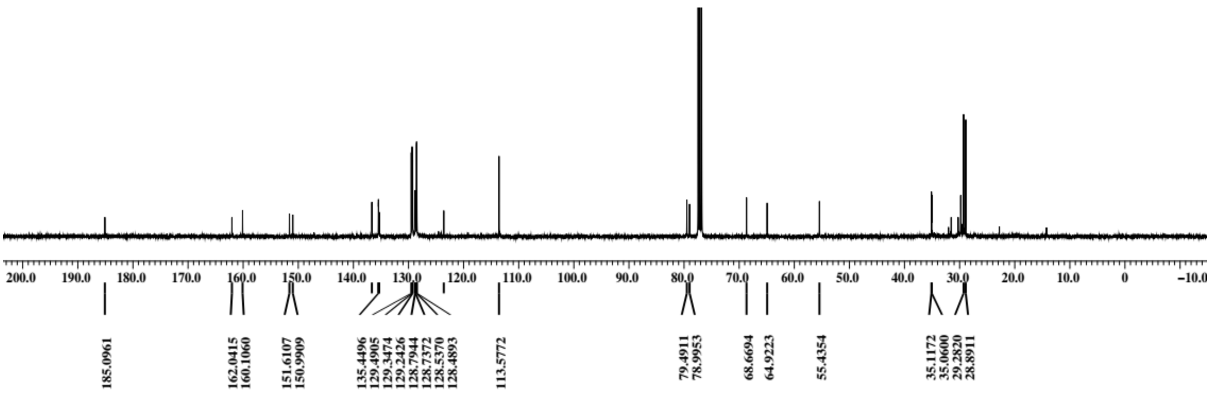

^{13}C DEPT NMR ($CDCl_3$, 100 MHz) of 4ba

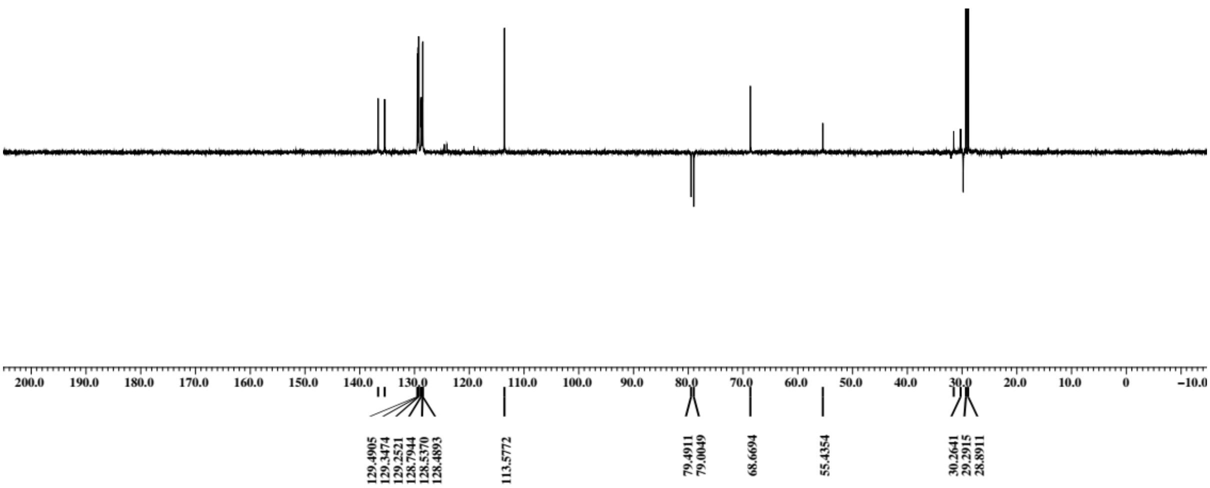

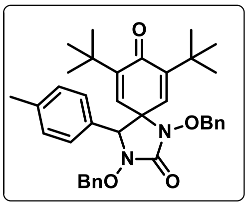

^{1}H NMR ($CDCl_3$, 400 MHz) of 4ca

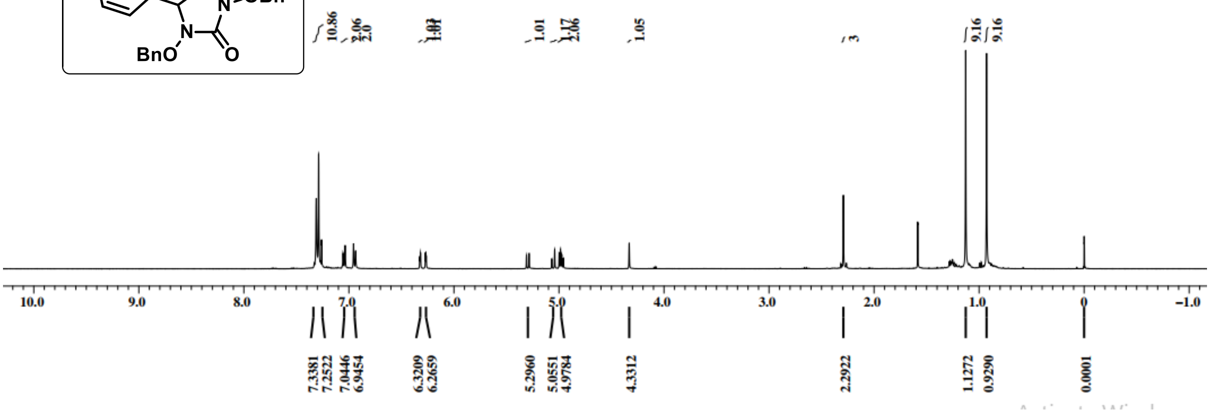

^{13}C NMR ($CDCl_3$, 100 MHz) of 4ca

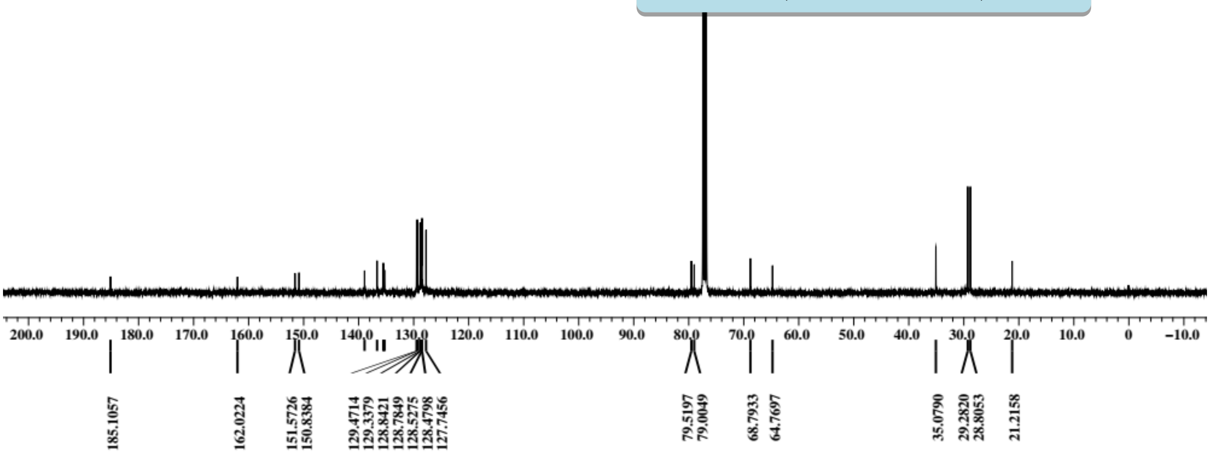

^{13}C DEPT NMR ($CDCl_3$, 100 MHz) of 4ca

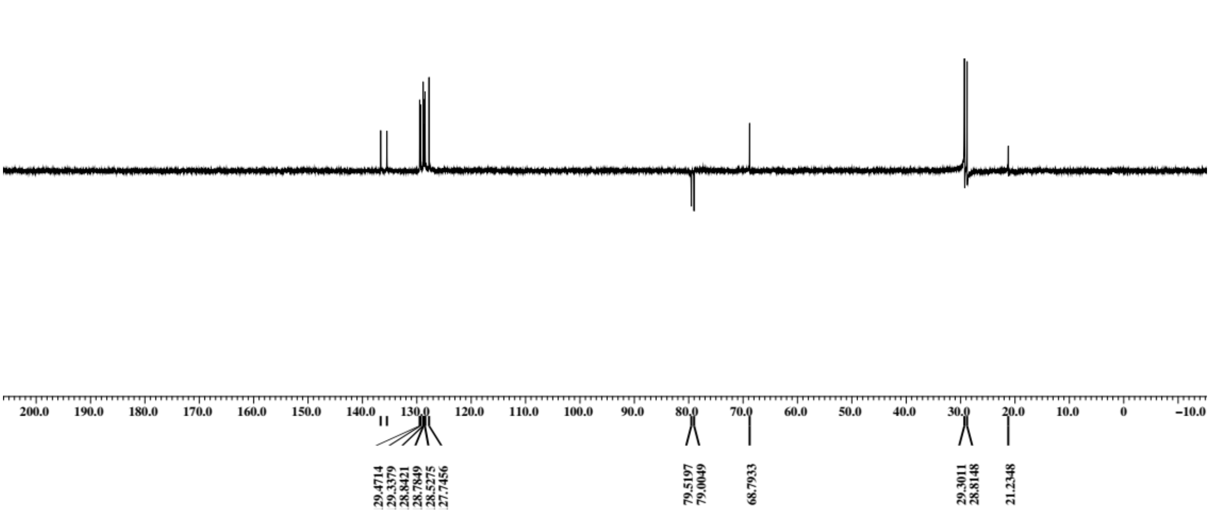

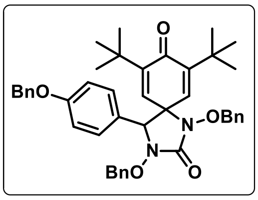

^{1}H NMR ($CDCl_3$, 400 MHz) of 4da

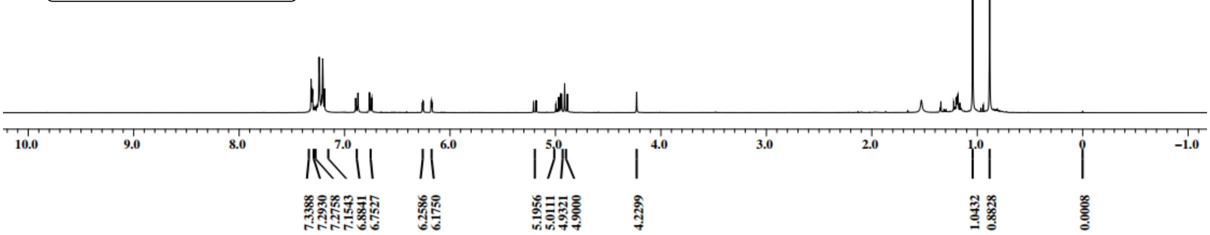

^{13}C NMR ($CDCl_3$, 100 MHz) of 4da

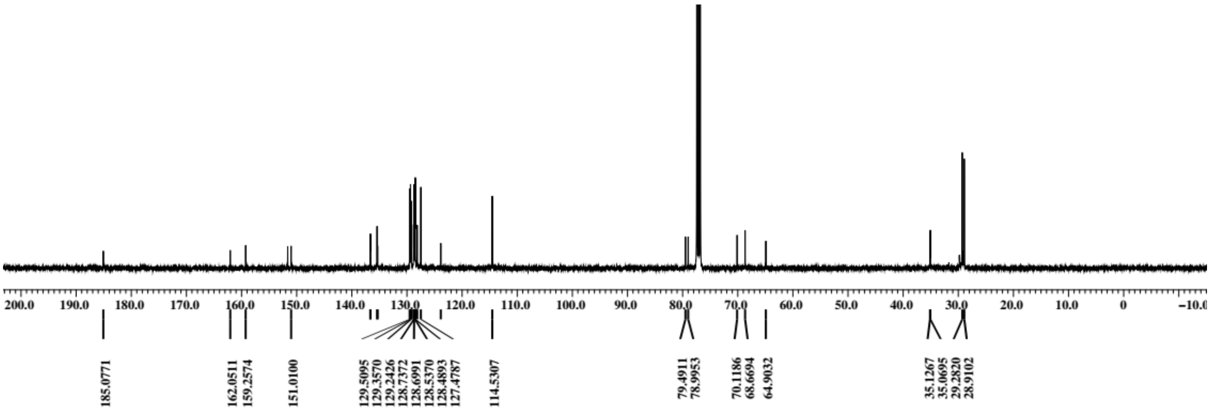

^{13}C DEPT NMR ($CDCl_3$, 100 MHz) of 4da

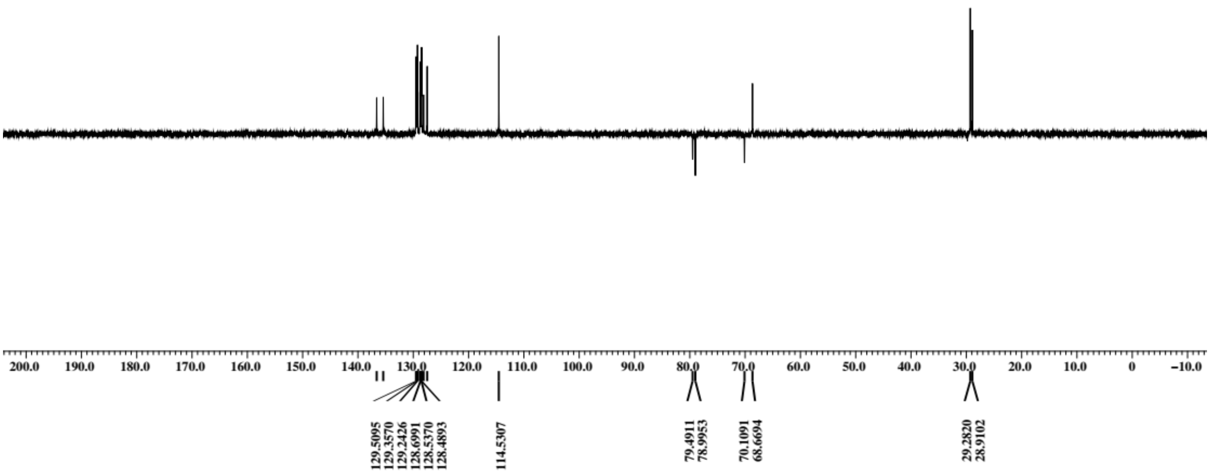

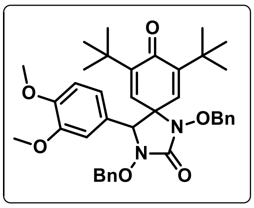

[1]H NMR (CDCl₃, 400 MHz) of 4ea

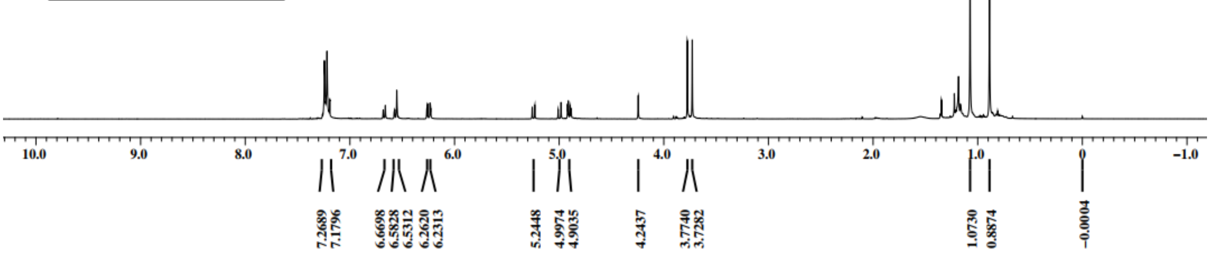

[13]C NMR (CDCl₃, 100 MHz) of 4ea

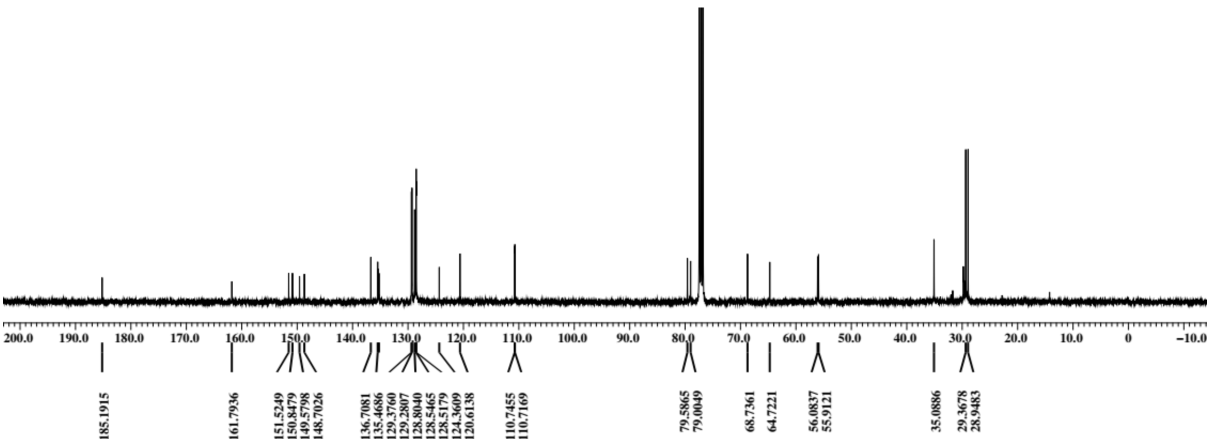

[13]C DEPT NMR (CDCl₃, 100 MHz) of 4ea

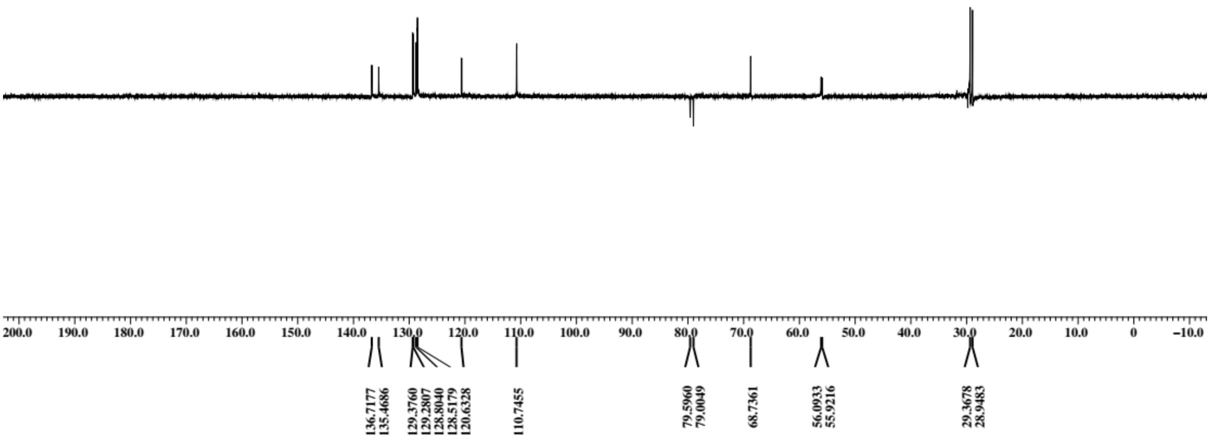

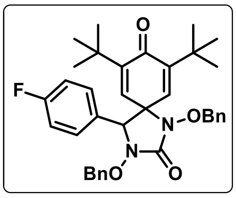

^{1}H NMR ($CDCl_3$, 400 MHz) of 4fa

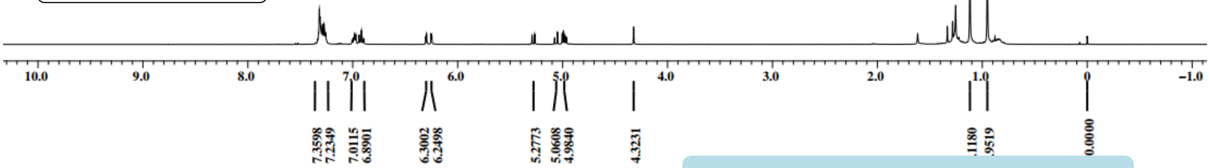

^{13}C NMR ($CDCl_3$, 100 MHz) of 4fa

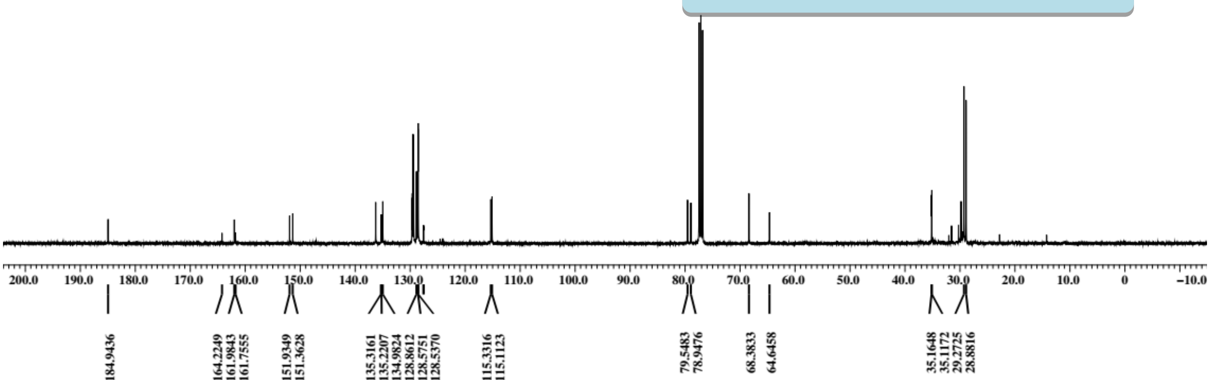

^{13}C DEPT NMR ($CDCl_3$, 100 MHz) of 4fa

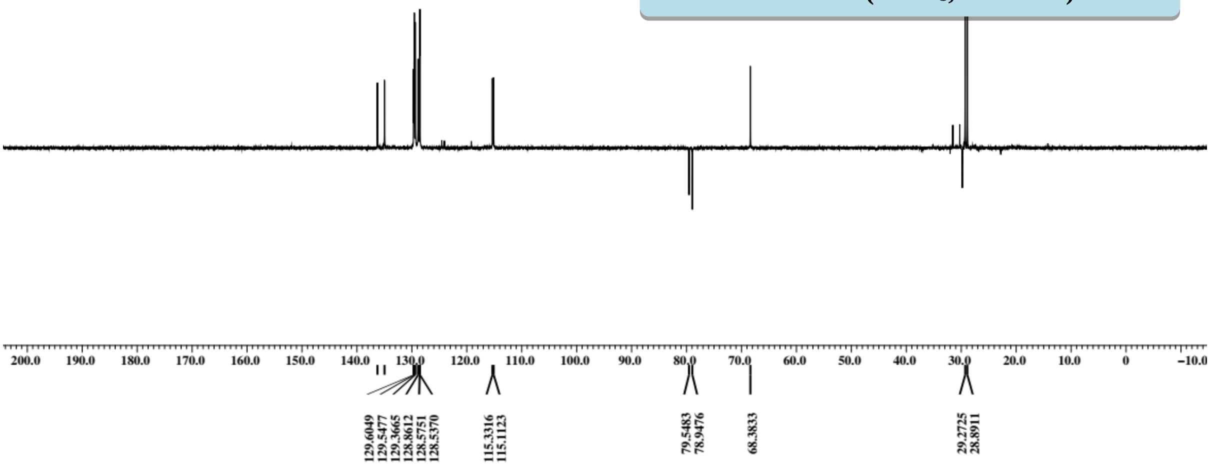

^{19}F NMR ($CDCl_3$, 376 MHz) of 4fa

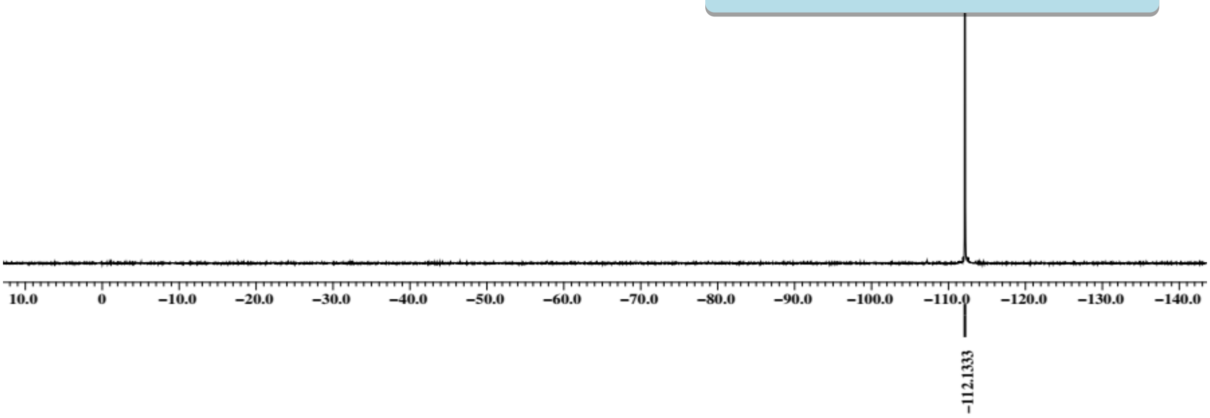

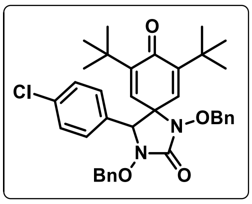

^{1}H NMR ($CDCl_3$, 400 MHz) of 4ga

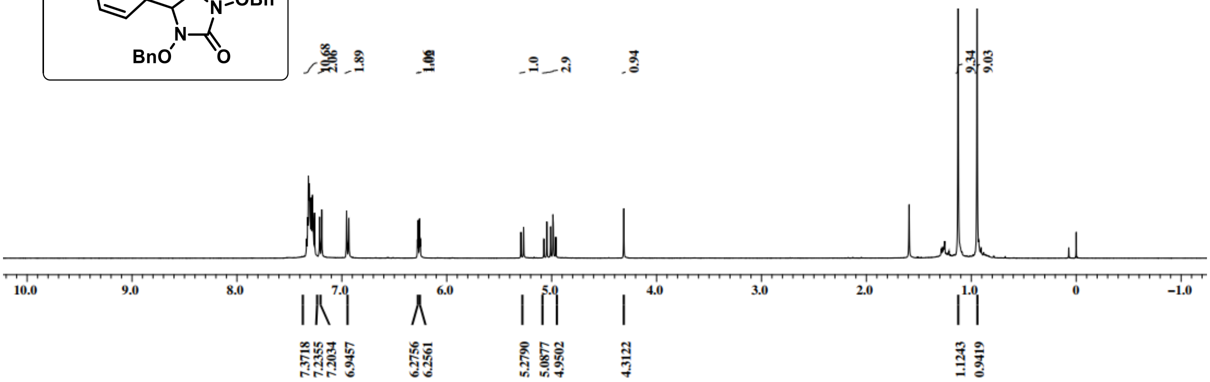

^{13}C NMR ($CDCl_3$, 100 MHz) of 4ga

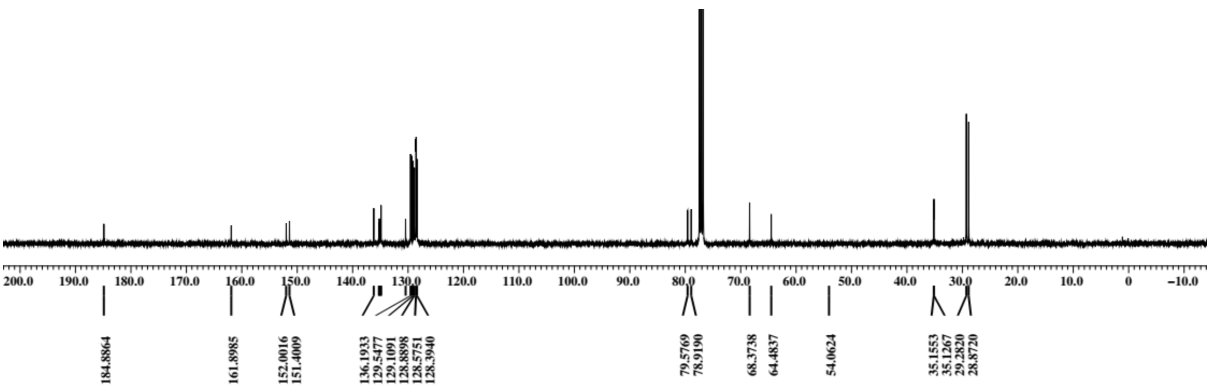

^{13}C DEPT NMR ($CDCl_3$, 100 MHz) of 4ga

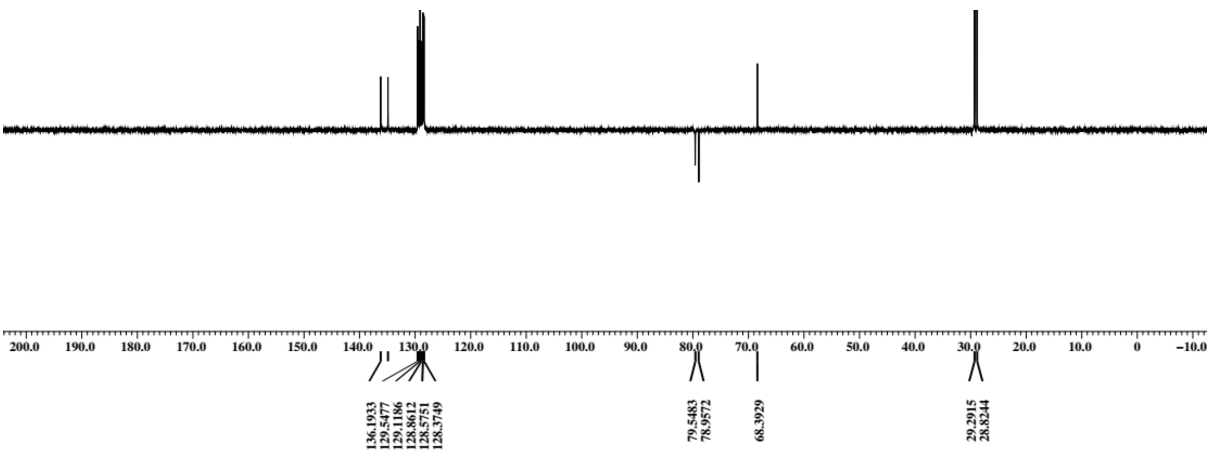

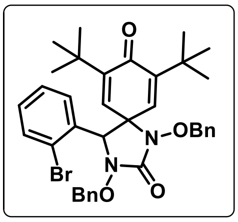

^{1}H NMR ($CDCl_3$, 400 MHz) of 4ha

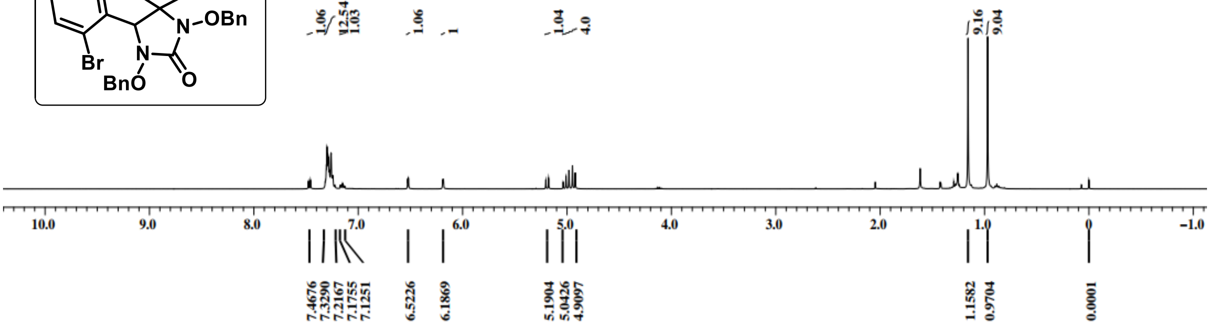

^{13}C NMR ($CDCl_3$, 100 MHz) of 4ha

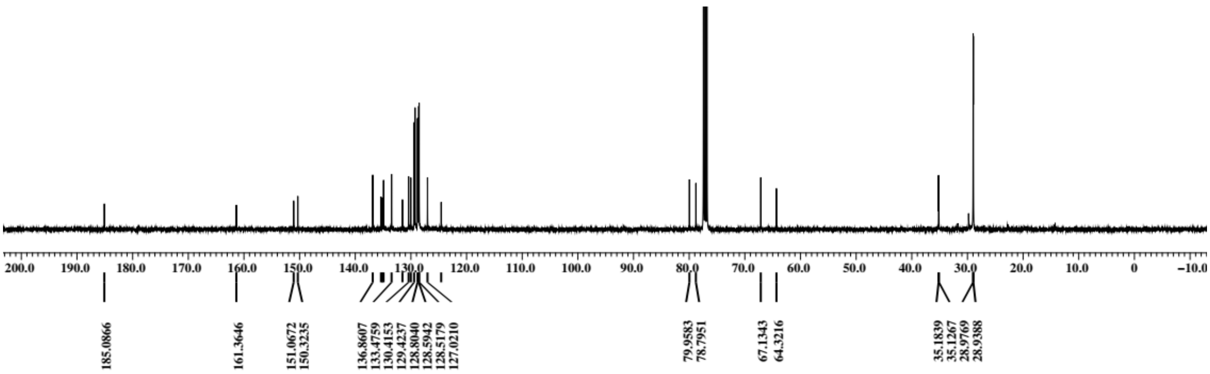

^{13}C DEPT NMR ($CDCl_3$, 100 MHz) of 4ha

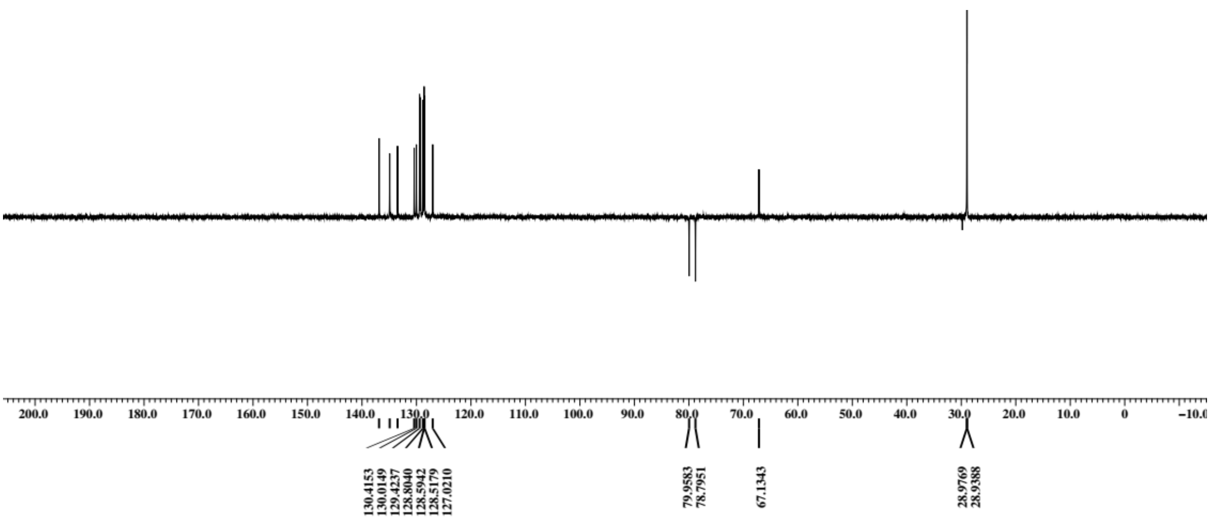

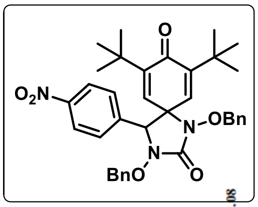

^{1}H NMR ($CDCl_3$, 400 MHz) of 4ia

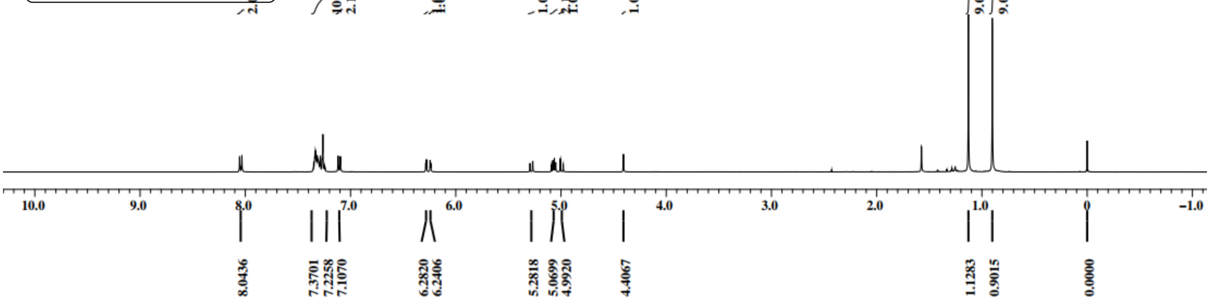

^{13}C NMR ($CDCl_3$, 100 MHz) of 4ia

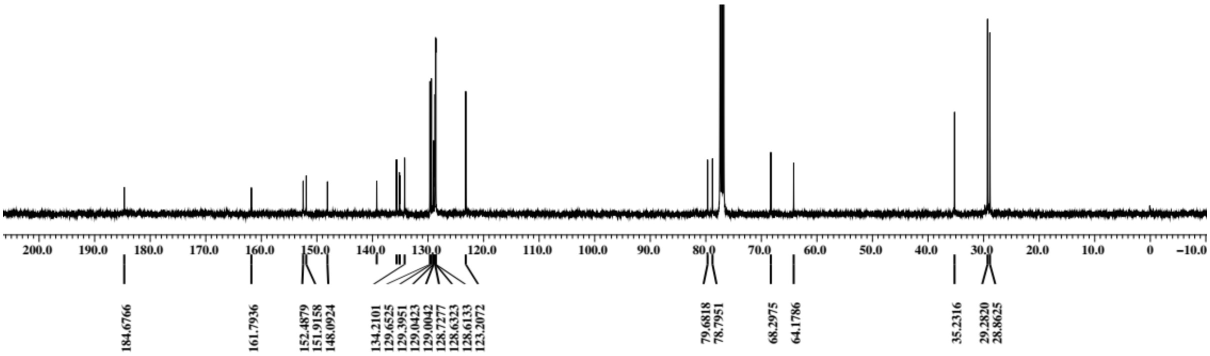

^{13}C DEPT NMR ($CDCl_3$, 100 MHz) of 4ia

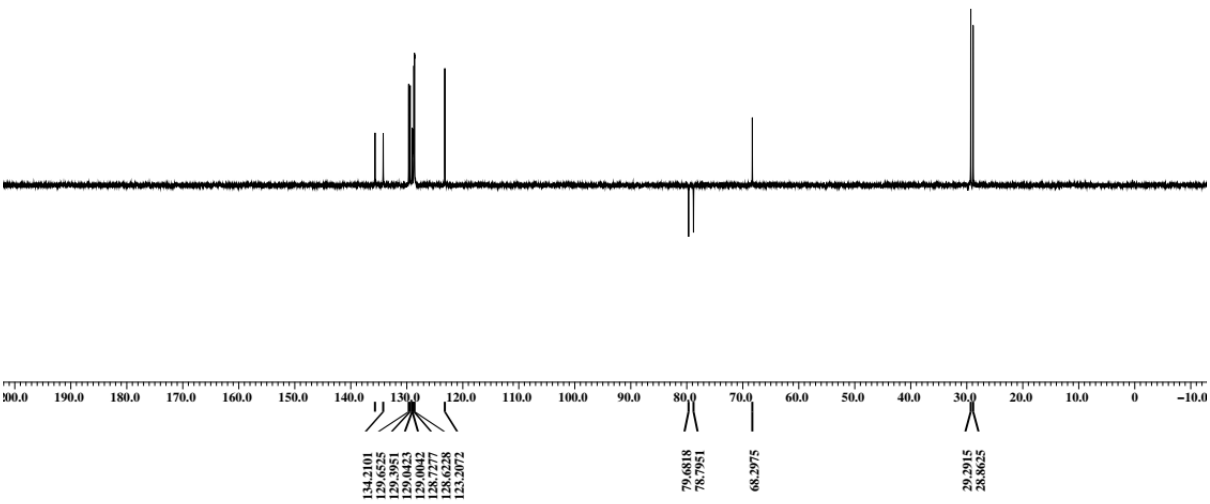

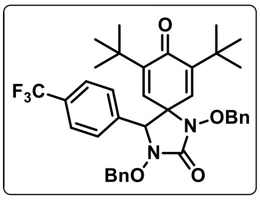

^{1}H NMR ($CDCl_3$, 400 MHz) of 4ja

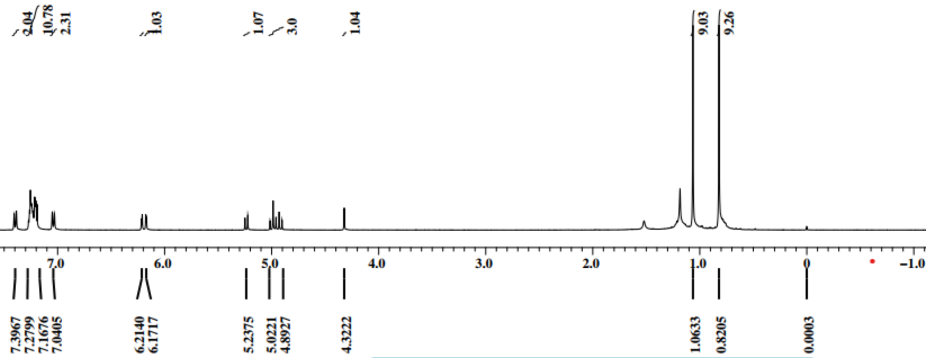

^{13}C NMR ($CDCl_3$, 100 MHz) of 4ja

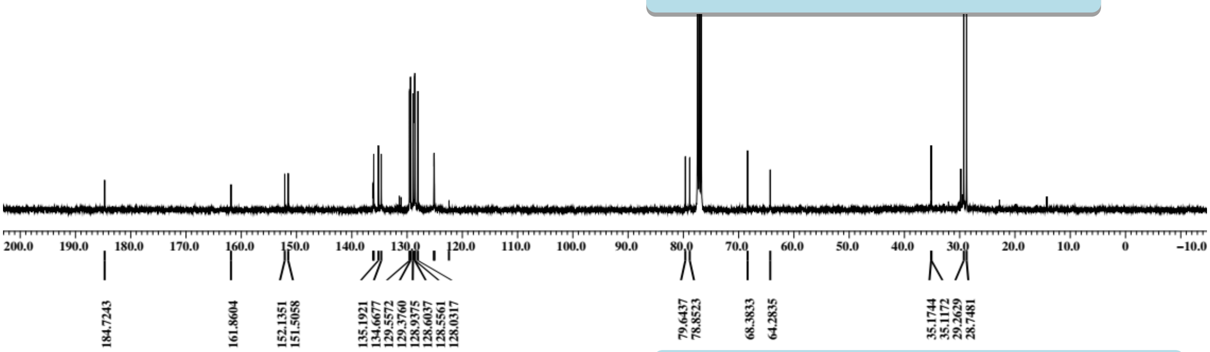

^{13}C DEPT NMR ($CDCl_3$, 100 MHz) of 4ja

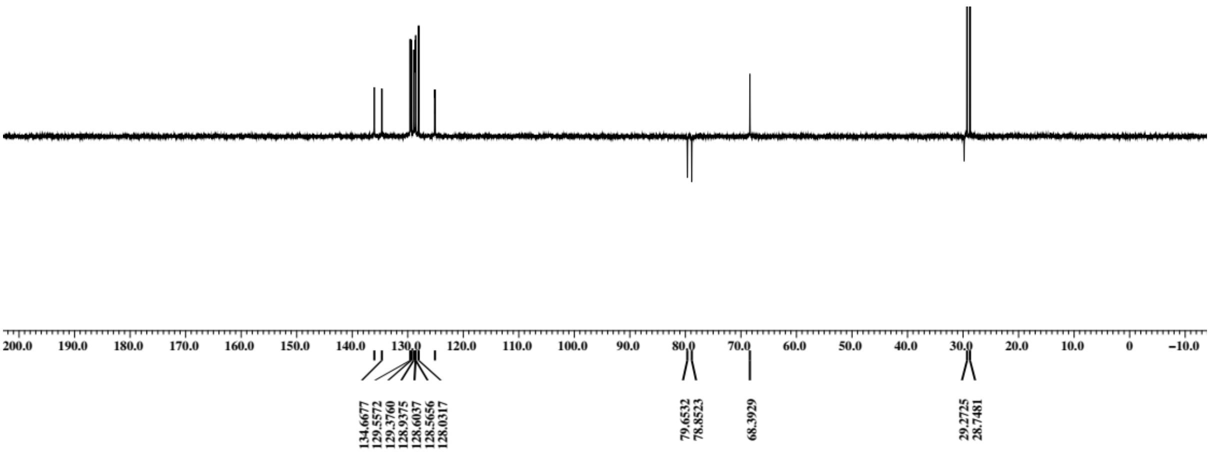

^{19}F NMR ($CDCl_3$, 376 MHz) of 4ja

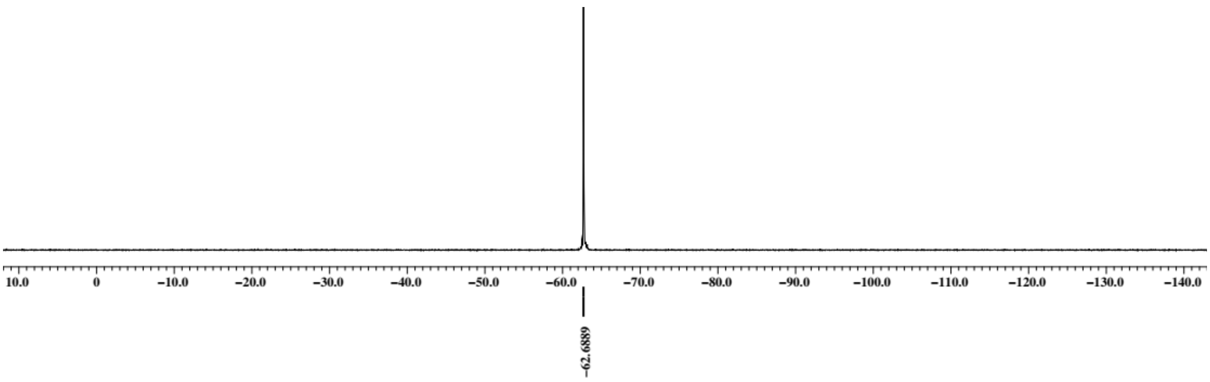

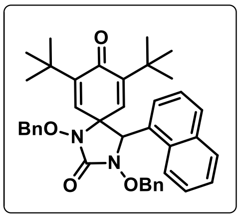

[1]H NMR ($CDCl_3$, 400 MHz) of 4ka

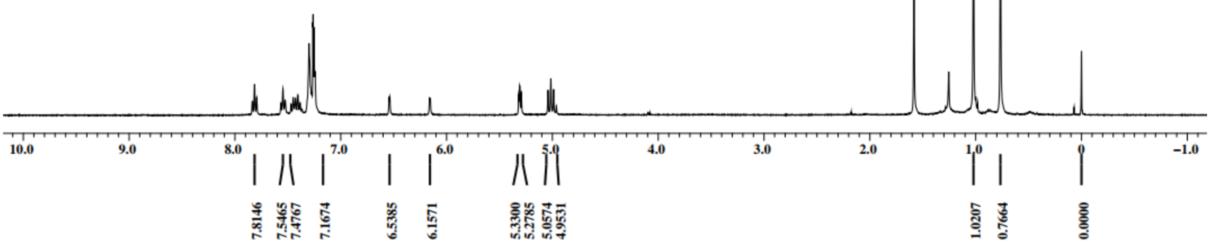

[13]C NMR ($CDCl_3$, 100 MHz) of 4ka

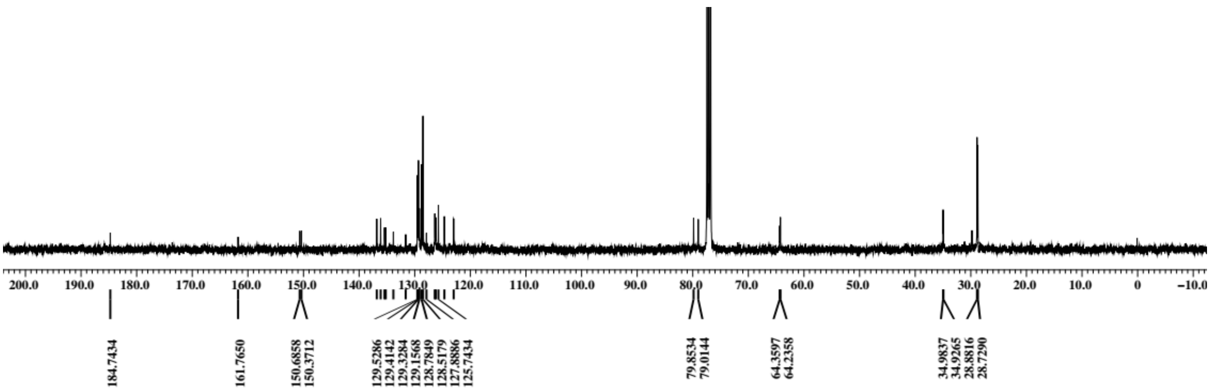

[13]C DEPT NMR ($CDCl_3$, 100 MHz) of 4ka

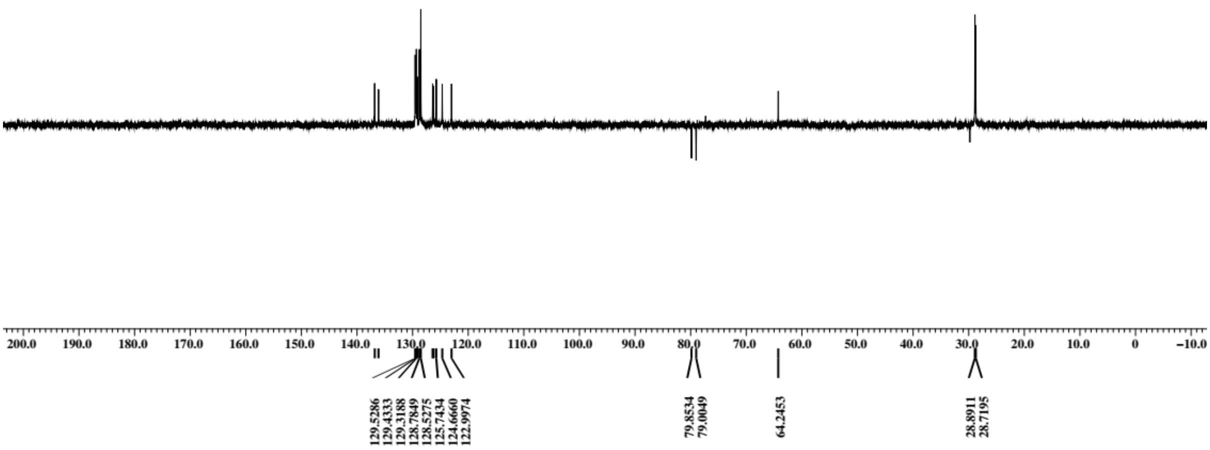

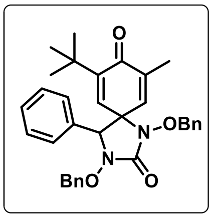

^{1}H NMR ($CDCl_3$, 400 MHz) of 4la

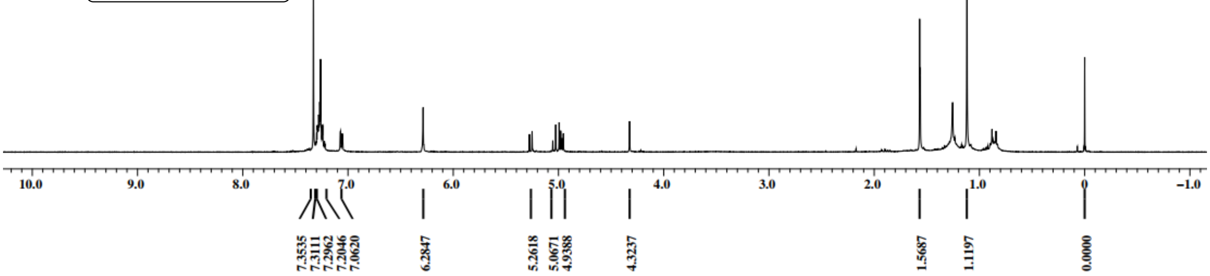

^{13}C NMR ($CDCl_3$, 100 MHz) of 4la

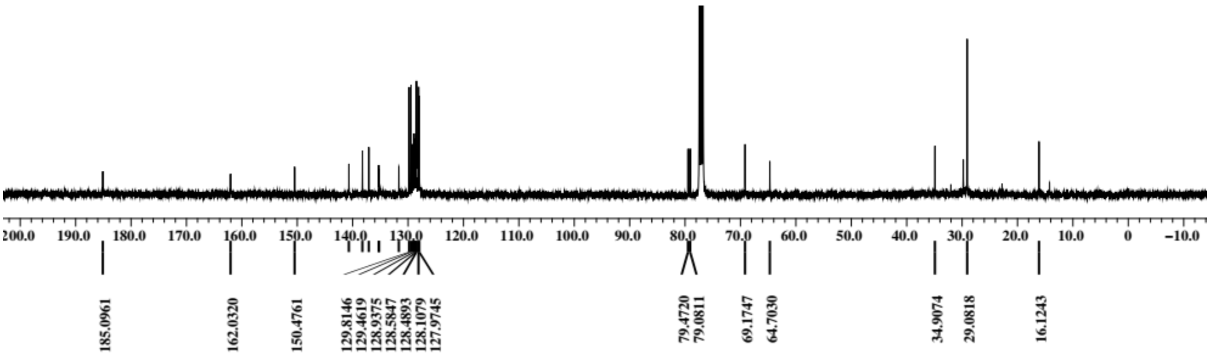

^{13}C DEPT NMR ($CDCl_3$, 100 MHz) of 4la

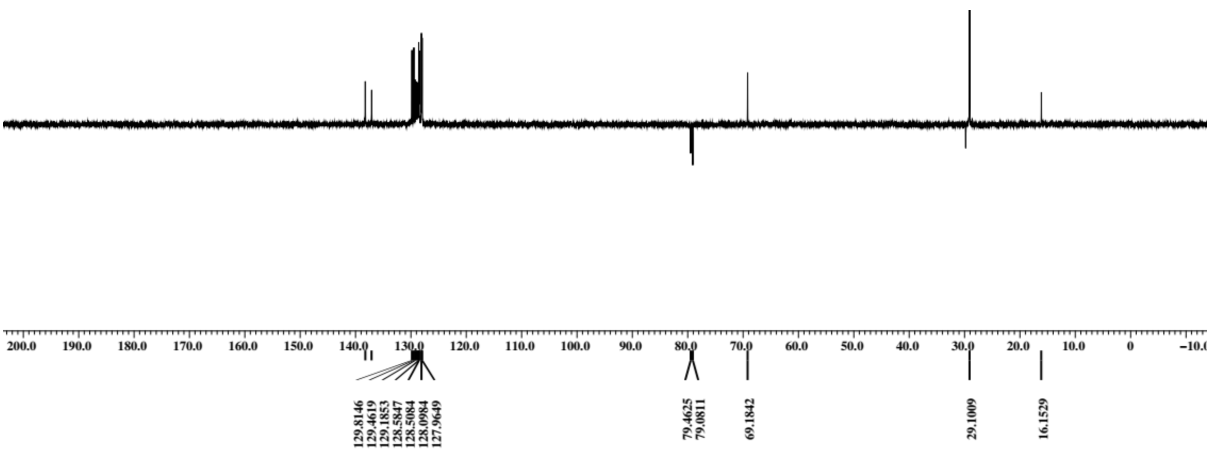

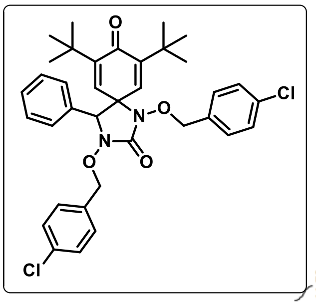

^{1}H NMR (CDCl$_3$, 400 MHz) of 4ab

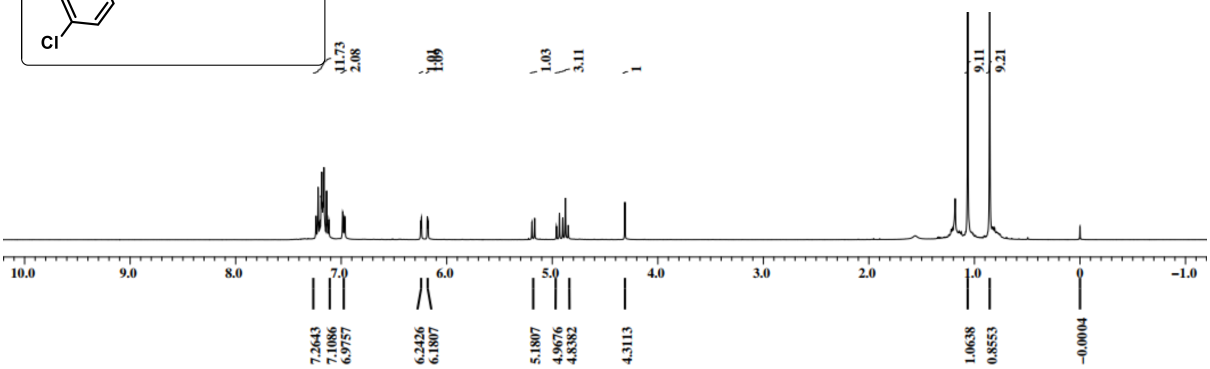

^{13}C NMR (CDCl$_3$, 100 MHz) of 4ab

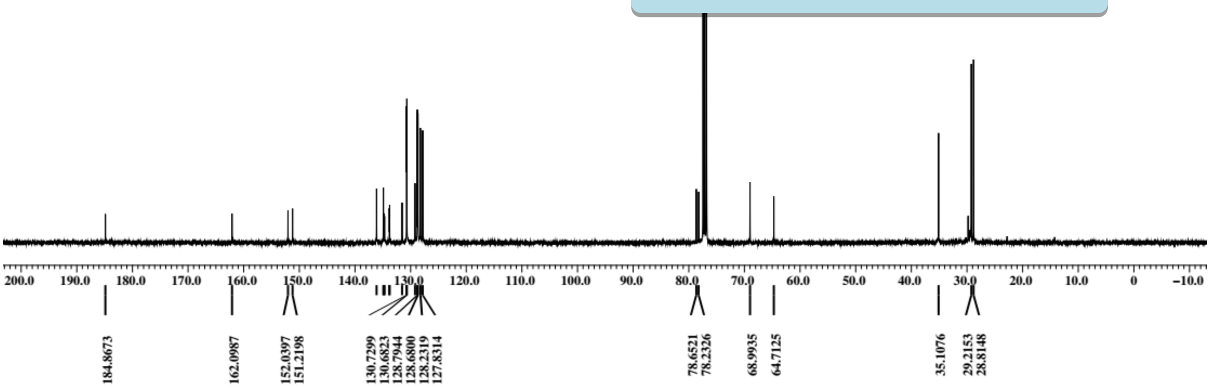

^{13}C DEPT NMR (CDCl$_3$, 100 MHz) of 4ab

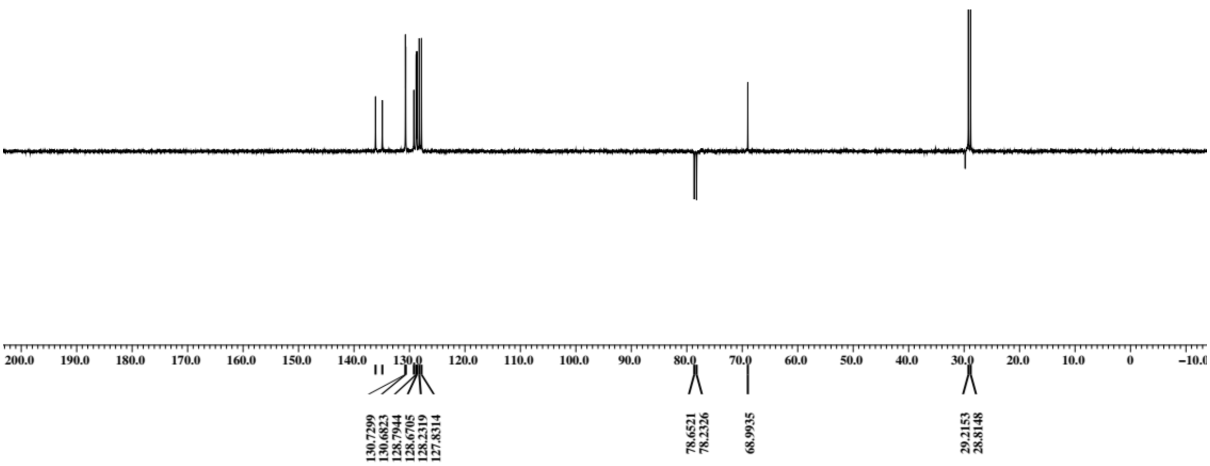

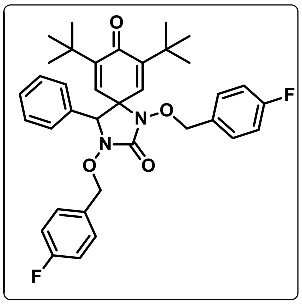

^{1}H NMR ($CDCl_3$, 400 MHz) of 4ac

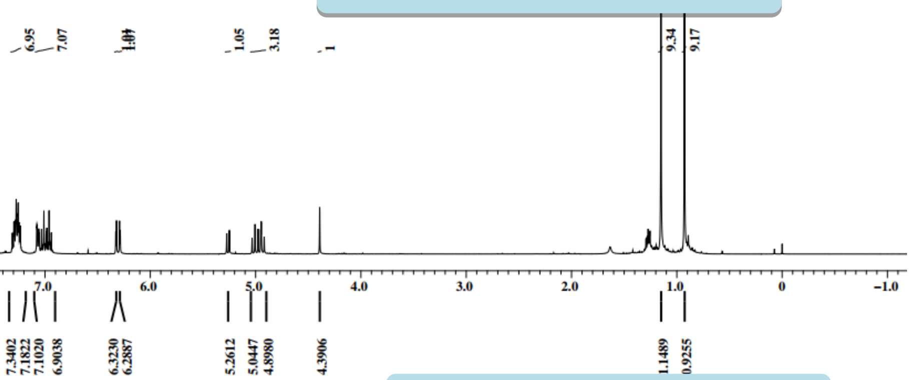

^{13}C NMR ($CDCl_3$, 100 MHz) of 4ac

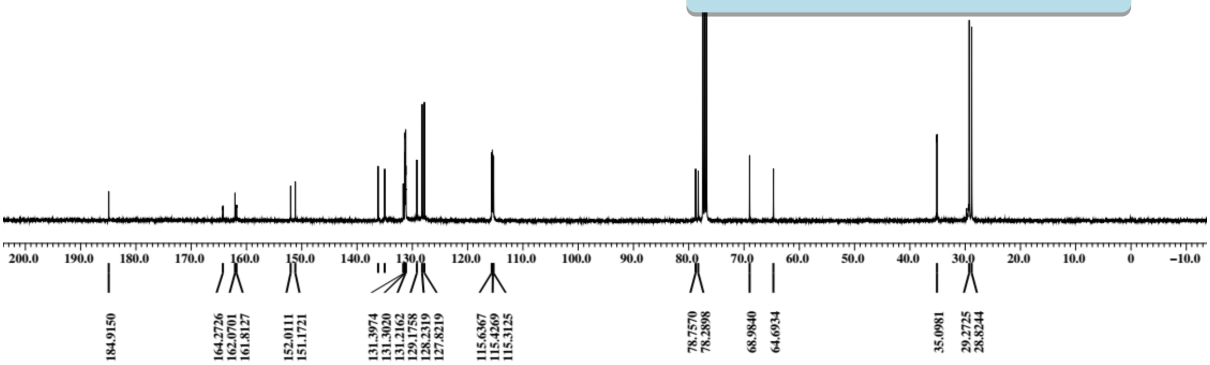

^{13}C DEPT NMR ($CDCl_3$, 100 MHz) of 4ac

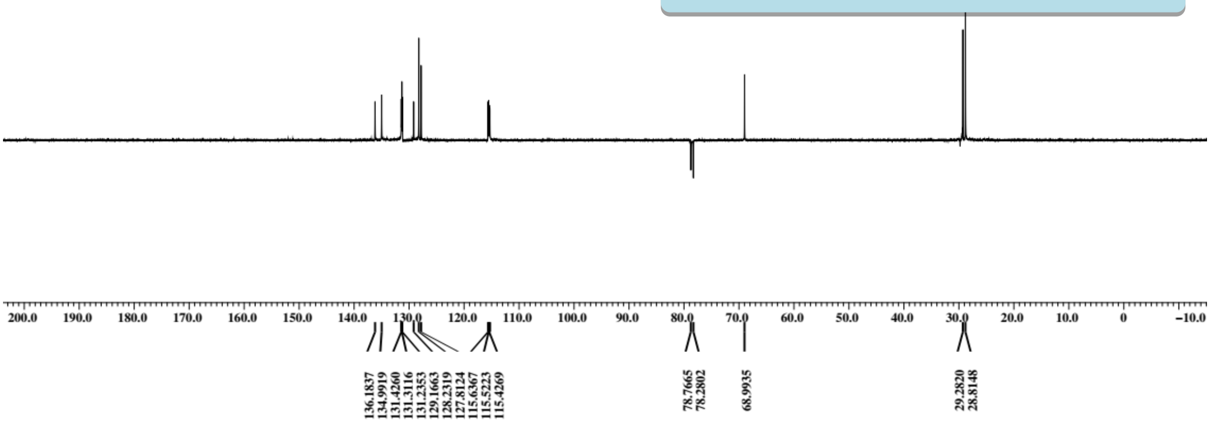

^{19}F NMR ($CDCl_3$, 376 MHz) of 4ac

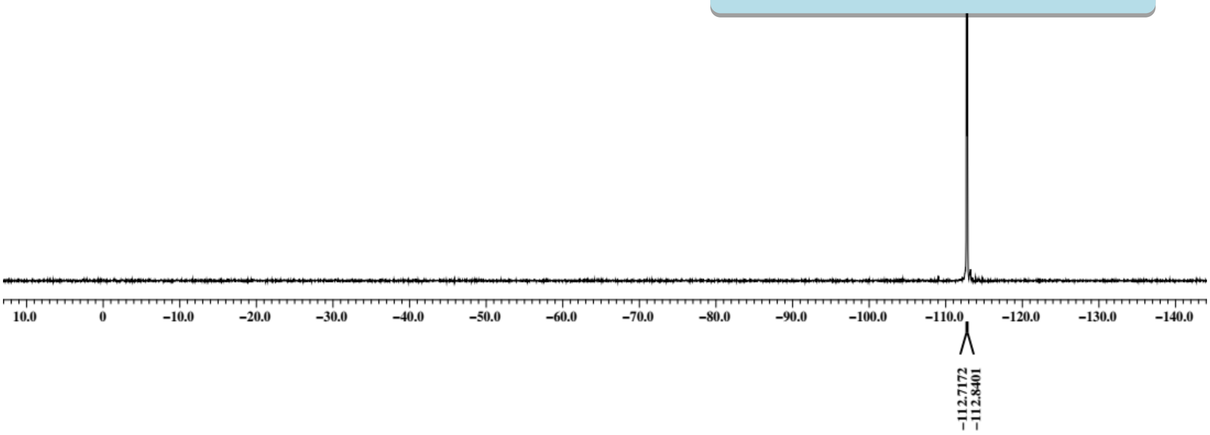

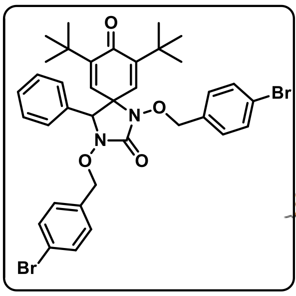

^{1}H NMR ($CDCl_3$, 400 MHz) of 4ad

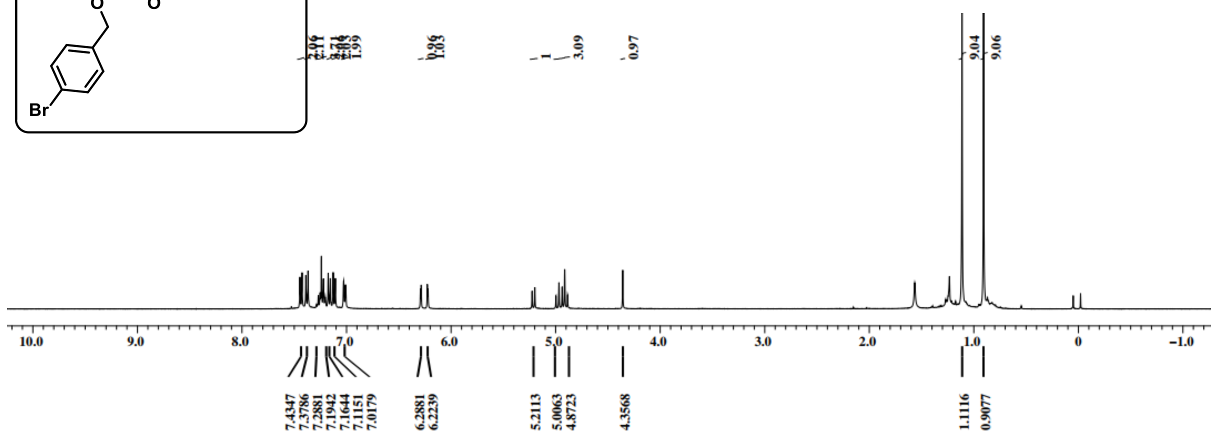

^{13}C NMR ($CDCl_3$, 100 MHz) of 4ad

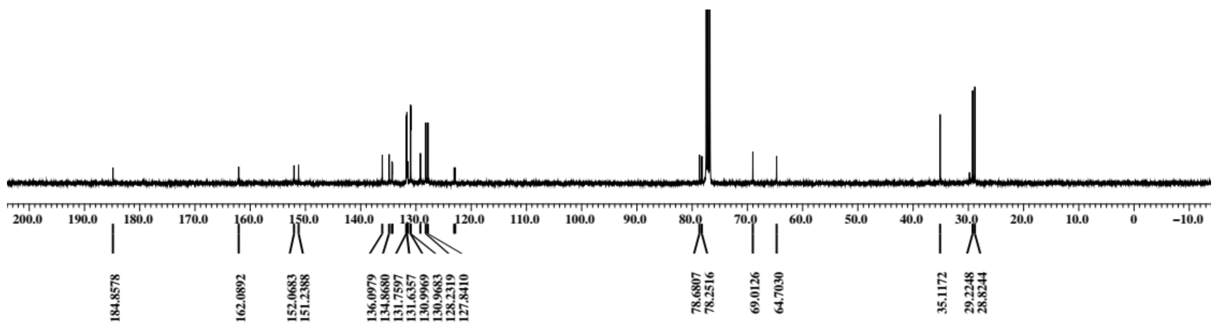

^{13}C DEPT NMR ($CDCl_3$, 100 MHz) of 4ad

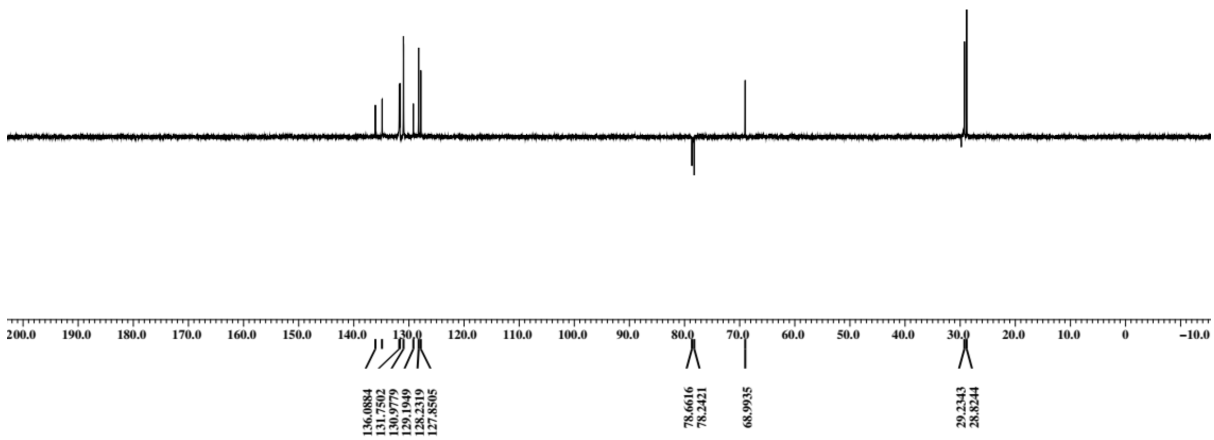

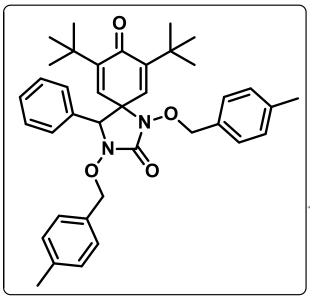

^{1}H NMR (CDCl$_3$, 400 MHz) of 4ae

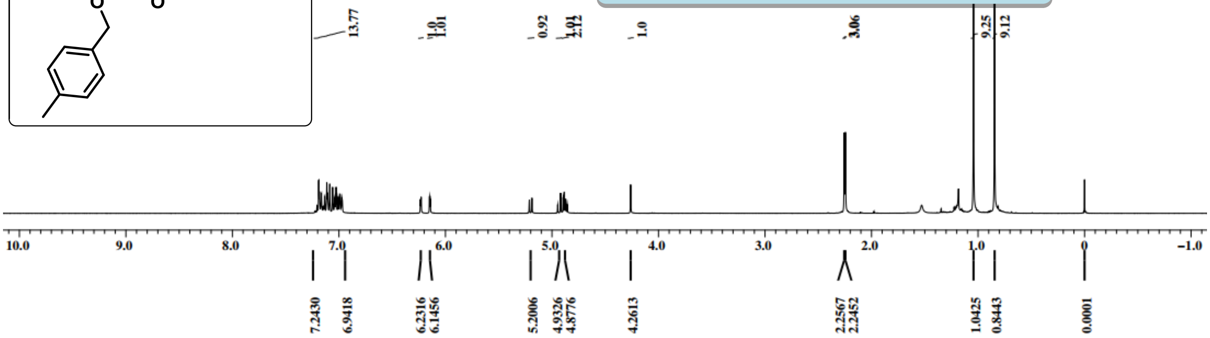

^{13}C NMR (CDCl$_3$, 100 MHz) of 4ae

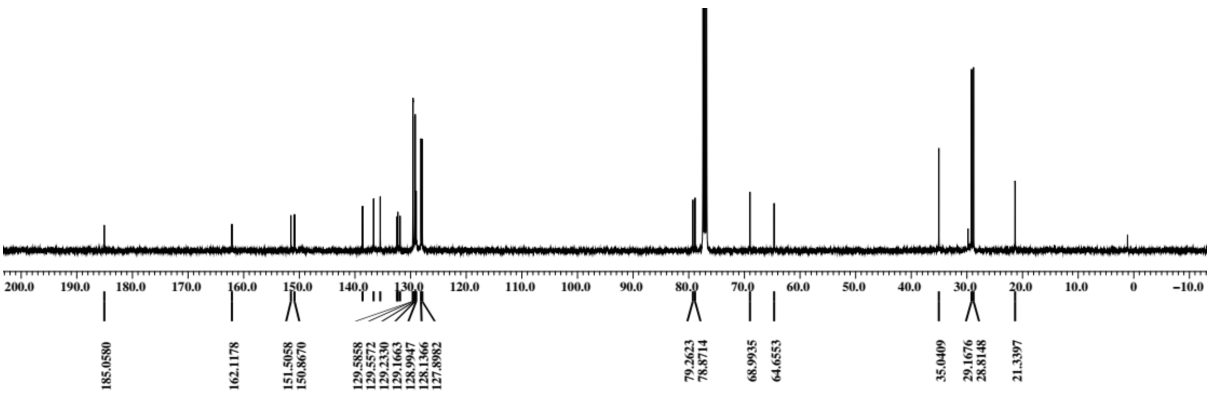

^{13}C DEPT NMR (CDCl$_3$, 100 MHz) of 4ae

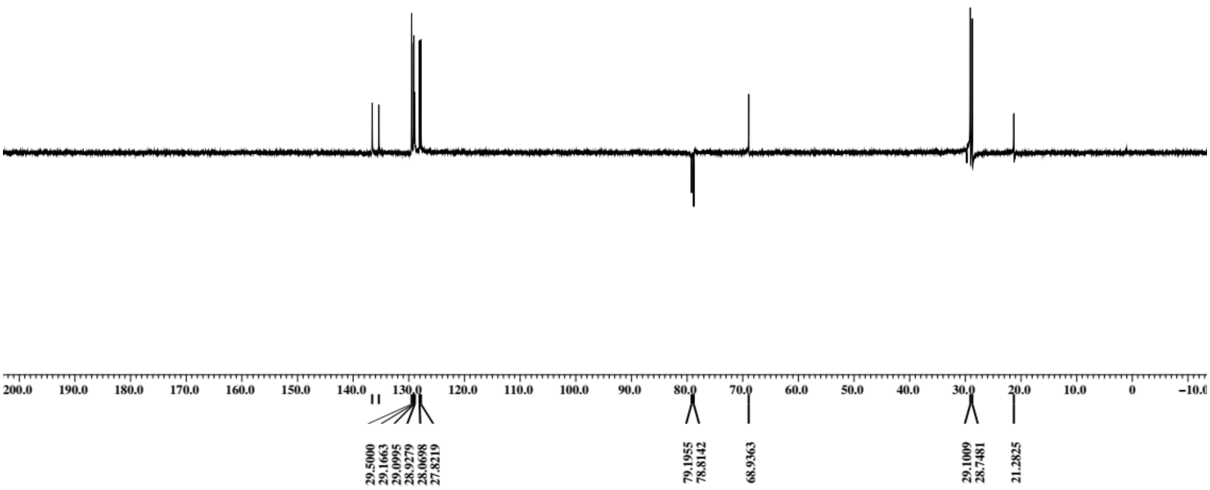

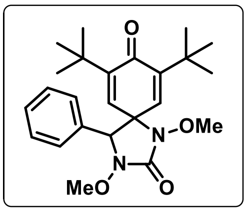

^{1}H NMR ($CDCl_3$, 400 MHz) of 4af

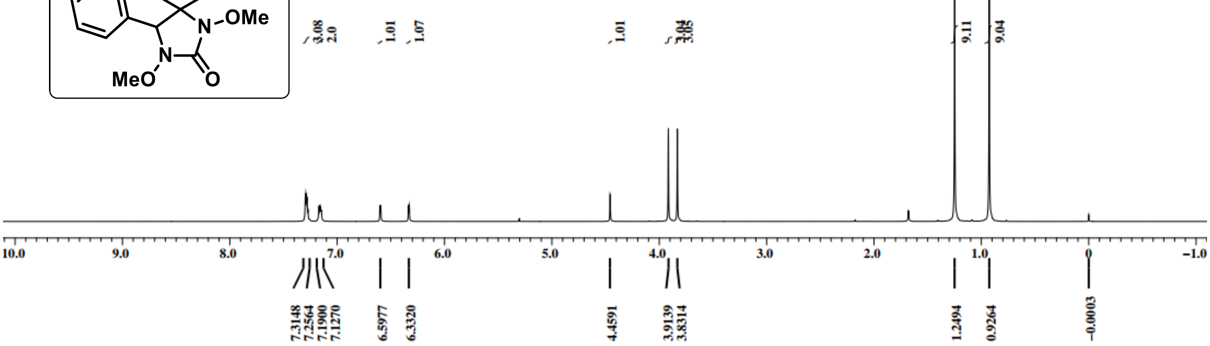

^{13}C NMR ($CDCl_3$, 100 MHz) of 4af

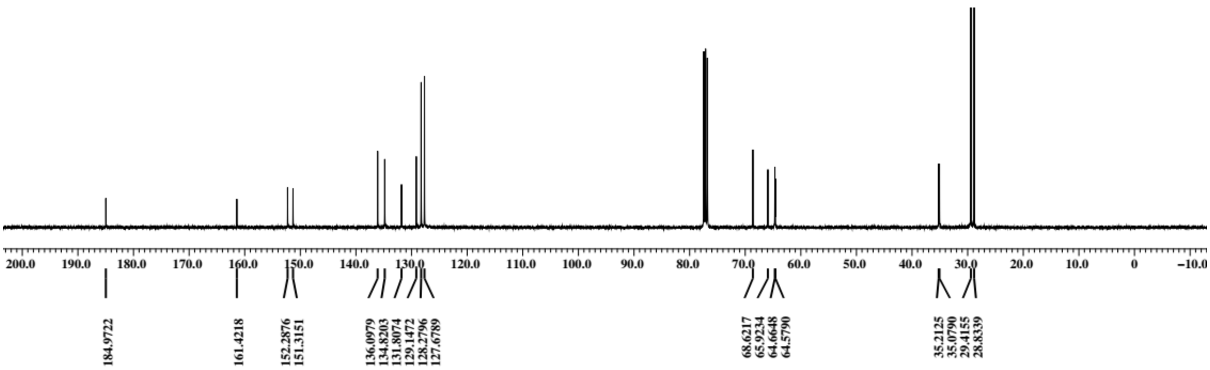

^{13}C DEPT NMR ($CDCl_3$, 100 MHz) of 4af

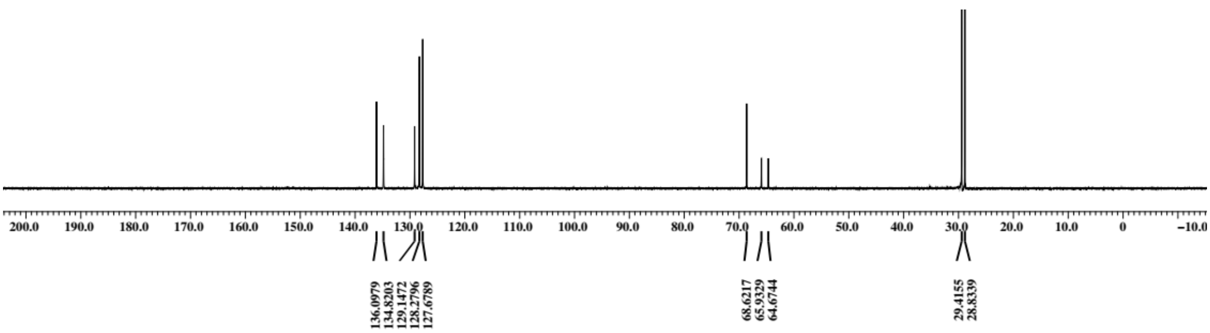

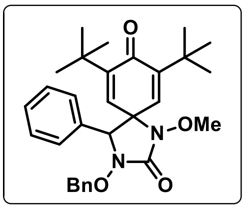

^{1}H NMR ($CDCl_3$, 400 MHz) of 4ag

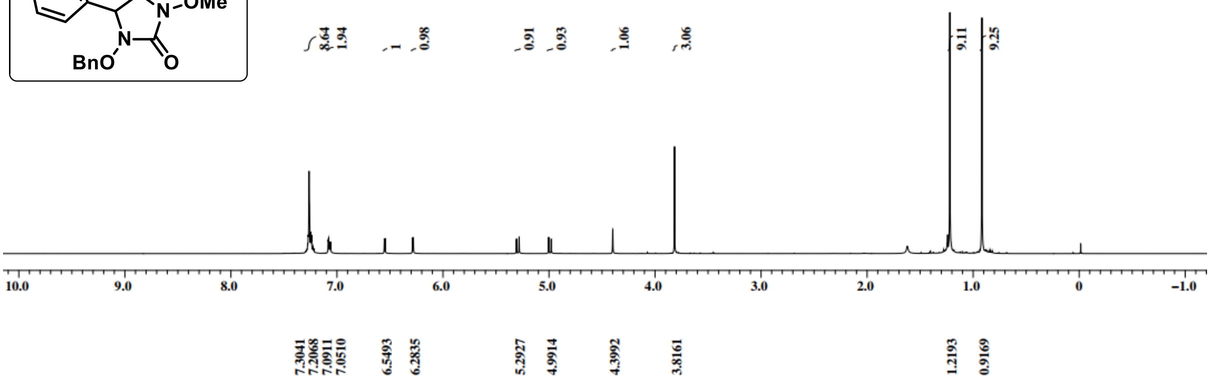

^{13}C NMR ($CDCl_3$, 100 MHz) of 4ag

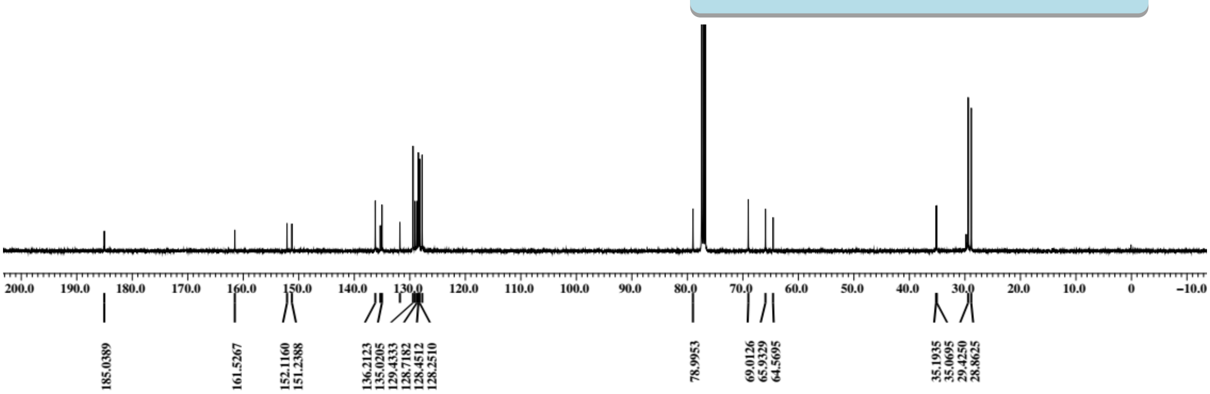

^{13}C DEPT NMR ($CDCl_3$, 100 MHz) of 4ag

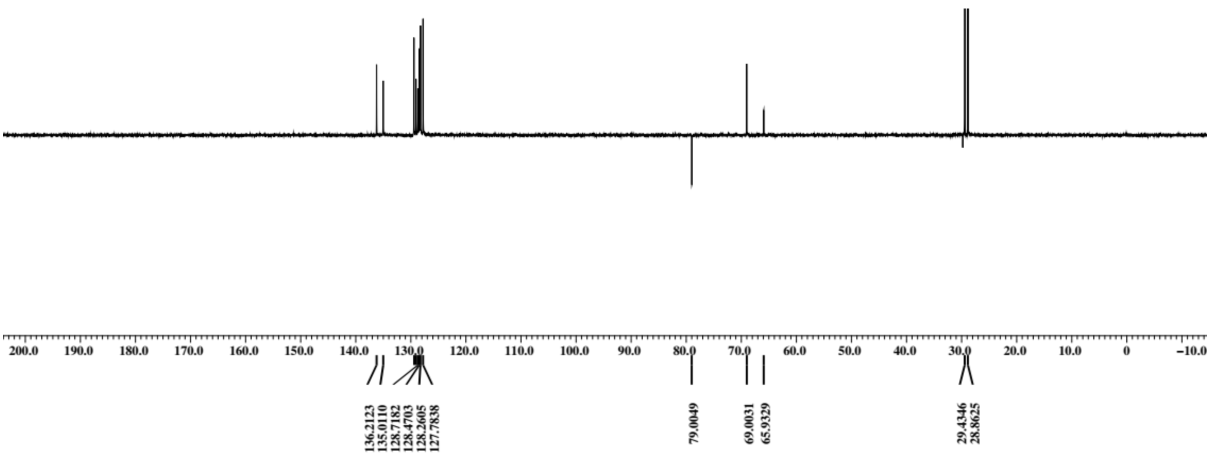

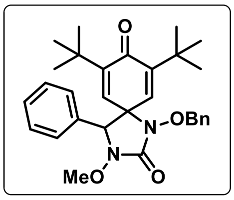

[1]H NMR (CDCl₃, 400 MHz) of 4ag’

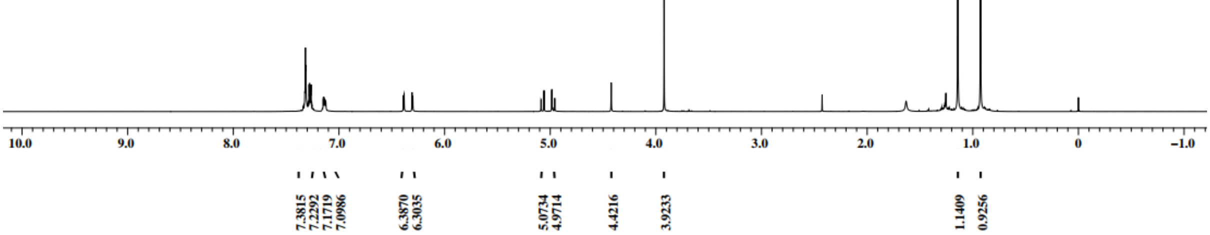

[13]C NMR (CDCl₃, 100 MHz) of 4ag’

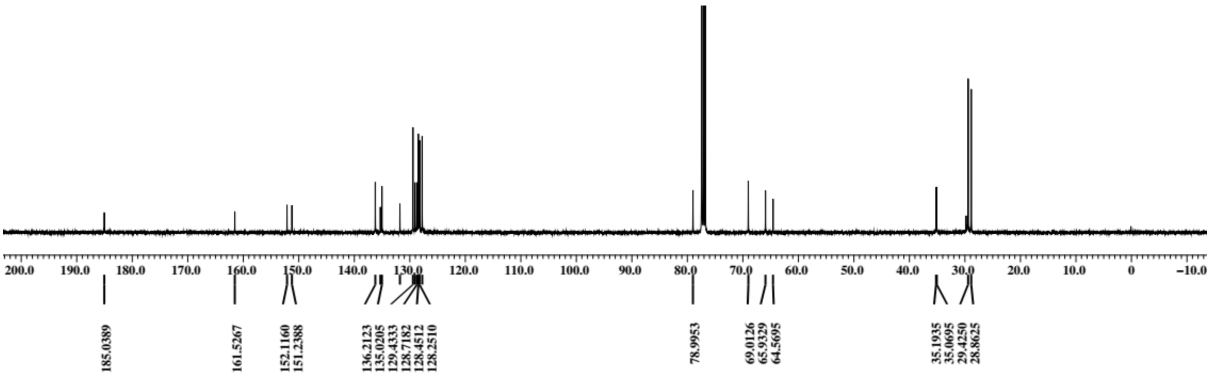

[13]C DEPT NMR (CDCl₃, 100 MHz) of 4ag’

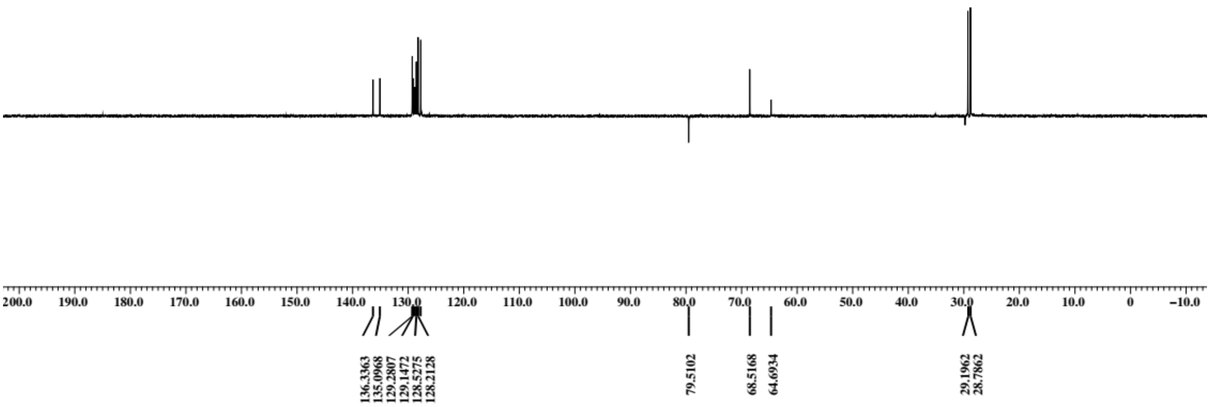

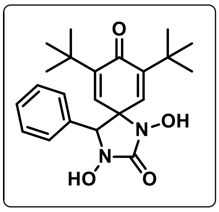

^{1}H NMR ($CDCl_3$, 400 MHz) of 5aa

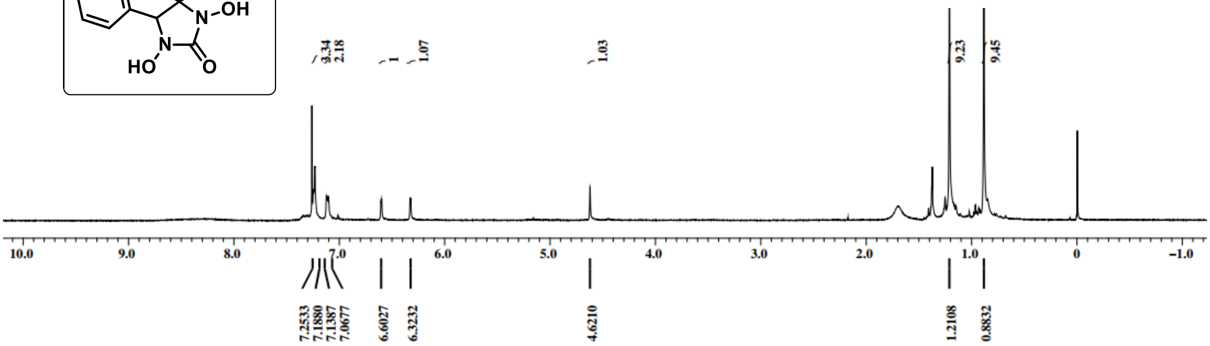

^{13}C NMR ($CDCl_3$, 100 MHz) of 5aa

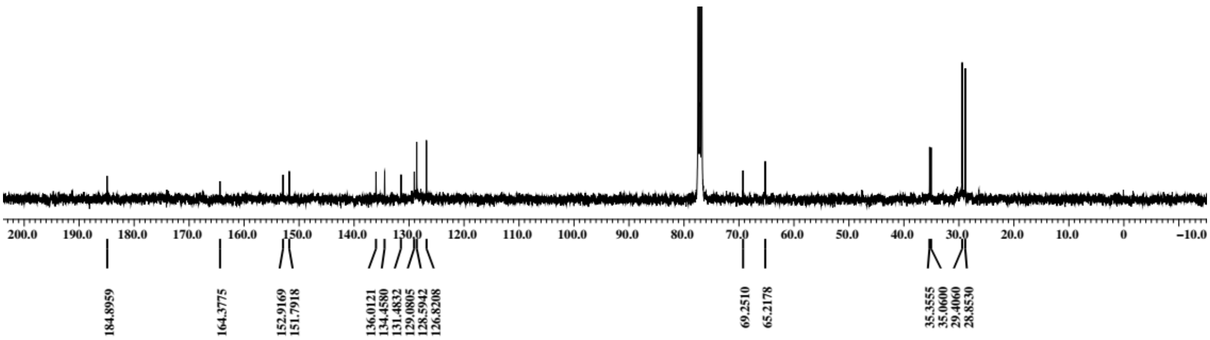

^{13}C DEPT NMR ($CDCl_3$, 100 MHz) of 5aa

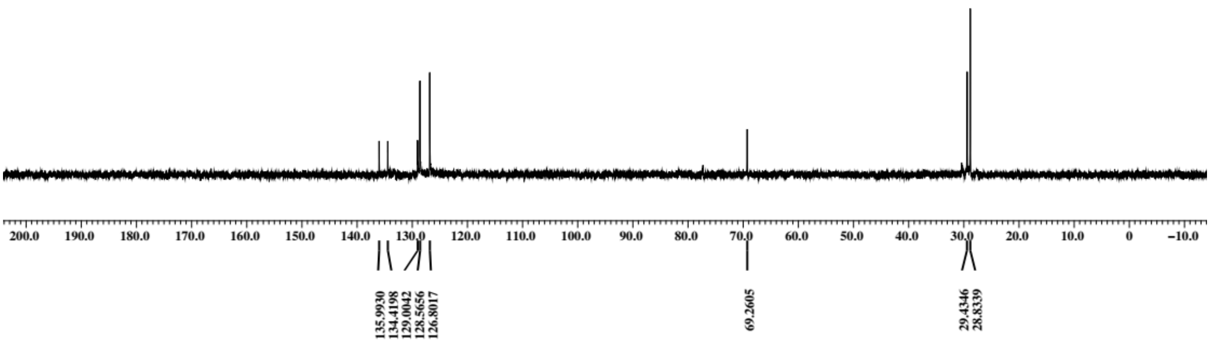

Chapter 3

Accessing Complex Tetrahydrofurobenzo-Pyran/Furan Scaffolds via Lewis-Acid Catalyzed Bicyclization of Cyclopropane Carbaldehydes with Quinone Methides/Esters

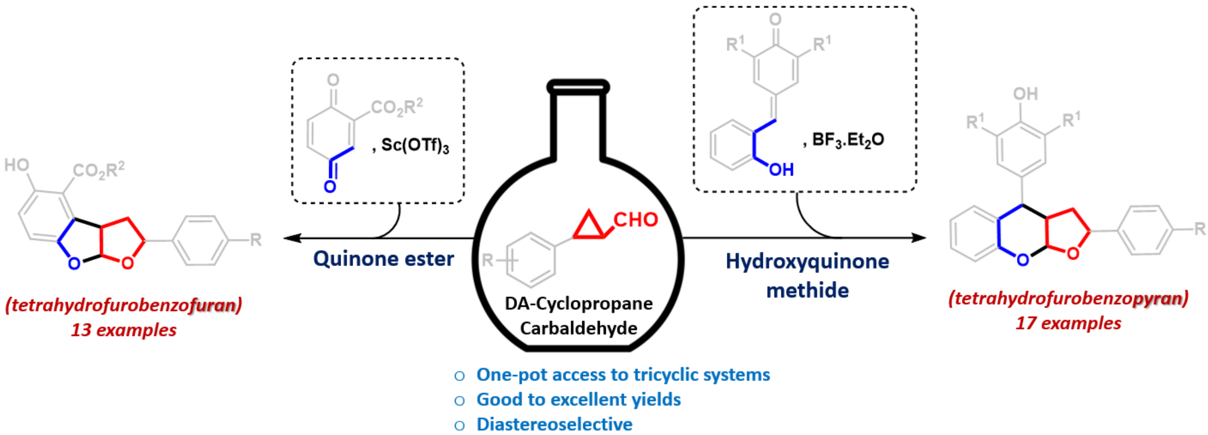

This work was published in *The Journal of Organic Chemistry* (A journal of *American Chemical Society*). Please see citation "Kaur, N.; Kumar, P.; Dutt, S.; Banerjee, P. *J. Org. Chem*. **2022**, *87*, 7905-7918."

3.1 Introduction

Benzannulated oxacycles, especially benzannulated [6,5]- and [5,5]- fused oxygen heterocycles, represent a highly privileged class of structural motifs in a variety of bioactive molecules and natural products.[1] Xyloketals, isolated from mangrove fungus, comprising the tetrahydrofurobenzopyran unit, is engaged in the treatment of several neurological disorders like Alzheimer's disease.[2] Alboatrin, a phytotoxic metabolite, is responsible for vascular-wilt disease in alfalfa[3], whereas aflatoxins bearing the tetrahydrofurobenzofuran units are well-known for their carcinogenicity, toxicity, and antimitoticity[4] (Figure 1).

Figure 3.1.1 Bioactive tetrahydrofurobenzo-pyran/furan systems.

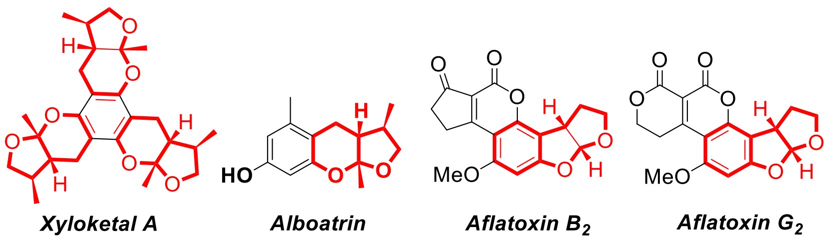

Owing to their unique structure and intriguing activity in biological systems, the construction of such complex structural motifs with multiple stereogenic centers has always been a challenging task for the synthetic fraternity, and consequently, the reports on the synthesis of these frameworks are still rare and underexplored. However, a few methodologies demonstrating the synthesis of benzofused six-five and five-five oxygen tricycles have been reported in recent years. [5-6] In 2016, Mazet *et al.* introduced an enantioselective palladium-catalyzed intermolecular carboetherification of dihydrofurans towards the formation of fused tetrahydrofurobenzofurans[7] (Scheme 3.1.1a).

Scheme 3.1.1 Previous reports on synthesis of tetrahydrofurobenzo-pyran/furan systems

a). Mazet et al. (2016)

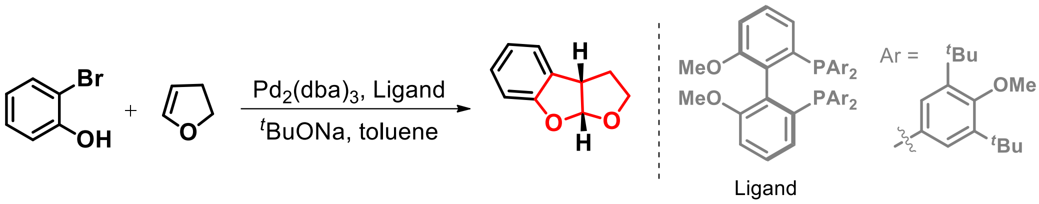

Recently, Wang and Bu *et al.* reported the synthesis of furanobenzopyran-fused polycyclic motifs from *o*-hydroxy chalcones and hydroxyketones[8] (Scheme 3.1.1b). In this context, Jia and Xu *et al.* also demonstrated a gold-catalyzed cyclization of *p*-quinone methides with *in situ* generated cyclic enol ethers towards the construction of spiro and fused ketals.[9]

b). Wang and Bu et al. (2019)

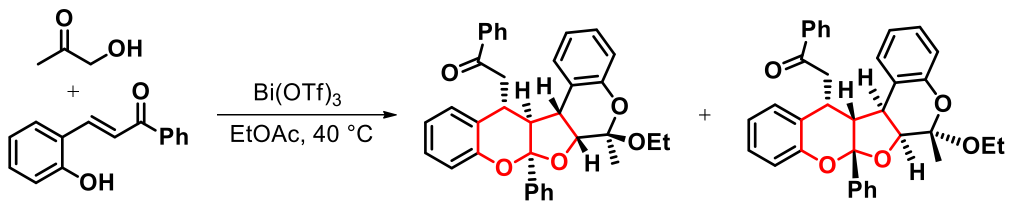

Over the time, donor-acceptor cyclopropane carbaldehydes have emerged as versatile synthons for the diverse hetero/carbocyclic synthesis.[10-11] In this regard, our group has significantly explored the strain-driven reactivity of aryl-substituted cyclopropane carbaldehydes (ACC) towards heterocyclic synthesis via Lewis-acid or metal-free activation of the cyclopropane ring.[12] At the same time, quinone derivatives have also acquired enormous attention for their electrophilic nature towards assembling densely functionalized molecules.[13-14] Quinone methides and quinone esters are widely known to act as four- and three-atom contributors for accessing intriguing heterocyclic systems. As part of our efforts and inspired by our previous results, we anticipated that the electrophilic dipolar reactivity of quinone derivatives and the *in-situ* ring expansion of ACC could be used in synergy for a possible bicyclization process. In trials, our proposal worked out successfully, as we report here a Lewis-acid catalyzed bicyclization of ACCs with quinone methides/esters to deliver complex tetrahydrofurobenzo-pyran/furan scaffolds Scheme (3.1.1c).

c). Our Idea

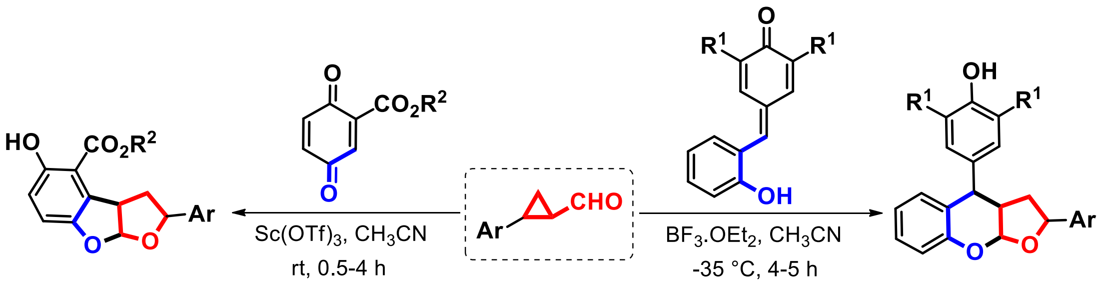

3.2 Results and Discussions

To start with, *o*-hydroxyphenyl substituted *para*-quinone methide (*p*-QM) **1a** and *p*-methoxyphenyl substituted cyclopropane carbaldehyde **2a** were chosen as model substrates. Initially, at room temperature with Lewis-acids such as $InCl_3$, $Sc(OTf)_3$, $Bi(OTf)_3$, $TiCl_4$, $Yb(OTf)_3$ in DCM solvent, either no or negligible product formation was observed (Table 3.2.1, entries 1-3). So, we tried the reaction at -78 °C with $Sc(OTf)_3$ and $Bi(OTf)_3$ but again failed to get the expected product (Table 3.2.1, entry 4). However, with $TiCl_4$ at -78 °C, we obtained the desired product in 35% yield (Table 3.2.1, entry 5). Changing the temperature to -40 °C led to improved yields (Table 3.2.1, entry 6). Gratifyingly, 20 mol % of $BF_3{\cdot}OEt_2$ in DCM at -35°C provided the desired product in 60% yield, albeit with low diastereoselectivity (Table 3.2.1, entry 7). Further, various solvents like DCE, CH_3CN, Toluene, $CHCl_3$, and THF were screened (Table 3.2.1, entry 8-12), where CH_3CN proved to be optimal and rendered the product in 82% yield with exceptional diastereoselectivity. Reducing the catalyst loading to 10 mol% resulted in compromised yields and diastereoselectivity (Table 3.2.1, entry 13).

Table 3.2.1 Optimization of reaction conditions[a]

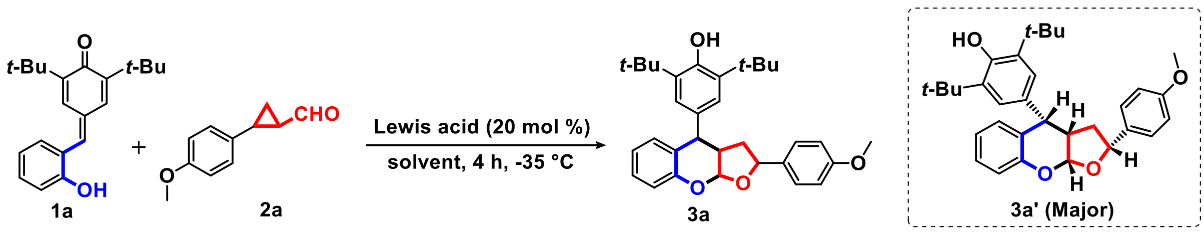

entry	Lewis-acid	T (°C)	solvent	yield (%)[b]	*dr*[c]
1	$Sc(OTf)_3/Bi(OTf)_3$	rt	CH_2Cl_2	20/10	-
2	$InCl_3$/ $TiCl_4$	rt	CH_2Cl_2	10/15	-
3	$Yb(OTf)_3/In(OTf)_3$	rt	CH_2Cl_2	0	-
4	$Sc(OTf)_3/Bi(OTf)_3$	-78	CH_2Cl_2	n.r.[d]	-
5	$TiCl_4$	-78	CH_2Cl_2	35	5:2:1.2:1
6	$TiCl_4$	-40	CH_2Cl_2	48	6:2:1:1
7	$BF_3{\cdot}OEt_2$	-40	CH_2Cl_2	60	9:5:1.1:1
8	$BF_3{\cdot}OEt_2$	-35	CH_3CN	82	13:2:1:1
9	$BF_3{\cdot}OEt_2$	-35	DCE	50	5:3:1:1
10	$BF_3{\cdot}OEt_2$	-35	$CHCl_3$	40	9:5:2:1
11	$BF_3{\cdot}OEt_2$	-35	toluene	35	10:4:4:1
12	$BF_3{\cdot}OEt_2$	-35	THF	trace	-
13[e]	$BF_3{\cdot}OEt_2$	-35	CH_3CN	55	7:3:2:1

[a]Reaction condition: **1a** (1 equiv., 0.3 mmol), **2a** (1.2 equiv., 0.36 mmol), Lewis-acid (0.2 equiv., 0.06 mmol), solvent (2 mL). [b]Isolated overall yields. [c]Determined by crude ^1H NMR. [d]no reaction. [e]with 10 mol% $BF_3{\cdot}OEt_2$.

With the optimized conditions, we investigated the generality of the method with various ACCs (Scheme 2). Electron-rich aromatic groups such as 4-methoxy, 3,4-dimethoxy, and 3,4,5-trimethoxy phenyl groups offered the product **3a**, **3b**, and **3c** in moderate to good yields. Substituents like 3-ethoxy-4-methoxyphenyl and 4-benzyloxyphenyl also afforded the desired products **3d** and **3e** in 78-85% yields. ACC with methylenedioxyphenyl and 4-butoxyphenyl substituents afforded **3f** and **3g** in appreciable yields. Cyclopropanes bearing halogens like fluoro- and bromo- along with the methoxy group at the *para*-position of the aryl ring delivered the anticipated products **3h** and **3i** in satisfactory yields. Expectedly, the styryl cyclopropane carbaldehyde successfully furnished **3j** in 70% yield. However, ACCs like those bearing electron-deficient and less electron-rich aromatic groups were found ineffective. Next, we examined the substrate scope with respect to *p*-QMs, where the variation of substituents on the aryl ring had no pronounced effect and *p*-QMs having bromo- and fluoro- on the aryl ring offered **3k** and **3l** in 64% and 62% yield, respectively. In addition, methoxy substituted *p*-QM delivered **3m** in 71% yield. Further, methyl-substituted *p*-QMs were well suited and afforded **3n** and **3o** in 67% and 65% yields, respectively. In addition to *p*-QMs, *o*-quinone methides also followed the designed strategy and *o*-hydroxy benzhydryl alcohols **1g** and **1h** (precursors of *o*-QMs), afforded **3p** and **3q** in acceptable yields (Scheme 3.2.1).

Scheme 3.2.1 Bicyclization of ACC with *para*-Quinone methides.

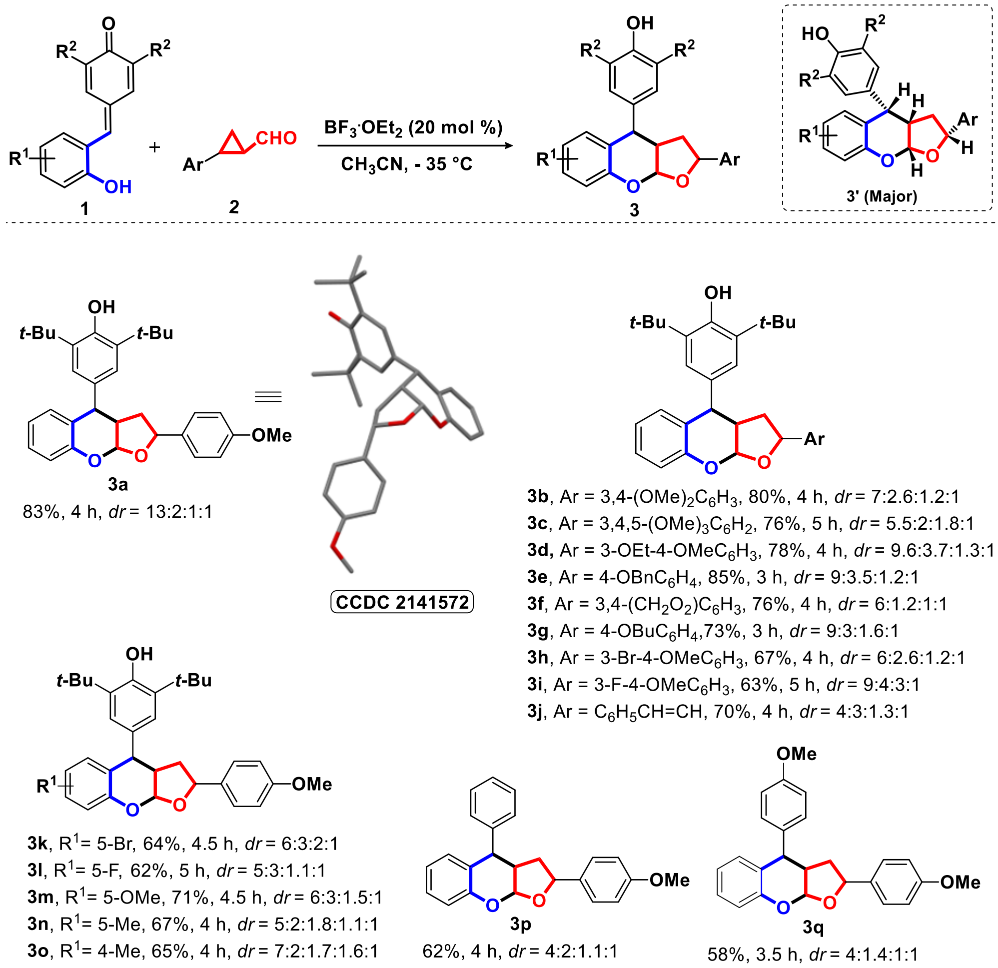

[a]Reaction condition: **1** (1 equiv.), **2** (1.2 equiv.), $BF_3 \cdot OEt_2$ (0.2 equiv.) in anhydrous CH_3CN (0.15 M) at -35 °C. Hydrogen atoms are omitted in the single-crystal X-ray structure of **3a** for the sake of clarity. *dr* determined by crude ^{1}H NMR analysis.

The development of this effortless strategy for the synthesis of benzofused six-five oxacycles made us eager to know whether a similar chemistry can be employed to synthesize benzofused five-five oxacycles using ACC with another class of quinone derivative which can act as a three-atom synthon for the bicyclization process. For this purpose, we anticipated that quinone ester could serve as a suitable substrate for the construction of tetrahydrofurobenzofuran scaffolds.

The success of our prior methodology led us to initiate the optimization of this approach with previously optimized conditions, but no product formation was observed (Table 3.2.2, entry 1). Next, 10 mol % of $InCl_3$ was tested with quinone ester **4a** and ACC **2a** at room temperature, and delightfully rendered the expected product **5a** in 48% yield and with good diastereoselectivity (Table 3.2.2, entry 2). Inspired by this result, we screened the reaction with other Lewis acids at room temperature, and with $Sc(OTf)_3$ in DCM, **5a** was obtained in 60% yield (Table 3.2.2, entry 3). When we performed the reaction in acetonitrile, the desired product was isolated in 88% yield (Table 3.2.2, entry 4). Lowering the catalyst loading to 5 mol% delivered the product in compromised yields (Table 3.2.2, entry 5). Other solvents like DCE, $CHCl_3$, and toluene proved to be detrimental (Table 3.2.2, entries 6-8). Moreover, Lewis-acids like $Yb(OTf)_3$ and $Cu(OTf)_2$ could also catalyze the reaction but resulted in lower yields (Table 3.2.2, entries 9-12), whereas, MgI_2, $BF_3 \cdot OEt_2$, $In(OTf)_3$, and $Bi(OTf)_3$ proved to be inefficient (Table 3.2.2, entries 13-14).

Table 3.2.2 Optimization of Reaction Conditions.[a]

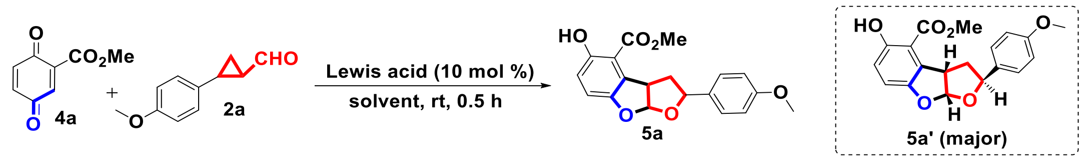

entry	Lewis acid	solvent	Yield[b] (%)	*dr*[c]
1[d]	$BF_3 \cdot OEt_2$	CH_3CN	0	-
2	$InCl_3$	CH_2Cl_2	48	19:3.5:1.2:1
3	$Sc(OTf)_3$	CH_2Cl_2	60	17:2.2:1.2:1
4	$Sc(OTf)_3$	CH_3CN	88	>20:3:2:1
5[e]	$Sc(OTf)_3$	CH_3CN	58	20:2:1.2:1
6	$Sc(OTf)_3$	DCE	57	19:3:1.6:1
7	$Sc(OTf)_3$	$CHCl_3$	42	15:1.5:1.1:1
8	$Sc(OTf)_3$	toluene	65	14:1.2:1.2:1
9	$Yb(OTf)_3$	CH_2Cl_2	62	14:1.3:1.1:1
10	$Yb(OTf)_3$	CH_3CN	72	19.5:2:1:1
11	$Cu(OTf)_2$	CH_2Cl_2	70	14:2:1:1
12	$Cu(OTf)_2$	CH_3CN	80	20:2:1.5:1
13	$MgI_2/BF_3 \cdot OEt_2$	CH_2Cl_2	trace	-
14	$In(OTf)_3/Bi(OTf)_3$	CH_2Cl_2	trace	-

[a]Reaction condition: **4a** (1 equiv., 0.6 mmol), **2a** (1.5 equiv., 0.9 mmol), Lewis-acid (0.1 equiv., 0.06 mmol) in solvent (2 mL). [b]Isolated overall yields. [c]Determined by crude ^1H NMR analysis. [d]with 10 mol% $BF_3 \cdot OEt_2$ at -35 °C for 4 h. [e]with 0.05 mol % catalyst loading.

With the optimized conditions, we investigated the generality of this reaction by varying the aryl substitution on ACC. Compatible results were obtained for the ACCs bearing electron-rich aryl groups like 4-methoxy, 3,4-dimethoxy, 3,4,5-trimethoxy, and 4-benzyloxy phenyl substituents to construct the corresponding products **5a**, **5b**, **5c**, and **5d** in good to excellent yields. ACCs with methylenedioxy and 4-butoxy phenyl groups provided **5e** and **5f** in 80% and 82%, respectively. Further, cyclopropanes possessing halide substituents along with the methoxy group on the phenyl ring furnished **5g** and **5h** in good yields. Other analogs like styryl and naphthyl substituted ACCs also proved compatible and provided **5i** and **5j** in 73% and 70% yields, respectively. To add on, cyclopropanes having less electronically rich substituents such as 4-tolyl and mesityl also delivered the expected **5k** and **5l** in satisfactory yields. In regard to quinone esters, replacing the methyl ester with ethyl ester didn't change much and furnished the corresponding product **5m** in 84% yield (Scheme 3.2.2).

Based on literature reports[12-14] and our findings, we proposed two similar reaction pathways for the reaction of ACC with quinone derivatives (Scheme 3.2.3). In the beginning, Lewis-acid activates the cyclopropane ring through co-ordination to the aldehyde group (A), which undergoes the well-known Cloke-Wilson type rearrangement to furnish a cyclic enol ether B. This step seems to be common to both strategies. The carbon-carbon double bond of the quinone methide, which is already activated by the Lewis acid, undergoes an intermolecular nucleophilic attack by the nucleophilic carbon-carbon double bond adjacent to the oxygen atom of intermediate B resulting in aromatization of the quinone ring to afford an oxocarbenium intermediate C.

Scheme 3.2.2 Bicyclization of ACC with Quinone esters.

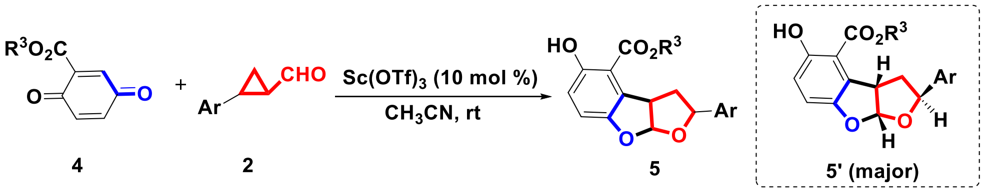

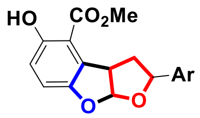

5a, Ar = 4-OMeC_6H_4, 88%, 0.5 h, *dr* = >20:3:2:1
5b, Ar = 3,4-$(OMe)_2C_6H_3$, 85%, 0.5 h, *dr* = >20:3:1.5:1
5c, Ar = 3,4,5-$(OMe)_3C_6H_2$, 82%, 0.7 h, *dr* = 13:1
5d, Ar = 4-OBnC_6H_4, 86%, 0.7 h, *dr* = 9:1
5f, Ar = 4-OBuC_6H_4, 82%, 0.7 h, *dr* = 19:3:2:1
5g, Ar = 3-Br-4-OMeC_6H_3, 78%, 1 h, *dr* = 9:1
5h, Ar = 3-F-4-OMeC_6H_3, 81%, 0.8 h, *dr* = 10:1
5i, Ar =C_6H_5CH=CH, 73%, 2 h, *dr* = 9:2:1
5j, Ar = $C_{11}H_{10}$(naphthyl), 70%, 4 h, *dr* = 5:1
5k, Ar = 4-MeC_6H_4, 66%, 3 h, *dr* = 13:2:1
5l, Ar = 2,4,6-MeC_6H_2, 68%, 2 h, *dr* = >20:1.2:1

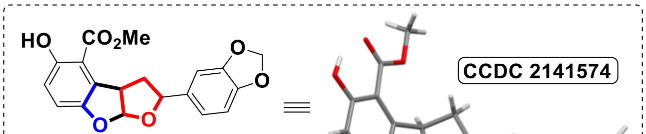

5e
80%, 0.6 h, *dr* = 12:1.4:1

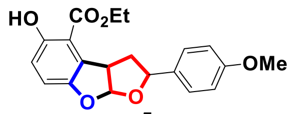

5m
84%, 0.7 h, *dr* = 9:1

[a]Reaction conditions: **4** (1 equiv.), **2** (1.5 equiv.,), $Sc(OTf)_3$ (0.1 equiv.) in anhydrous CH_3CN (0.3 M) at room temperature. *dr* determined by crude ^{1}H NMR analysis

This intermediate C then undergoes subsequent intramolecular ring closure to manifest the tricyclic product **3**. Intermediate C can practically have two different orientations of the substituents on half-boat conformation (deduced from the X-ray crystal structure of product) of the five-membered ring that accounts for the diastereoselectivity in the final product. In the *cis* conformation (CC), the aryl substituent from the cyclopropane moiety and the bulky group derived from the *p*-QM unit are on the same side, while in the *trans* conformation (CT), the two substituents are away from each other. At the first site, CT seems to be a more stable orientation to furnish the major product; however, a close inspection of the structure revealed that in the *trans* conformation, the heavily bulky substituent with two *tert*-butyl groups is in the *endo* cavity of the half-boat geometry. Consequently, CT must be highly destabilized, and the major diastereomer should come from the *cis*-fusion of intermediate CC (Scheme 3.2.3b). Other orientations of the final ring-closure like *cis*-fusion of CT or *trans*-fusion of CC and CT contribute to the minor diastereomers of **3**. With four stereocentres in the molecule, there are eight possible diastereomers that may form through two opposite geometries of the phenolic substituent at C-4 position of the fused pyran ring *via* four approaches of bicyclization represented in Scheme 3.2.3b. In a similar manner to that with quinone methide, quinone ester **4** gets activated through chelation with the Lewis-acid and undergoes a Michael type addition with B to render intermediate D, which eventually undergoes tautomerization to furnish the aromatized intermediate E. Finally, the intramolecular nucleophilic attack of the hydroxy group facilitates the formation of the anticipated tetrahydrofurobenzofuran **5** (Scheme 3.2.3a).

Scheme 3.2.3 Plausible Mechanism.

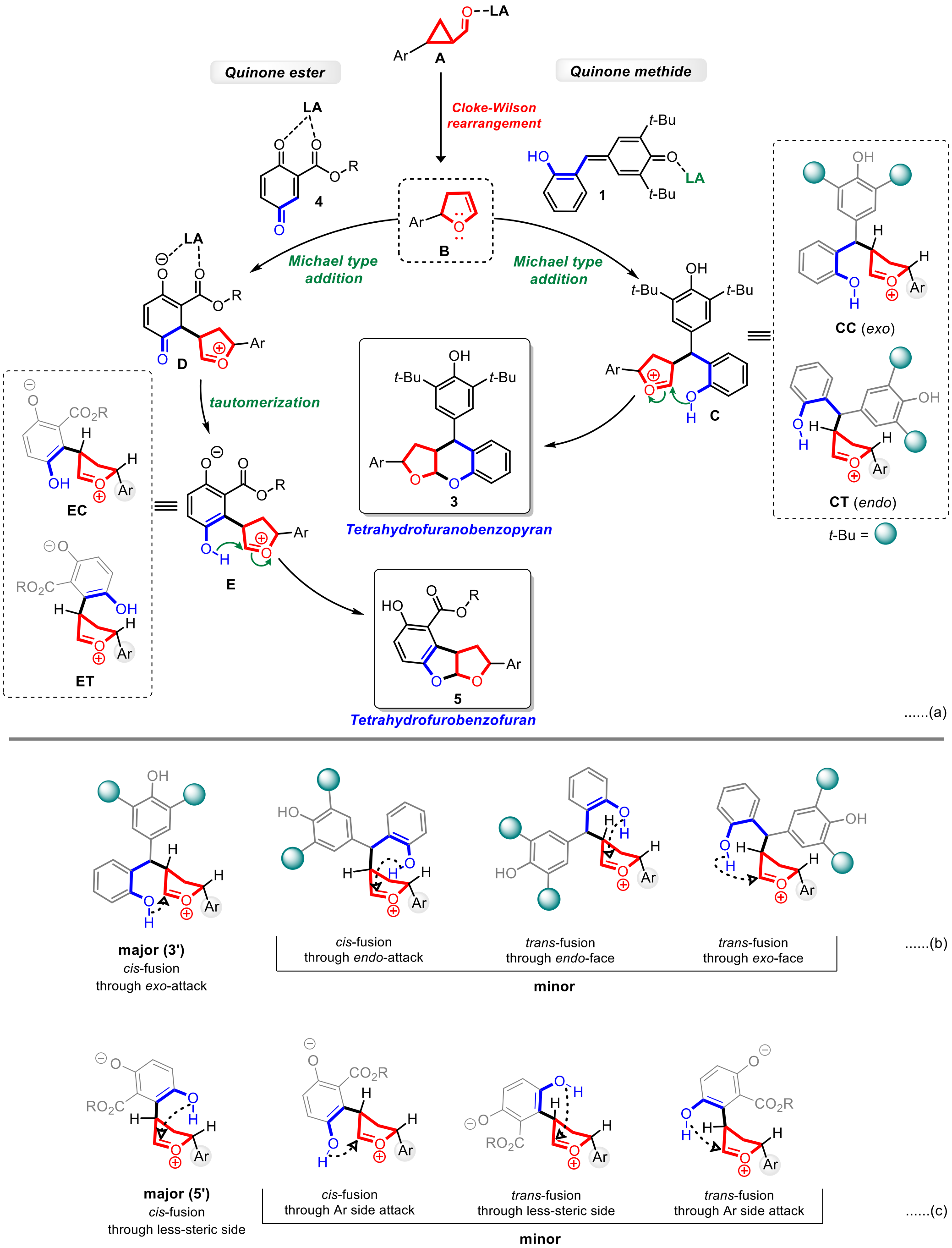

As was the case with quinone methides, the final cyclization through nucleophilic attack of the hydroxy group can take place through two orientations of intermediate E – the *cis* conformation EC of the dihydrofuran ring or the *trans* conformation ET. Here, as the substituent derived from the quinone ester is now planar and comparatively less bulky to be easily incorporated in the *endo* cavity of the half-boat conformation, ET outstands to be a stable conformation to deliver the major diastereomer through *cis*-fusion. Other orientations of ring-closure would make up the minor isomers of **5** (Scheme 3.2.3c).

To examine the synthetic potential of the protocol, post-functionalization of the cycloadduct was performed. The oxidation of the cycloadduct was attempted with DDQ in acetonitrile to afford the corresponding dehydrogenated product **6a** in 75% yield (Scheme 3.2.4a). Further, for demonstration of the synthetic utility of the designed protocol in large scale, gram scale experiment was also carried out, where the desired product **5a** was obtained in 68% overall yield (Scheme 3.2.4b).

Scheme 3.2.4 Follow up chemistry.

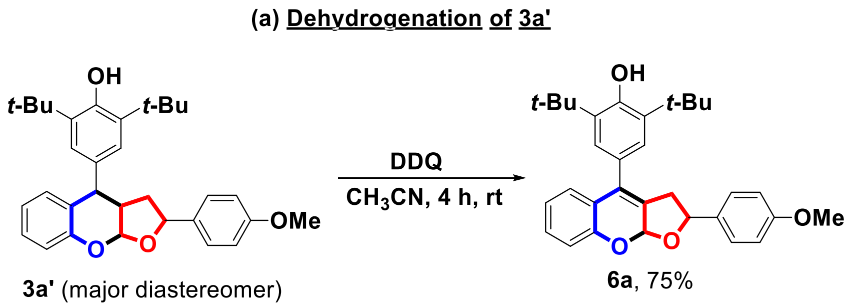

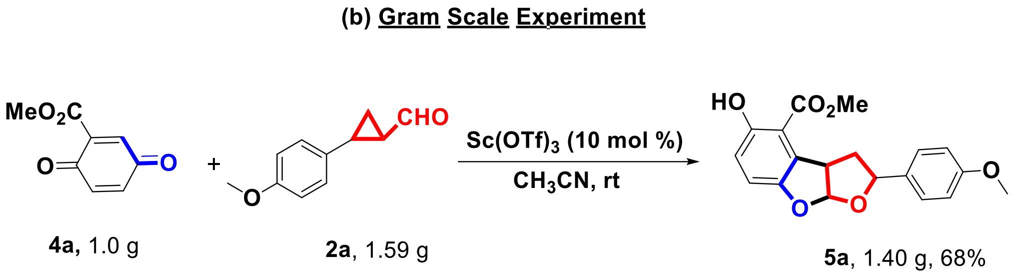

The oxidation with DDQ lead to the formation of a dehydrogenated product **6**, which only had two stereocenters and so, only two diastereomers are possible. This observation motivated us to think of it as an alternate for a process with better overall diastereoselectivity. So, in order to improve the overall diastereoselectivity, we directly subjected the crude mixture (after passing through a silica gel column) of the tetrahydrofurobenzopyran derivative (**3**) to dehydrogenation with DDQ. This experiment led to the exclusive formation of only one diastereomer, however, the yields for the final dehydrogenated product (**6**) were highly compromised (Scheme 3.2.5).

Scheme 3.2.5 Direct dehydrogenation for diastereoselective synthesis of 6

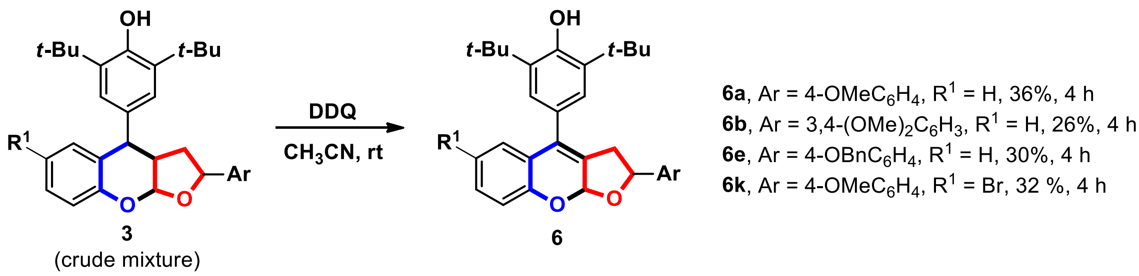

3.3 Conclusion

To conclude, an extremely versatile and time-efficient technique has been developed for single-step diastereoselective synthesis of tetrahydrofurobenzopyran and tetrahydrofurobenzofuran frameworks *via* cascade [2+n] cycloaddition process of the quinone derivatives following an intramolecular rearrangement of the cyclopropane carbaldehydes. The protocol demonstrated high compatibility with both quinone methides and quinone esters. Additionally, the tetrahydrofuranobenzopyran derivative was easily transformed to 3,9*a*-dihydro-2*H*-furo[2,3-*b*]chromene, which is also an essential component in many biological scaffolds. Further exploration and work on the asymmetric version of this transformation are underway in the lab.

3.4 Experimental Section

3.4.1 General Information

All reactions were carried out under an inert atmosphere with oven-dried glassware. All solvents and reagents were obtained from commercial sources and were purified following the standard procedure prior to use. The developed chromatogram was analyzed by UV lamp (254 nm) or *p*-anisaldehyde solution. Products were purified by flash chromatography on silica gel (mesh size 230–400). Melting points were determined using a Stuart SMP30 advanced digital melting point apparatus. Mass spectral data (HRMS) were obtained using the XEVO G2-XS QTOF instrument. The ^{1}H NMR and ^{13}C{^{1}H} NMR spectra were recorded at 400 MHz and 100 MHz respectively on 400 MHz JEOL JNM ECS400 instrument in $CDCl_3$ solvent (unless otherwise mentioned). Chemical shifts of ^{1}H and ^{13}C{^{1}H} NMR spectra are expressed in parts per million (ppm). All coupling constants are absolute values and are expressed in hertz. The description of the signals includes the following: s = singlet, d = doublet, dd = doublet of doublet, t = triplet, dt = doublet of triplet, q = quartet, dq = doublet of quartet, br = broad, and m = multiplet.

3.4.2 General procedure for the synthesis of *p*-quinone methides:

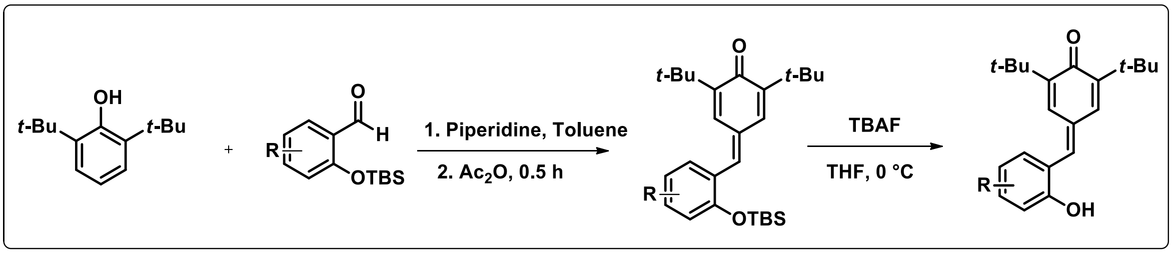

A solution of phenols (1.0 equiv., 4.84 mmol) and aldehydes (1.0 equiv., 4.84 mmol) in toluene (5 mL/mmol substrate) was placed in a Dean-Stark apparatus which was heated to reflux. Piperidine (2.0 equiv., 9.69 mmol) was added dropwise slowly. Then, the temperature was raised to 140 °C (oil bath) and stirred for 12 h. After that, the reaction mixture was cooled to 120 °C, and acetic anhydride (2.0 equiv., 9.69 mmol) was dropwise added. The stirring was continued for 30 min, and the solution was poured on ice water and extracted with CH_2Cl_2 (3 × 50 mL). The organic phases were combined, washed with brine, and dried over anhydrous Na_2SO_4. Then the solvent was evaporated under reduced pressure, and the corresponding products **1a-1f** were obtained after flash column chromatography.

To a solution of **1a-1f** (1.0 equiv., 0.941 mmol) in THF (10 mL/mmol substrate) at 0 °C was added tetrabutylammonium fluoride trihydrate (1.1 equiv., 1.03 mmol). The reaction mixture was stirred for 10 min, and a saturated NH_4Cl solution was added dropwise to quench the reaction. The resulting solution was extracted with Et_2O (3 × 20 mL). Then the combined organic phases were washed with brine and dried over anhydrous Na_2SO_4. The solvent was removed to give the crude product which was purified by flash column chromatography to afford the desired compounds **1a-1f.**

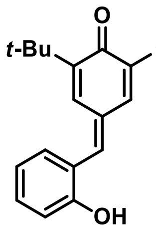

(1a)

2,6-di-*tert*-butyl-4-(2-hydroxybenzylidene)cyclohexa-2,5-dienone (1a)[13]: According to the above general procedure, 2-hydroxy benzaldehyde (1 g, 8.18 mmol), **1a** was obtained as yellow solid (1.65 g, 5.31 mmol, 65% Overall yield): the product was purified by silica gel column chromatography using hexane/ethyl acetate (90:10) as eluent, ^{1}H-NMR (400 MHz, DMSO- d_6): δ 10.16 (s, 1H), 7.56 (s, 1H), 7.43 (d, *J* = 2.1 Hz, 1H), 7.32 (d, *J* = 7.6 Hz, 1H), 7.24 (t, *J* = 8.3 Hz, 1H), 7.19 (s, 1H), 6.89 (dd, *J* = 15.6, 7.9 Hz, 2H), 1.24 (s, 9H), 1.20 (s, 9H).

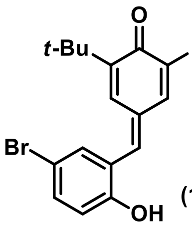

(1b)

4-(5-bromo-2-hydroxybenzylidene)-2,6-di-*tert*-butylcyclohexa-2,5-dienone (1b): According to the above general procedure, 4-bromo-2-hydroxybenzaldehyde (1 g, 4.97 mmol), **1b** was obtained as yellow solid (1.2 g, 3.08 mmol, 63% Overall yield): the product was purified by silica gel column chromatography using hexane/ethyl acetate (90:10) as eluent, ^{1}H-NMR (400 MHz, DMSO-d_6): δ 10.49 (s, 1H), 7.46 – 7.36 (m, 4H), 7.20 (s, 1H), 6.87 (d, *J* = 8.4 Hz, 1H), 1.23 (s, 9H), 1.20 (s, 9H).

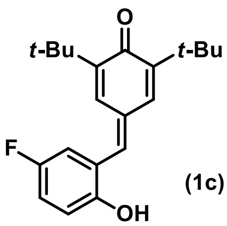

(1c)

2,6-di-*tert*-butyl-4-(5-fluoro-2-hydroxybenzylidene)cyclohexa-2,5-dienone (1c): According to the above general procedure, 4-fluoro-2-hydroxybenzaldehyde (1 g, 7.13 mmol), **1c** was obtained as yellow solid (1.35 g, 4.11 mmol, 58% Overall yield): the product was purified by silica gel column chromatography using hexane/ethyl acetate (90:10) as eluent, ^{1}H-NMR (400 MHz, DMSO-d_6): δ 10.16 (s, 1H), 7.47 (s, 1H), 7.38 (d, *J* = 2.1 Hz, 1H), 7.22 – 7.06 (m, 4H), 6.90 (dd, *J* = 8.9, 4.8 Hz, 1H), 1.23 (s, 9H), 1.20 (s, 9H).

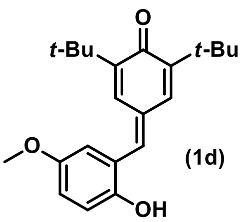

(1d)

2,6-di-*tert*-butyl-4-(2-hydroxy-5-methoxybenzylidene)cyclohexa-2,5-dienone (1d): According to the above general procedure, 2-hydroxy-4-methoxybenzaldehyde (1 g, 6.57 mmol), **1d** was obtained as yellow solid (1.5 g, 4.40 mmol, 67% Overall yield): the product was purified by silica gel column chromatography using hexane/ethyl acetate (90:10) as eluent, ^{1}H-NMR (400 MHz, DMSO-d_6): δ 9.74 (s, 1H), 7.54 (s, 1H), 7.50 (d, *J* = 2.0 Hz, 1H), 7.19 (d, *J* = 2.2 Hz, 1H), 6.89 – 6.84 (m, 3H), 3.68 (s, 3H), 1.24 (s, 9H), 1.21 (s, 9H).

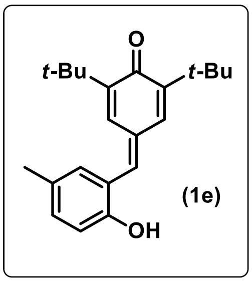

2,6-di-*tert*-butyl-4-(2-hydroxy-5-methylbenzylidene)cyclohexa-2,5-dienone (1e): According to the above general procedure, 2-hydroxy-4-methylbenzaldehyde (1 g, 7.34 mmol), **1e** was obtained as yellow solid (1.3 g, 4.00 mmol, 55% Overall yield): the product was purified by silica gel column chromatography using hexane/ethyl acetate(90:10) as eluent, ^{1}H-NMR (400 MHz, DMSO-d$_6$): δ 9.94 (s, 1H), 7.54 (s, 1H), 7.46 (d, *J* = 2.0 Hz, 1H), 7.18 (s, 1H), 7.12 (s, 1H), 7.07 – 7.04 (m, 1H), 6.81 (d, *J* = 8.2 Hz, 1H), 2.20 (s, 3H), 1.23 (s, 9H), 1.21 (s, 9H).

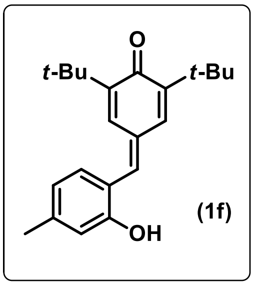

2,6-di-*tert*-butyl-4-(2-hydroxy-4-methylbenzylidene)cyclohexa-2,5-dienone (1f): According to the above general procedure, 2-hydroxy-5-methylbenzaldehyde (1 g, 7.34 mmol), **1f** was obtained as yellow solid (1.0 g, 3.08 mmol, 42% Overall yield): the product was purified by silica gel column chromatography using hexane/ethyl acetate (90:10) as eluent, ^{1}H-NMR (400 MHz, DMSO-d$_6$): δ 10.09 (s, 1H), 7.53 (s, 1H), 7.45 (d, *J* = 1.5 Hz, 1H), 7.22 (d, *J* = 7.8 Hz, 1H), 7.16 (s, 1H), 6.74 – 6.69 (m, 2H), 2.23 (s, 3H), 1.23 (s, 9H), 1.20 (s, 9H).

3.4.3 General procedure for the Synthesis of Diols:

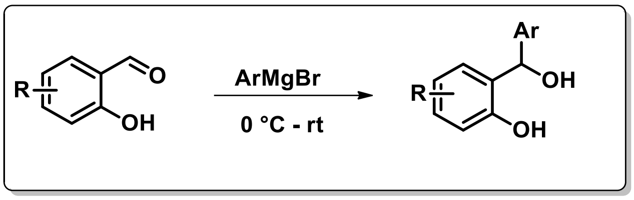

To a solution of corresponding salicylaldehyde (10.0 mmol, 1.0 equiv.) in THF (20.0 ml) was added a solution of 1M arylmagnesium bromide in THF (30.0 mmol, 3.0 equiv.) dropwise at 0 ºC. The resulting solution was allowed to warm to room temperature and stirred for 2 hours, and monitored by TLC. After completion of the reaction, the reaction mixture was quenched with saturated aqueous NH_4Cl solution (30.0 ml) at 0 ºC. It was then extracted with ethyl acetate (3 x 30.0 mL). The combined organic layers were washed with brine, dried over Na_2SO_4, and concentrated in vacuo. The residue was purified by column chromatography to afford the desired product. (60-90% yield).

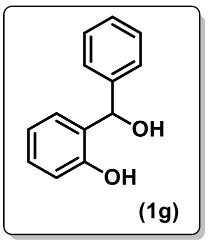

2-(hydroxy(phenyl)methyl)phenol (1g)[13e]: According to the above general procedure, 2-hydroxybenzaldehyde (0.5mL, 4.7 mmol) and bromobenzene (2.0 mL, 19.0 mmol). **1g** was obtained as White solid (940 mg, 96% yield): the product was purified by silica gel column chromatography using hexane/ethyl acetate (80:20) as eluent, ^{1}H-NMR (400 MHz, CDCl$_3$): δ 7.86 (s, 1H), 7.39 – 7.31 (m, 5H), 7.21 – 7.17 (m, 1H), 6.91 – 6.79 (m, 3H), 6.02 (d, *J* = 3.2 Hz, 1H).

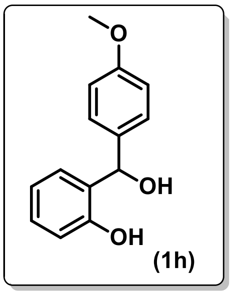

2-(hydroxy(4-methoxyphenyl)methyl)phenol (1h): According to the above general procedure, Salicylaldehyde (1.0 mL, 9.4 mmol) and 4-bromoanisole (4.7 mL, 37.0 mmol). **1h** was obtained as colourless oil (2.16 g, 98% yield): the product was purified by silica gel column chromatography using hexane/ethyl acetate (80:20) as eluent, ^{1}H-NMR (400 MHz, $CDCl_3$): δ 8.03 (s, 1H), 7.30 (d, *J* = 8.7 Hz, 2H), 7.20 – 7.16 (m, 1H), 6.91 – 6.86 (m, 3H), 6.83 – 6.77 (m, 2H), 5.97 (d, *J* = 2.3 Hz, 1H), 3.79 (s, 3H), 2.81 (s, 1H).

3.4.4 General procedure for the synthesis of quinone ester:

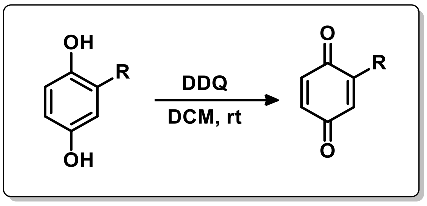

To a solution of the hydroquinone (1 equiv., 6.01 mmol) in DCM (30 mL) was added DDQ (1.5 equiv., 9.02 mmol) portion wise at room temperature. After 2 h, the reaction mixture was diluted with DCM (150 mL), then washed with a mixture of water (100 mL) and saturated aqueous sodium bicarbonate (10 mL) five times. Combined organics were washed with brine (200 mL), dried over Na_2SO_4, and concentrated in vacuo to afford generally orange or red solids **4.**

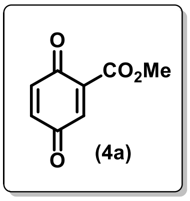

Methyl 3,6-dioxocyclohexa-1,4-dienecarboxylate (4a)[14]: According to the above general procedure, methyl 2,5-dihydroxybenzoate (1 g, 5.94 mmol), **4a** was obtained as brown solid (0.87 g, 5.23 mmol, 89% yield): ^{1}H-NMR (400 MHz, $CDCl_3$): δ 7.10 (d, *J* = 1.8 Hz, 1H), 6.82 (d, *J* = 1.9 Hz, 2H), 3.90 (s, 3H).

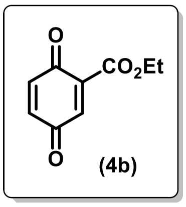

Ethyl 3,6-dioxocyclohexa-1,4-dienecarboxylate (4b): According to the above general procedure, ethyl 2,5-dihydroxybenzoate (1 g, 5.48 mmol), **4b** was obtained as reddish brown solid (0.85 g, 4.71 mmol, 86% yield): ^{1}H-NMR (400 MHz, $CDCl_3$): δ 7.08 (d, *J* = 1.9 Hz, 1H), 6.81 (d, *J* = 1.6 Hz, 2H), 4.36 (q, *J* = 7.2 Hz, 2H), 1.35 (t, *J* = 7.1 Hz, 3H).

3.4.5 General procedure for the synthesis of *trans*-2- arylcyclopropanecarbaldehydes:

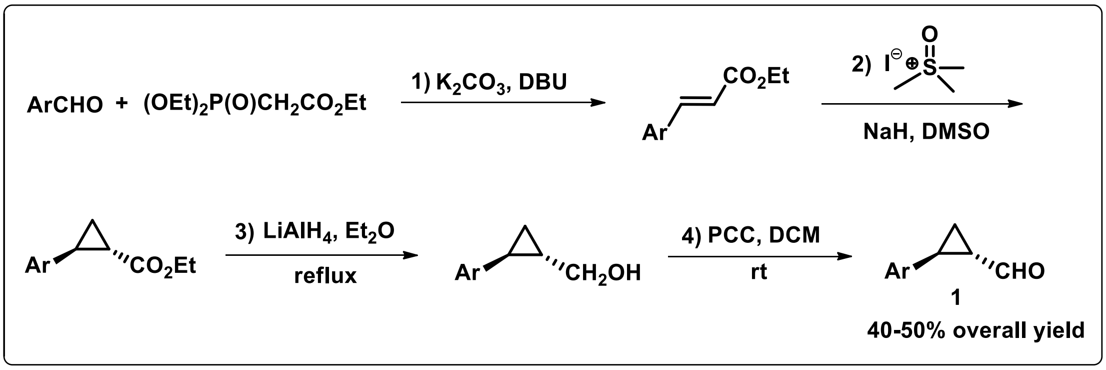

1). To a mixture of triethyl phosphonoacetate (1.1 equiv., 24.23 mmol), DBU (0.035 equiv., 0.771 mmol), and finely ground K_2CO_3 (2 equiv., 44.06 mmol) was added ArCHO (1 equiv., 22.03 mmol), and the resulting mixture was stirred using a magnetic stirrer for 4 h at room temperature under argon atmosphere. Ethyl acetate was added to the crude mixture and the solid was filtered off. The solid was rinsed with ethyl acetate, and the combined filtrate was concentrated. The resulting oil was distilled under reduced pressure using a bulb-to-bulb apparatus (10 mm Hg/240 °C) to give corresponding alkene (yield 84%) (E:Z = 99:1).

2). A suspension of TMSOI (1.2 equiv., 23.27 mmol) and NaH (1.5 equiv., 28.95 mmol) in anhydrous DMSO (15 mL) was stirred for 1 h. A DMSO solution (14 mL) of alkene (1 equiv., 19.3 mmol) was added at 0 °C. The reaction mixture was stirred at 55 °C (oil bath) for 24 h. Another suspension of TMSOI (0.3 equiv., 5.79 mmol) and NaH (0.3 equiv., 5.79 mmol) in DMSO (10 mL) was added to the reaction mixture, and the reaction was stirred at 65 °C (oil bath) for 84 h. The solution was poured into a brine solution and extracted with ethyl acetate. The combined organic layer was washed with water and dried over $MgSO_4$, concentrated, and purified by silica gel column to afford corresponding cyclopropane derivative as a white solid (60-80% yield).

3). To a stirred solution of LAH (1.5 equiv., 5.98 mmol) in 7 mL diethyl ether was added dropwise a solution of cyclopropane ester (1 equiv., 3.99 mmol) in 3 mL diethyl ether under N_2 atmosphere. After the addition was completed, the reaction mixture was refluxed for another 6 h. The reaction mixture was then cooled to rt, and the excess LAH was destroyed by water. 15 mL of 10% H_2SO_4 and 8 mL of ether were added, and the aqueous layer was extracted several times with diethyl ether. The combined organic layer was washed with water and 5% $NaHCO_3$, dried over $MgSO_4$, and concentrated in a rotary evaporator (90-95% yield). Without any further purification, the crude material (a colorless oil) was used for the next step.

4). To a solution of cyclopropane alcohol (6.8 mmol, 1 equiv.) in dry DCM (14 mL), PCC (2 equiv., 13.6 mmol) was added in a portion-wise manner through a solid addition tube under N_2 atmosphere. After 3 h reaction mixture was filtered through a small plug of celite and concentrated in vacuo. The crude mixture was purified by silica gel column chromatography using ethyl acetate in hexane as an eluent. Starting from aryl aldehyde the 2-arylcyclopropanecarbaldehydes was obtained in 40-55% overall yield.

***trans*-2-(4-methoxyphenyl)cyclopropane-1-carbaldehyde (2a):**[12]

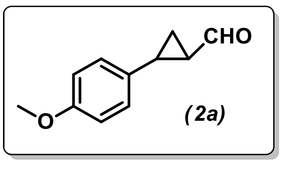

According to the above general procedure, 4-methoxybenzaldehyde (1.0 g, 7.35 mmol), **2a** was obtained as colorless crystals (0.62 g, 3.53 mmol, 48% Overall yield): the product was purified by silica gel column chromatography using hexane/ethyl acetate (95:5) as eluent, ^{1}H-NMR (400 MHz, $CDCl_3$): δ 9.28 (d, *J* = 4.7 Hz, 1H), 7.03 (d, *J* = 8.8 Hz, 2H), 6.82 (d, *J* = 8.8 Hz, 2H), 3.77 (s, 3H), 2.61 – 2.55 (m, 1H), 2.11 – 2.05 (m, 1H), 1.71 – 1.66 (m, 1H), 1.49 – 1.44 (m, 1H).

trans*-2-(3,4-dimethoxyphenyl)cyclopropanecarbaldehyde (2b):*

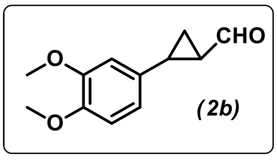

According to the above general procedure, 3,4-dimethoxybenzaldehyde (1.0 g, 6.02 mmol), **2b** was obtained in off white solid (0.53 g, 2.59 mmol, 43% Overall yield): the product was purified by silica gel column chromatography using hexane/ethyl acetate (90:10) as eluent, ^{1}H-NMR (400 MHz, $CDCl_3$): δ 9.30 (d, *J* =

4.7 Hz, 1H), 6.78 (d, *J* = 7.9 Hz, 1H), 6.67 – 6.64 (m, 2H), 3.86 (s, 3H), 3.85 (s, 3H), 2.63 – 2.56 (m, 1H), 2.13 – 2.08 (m, 1H), 1.72 – 1.65 (m, 1H), 1.51 – 1.47 (m, 1H).

***trans*-2-(3,4,5-trimethoxyphenyl)cyclopropanecarbaldehyde (2c):**

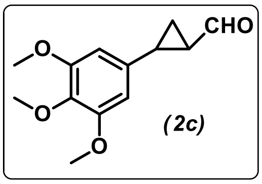

According to the above general procedure, 3,4,5-trimethoxybenzaldehyde (1.0 g, 5.09 mmol), **2d** was obtained in white solid (0.54 g, 2.28 mmol, 45% Overall yield): the product was purified by silica gel column chromatography using hexane/ethyl acetate (85:15) as eluent, ^{1}H-NMR (400 MHz, $CDCl_3$): δ 9.32 (d, *J* = 5.3 Hz, 1H), 6.33 (s, 2H), 3.83 (s, 6H), 3.80 (s, 3H), 2.61 – 2.56 (m, 1H), 2.17 – 2.11 (m, 1H), 1.72 – 1.67 (m, 1H), 1.51 – 1.47 (m, 1H).

***trans*-2-(3-ethoxy-4-methoxyphenyl)cyclopropanecarbaldehyde (2d):**

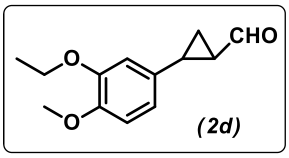

According to the above general procedure, 3-ethoxy-4-methoxybenzaldehyde (1.0 g, 5.54 mmol), **2d** was obtained in white solid (0.46 g, 2.55 mmol, 46% Overall yield): the product was purified by silica gel column chromatography using hexane/ethyl acetate (85:15) as eluent, ^{1}H-NMR (400 MHz, $CDCl_3$): δ 9.29 (d, *J* = 4.8 Hz, 1H), 6.78 (d, *J* = 8.8 Hz, 1H), 6.66 – 6.63 (m, 2H), 4.07 (q, *J* = 7.0 Hz, 2H), 3.84 (s, 3H), 2.61 – 2.54 (m, 1H), 2.12 – 2.05 (m, 1H), 1.72 – 1.65 (m, 1H), 1.50 – 1.46 (m, 1H), 1.45 (t, *J* = 7.0 Hz, 3H).

***trans*-2-(4-(benzyloxy)phenyl)cyclopropanecarbaldehyde (2e):**

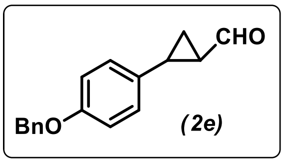

According to the above general procedure, 4-(benzyloxy)benzaldehyde (1.0 g, 4.71 mmol), **2e** was obtained in white solid (0.55 g, 2.16 mmol, 46% Overall yield): the product was purified by silica gel column chromatography using hexane/ethyl acetate (95:5) as eluent, ^{1}H-NMR (400 MHz, $CDCl_3$): δ 9.29 (d, *J* = 4.7 Hz, 1H), 7.41 – 7.33 (m, 5H), 7.03 (d, *J* = 8.7 Hz, 2H), 6.89 (d, *J* = 8.7 Hz, 2H), 5.04 (s, 2H), 2.60 – 2.55 (m, 1H), 2.11 – 2.03 (m, 1H), 1.72 – 1.66 (m, 1H), 1.49 – 1.44 (m, 1H).

***trans*-2-(benzo[d][1,3]dioxol-5-yl)cyclopropanecarbaldehyde (2f):**

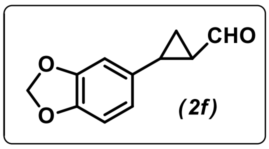

According to the above general procedure, benzo[d][1,3]dioxole-5-carbaldehyde (1 g, 6.66 mmol), **2f** was obtained in off-white solid (0.60 g, 3.15 mmol, 47% Overall yield): the product was purified by silica gel column chromatography using hexane/ethyl acetate (90:10) as eluent, ^{1}H-NMR (400 MHz, $CDCl_3$): δ 9.29 (d, J = 4.6 Hz, 1H), 6.71 (d, J = 7.9 Hz, 1H), 6.61 (dd, J = 8.0, 1.7 Hz, 1H), 6.56 (d, J = 1.7 Hz, 1H), 5.92 (s, 2H), 2.59 – 2.53 (m, 1H), 2.10 – 2.05 (m, 1H), 1.70 – 1.64 (m, 1H), 1.46 – 1.42 (m, 1H).

***trans*-2-(4-butoxyphenyl)cyclopropanecarbaldehyde (2g):**

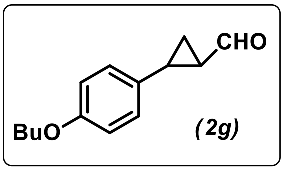

According to the above general procedure, 4-butoxybenzaldehyde (1 g, 5.61 mmol), **2g** was obtained in White solid (0.50 g, 2.29 mmol, 41% Overall yield): the product was purified by silica gel column chromatography using hexane/ethyl acetate (95:5) as eluent, ^{1}H-NMR (400 MHz, $CDCl_3$): δ 9.28 (d, *J* = 4.7 Hz, 1H), 7.02 (d, *J* = 8.7 Hz, 2H), 6.81 (d, *J* = 8.7 Hz, 2H), 3.92 (t, *J* = 6.5 Hz, 2H), 2.61 – 2.55 (m, 1H), 2.10 – 2.06 (m, 1H), 1.76 – 1.67 (m, 3H), 1.49 – 1.44 (m, 3H), 0.96 (t, *J* = 7.4 Hz, 3H).

***trans*-2-(3-bromo-4-methoxyphenyl)cyclopropanecarbaldehyde (2h):**

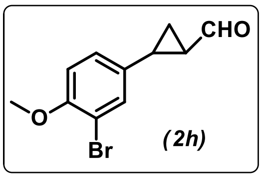

According to the above general procedure, 3-bromo-4-methoxybenzaldehyde (1 g, 4.65 mmol), **2h** was obtained in white solid (0.48 g, 1.88 mmol, 40% Overall yield): the product was purified by silica gel column chromatography using hexane/ethyl acetate (95:5) as eluent, ^{1}H-NMR (400 MHz, $CDCl_3$): δ 9.32 (d, *J* = 4.5 Hz, 1H), 7.28 (d, *J* = 2.2 Hz, 1H), 7.03 (dd, *J* = 8.5, 2.2 Hz, 1H), 6.81 (d, *J* = 8.5 Hz, 1H), 3.86 (s, 3H), 2.58 – 2.53 (m, 1H), 2.12 – 2.07 (m, 1H), 1.71 – 1.66 (m, 1H), 1.49 – 1.43 (m, 1H).

***trans*-2-(3-fluoro-4-methoxyphenyl)cyclopropanecarbaldehyde (2i)**:

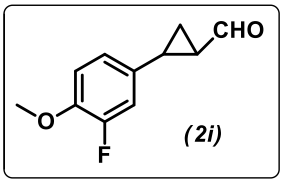

According to the above general procedure, 3-fluoro-4-methoxybenzaldehyde (1 g, 6.48 mmol), **2i** was obtained in white solid (0.57 g, 2.93 mmol, 45% Overall yield): the product was purified by silica gel column chromatography using hexane/ethyl acetate (95:5) as eluent, ^{1}H-NMR (400 MHz, $CDCl_3$): δ 9.31 (d, *J* = 5.2 Hz, 1H), 6.89 – 6.80 (m, 3H), 3.85 (s, 3H), 2.60 – 2.52 (m, 1H), 2.11 – 2.06 (m, 1H), 1.71 – 1.67 (m, 1H), 1.46 – 1.43 (m, 1H).

***trans*-(E)-2-styrylcyclopropanecarbaldehyde (2j):**

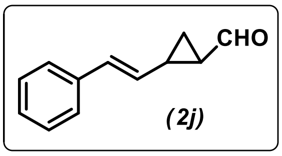

According to the above general procedure, Cinnamaldehyde (1 g, 7.56 mmol), **2j** was obtained in pale yellow liquid (0.57 g, 3.30 mmol, 43% Overall yield): the product was purified by silica gel column chromatography using hexane/ethyl acetate (95:5) as eluent, ^{1}H-NMR (400 MHz, $CDCl_3$): δ 9.24 (d, *J* = 4.7 Hz, 1H), 7.30 – 7.28 (m, 5H), 6.55 (d, *J* = 15.8 Hz, 1H), 5.76 (dd, *J* = 15.8, 8.6 Hz, 1H), 2.31 – 2.24 (m, 1H), 2.06 – 2.01 (m, 1H), 1.63 – 1.60 (m, 1H), 1.32 – 1.28 (m, 1H).

***trans*-2-(naphthalen-2-yl)cyclopropanecarbaldehyde (2k):**

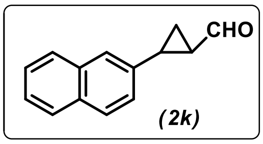

According to the above general procedure, 2-naphthaldehyde (1.0 g, 6.41 mmol), **2k** was obtained in off white solid (0.53 g, 2.69 mmol, 42% Overall yield): the product was purified by silica gel column chromatography using hexane/ethyl acetate (95:5) as eluent, ^{1}H-NMR

(400 MHz, $CDCl_3$): δ 9.37 (d, *J* = 4.6 Hz, 1H), 7.80 – 7.75 (m, 3H), 7.58 (s, 1H), 7.49 – 7.41 (m, 2H), 7.20 (dd, *J* = 8.6, 1.8 Hz, 1H), 2.82 – 2.76 (m, 1H), 2.30 – 2.24 (m, 1H), 1.82 – 1.77 (m, 1H), 1.68 – 1.63 (m, 1H).

***trans*-2-(*p*-tolyl)cyclopropanecarbaldehyde (2l):**

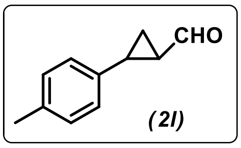

According to the above general procedure, 4-methylbenzaldehyde (1.0 g, 8.32 mmol), **2l** was obtained in colorless liquid (0.69 g, 4.32 mmol, 52% Overall yield)**:** the product was purified by silica gel column chromatography using hexane/ethyl acetate (95:5) as eluent, ^{1}H-NMR (400 MHz, $CDCl_3$): δ 9.29 (d, *J* = 4.6 Hz, 1H), 7.10 (d, *J* = 7.9 Hz, 2H), 7.00 (d, *J* = 8.1 Hz, 2H), 2.63 – 2.56 (m, 1H), 2.31 (s, 3H), 2.15 – 2.10 (m, 1H), 1.74 – 1.67 (m, 1H), 1.53 – 1.47 (m, 1H).

***trans*-2-mesitylcyclopropanecarbaldehyde (2m):**

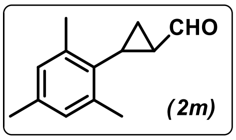

According to the above general procedure, 2,4,6-trimethylbenzaldehyde (1.0 g, 6.75 mmol), **2m** was obtained in pale yellow liquid (0.53 g, 2.84 mmol, 42% Overall yield): the product was purified by silica gel column chromatography using hexane/ethyl acetate (95:5) as eluent, ^{1}H-NMR (400 MHz, $CDCl_3$): δ 9.28 (d, *J* = 5.5 Hz, 1H), 6.84 (s, 2H), 2.44 – 2.36 (m, 1H), 2.32 (s, 6H), 2.25 (s, 3H), 1.97 – 1.91 (m, 1H), 1.79 – 1.74 (m, 1H), 1.39 – 1.34 (m, 1H).

3.4.6 Representative procedure for the synthesis of tetrahydrofurobenzopyran derivatives 3:

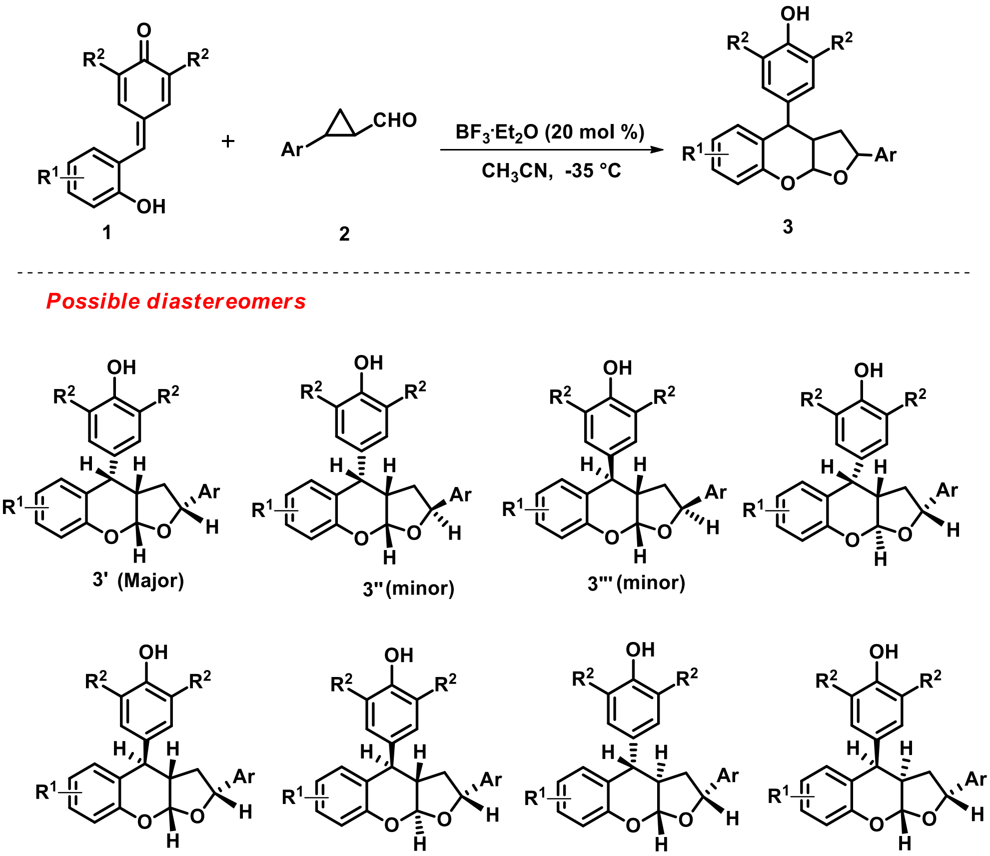

A long neck round-bottom flask equipped with a magnetic stir bar was charged **1** (1 equiv., 0.3 mmol), **2** (1.2 equiv., 0.36 mmol), and dry CH_3CN (2 mL) under a nitrogen atmosphere. The reaction mixture is stirred for 15 minutes at -35 °C. To the reaction mixture at -35 °C, added slowly (not at once, but within a period of about 30 seconds) $BF_3{\cdot}OEt_2$ (0.2 equiv., 0.06 mmol). On completion (after about 2-3 h, as monitored by TLC), the reaction mixture was filtered through a small plug of celite and concentrated in a rotary evaporator. Diastereomeric ratios were determined from the crude ^{1}H NMR analysis, which shows the formation of four diastereomers. The crude mixture was further purified by column chromatography on silica gel with ethyl acetate/hexane as eluent to afford **3**.

As the molecule incorporates four stereocentres, there should be eight possible diastereomers. The structures of these possible diastereomers are shown in the scheme. However, from the crude ^{1}H NMR analysis, we could observe the formation of four diastereomers, out of which, we were able to isolate three isomers (**3d'**, **3d''**, **3d'''**) for compound **3d**. The assignment of their relative stereochemistry is done on the basis of the 2D-NMR analysis. In most of the cases, the diastereomers had R_f values very close to each other, making them inseparable. Consequently, we could not get the publishable data for the minor isomers in most of the cases, and so, the spectroscopic data for only the major isomers are analysed and reported.

2,6-di-*tert*-butyl-4-(2-(4-methoxyphenyl)-3,3a,4,9a-tetrahydro-2*H*-furo[2,3-b]chromen-4-yl)phenol

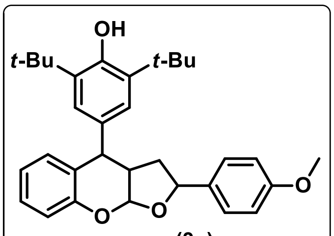

(3a)

(3a): Reaction time: 4 h. **1a** (0.1 g, 0.3 mmol), **2a** (0.063 g, 0.36 mmol), **3a** (0.121 g, 0.25 mmol). Overall Yield: 83 %. Nature: White solid. mp: 208-210 °C: the product was purified by silica gel column chromatography using hexane/ethyl acetate (95:5) as eluent. ^{1}H-NMR (400 MHz, $CDCl_3$): δ 7.26 (d, *J* = 8.6 Hz, 2H), 7.19 (t, *J* = 7.5 Hz, 1H), 7.00 (d, *J* = 8.8 Hz, 3H), 6.87 – 6.80 (m, 4H), 5.94 (d, *J* = 4.8 Hz, 1H), 5.17 (s, 1H), 5.00 (dd, *J* = 10.5, 5.9 Hz, 1H), 4.39 (d, *J* = 4.5 Hz, 1H), 3.78 (s, 3H), 2.98 – 2.90 (m, 1H), 2.12 – 2.04 (m, 1H), 1.84 – 1.76 (m, 1H), 1.41 (s, 18H): $^{13}C\{^1H\}$ NMR (100 MHz, $CDCl_3$): δ 159.2, 153.0, 152.8, 136.0, 134.1, 130.9, 128.5, 128.1, 127.8, 125.9, 124.6, 120.9, 116.8, 113.9, 102.1, 82.7, 55.3, 46.9, 42.5, 34.7, 34.4, 30.4: HRMS (ESI, Q-TOF) *m/z*: $[M - H]^-$ Calculated for $C_{32}H_{37}O_4$ 485.2692, found 485.2697.

2,6-di-*tert*-butyl-4-(2-(3,4-dimethoxyphenyl)-3,3a,4,9a-tetrahydro-2*H*-furo[2,3-*b*]chromen-4-yl)

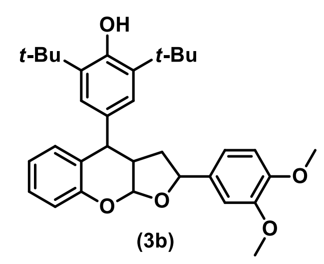

(3b)

phenol (3b): Reaction time: 4 h. **1a** (0.1 g, 0.3 mmol), **2b** (0.074 g, 0.36 mmol), **3b** (0.124 g, 0.24 mmol). Overall Yield: 80%. Nature: White solid. mp: 185-187 °C: the product was purified by silica gel column chromatography using hexane/ethyl acetate (95:5) as eluent. ^{1}H-NMR (400 MHz, $CDCl_3$): δ 7.19 – 7.13 (m, 1H), 6.99 (s, 2H), 6.95 (dd, *J* = 4.9, 1.5 Hz, 2H), 6.88 – 6.82 (m, 2H), 6.78 – 6.75 (m, 2H), 5.96 (d, *J* = 4.9 Hz, 1H), 5.17 (s, 1H), 4.99 (dd, *J* = 10.4, 6.0 Hz, 1H), 4.38 (d, *J* = 4.5 Hz, 1H), 3.86 (s, 3H), 3.84 (s, 3H), 2.97 – 2.91 (m, 1H), 2.14 – 2.08 (m, 1H), 1.84 – 1.77 (m, 1H), 1.40 (s, 18H): $^{13}C\{^1H\}$ NMR (100 MHz, $CDCl_3$): δ 153.0, 152.8, 149.2, 148.6, 136.0, 134.6, 130.7, 128.6, 128.0, 125.9, 124.9, 121.1, 118.8, 116.6, 110.5, 109.2, 102.3, 83.0, 55.9, 55.8, 46.8, 42.5, 35.0, 34.4, 30.4: HRMS (ESI, Q-TOF) *m/z*: [M - H]$^-$ Calculated for $C_{33}H_{39}O_5$ 515.2797, found 515.2790.

2,6-di-*tert*-butyl-4-(2-(3,4,5-trimethoxyphenyl)-3,3a,4,9a-tetrahydro-*2H*-furo[2,3-*b*]chromen-4-yl) phenol (3c): Reaction time: 5 h. **1a** (0.1 g, 0.3 mmol), **2c** (0.074 g, 0.36 mmol), **3c** (0.124 g, 0.23 mmol). Overall Yield: 76%. Nature: Yellow solid. mp: 180-182 °C: the product was purified by silica gel column chromatography using hexane/ethyl acetate (90:10) as eluent ^{1}H-NMR (400 MHz, $CDCl_3$): δ 7.20 – 7.16 (m, 1H), 7.00 (s, 2H), 6.96 (d, *J* = 8.1 Hz, 1H), 6.86 (d, *J* = 4.1 Hz, 2H), 6.46 (s, 2H), 6.10 (d, *J* = 4.7 Hz, 1H), 5.24 – 5.20 (m, 1H), 5.15 (s, 1H), 4.39 (d, *J* = 4.4 Hz, 1H), 3.82 (s, 6H), 3.79 (s, 3H), 3.01 – 2.93 (m, 1H), 2.40 – 2.33 (m, 1H), 1.80 – 1.75 (m, 1H), 1.40 (s, 18H): $^{13}C\{^1H\}$ NMR (100 MHz, $CDCl_3$): δ 153.2, 153.0, 152.9, 137.9, 136.0, 130.6, 128.6, 128.0, 125.8, 124.8, 121.1, 116.5, 103.2, 103.0, 102.4, 83.2, 60.8, 56.1, 46.8, 42.4, 35.0, 34.4, 30.4: HRMS (ESI, Q-TOF) *m/z*: [M - H]$^-$ Calculated for $C_{34}H_{42}O_6$ 545.2903, found 545.2903.

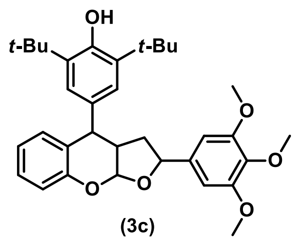

(3c)

2,6-di-tert-butyl-4-(2-(3-ethoxy-4-methoxyphenyl)-3,3a,4,9a-tetrahydro-2H-furo[2,3-b]chromen-4-yl) phenol (3d): Reaction time: 4 h. **1a** (0.1 g, 0.3 mmol), **2d** (0.079 g, 0.36 mmol), **3d** (0.124 g, 0.233 mmol). Overall Yield: 78%. Nature**:** White solid. mp: 180-182 °C: the product was purified by silica gel column chromatography using hexane/ethyl acetate (95:5) as eluent. ^{1}H-NMR (400 MHz, $CDCl_3$): δ 7.20 – 7.13 (m, 1H), 6.99 (s, 2H), 6.98 - 6.91 (m, 2H), 6.89 - 6.82 (m, 2H), 6.82 - 6.74 (m, 2H), 5.95 (d, J = 4.9 Hz, 1H), 5.17 (s, 1H), 4.97 (dd, J = 10.4, 6.0 Hz, 1H), 4.38 (d, J = 4.5 Hz, 1H), 4.14 – 4.01 (m, 2H), 3.83 (s, 3H), 2.97 – 2.93 (m, 1H), 2.13 – 2.08 (m, 1H), 1.84 – 1.76 (m, 1H), 1.45 (t, J = 7.0 Hz, 3H), 1.40 (s, 18H): $^{13}C\{^1H\}$ NMR (100 MHz, $CDCl_3$): δ 153.0, 152.8, 148.8, 148.5, 136.0, 134.5, 130.7, 128.5, 128.0, 125.9, 124.9, 121.1, 118.8, 116.6, 110.8, 110.6, 102.3, 82.9, 64.1, 56.0, 46.8, 42.5, 34.9, 34.4, 30.4, 14.9: HRMS (ESI, Q-TOF) m/z: [M - H]$^-$ Calculated for $C_{34}H_{41}O_5$ 529.2954, found 529.2959.

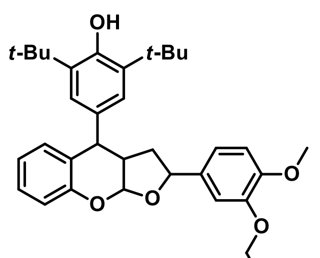

(3d)

4-(2-(4-(benzyloxy)phenyl)-3,3a,4,9a-tetrahydro-2H-furo[2,3-b]chromen-4-yl)-2,6-di-*tert*-butylphenol (**3e**): Reaction time: 3 h. **1a** (0.1 g, 0.3 mmol), **2e** (0.091 g, 0.36 mmol), **3e** (0.144 g, 0.255 mmol). Overall Yield: 85%. Nature: White solid. mp: 120-122 °C: the product was purified by silica gel column chromatography using hexane/ethyl acetate (95:5) as eluent. ^{1}H-NMR (400 MHz, $CDCl_3$): δ 7.44 - 7.29 (m, 5H), 7.26 (d, *J* = 8.6 Hz, 2H), 7.21 - 7.16 (m, 1H), 7.02 - 6.99 (m, 3H), 6.92 (d, *J* = 8.7 Hz, 2H), 6.87 - 6.81 (m, 2H), 5.95 (d, *J* = 4.9 Hz, 1H), 5.17 (s, 1H), 5.04 (s, 2H), 5.00 (dd, *J* = 10.5, 5.9 Hz, 1H), 4.39 (d, *J* = 4.5 Hz, 1H), 2.99 - 2.91 (m, 1H), 2.14 - 2.04 (m, 1H), 1.84 – 1.76 (m, 1H), 1.41 (s, 18H): $^{13}C\{^1H\}$ NMR (100 MHz, $CDCl_3$): δ 158.5, 153.0, 152.8, 137.1, 136.0, 134.4, 130.9, 128.6, 128.5, 128.1, 128.0, 127.9,

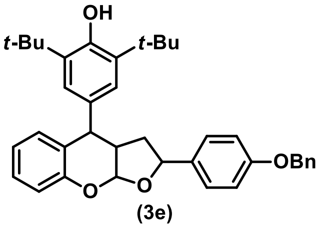

(3e)

127.5, 125.9, 124.5, 121.0, 116.8, 114.8, 102.1, 82.7, 70.0, 46.9, 42.5, 34.7, 34.4, 30.5: HRMS (ESI, Q-TOF) *m/z*: $[M - H]^-$ Calculated for $C_{38}H_{41}O_4$ 561.3005, found 561.3008.

4-(2-(benzo[d][1,3]dioxol-5-yl)-3,3a,4,9a-tetrahydro-2H-furo[2,3-b]chromen-4-yl)-2,6-di-tert-butyl phenol (3f): Reaction time: 4 h. **1a** (0.1 g, 0.3 mmol), **2f** (0.068 g, 0.36 mmol), **3f** (0.115 g, 0.23 mmol). Overall Yield: 76%. Nature: White solid. mp: 158-160 °C. the product was purified by silica gel column chromatography using hexane/ethyl acetate (95:5) as eluent. ^{1}H-NMR (400 MHz, $CDCl_3$): δ 7.22 – 7.15 (m, 1H), 7.00 (dd, *J* = 8.1, 0.9 Hz, 1H), 6.98 (s, 2H), 6.88 - 6.82 (m, 3H), 6.76 - 6.70 (m, 2H), 5.94 - 5.90 (m, 3H), 5.17 (s, 1H), 4.96 (dd, *J* = 10.4, 5.9 Hz, 1H), 4.38 (d, *J* = 4.6 Hz, 1H), 2.95 - 2.89 (m, 1H), 2.11 - 2.01 (m, 1H), 1.84 – 1.77 (m, 1H), 1.40 (s, 18H): $^{13}C\{^1H\}$ NMR (100 MHz, $CDCl_3$): δ 152.9, 152.8, 147.9, 147.2, 136.0, 136.0, 130.9, 128.5, 128.2, 125.8, 124.4, 121.0, 120.0, 116.8, 107.9, 107.0, 102.0, 101.0, 82.9, 46.8, 42.4, 34.8, 34.4, 30.4: HRMS (ESI, Q-TOF) *m/z*: $[M - H]^-$ Calculated for $C_{32}H_{35}O_5$ 499.2484, found 499.2497.

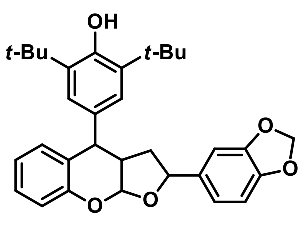

(3f)

4-(2-(4-butoxyphenyl)-3,3a,4,9a-tetrahydro-2*H*-furo[2,3-b]chromen-4-yl)-2,6-di-*tert*-butylphenol (3g): Reaction time: 3 h. **1a** (0.1 g, 0.3 mmol), **2g** (0.078 g, 0.36 mmol), **3g** (0.116 g, 0.22 mmol). Overall yield: 73%. Nature: White solid. mp: 130-132 °C: the product was purified by silica gel column chromatography using hexane/ethyl acetate (95:5) as eluent. ^{1}H-NMR (400 MHz, $CDCl_3$): δ 7.25 - 7.22 (m, 2H), 7.20 - 7.15 (m, 1H), 7.01 - 6.98 (m, 3H), 6.86 - 6.80 (m, 4H), 5.94 (d, *J* = 4.9 Hz, 1H), 5.16 (s, 1H), 4.99 (dd, *J* = 10.5, 5.9 Hz, 1H), 4.38 (d, *J* = 4.5 Hz, 1H), 3.92 (t, *J* = 6.5 Hz, 2H), 2.98 - 2.89 (m, 1H), 2.10 – 2.05 (m, 1H), 1.84 - 1.70 (m, 3H), 1.49 - 1.43 (m, 2H), 1.40 (s, 18H), 0.95 (t, *J* = 7.4 Hz, 3H): $^{13}C\{^1H\}$ NMR (100 MHz, $CDCl_3$): δ 158.8, 153.0, 152.8, 136.0, 133.8, 130.9, 128.5, 128.1, 127.8, 125.9, 124.6, 120.9, 116.8, 114.4, 102.1, 82.8, 67.7, 46.8, 42.5, 34.7, 34.4, 31.3, 30.4, 19.3, 13.9: HRMS (ESI, Q-TOF) *m/z*: $[M - H]^-$ Calculated for $C_{35}H_{43}O_4$ 527.3161, found 527.3165.

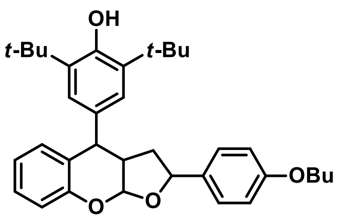

(3g)

4-(2-(3-bromo-4-methoxyphenyl)-3,3a,4,9a-tetrahydro-2*H*-furo[2,3-b]chromen-4-yl)-2,6-di-*tert*-butylphenol (3h): Reaction time**:** 4 h. **1a** (0.1 g, 0.3 mmol), **2h** (0.092 g, 0.36 mmol), **3h** (0.113 g, 0.20 mmol). Overall yield: 67%. Nature: White solid. mp: 158-160 °C: the product was purified by silica gel column chromatography using hexane/ethyl acetate (95:5) as eluent. ^{1}H-NMR (400 MHz, $CDCl_3$): δ 7.53 (d, *J* = 2.1 Hz, 1H), 7.24 - 7.17 (m, 2H), 7.01 (d, *J* = 8.4 Hz, 1H), 6.98 (s, 2H), 6.87 - 6.79 (m, 3H), 5.94 (d, *J* = 4.8 Hz, 1H), 5.17 (s, 1H), 4.96 (dd, *J* = 10.3, 6.1 Hz, 1H), 4.38 (d, *J* = 4.5 Hz, 1H), 3.86 (s, 3H), 2.95 - 2.90 (m, 1H), 2.13 - 2.07 (m, 1H), 1.78 – 1.69 (m, 1H), 1.40 (s, 18H): $^{13}C\{^1H\}$ NMR (100 MHz, $CDCl_3$): δ 155.4, 152.9, 136.1, 136.0, 131.6, 130.7, 128.6, 128.3, 126.6, 125.9, 124.5, 121.1, 116.8, 111.8, 111.6, 102.1,

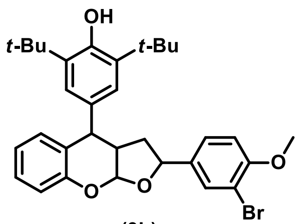

(3h)

82.0, 56.4, 46.8, 42.4, 34.9, 34.4, 30.4: HRMS (ESI, Q-TOF) *m/z*: [M - H]⁻ Calculated for $C_{32}H_{36}O_4Br$ 563.1797, found 563.1804.

2,6-di-*tert*-butyl-4-(2-(3-fluoro-4-methoxyphenyl)-3,3a,4,9a-tetrahydro-2*H*-furo[2,3-b]chromen-4-yl)phenol (3i):

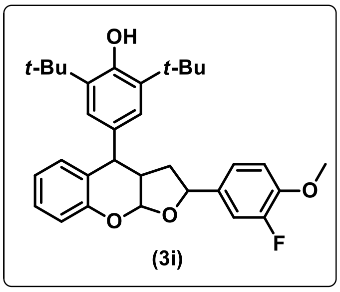

Reaction time: 5 h. **1a** (0.1 g, 0.3 mmol), **2i** (0.070 g, 0.36 mmol), **3i** (0.096 g, 0.19 mmol). Overall yield: 63%. Nature: Yellow solid. mp: 206-208 °C: the product was purified by silica gel column chromatography using hexane/ethyl acetate (95:5) as eluent. ^{1}H-NMR (400 MHz, $CDCl_3$): δ 7.21 – 7.16 (m, 1H), 7.10 (dd, *J* = 12.2, 2.1 Hz, 1H), 7.02 – 6.99 (m, 1H), 6.97 (s, 2H), 6.89 - 6.81 (m, 4H), 5.93 (d, *J* = 4.8 Hz, 1H), 5.16 (s, 1H), 4.97 (dd, *J* = 10.4, 6.0 Hz, 1H), 4.39 (d, *J* = 4.6 Hz, 1H), 3.85 (s, 3H), 2.95 - 2.90 (m, 1H), 2.12 - 2.06 (m, 1H), 1.85 – 1.76 (m, 1H), 1.40 (s, 18H): ^{13}C{^{1}H} NMR (100 MHz, $CDCl_3$): δ 153.6, 152.8, 151.1, 147.2, 147.1, 136.0, 135.3, 135.2, 130.8, 128.6, 128.2, 125.8, 124.3, 122.2, 122.1, 121.1, 116.8, 114.4, 114.2, 113.1, 102.0, 82.1, 56.3, 46.8, 42.4, 34.8, 34.4, 30.4. HRMS (ESI, Q-TOF) *m/z*: [M - H]⁻ Calculated for $C_{32}H_{36}O_4F$ 503.2598, found 503.2604.

(*E*)-2,6-di-*tert*-butyl-4-(2-styryl-3,3a,4,9a-tetrahydro-2*H*-furo[2,3-b]chromen-4-yl)phenol (3j):

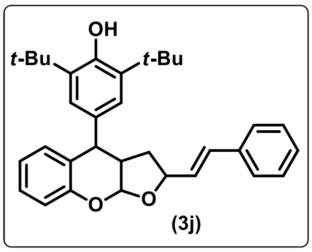

Reaction time: 4 h. **1a** (0.1 g, 0.3 mmol), **2j** (0.062 g, 0.36 mmol), **3j** (0.101 g, 0.21 mmol). Overall yield: 70%. Nature: White solid. mp: 182-184 °C: the product was purified by silica gel column chromatography using hexane/ethyl acetate (95:5) as eluent. ^{1}H-NMR (400 MHz, $CDCl_3$): δ 7.36 (d, *J* = 7.2 Hz, 1H), 7.30 - 7.16 (m, 5H), 7.00 (s, 2H), 6.98 - 6.94 (m, 1H), 6.88 - 6.82 (m, 2H), 6.54 (d, *J* = 15.8 Hz, 1H), 6.14 (dd, *J* = 15.7, 7.9 Hz, 1H), 5.87 (d, *J* = 4.7 Hz, 1H), 5.17 (s, 1H), 4.66 (dd, *J* = 16.9, 6.9 Hz, 1H), 4.37 (d, *J* = 4.7 Hz, 1H), 2.92 - 2.84 (m, 1H), 2.01 - 1.93 (m, 1H), 1.76 – 1.68 (m, 1H),1.42 (s, 18H): ^{13}C{^{1}H} NMR (100 MHz, $CDCl_3$): δ 153.0, 152.8, 136.4, 136.0, 131.8, 131.0, 130.4, 128.6, 128.5, 128.0, 127.8, 126.7, 125.8, 124.4, 121.0, 116.9, 102.0, 81.9, 46.5, 42.4, 34.4, 32.2, 30.4: HRMS (ESI, Q-TOF) *m/z*: [M - H]⁻ Calculated for $C_{33}H_{37}O_3$ 481.2743, found 481.2739.

4-(6-bromo-2-(4-methoxyphenyl)-3,3a,4,9a-tetrahydro-2*H*-furo[2,3-b]chromen-4-yl)-2,6-di-*tert*-butyl phenol (3k):

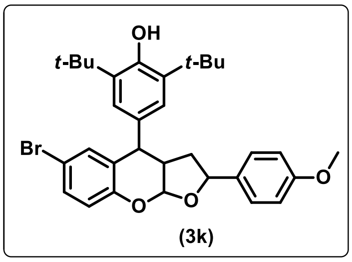

Reaction time: 4 h. **1b** (0.1 g, 0.25 mmol), **2a** (0.053 g, 0.30 mmol), **3k** (0.090 g, 0.159 mmol). Overall yield: 64%. Nature: Yellow solid. mp: 158-160 °C: the product was purified by silica gel column chromatography using hexane/ethyl acetate (95:5) as eluent. ^{1}H-NMR (400 MHz, $CDCl_3$): δ 7.29 -7.21 (m, 3H), 7.00 (dd, *J* = 2.4, 1.2 Hz, 1H), 6.96 (s, 2H), 6.90 - 6.82 (m, 3H), 5.92 (d, *J* = 4.9 Hz, 1H), 5.20 (s, 1H), 4.99 (dd, *J* = 10.5, 5.9 Hz, 1H), 4.35 (d, *J* = 4.5 Hz, 1H), 3.78 (s, 3H), 2.96 - 2.88 (m, 1H), 2.11 – 2.06 (m, 1H), 1.77 - 1.69 (m, 1H), 1.41 (s, 18H): ^{13}C{^{1}H} NMR (100 MHz, $CDCl_3$): δ 159.3, 153.0, 152.2, 136.2, 133.8, 131.2, 131.0, 130.0, 127.7, 126.9, 125.7, 118.6, 113.9, 113.1, 102.1, 82.7, 55.3, 46.6, 42.4, 34.6, 34.4, 30.4: HRMS (ESI, Q-TOF) m/z: $[M - H]^-$ Calculated for $C_{32}H_{36}O_4Br$ 563.1797, found 563.1796.

2,6-di-*tert*-butyl-4-(6-fluoro-2-(4-methoxyphenyl)-3,3a,4,9a-tetrahydro-2*H*-furo[2,3-b]chromen-4-yl) phenol (3l): Reaction time: 5 h. **1c** (0.1 g, 0.3 mmol), **2a** (0.063 g, 0.36 mmol), **3l** (0.096 g, 0.19mmol). Overall yield: 62%. Nature: Yellow solid. mp: 118-120 °C: the product was purified by silica gel column chromatography using hexane/ethyl acetate (95:5) as eluent. ^{1}H-NMR (400 MHz, $CDCl_3$): δ 7.22 (d, *J* = 8.7 Hz, 2H), 6.97 (d, *J* = 3.6 Hz, 2H), 6.96 – 6.92 (m, 1H), 6.88 (dd, *J* = 8.5, 2.7 Hz, 1H), 6.84 (d, *J* = 8.8 Hz, 2H), 6.61 – 6.55 (m, 1H), 5.93 (d, J = 5.1 Hz, 1H), 5.19 (s, 1H), 4.97 (dd, *J* = 10.5, 5.8 Hz, 1H), 4.33 (d, *J* = 4.5 Hz, 1H), 3.77 (s, 3H), 2.99 – 2.91 (m, 1H), 2.14 – 2.06 (m, 1H), 1.78 – 1.69 (m, 1H), 1.41 (s, 18H): ^{13}C{^{1}H} NMR (100 MHz, $CDCl_3$): δ 159.3, 157.3 (d, *J* = 238.11 Hz), 153.0, 148.8, 136.2, 133.8, 130.1, 127.7, 126.7 (d, *J* = 8.01 Hz), 125.7, 117.8, 117.7, 114.9, 114.7, 114.5, 113.9, 102.3, 82.5, 55.3, 46.5, 42.6, 34.8, 34.4, 30.4: HRMS (ESI, Q-TOF) m/z: $[M - H]^-$ Calculated for $C_{32}H_{36}O_4F$ 503.2598, found 503.2606.

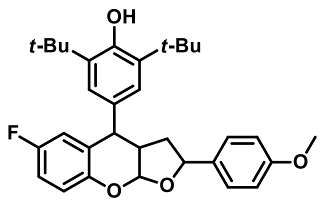

(3l)

2,6-di-*tert*-butyl-4-(6-methoxy-2-(4-methoxyphenyl)-3,3a,4,9a-tetrahydro-2*H*-furo[2,3-b]chromen-4-yl)phenol (3m): Reaction time: 4.5 h. **1d** (0.1 g, 0.3 mmol), **2a** (0.063 g, 0.36 mmol), **3m** (0.111 g, 0.214 mmol). Overall yield: 71%. Nature: Yellow solid. mp: 180-182 °C: the product was purified by silica gel column chromatography using hexane/ethyl acetate (95:5) as eluent. ^{1}H-NMR (400 MHz, $CDCl_3$): δ 7.21 (d, *J* = 8.7 Hz, 2H), 7.00 (s, 2H), 6.94 (d, *J* = 8.7 Hz, 1H), 6.82 (d, *J* = 8.7 Hz, 2H), 6.76 - 6.72 (m, 1H), 6.42 (dd, *J* = 3.0, 1.0 Hz, 1H), 5.92 (d, *J* = 5.2 Hz, 1H), 5.16 (s, 1H), 4.94 (dd, J = 10.5, 5.8 Hz, 1H), 4.32 (d, *J* = 4.5 Hz, 1H), 3.77 (s, 3H), 3.63 (s, 3H), 2.98 - 2.90 (m, 1H), 2.10 – 2.06 (m, 1H), 1.79 - 1.70 (m, 1H), 1.40 (s, 18H): ^{13}C{^{1}H} NMR (100 MHz, $CDCl_3$): δ 159.2, 154.0, 152.8, 146.8, 136.0, 134.0, 130.4, 127.7, 126.5, 125.8, 117.5, 113.8, 113.8, 113.3, 102.4, 82.3, 55.7, 55.3, 46.9, 42.8, 34.9, 34.4, 30.4: HRMS (ESI, Q-TOF) m/z: $[M - H]^-$ Calculated for $C_{33}H_{39}O_5$ 515.2797, found 515.2799.

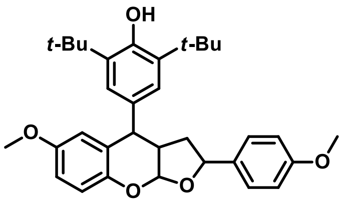

(3m)

2,6-di-*tert*-butyl-4-(2-(4-methoxyphenyl)-6-methyl-3,3a,4,9a-tetrahydro-2*H*-furo[2,3-b]chromen-4-yl)phenol (3n): Reaction time: 4 h. **1e** (0.1 g, 0.3 mmol), **2a** (0.063 g, 0.36 mmol), **3n** (0.1 g, 0.20mmol). Overall yield: 67%. Nature: Yellow solid. mp: 208-210 °C: the product was purified by silica gel column chromatography using hexane/ethyl acetate (95:5) as eluent. ^{1}H-NMR (400 MHz, $CDCl_3$): δ 7.24 (d, *J* = 8.9 Hz, 2H), 7.00 – 6.96 (m, 3H), 6.90 (d, *J* = 8.2 Hz, 1H), 6.82 (d, *J* = 8.7 Hz, 2H), 6.68 (s, 1H), 5.91 (d, *J* = 5.0 Hz, 1H), 5.16 (s, 1H), 4.96 (dd, *J* = 10.5, 5.9 Hz, 1H), 4.34 (d, *J* = 4.5 Hz, 1H), 3.77 (s, 3H), 3.00 – 2.87 (m, 1H), 2.16 (s, 3H), 2.07 – 2.00 (m, 1H), 1.81 – 1.71 (m, 1H), 1.40 (s, 18H): ^{13}C{^{1}H} NMR (100 MHz, $CDCl_3$): δ 159.2, 152.7, 150.7, 135.9, 134.1, 130.9, 130.2, 128.8, 128.6, 127.8, 125.9, 124.3, 116.6, 113.8,

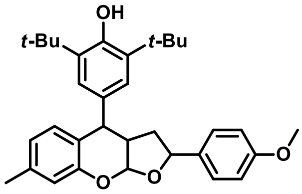

(3o)

102.0, 82.5, 55.3, 47.0, 42.4, 34.7, 34.4, 30.5, 20.8: HRMS (ESI, Q-TOF) *m/z*: $[M - H]^-$ Calculated for $C_{33}H_{39}O_4$ 499.2848, found 499.2848.

2,6-di-tert-butyl-4-(2-(4-methoxyphenyl)-7-methyl-3,3a,4,9a-tetrahydro-2H-furo[2,3-b]chromen-4-yl)phenol (3o): Reaction time: 4 h. **1f** (0.1 g, 0.3 mmol), **2a** (0.063 g, 0.36 mmol), **3o** (0.098 g, 0.19 mmol). Overall yield: 65%. Nature: Yellow solid. mp: 218-220 °C: the product was purified by silica gel column chromatography using hexane/ethyl acetate (95:5) as eluent. ^{1}H-NMR (400 MHz, $CDCl_3$): δ 7.28 – 7.25 (m, 2H), 6.98 (s, 2H), 6.87 – 6.81 (m, 3H), 6.74 (d, *J* = 7.8 Hz, 1H), 6.64 (d, *J* = 7.8 Hz, 1H), 5.90 (d, *J* = 4.7 Hz, 1H), 5.14 (s, 1H), 4.99 (dd, *J* = 10.5, 5.9 Hz, 1H), 4.35 (d, *J* = 4.6 Hz, 1H), 3.78 (s, 3H), 2.93 – 2.85 (m, 1H), 2.31 (s, 3H), 2.08 – 2.01 (m, 1H), 1.86 – 1.76 (m, 1H), 1.40 (s, 18H): $^{13}C\{^1H\}$ NMR (100 MHz, $CDCl_3$): δ 159.2, 152.8, 152.7, 138.0, 135.9, 134.2, 131.2, 128.4, 127.8, 125.8, 121.7, 121.0, 117.2, 113.8, 101.9, 82.7, 55.3, 46.9, 42.2, 34.6, 34.4, 30.4, 21.2: HRMS (ESI, Q-TOF) *m/z*: $[M - H]^-$ Calculated for $C_{33}H_{39}O_4$ 499.2848, found 499.2848.

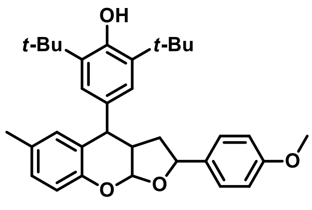

(3n)

2-(4-methoxyphenyl)-4-phenyl-3,3a,4,9a-tetrahydro-2*H*-furo[2,3-b]chromene (3p): Reaction time: 4 h. **1g** (0.1 g, 0.5 mmol), **2a** (0.105 g, 0.6 mmol), **3p** (0.110 g, 0.31 mmol). Overall yield: 62%. Nature: White solid. mp: 156-158 °C: the product was purified by silica gel column chromatography using hexane/ethyl acetate (95:5) as eluent. ^{1}H-NMR (400 MHz, $CDCl_3$): δ 7.34 – 7.18 (m, 9H), 7.03 – 7.01 (m, 1H), 6.85 – 6.82 (m, 3H), 5.90 (d, *J* = 4.5 Hz, 1H), 5.00 (dd, *J* = 10.4, 6.0 Hz, 1H), 4.54 (d, *J* = 5.3 Hz, 1H), 3.77 (s, 3H), 2.97 – 2.89 (m, 1H), 2.01 – 1.94 (m, 1H), 1.87 – 1.78 (m, 1H): $^{13}C\{^1H\}$ NMR (100 MHz, $CDCl_3$): δ 159.2, 152.9, 141.1, 134.1, 129.4, 128.9, 128.7, 128.3, 127.7, 127.2, 123.1, 121.1, 117.1, 113.8, 101.3, 82.8, 55.4, 46.4, 42.5, 35.2: HRMS (ESI, Q-TOF) *m/z*: $[M + H]^+$ Calculated for $C_{24}H_{23}O_3$ 359.1647, found 359.1647.

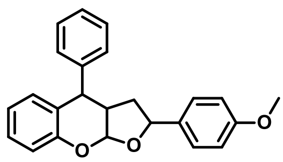

(3p)

2,4-bis(4-methoxyphenyl)-3,3a,4,9a-tetrahydro-2H-furo[2,3-b]chromene (3q): Reaction time: 3.5 h. **1h** (0.1 g, 0.4 mmol), **2a** (0.088 g, 0.5 mmol), **3q** (0.09 g, 0.23 mmol). Overall yield: 58%. Nature: White solid. mp: 180-182 °C: the product was purified by silica gel column chromatography using hexane/ethyl acetate (90:10) as eluent. ^{1}H-NMR (400 MHz, $CDCl_3$): δ 7.25 (t, *J* = 2.4 Hz, 2H), 7.21 – 7.17 (m, 1H), 7.14 (d, *J* = 8.6 Hz, 2H), 7.05 – 6.99 (m, 2H), 6.87 – 6.82 (m, 5H), 5.89 (d, *J* = 4.6 Hz, 1H), 5.00 (dd, *J* = 10.4, 6.0 Hz, 1H), 4.48 (d, *J* = 5.2 Hz, 1H), 3.81 (s, 3H), 3.77 (s, 3H), 2.94 – 2.86 (m, 1H), 2.02 – 1.97 (m, 1H), 1.84 – 1.75 (m, 1H): $^{13}C\{^1H\}$ NMR (100 MHz, $CDCl_3$): δ 159.2, 158.7, 152.9, 134.1, 133.0, 130.4, 128.8, 128.3, 127.7, 123.5, 121.0, 117.0, 113.8, 101.4, 82.7, 55.3, 46.5, 41.6, 35.1: HRMS (ESI, Q-TOF) *m/z*: $[M + H]^+$ Calculated for $C_{25}H_{25}O_4$ 389.1753, found 389.1753.

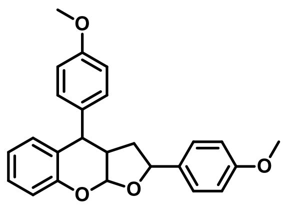

(3q)

3.4.7 Representative procedure for the synthesis of tetrahydrofurobenzofuran derivatives 5.

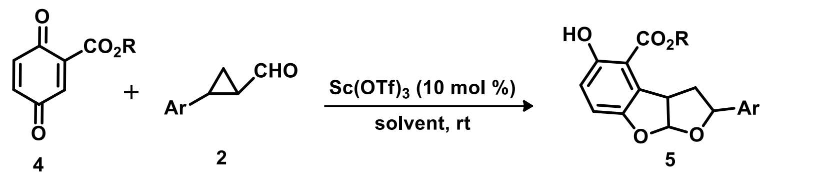

Possible diastereomers

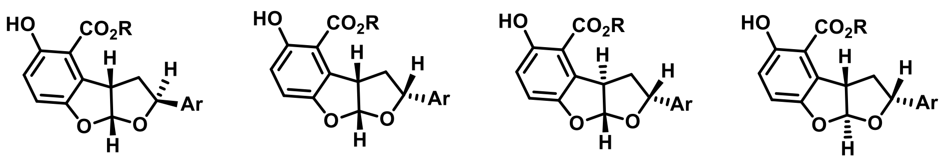

5' (major) 5'' (minor)

A round-bottom flask equipped with magnetic stir bar was charged **4** (1 equiv., 0.6 mmol), **2** (1.5 equiv., 0.9 mmol), $Sc(OTf)_3$ (0.1 equiv., 0.06mmol) and CH_3CN (2 mL) under nitrogen atmosphere. The reaction mixture is stirred for 30 minutes at room temperature. On completion (as monitored by TLC), the reaction mixture was filtered through a small plug of celite and concentrated in a rotary evaporator. The crude NMR analysis data shows the formation of four diastereomers. Diastereomeric ratios were determined from the crude ^{1}H NMR analysis, which shows the formation of four diastereomers. The crude mixture was further purified by column chromatography on silica gel with ethyl acetate/hexane as eluent to afford **5**.

As the molecule incorporates three stereocentres, there should be four possible diastereomers. The structures of these possible diastereomers are shown in the scheme. Out of these four diastereomers, we were able to isolate two isomers (**5m'**, **5m''**) for compound **5m**. The assignment of their relative stereochemistry is done on the basis of 2D-NMR analysis. Similar to the other reaction, in most of the cases, the diastereomers had R_f values very close to each other, making them inseparable. Consequently, the spectroscopic data for only the major isomers is analyzed and reported.

Methyl-5-hydroxy-2-(4-methoxyphenyl)-2,3,3a,8a-tetrahydrofuro[2,3-*b*]benzofuran-4-carboxylate

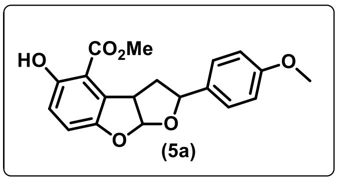

(5a): Reaction time: 30 min. **4a** (0.1 g, 0.6 mmol), **2a** (0.158 g, 0.9 mmol), **5a** (0.181 g, 0.53 mmol). Overall Yield: 88%. Nature: White solid. mp: 150-152 °C: the product was purified by silica gel column chromatography using hexane/ethyl acetate (90:10) as eluent ^{1}H-NMR (400 MHz, $CDCl_3$): δ 10.52 (s, 1H), 7.26 (d, J = 8.4 Hz, 2H), 7.00 (d, J = 8.9 Hz, 1H), 6.88 – 6.84 (m, 3H), 6.47 (d, J = 6.0 Hz, 1H), 4.86 (dd, J = 10.9, 5.4 Hz, 1H), 4.46 – 4.38 (m, 1H), 3.93 (s, 3H), 3.78 (s, 3H), 2.36 – 2.27 (m, 2H): $^{13}C\{^1H\}$ NMR (100 MHz, $CDCl_3$): δ 170.2, 159.5, 157.0, 152.3, 131.3, 128.0, 127.5, 117.8, 117.0, 113.9, 110.8, 109.0, 79.3, 55.3, 52.4, 50.1, 42.6: HRMS (ESI, Q-TOF) *m/z*: $[M + H]^+$ Calculated for $C_{19}H_{19}O_6$ 343.1182, found 343.1187.

Methyl-2-(3,4-dimethoxyphenyl)-5-hydroxy-2,3,3a,8a-tetrahydrofuro[2,3-*b*]benzofuran-4-carboxyla

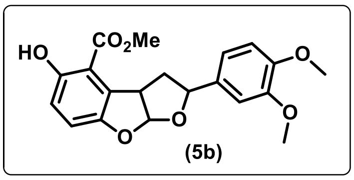

-te (5b): Reaction time: 30 min. **4a** (0.1 g, 0.6 mmol), **2b** (0.186 g, 0.9 mmol), **5b** (0.189 g, 0.51 mmol). Overall Yield: 85%. Nature: White solid. mp: 138-140 °C: the product was purified by silica gel column chromatography using hexane/ethyl acetate (85:15) as eluent ^{1}H-NMR (400 MHz, $CDCl_3$): δ 10.51 (s, 1H), 6.99 (d, J = 8.9 Hz, 1H), 6.89 (d, J = 1.5 Hz, 1H), 6.85 – 6.79 (m, 3H), 6.48 (d, J = 6.0 Hz, 1H), 4.85 (dd, J = 10.9, 5.3 Hz, 1H), 4.44 – 4.38 (m, 1H), 3.93 (s, 3H), 3.86 (s, 3H), 3.85 (s, 3H), 2.37 – 2.27 (m, 2H): $^{13}C\{^{1}H\}$ NMR (100 MHz, $CDCl_3$): δ 170.1, 157.0, 152.3, 149.1, 148.8, 131.8, 128.0, 118.5, 117.8, 116.9, 110.9, 110.8, 109.1, 109.0, 79.5, 55.9, 55.9, 52.4, 49.9, 42.6: HRMS (ESI, Q-TOF) m/z: $[M + H]^+$ Calculated for $C_{20}H_{21}O_7$ 373.1287, 373.1285.

Methyl-5-hydroxy-2-(3,4,5-trimethoxyphenyl)-2,3,3a,8a-tetrahydrofuro[2,3-*b*]benzofuran-4-carboxy

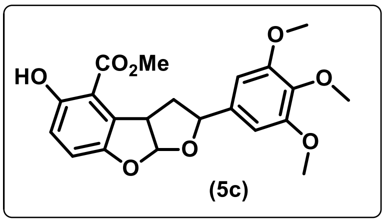

-late (5c): 4a (0.1 g, 0.6 mmol), **2c** (0.213 g, 0.9 mmol), **5c** (0.197 g, 0.49 mmol). Overall Yield: 82%. Nature: White solid. mp: 182-184 °C: the product was purified by silica gel column chromatography using hexane/ethyl acetate (85:15) as eluent ^{1}H-NMR (400 MHz, $CDCl_3$): δ 10.51 (s, 1H), 6.99 (d, *J* = 8.9 Hz, 1H), 6.86 – 6.83 (m, 1H), 6.55 (s, 2H), 6.49 (d, *J* = 5.9 Hz, 1H), 4.84 (dd, *J* = 11.2, 5.1 Hz, 1H), 4.45 – 4.40 (m, 1H), 3.94 (s, 3H), 3.83 (s, 6H), 3.81 (s, 3H), 2.37 – 2.25 (m, 2H): $^{13}C\{^{1}H\}$ NMR (100 MHz, $CDCl_3$): δ 170.1, 157.0, 153.3, 152.3, 137.5, 135.1, 127.9, 117.9, 117.0, 110.8, 109.0, 102.8, 79.6, 60.9, 56.1, 52.4, 49.9, 42.8: HRMS (ESI, Q-TOF) *m/z*: $[M + H]^+$ Calculated for $C_{21}H_{23}O_8$ 403.1393, found 403.1391.

Methyl-2-(4-(benzyloxy)phenyl)-5-hydroxy-2,3,3a,8a-tetrahydrofuro[2,3-*b*]benzofuran-4-carboxyla-

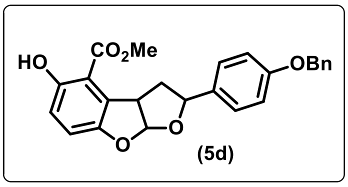

te (5d): Reaction time: 45 min. **4a** (0.1 g, 0.6 mmol), **2e** (0.227 g, 0.9 mmol), **5d** (0.217 g, 0.52 mmol). Overall Yield: 86%. Nature: White solid. mp: 165-167 °C: the product was purified by silica gel column chromatography using hexane/ethyl acetate (90:10) as eluent ^{1}H-NMR (400 MHz, $CDCl_3$): δ 10.54 (s, 1H), 7.42 – 7.31 (m, 5H), 7.26 (d, *J* = 8.7 Hz, 2H), 7.00 (d, *J* = 8.8 Hz, 1H), 6.94 (d, *J* = 8.7 Hz, 2H), 6.85 (d, *J* = 8.6 Hz, 1H), 6.48 (d, *J* = 6.0 Hz, 1H), 5.05 (s, 2H), 4.87 (dd, *J* = 10.9, 5.4 Hz, 1H), 4.44 – 4.39 (m, 1H), 3.93 (s, 3H), 2.36 – 2.27 (m, 2H): $^{13}C\{^{1}H\}$ NMR (100 MHz, $CDCl_3$): δ 170.2, 158.7, 157.0, 152.3, 136.9, 131.7, 128.6, 128.1, 128.0, 127.5, 127.5, 117.8, 117.0, 114.9, 110.9, 109.1, 79.3, 70.1, 52.4, 50.0, 42.6: HRMS (ESI, Q-TOF) *m/z*: $[M + H]^+$ Calculated for $C_{25}H_{23}O_6$ 419.1495, found 419.1494.

Methyl-2-(benzo[d][1,3]dioxol-5-yl)-5-hydroxy-2,3,3a,8a-tetrahydrofuro[2,3-*b*]benzofuran-4-

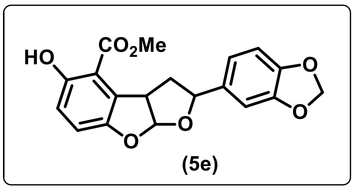

carboxylate (5e): Reaction time: 35 min. **4a** (0.1 g, 0.6 mmol), **2f** (0.171 g, 0.9 mmol), **5e** (0.171 g, 0.48 mmol). Overall Yield: 80%. Nature: White solid. mp: 168-170 °C: the product was purified by silica gel column chromatography using hexane/ethyl acetate (90:10) as eluent ^{1}H-NMR (400 MHz, $CDCl_3$): δ 10.52 (s, 1H), 6.98 (d, *J* = 8.8 Hz, 1H), 6.83 (d, *J* = 8.8 Hz, 2H), 6.77 – 6.72 (m, 2H), 6.45 (d, *J* = 6.0 Hz, 1H), 5.92 (s, 2H), 4.81 (dd, *J* = 11.1, 5.2 Hz, 1H), 4.42 – 4.35 (m, 1H), 3.93 (s, 3H), 2.34 – 2.23 (m, 2H): $^{13}C\{^{1}H\}$ NMR (100 MHz, $CDCl_3$): δ 170.1, 157.0, 152.2, 147.9, 147.4, 133.3, 128.0, 119.8, 117.8, 116.9, 110.8, 109.0, 108.1, 106.5, 101.1, 79.5, 52.4, 49.9, 42.7: HRMS (ESI, Q-TOF) *m/z*: $[M + H]^+$ Calculated for $C_{19}H_{17}O_7$ 357.0974, found 357.0973.

Methyl-2-(4-butoxyphenyl)-5-hydroxy-2,3,3a,8a-tetrahydrofuro[2,3-*b*]benzofuran-4-carboxylate

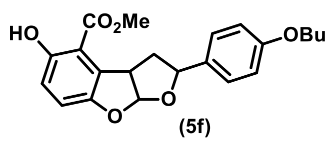

(5f)

(5f): Reaction time: 45 min. **4a** (0.1 g, 0.6 mmol), **2g** (0.197 g, 0.9 mmol), **5f** (0.190 g, 0.49 mmol). Overall Yield: 82%. Nature**:** White solid. mp: 142-144 °C: the product was purified by silica gel column chromatography using hexane/ethyl acetate (90:10) as eluent. ^{1}H-NMR (400 MHz, $CDCl_3$): δ 10.53 (s, 1H), 7.24 (d, *J* = 8.6 Hz, 2H), 6.99 (d, *J* = 8.8 Hz, 1H), 6.86 – 6.82 (m, 3H), 6.47 (d, *J* = 6.0 Hz, 1H), 4.85 (dd, *J* = 10.7, 5.5 Hz, 1H), 4.45 – 4.37 (m, 1H), 3.95 – 3.91 (m, 5H), 2.36 – 2.27 (m, 2H), 1.78 – 1.71 (m, 2H), 1.50 – 1.43 (m, 2H), 0.95 (t, *J* = 7.4 Hz, 3H): $^{13}C\{^1H\}$ NMR (100 MHz, $CDCl_3$): δ 170.2, 159.1, 157.0, 152.3, 131.1, 128.1, 127.5, 117.8, 116.9, 114.5, 110.8, 109.0, 79.4, 67.7, 52.4, 50.0, 42.6, 31.3, 19.3, 13.9: HRMS (ESI, Q-TOF) *m/z*: $[M + H]^+$ Calculated for $C_{22}H_{25}O_6$ 385.1651, found 385.1651.

Methyl-2-(3-bromo-4-methoxyphenyl)-5-hydroxy-2,3,3a,8a-tetrahydrofuro[2,3-*b*]benzofuran-4-

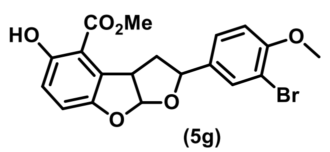

(5g)

carboxylate (5g): Reaction time: 1 h. **4a** (0.1 g, 0.6 mmol), **2h** (0.229 g, 0.9 mmol), **5g** (0.197 g, 0.47 mmol). Overall Yield**:** 78%. Nature: Off-white solid. mp: 108-110 °C: the product was purified by silica gel column chromatography using hexane/ethyl acetate (90:10) as eluent. ^{1}H-NMR (400 MHz, $CDCl_3$): δ 10.52 (s, 1H), 7.54 (d, *J* = 2.2 Hz, 1H), 7.21 (dd, *J* = 8.5, 2.1 Hz, 1H), 6.98 (d, *J* = 8.8 Hz, 1H), 6.84 (d, *J* = 8.3 Hz, 2H), 6.46 (d, *J* = 6.0 Hz, 1H), 4.82 (dd, *J* = 11.2, 5.1 Hz, 1H), 4.44 – 4.39 (m, 1H), 3.94 (s, 3H), 3.87 (s, 3H), 2.38 – 2.22 (m, 2H): $^{13}C\{^1H\}$ NMR (100 MHz, $CDCl_3$): δ 170.1, 157.0, 155.6, 152.2, 133.0, 131.1, 127.8, 126.5, 117.9, 117.0, 111.7, 111.7, 110.8, 109.0, 78.6, 56.3, 52.4, 49.9, 42.6: HRMS (ESI, Q-TOF) *m/z*: $[M + H]^+$ Calculated for $C_{19}H_{18}O_6$ Br 421.0287, found 421.0286.

Methyl-2-(3-fluoro-4-methoxyphenyl)-5-hydroxy-2,3,3a,8a-tetrahydrofuro[2,3-*b*]benzofuran-4-carbo

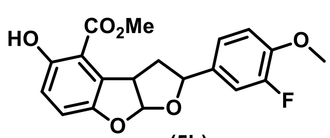

(5h)

-xylate (5h): Reaction time: 50 min. **4a** (0.1 g, 0.6 mmol), **2i** (0.174 g, 0.9 mmol), **5h** (0.176 g, 0.49 mmol). Overall Yield: 81%. Nature: White solid. mp: 138-140 °C: the product was purified by silica gel column chromatography using hexane/ethyl acetate (90:10) as eluent ^{1}H-NMR (400 MHz, $CDCl_3$): δ 10.52 (s, 1H), 7.09 (dd, *J* = 12.2, 2.1 Hz, 1H), 7.00 (t, *J* = 8.4 Hz, 2H), 6.89 (t, *J* = 8.5 Hz, 1H), 6.84 (d, *J* = 8.9 Hz, 1H), 6.46 (d, *J* = 6.0 Hz, 1H), 4.83 (dd, *J* = 11.2, 5.0 Hz, 1H), 4.44 – 4.38 (m, 1H), 3.94 (s, 3H), 3.86 (s, 3H), 2.39 – 2.33 (m, 1H), 2.29 – 2.19 (m, 1H): $^{13}C\{^1H\}$ NMR (100 MHz, $CDCl_3$): δ 170.1, 157.0, 153.6, 152.2, 151.2, 147.4, 147.3, 132.5, 132.4, 127.8, 122.1, 122.1, 117.9, 117.0, 114.0, 113.8, 113.2, 110.8, 109.0, 78.8, 56.3, 52.4, 49.9, 42.6: HRMS (ESI, Q-TOF) *m/z*: $[M + H]^+$ Calculated for $C_{19}H_{18}O_6$ F 361.1087, found 361.1087.

(*E*)-methyl-5-hydroxy-2-styryl-2,3,3a,8a-tetrahydrofuro[2,3-*b*]benzofuran-4-carboxylate (5i):

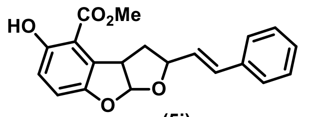

(5i)

Reaction time: 2 h. **4a** (0.1 g, 0.6 mmol), **2j** (0.155 g, 0.9 mmol), **5i** (0.149 g, 0.44 mmol). Overall Yield: 73%. Nature**:** White solid. mp: 208-210 °C: the product was purified by silica gel column chromatography using hexane/ethyl acetate (90:10) as eluent ^{1}H-NMR (400 MHz, $CDCl_3$): δ 10.52 (s, 1H), 7.36 – 7.23 (m, 5H), 6.98 (d, J = 8.8 Hz, 1H), 6.84 (d, J = 8.7 Hz, 1H), 6.60 (d, J = 15.8 Hz, 1H), 6.38 (d, J = 6.0 Hz, 1H), 6.18 (dd, J = 15.9, 7.2 Hz, 1H), 4.52 (dd, J = 15.7, 7.3 Hz, 1H), 4.38 – 4.34 (m, 1H), 3.96 (s, 3H), 2.25 – 2.20 (m, 2H): ^{13}C{^{1}H} NMR (100 MHz, $CDCl_3$): δ 170.1, 157.0, 152.2, 136.3, 133.0, 128.6, 128.0, 128.0, 127.0, 126.6, 117.9, 116.9, 110.8, 109.0, 78.9, 52.4, 49.9, 40.6: HRMS (ESI, Q-TOF) m/z: $[M + H]^+$ Calculated for $C_{20}H_{19}O_5$ 339.1232, found 339.1230.

Methyl-5-hydroxy-2-(naphthalen-2-yl)-2,3,3a,8a-tetrahydrofuro[2,3-*b*]benzofuran-4-carboxylate (5j):

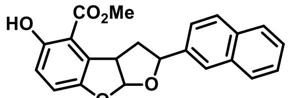

(5j)

Reaction time**:** 4 h. **4a** (0.1 g, 0.6 mmol), **2k** (0.176 g, 0.9 mmol), **5j** (0.152 g, 0.42 mmol). Overall Yield: 70%. Nature: White solid. mp: 90-92 °C: the product was purified by silica gel column chromatography using hexane/ethyl acetate (90:10) as eluent. ^{1}H-NMR (400 MHz, $CDCl_3$): δ 10.55 (s, 1H), 7.84 – 7.78 (m, 4H), 7.48 – 7.44 (m, 3H), 7.03 (d, *J* = 8.8 Hz, 1H), 6.88 (d, *J* = 8.7 Hz, 1H), 6.56 (d, *J* = 6.0 Hz, 1H), 5.09 (dd, *J* = 11.1, 5.2 Hz, 1H), 4.49 – 4.44 (m, 1H), 3.93 (s, 3H), 2.48 – 2.36 (m, 2H): ^{13}C{^{1}H} NMR (100 MHz, $CDCl_3$): δ 170.1, 157.1, 152.3, 137.0, 133.2, 133.1, 128.4, 128.0, 127.7, 126.3, 126.1, 125.0, 123.8, 117.9, 117.0, 111.0, 109.1, 79.7, 52.4, 50.1, 42.8: HRMS (ESI, Q-TOF) *m/z*: $[M + H]^+$ Calculated for $C_{22}H_{19}O_5$ 363.1232, found 363.1232.

Methyl-5-hydroxy-2-(p-tolyl)-2,3,3a,8a-tetrahydrofuro[2,3-*b*]benzofuran-4-carboxylate (5k):

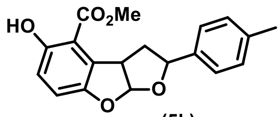

(5k)

Reaction time**:** 3 h. **4a** (0.1 g, 0.6 mmol), **2l** (0.144 g, 0.9 mmol), **5k** (0.130 g, 0.40 mmol). Overall Yield: 66%. Nature: White solid. mp: 173-175 °C: the product was purified by silica gel column chromatography using hexane/ethyl acetate (90:10) as eluent. ^{1}H-NMR (400 MHz, $CDCl_3$): δ 10.53 (s, 1H), 7.23 (d, *J* = 8.1 Hz, 2H), 7.14 (d, *J* = 8.0 Hz, 2H), 7.00 (d, *J* = 8.9 Hz, 1H), 6.85 (d, *J* = 8.7 Hz, 1H), 6.49 (d, *J* = 6.0 Hz, 1H), 4.89 (dd, *J* = 11.1, 5.2 Hz, 1H), 4.43 – 4.38 (m, 1H), 3.93 (s, 3H), 2.40 – 2.35 (m, 1H), 2.33 (s, 3H), 2.31 – 2.27 (m, 1H): ^{13}C{^{1}H} NMR (100 MHz, $CDCl_3$): δ 170.2, 157.0, 152.3, 137.8, 136.5, 129.2, 128.1, 117.8, 117.0, 110.9, 109.0, 79.5, 52.4, 50.0, 42.8, 21.2: HRMS (ESI, Q-TOF) *m/z*: $[M + H]^+$ Calculated for $C_{19}H_{19}O_5$ 327.1232, found 327.1231.

Methyl-5-hydroxy-2-mesityl-2,3,3a,8a-tetrahydrofuro[2,3-*b*]benzofuran-4-carboxylate (5l): Reaction

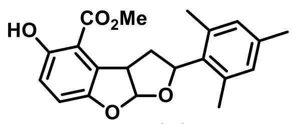

(5l)

time: 2 h. **4a** (0.1 g, 0.6 mmol), **2m** (0.169 g, 0.9 mmol), **5l** (0.145 g, 0.41 mmol). Overall Yield: 68%. Nature: White solid. mp: 212-214 °C: the product was purified by silica gel column chromatography using hexane/ethyl acetate (90:10) as eluent. ^{1}H-NMR (400 MHz, $CDCl_3$): δ 10.55 (s, 1H), 7.01 (d, *J* = 8.8 Hz, 1H), 6.85 (d, *J* = 9.1 Hz, 1H), 6.81 (s, 2H), 6.52 (d, *J* = 6.1 Hz, 1H), 5.36 (dd, *J* = 11.4, 6.2 Hz, 1H), 4.46 – 4.41 (m, 1H), 3.92 (s, 3H), 2.54 – 2.41 (m, 1H), 2.30 (s, 6H), 2.24 (s, 3H), 2.21 – 2.17 (m, 1H): $^{13}C\{^1H\}$ NMR (100 MHz, $CDCl_3$): δ 170.2, 156.9, 152.1, 137.2, 136.4, 131.4, 130.2, 128.7, 117.8, 117.1, 111.2, 109.0, 77.1, 52.4, 50.0, 39.3, 20.8, 20.7: HRMS (ESI, Q-TOF) *m/z*: $[M + H]^+$ Calculated for $C_{21}H_{23}O_5$ 355.1545, found 355.1545.

Ethyl-5-hydroxy-2-(4-methoxyphenyl)-2,3,3a,8a-tetrahydrofuro[2,3-*b*]benzofuran-4-carboxylate

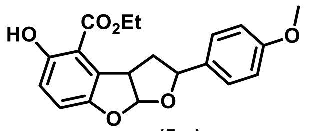

(5m)

(5m): Reaction time: 45 min. **4b** (0.1 g, 0.6 mmol), **2a** (0.158 g, 0.9 mmol), **5m** (0.178 g, 0.50 mmol). Overall Yield: 84%. Nature: White solid. mp: 125-127 °C: the product was purified by silica gel column chromatography using hexane/ethyl acetate (90:10) as eluent. ^{1}H-NMR (400 MHz, $CDCl_3$): δ 10.64 (s, 1H), 7.26 (d, *J* = 8.8 Hz, 2H), 6.98 (d, *J* = 8.8 Hz, 1H), 6.85 (dd, *J* = 11.7, 8.7 Hz, 3H), 6.47 (d, *J* = 6.0 Hz, 1H), 4.86 (dd, *J* = 11.3, 5.0 Hz, 1H), 4.46 – 4.36 (m, 3H), 3.78 (s, 3H), 2.41 – 2.35 (m, 1H), 2.31 – 2.24 (m, 1H), 1.39 (t, *J* = 7.2 Hz, 3H): $^{13}C\{^1H\}$ NMR (100 MHz, $CDCl_3$): δ 169.8, 159.4, 157.1, 152.3, 131.3, 128.0, 127.5, 117.8, 116.8, 113.9, 110.8, 109.2, 79.3, 61.8, 55.3, 50.0, 43.0, 14.1: HRMS (ESI, Q-TOF) *m/z*: $[M + H]^+$ Calculated for $C_{20}H_{21}O_6$ 357.1338, found 357.1339.

3.4.8 General procedure for dehydrogenation

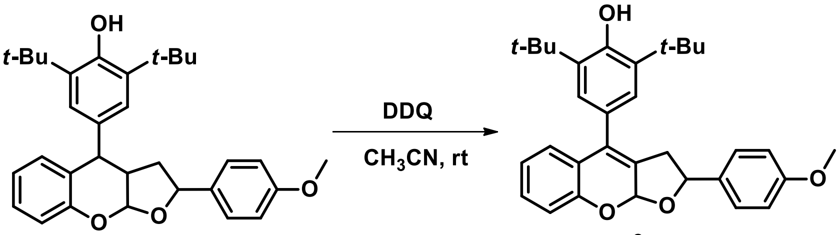

A round-bottom flask equipped with a magnetic stir bar was charged **3a** (major diastereomer) (0.100 g, 0.2 mmol), DDQ (0.070 g, 0.3 mmol), and anhydrous CH_3CN (4 mL) under nitrogen atmosphere. The reaction mixture is stirred for 4 h at room temperature. On completion, the reaction mixture was filtered through a small plug of celite and concentrated in a rotary evaporator. The crude mixture was further purified by column chromatography on silica gel with ethyl acetate/hexane (5:95, V/V) as eluent to afford **6**.

2,6-di-*tert*-butyl-4-(2-(4-methoxyphenyl)-2,3-dihydro-9aH-furo[2,3-b]chromen-4-yl)phenol (6a):

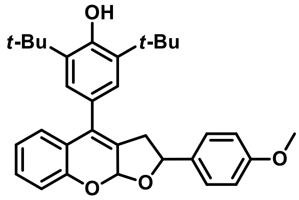

(6)

Reaction time: 4 h. **3a'** (0.1 g, 0.2 mmol), **6** (0.073 g, 0.15 mmol). Yield: 75%. Nature: yellow solid. mp: 140-142 °C: the product was purified by silica gel column chromatography using hexane/ethyl acetate (95:5) as eluent. ^{1}H-NMR (400 MHz, $CDCl_3$): δ 7.36 (d, J = 8.7 Hz, 2H), 7.23 – 7.17 (m, 2H), 7.11 – 7.07 (m, 3H), 6.98 – 6.94 (m, 1H), 6.90 (d, J = 8.7 Hz, 2H), 6.19 (s, 1H), 5.30 (s, 1H), 5.29 – 5.26 (m, 1H), 3.81 (s, 3H), 3.02 – 2.97 (m, 1H), 2.87 – 2.80 (m, 1H), 1.41 (s, 18H): $^{13}C\{^1H\}$ NMR (100 MHz, $CDCl_3$): δ 159.5, 153.8, 152.3, 135.5, 132.4, 132.0, 129.6, 128.9, 127.6, 127.2, 126.8, 125.4, 121.7, 117.2, 113.9, 102.5, 83.0, 55.3, 39.8, 34.4, 30.4: HRMS (ESI, Q-TOF) m/z: $[M + H]^+$ Calculated for $C_{32}H_{37}O_4$ 485.2692, found 485.2688.

3.4.9 Direct dehydrogenation for diastereoselective synthesis of 6:

A round-bottom flask equipped with a magnetic stir bar was charged **3** (crude reaction mixture) (0.05 g, 0.102 mmol), DDQ (0.034 g, 0.153 mmol), and anhydrous CH_3CN (2 mL) under nitrogen atmosphere. The reaction mixture is stirred for 4 h at room temperature. On completion, the reaction mixture was filtered through a small plug of celite and concentrated in a rotary evaporator. The crude mixture was further purified by column chromatography on silica gel with ethyl acetate/hexane (5:95, V/V) as eluent to afford **6**.

2,6-di-*tert*-butyl-4-(2-(4-methoxyphenyl)-2,3-dihydro-9aH-furo[2,3-b]chromen-4-yl)phenol (6a):

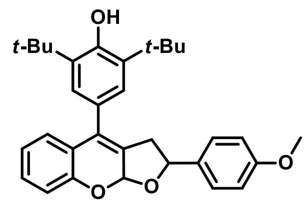

(6a)

Reaction time: 4 h. **3a** (0.05 g, 0.102 mmol), **6a** (0.018 g, 0.037 mmol). Yield: 36%. Nature: yellow solid, the product was purified by silica gel column chromatography using hexane/ethyl acetate (95:5) as eluent, ^{1}H-NMR (400 MHz, $CDCl_3$): δ 7.36 (d, J = 8.7 Hz, 2H), 7.23 – 7.17 (m, 2H), 7.11 – 7.07 (m, 3H), 6.98 – 6.94 (m, 1H), 6.90 (d, J = 8.7 Hz, 2H), 6.19 (s, 1H), 5.30 (s, 1H), 5.29 – 5.26 (m, 1H), 3.81 (s, 3H), 3.02 – 2.97 (m, 1H), 2.87 – 2.80 (m, 1H), 1.41 (s, 18H): $^{13}C\{^{1}H\}$ NMR (100 MHz, $CDCl_3$): δ 159.5, 153.8, 152.3, 135.5, 132.4, 132.0, 129.6, 128.9, 127.6, 127.2, 126.8, 125.4, 121.7, 117.2, 113.9, 102.5, 83.0, 55.3, 39.8, 34.4, 30.4.

2,6-di-*tert*-butyl-4-((9aS)-2-(3,4-dimethoxyphenyl)-3,9a-dihydro-2H-furo[2,3-b]chromen-4-yl) phenol) (6b):

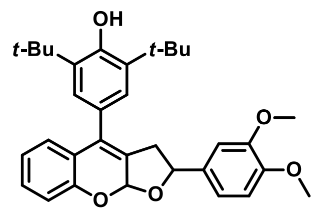

(6b)

Reaction time: 4 h. **3b** (0.05 g, 0.096 mmol), **6b** (0.013 g, 0.025 mmol). Yield: 26%. Nature: yellow solid, the product was purified by silica gel column chromatography using hexane/ethyl acetate (95:5) as eluent, ^{1}H-NMR (400 MHz, $CDCl_3$): δ 7.22 – 7.17 (m, 2H), 7.11 – 7.08 (m, 2H), 7.02 (d, J = 1.9 Hz, 1H), 6.99 – 6.91 (m, 3H), 6.85 (d, J = 8.3 Hz, 1H), 6.20 (s, 1H), 5.30 (s, 1H), 5.30 – 5.26 (m, 1H), 3.90 (s, 3H), 3.87 (s, 3H), 3.04 – 2.97 (m, 1H), 2.88 – 2.79 (m, 1H), 1.42 (s, 18H): $^{13}C\{^{1}H\}$ NMR (100 MHz, $CDCl_3$): δ 153.8, 152.3, 149.0, 148.8, 135.6, 132.8, 129.4, 129.0, 127.2, 126.8, 125.4, 121.7, 118.55, 117.2, 110.9, 109.2, 102.5, 83.1, 56.0, 39.7, 34.5, 30.4: HRMS (ESI, Q-TOF) m/z: $[M + H]^+$ Calculated for $C_{33}H_{39}O_5$ 515.2797, found 515.2792.

4-((2S,9aS)-2-(4-(benzyloxy)phenyl)-3,9a-dihydro-2H-furo[2,3-b]chromen-4-yl)-2,6-di-*tert*-butyl phenol (6e):

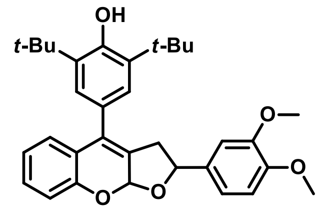

(6b)

Reaction time: 4 h. **3e** (0.05 g, 0.088 mmol), **6e** (0.015 g, 0.026 mmol). Yield: 30%. Nature: yellow solid, the product was purified by silica gel column chromatography using hexane/ethyl acetate (95:5) as eluent, ^{1}H-NMR (400 MHz, $CDCl_3$): δ 7.44 – 7.34 (m, 8H), 7.19 (t, *J* = 7.2 Hz, 2H), 7.09 (d, *J* = 7.9 Hz, 2H), 6.99 – 6.96 (m, 3H), 6.19 (s, 1H), 5.30 (s, 1H), 5.29 – 5.25 (m, 1H), 5.06 (s, 2H), 3.02 – 2.97 (m, 1H), 2.86 – 2.80 (m, 1H), 1.42 (s, 18H). $^{13}C\{^{1}H\}$ NMR (100 MHz, $CDCl_3$): δ 158.78, 153., 152.4, 137.0, 135.6, 132.7, 132.1, 129.6, 128.9, 128.6, 128.0, 127.6, 127.5, 127.3, 126.8, 125.4, 121.6, 117.2, 114.8, 102.5, 83.0, 70.1, 39.8, 34.4, 30.4. HRMS (ESI, Q-TOF) m/z: $[M + H]^+$ Calculated for $C_{38}H_{41}O_4$ 561.3005, found 561.3006.

4-(6-bromo-2-(4-methoxyphenyl)-3,9a-dihydro-2H-furo[2,3-b]chromen-4-yl)-2,6-di-*tert*-butylphenol

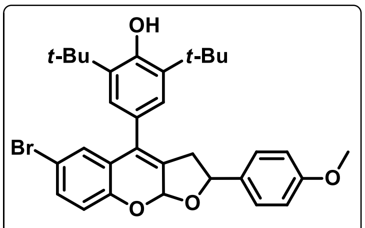

(6k)

(6k): Reaction time: 4 h. **3k** (0.05 g, 0.088 mmol), **6k** (0.016 g, 0.028 mmol). Yield: 32%. Nature: yellow solid, the product was purified by silica gel column chromatography using hexane/ethyl acetate (95:5) as eluent, ^{1}H-NMR (400 MHz, $CDCl_3$): δ 7.38 – 7.29 (m, 5H), 7.07 (s, 1H), 6.97 (d, J = 8.5 Hz, 1H), 6.90 (d, J = 8.7 Hz, 2H), 6.17 (s, 1H), 5.34 (s, 1H), 5.26 (dd, J = 10.3, 4.7 Hz, 1H), 3.81 (s, 3H), 3.03 – 2.98 (m, 1H), 2.89 – 2.82 (m, 1H), 1.42 (s, 18H). $^{13}C\{^1H\}$ NMR (100 MHz, $CDCl_3$): δ 159.6, 154.0, 151.4, 135.8, 132.0, 131.5, 131.3, 130.4, 129.6, 127.6, 127.2, 126.5, 119.0, 113.9, 102.5, 83.2, 55.4, 39.9, 34.5, 30.4. HRMS (ESI, Q-TOF) m/z: $[M + H]^+$ Calculated for $C_{32}H_{36}O_4Br$ 563.1797, found 563.1796.

3.4.10 Procedure for gram scale experiment: A round-bottom flask equipped with magnetic stir bar was charged **4a** (1.0 g, 6.02 mmol), **2a** (1.59 g, 9.03 mmol), $Sc(OTf)_3$ (0.295 g, 0.602 mmol) and anhydrous CH_3CN (20 mL) under nitrogen atmosphere. The reaction mixture is stirred at room temperature. On completion (as monitored by TLC), the reaction mixture was filtered through celite and concentrated in a rotary evaporator. The resulting crude mixture was then purified on a silica gel column using hexane/ethyl acetate as an eluent to isolate **5a** in 68% overall yield (1.40 g, 4.08 mmol).

3.5 References

1. a) Lin, Y.; Wu, X.; Feng, S.; Jiang, G.; Luo, J.; Zhou, S.; Vrijmoed L. L. P.; Jones, E. B. G.; Krohn, K.; Steingrover, K.; Zsila, F. *J. Org. Chem*. **2001**, *66*, 6252-6256. (b) Ghosh, A. K.; Parham, G. L.; Martyr, C. D.; Nyalapatla, P. R.; Osswald, H. L.; Agniswamy, J.; Wang, Y.-F.; Amano, M.; Weber I. T.; Mitsuya, H. *J. Med. Chem*. **2013**, *56*, 6792-6802.
2. (a) R. E.; Townsend, C. A. *Chem. Rev.* **1997**, *97*, 2537-2556. (b) Quach, R.; Furkert, D. P.; and Brimble, M. A. *Org. Biomol. Chem.*, **2017**, *15*, 3098-3104. (c) Panda, B.; and Sarkar, T. K.; *J. Org. Chem*., **2013**, *78*, 2413–2421.
3. Ichihara, A.; Nonaka, M.; Sakamura, S.; Sato, R.; Tajimi, A. *Chem. Lett.* **1988**, *17*, 27-30.
4. Jonathan, L. T.; Gbeassor, M.; Che, C.-T.; Fong, H. H. S.; *J. Nat. Prod.* **1990,** *53*, 1572-1574.
5. (a) Yadav, J. S.; Reddy, B. V. S.; Reddy, P. N.; $Bi(OTf)_3$-[Bmim]PF_6 *Chem. Lett.* **2004**, *33*, 1436-1437. (b) Gaddam, V.; Sreenivas, D. K.; Nagarajan, R. *Tetrahedron Lett.* **2006**, *47*, 9291-9295.
6. (a) Zhou, G.; Corey E. J. *J. Am. Chem. Soc*. **2005**, *127*, 11958-11959. (b) Airoldi, C.; Cardona, F.; Sironi, E.; Colombo, L.; Salmona, M. *Chem. Commun.* **2011**, *47*, 10266-10268.
7. Gustavo, B.-C. M.; Bizet, V. Mazet, C. *J. Am. Chem. Soc.* **2016**, *138*, 4014−4017.
8. Guo, J.; Miao, H.; Zhao, Y.; Bai, X.; Zhu, Y.; Wang, Q.; Bu, Z.; *Chem. Commun.*, **2019**, *55*, 5207-5210.

9. Mao, W.; Lin, S.; Zhang, L.; Lu, H.; Jia, J.; Xu, Z. *Org. Chem. Front*., **2020**, *7,* 856–861.
10. (a) Schneider, T.F.; Kaschel, J.; Werz, D.B. *Angew. Chem. Int. Ed*. **2014**, *53*, 5504-5523. (b) Pandey, A.K.; Ghosh, A.; Banerjee, P. *Isr. J. Chem.* **2016**, *56*, 512-521. (c) Budynina, E.M.; Ivanov, K.L.; Sorokin, I.D.; Melnikov, M.Y. *Synthesis.* **2017**, *49*, 3035-3068. (d) Garve, L.K.B.; Jones, P.G.; Werz, D.B. *Angew. Chem. Int. Ed.* **2017**, 56, 9226-9230.
11. (a) Wang, Z.-H.; Zhang, H.-H.; Xu, P.-F.; Luo, Y.-C. *Chem. Commun*. **2018**, *54*, 10128-10131. (b) Liu, P.; Cui, Y.; Chen, K.; Zhou, X.; Pan, W.; Ren, J.; Wang, Z. *Org. Lett.* **2018**, *20*, 2517-2521.
12. (a) Kumar, P.; Dey, R.; Banerjee, P. *Org. Lett*. **2018**, *20*, 5163-5166. (b) Dey, R.; Banerjee, P. *Adv. Synth. Catal.* **2019**, *361*, 2849-2854. (c) Dey, R.; Rajput, S.; Banerjee, P. *Tetrahedron,* **2020**, *76*, 131080. (d) Singh, P.; Kaur, N.; Banerjee, P. *J. Org. Chem.* **2020**, 85, 3393-3406.
13. (a) Diao, L.; Yang, C.; Wan, P. *J. Am. Chem. Soc.* **1995**, *117*, 5369-5370. (b) Mei, G.-J.; Xu, S.-L.; Zheng, W.-Q.; Bian, C.-Y.; Shi, F. *J. Org. Chem.*, **2018**, *83*, 1414–1421. (c) Kaur, N.; Singh, P.; Banerjee, P. *Adv. Synth. Catal.,* **2021**, *363*, 2813–2824. (d) Lu, Z.; Zhang, Q.; Ke, M.; Hu, S.; Xiao, X.; Chen, F. *J. Org. Chem.* **2021**, *86*, 7625–7635. (e) Sun, M.; Ma, C.; Zhou, S.-J.; Lou, S.-F.; Xiao, J.; Jiao, Y.-C.; Shi, F. *Angew. Chem., Int. Ed*. **2019**, *58*, 8703−8708.
14. (a) Zheng, H.; Xu, C.; Wang, Y.; Kang, T.; Liu, X.; Lin, L.; Feng, X. *Chem. Commun.* **2017**, *53*, 6585−6588. (b) Vazquez, J.C.; Davis, J.; Nesterov, V. N. Wang, H.; Luo, W. *Org. Lett.* **2021**, *23*, 8, 3136–3140. (c) Xi, C. C.; Zhao, X. J.; Tian, J. M.; Chen, Z. M.; Zhang, K.; Zhang, F. M.; Tu, Y. Q.; Dong, J. W. *Org. Lett.* **2020**, 22, 4995−5000.

3.6 NMR spectra of the compounds

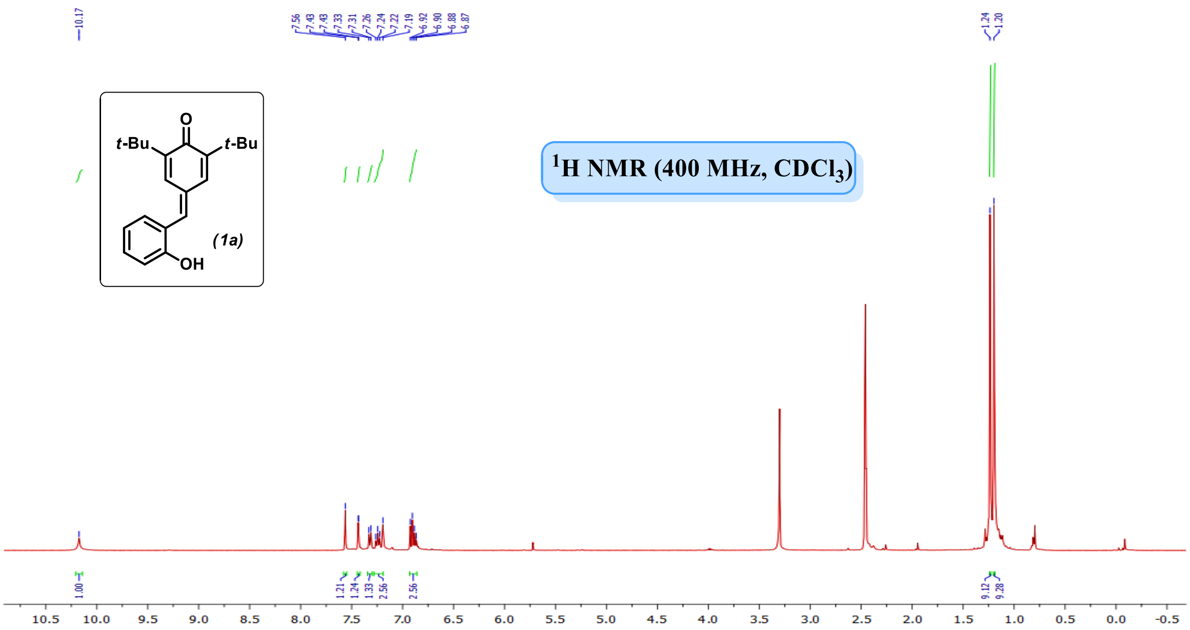

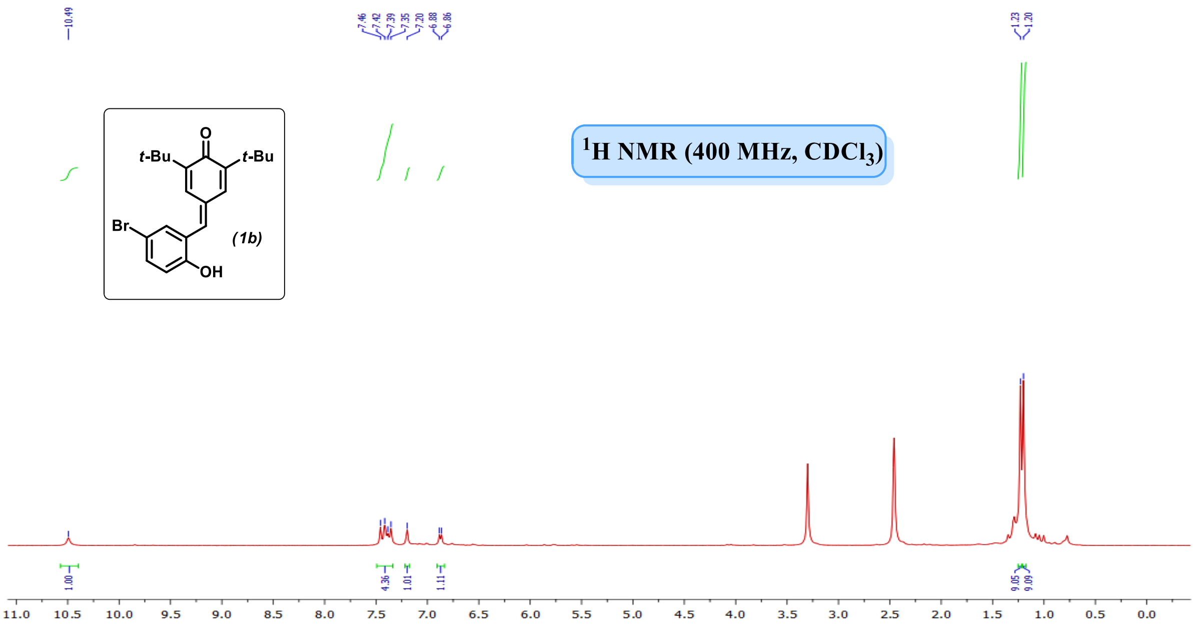

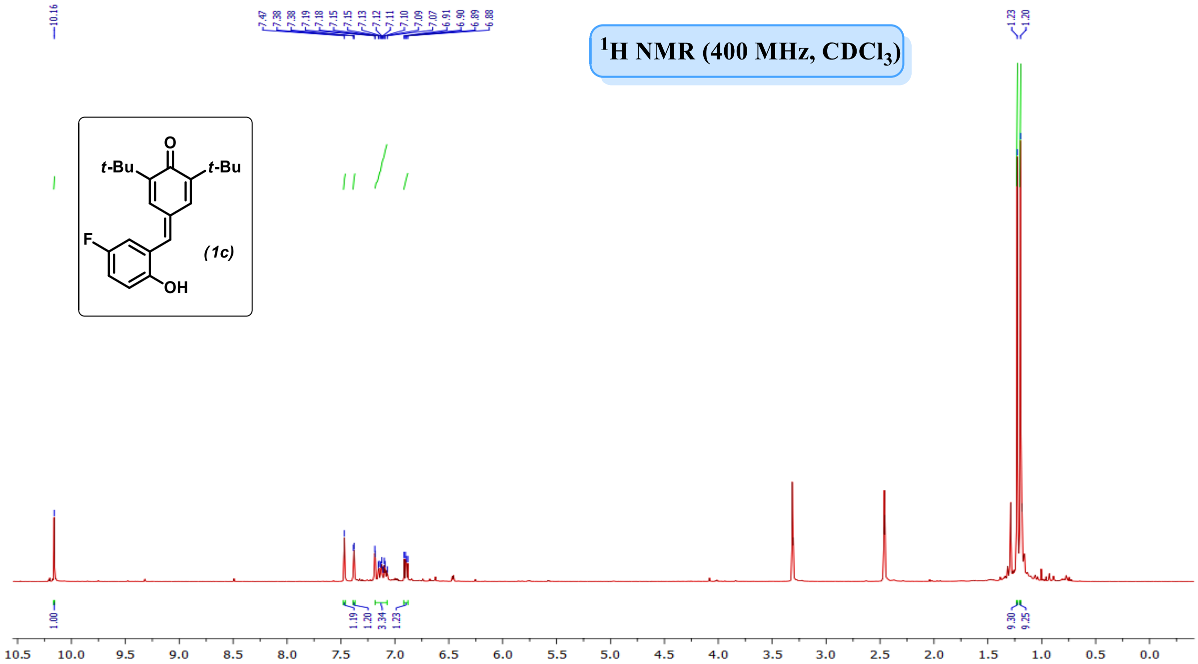
1H NMR (400 MHz, CDCl3)
(1c)

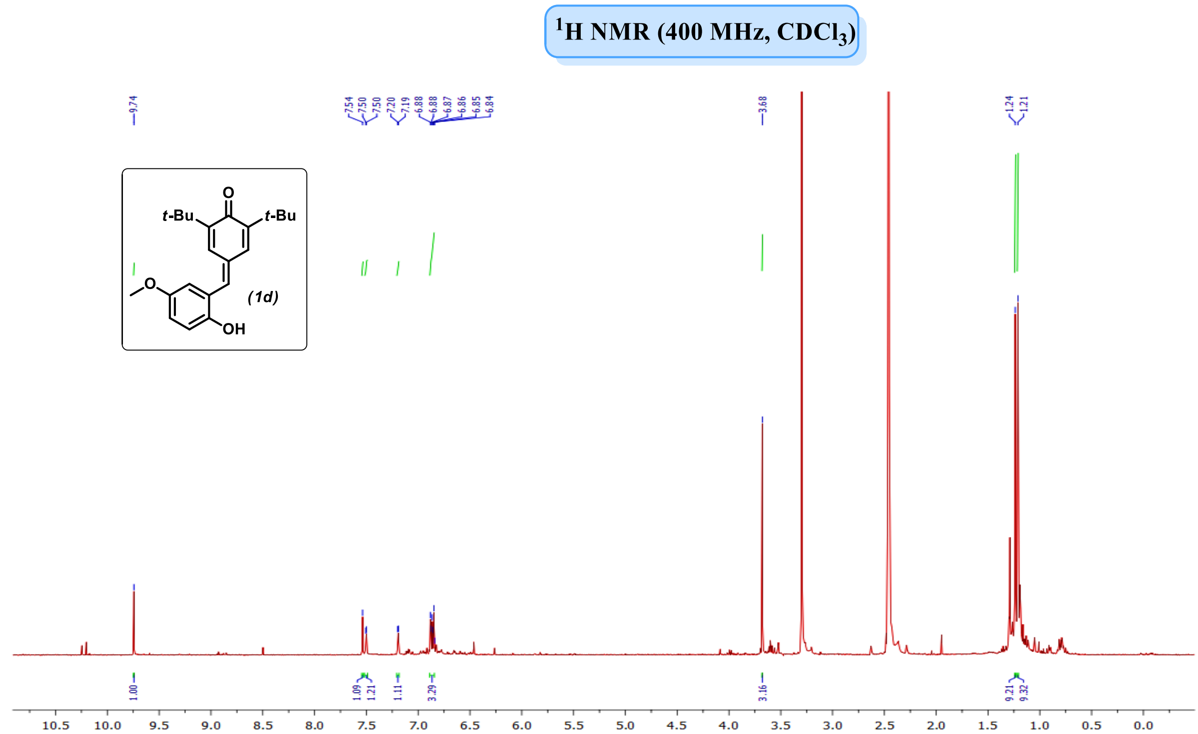
1H NMR (400 MHz, CDCl3)
(1d)

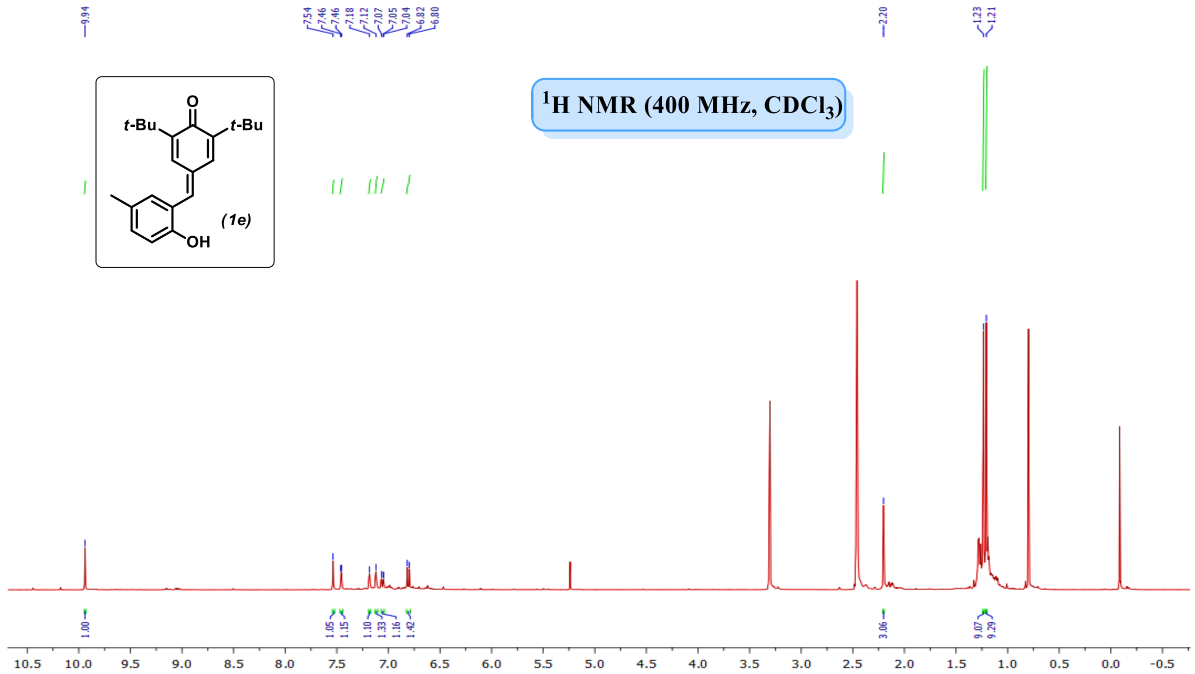

1H NMR (400 MHz, CDCl3)
t-Bu
t-Bu
O
OH
(1e)

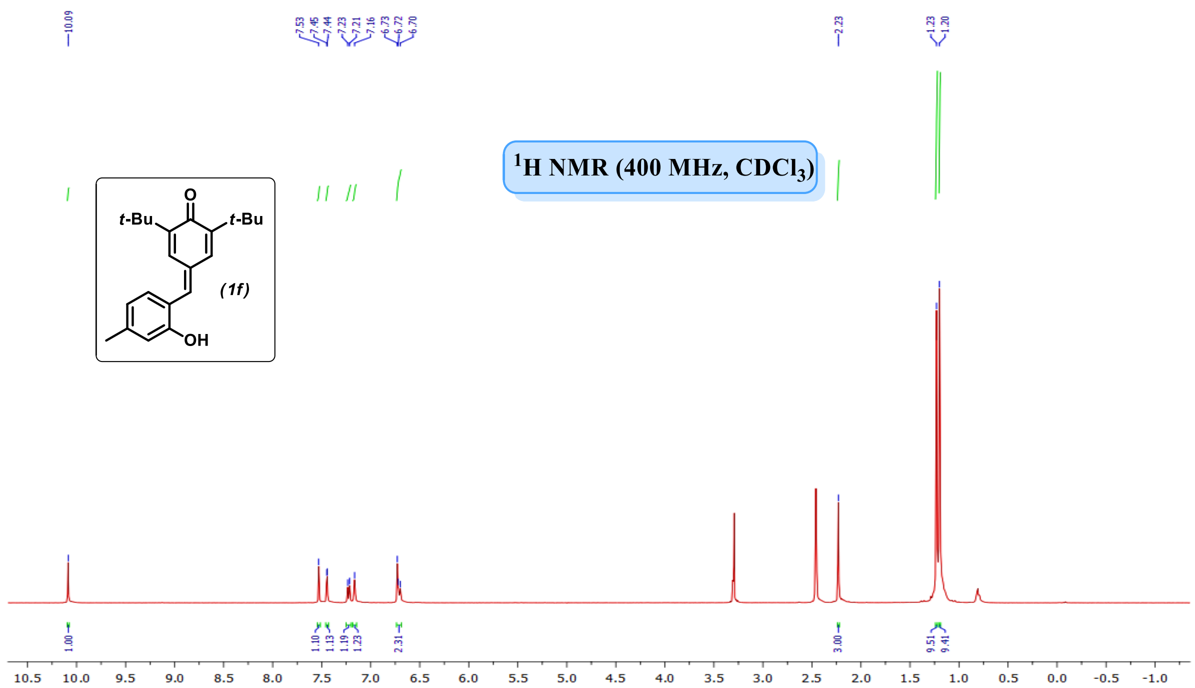

1H NMR (400 MHz, CDCl3)
t-Bu
t-Bu
O
OH
(1f)

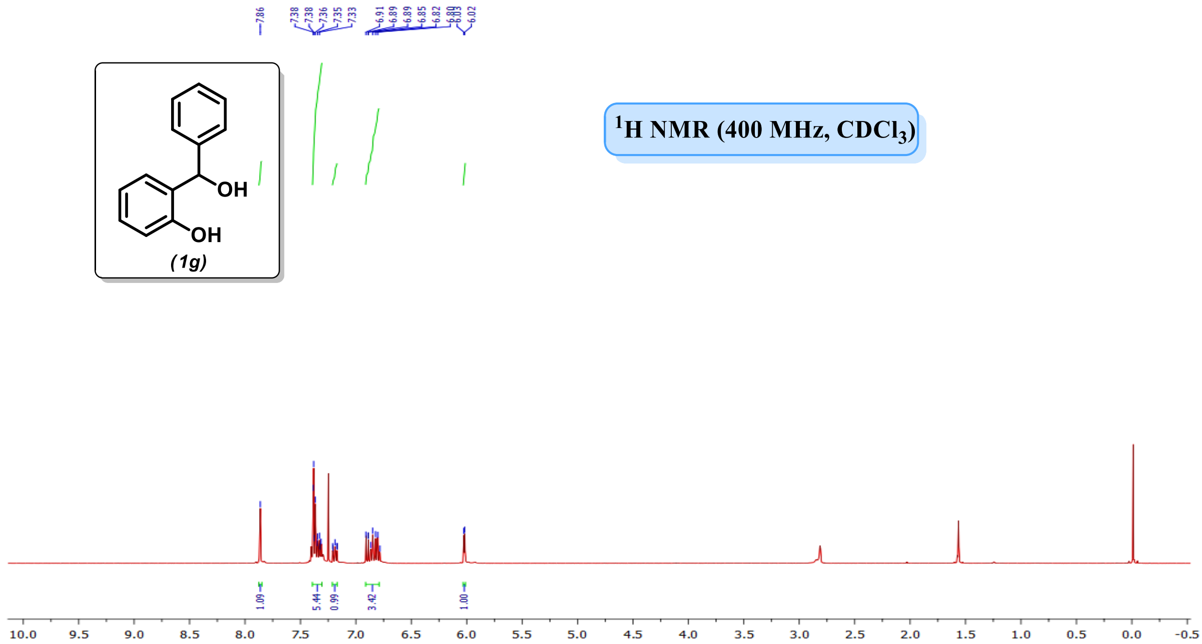

OH
OH
(1g)
1H NMR (400 MHz, CDCl3)
10.0 9.5 9.0 8.5 8.0 7.5 7.0 6.5 6.0 5.5 5.0 4.5 4.0 3.5 3.0 2.5 2.0 1.5 1.0 0.5 0.0 -0.5

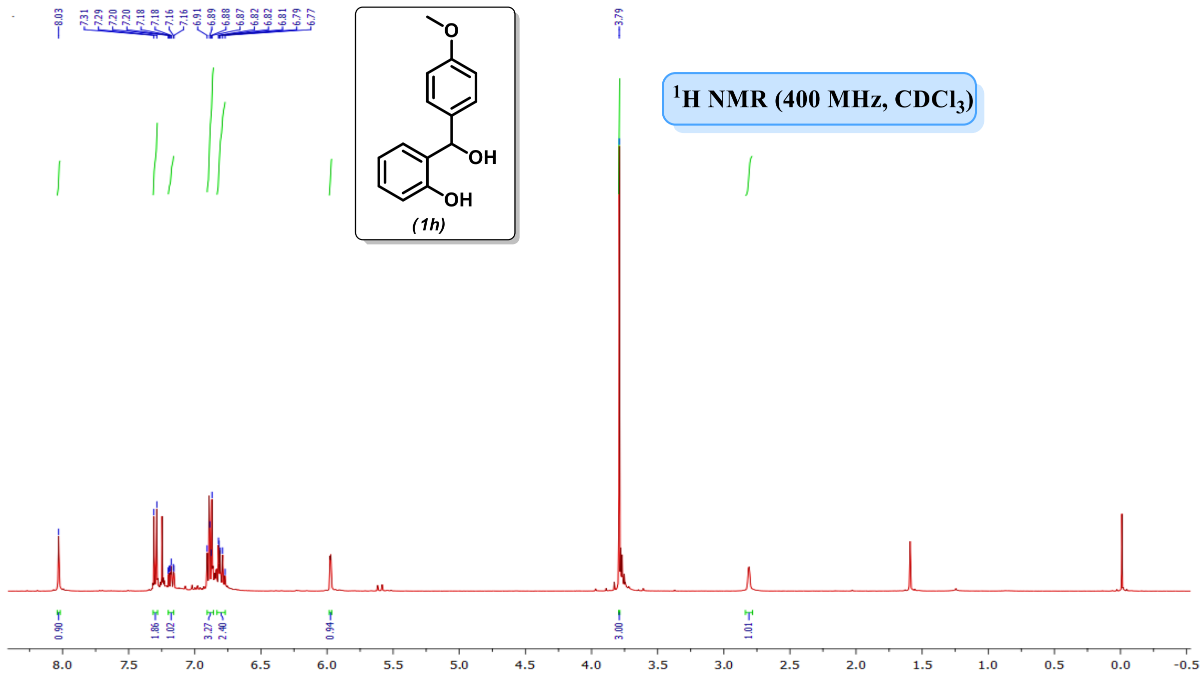

O
OH
OH
(1h)
1H NMR (400 MHz, CDCl3)
8.0 7.5 7.0 6.5 6.0 5.5 5.0 4.5 4.0 3.5 3.0 2.5 2.0 1.5 1.0 0.5 0.0 -0.5

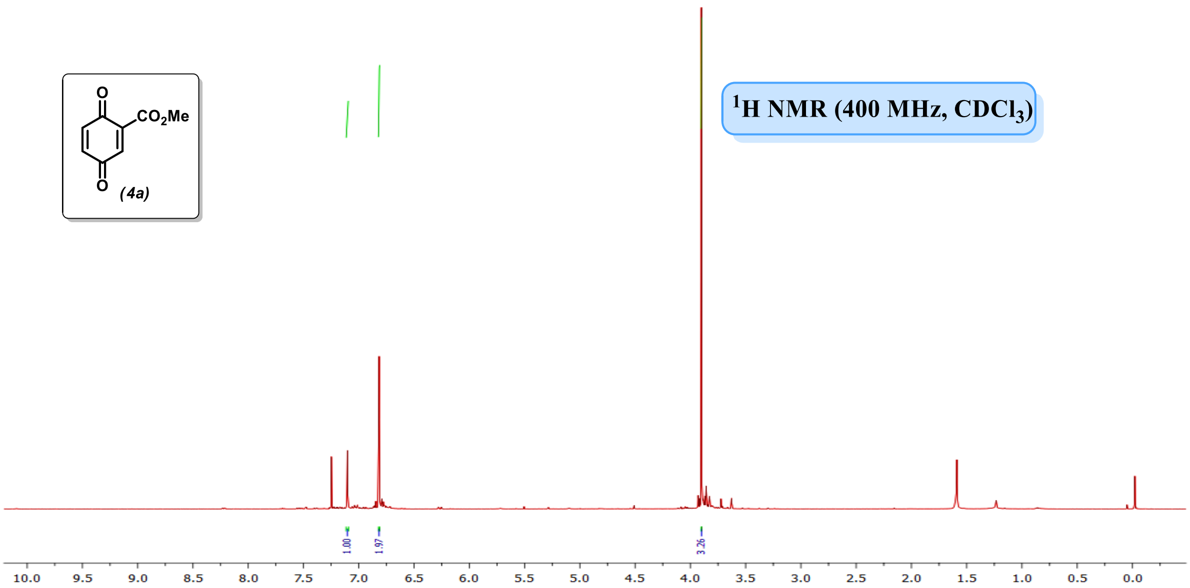
CO2Me
(4a)
1H NMR (400 MHz, CDCl3)
1.00
1.97
3.26
10.0 9.5 9.0 8.5 8.0 7.5 7.0 6.5 6.0 5.5 5.0 4.5 4.0 3.5 3.0 2.5 2.0 1.5 1.0 0.5 0.0

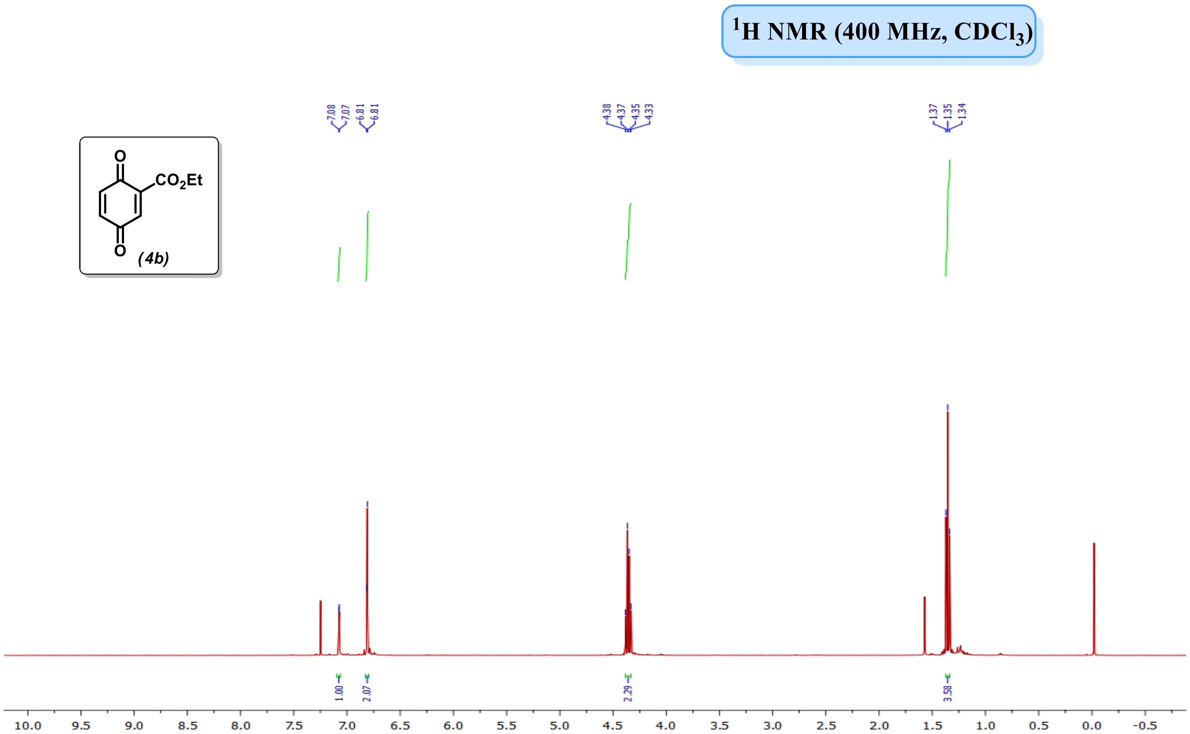
1H NMR (400 MHz, CDCl3)
7.08
7.07
6.81
6.81
4.38
4.37
4.35
4.33
1.37
1.35
1.34
CO2Et
(4b)
1.00
2.07
2.29
3.58
10.0 9.5 9.0 8.5 8.0 7.5 7.0 6.5 6.0 5.5 5.0 4.5 4.0 3.5 3.0 2.5 2.0 1.5 1.0 0.5 0.0 -0.5

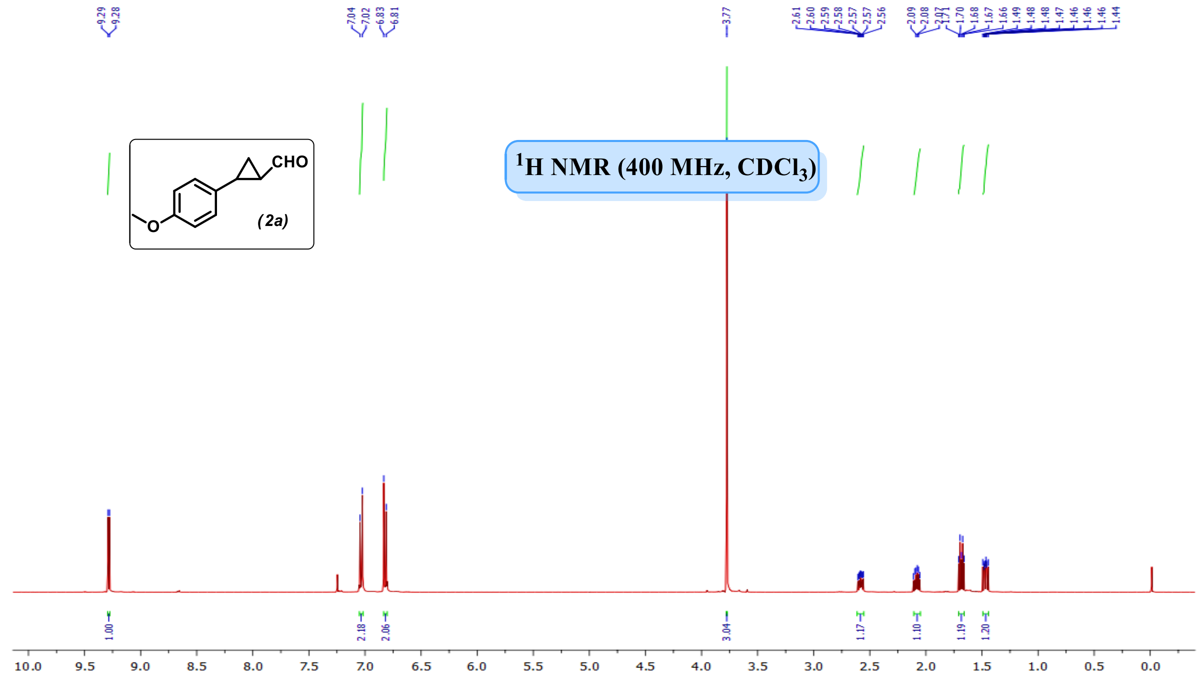
(2a)
^{1}H NMR (400 MHz, CDCl$_3$)

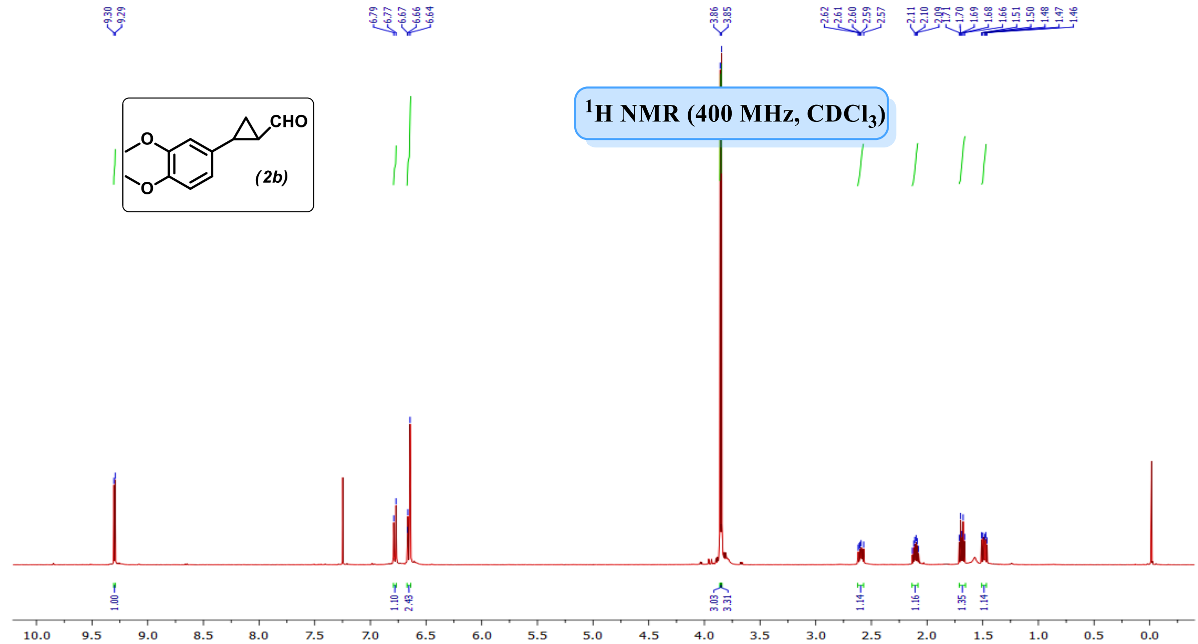
(2b)
^{1}H NMR (400 MHz, CDCl$_3$)

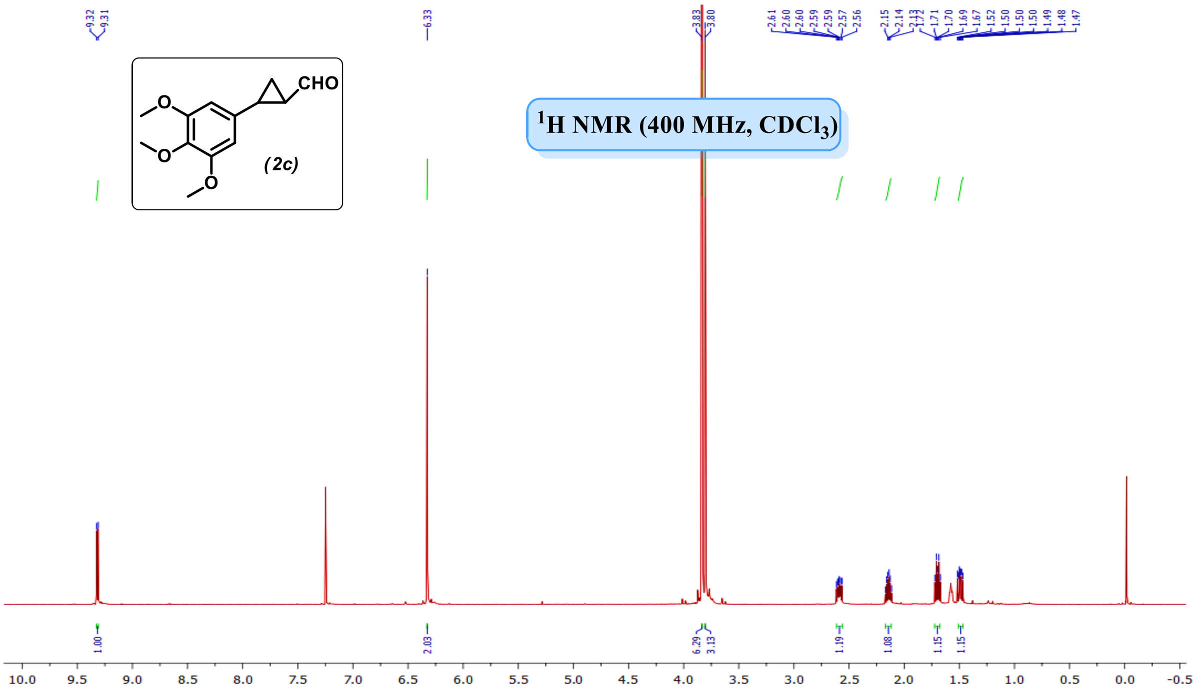
CHO
(2c)
^{1}H NMR (400 MHz, CDCl$_3$)

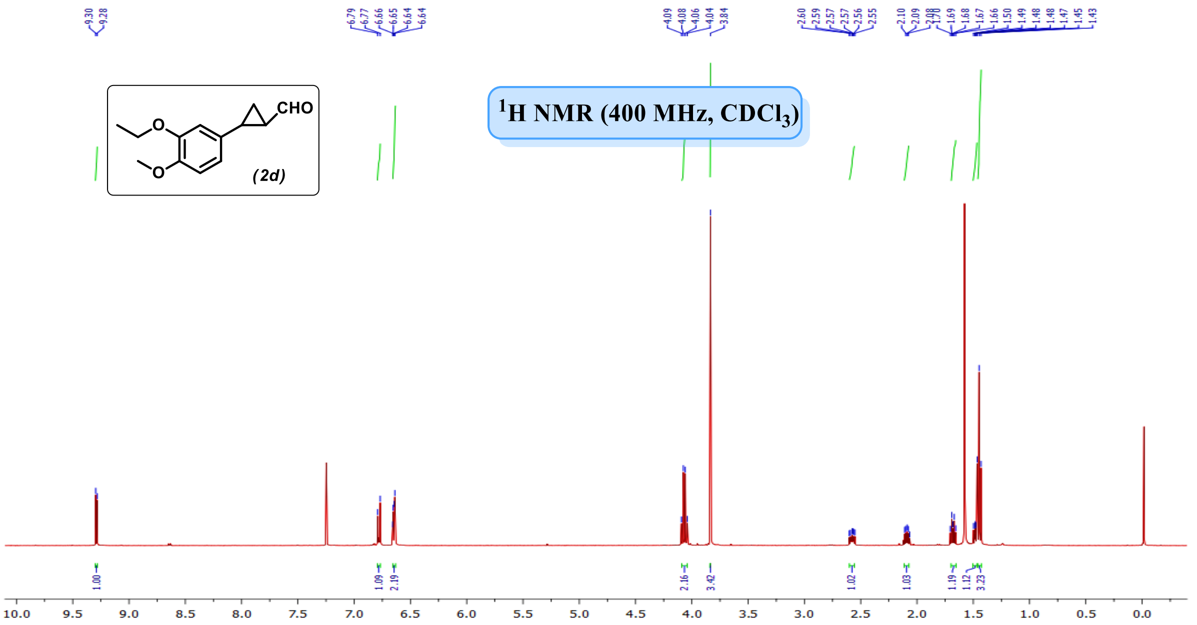
CHO
(2d)
^{1}H NMR (400 MHz, CDCl$_3$)

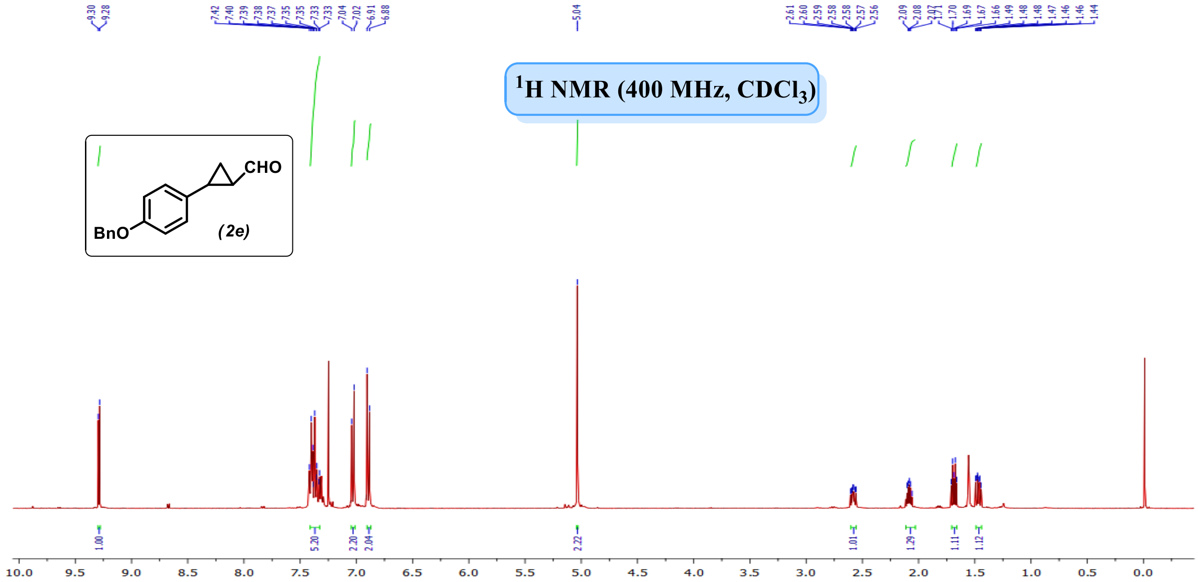

¹H NMR (400 MHz, CDCl3)
CHO
BnO
(2e)

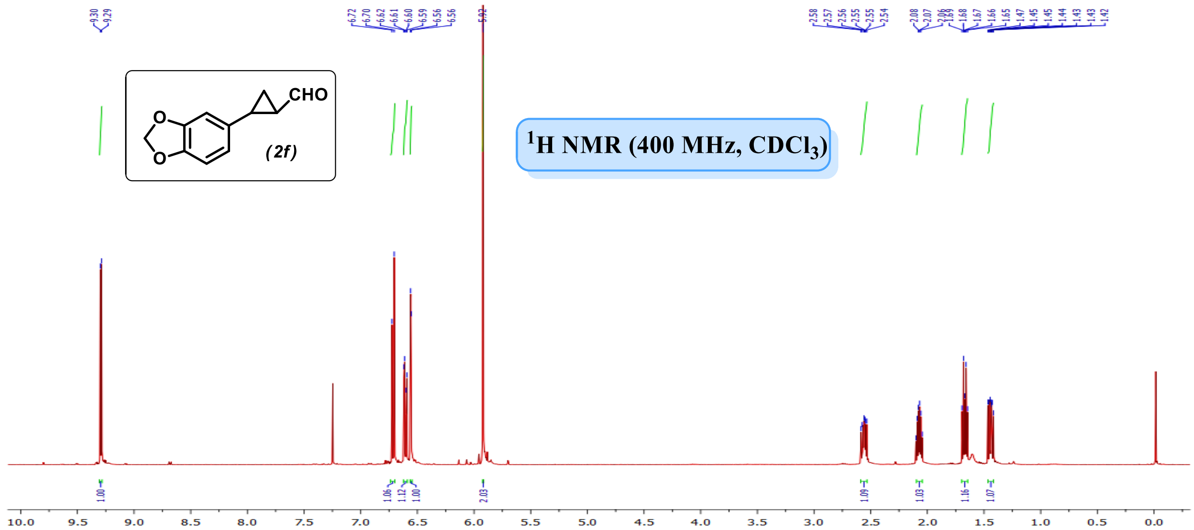

CHO
(2f)
¹H NMR (400 MHz, CDCl3)

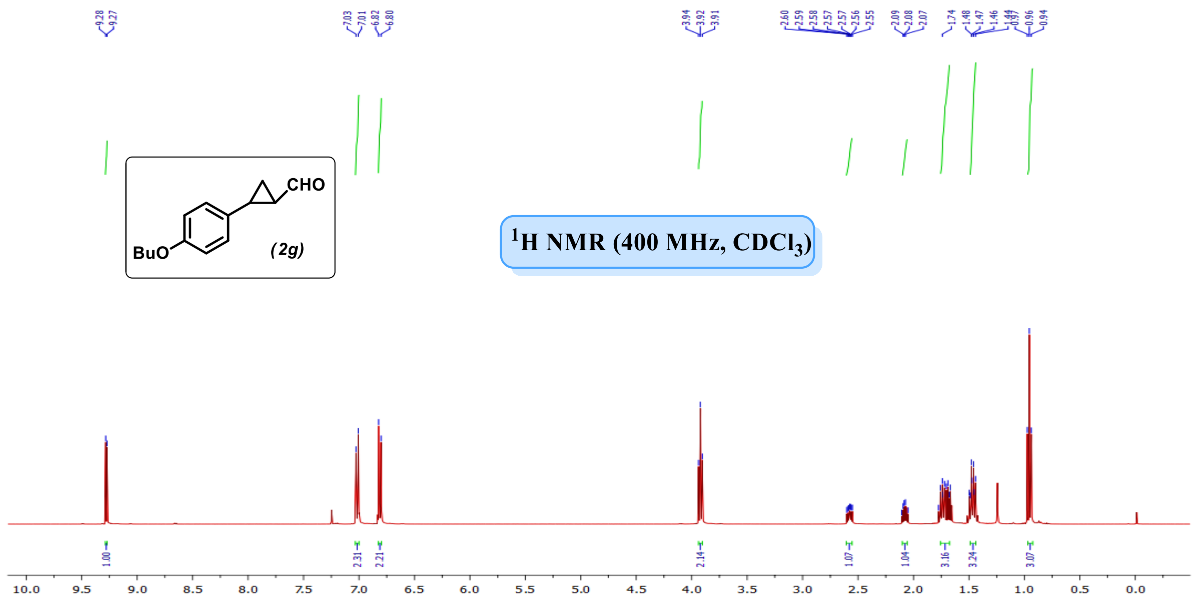

CHO
BuO
(2g)
¹H NMR (400 MHz, CDCl3)

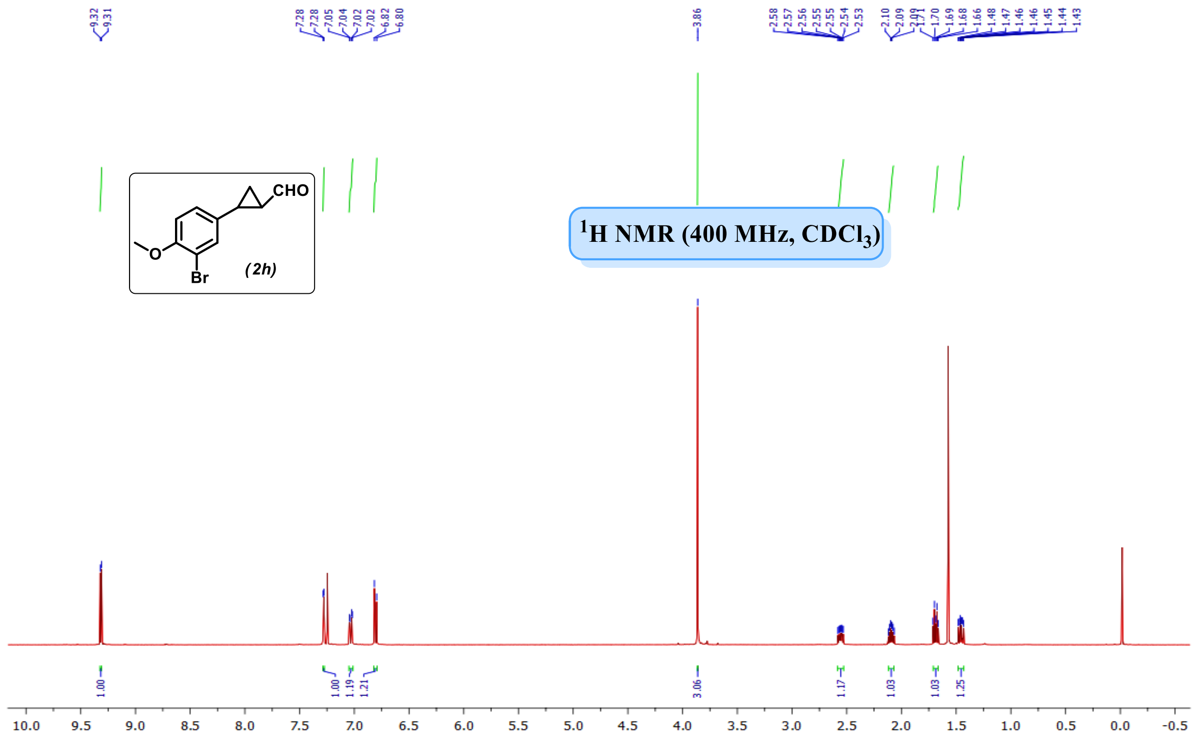
CHO
O
Br
(2h)
¹H NMR (400 MHz, CDCl₃)

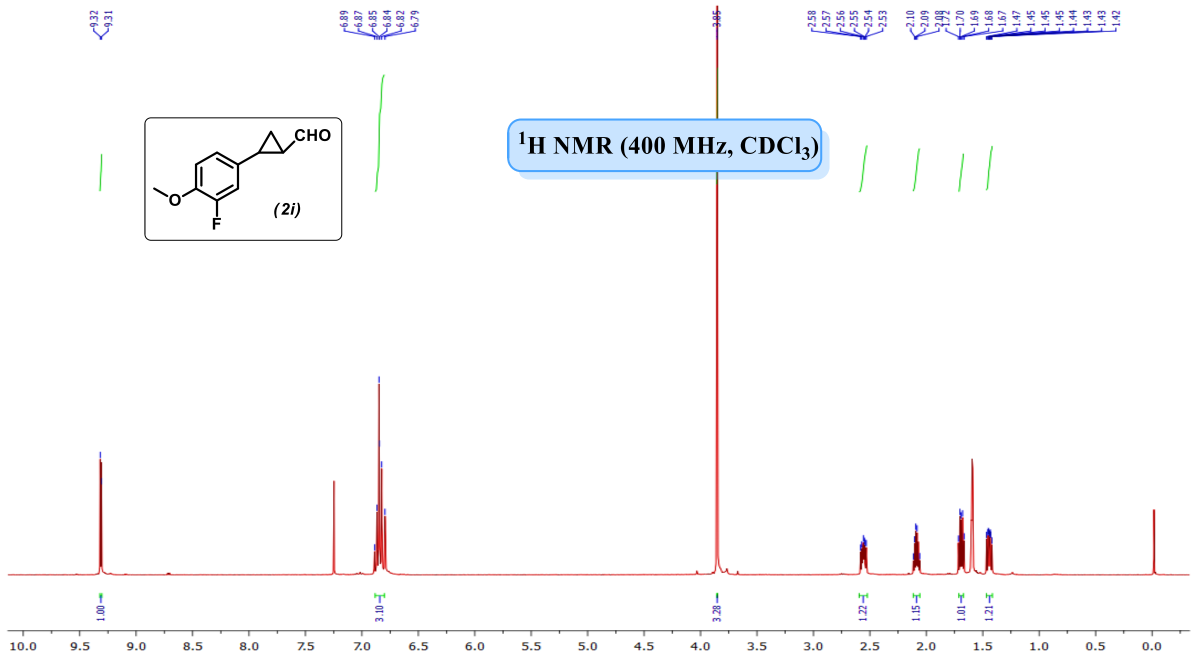
CHO
O
F
(2i)
¹H NMR (400 MHz, CDCl₃)

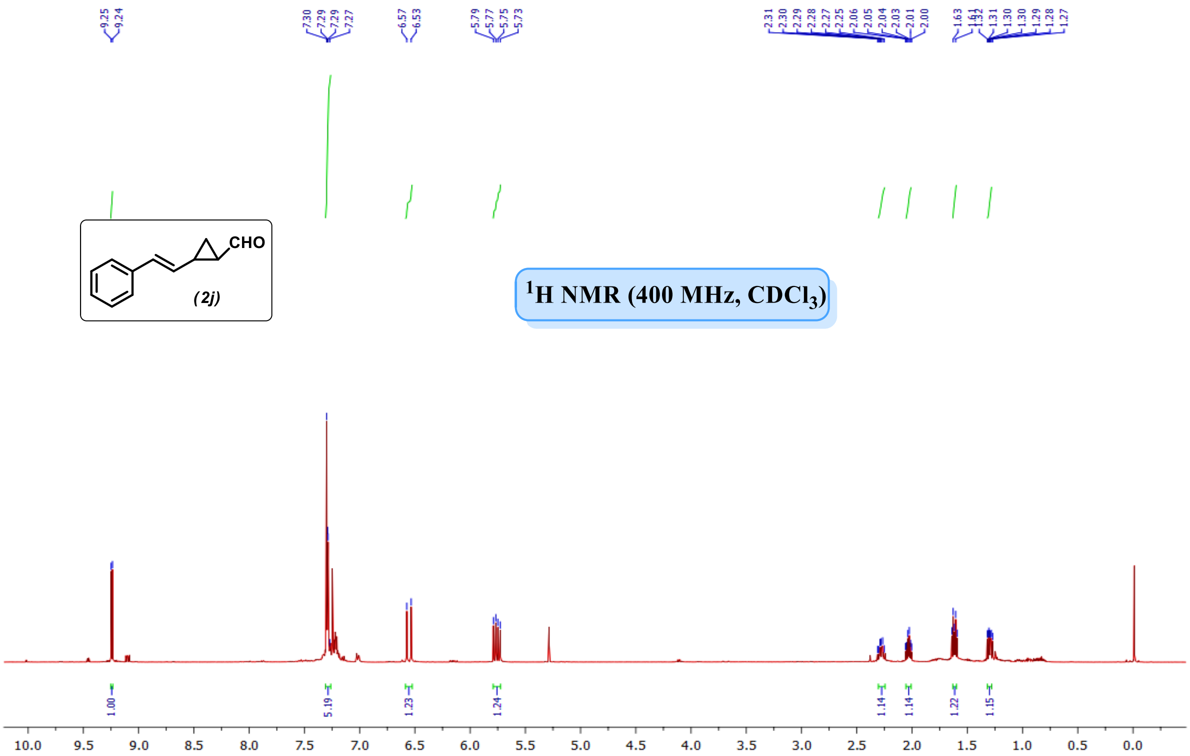
CHO
(2j)
1H NMR (400 MHz, CDCl3)

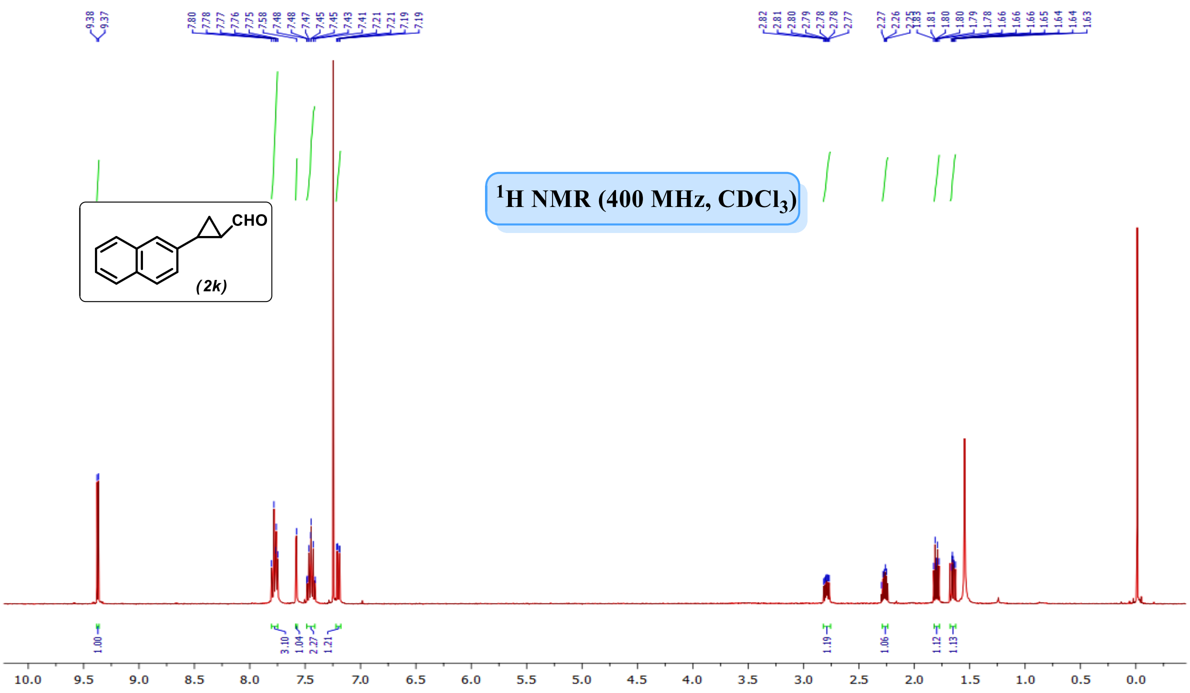
CHO
(2k)
1H NMR (400 MHz, CDCl3)

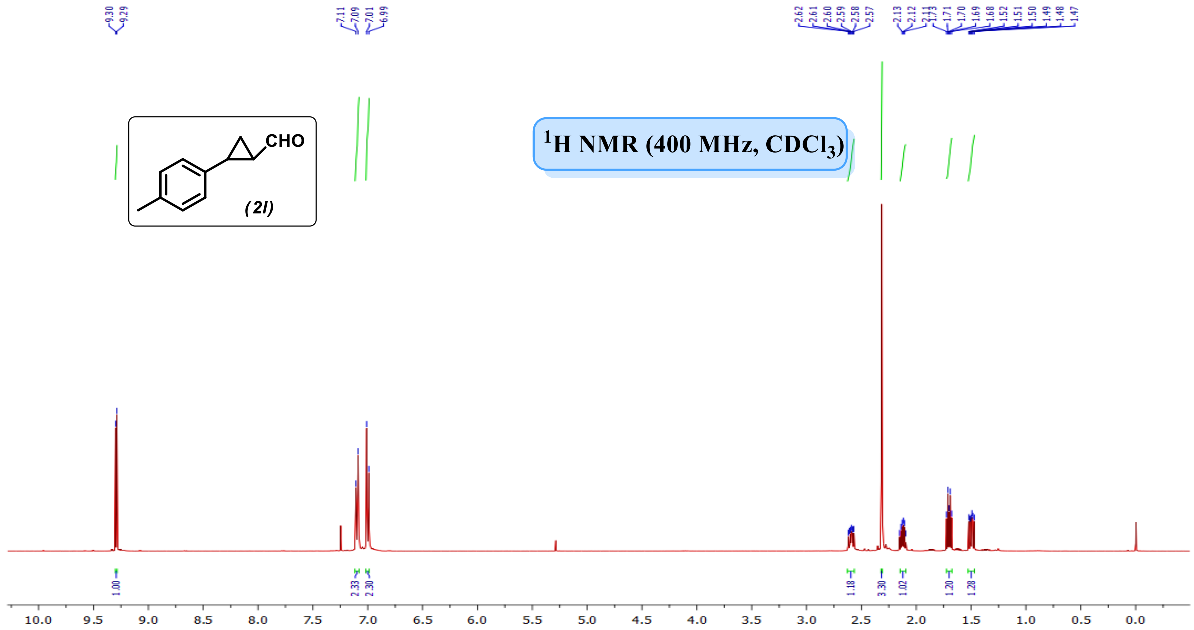
CHO
(2l)
^{1}H NMR (400 MHz, CDCl$_3$)

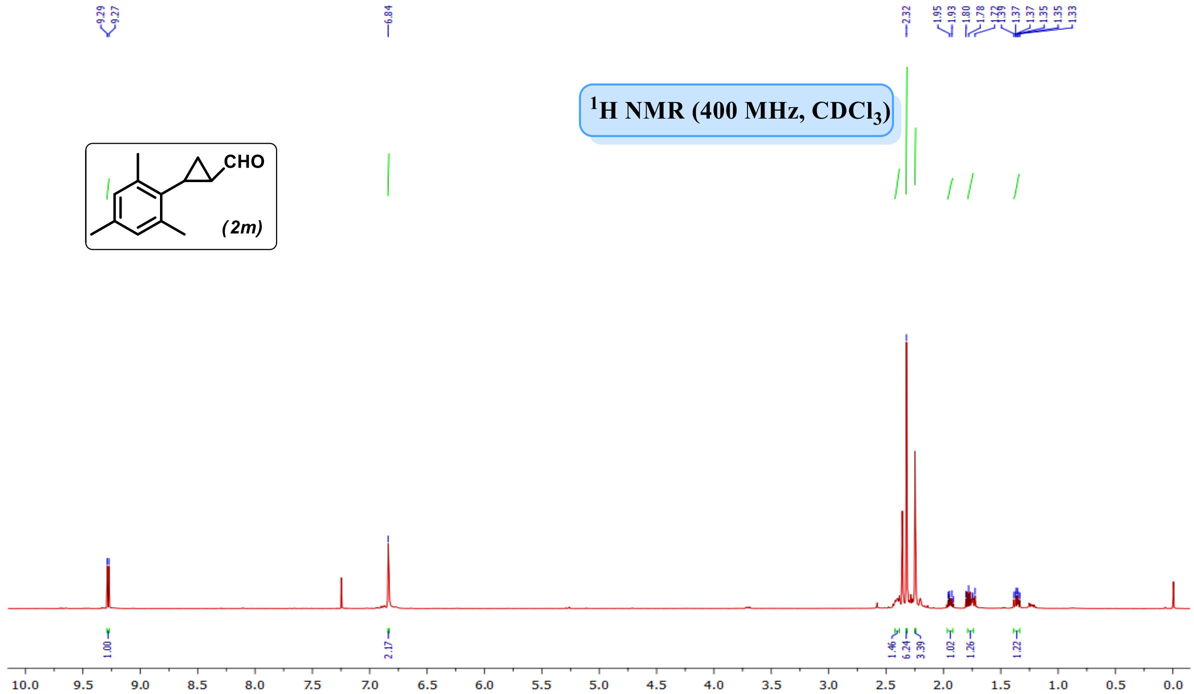
CHO
(2m)
^{1}H NMR (400 MHz, CDCl$_3$)

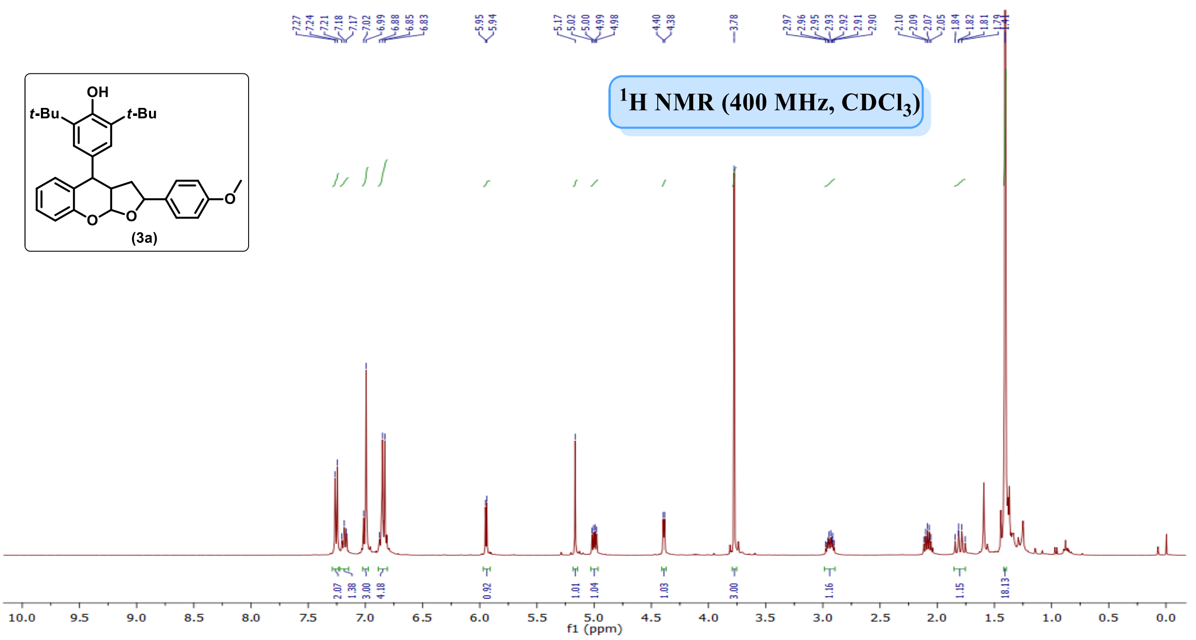
OH
t-Bu
t-Bu
O
O
O
(3a)
^{1}H NMR (400 MHz, CDCl$_3$)
f1 (ppm)

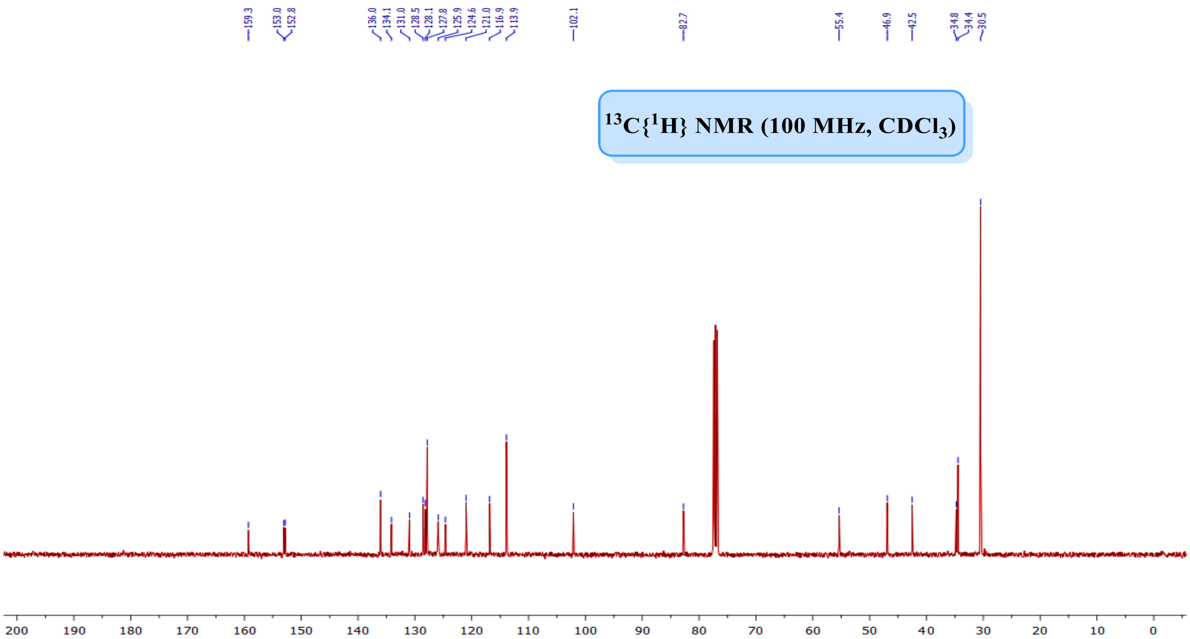
^{13}C{^{1}H} NMR (100 MHz, CDCl$_3$)

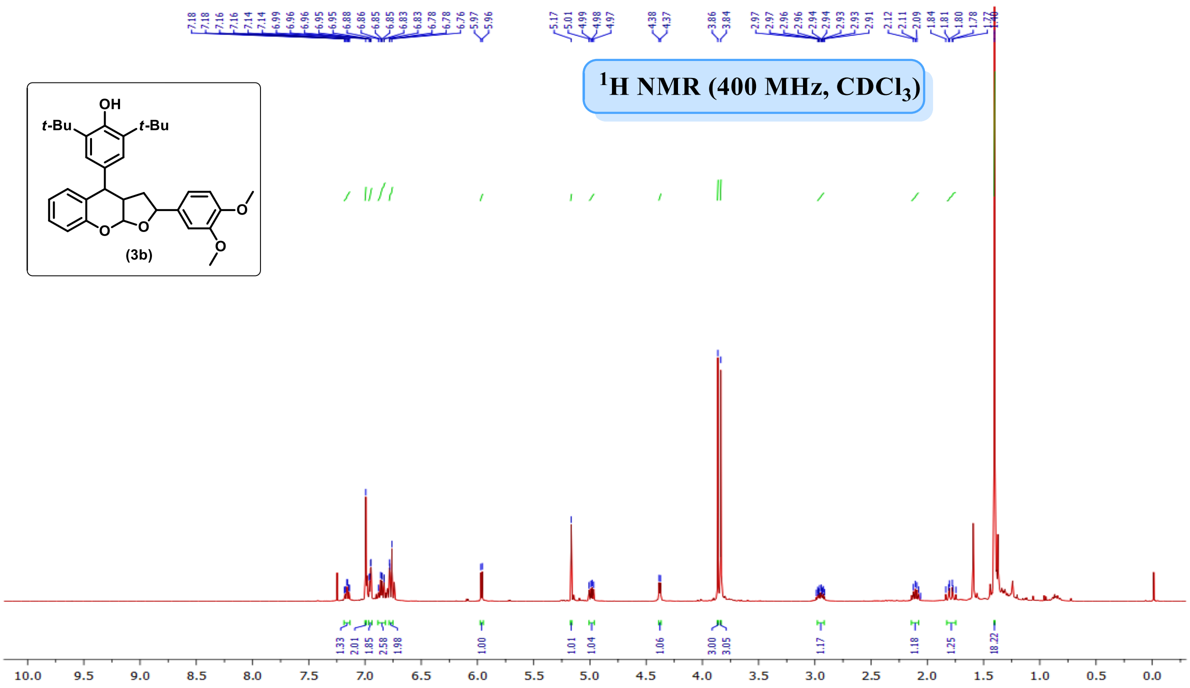

OH
t-Bu
t-Bu
(3b)
¹H NMR (400 MHz, CDCl₃)

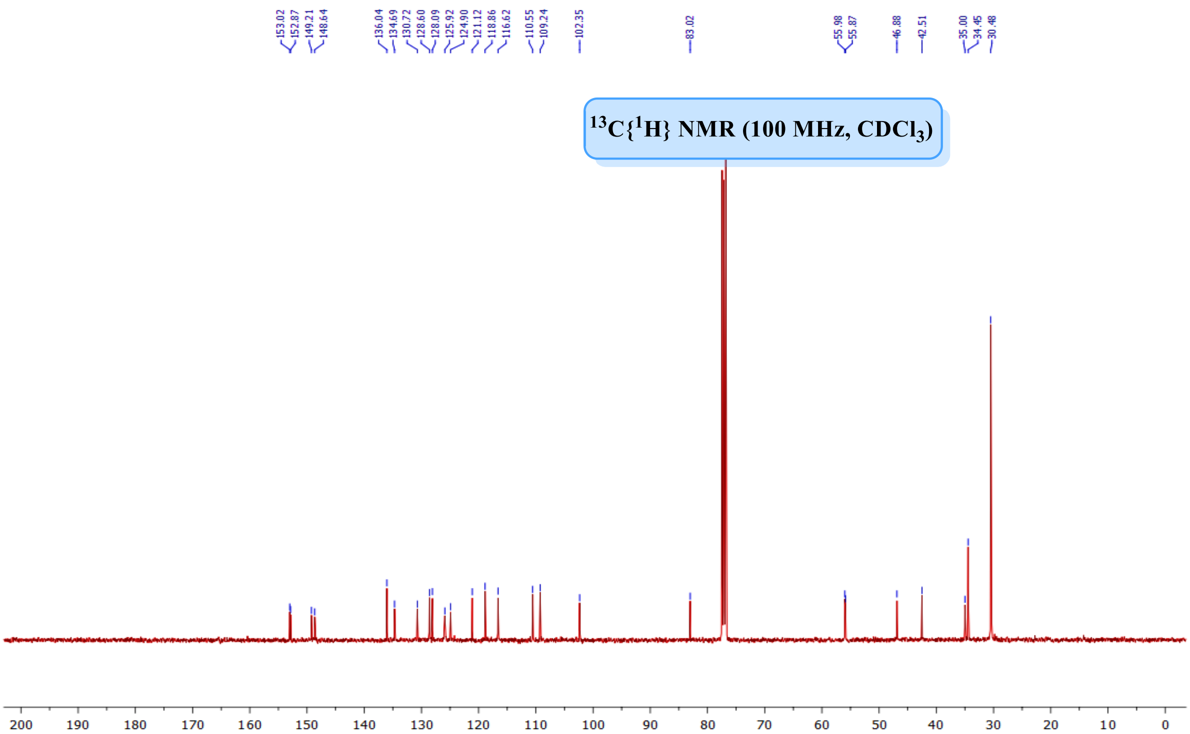

¹³C{¹H} NMR (100 MHz, CDCl₃)

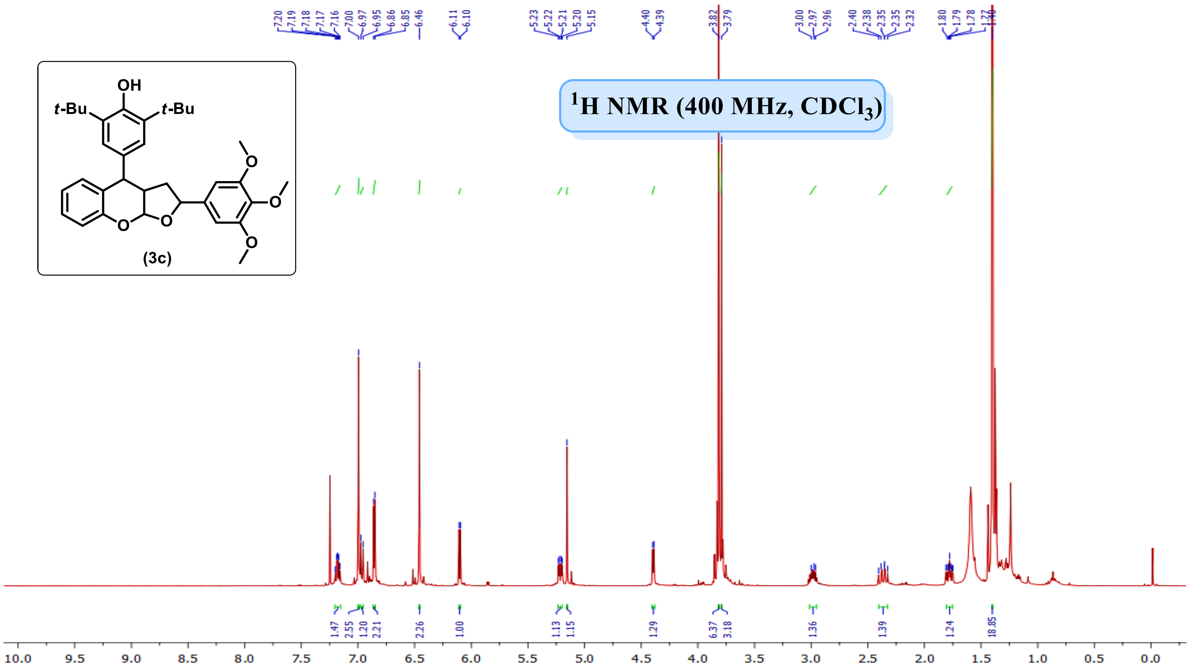
OH
t-Bu
t-Bu
(3c)
^{1}H NMR (400 MHz, CDCl$_3$)

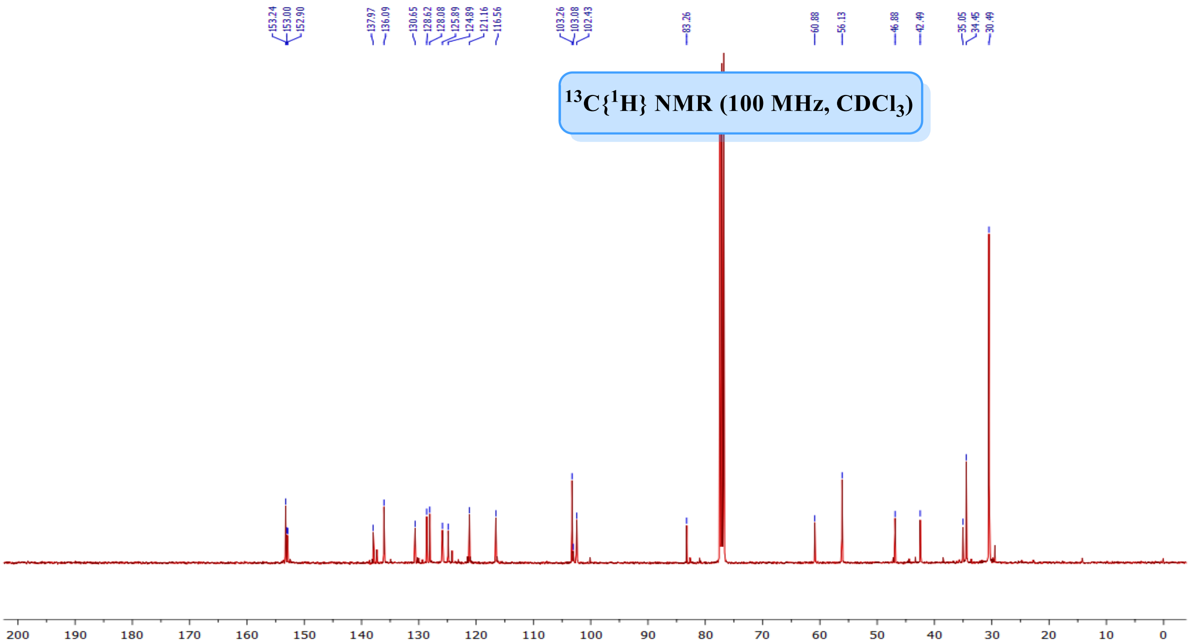
^{13}C{^{1}H} NMR (100 MHz, CDCl$_3$)

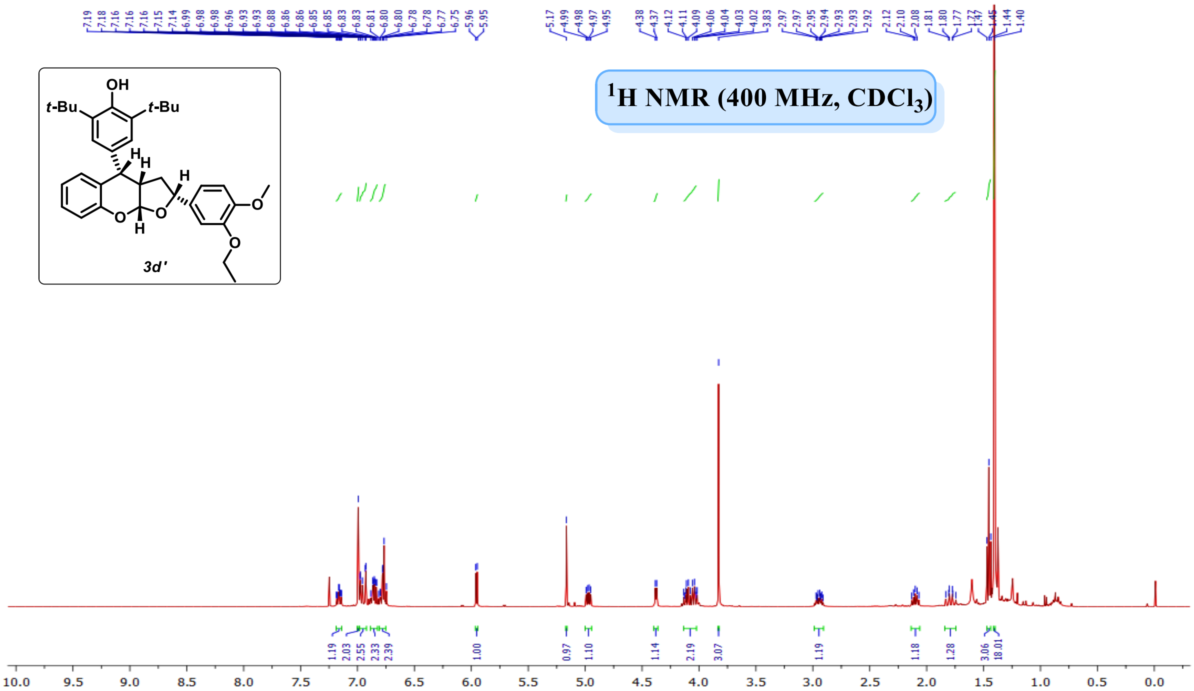

OH
t-Bu
t-Bu
H
H
H
O
O
H
O
O
3d'
¹H NMR (400 MHz, CDCl₃)

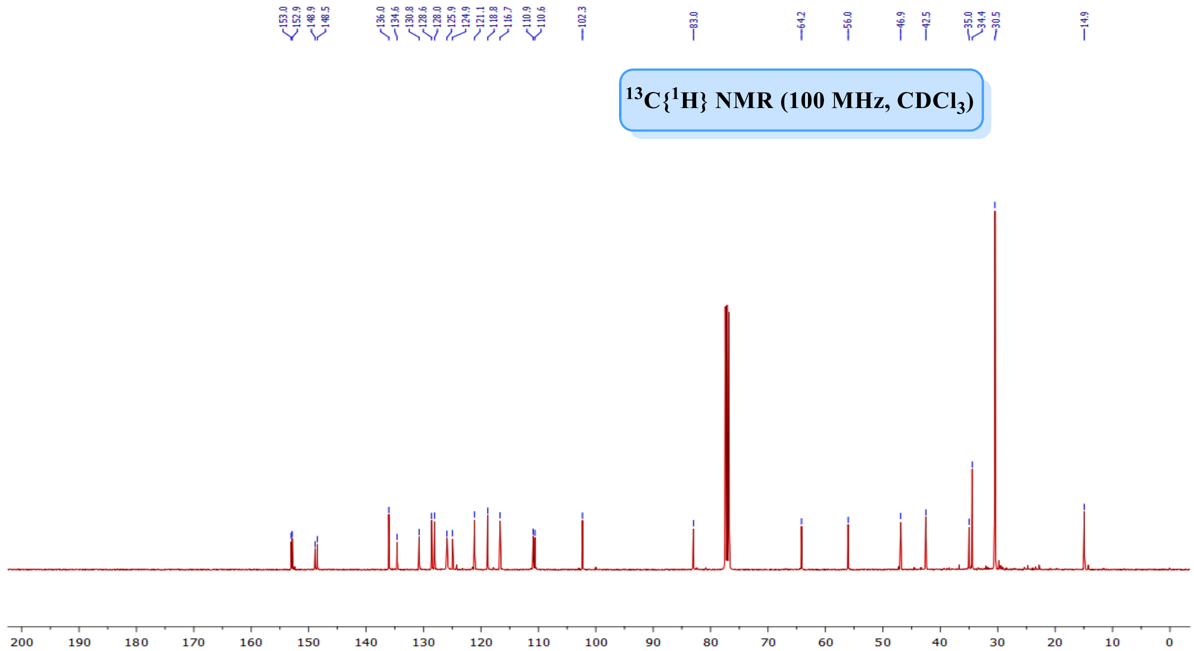

¹³C{¹H} NMR (100 MHz, CDCl₃)

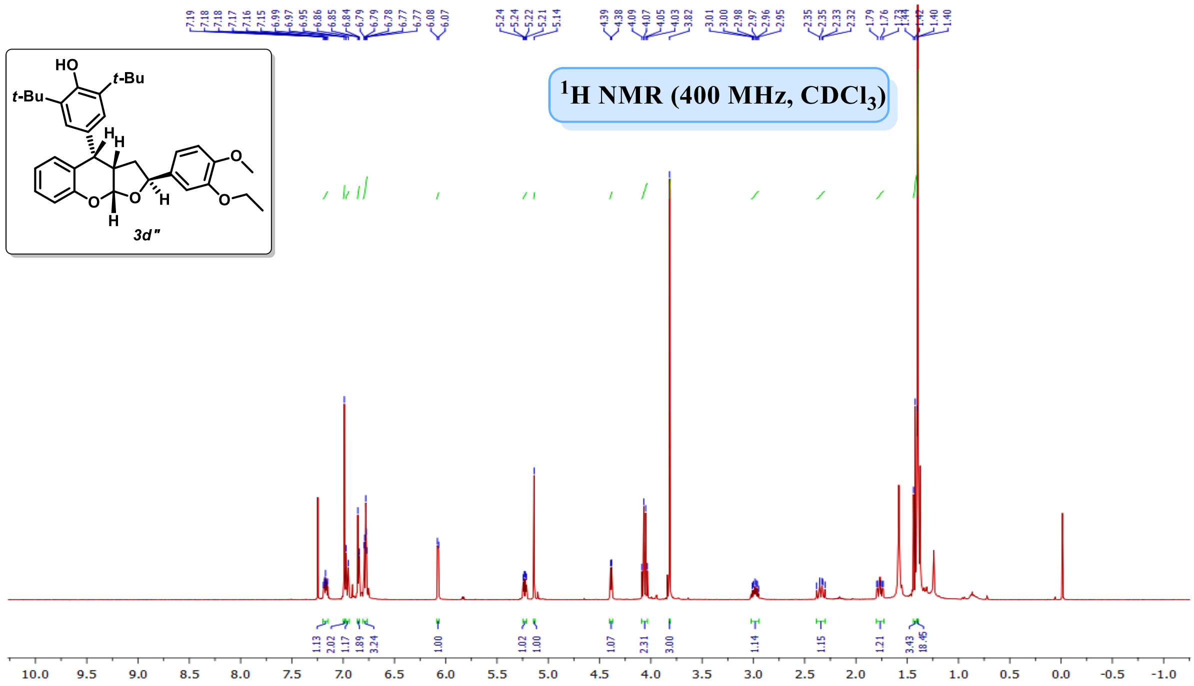
1H NMR (400 MHz, CDCl3)
HO
t-Bu
t-Bu
3d''

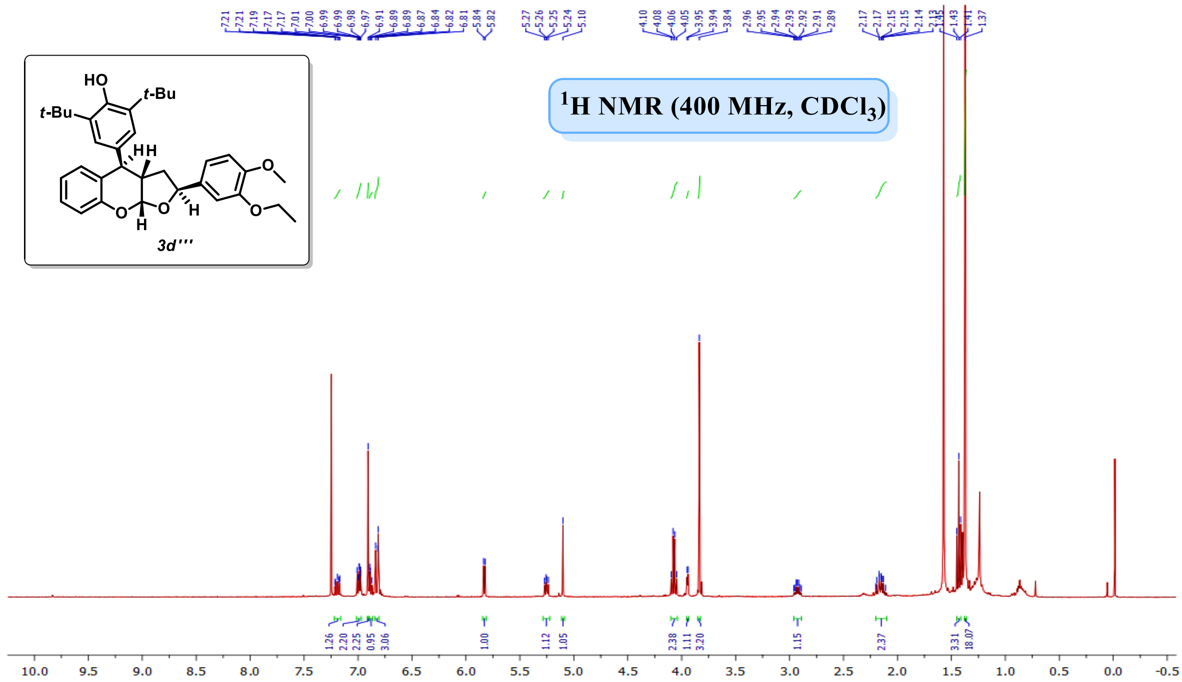
1H NMR (400 MHz, CDCl3)
HO
t-Bu
t-Bu
3d'''

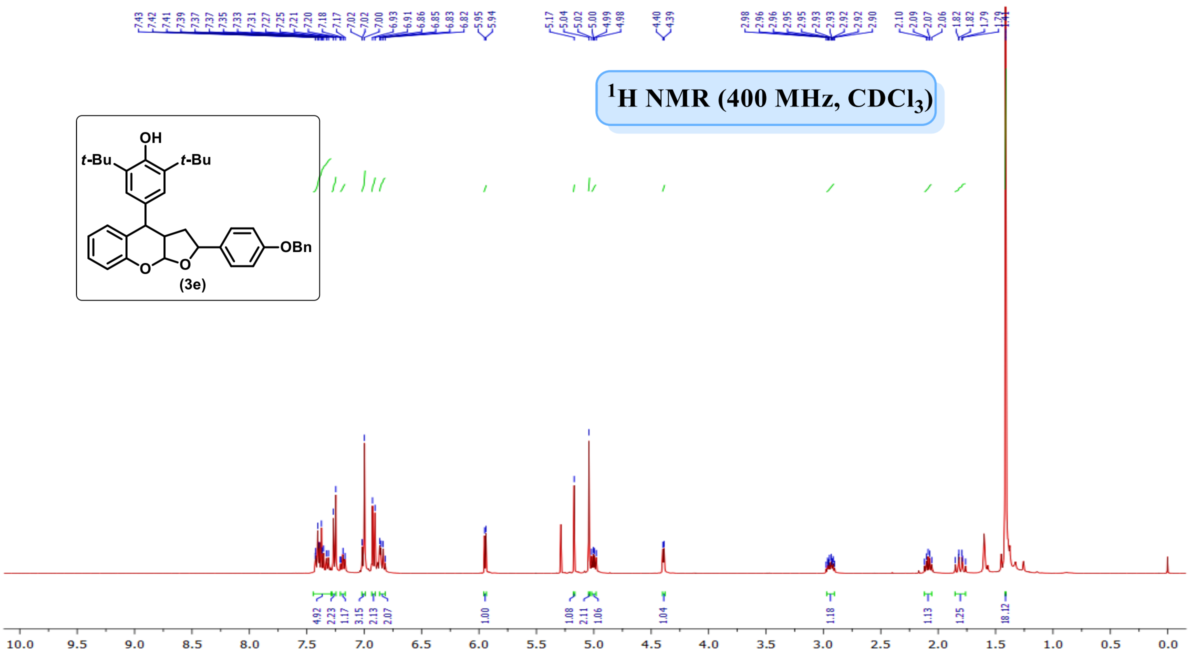
1H NMR (400 MHz, CDCl3)
OH
t-Bu
t-Bu
OBn
(3e)

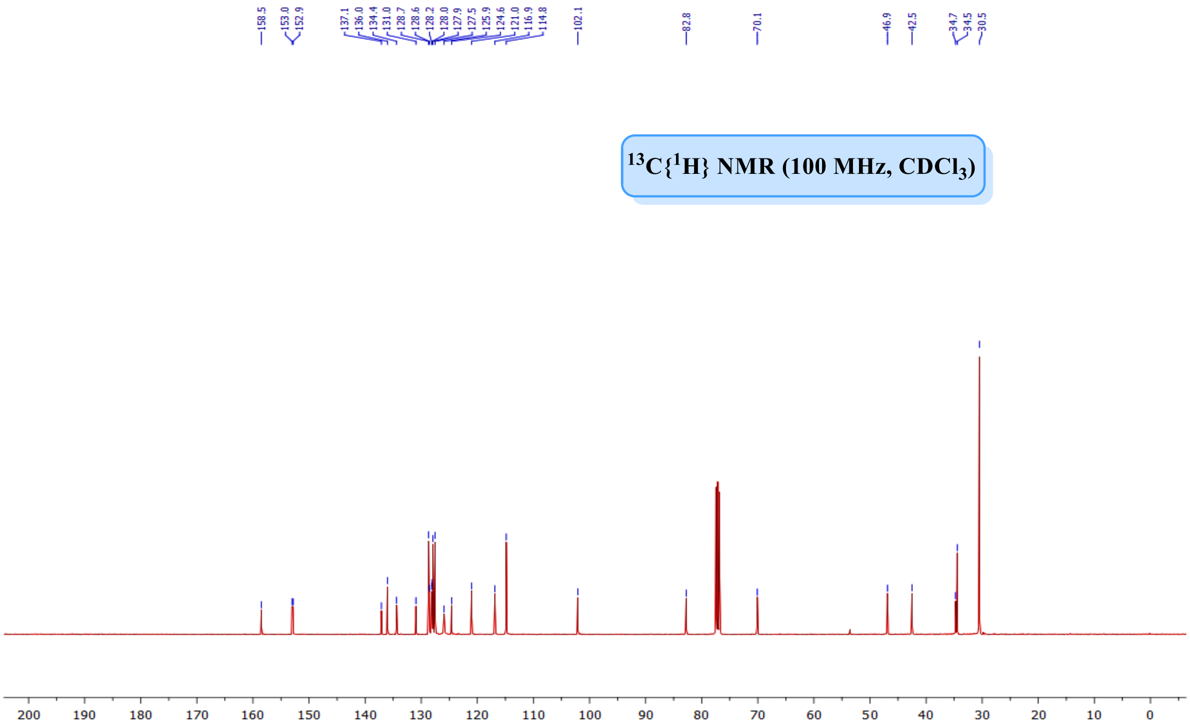
13C{1H} NMR (100 MHz, CDCl3)

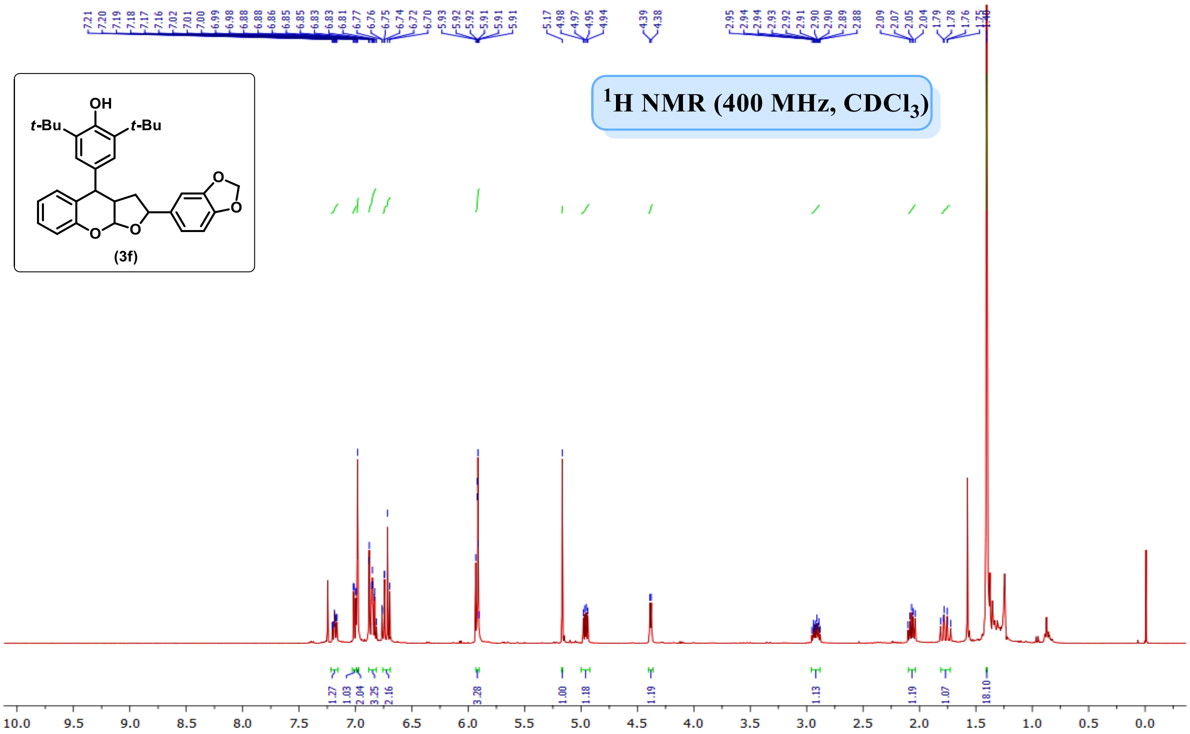
OH
t-Bu
t-Bu
O
O
O
O
(3f)
1H NMR (400 MHz, CDCl3)

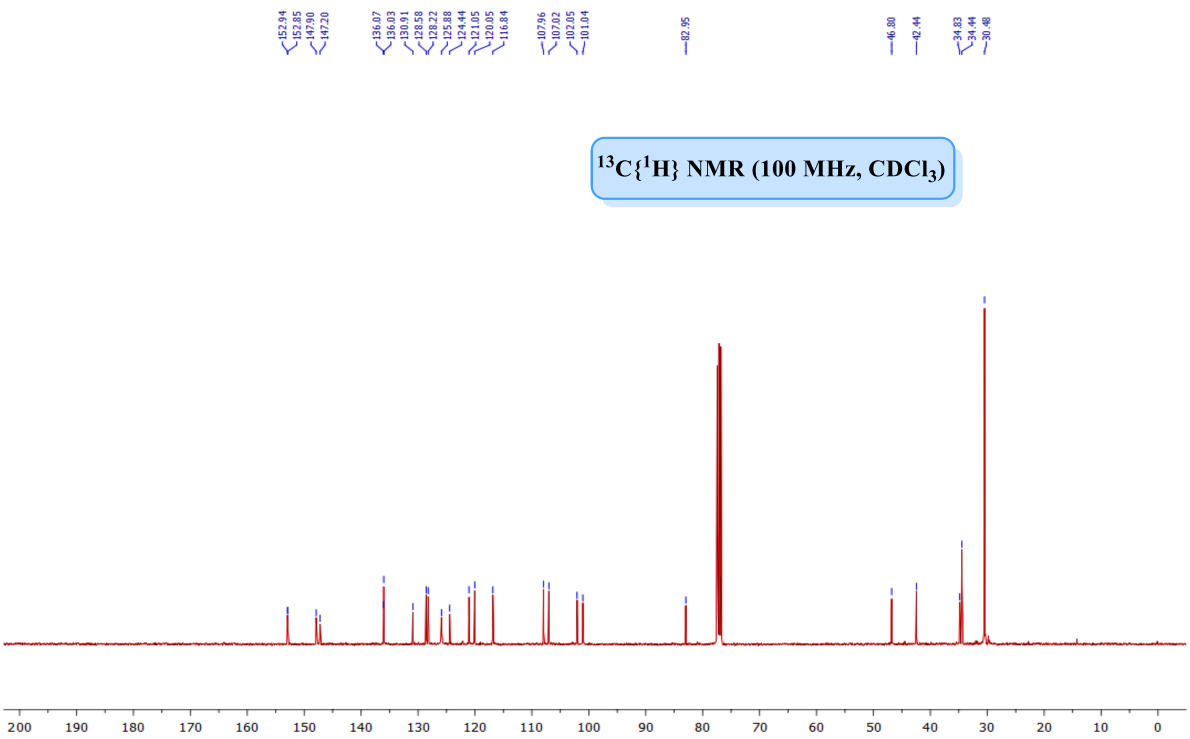
13C{1H} NMR (100 MHz, CDCl3)

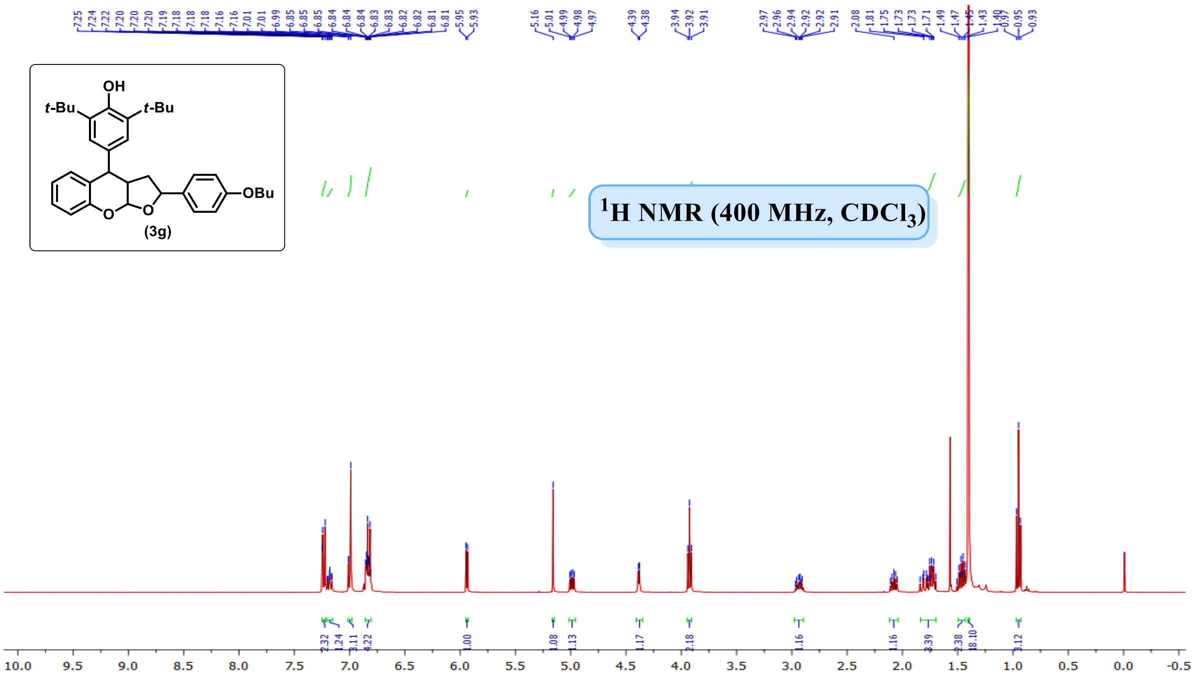
OH
t-Bu
t-Bu
OBu
(3g)
^{1}H NMR (400 MHz, CDCl$_3$)

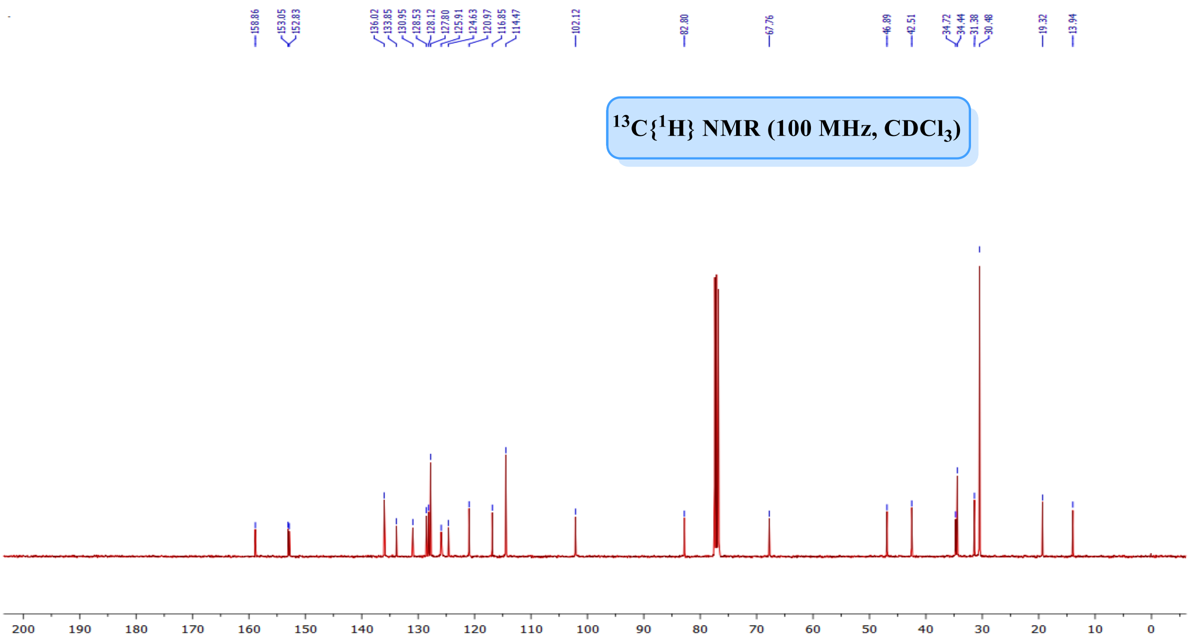
^{13}C{^{1}H} NMR (100 MHz, CDCl$_3$)

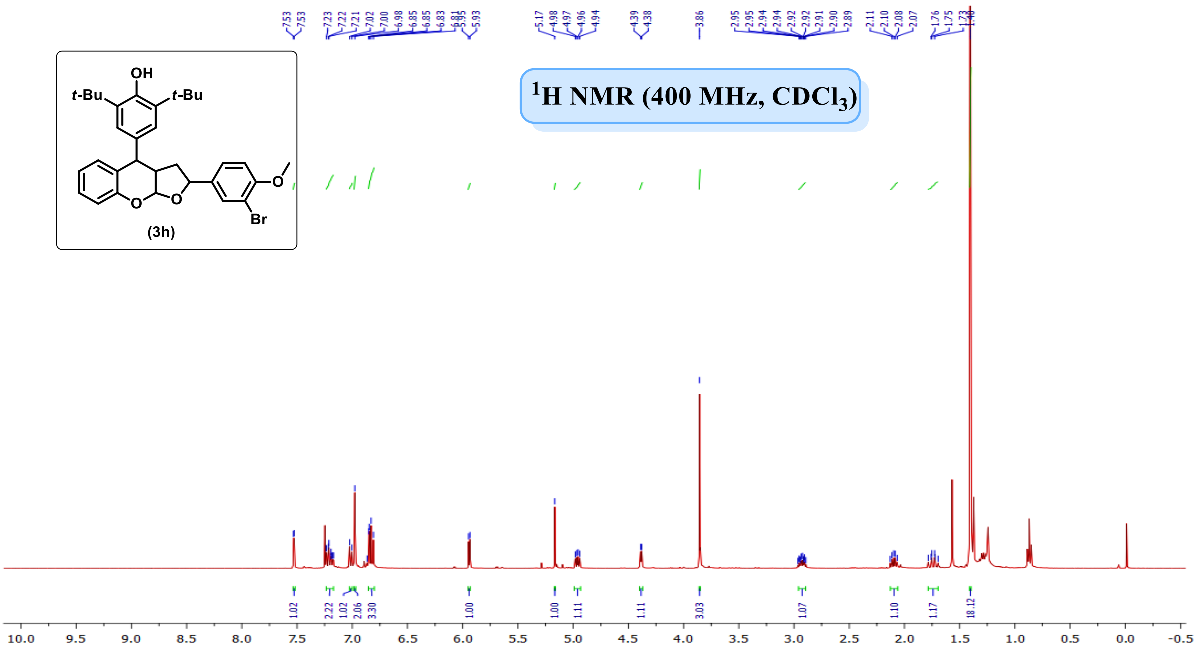
OH
t-Bu
t-Bu
O
O
O
Br
(3h)
1H NMR (400 MHz, CDCl3)

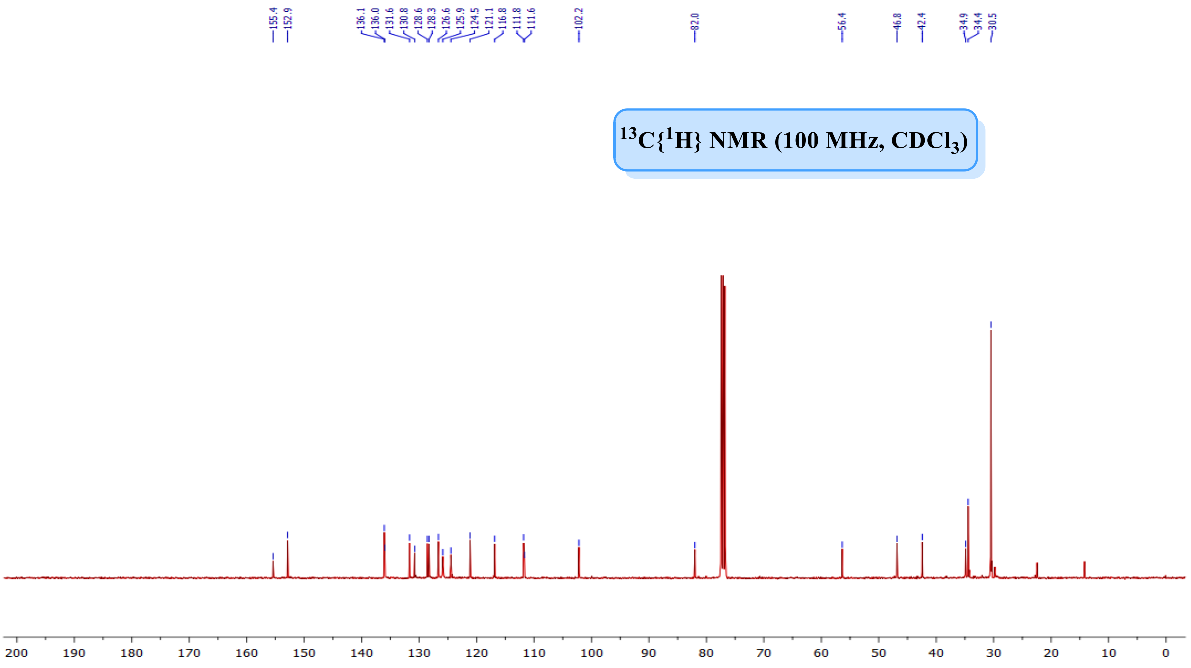
13C{1H} NMR (100 MHz, CDCl3)

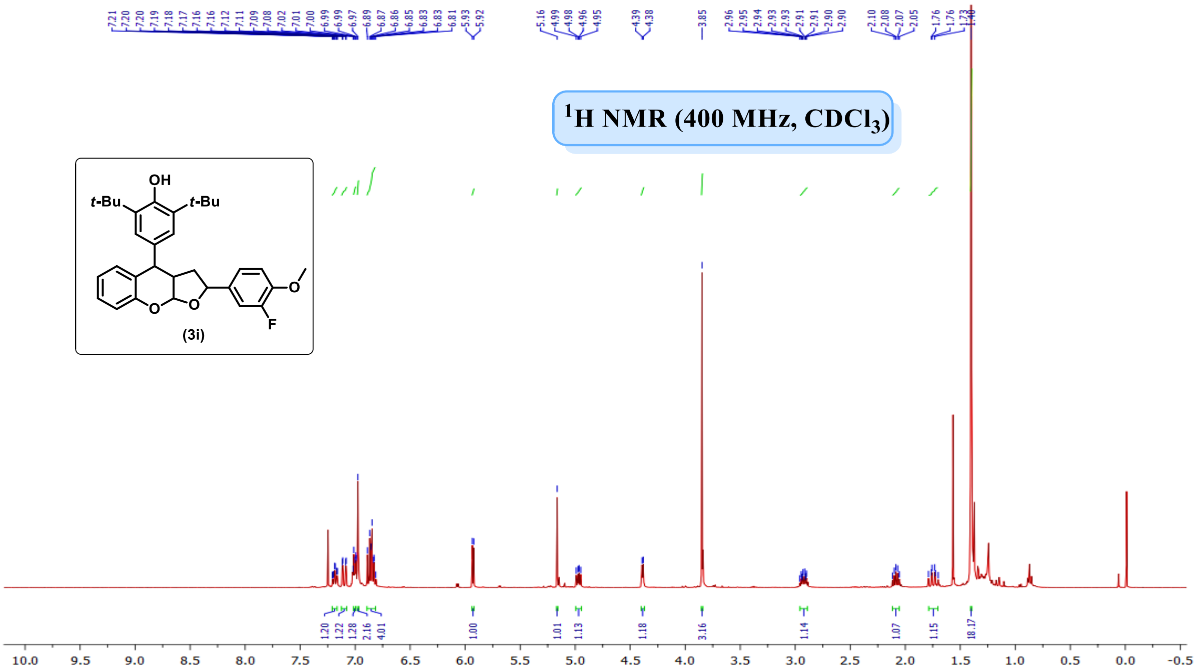
^{1}H NMR (400 MHz, $CDCl_3$)
OH
t-Bu
t-Bu
O
O
O
F
(3i)

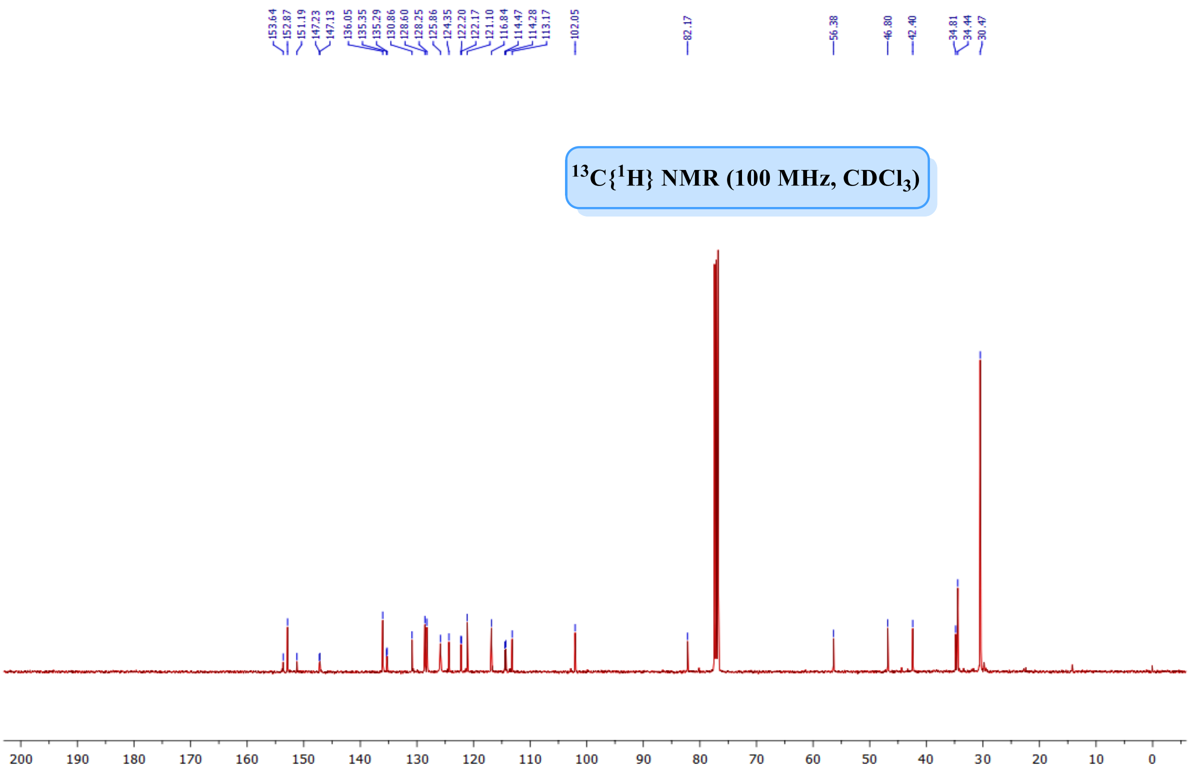
^{13}C{^{1}H} NMR (100 MHz, $CDCl_3$)

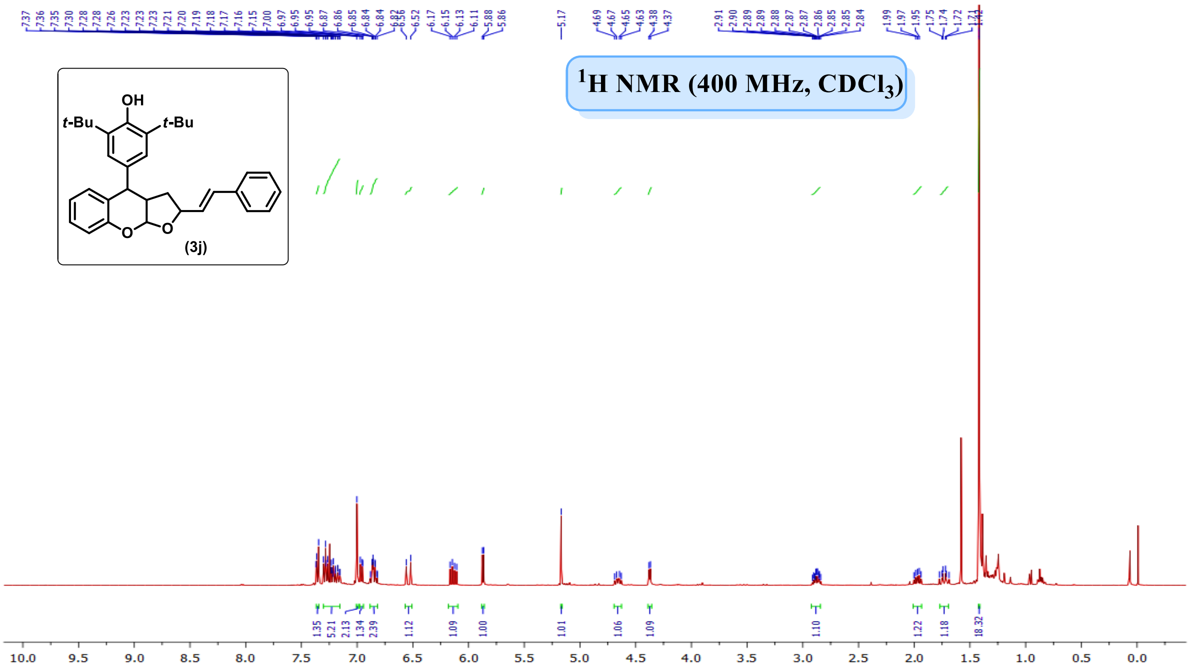

^{1}H NMR (400 MHz, CDCl$_3$)
OH
t-Bu
t-Bu
O
O
(3j)

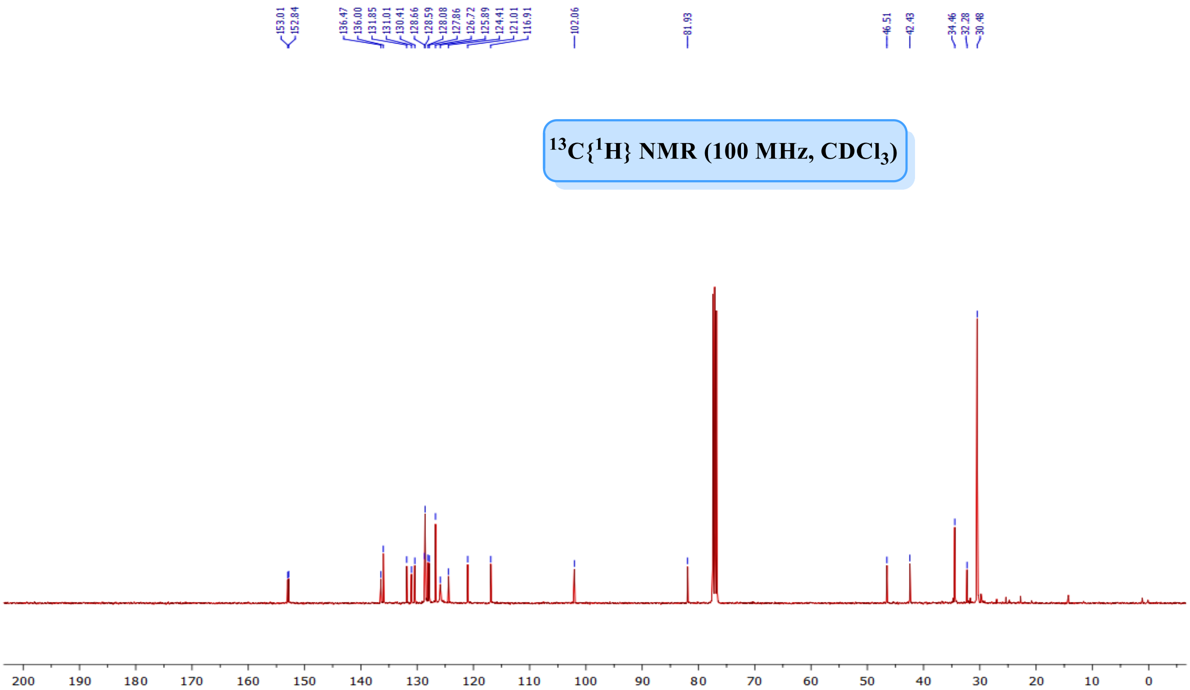

^{13}C{^{1}H} NMR (100 MHz, CDCl$_3$)

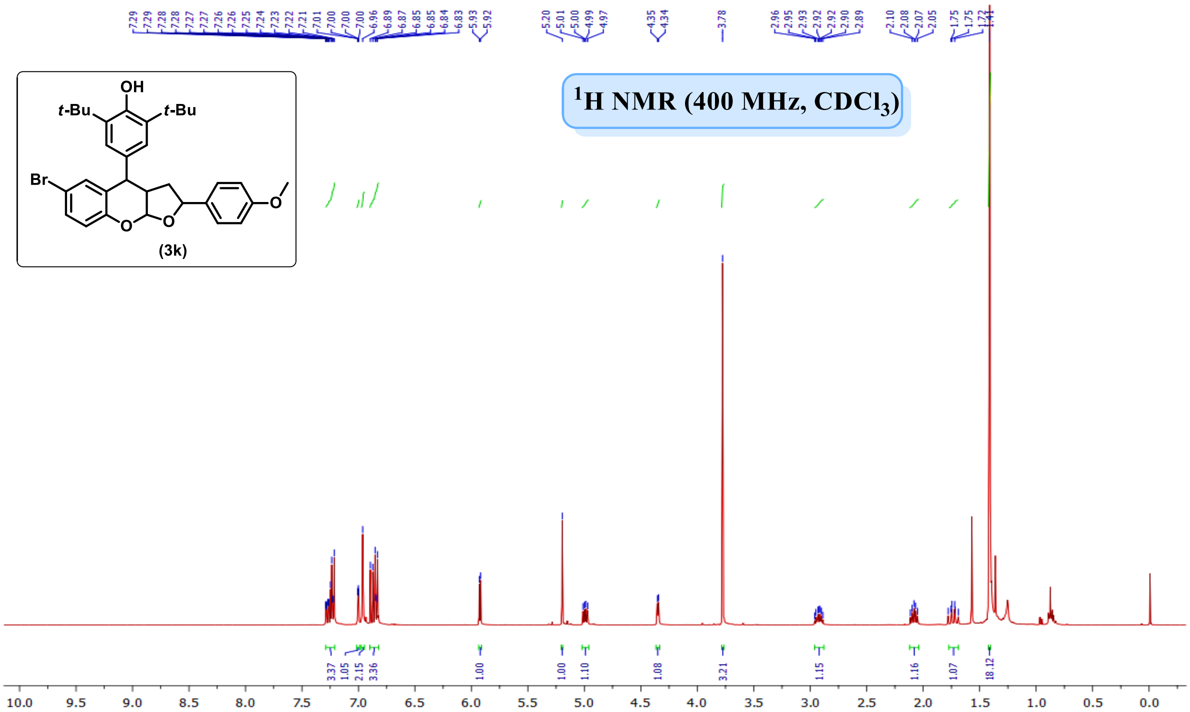

(3k)

^{1}H NMR (400 MHz, $CDCl_3$)

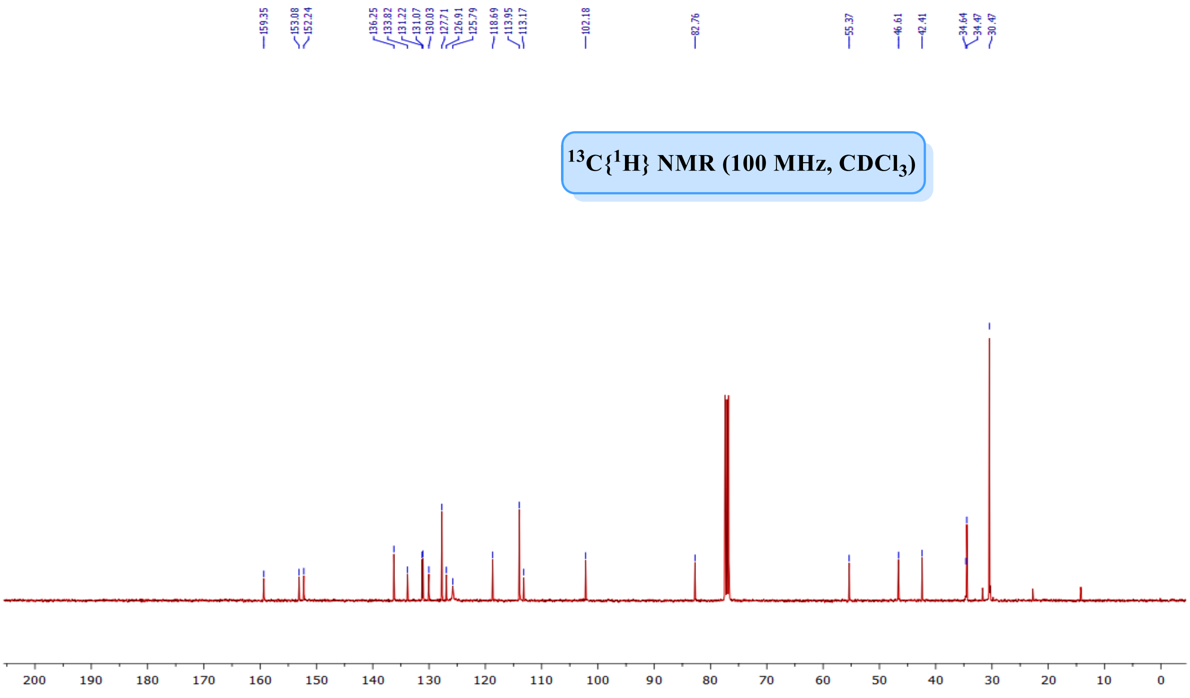

$^{13}C\{^{1}H\}$ NMR (100 MHz, $CDCl_3$)

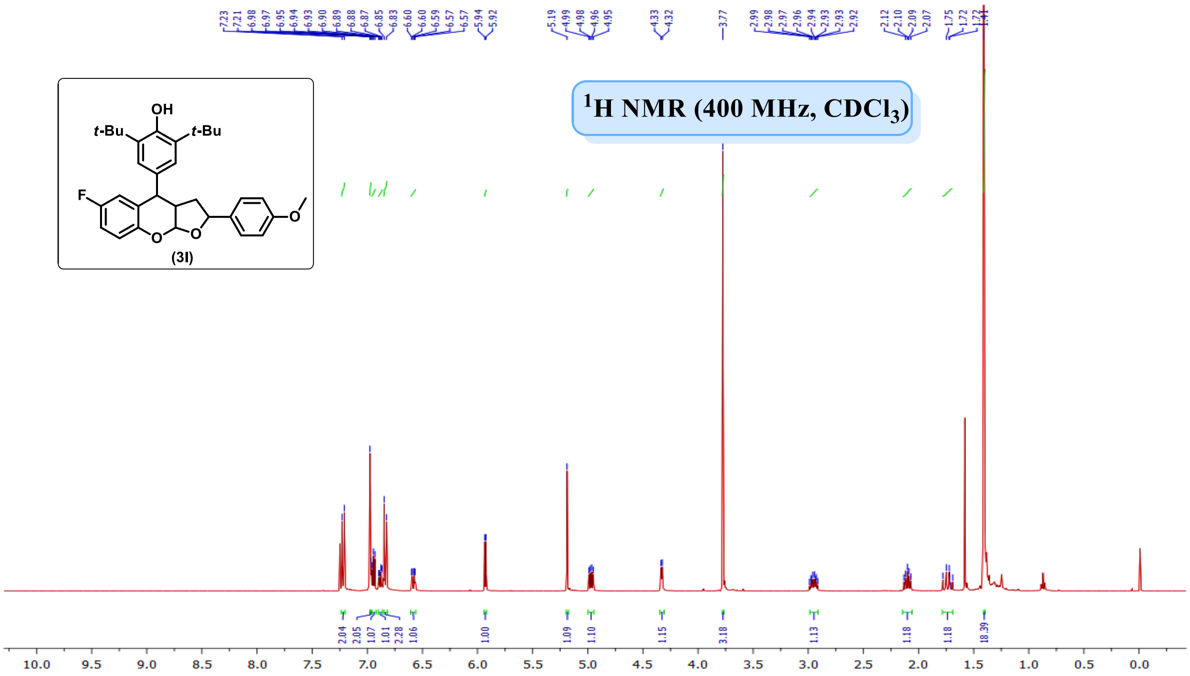

OH
t-Bu
t-Bu
F
O
O
O
(3l)
¹H NMR (400 MHz, CDCl₃)
10.0 9.5 9.0 8.5 8.0 7.5 7.0 6.5 6.0 5.5 5.0 4.5 4.0 3.5 3.0 2.5 2.0 1.5 1.0 0.5 0.0

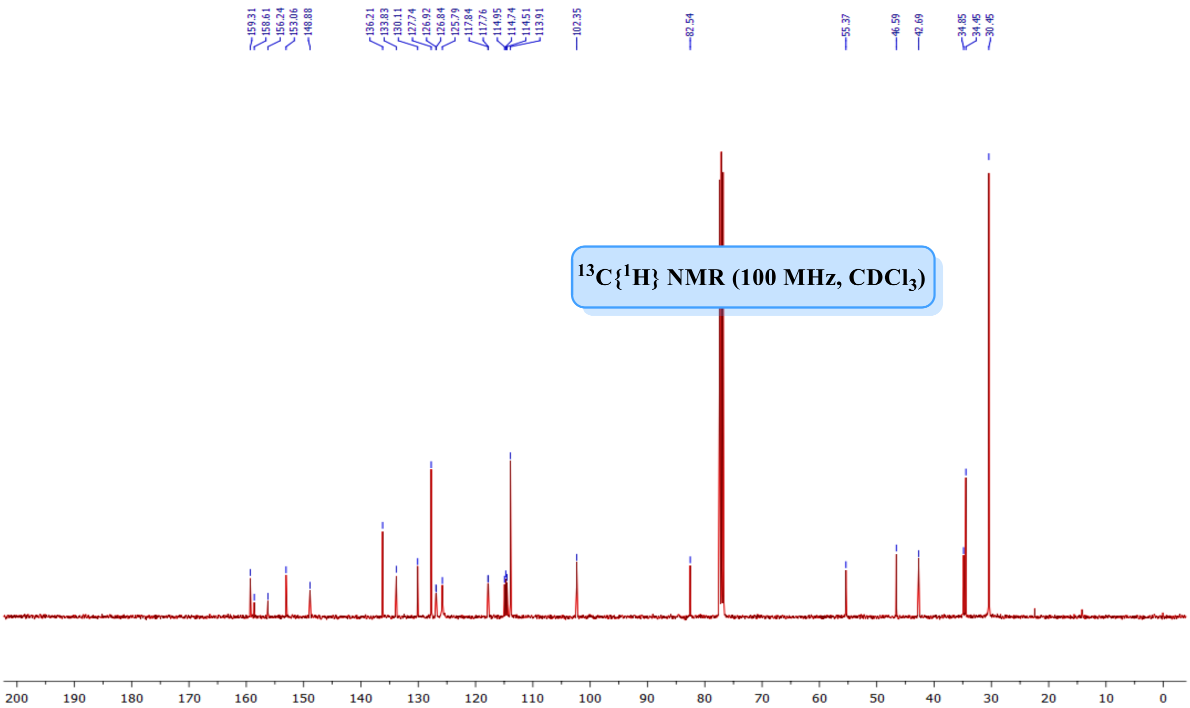

¹³C{¹H} NMR (100 MHz, CDCl₃)
159.31 158.61 156.24 153.06 148.88 136.21 133.83 130.11 127.74 126.92 126.84 125.79 117.84 117.76 114.95 114.74 114.51 113.91 102.35 82.54 55.37 46.59 42.69 34.85 34.45 30.45
200 190 180 170 160 150 140 130 120 110 100 90 80 70 60 50 40 30 20 10 0

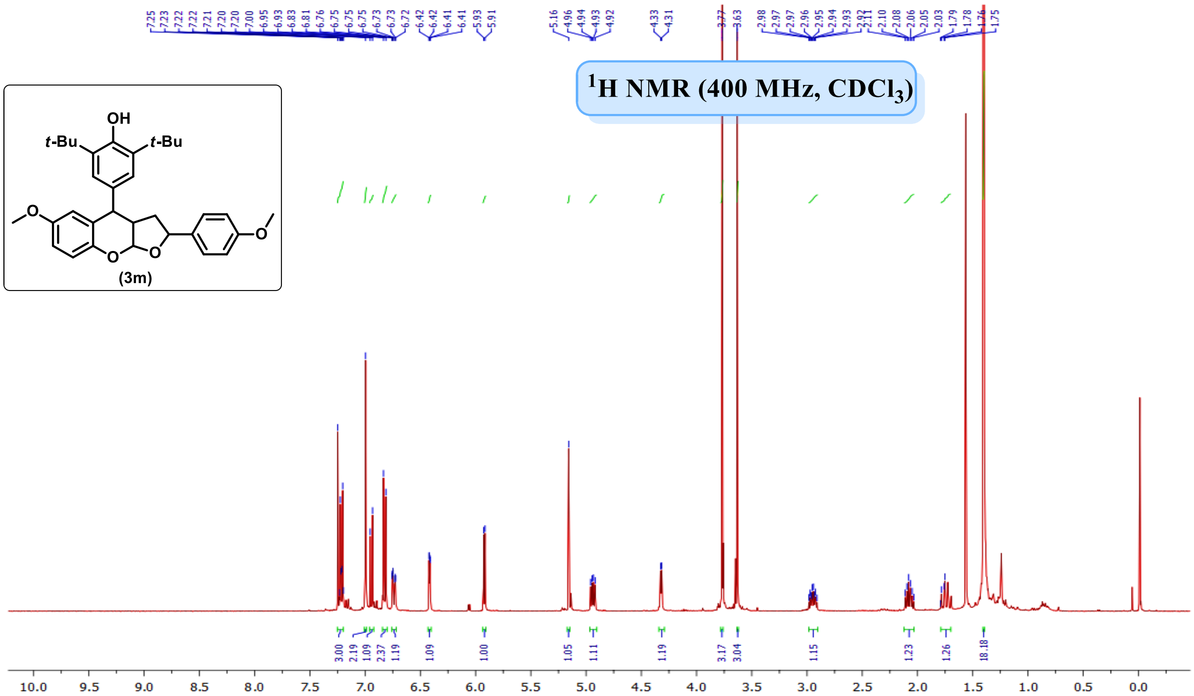
OH
t-Bu
t-Bu
(3m)
^{1}H NMR (400 MHz, $CDCl_3$)

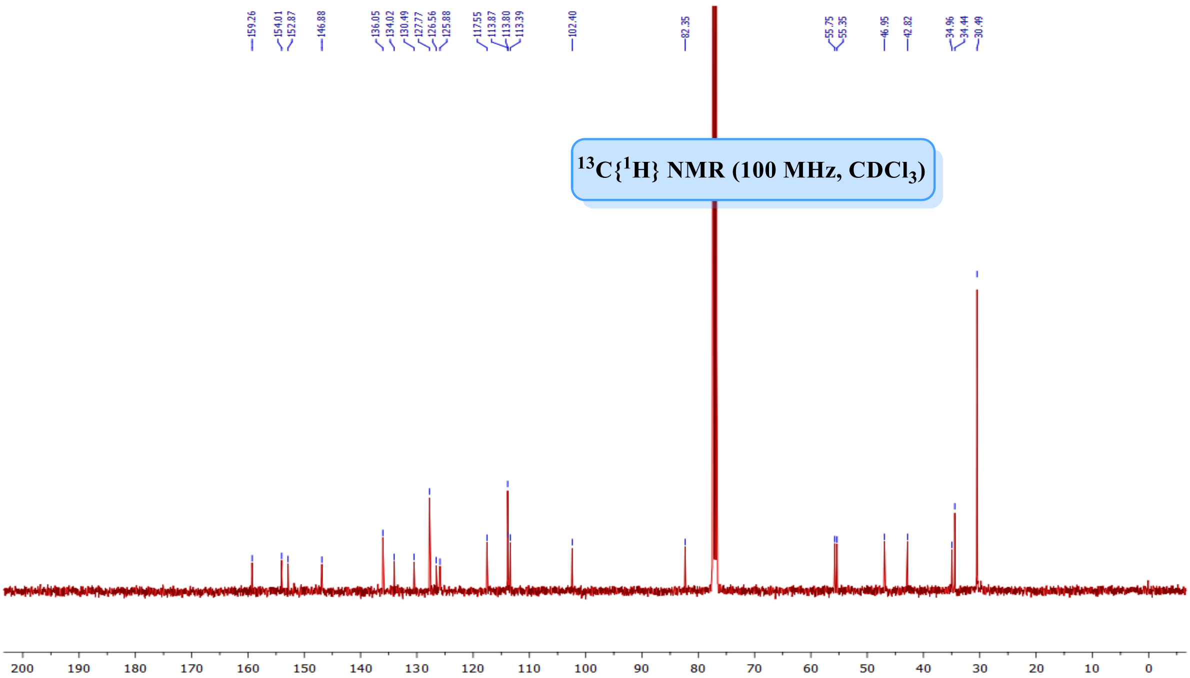
$^{13}C\{^{1}H\}$ NMR (100 MHz, $CDCl_3$)

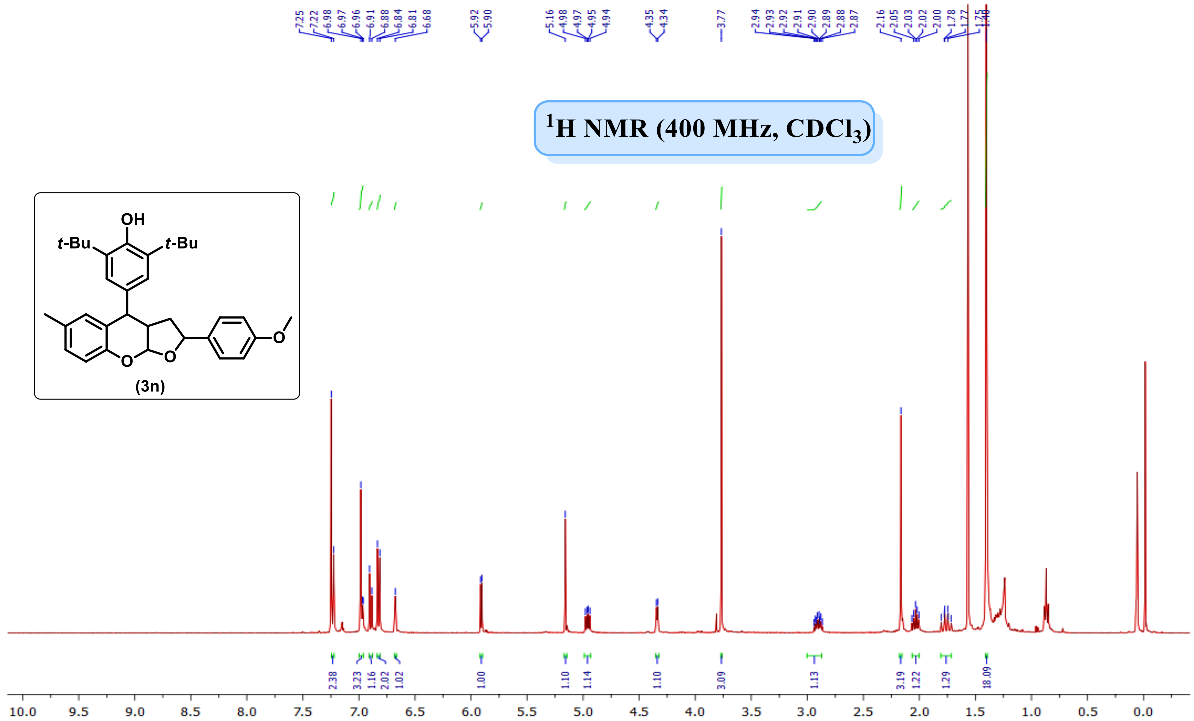
1H NMR (400 MHz, CDCl3)
OH
t-Bu
t-Bu
(3n)

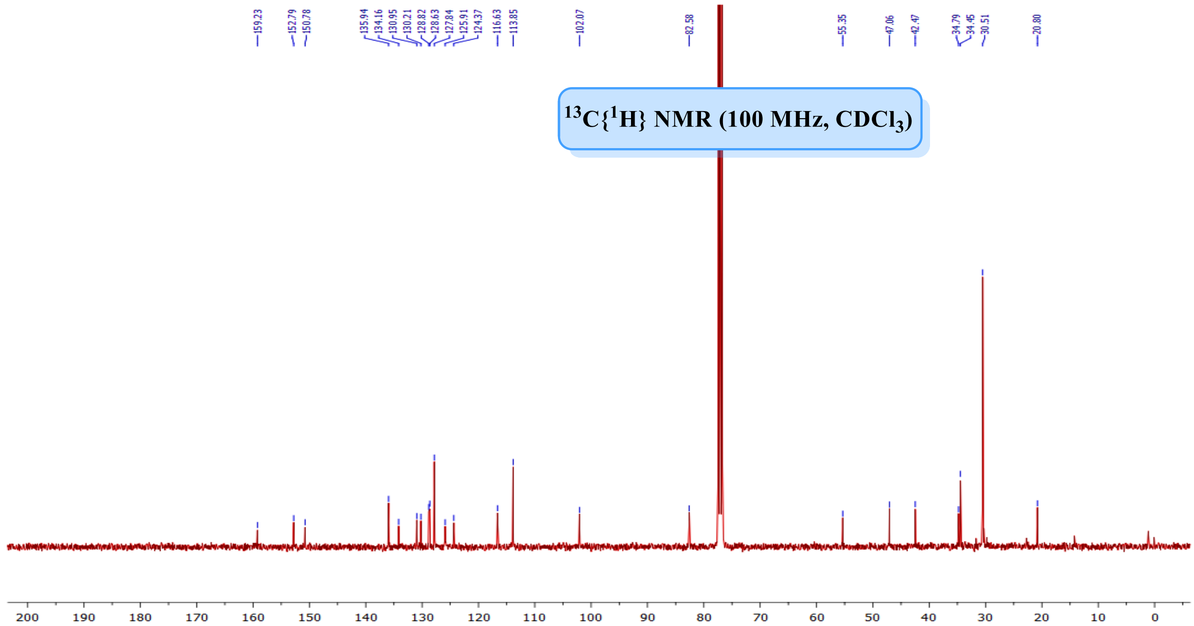
13C{1H} NMR (100 MHz, CDCl3)

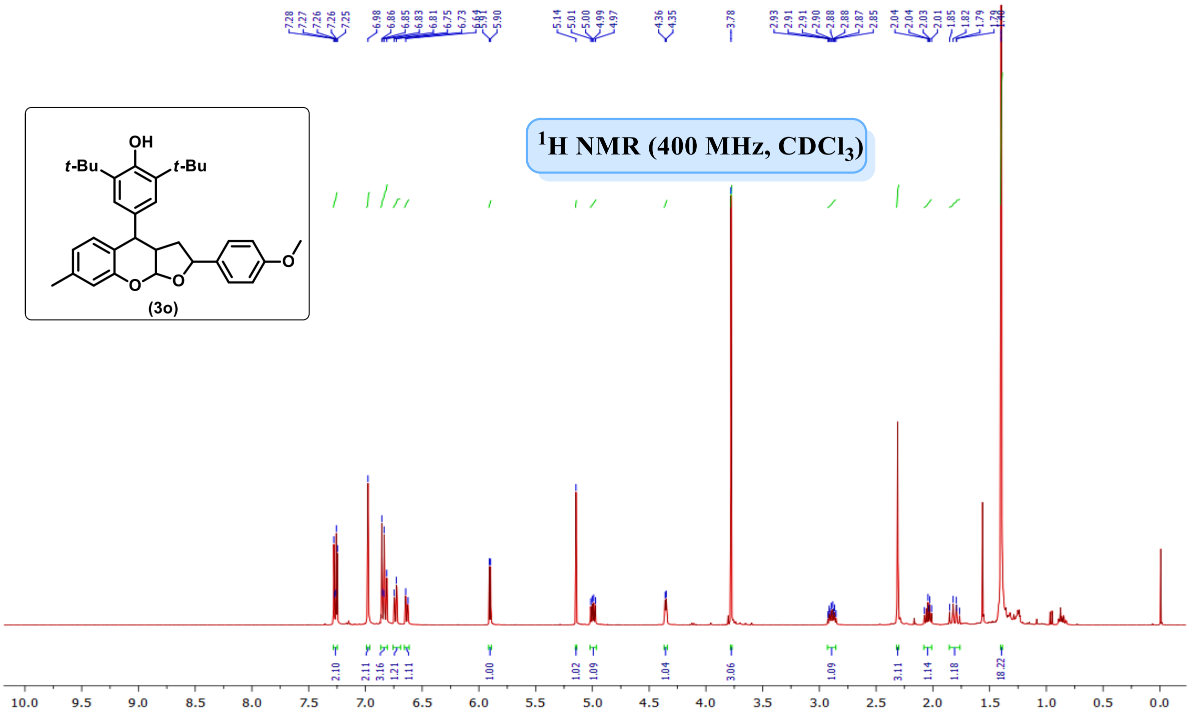
OH
t-Bu
t-Bu
O
O
O
(3o)
1H NMR (400 MHz, CDCl3)

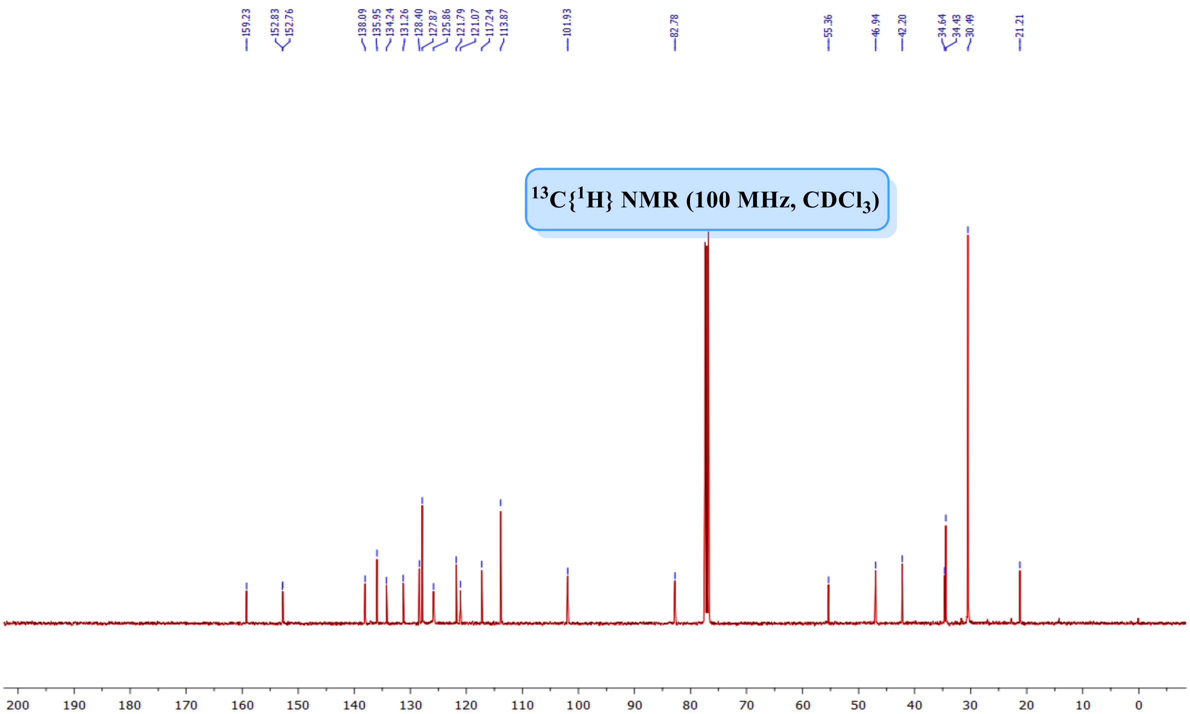
159.23
152.83
152.76
138.09
135.95
134.24
131.26
128.40
127.87
125.86
121.79
121.07
117.24
113.87
101.93
82.78
55.36
46.94
42.20
34.64
34.43
30.49
21.21
13C{1H} NMR (100 MHz, CDCl3)

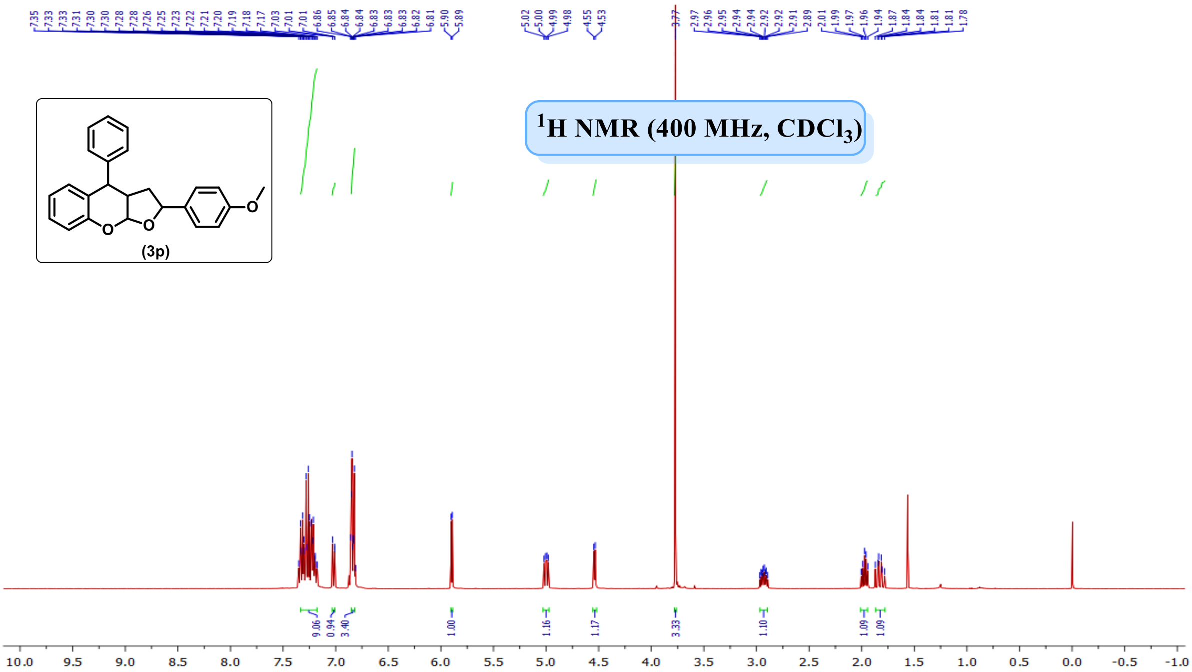
(3p)
1H NMR (400 MHz, CDCl3)

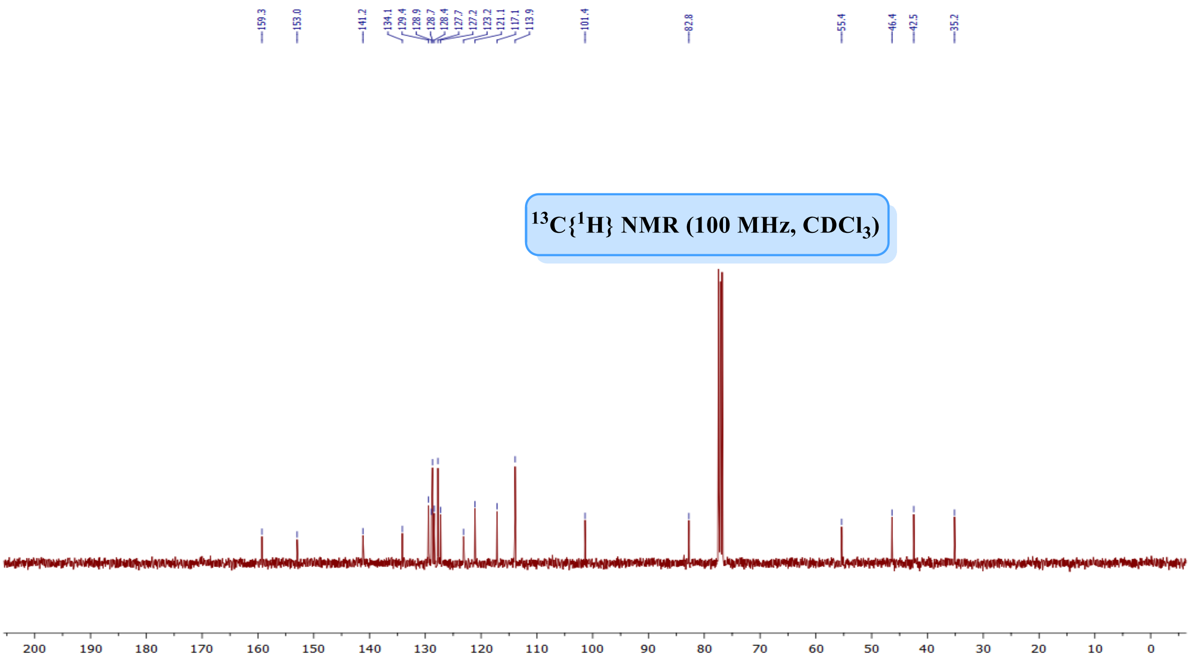
13C{1H} NMR (100 MHz, CDCl3)

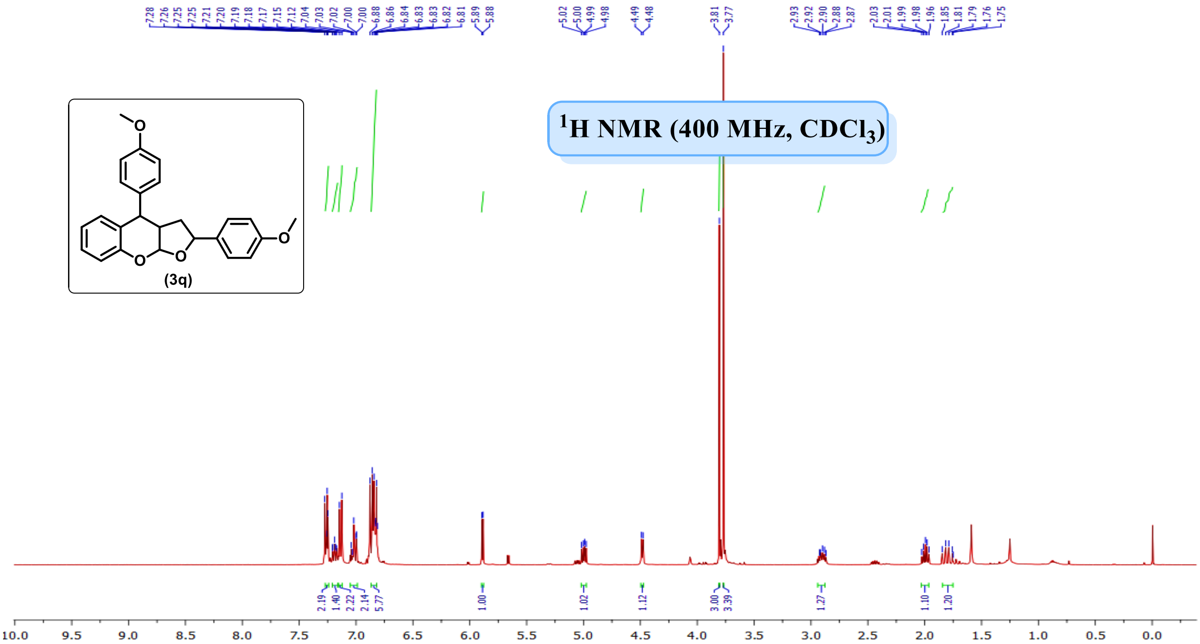
(3q)
¹H NMR (400 MHz, CDCl₃)

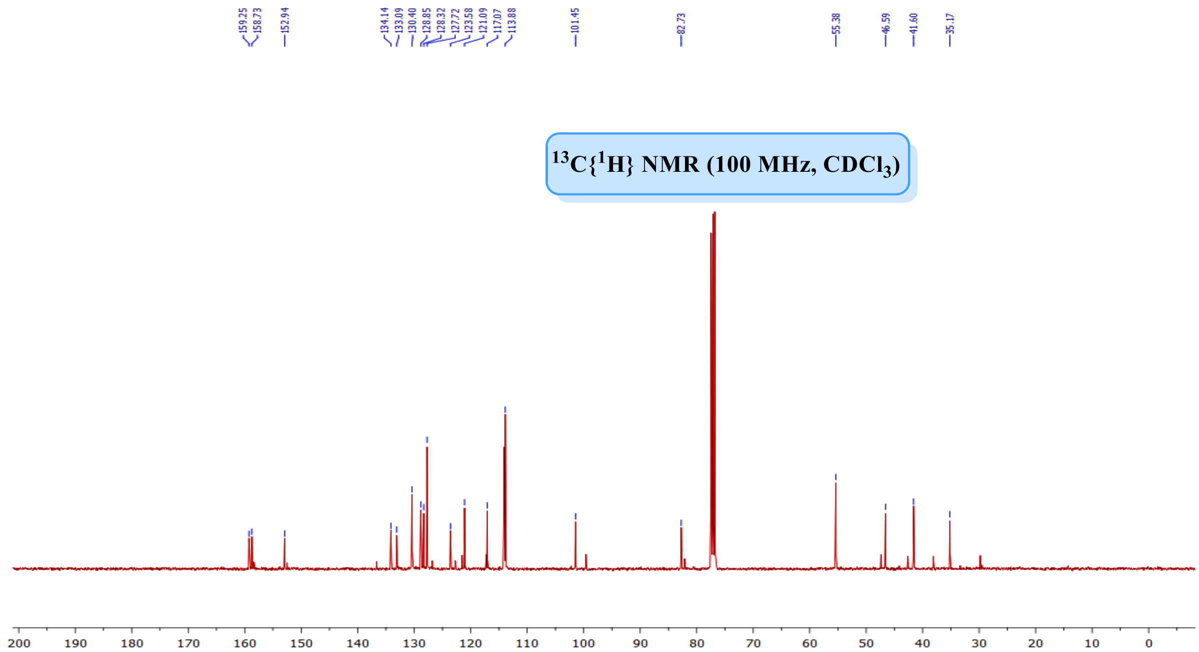
¹³C{¹H} NMR (100 MHz, CDCl₃)

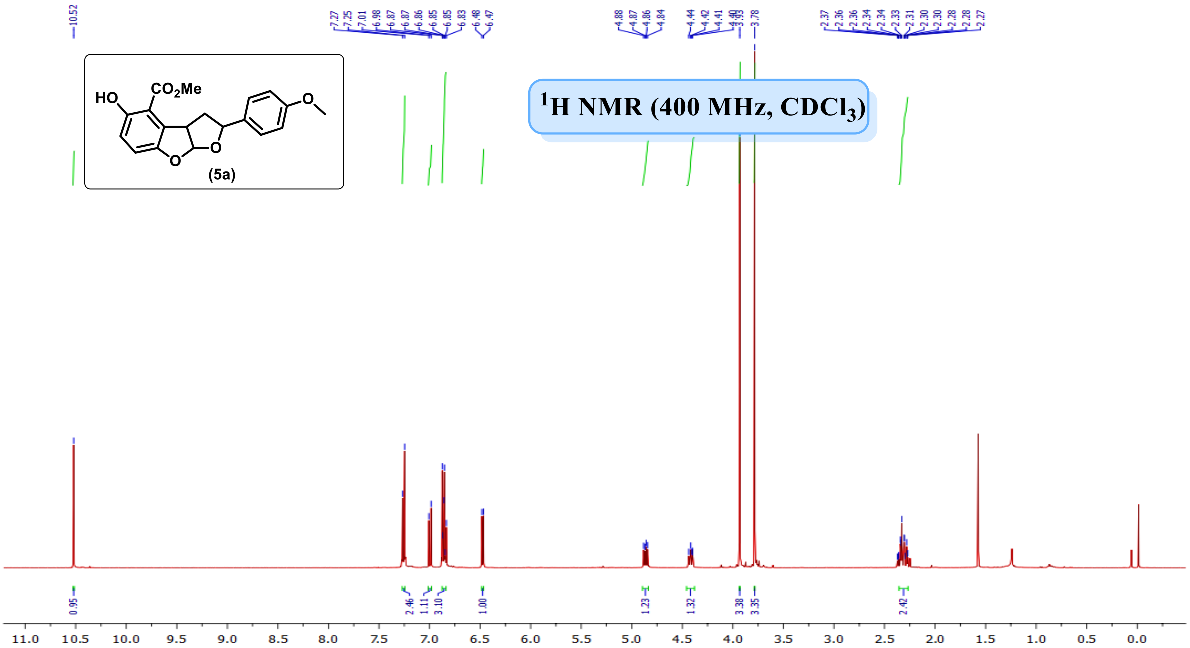
HO
CO2Me
O
O
O
(5a)
1H NMR (400 MHz, CDCl3)

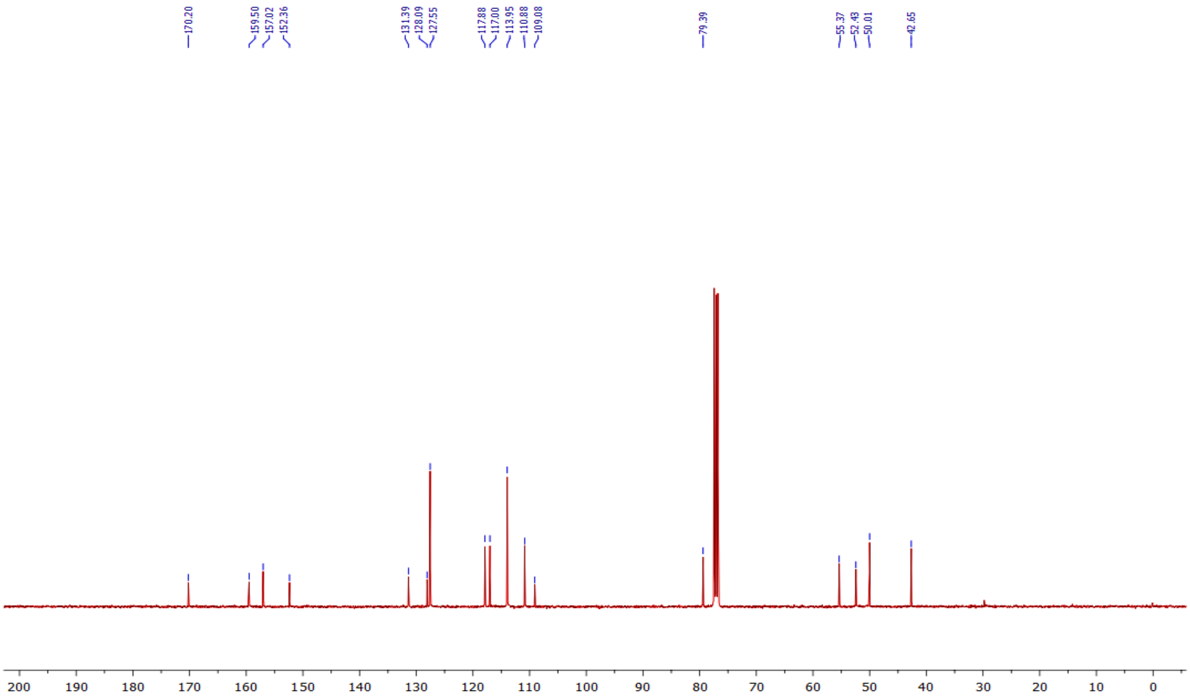

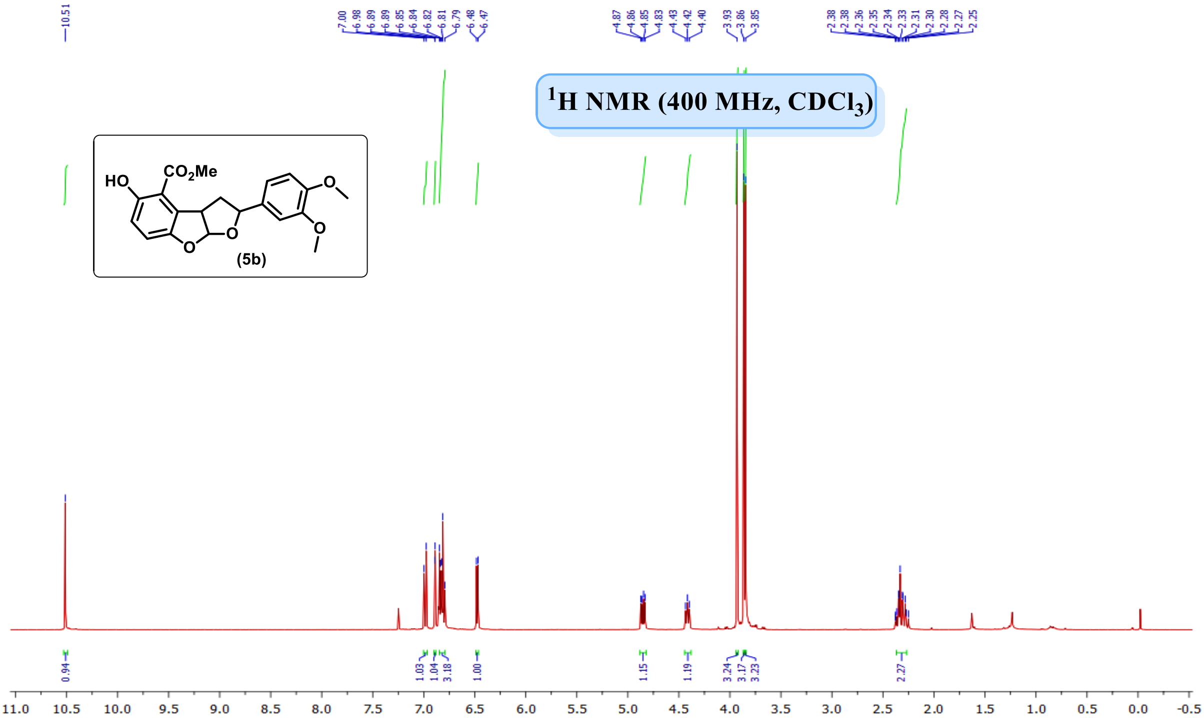
1H NMR (400 MHz, CDCl3)
HO
CO2Me
(5b)

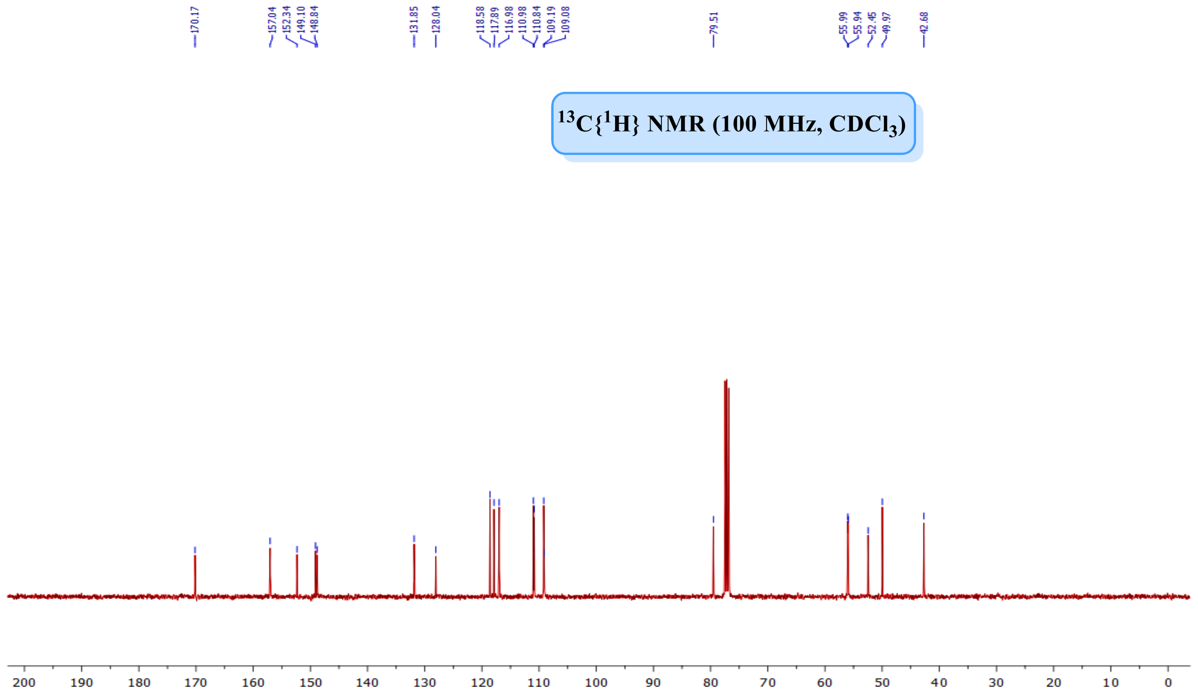
13C{1H} NMR (100 MHz, CDCl3)

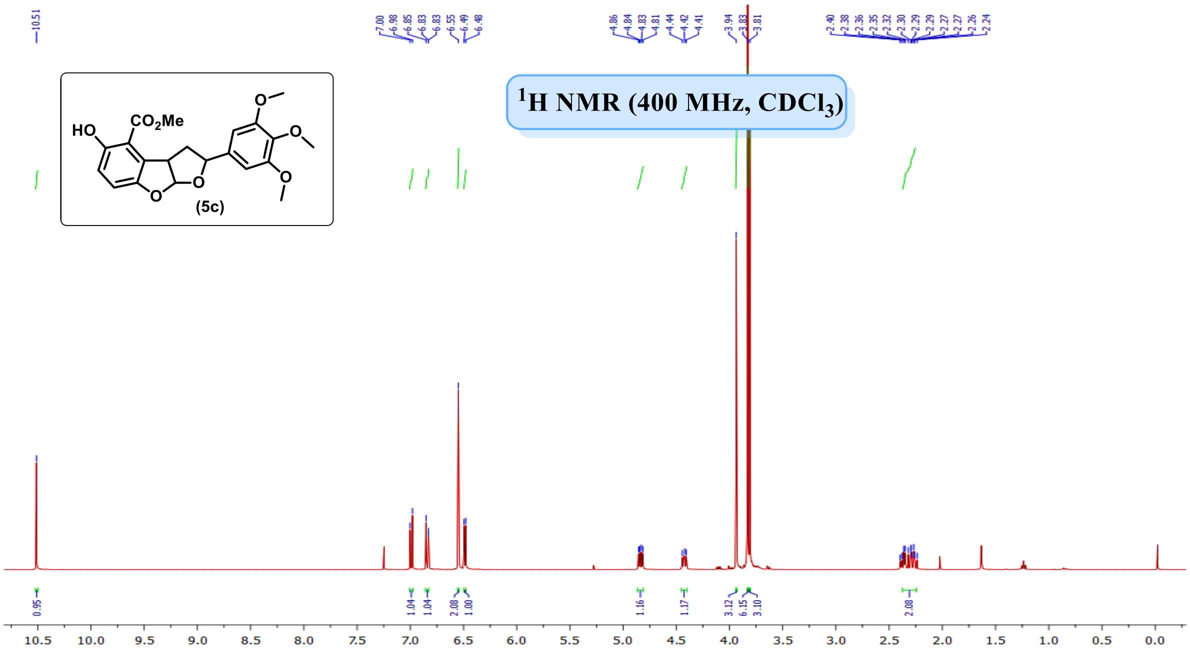
HO
CO_2Me
O
(5c)
^{1}H NMR (400 MHz, $CDCl_3$)

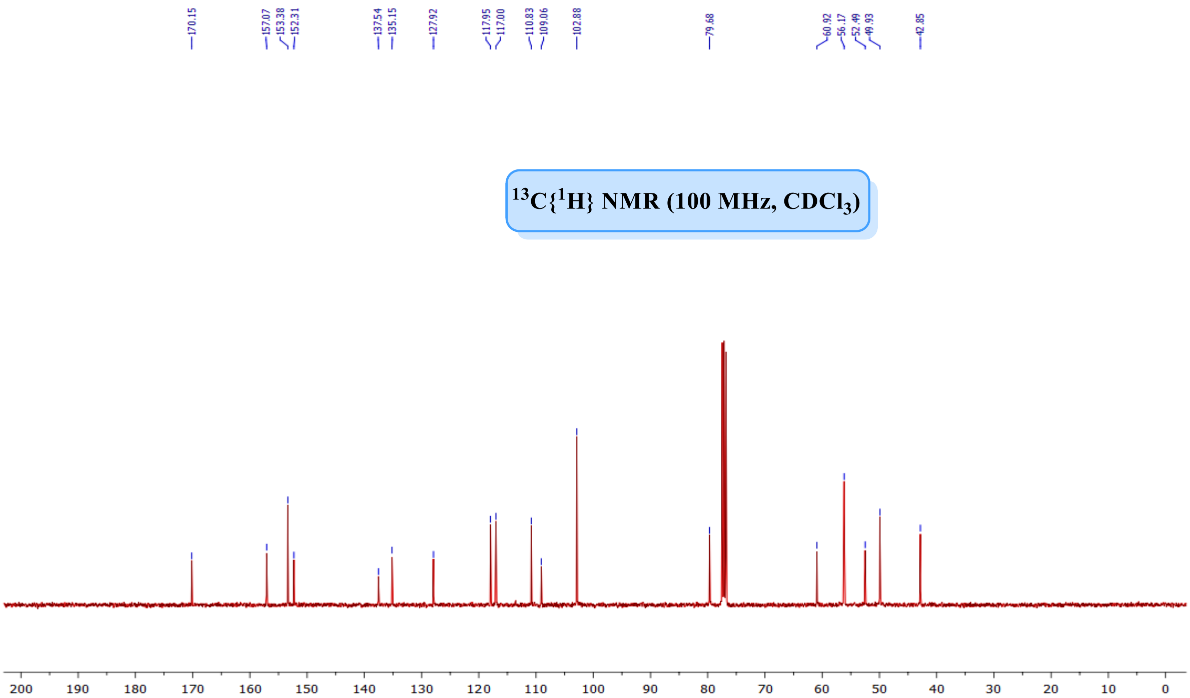
170.15
157.07
153.38
152.31
137.54
135.15
127.92
117.95
117.00
110.83
109.06
102.88
79.68
60.92
56.17
52.49
49.93
42.85
$^{13}C\{^1H\}$ NMR (100 MHz, $CDCl_3$)

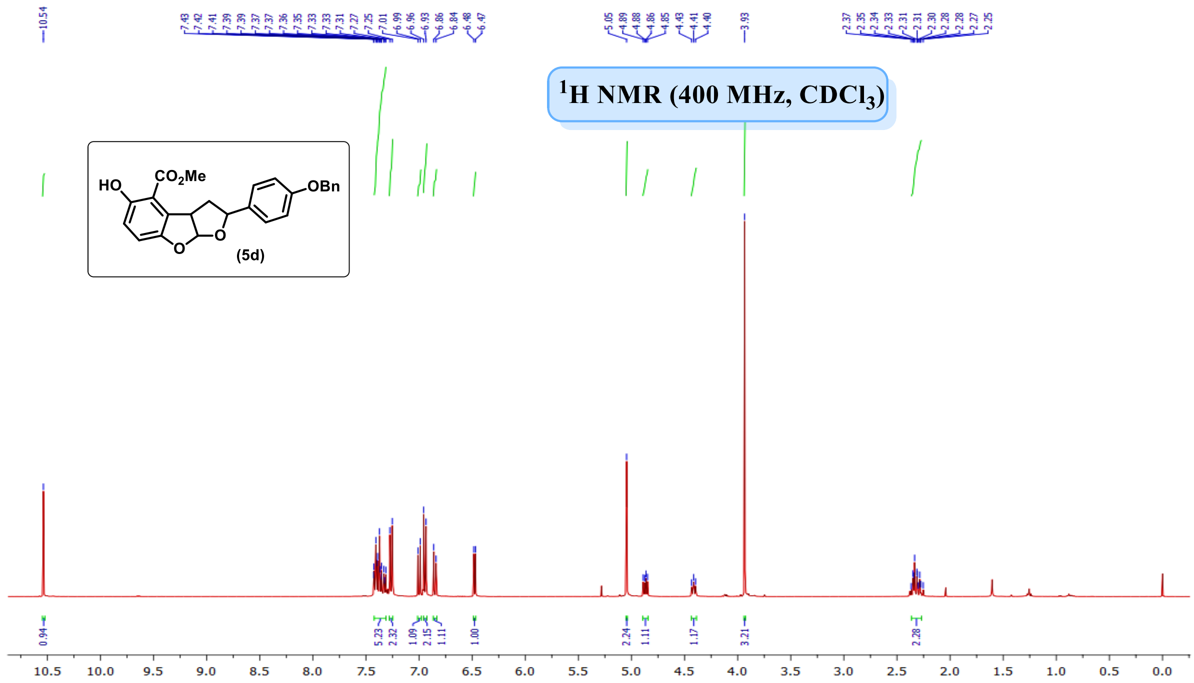
1H NMR (400 MHz, CDCl3)
HO
CO2Me
OBn
(5d)

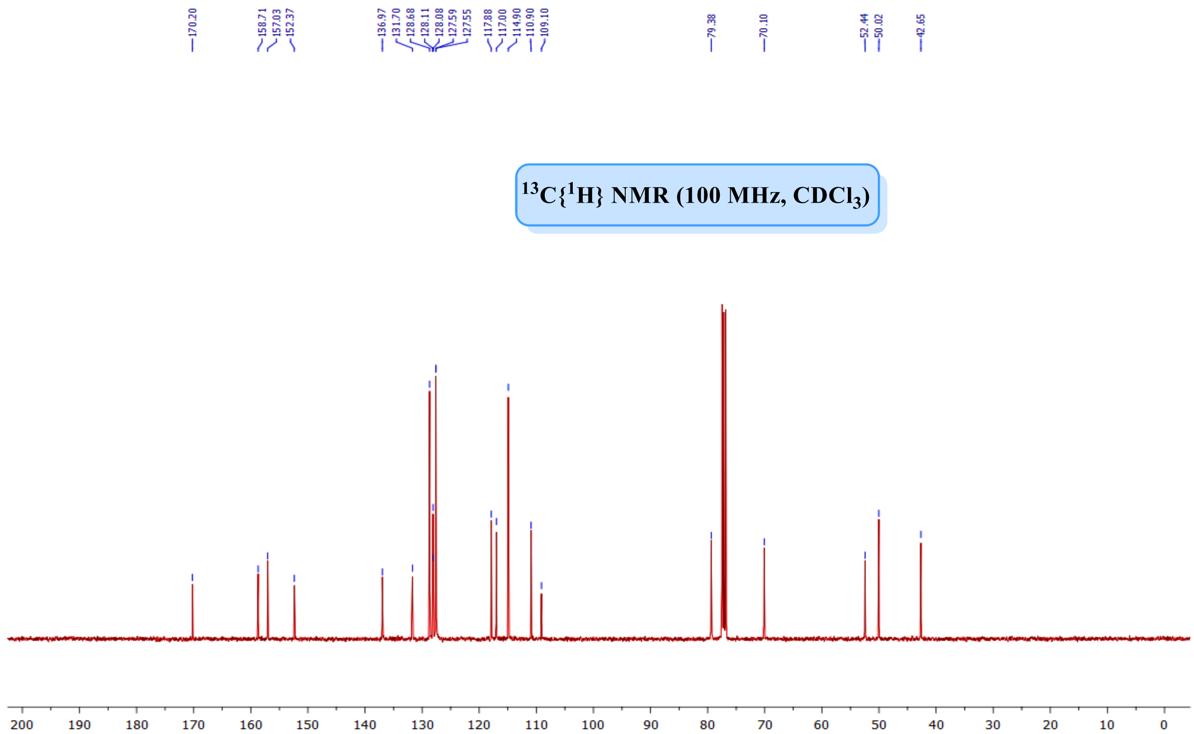
13C{1H} NMR (100 MHz, CDCl3)

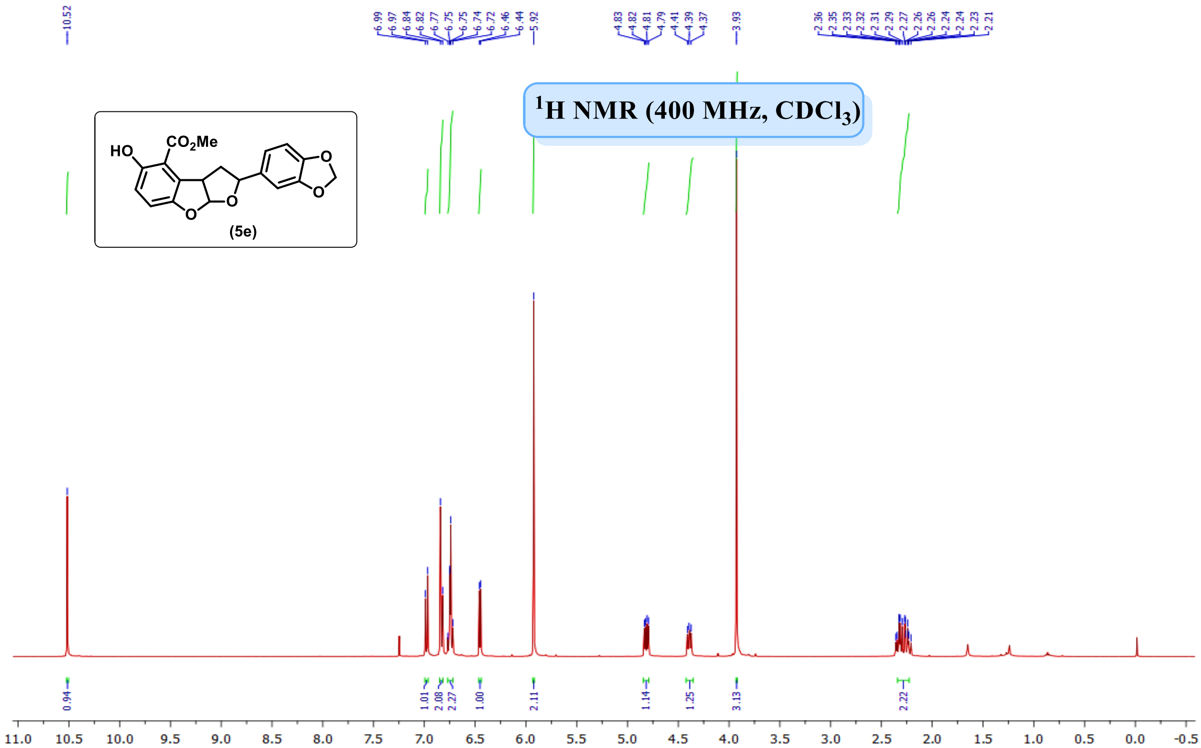
10.52
6.99
6.97
6.84
6.82
6.77
6.75
6.75
6.74
6.72
6.46
6.44
5.92
4.83
4.82
4.81
4.79
4.41
4.39
4.37
3.93
2.36
2.35
2.33
2.32
2.31
2.29
2.27
2.26
2.26
2.24
2.24
2.23
2.21
[1]H NMR (400 MHz, CDCl3)
HO
CO2Me
O
O
O
O
(5e)
0.94
1.01
2.08
2.27
1.00
2.11
1.14
1.25
3.13
2.22
11.0
10.5
10.0
9.5
9.0
8.5
8.0
7.5
7.0
6.5
6.0
5.5
5.0
4.5
4.0
3.5
3.0
2.5
2.0
1.5
1.0
0.5
0.0
-0.5

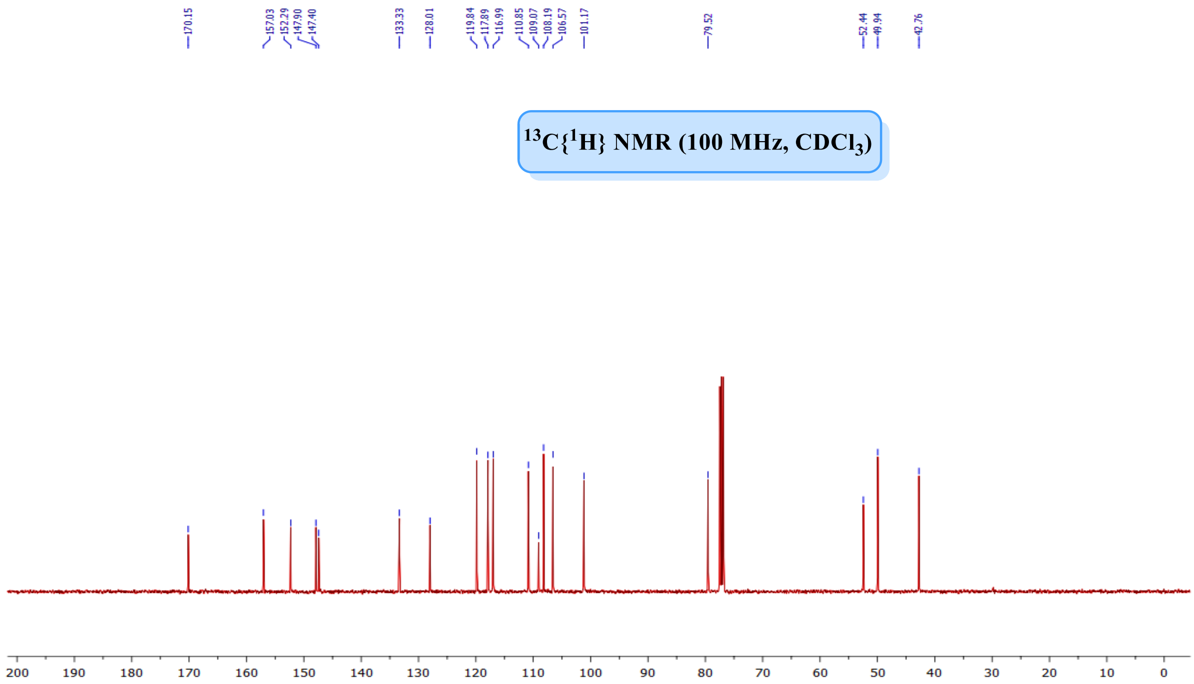
170.15
157.03
152.29
147.90
147.40
133.33
128.01
119.84
117.89
116.99
110.85
109.07
108.19
106.57
101.17
79.52
52.44
49.94
42.76
[13]C{[1]H} NMR (100 MHz, CDCl3)
200
190
180
170
160
150
140
130
120
110
100
90
80
70
60
50
40
30
20
10
0

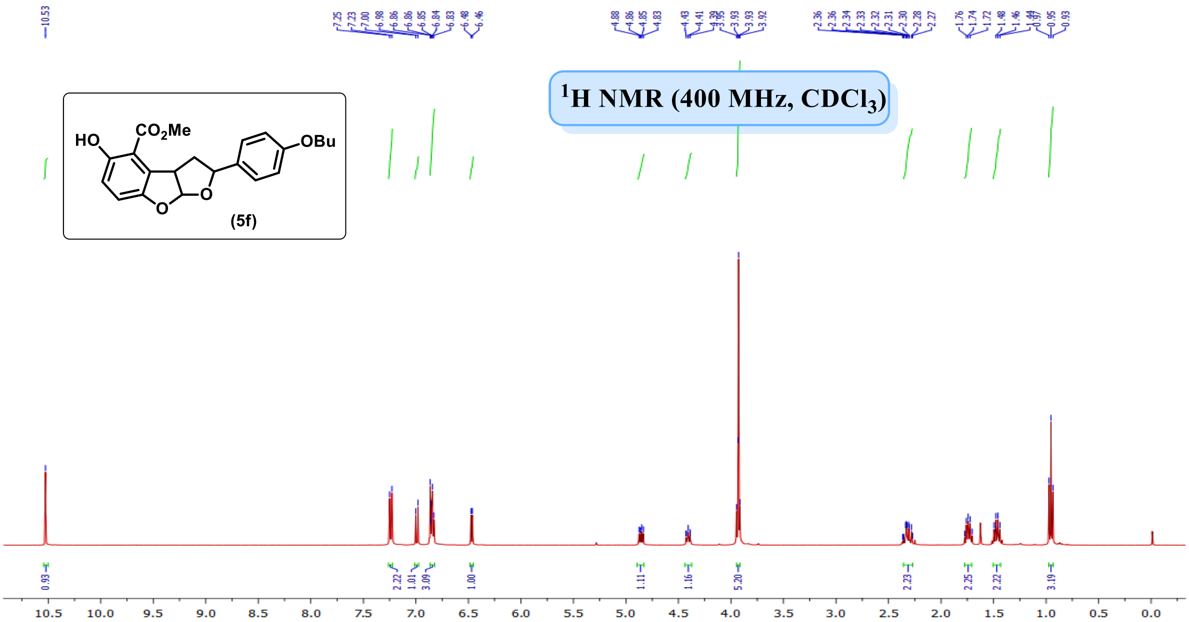
^{1}H NMR (400 MHz, CDCl$_3$)
(5f)

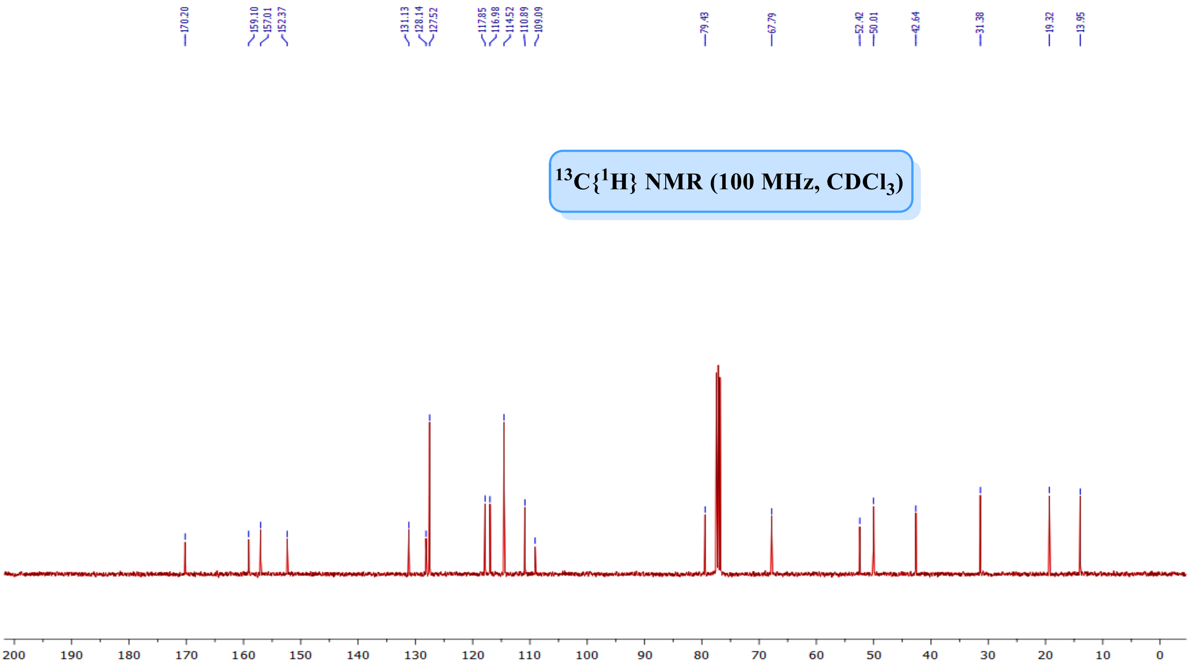
^{13}C{^{1}H} NMR (100 MHz, CDCl$_3$)

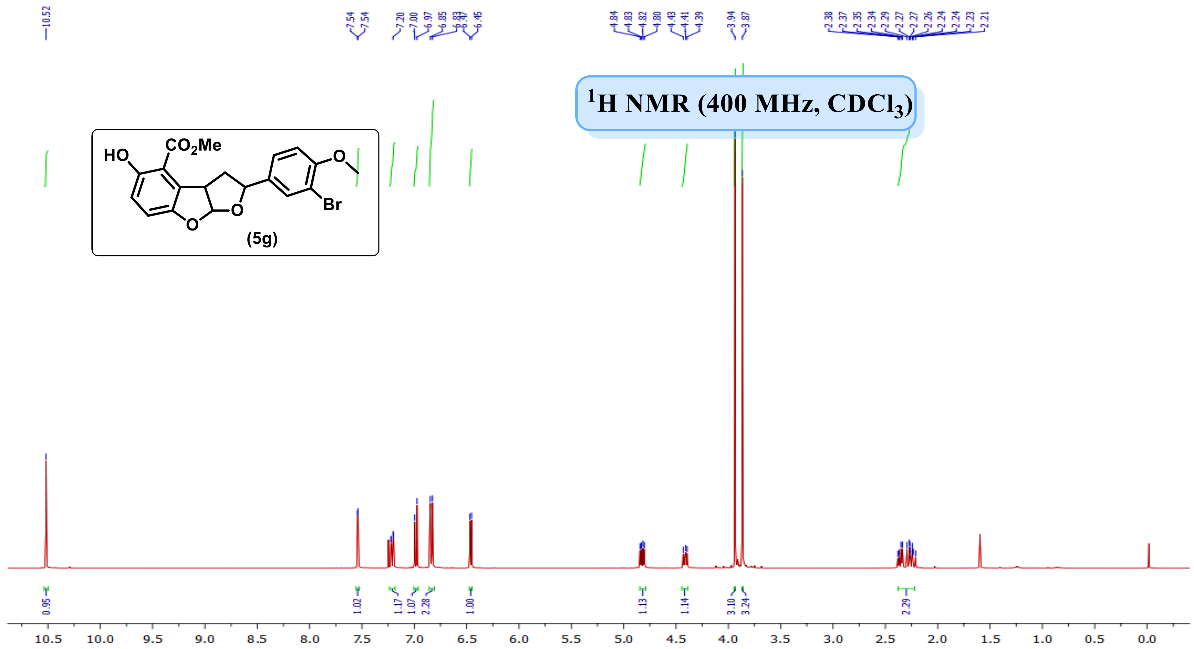
1H NMR (400 MHz, CDCl3)
HO
CO2Me
O
O
O
Br
(5g)
10.5 10.0 9.5 9.0 8.5 8.0 7.5 7.0 6.5 6.0 5.5 5.0 4.5 4.0 3.5 3.0 2.5 2.0 1.5 1.0 0.5 0.0

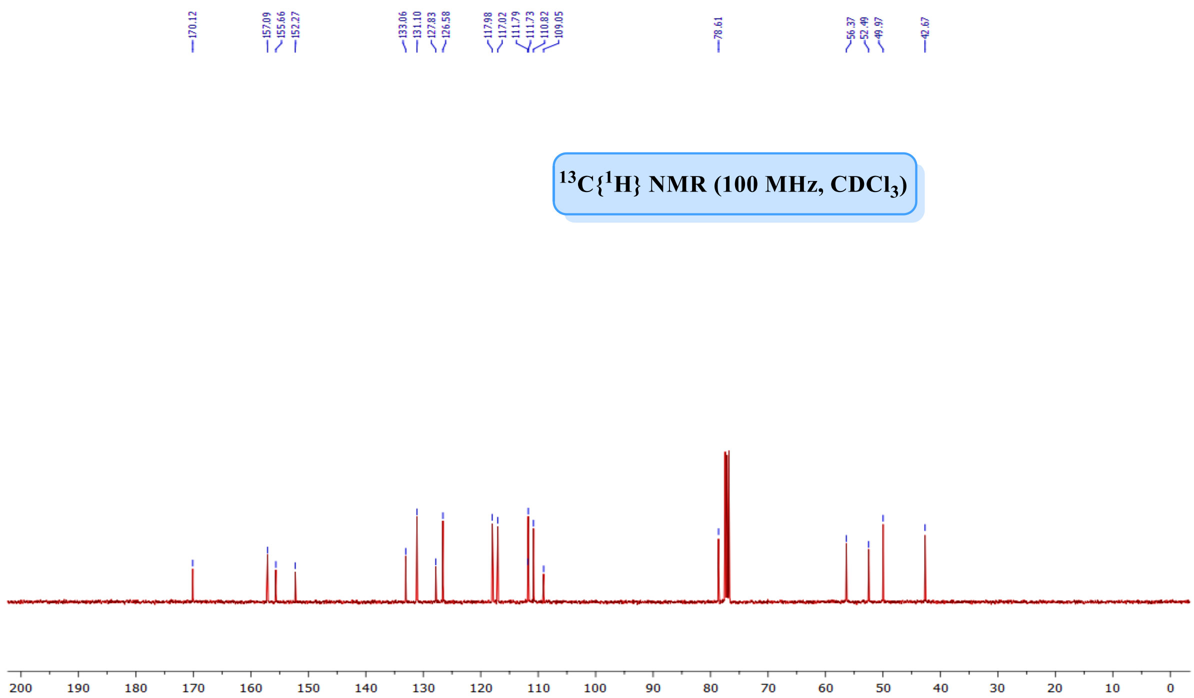
13C{1H} NMR (100 MHz, CDCl3)
170.12
157.09
155.66
152.27
133.06
131.10
127.83
126.58
117.98
117.02
111.79
111.73
110.82
109.05
78.61
56.37
52.49
49.97
42.67
200 190 180 170 160 150 140 130 120 110 100 90 80 70 60 50 40 30 20 10 0

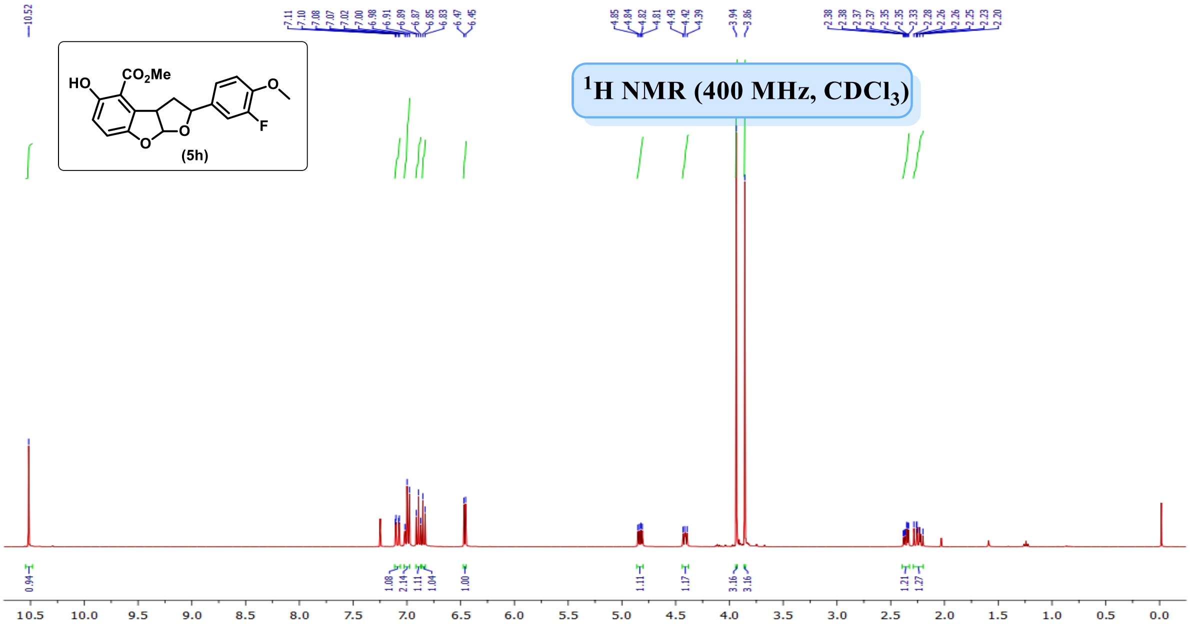
HO
CO2Me
O
O
F
(5h)
1H NMR (400 MHz, CDCl3)

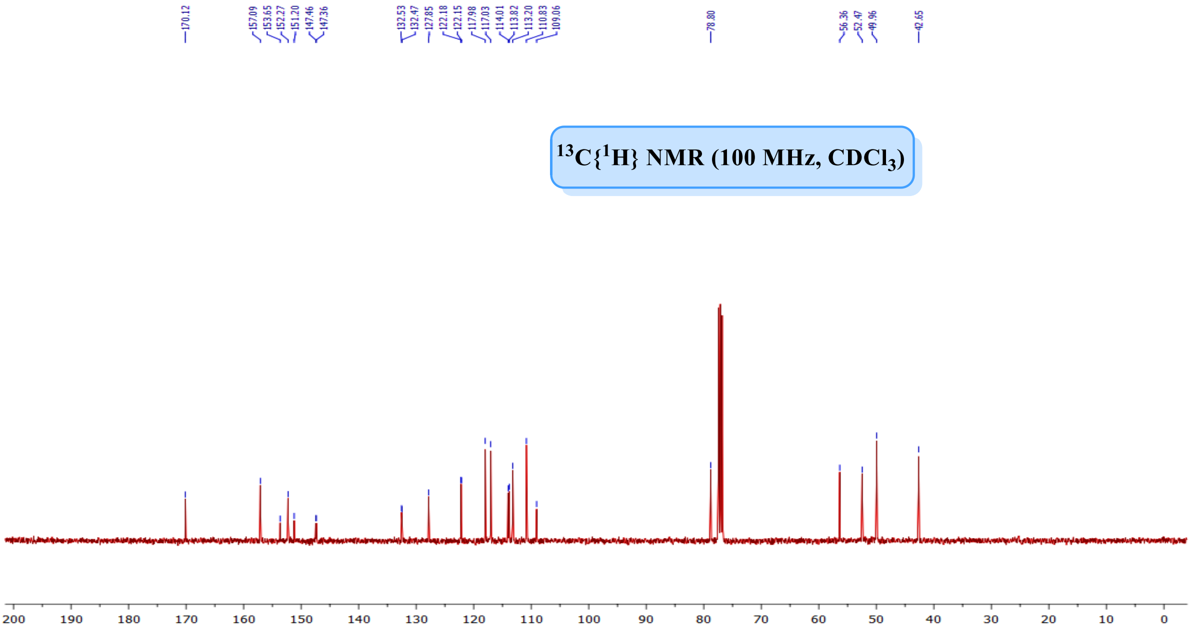
13C{1H} NMR (100 MHz, CDCl3)

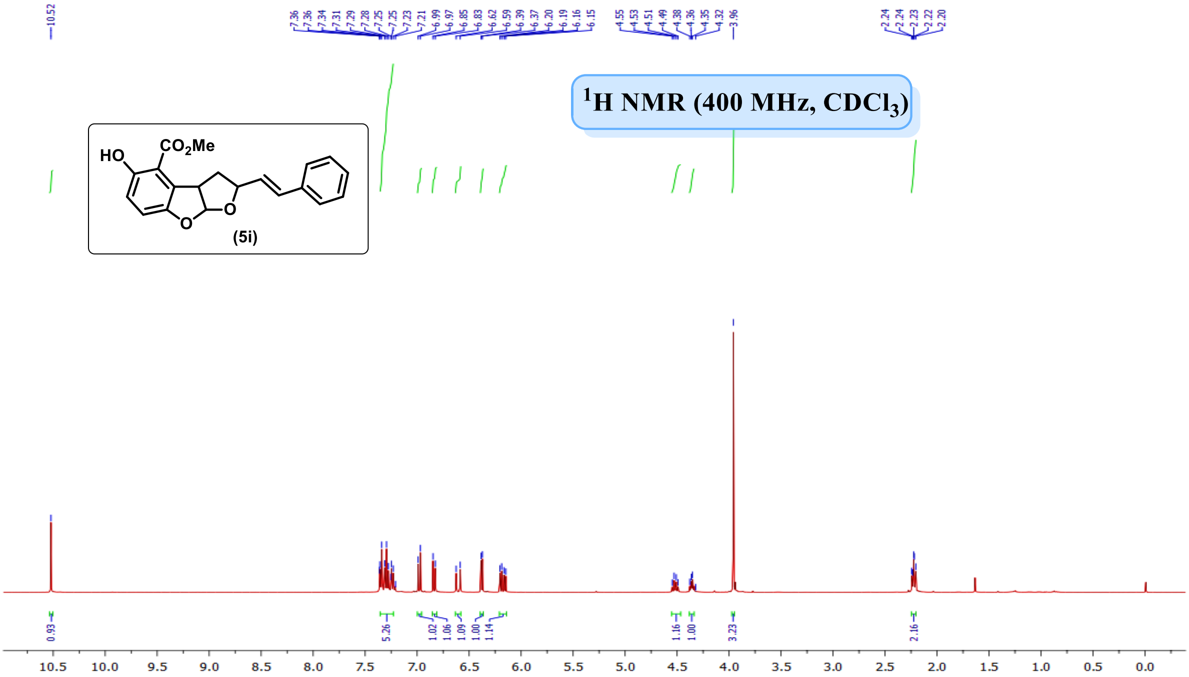
HO
CO_2Me
O
O
(5i)
^{1}H NMR (400 MHz, $CDCl_3$)

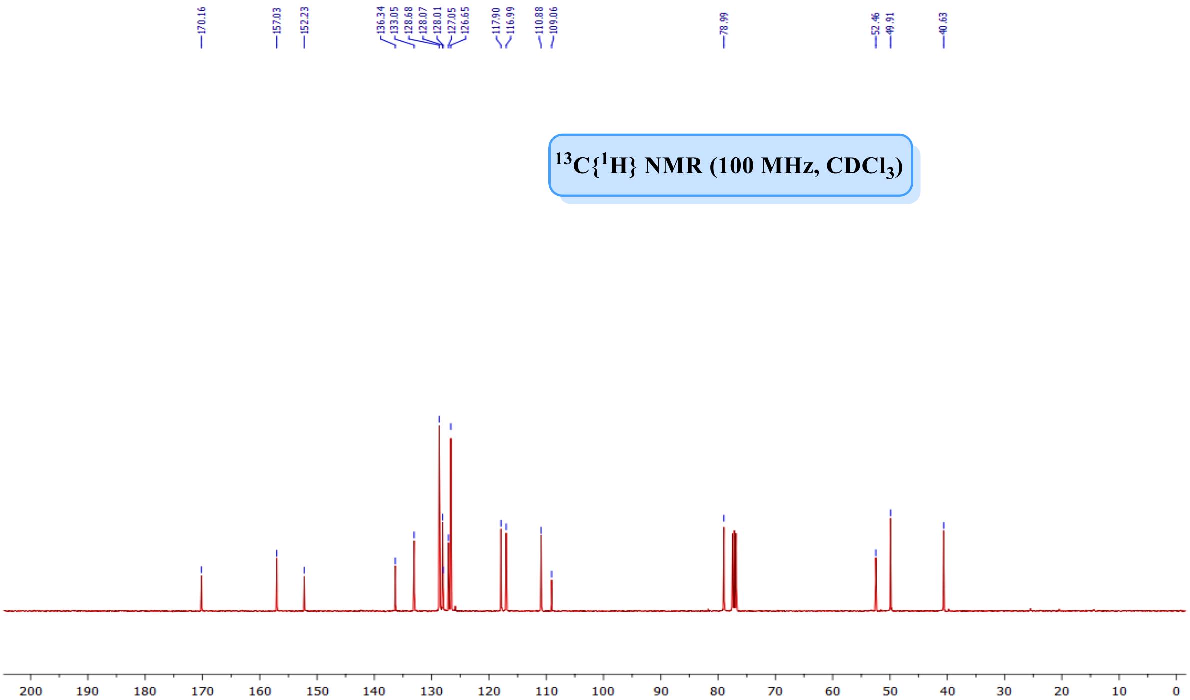
$^{13}C\{^1H\}$ NMR (100 MHz, $CDCl_3$)

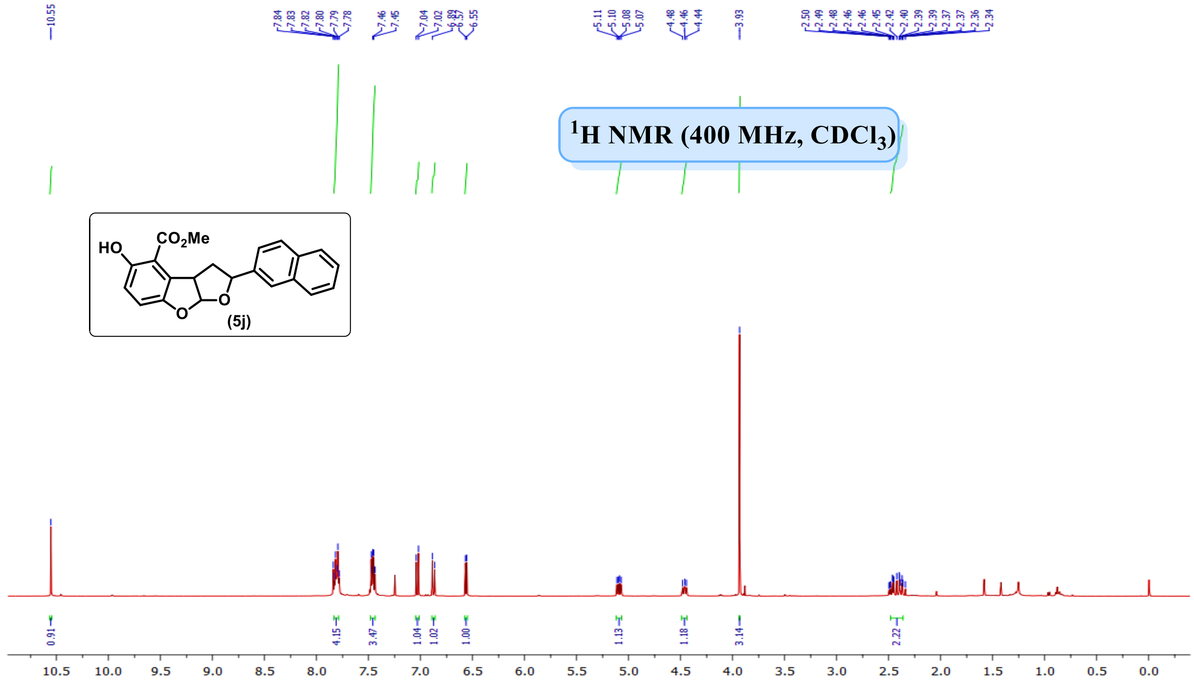
1H NMR (400 MHz, CDCl3)
HO
CO2Me
O
O
(5j)

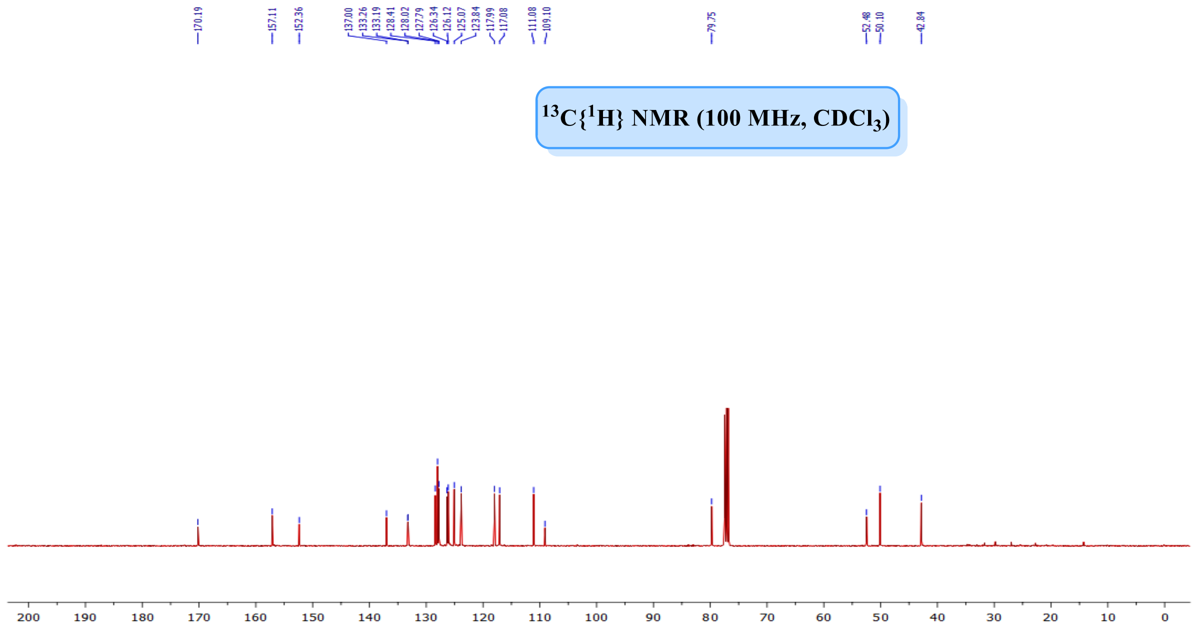
13C{1H} NMR (100 MHz, CDCl3)

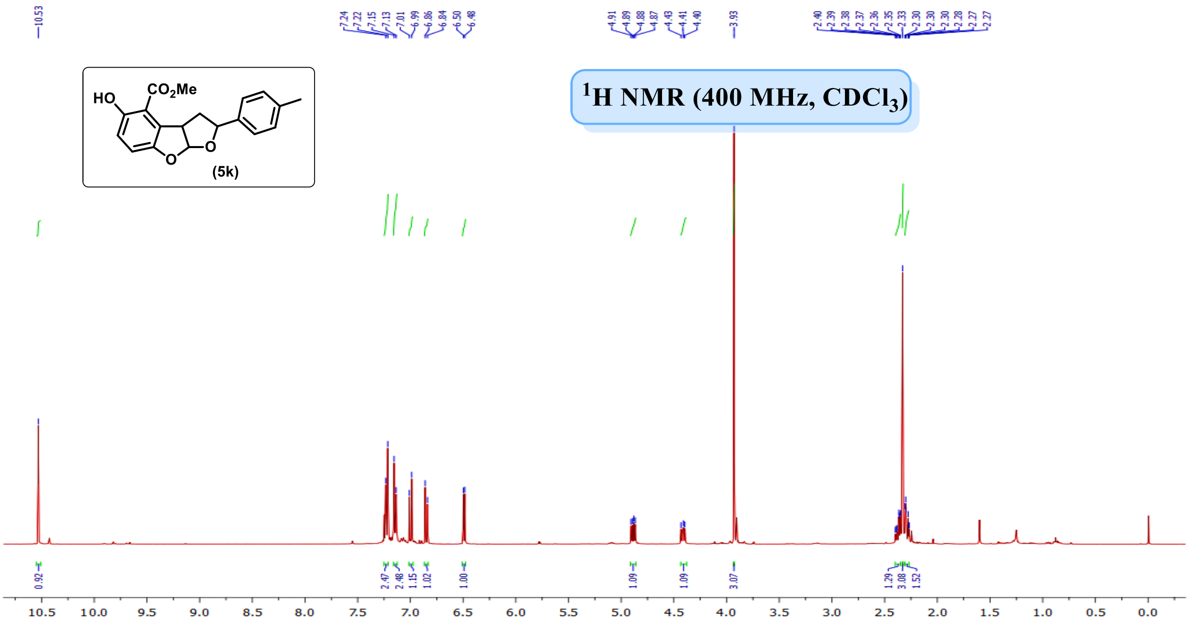
HO
CO2Me
(5k)
1H NMR (400 MHz, CDCl3)

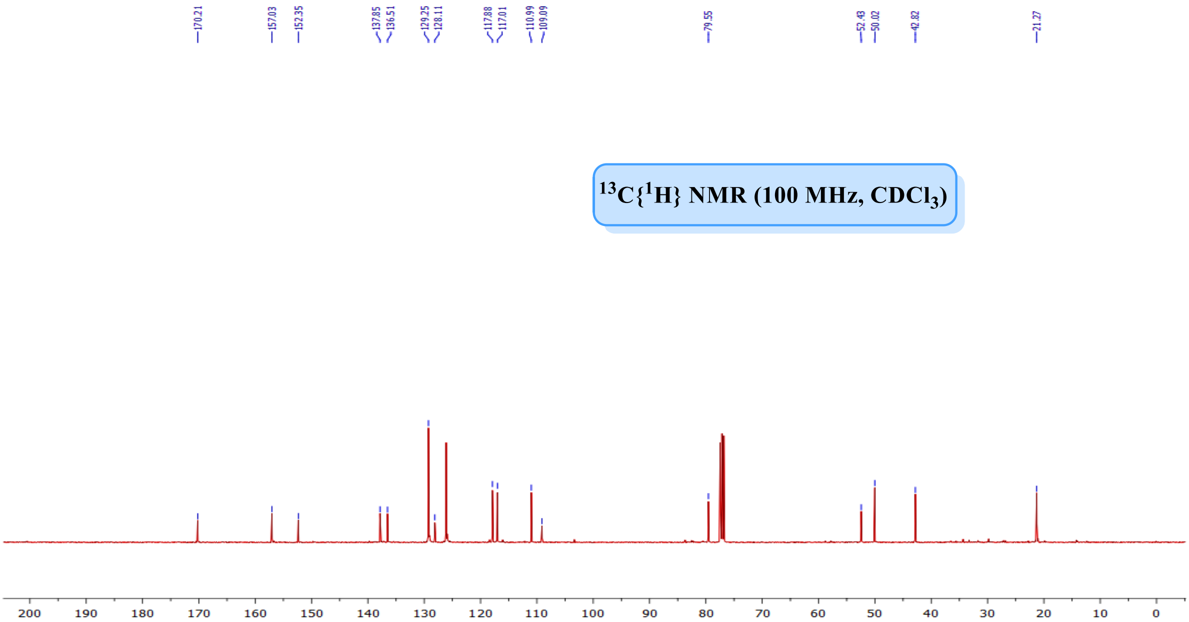
13C{1H} NMR (100 MHz, CDCl3)

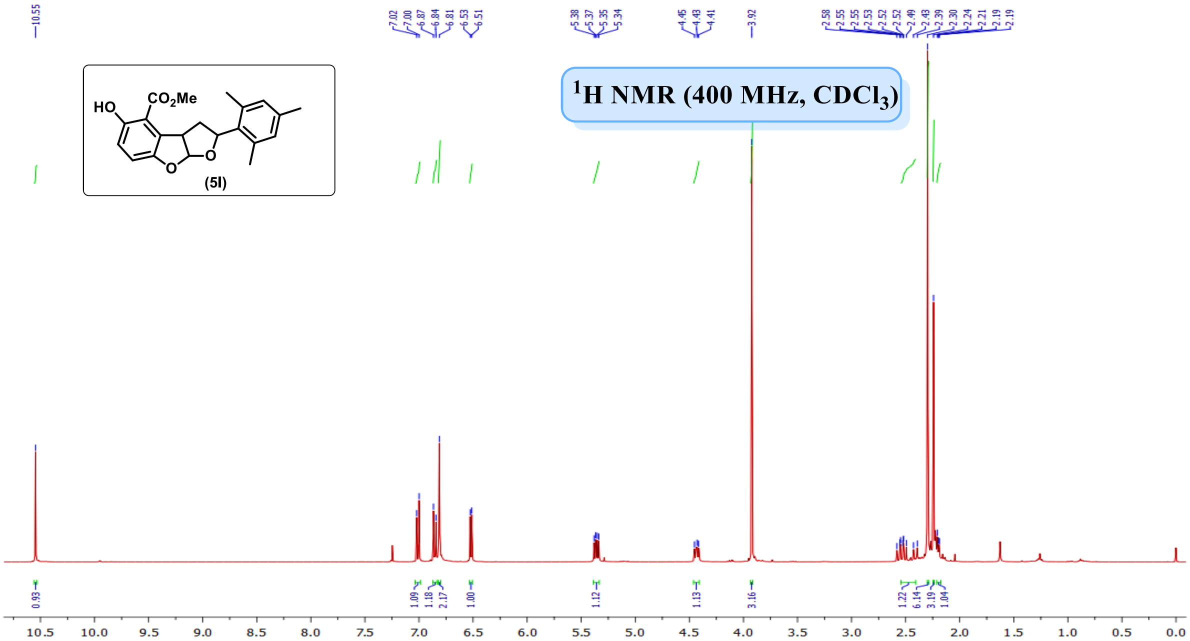
HO
CO_2Me
O
O
(5l)
^{1}H NMR (400 MHz, $CDCl_3$)

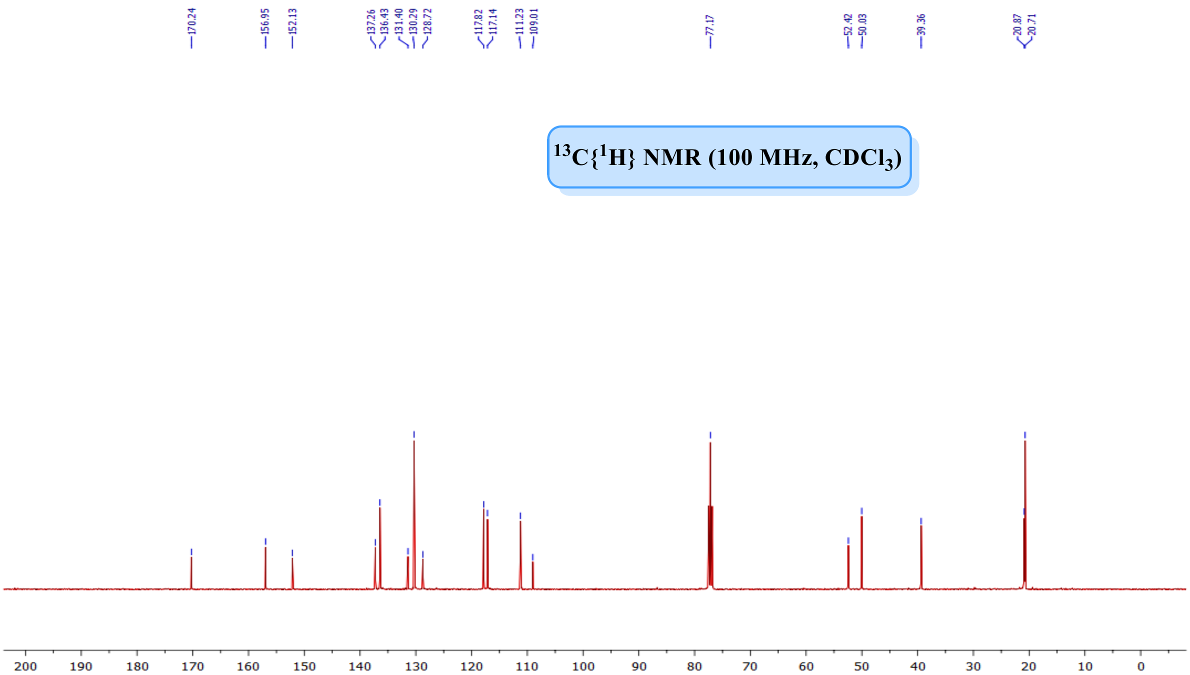
$^{13}C\{^{1}H\}$ NMR (100 MHz, $CDCl_3$)

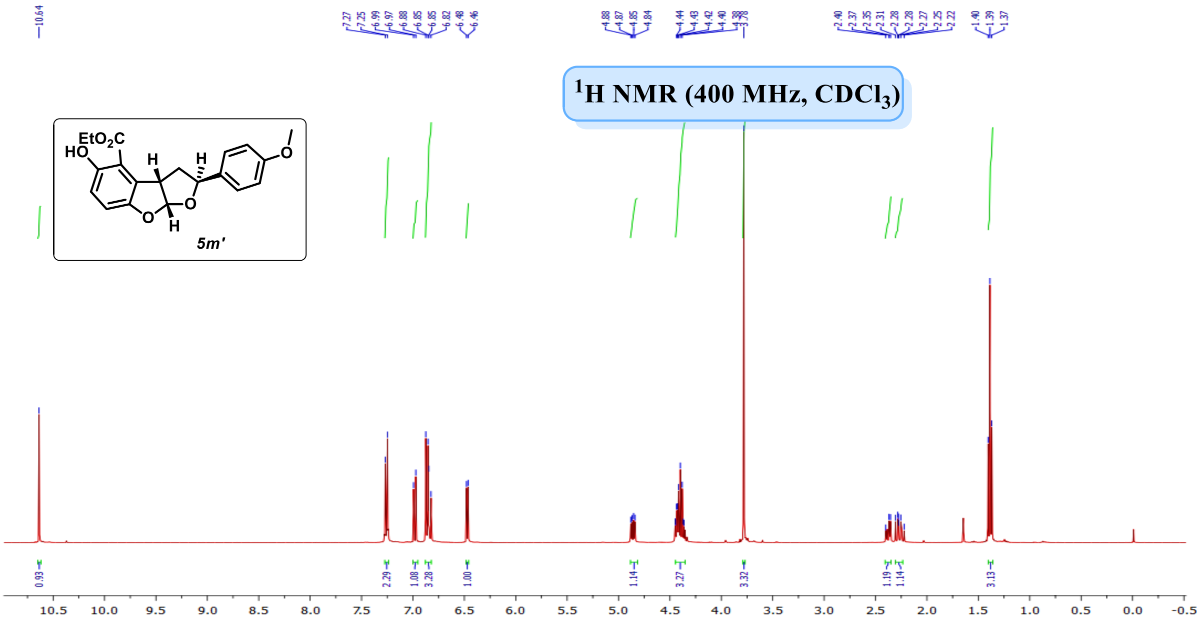
EtO2C
HO
H
H
O
O
H
O
5m'
1H NMR (400 MHz, CDCl3)

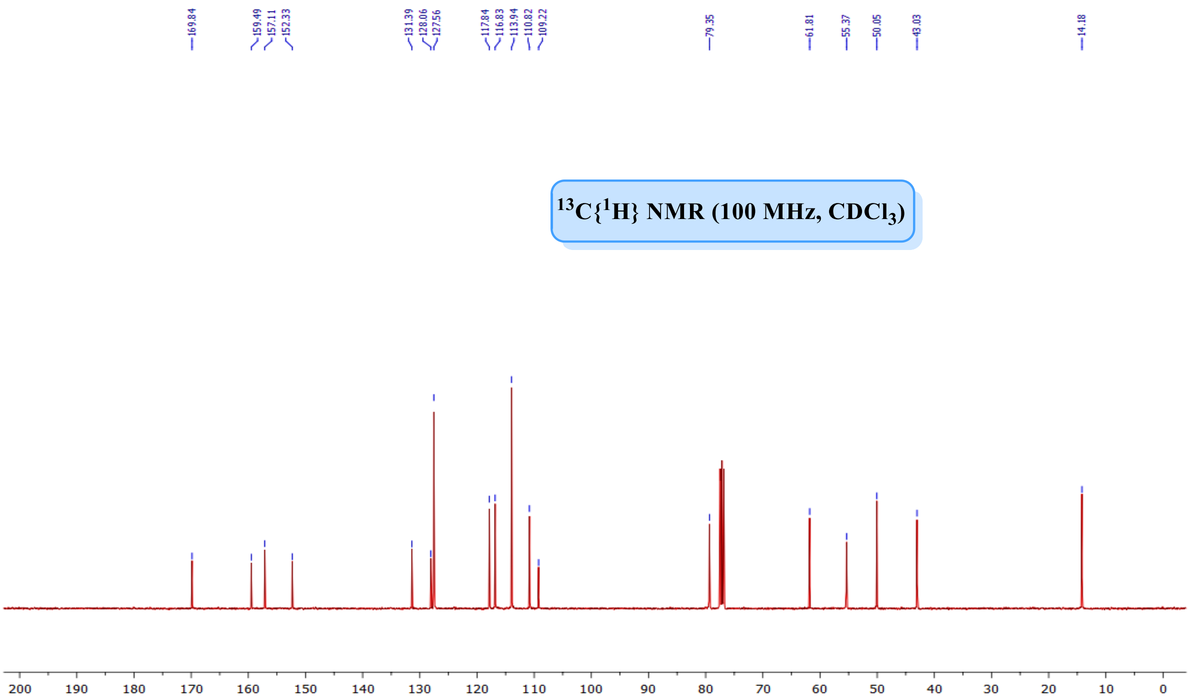
13C{1H} NMR (100 MHz, CDCl3)

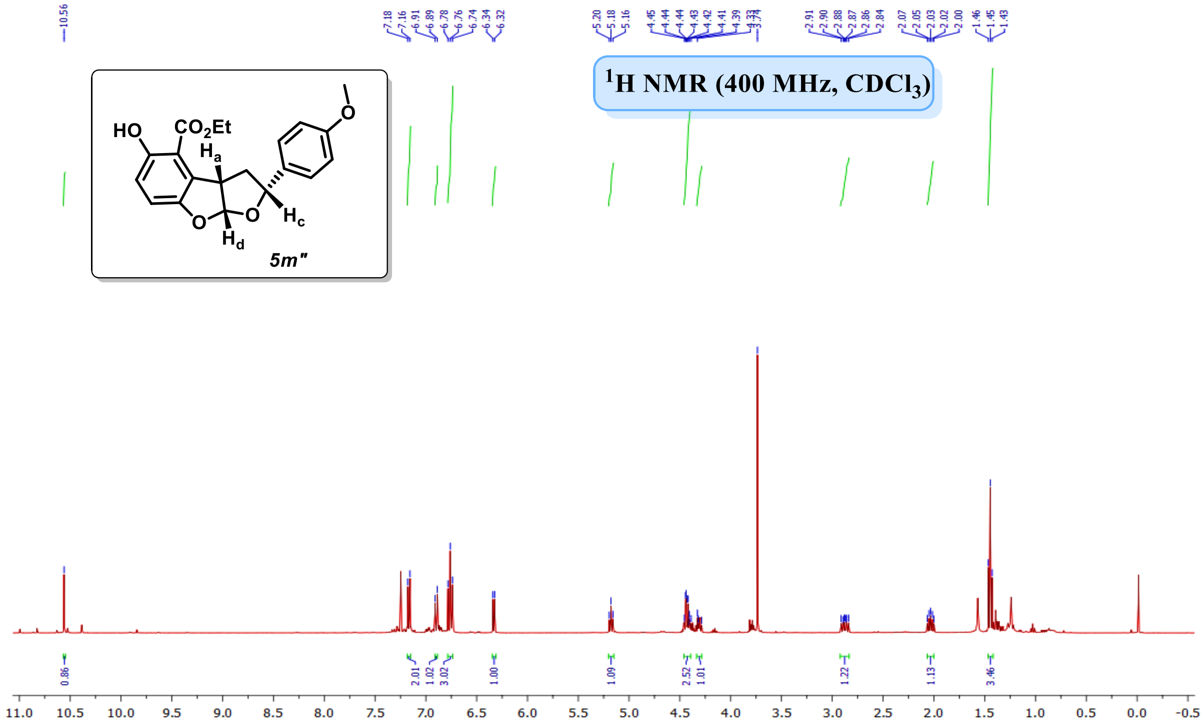
HO
CO2Et
Ha
O
Hc
Hd
5m"
1H NMR (400 MHz, CDCl3)

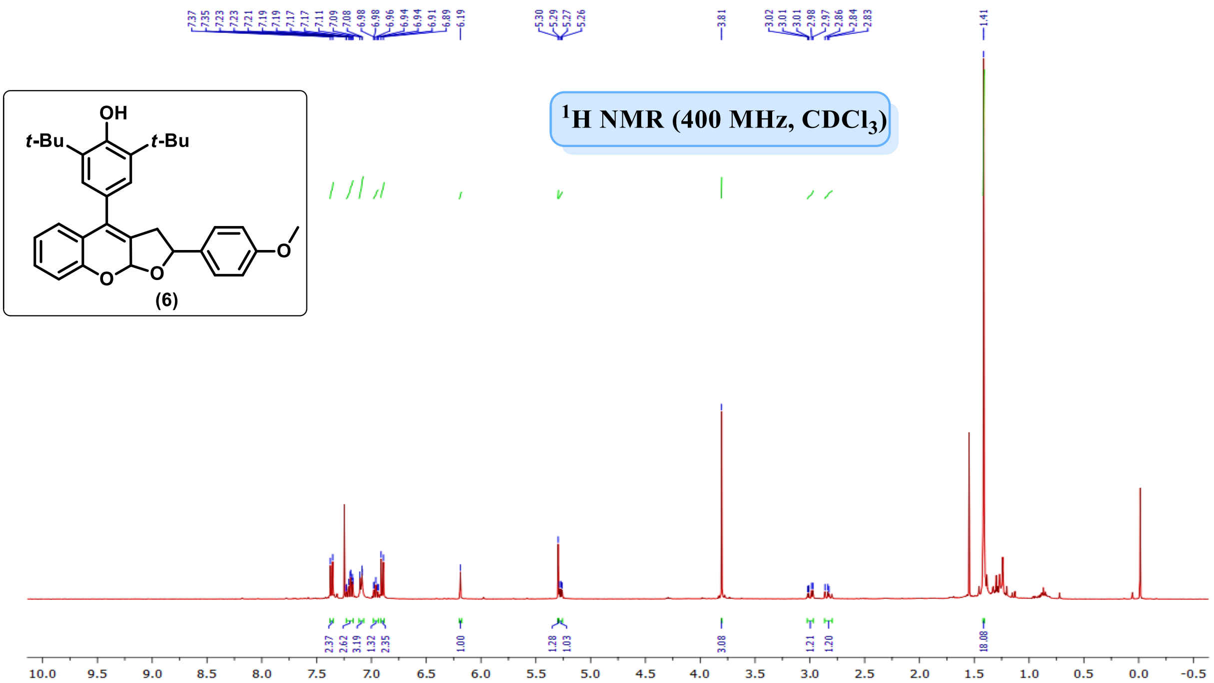
OH
t-Bu
t-Bu
O
(6)
1H NMR (400 MHz, CDCl3)

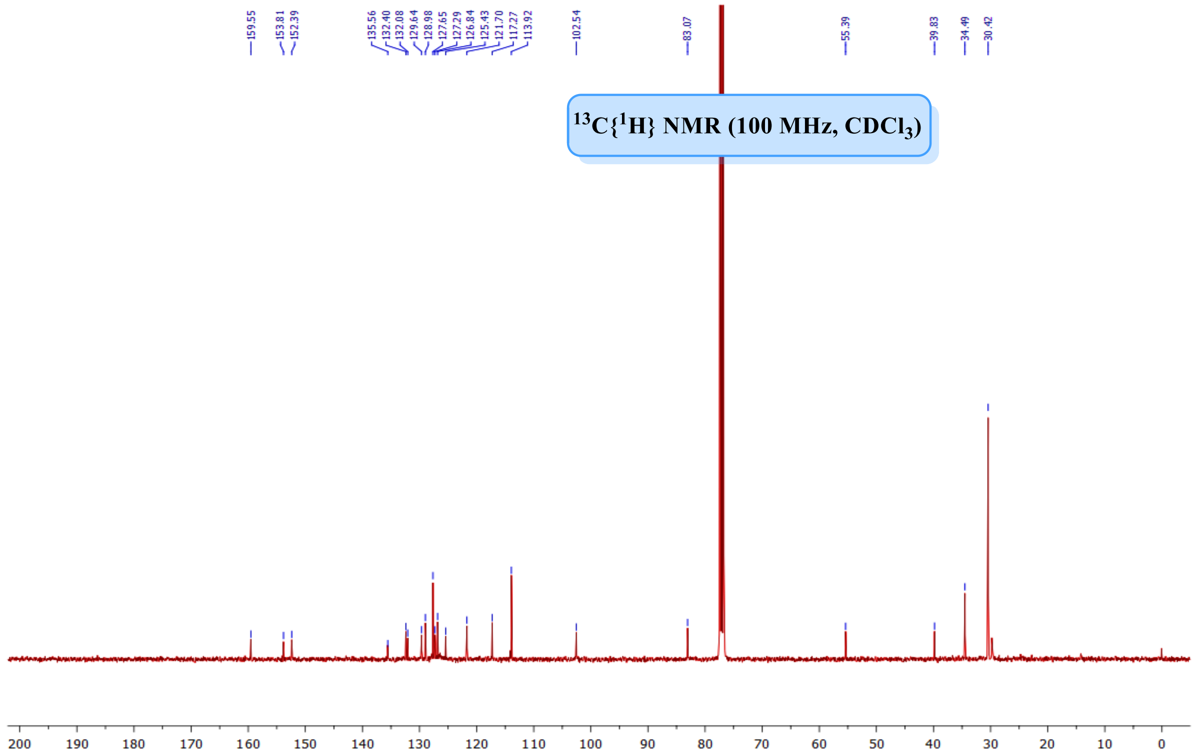
13C{1H} NMR (100 MHz, CDCl3)

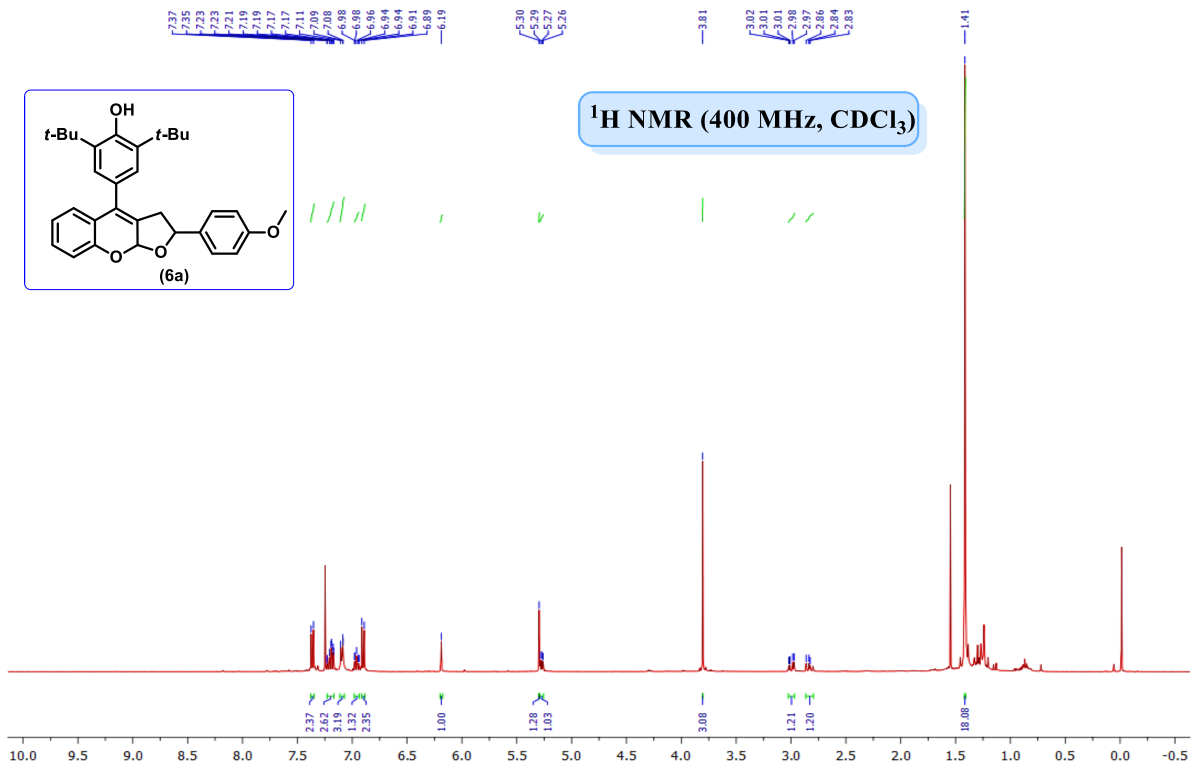
1H NMR (400 MHz, CDCl3)
(6a)

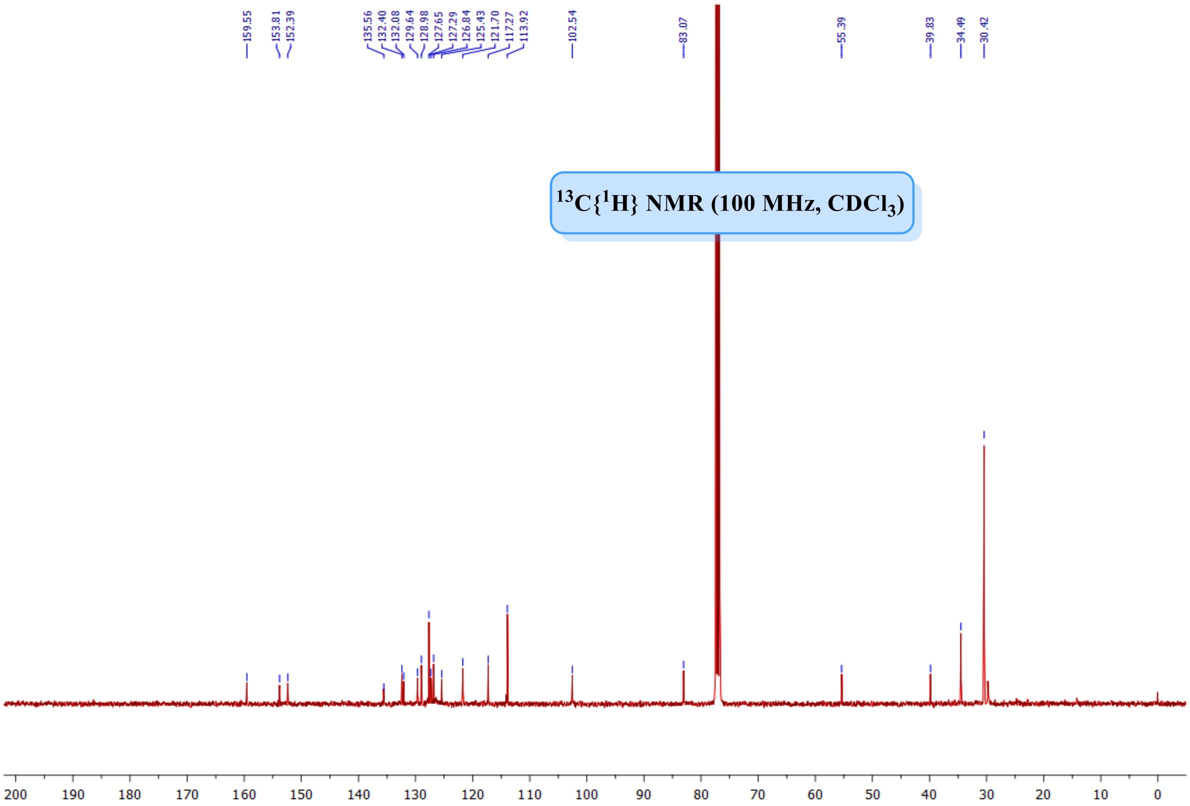
$^{13}C\{^{1}H\}$ NMR (100 MHz, $CDCl_3$)
159.55
153.81
152.39
135.56
132.40
132.08
129.64
128.98
127.65
127.29
126.84
125.43
121.70
117.27
113.92
102.54
83.07
55.39
39.83
34.49
30.42
200 190 180 170 160 150 140 130 120 110 100 90 80 70 60 50 40 30 20 10 0

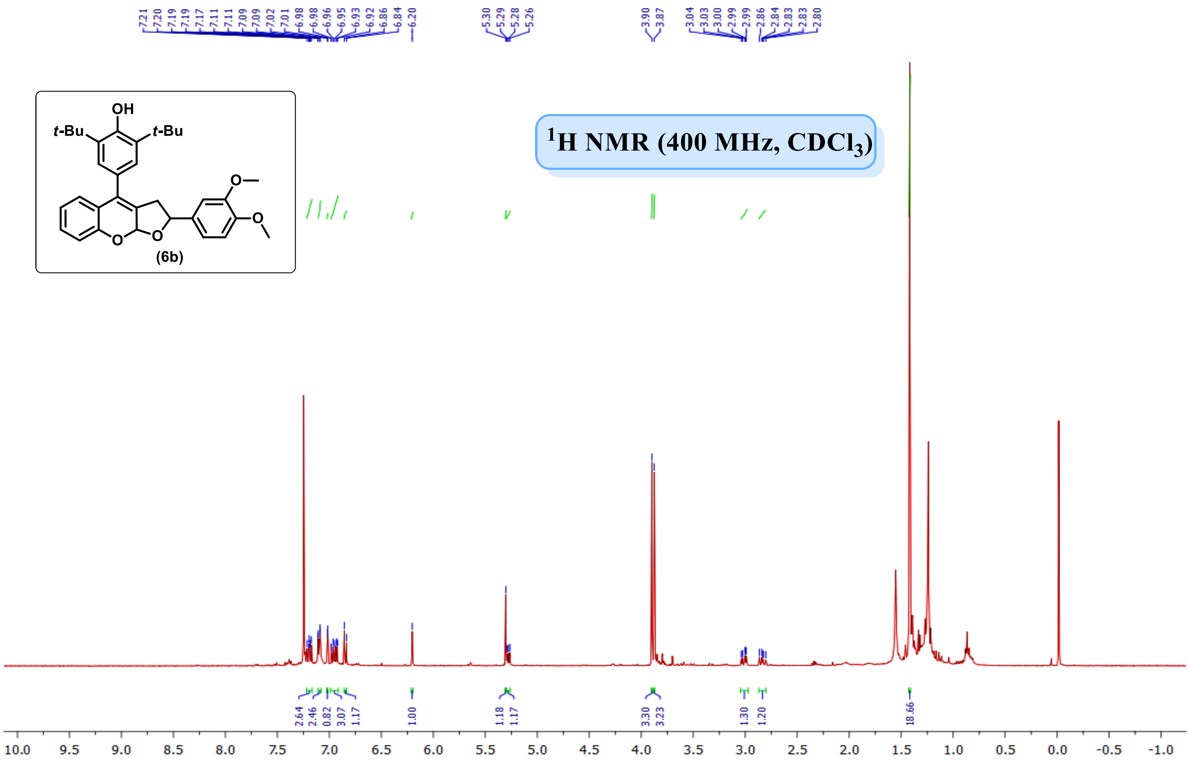
^{1}H NMR (400 MHz, $CDCl_3$)
OH
t-Bu
t-Bu
O
O
O
O
(6b)
7.21 7.20 7.19 7.19 7.17 7.11 7.11 7.09 7.09 7.02 7.01 6.98 6.98 6.96 6.95 6.93 6.92 6.86 6.84 6.20
5.30 5.29 5.28 5.26
3.90 3.87
3.04 3.03 3.00 2.99 2.99 2.86 2.84 2.83 2.83 2.80
2.64 2.46 0.82 3.07 1.17 1.00 1.18 1.17 3.30 3.23 1.30 1.20 18.66
10.0 9.5 9.0 8.5 8.0 7.5 7.0 6.5 6.0 5.5 5.0 4.5 4.0 3.5 3.0 2.5 2.0 1.5 1.0 0.5 0.0 -0.5 -1.0

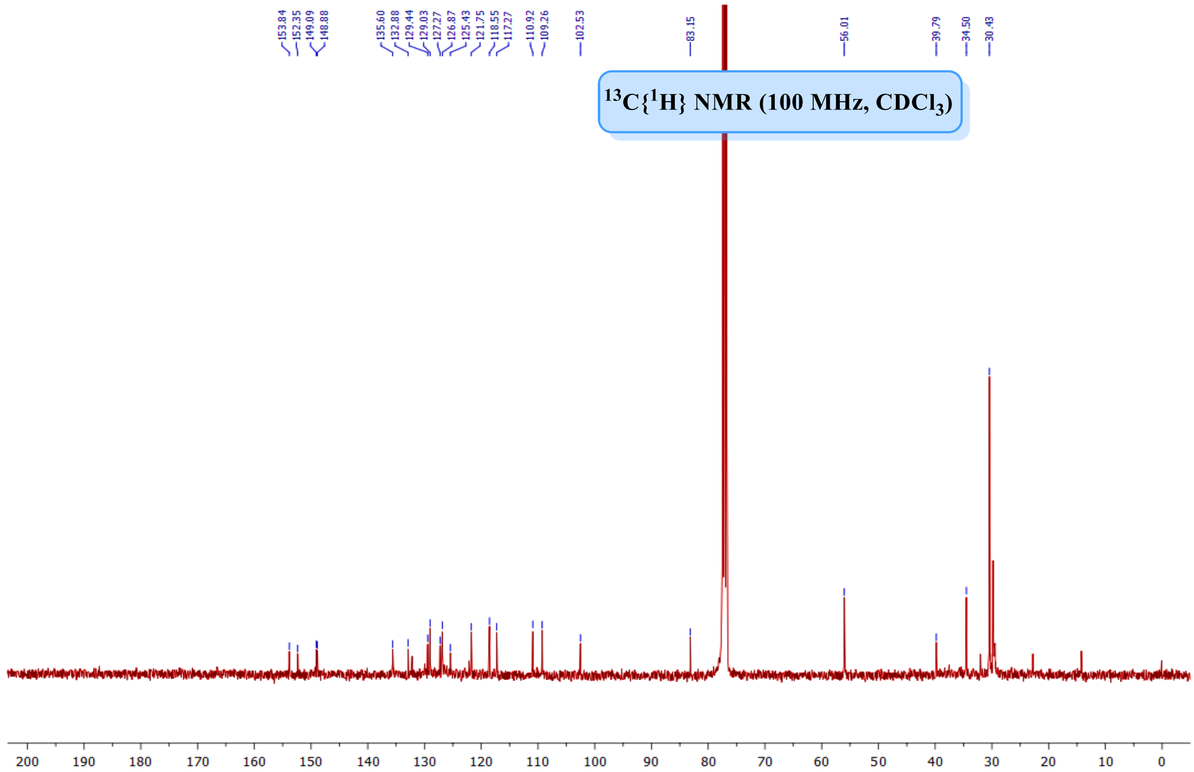
153.84
152.35
149.09
148.88
135.60
132.88
129.44
129.03
127.27
126.87
125.43
121.75
118.55
117.27
110.92
109.26
102.53
83.15
56.01
39.79
34.50
30.43
13C{1H} NMR (100 MHz, CDCl3)
200 190 180 170 160 150 140 130 120 110 100 90 80 70 60 50 40 30 20 10 0

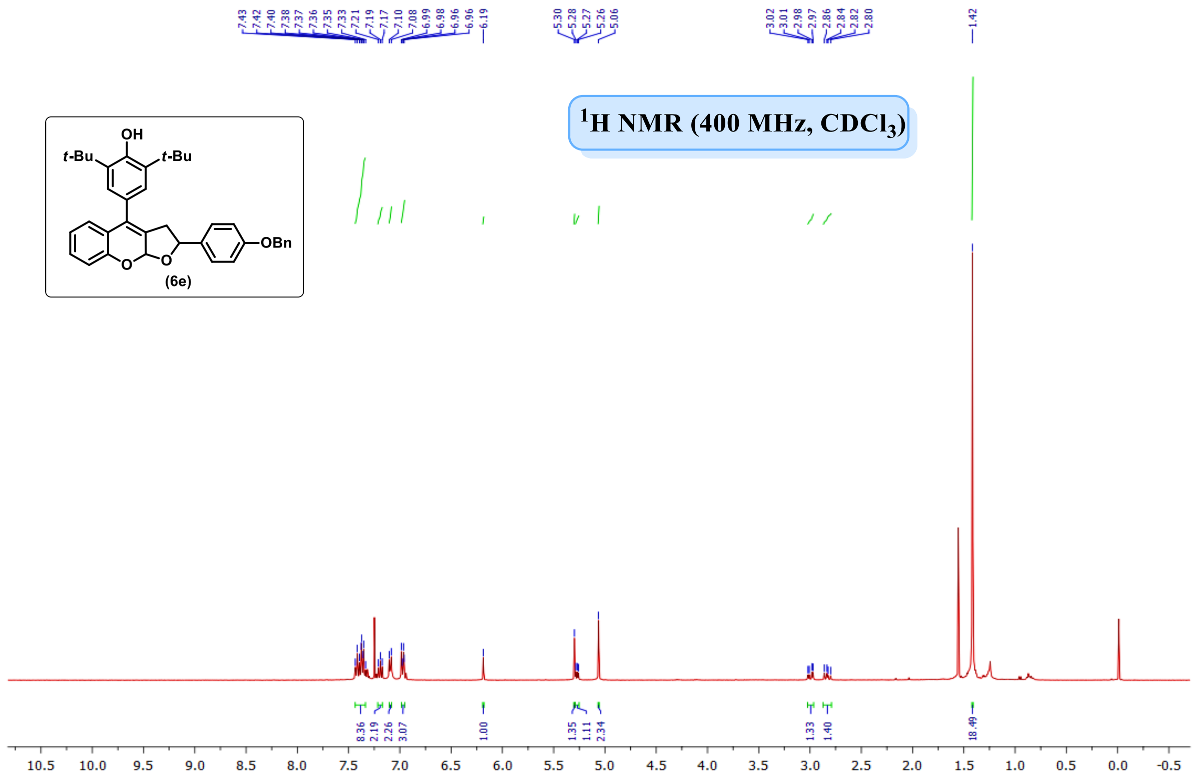
7.43
7.42
7.40
7.38
7.37
7.36
7.35
7.33
7.21
7.19
7.17
7.10
7.08
6.99
6.98
6.96
6.96
6.19
5.30
5.28
5.27
5.26
5.06
3.02
3.01
2.98
2.97
2.86
2.84
2.82
2.80
1.42
1H NMR (400 MHz, CDCl3)
OH
t-Bu
t-Bu
O
O
OBn
(6e)
8.36
2.19
2.26
3.07
1.00
1.35
1.11
2.34
1.33
1.40
18.49
10.5 10.0 9.5 9.0 8.5 8.0 7.5 7.0 6.5 6.0 5.5 5.0 4.5 4.0 3.5 3.0 2.5 2.0 1.5 1.0 0.5 0.0 -0.5

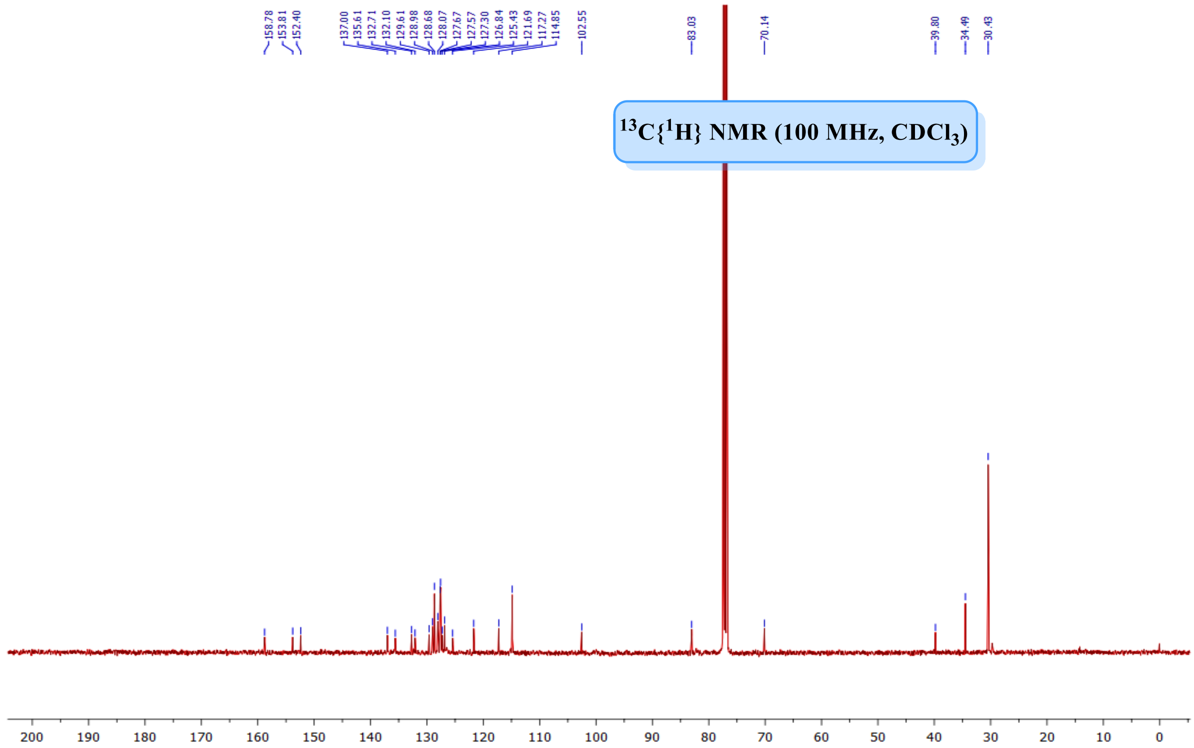
158.78
153.81
152.40
137.00
135.61
132.71
132.10
129.61
128.98
128.68
128.07
127.67
127.57
127.30
126.84
125.43
121.69
117.27
114.85
102.55
83.03
70.14
39.80
34.49
30.43
13C{1H} NMR (100 MHz, CDCl3)
200 190 180 170 160 150 140 130 120 110 100 90 80 70 60 50 40 30 20 10 0

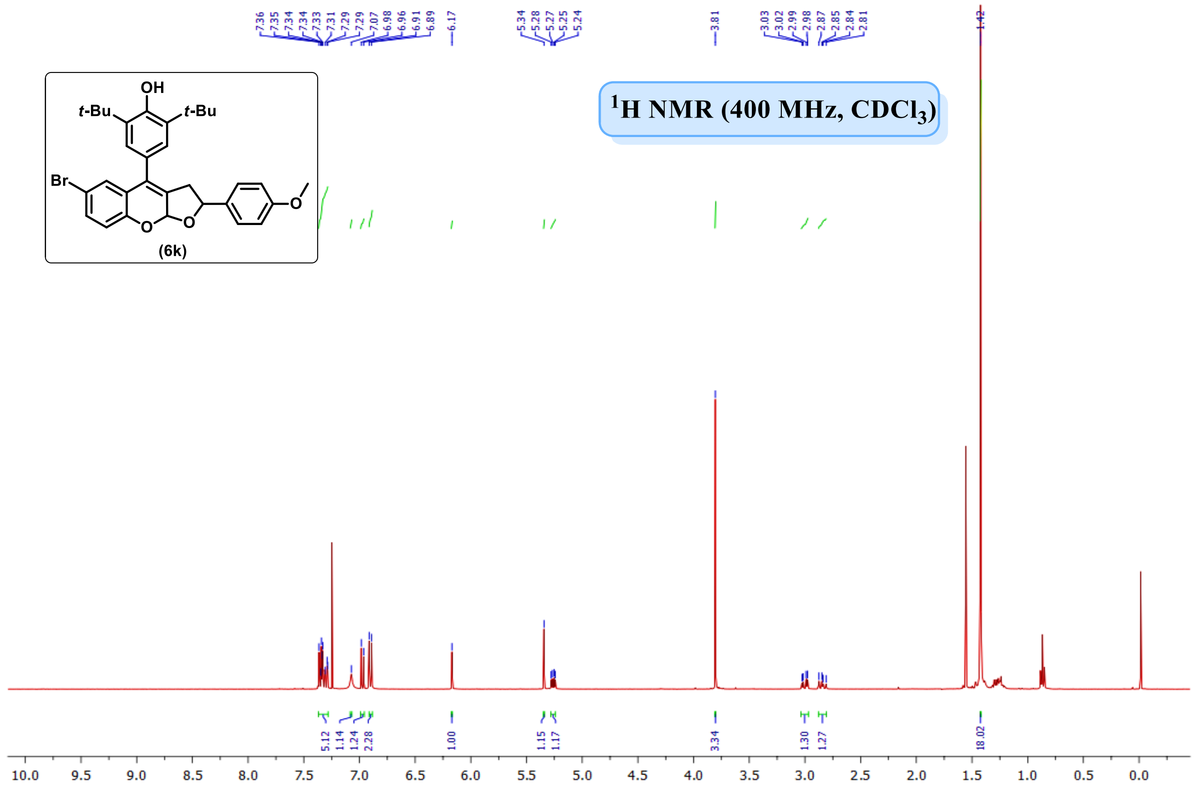
7.36
7.35
7.34
7.34
7.33
7.31
7.29
7.29
7.07
6.98
6.96
6.91
6.89
6.17
5.34
5.28
5.27
5.25
5.24
3.81
3.03
3.02
2.99
2.98
2.87
2.85
2.84
2.81
1.42
1H NMR (400 MHz, CDCl3)
OH
t-Bu
t-Bu
Br
O
O
O
(6k)
5.12
1.14
1.24
2.28
1.00
1.15
1.17
3.34
1.30
1.27
18.02
10.0 9.5 9.0 8.5 8.0 7.5 7.0 6.5 6.0 5.5 5.0 4.5 4.0 3.5 3.0 2.5 2.0 1.5 1.0 0.5 0.0

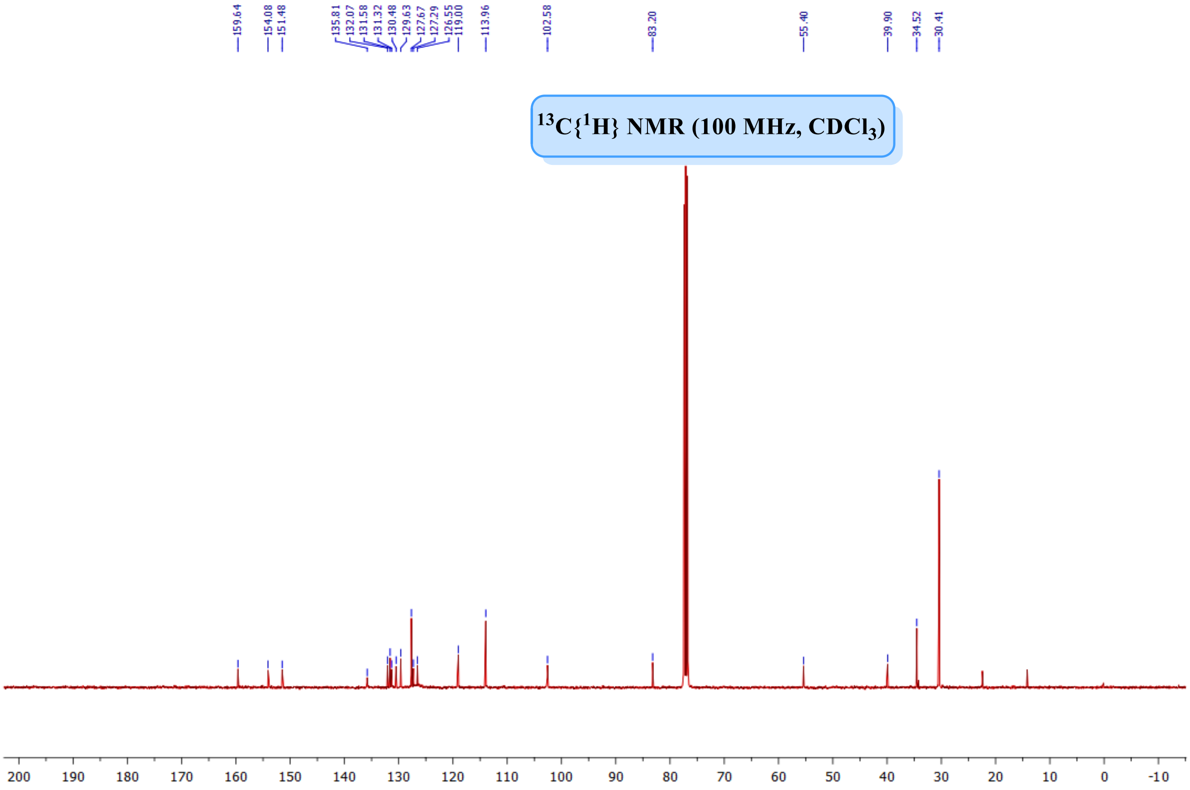

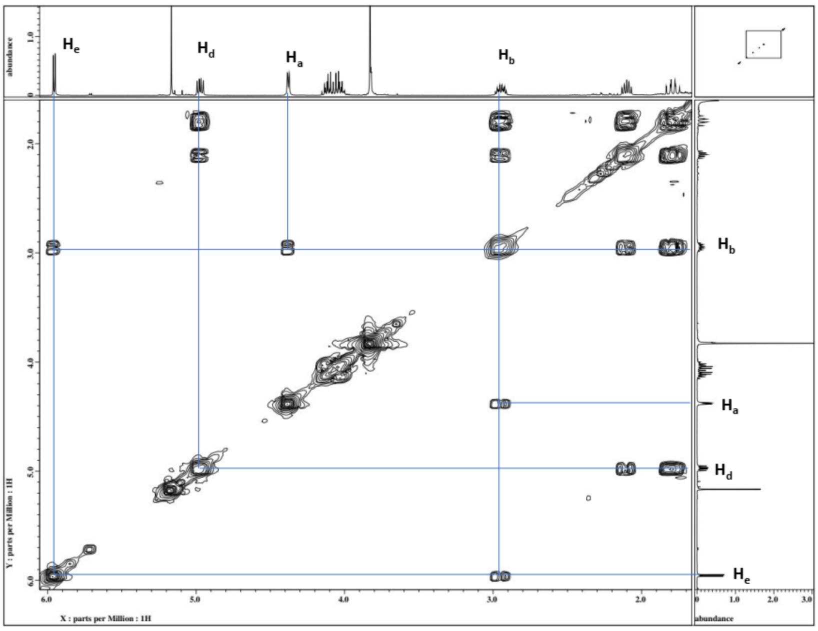

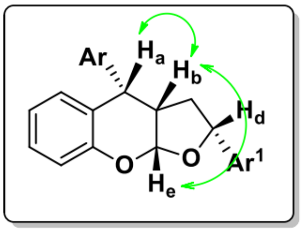

COSY (400 MHz, $CDCl_3$) of 3d'

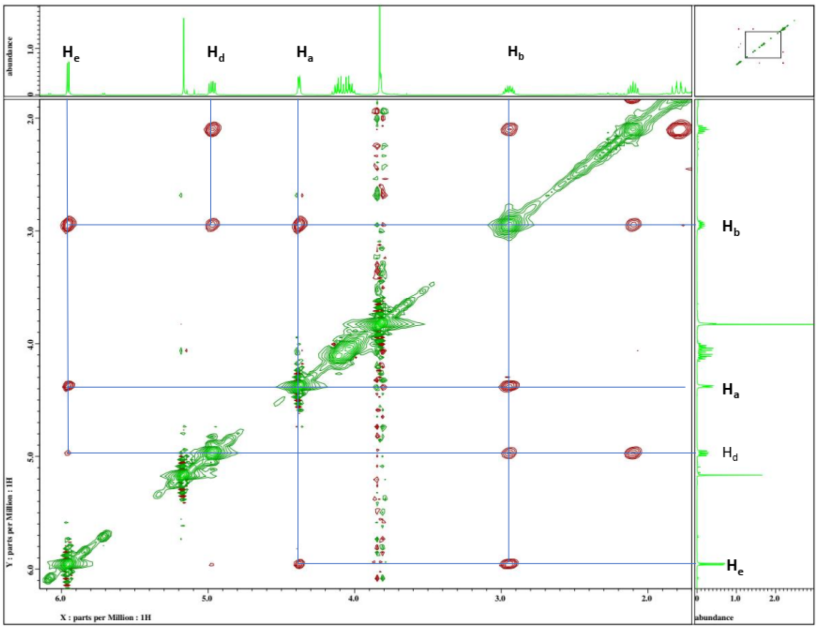

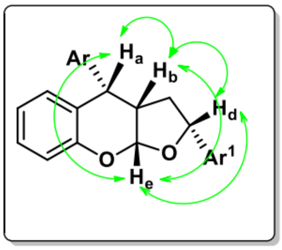

^{1}H-NOE NMR (400 MHz, CDCl$_3$) of 3d'

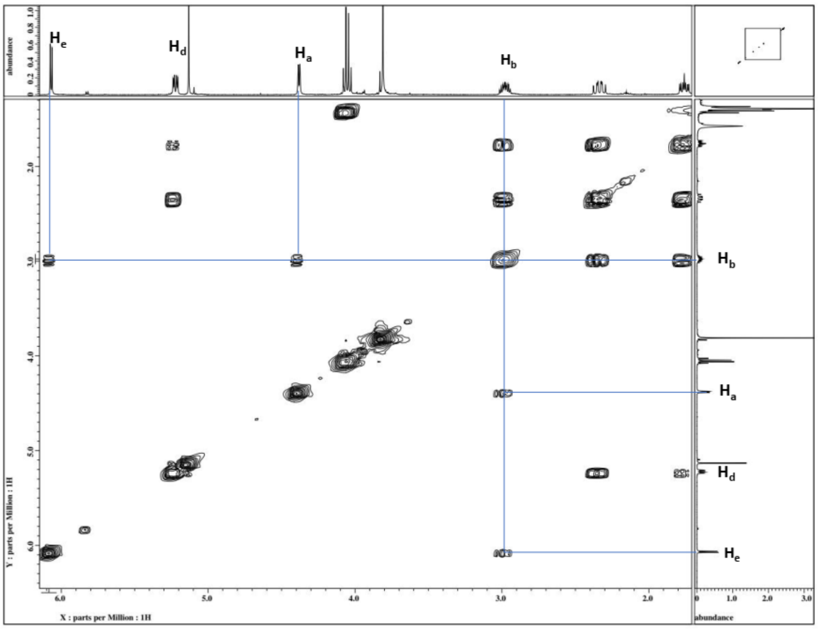

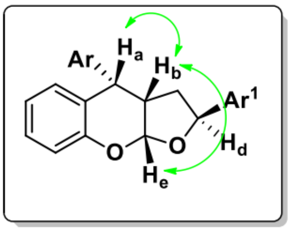

COSY (400 MHz, CDCl$_3$) of 3d''

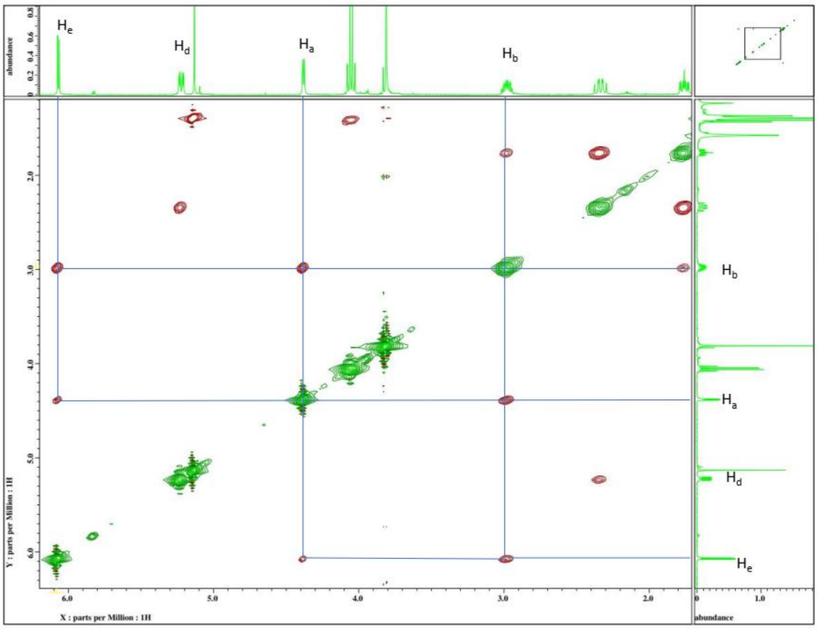

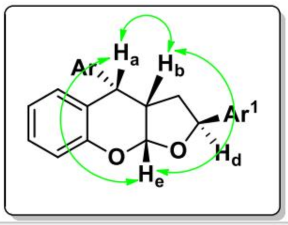

^{1}H-NOE NMR (400 MHz, CDCl$_3$) of 3d''

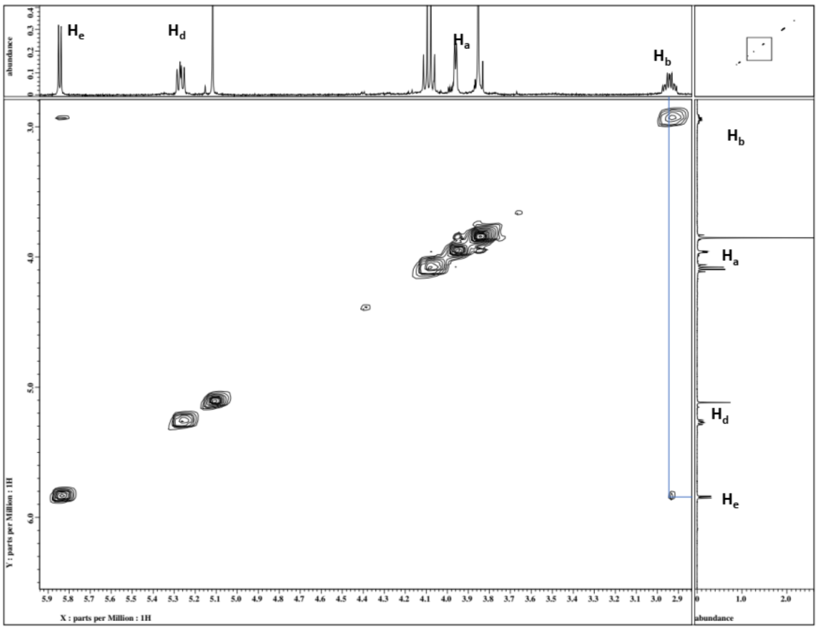

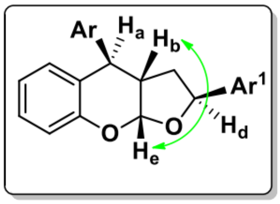

COSY (400 MHz, CDCl$_3$) of 3d'''

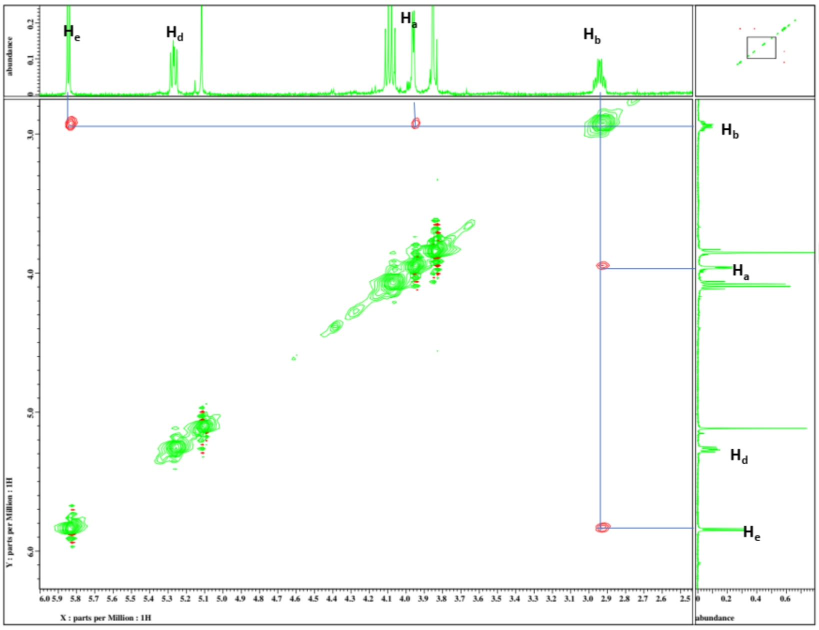

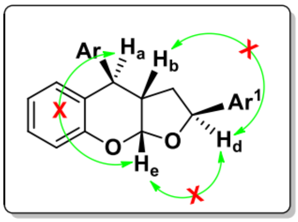

^{1}H-NOE NMR (400 MHz, $CDCl_3$) of 3d'''

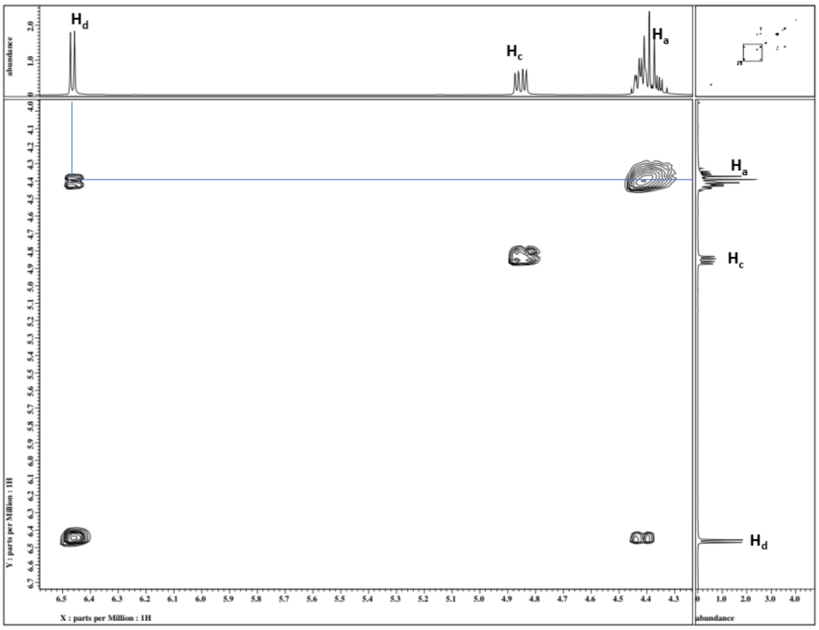

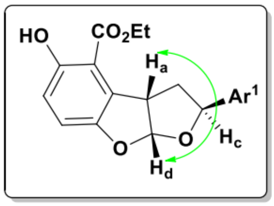

COSY (400 MHz, $CDCl_3$) of 5m'

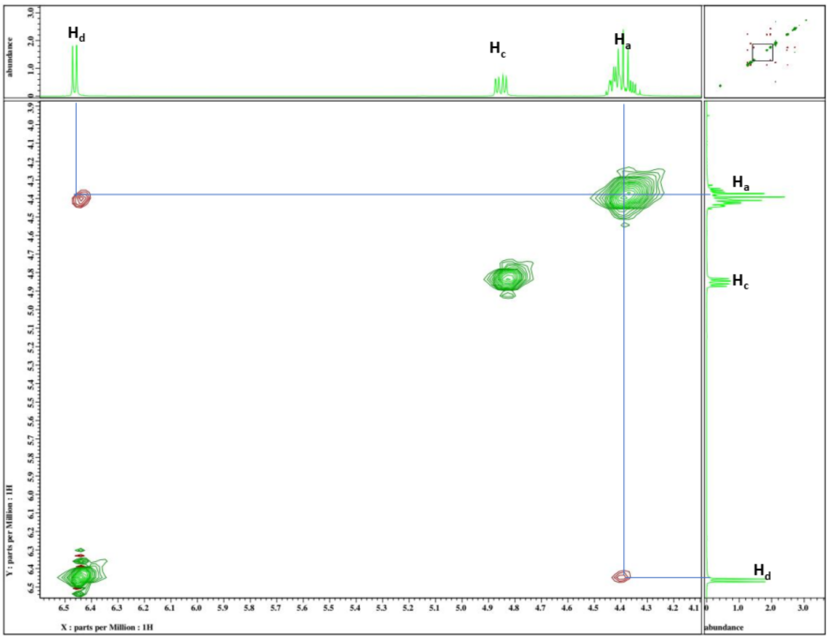

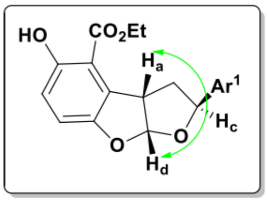

^{1}H-NOE NMR (400 MHz, $CDCl_3$) of 5m'

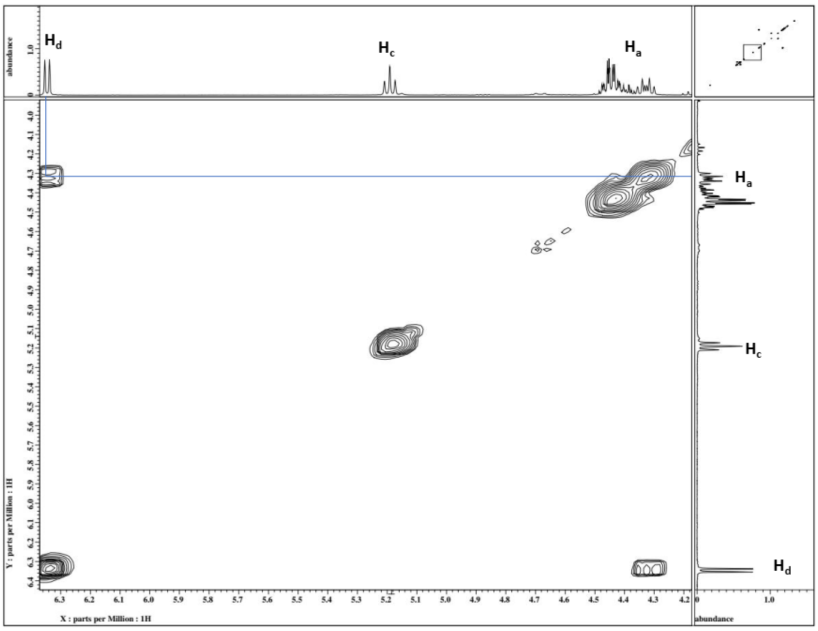

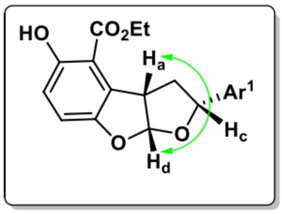

COSY (400 MHz, $CDCl_3$) of 5m"

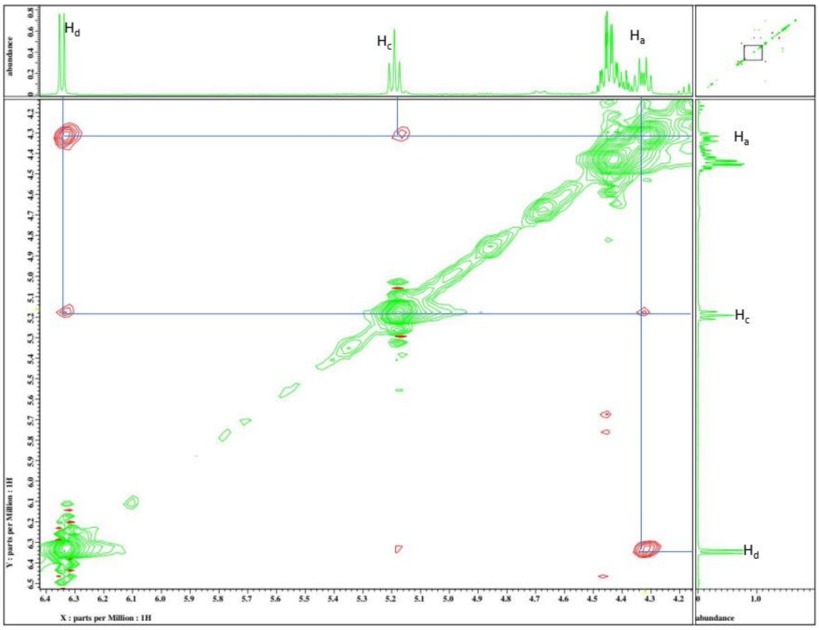

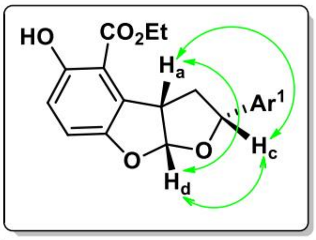

^{1}H-NOE NMR (400 MHz, $CDCl_3$) of 5m''

Chapter 4

Switchable Reactivity of Cyclopropane Diesters towards (3+3) and (3+2) Cycloadditions with Benzoquinone Esters

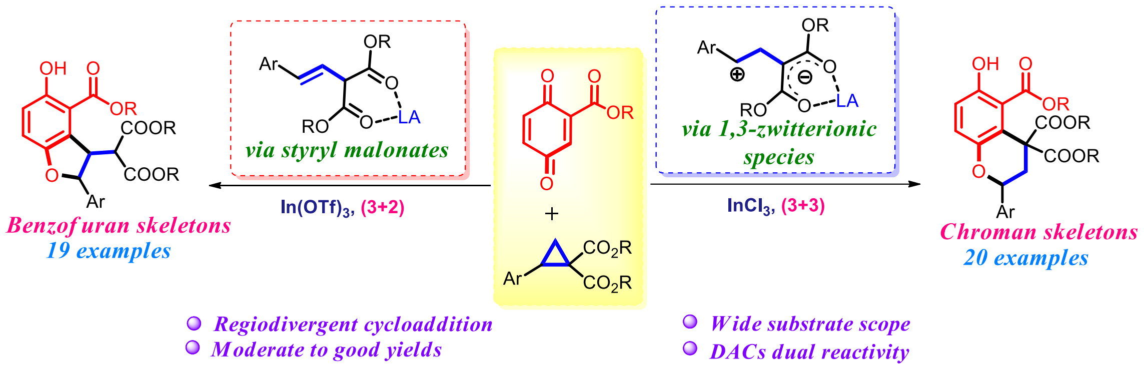

This work was published in *Organic Letters* (A journal of *American Chemical Society*). Please see citation "Kaur, N.; Kumar, P.; Hazra. A.; Banerjee, P. *Org. Lett.* **2022**, *24*, 8249-8254."

4.1 Introduction

Heterocyclic compounds are privileged structural motifs that have been found as an important core in many natural products.[1] Particularly, oxygen-containing heterocyclic frameworks are widely known for their biological and pharmaceutical activities.[2] However, benzopyran derivatives often possess antitumor, antibiotic and antioxidant properties.[3] Due to their inherent biological properties, chromans have acquired immense attraction in medicinal and organic chemistry. Furthermore, the benzopyran moiety is also a part of PPARγ and PPARα/γ agonists. These PPARs play a very crucial role in the control of different pathological disorders, like hyperlipidaemia, obesity, type 2 diabetes, neurodegenerative and cardiovascular diseases.[4] (Figure 4.1.1)

Figure 4.1.1. Representative natural products and pharmaceuticals containing chroman and benzofuran skeletons.

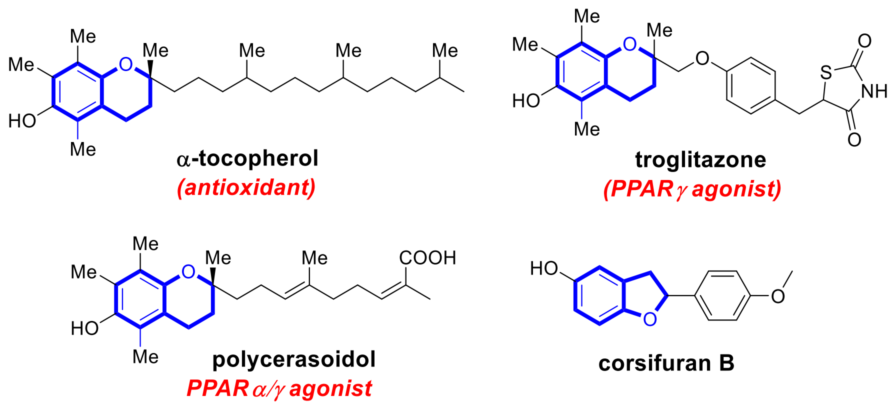

In addition, bioactive benzopyran scaffolds are used as neuroprotectors in various neurological disorders such as Alzheimer's disease.[5] On the other hand, benzofuran derivatives also represent a wide variety of heterocycles and are found as a core structure in many bioactive molecules.[6] They show a wide range of pharmacological properties and are featured in most clinically used drugs. Indeed, these functionalized derivatives are widely known for their physiological and chemotherapeutic properties, which has made the development of new and time-efficient approaches for the synthesis of these pivotal skeletons more desired and attractive in the synthetic community.[7] Over time, donor-acceptor cyclopropanes (DACs) have appeared as one of the most versatile building blocks for the synthesis of various carbo- and heterocycles.[8] Due to the presence of vicinal donor and acceptor groups and high ring strain in the cyclopropane, the cleavage of the carbon-carbon bond occurs effortlessly. These 1,3 zwitterionic species exhibit several transformations like ring opening, rearrangements, ring expansion, and cycloaddition reactions.[9] Out of these, cycloaddition reactions with reaction partners such as imines, carbonyls, dienes, alkynes, and nitrones are most investigated.[10] Also, the cycloaddition reactions for the construction of numerous nitrogen heterocycles are extensively studied using DACs as 1,3 dipolar species.[11] On the contrary, the formation of oxygen heterocycles (chromans) using DACs as 1,3 dipolar species for the cycloaddition reactions is less explored. Also, these activated cyclopropanes undergo many rearrangement reactions, most commonly the *in-situ* generation of styryl malonates.[12] Interestingly, these styryl malonates can further be a part of cycloaddition reactions by using a suitable reaction partner.[13] Our group has significantly utilized the strain-driven reactivity of DACs for a variety of annulation and cycloaddition reactions to synthesize valuable heterocycles.[14]

On the other hand, quinone esters (QE) have attained substantial attention due to their electrophilic nature.[15] In past years, there are a very few reports on the reactivity of quinone derivatives with strained ring systems. In 2016, Zhao's group demonstrated the formal (3+2) cycloaddition of *para*-quinone methides with vinyl epoxides/cyclopropanes using palladium precursor and a chiral *bis*-phosphine (Scheme 4.1.1a).[16] Recently, Wang and Luo's group reported the $Sc(OTf)_3$-catalyzed formal (3+3) cycloaddition reaction of diaziridines and quinones towards the construction of tricyclic 1,3,4-oxadiazinanes (Scheme 4.1.1b).[17]

Scheme 4.1.1. Reactivity of quinone derivatives with strained rings

a). Zhao's group

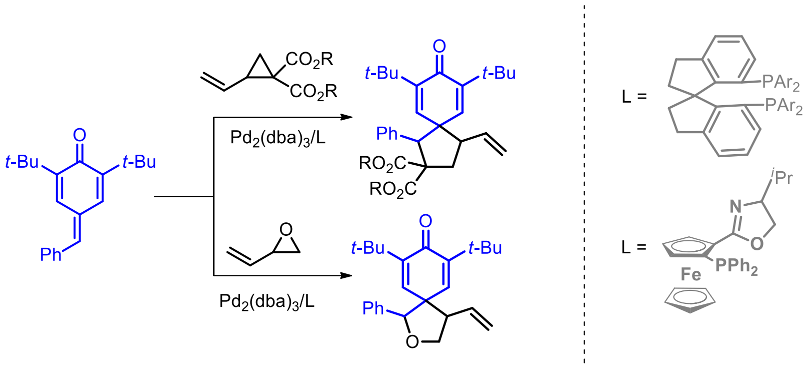

b). Wang and Luo's group

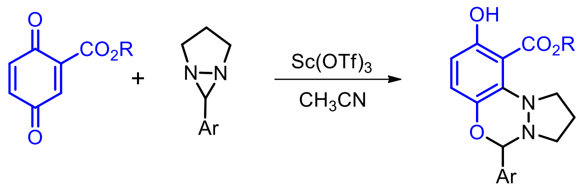

Very recently, our group also presented the synthesis of tetrahydrofurobenzopyran and tetrahydrofurobenzofuran systems *via* an *in-situ* ring-expansion (Cloke-Wilson rearrangement) of the cyclopropane carbaldehydes followed by a [2+n] cycloaddition with the quinone derivatives (Scheme 4.1.1c).[18] Despite these elegant approaches, we believe quinone esters and DACs would provide a simple

c). Our Previous work

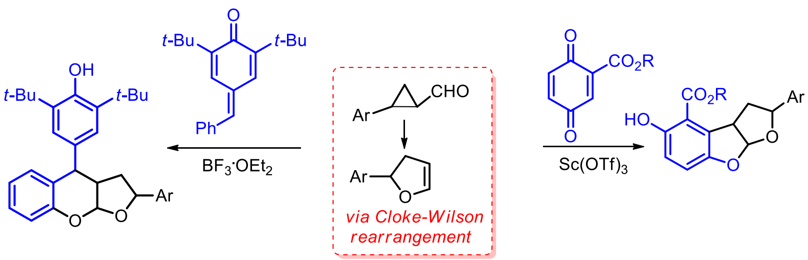

and efficient route for the (3+3) and (3+2) regiodivergent cycloaddition reaction of DACs with quinone esters towards the construction of functionalized oxacycles (chroman and benzofuran derivatives). In this context, we delineate a catalyst-controlled cycloaddition reaction of DACs; a source of 1,3-zwitterionic species as well as 2-styryl malonate by fine-tuning of Lewis acid with the same reaction partner (quinone esters) to furnish densely functionalized five- and six-membered oxacycles Scheme (4.1.1d).

d) Our Idea

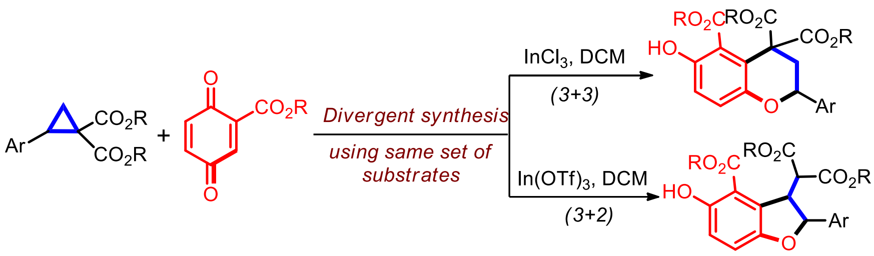

4.2 Results and Discussion

We started our investigation using dimethyl 2-(4-methoxyphenyl)cyclopropane-1,1-dicarboxylate (DAC) **1a** and quinone ester **2a** as model substrates. Initially, the reaction was performed using $BF_3{\cdot}OEt_2$ (20 mol %) in dichloromethane at room temperature leads to the formation of a complex mixture (Table 4.2.1, entry 1). Then the reaction was carried out using $Sc(OTf)_3$, and it was found that a new product **4aa** was encountered along with the desired product **3aa** (Table 4.2.1, entry 2). After analyzing the data, it was confirmed that a (3+2) cycloaddition has taken place. The compound **4aa** was characterized by spectral data, HRMS, and single crystal X-ray analysis. Different Lewis acids like $Cu(OTf)_2$, $Yb(OTf)_3$, $Mg(OTf)_2$, and $In(OTf)_3$ in dichloromethane were examined for the transformation (Table 4.2.1, entries 3-6). In all the cases, **4aa** was the main product, and **3aa** was attained in very low yields. Further screening of Lewis acids such as MgI_2, $MgBr_2$, and $FeCl_3$ proved useful for the transformation, and the improved yield of the desired product **3aa** was obtained with $FeCl_3$ (Table 4.2.1, entries 7-9). Therefore, we next examined $InCl_3$ (20 mol %) in DCM and we were pleased to obtain the targeted cycloadduct **3aa** in 60% yield (Table 4.2.1, entry 10). The spectroscopic data and single crystal X-ray analysis data confirmed the formation of the desired chroman. Delightfully, decreasing the catalyst loading to 10 mol %, resulted in 70 % yield (Table 4.2.1, entry 11). Next, the optimization regarding the five-membered oxacycles were carried out. Initially, the DACs remained unconsumed, resulting in a lower yield of **4aa**. Further, attempting the reaction with 1.2 equivalents of **2a** and 20 mol %. of catalyst, afforded the product **4aa** in 78% yield (Table 4.2.1, entry 12). Further, both reactions were performed in various solvents like DCE, $CHCl_3$, CH_3CN, and toluene, resulted in the decreased yield of the final product (Table 4.2.1, entry 13-18). However, DCM was the solvent of choice in both cases among various solvents. $AlCl_3$ and $TiCl_4$ proved ineffective for both transformations (Table 4.2.1, entry 19-20). After giving many trials, we finally got the optimal reaction conditions for both transformations, where $InCl_3$ (10 mol %) was the most effective Lewis acid for the (3+3) cycloaddition. On the contrary, (3+2) cycloaddition was successfully carried out using $In(OTf)_3$ (20 mol %) in dichloromethane in good yields.

Table 4.2.1. Optimization of the Reaction Conditions[a]

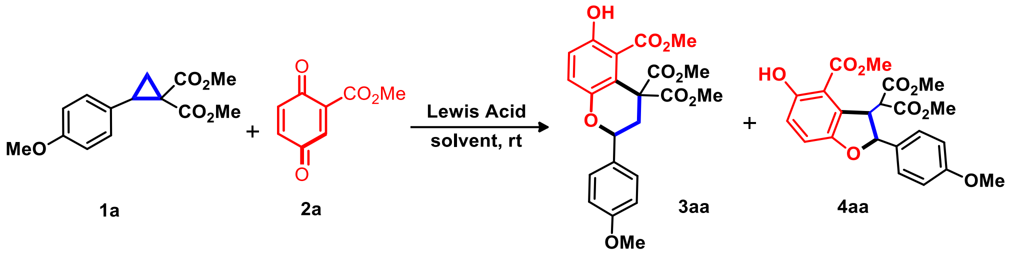

Entry	Catalyst	Loading (mol %)	Solvent[c]	Time (h)	Yield(%)[d]	
					3aa	4aa
1	$BF_3.OEt_2$	0.2	DCM	1	-	-
2	$Sc(OTf)_3$	0.2	DCM	1	15	50
3	$Cu(OTf)_2$	0.2	DCM	1.5	10	40
4	$Yb(OTf)_3$	0.2	DCM	2	trace	42
5	$Mg(OTf)_2$	0.2	DCM	0.5	10	25
6	$In(OTf)_3$	0.2	DCM	5	trace	56
7	MgI_2	0.2	DCM	12	30	-
8	$MgBr_2$	0.2	DCM	8	25	-
9	$FeCl_3$	0.2	DCM	0.5	45	-
10	$InCl_3$	0.2	DCM	0.5	60	trace
11	$InCl_3$	0.1	DCM	0.8	70	trace
12[b]	$In(OTf)_3$	0.2	DCM	1	trace	75
13	$InCl_3$	0.1	DCE	0.8	55	-
14	$InCl_3$	0.1	CH_3CN	2	20	-
15	$InCl_3$	0.1	$CHCl_3$	1	30	-
16	$In(OTf)_3$	0.2	DCE	1	trace	60
17	$In(OTf)_3$	0.2	CH_3CN	2	-	20
18	$In(OTf)_3$	0.2	toluene	2	-	30
19	$AlCl_3$	0.2	DCM	1	-	-
20	$TiCl_4$	0.2	DCM	1	-	-

[a]Reactions were carried out with 1 equiv. of **1a** and 1 equiv. of **2a** in solvent (0.1 M). [b]Reactions were carried out with 1 equiv. of **1a** and 1.2 equiv. of **2a** in solvent (0.2 M). [c]DCM = dichloromethane, DCE = dichloroethane, CH_3CN = acetonitrile. [d]Isolated yield.

With the optimized reaction conditions in hand, we first explored the substrate scope of the (3+3) cycloaddition reaction employing a wide range of DA cyclopropanes possessing different substituents on the aryl ring. Cyclopropanes bearing electron-rich substituents at the *para*-position and multiple position of the aryl ring, such as 4-methoxy, 3,4-dimethoxy, 3,4,5-trimethoxy, and 4-benzyloxy delivered the desired product **3aa, 3ba, 3ca** and **3da** in moderate to good yields. Next, cyclopropanes having other substituents on the aryl ring along with the methoxy group at the *para*-position were also evaluated. Gratifyingly, groups such as ethoxy, bromo, and methyl at the *meta*-position furnished the targeted (3+3) cycloadduct **3ea, 3fa**, and **3ga** in 65-70% yields. Substituents like methylenedioxy and benzofuran on the aryl ring gave the corresponding product **3ha, 3ia** in good yields. Cyclopropane having a mesityl substituent on the aryl ring rendered the corresponding product **3ja** in 62% yield. Less electron-rich and halogen-substituted DACs proved inappropriate for the transformation. Later, we evaluated the substrate scope using quinone esters with a range of alkoxy groups. To our pleasure, all the variations in the esters group, such as ethyl, butyl, benzyl, allyl, *para*-substituted benzyl, *ortho*-substituted benzyl, and phenethyl esters afforded the desired product **3ab-3ai** in moderate to good yields. On the other hand, quinone ketones and unsubstituted quinones were also tested, unfortunately, no product formation was observed. Also, methoxy substituted QE and naphthoquinone ester gave the products **3aj** and **3ak** in appreciable yields. (Scheme 4.2.1)

Scheme 4.2.1. Substrate scope of DACs and quinones for (3+3) cycloaddition.[a,b]

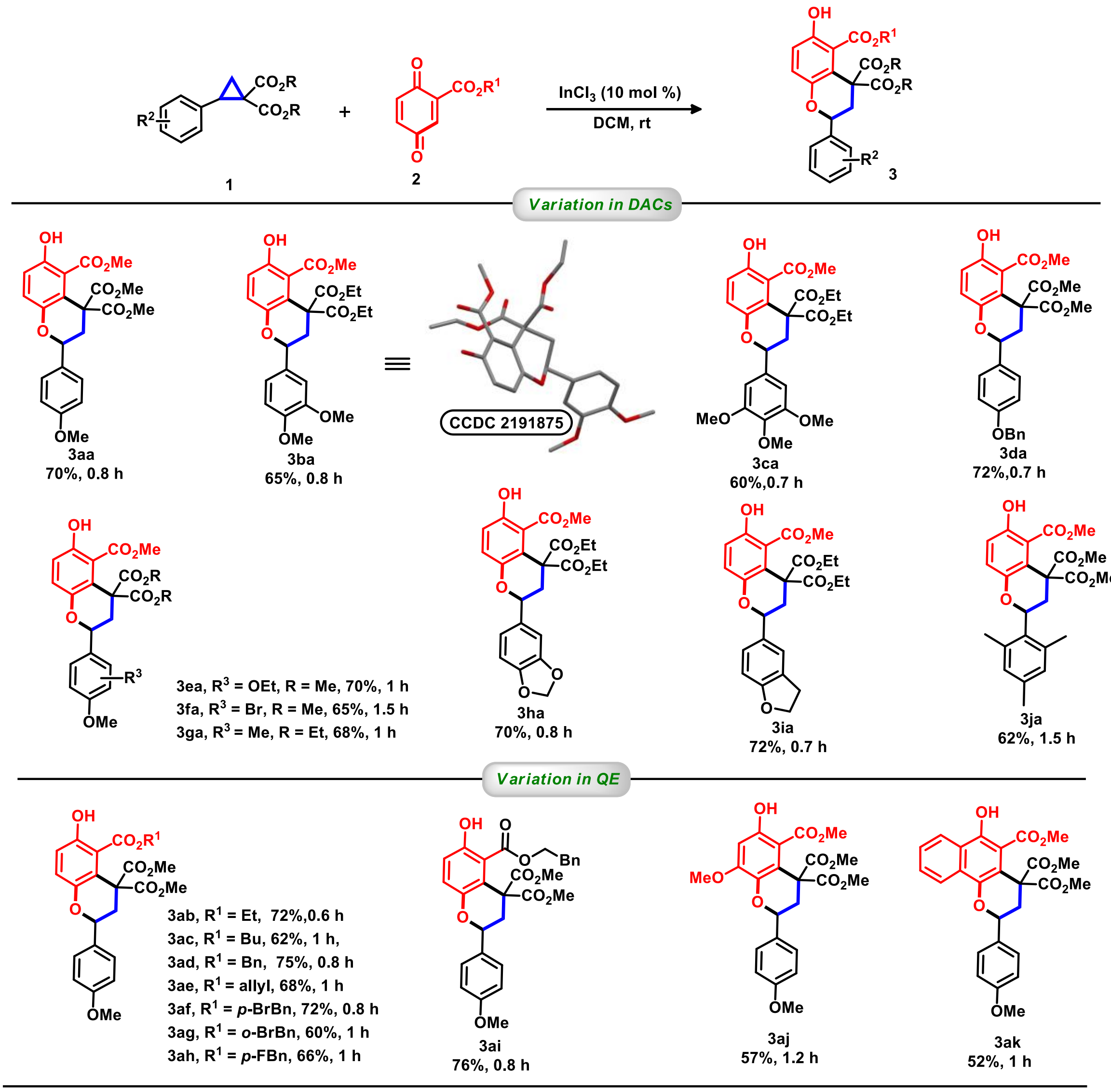

[a]Standard reaction conditions: **1a** (0.37 mmol), **2a** (0.37 mmol), Indium chloride (10 mol %) at room temperature in DCM (4 ml). [b]Isolated yield.

Further, the generality and viability of the (3+2) cycloaddition reaction were investigated with respect to various DA cyclopropanes. The treatment of dimethyl 2-(4-methoxyphenyl)cyclopropane-1,1-dicarboxylate (DAC) **1a** with quinone ester **2a** provided the corresponding product **4aa** in 75% yield. Cyclopropanes possessing 3,4-dimethoxy, 4-benzyloxy, and methylenedioxy groups on the vicinal phenyl ring of the DACs furnished the anticipated product **4ba**, **4ca**, and **4da** in moderate to good yields. Electron-rich DACs having *N*,*N*-dimethyl group at the *para*-position was also well-tolerated and provided the cycloadduct **4ea** in 70% yield. Cyclopropanes with multiple substitutions at the aryl ring proved suitable for the desired transformation. The presence of substituents like ethoxy, bromo, and methyl accompanying the methoxy group at the *para* position gave the corresponding products **4fa, 4ga,** and **4ha** in 68%, 62%, and 74% yields, respectively. Other aryl substituents like benzofuran derivatives afforded the desired product **4ia** in 72% yields. The reaction was also tried with less electron-rich DACs such as those substituted with 4-tolyl, 4-isopropylphenyl, and 2,4,6-trimethylphenyl groups, but unfortunately, we did not get the desired product. Next, QEs with different ester groups were also screened, where those with ethyl, butyl, benzyl, and allyl esters offered the targeted products **4ab**, **4ac**, **4ad,** and **4ae** in moderate to good yields. QEs with substituted benzyl and phenethyl esters also procured the corresponding products **4af-4ai** in good yields. Other derivatives like methoxy substituted QE and naphthoquinone esters gave the products **4aj** and **4ak** in 54% and 58% yields, respectively. (Scheme 4.2.2)

Scheme 4.2.2. Substrate scope of DACs and quinones for (3+2) cycloaddition.[a,b]

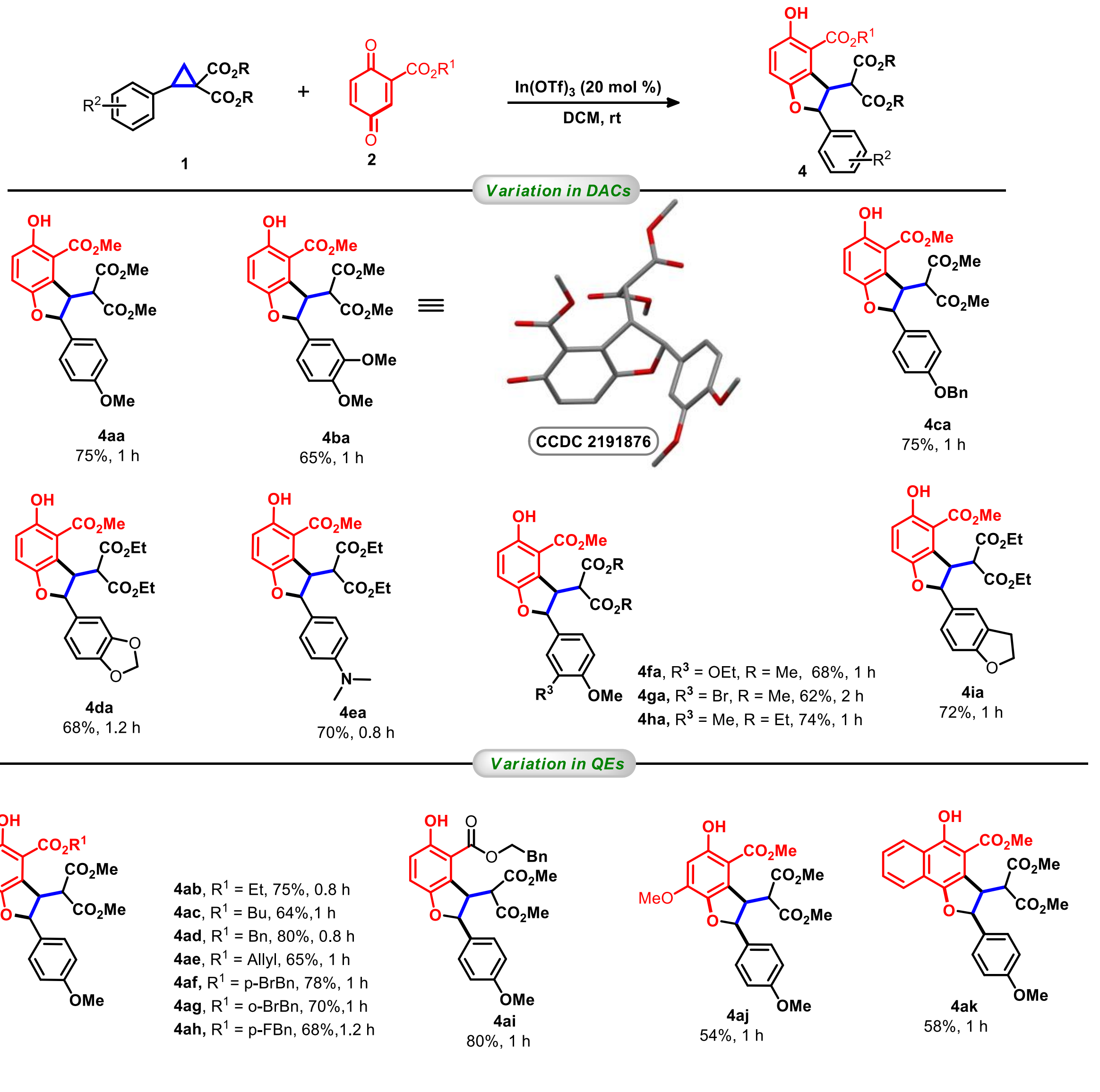

[a]Standard reaction conditions: **1a** (0.37 mmol), **2a** (0.44 mmol), Indium triflate (20 mol %) at room temperature in DCM (2 ml). [b]Isolated yield.

To gain mechanistic insights, control experiments were carried out. Firstly, 2-styryl malonate was synthesized according to the reported literature, and it was treated with QE **2a** under the optimized conditions, which furnished **4aa** in 70% yield (Scheme 4.2.3a), confirming that pathway II proceeds *via* 2-styryl malonate intermediate.

Scheme 4.2.3. Control Experiments

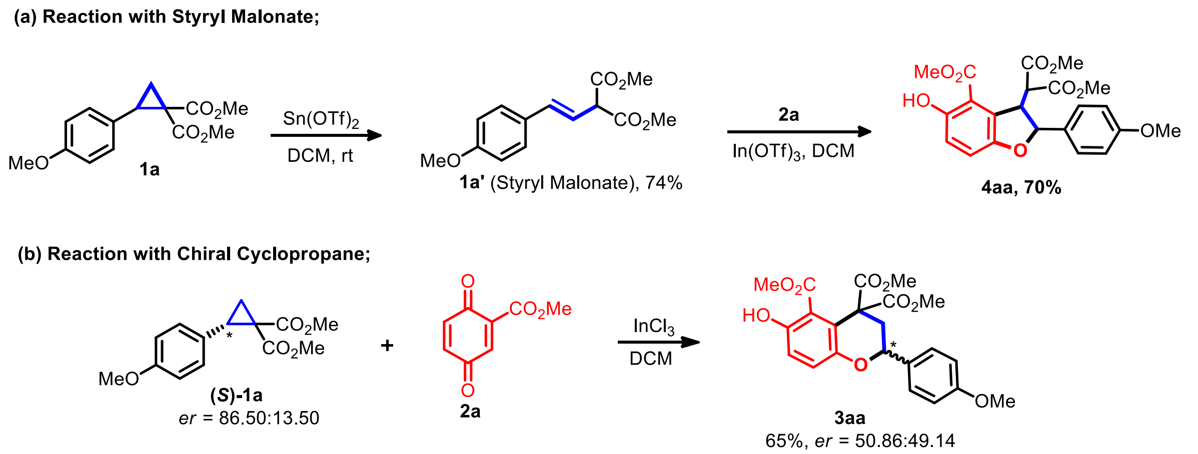

Also, the cycloaddition reaction of enantiopure cyclopropane (*S*)-**1a** and QE **2a** was performed in the presence of $InCl_3$, which led to the expected product, which was found to be essentially racemic (Scheme 4.2.3b). This racemization of the final product indicated that pathway I followed an S_N1 mechanism that would involve the formation of a carbocationic or zwitterionic intermediate.

Based on the above experiments and literature reports[13], a mechanism has been proposed for the designed formal (3+3) and (3+2) cycloaddition reactions (Scheme 4.2.4). In pathway I, $InCl_3$ activates the C-C bond of the DAC and generates a zwitterionic intermediate **A**. At the same time, the quinone ester **2** is activated by the Lewis acid and attacks intermediate **A** on the cationic part to form a new C-O bond *via* S_N1 fashion to give intermediate **B,** which further undergoes ring closure followed by the aromatization of **C** to deliver the anticipated chroman derivative **3**. In pathway II, to synthesize benzofuran derivatives, the DAC rearranges itself into the styryl malonate **D,** which subsequently participates in a formal (3+2) cycloaddition to produce **4**.

Scheme 4.2.4. Plausible mechanism for the desired transformations.

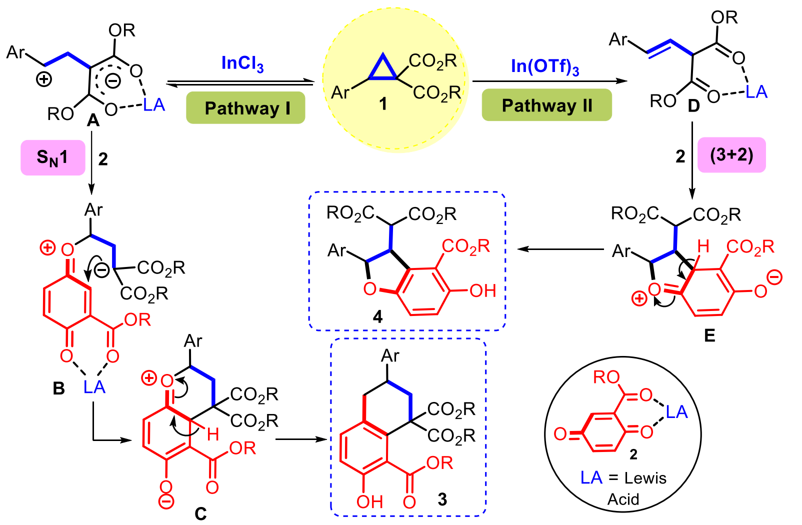

To further showcase the synthetic utility of the designed protocol, a gram-scale experiment was performed where cyclopropane diester and QE were subjected to the optimized reaction conditions. In this scaled-up reaction, **3aa** was obtained in 52% yields. Furthermore, the final product **3aa** was subjected to the methylation of the phenolic hydroxyl group using methyl iodide and base, which resulted in the synthesis of **5aa** in 80% yields. The treatment of **3aa** with DIBAL-*H* resulted in the formation of tetrahydro-2*H*-pyrano[3,4,5-*de*]chromene scaffolds **6aa** in 50% yield. (Scheme 4.2.5).

Scheme 4.2.5. Follow-up Chemistry.

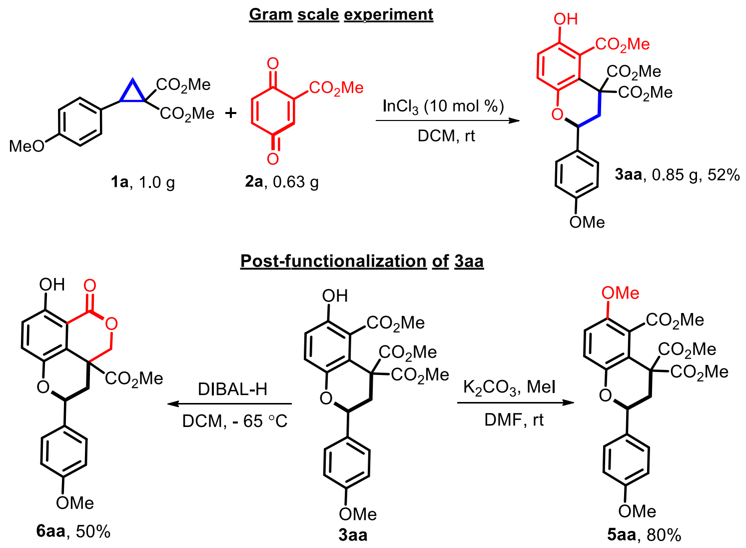

4.3 Conclusion

In summary, we have developed a straightforward and efficient method for the construction of diverse chroman and benzofuran skeletons *via* Lewis acid-catalyzed cycloaddition reaction of DACs and quinones. By careful tuning of Lewis acids, we could achieve either (3+3) or (3+2) cycloaddition reaction with the same reaction partners, and consequently, the designed protocol represents the regiodivergent synthesis of functionalized benzofuzed six- and five-membered oxacycles. The practicality of this methodology was also confirmed by the gram scale experiment. The final chroman skeleton could be further derivatized to the 6-methoxy-2-(4-methoxyphenyl)chroman and tetrahydro-2*H*-pyrano[3,4,5-*de*]chromene scaffolds, indicating the synthetic utility of the designed protocol. The novel methodology exhibits a new synthetic route to access functionalized benzofuzed six- and five-membered oxacycles that make part of numerous bioactive molecules.

4.4 Experimental Section

4.4.1. General Information

All reactions were carried out under an inert atmosphere with oven-dried glassware. All solvents and reagents were obtained from commercial sources and were purified following the standard procedure prior to use. The developed chromatogram was analyzed by UV lamp (254 nm) or *p*-anisaldehyde solution. Products were purified by flash chromatography on silica gel (mesh size 230–400). Melting points were determined using a Stuart SMP30 advanced digital melting point apparatus. Mass spectral data (HRMS) were obtained using the XEVO G2-XS QTOF instrument. The ^{1}H NMR and ^{13}C NMR spectra were recorded at 400 MHz and 100 MHz respectively on 400 MHz JEOL JNM ECS400 instrument in $CDCl_3$ solvent (unless otherwise mentioned). Chemical shifts of ^{1}H and ^{13}C{^{1}H} NMR spectra are expressed in parts per million (ppm). All coupling constants are absolute values and are expressed in hertz. The description of the signals includes the following: s = singlet, d = doublet, dd = doublet of doublet, t = triplet, dt = doublet of triplet, q = quartet, dq = doublet of quartet, br = broad, and m = multiplet.

4.4.2. General procedure for the preparation of cyclopropane diesters:[19]

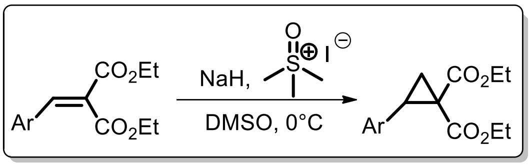

Sodium hydride (1.5 equiv) was taken in three-neck R.B flask and washed 3 to 4 times with dry hexane under N_2 atmosphere. 100 ml of DMSO was added. The solution of trimethyl sulfoxonium iodide (1.5 equiv.) in DMSO (20 mL) was added to the flask at 0 °C. After 12 min. diethylbenzylidenemalonate (1 equiv.) in 10 mL DMSO was added to the stirred solution and the reaction mixture was allowed to stir for 2 h at room temperature. Upon Completion of the reaction (as monitored by TLC), the reaction mixture was quenched with ice cold water and the organic solution was extracted with diethyl ether. Further organic solution was dried over anhydrous Na_2SO_4. The solution was concentrated in vacuo. The crude mixture was further purified by silica gel column chromatography taking EtOAc/hexane as eluent. The compounds 1a-1m are prepared according to the reported literature and the data of all the compounds is in complete agreement with reported data in the literature.

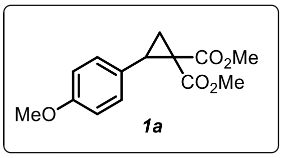

Dimethyl 2-(4-methoxyphenyl)cyclopropane-1,1-dicarboxylate (1a): Colorless oil, dimethyl 2-(4-methoxybenzylidene)malonate (1.0 g, 4.0 mmol), **1a** (0.755 g, 2.8 mmol), 70% yield, ^{1}H-NMR (400 MHz, $CDCl_3$): δ 7.10 (d, *J* = 8.8 Hz, 2H), 6.78 (d, *J* = 8.8 Hz, 2H), 3.76 (s, 3H), 3.75 (s, 3H), 3.37 (s, 3H), 3.17 (t, *J* = 8.6 Hz, 1H), 2.14 (dd, *J* = 8.0, 5.2 Hz, 1H), 1.71 (dd, *J* = 9.3, 5.1 Hz, 1H).

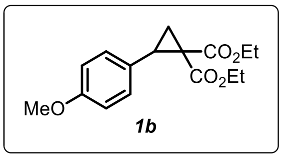

Diethyl 2-(4-methoxyphenyl)cyclopropane-1,1-dicarboxylate (1b) Colorless oil, Diethyl 2-(4-methoxybenzylidene)malonate (1.0 g, 3.6 mmol), **1b** (0.77 g, 2.6 mmol), 72% yield. ^{1}H-NMR (400 MHz, $CDCl_3$): δ 7.11 (d, *J* = 8.5 Hz, 2H), 6.78 (d, *J* = 8.7 Hz, 2H), 4.26 – 4.16 (m, 2H), 3.90 – 3.79 (m, 2H), 3.75 (s, 3H), 3.17 – 3.13 (m, 1H), 2.11 (dd, *J* = 8.0, 5.1 Hz, 1H), 1.66 (dd, *J* = 9.2, 5.1 Hz, 1H), 1.27 (t, *J* = 7.2 Hz, 3H), 0.90 (t, *J* = 7.1 Hz, 3H).

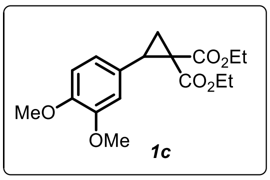

Dimethyl 2-(3,4-dimethoxyphenyl)cyclopropane-1,1-dicarboxylate (1c) White solid, Diethyl 2-(3,4-dimethoxybenzylidene)malonate (1.0 g, 3.2 mmol), **1c** (0.76 g, 2.3 mmol), 72% yield. ^{1}H-NMR (400 MHz, $CDCl_3$): δ 6.77 – 6.69 (m, 3H), 4.27 – 4.14 (m, 2H), 3.91 – 3.84 (m, 2H), 3.84 (s, 3H), 3.83 (s, 3H), 3.16 (t, *J* = 8.6 Hz, 1H), 2.11 (dd, *J* = 7.9, 5.1 Hz, 1H), 1.66 (dd, *J* = 9.2, 5.1 Hz, 1H), 1.28 (t, *J* = 7.1 Hz, 3H), 0.91 (t, *J* = 6.8 Hz, 3H).

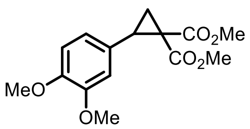

1d

Dimethyl 2-(3,4-dimethoxyphenyl)cyclopropane-1,1-dicarboxylate (1d) White solid, Dimethyl 2-(3,4-dimethoxybenzylidene)malonate (1.0 g, 3.5 mmol), **1d** (0.78 g, 2.6 mmol), 74% yield. ^{1}H-NMR (400 MHz, $CDCl_3$): δ 6.77−6.71 (m, 3H), 3.85 (s, 6H), 3.78 (s, 3H), 3.40 (s, 3H), 3.18 (t, 1H), 2.15 (dd, *J* = 7.9, 5.1 Hz, 1H), 1.72 (dd, 9.2, 5.1 Hz, 1H).

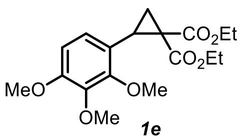

1e

Diethyl 2-(2,3,4-trimethoxyphenyl)cyclopropane-1,1-dicarboxylate (1e) Light yellow crystalline solid, Diethyl 2-(3,4,5-trimethoxybenzylidene) malonate (1.0 g, 2.9 mmol), **1e** (0.74 g, 2.1 mmol), 72% yield. ^{1}H-NMR (400 MHz, $CDCl_3$): δ 6.41 (s, 2H), 4.23 – 4.20 (m, 2H), 3.93 – 3.87 (m, 2H), 3.82 (s, 6H), 3.78 (s, 3H), 3.16 (t, *J* = 8.6 Hz, 1H), 2.10 (dd, *J* = 7.9, 5.2 Hz, 1H), 1.67 (dd, *J* = 9.2, 5.2 Hz, 1H), 1.28 (t, *J* = 7.1 Hz, 3H), 0.90 (t, *J* = 7.1 Hz, 3H).

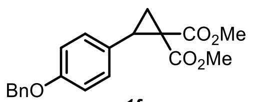

1f

Dimethyl 2-(4-(benzyloxy)phenyl)cyclopropane-1,1-dicarboxylate (1f) Yellow solid, Dimethyl 2-(4-(benzyloxy)benzylidene)malonate (1.0 g, 3.1 mmol), **1f** (0.75 g, 2.2 mmol), 71% yield. ^{1}H-NMR (400 MHz, $CDCl_3$): δ 7.42 – 7.29 (m, 5H), 7.11 (d, *J* = 8.7 Hz, 2H), 6.87 (d, *J* = 8.7 Hz, 2H), 5.02 (s, 2H), 3.77 (s, 3H), 3.36 (s, 3H), 3.17 (t, *J* = 8.7 Hz, 1H), 2.15 (dd, *J* = 8.0, 5.2 Hz, 1H), 1.71 (dd, *J* = 9.3, 5.2 Hz, 1H).

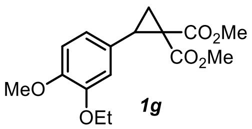

1g

Dimethyl 2-(3-ethoxy-4-methoxyphenyl)cyclopropane-1,1-dicarboxylate (1g) White solid, dimethyl 2-(3-ethoxy-4-methoxybenzylidene)malonate (1.0 g, 3.4 mmol), **1g** (0.72 g, 2.3 mmol), 68% yield. ^{1}H-NMR (400 MHz, $CDCl_3$): δ 6.76 – 6.67 (m, 3H), 4.08 – 4.03 (m, 2H), 3.83 (s, 3H), 3.77 (s, 3H), 3.38 (s, 3H), 3.19 – 3.14 (m, 1H), 2.13 (dd, *J* = 8.0, 5.2 Hz, 1H), 1.70 (dd, *J* = 9.2, 5.1 Hz, 1H), 1.44 (t, *J* = 7.0 Hz, 3H).

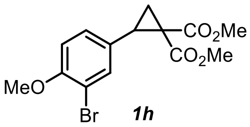

1h

Dimethyl 2-(3-bromo-4-methoxyphenyl)cyclopropane-1,1-dicarboxylate (1h) White solid, dimethyl 2-(3-bromo-4-methoxybenzylidene)malonate (1.0 g, 3.0 mmol), **1h** (0.69 g, 2.0 mmol), 67% yield. ^{1}H-NMR (400 MHz, $CDCl_3$): δ 7.39 (d, *J* = 2.3 Hz, 1H), 7.09 (dd, *J* = 8.8, 2.3 Hz, 1H), 6.78 (d, *J* = 8.5 Hz, 1H), 3.85 (s, 3H), 3.77 (s, 3H), 3.43 (s, 3H), 3.16 – 3.10 (m, 1H), 2.11 (dd, *J* = 8.0, 5.3 Hz, 1H), 1.71 (dd, *J* = 9.2, 5.2 Hz, 1H).

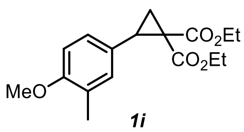

1i

Diethyl 2-(4-methoxy-3-methylphenyl)cyclopropane-1,1-dicarboxylate (1i) Colorless oil, diethyl 2-(4-methoxy-3-methylbenzylidene)malonate (1.0 g, 3.4 mmol), **1i** (0.75 g, 2.3 mmol), 67% yield. ^{1}H-NMR (400 MHz, $CDCl_3$): δ 6.99 – 6.95 (m, 1H), 6.69 (d, *J* = 8.2 Hz, 2H), 4.26 – 4.17 (m, 2H), 3.90 – 3.82 (m, 2H), 3.77 (s, 3H), 3.13 (t, *J* = 8.6 Hz, 1H), 2.14 (s, 3H), 2.10 (dd, *J* = 8.1, 5.1 Hz, 1H), 1.65 (dd, *J* = 9.5, 4.7 Hz, 1H), 1.27 (t, *J* = 7.1 Hz, 3H), 0.90 (t, *J* = 6.8 Hz, 3H).

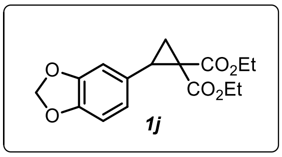

Diethyl 2-(benzo[*d*][1,3]dioxol-5-yl)cyclopropane-1,1-dicarboxylate (1j) Colorless oil, Diethyl 2-(benzo[d][1,3]dioxol-5-ylmethylene)malonate (1.0 g, 3.4 mmol), **1j** (0.82 g, 2.6 mmol), 76% yield. ^{1}H-NMR (400 MHz, $CDCl_3$): δ 6.70 – 6.65 (m, 3H), 5.90 (s, 2H), 4.27 – 4.14 (m, 2H), 3.95 – 3.87 (m, 2H), 3.15 – 3.10 (m, 1H), 2.07 (dd, *J* = 7.9, 5.2 Hz, 1H), 1.65 (dd, *J* = 9.2, 5.1 Hz, 1H), 1.27 (t, *J* = 7.1 Hz, 3H), 0.96 (t, *J* = 7.1 Hz, 3H).

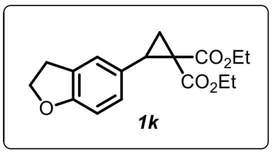

Diethyl 2-(2,3-dihydrobenzofuran-5-yl)cyclopropane-1,1-dicarboxylate (1k) Colorless oil, Diethyl 2-((2,3-dihydrobenzofuran-5-yl)methylene)malonate (1.0 g, 3.4 mmol), **1k** (0.80 g, 2.6 mmol), 76% yield. ^{1}H-NMR (400 MHz, $CDCl_3$): 7.03 (s, 1H), 6.95 – 6.91 (m, 1H), 6.65 (d, *J* = 8.2 Hz, 1H), 4.52 (t, *J* = 8.7 Hz, 2H), 4.29 – 4.15 (m, 2H), 3.89 – 3.84 (m, 2H), 3.17 – 3.11 (m, 3H), 2.09 (dd, *J* = 7.9, 5.1 Hz, 1H), 1.65 (dd, *J* = 9.2, 5.1 Hz, 1H), 1.27 (t, *J* = 7.1 Hz, 3H), 0.92 (t, *J* = 7.1 Hz, 3H).

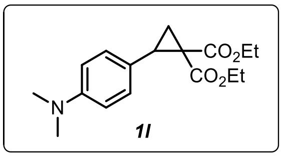

Diethyl 2-(4-(dimethylamino)phenyl)cyclopropane-1,1-dicarboxylate (1l) Yellow solid, Diethyl 2-(4-(dimethylamino)benzylidene)malonate (1.0 g, 3.4 mmol), **1l** (0.72 g, 2.4 mmol), 70% yield.^{1}H-NMR (400 MHz, $CDCl_3$): δ 7.05 (d, *J* = 8.9 Hz, 2H), 6.60 (d, *J* = 8.8 Hz, 2H), 4.27 – 4.15 (m, 2H), 3.89 – 3.81 (m, 2H), 3.12 (t, *J* = 8.6 Hz, 1H), 2.87 (s, 6H), 2.10 (dd, *J* = 7.9, 5.4 Hz, 1H), 1.64 (dd, *J* = 9.2, 5.0 Hz, 1H), 1.26 (t, *J* = 7.1 Hz, 3H), 0.90 (t, *J* = 7.1 Hz, 3H).

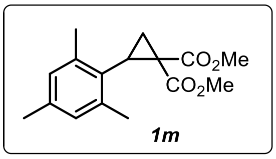

Dimethyl 2-mesitylcyclopropane-1,1-dicarboxylate (1m) Yellow solid, Dimethyl 2-(2,4,6-trimethylbenzylidene)malonate (1.0 g, 3.8 mmol), **1m** (0.80 g, 2.8 mmol), 74% yield. ^{1}H-NMR (400 MHz, $CDCl_3$): δ 6.76 (s, 2H), 3.81 (s, 3H), 3.34 (s, 3H), 3.04 (t, *J* = 9.3 Hz, 1H), 2.38 (dd, *J* = 8.9, 4.9 Hz, 1H), 2.30 (s, 6H), 2.20 (s, 3H), 1.92 (dd, *J* = 9.6, 5.0 Hz, 1H).

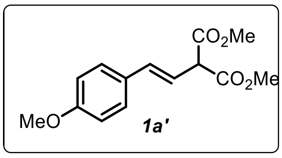

Dimethyl 2-(4-methoxystyryl) malonate (1a') Colorless oil, Dimethyl 2-(4-methoxyphenyl)cyclopropane-1,1-dicarboxylate (0.5 g, 1.9 mmol), 1a' (0.38 g, 1.4 mmol), 74% yield. ^{1}H-NMR (400 MHz, $CDCl_3$): δ 7.33 (d, *J* = 8.8 Hz, 2H), 6.84 (d, *J* = 8.7 Hz, 2H), 6.51 (d, *J* = 15.9 Hz, 1H), 6.24 (dd, *J* = 15.7, 9.1 Hz, 1H), 4.18 (dd, *J* = 9.1, 0.7 Hz, 1H), 3.80 (s, 3H), 3.76(s, 6H).

4.4.3 General procedure for the Synthesis of Quinone ester:[20]

To a solution of the hydroquinone (1 equiv.) in DCM (30 mL) was added DDQ (1.5 equiv.) portionwise at room temperature. After 2 h, the reaction mixture was diluted with DCM (150 mL), then washed with a mixture of water (100 mL) and saturated aqueous sodium bicarbonate (10 mL), five times. Combined organics were washed with brine (200 mL), dried over Na_2SO_4, and concentrated in vacuo to afford generally orange or red solids **2**. The compounds **2a-2k** are prepared according to the reported literature and the data of all the compounds is in complete agreement with reported data in the literature.

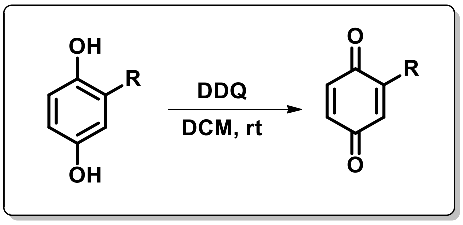

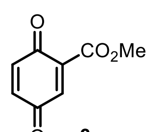

2a

Methyl 3,6-dioxocyclohexa-1,4-dienecarboxylate (2a)

Brown solid, methyl 2,5-dihydroxybenzoate (1 g, 5.9 mmol), **2a** (0.87 g, 5.2 mmol), 89% yield.^{1}H-NMR (400 MHz, $CDCl_3$): δ 7.10 (d, J = 1.8 Hz, 1H), 6.82 (d, J = 1.9 Hz, 2H), 3.90 (s, 3H).

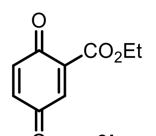

2b

Ethyl 3,6-dioxocyclohexa-1,4-dienecarboxylate (2b)

Reddish brown solid, ethyl 2,5-dihydroxybenzoate (1 g, 5.4 mmol), **2b** (0.85 g, 4.7 mmol), 86% yield. ^{1}H-NMR (400 MHz, $CDCl_3$): δ 7.07 (d, J = 1.8 Hz, 1H), 6.81 (d, J = 1.8 Hz, 2H), 4.39 – 4.32 (m, 2H), 1.35 (t, J = 7.2 Hz, 3H).

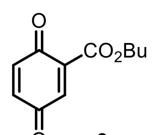

2c

Butyl 3,6-dioxocyclohexa-1,4-dienecarboxylate (2c)

Reddish brown oil, butyl 2,5-dihydroxybenzoate (1 g, 4.7 mmol), **2c** (0.80 g, 3.8 mmol), 80% yield. ^{1}H-NMR (400 MHz, $CDCl_3$): δ 7.06 (d, J = 1.8 Hz, 1H), 6.81 (d, J = 1.9 Hz, 2H), 4.29 (t, J = 6.6 Hz, 2H), 1.68 (dd, J = 15.0, 6.7 Hz, 2H), 1.42 (dd, J = 15.0, 7.5 Hz, 2H), 0.94 (t, J = 7.4 Hz, 3H).

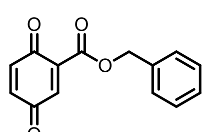
2d

Benzyl 3,6-dioxocyclohexa-1,4-dienecarboxylate (2d)

Reddish brown solid, benzyl 2,5-dihydroxybenzoate (1 g, 4.1 mmol), **2d** (0.80 g, 3.3 mmol), 81% yield. ^{1}H-NMR (400 MHz, $CDCl_3$): δ 7.42 – 7.34 (m, 5H), 7.10 (d, J = 1.6 Hz, 1H), 6.80 (d, J = 0.9 Hz, 2H), 5.32 (s, 2H).

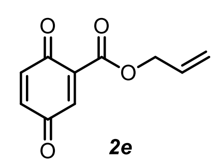
2e

Allyl 3,6-dioxocyclohexa-1,4-dienecarboxylate (2e)

Reddish brown oil, allyl 2,5-dihydroxybenzoate (1 g, 5.1 mmol), **2e** (0.76 g, 3.9 mmol), 78% yield. ^{1}H-NMR (400 MHz, $CDCl_3$): δ 7.11 (dd, J = 1.8, 0.7 Hz, 1H), 6.82 (d, J = 1.6 Hz, 2H), 5.99 – 5.93 (m, 1H), 5.45 – 5.39 (m, 1H), 5.33 – 5.30 (m, 1H), 4.80 – 4.78 (m, 2H).

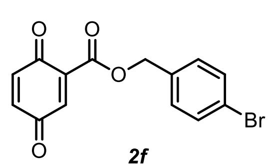

2f

4-bromobenzyl 3,6-dioxocyclohexa-1,4-dienecarboxylate (2f)

Reddish brown solid, 4-bromobenzyl 2,5-dihydroxybenzoate (1 g, 3.1 mmol), **2f** (0.75 g, 2.3 mmol), 76% yield. ^{1}H-NMR (400 MHz, $CDCl_3$): δ 7.49 (dd, J = 8.5, 2.3 Hz, 2H), 7.28 (d, J = 8.3 Hz, 2H), 7.09 (d, J = 1.8 Hz, 1H), 6.80 (d, J = 2.2 Hz, 2H), 5.26 (s, 2H).

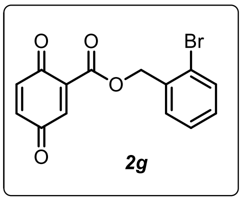

2-bromobenzyl 3,6-dioxocyclohexa-1,4-dienecarboxylate (2g)

Reddish brown solid, 4-bromobenzyl 2,5-dihydroxybenzoate (1 g, 3.1 mmol), **2g** (0.78 g, 2.4 mmol), 78% yield. ^{1}H-NMR (400 MHz, $CDCl_3$): δ 7.59 (d, *J* = 7.9 Hz, 1H), 7.49 (d, *J* = 7.7 Hz, 1H), 7.34 (t, *J* = 7.5 Hz, 1H), 7.24 – 7.21 (m, 1H), 7.18 – 7.14 (m, 1H), 6.82 (d, *J* = 0.8 Hz, 2H), 5.40 (s, 2H).

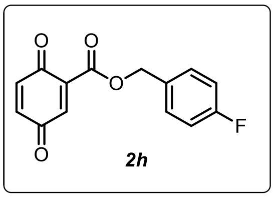

4-Fluorobenzyl 3,6-dioxocyclohexa-1,4-dienecarboxylate (2h)

Reddish brown solid, 4-fluorobenzyl 2,5-dihydroxybenzoate (1 g, 3.8 mmol), **2h** (0.8 g, 3.1 mmol), 81% yield. ^{1}H-NMR (400 MHz, $CDCl_3$): δ 7.43 – 7.35 (m, 2H), 7.12 – 7.02 (m, 3H), 6.81 (d, J = 1.6 Hz, 2H), 5.28 (s, 2H).

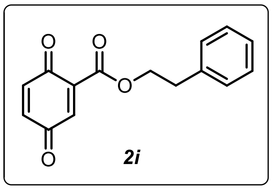

Phenethyl 3,6-dioxocyclohexa-1,4-dienecarboxylate (2i)

Reddish brown solid, phenethyl 2,5-dihydroxybenzoate (1 g, 3.9 mmol), **2i** (0.82 g, 3.2 mmol), 82% yield. ^{1}H-NMR (400 MHz, $CDCl_3$): δ 7.34 – 7.29 (m, 2H), 7.26 – 7.21 (m, 3H), 6.99 (d, *J* = 1.7 Hz, 1H), 6.80 (s, 2H), 4.51 (t, *J* = 7.0 Hz, 2H), 3.03 (t, *J* = 7.0 Hz, 2H).

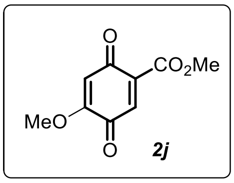

Methyl 4-methoxy-3,6-dioxocyclohexa-1,4-dienecarboxylate (2j)[20b]

Reddish brown solid, methyl 2,5-dihydroxy-4-methoxybenzoate (1 g, 5.0 mmol), **2j** (0.65 g, 3.3 mmol), 66% yield. ^{1}H-NMR (400 MHz, $CDCl_3$): δ 7.00 (s, 1H), 5.97 (s, 1H), 3.89 (s, 3H), 3.84 (s, 3H).

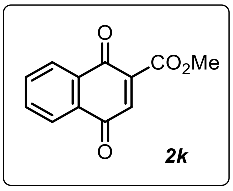

Methyl 1,4-dioxo-1,4-dihydronaphthalene-2-carboxylate (2k)[20c]

Reddish brown solid, methyl 1,4-dihydroxy-2-naphthoate (1 g, 4.5 mmol), **2k** (0.8 g, 3.7 mmol), 82% yield. ^{1}H-NMR (400 MHz, $CDCl_3$): δ 8.14 – 8.10 (m, 1H), 8.09 – 8.05 (m, 1H), 7.82 – 7.74 (m, 2H), 7.25 (d, *J* = 4.1 Hz, 1H), 3.94 (s, 3H).

4.2.4 Representative procedure for the synthesis of chroman derivatives 3:

A round-bottom flask equipped with magnetic stir bar was charged **1** (0.1 g, 0.37 mmol), **2** (0.061 g, 0.37 mmol), $InCl_3$ (0.008 g, 10 mol %) and dry DCM (4 ml, 0.1 M) under nitrogen atmosphere. On completion of the reaction (as monitored by TLC), the reaction mixture was filtered through a small plug of celite and concentrated in rotary evaporator. The crude mixture was further purified by column chromatography on silica gel with acetone/hexane (20:80) as eluent to afford **3**.

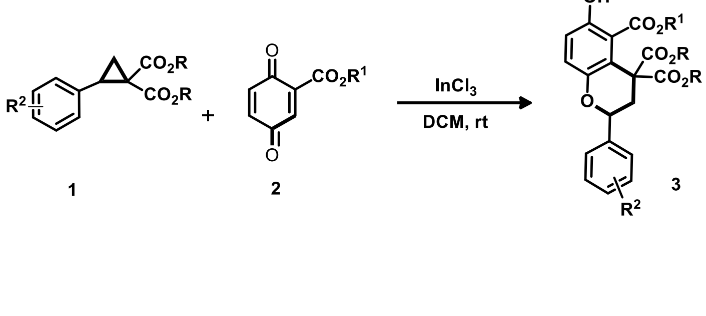

Trimethyl 6-hydroxy-2-(4-methoxyphenyl)chroman-4,4,5-tricarboxylate (3aa): 1a (0.1 g, 0.37 mmol), **2a** (0.061 g, 0.37 mmol), **3aa** (0.120 g, 0.26 mmol) Yield: 70% Nature: White solid Melting point: 174-176 ºC R_f: 0.5 (acetone:hexane = 20:80) ^{1}H-NMR (400 MHz, $CDCl_3$): δ 10.66 (s, 1H), 7.30 (d, *J* = 8.6 Hz, 2H), 7.11 (d, *J* = 9.2 Hz, 1H), 6.97 (d, *J* = 9.2 Hz, 1H), 6.90 (d, *J* = 8.7 Hz, 2H), 4.87 – 4.84 (m, 1H), 3.80 (s, 3H), 3.76 (s, 3H), 3.75 (s, 3H), 3.65 (s, 3H), 2.84 (dd, *J* = 13.8, 1.7 Hz, 1H), 2.30 (dd, *J* = 13.8, 11.9 Hz, 1H). ^{13}C-NMR (100 MHz, $CDCl_3$): 170.8, 170.45, 170.42, 159.8, 157.2, 148.5, 131.5, 127.4, 126.2, 119.9, 117.7, 114.1, 111.7, 73.0, 56.6, 55.4, 53.1, 52.9, 51.5, 40.7. HRMS (ESI, Q-TOF) *m/z*: $[M + Na]^+$ Calculated for $C_{22}H_{22}O_9Na$ 453.1162, found 453.1162.

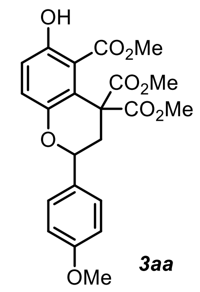

3aa

4,4-Diethyl 5-methyl 2-(3,4-dimethoxyphenyl)-6-hydroxychroman-4,4,5-tricarboxylate (3ba): 1c (0.1 g, 0.31 mmol), **2a** (0.052 g, 0.31 mmol), **3ba** (0.1 g, 0.20 mmol) Yield: 65% Nature: White solid Melting point: 170-172 ºC R_f: 0.5 (acetone:hexane = 20:80) ^{1}H-NMR (400 MHz, $CDCl_3$): δ 10.75 (s, 1H), 7.13 (d, *J* = 9.2 Hz, 1H), 6.98 (d, *J* = 9.2 Hz, 1H), 6.91 (s, 2H), 6.86 (d, *J* = 8.1 Hz, 1H), 4.90 – 4.87 (m, 1H), 4.30 – 4.23 (m, 2H), 4.17 – 4.10 (m, 2H), 3.90 (s, 3H), 3.88 (s, 3H), 3.75 (s, 3H), 2.85 (dd, *J* = 13.9, 1.6 Hz, 1H), 2.28 (dd, *J* = 13.8, 11.9 Hz, 1H), 1.24 (t, *J* = 7.1 Hz, 3H), 1.18 (t, *J* = 7.1 Hz, 3H). ^{13}C-NMR (100 MHz, $CDCl_3$): 170.6, 170.3, 169.9, 157.2, 149.25, 149.20, 148.4, 132.1, 126.1, 119.8, 118.5, 118.0, 111.1, 109.0, 73.2, 61.97, 61.93, 56.6, 56.0, 51.4, 40.8, 14.3, 14.1. HRMS (ESI, Q-TOF) *m/z*: $[M + H]^+$ Calculated for $C_{25}H_{29}O_{10}$ 489.1761, found 489.1758.

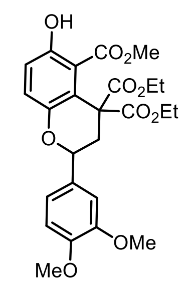

3ba

4,4-Diethyl 5-methyl 6-hydroxy-2-(3,4,5-trimethoxyphenyl)chroman-4,4,5-tricarboxylate (3ca) 1e (0.1 g, 0.28 mmol), **2a** (0.046 g, 0.28 mmol), **3ca** (0.09 g, 0.17 mmol) Yield: 60% Nature: White solid Melting point: 182-184 ºC R_f: 0.4 (acetone:hexane = 20:80). ^{1}H-NMR (400 MHz, $CDCl_3$): δ 10.53 (s, 1H), 7.06 (d, *J* = 8.9 Hz, 1H), 6.94 (d, *J* = 9.0 Hz, 1H), 6.61 (s, 2H), 4.85 – 4.81 (m, 1H), 4.21 – 4.10 (m, 2H), 4.02 (q, *J* = 7.2 Hz, 2H), 3.85 (s, 6H), 3.82 (s, 3H), 3.80 (s, 3H), 3.29 (dd, *J* = 13.2, 11.4 Hz, 1H), 2.42 (dd, *J* = 13.2, 5.1 Hz, 1H), 1.23 (t, *J* = 7.1 Hz, 3H), 1.18 (t, *J* = 7.1 Hz, 3H). ^{13}C-NMR (100 MHz, $CDCl_3$): 169.6, 169.3, 157.4, 153.4, 151.2, 137.9, 134.3, 131.2, 126.6, 118.9, 117.7, 108.5, 103.3, 79.8, 66.7, 61.7, 60.9, 56.2, 51.8, 45.0, 15.3, 14.2. HRMS (ESI, Q-TOF) *m/z*: $[M + Na]^+$ Calculated for $C_{26}H_{30}O_{11}Na$ 541.1686, found 541.1688.

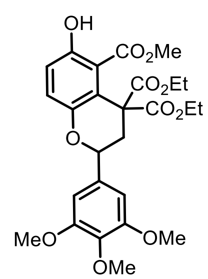

3ca

Trimethyl 2-(4-(benzyloxy)phenyl)-6-hydroxychroman-4,4,5-tricarboxylate (3da): 1f (0.1 g, 0.29 mmol), **2a** (0.048 g, 0.29 mmol), **3da** (0.110 g, 0.21 mmol), Yield: 72%, Nature: White solid, Melting point: 170-172 ºC, R_f: 0.5 (acetone:hexane = 20:80), ^{1}H-NMR (400 MHz, $CDCl_3$): δ 10.66 (s, 1H), 7.45 – 7.32 (m, 5H), 7.31 (d, *J* = 8.6 Hz, 2H), 7.11 (d, *J* = 9.2 Hz, 1H), 6.98 (d, *J* = 9.4 Hz, 3H), 5.07 (s, 2H), 4.88 – 4.84 (m, 1H), 3.76 (s, 3H), 3.75 (s, 3H), 3.65 (s, 3H), 2.85 (dd, *J* = 13.9, 1.7 Hz, 1H), 2.30 (dd, *J* = 13.8, 11.8 Hz, 1H). ^{13}C-NMR (100 MHz, $CDCl_3$): 170.8, 170.46, 170.41, 159.0,

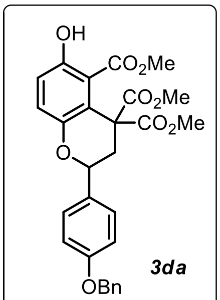

3da

157.2, 148.5, 136.8, 131.8, 128.7, 128.1, 127.52, 127.50, 126.2, 120.0, 117.7, 115.1, 111.7, 73.0, 70.1, 56.6, 53.1, 52.9, 51.5, 40.6. HRMS (ESI, Q-TOF) *m/z*: [M + Na]$^+$ Calculated for $C_{28}H_{26}O_9Na$ 529.1475, found 529.1475.

Trimethyl 2-(3-ethoxy-4-methoxyphenyl)-6-hydroxychroman-4,4,5-tricarboxylate (3ea): 1g (0.1 g, 0.3 mmol), **2a** (0.051 g, 0.3 mmol), **3ea** (0.102 g, 0.21 mmol), Yield: 70%, Nature: White solid, Melting point: 164-166 ºC, R_f: 0.5 (acetone:hexane = 20:80). ^{1}H-NMR (400 MHz, $CDCl_3$): δ 10.66 (s, 1H), 7.12 (d, *J* = 9.2 Hz, 1H), 6.97 (d, *J* = 9.2 Hz, 1H), 6.91 – 6.84 (m, 3H), 4.83 (d, *J* = 11.0 Hz, 1H), 4.13 – 4.06 (m, 2H), 3.86 (s, 3H), 3.76 (s, 3H), 3.75 (s, 3H), 3.65 (s, 3H), 2.84 (dd, *J* = 13.8, 1.3 Hz, 1H), 2.30 (dd, *J* = 13.7, 12.0 Hz, 1H), 1.46 (t, *J* = 7.0 Hz, 3H). ^{13}C-NMR (100 MHz, $CDCl_3$): 170.8, 170.4, 157.3, 149.5, 148.6, 148.4, 131.8, 126.2, 120.0, 118.6, 117.7, 111.6, 111.3, 110.6, 73.2, 64.5, 56.5, 56.1, 53.1, 53.0, 51.5, 40.7, 14.8. HRMS (ESI, Q-TOF) *m/z*: [M + Na]$^+$ Calculated for $C_{24}H_{26}O_{10}Na$ 497.1424, found 497.1424.

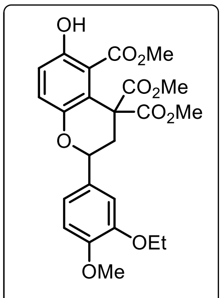

3ea

Trimethyl 2-(3-bromo-4-methoxyphenyl)-6-hydroxychroman-4,4,5-tricarboxylate (3fa): 1h (0.1 g, 0.29 mmol), **2a** (0.048 g, 0.29 mmol), **3fa** (0.095g, 0.19 mmol), Yield: 65%, Nature: White solid, Melting point: 141-143 ºC, R_f: 0.5 (acetone:hexane = 20:80), ^{1}H-NMR (400 MHz, $CDCl_3$): δ 10.66 (s, 1H), 7.58 (d, *J* = 2.0 Hz, 1H), 7.28 (dd, *J* = 8.4, 2.0 Hz, 1H), 7.12 (d, *J* = 9.2 Hz, 1H), 6.99 (d, *J* = 9.2 Hz, 1H), 6.89 (d, *J* = 8.5 Hz, 1H), 4.83 (d, *J* = 11.1 Hz, 1H), 3.90 (s, 3H), 3.77 (s, 3H), 3.75 (s, 3H), 3.66 (s, 3H), 2.83 (dd, *J* = 13.8, 1.5 Hz, 1H), 2.26 (dd, *J* = 13.8, 11.9 Hz, 1H). ^{13}C-NMR (100 MHz, $CDCl_3$): 170.8, 170.4, 170.2, 157.3, 156.0, 148.2, 133.0, 131.1, 126.4, 126.1, 120.1, 117.6, 111.9, 111.8, 111.7, 72.3, 56.4, 53.2, 53.0, 51.5, 40.6. HRMS (ESI, Q-TOF) *m/z*: [M + Na]$^+$ Calculated for $C_{22}H_{21}O_9BrNa$ 531.0267, found 531.0267

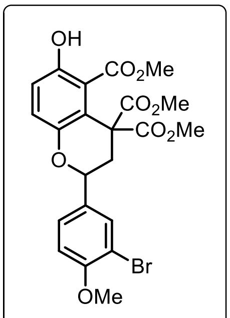

3fa

4,4-Diethyl 5-methyl 6-hydroxy-2-(4-methoxy-3-methylphenyl)chroman-4,4,5-tricarboxylate (3ga): 1i (0.1 g, 0.32 mmol), **2a** (0.053 g, 0.32 mmol), **3ga** (0.105g, 0.22 mmol), Yield: 68%, Nature: White solid, Melting point: 166-168 ºC, R_f: 0.5 (acetone:hexane = 20:80), ^{1}H-NMR (400 MHz, $CDCl_3$): δ 10.75 (s, 1H), 7.18 – 7.08 (m, 3H), 6.96 (d, *J* = 9.2 Hz, 1H), 6.81 (d, *J* = 8.2 Hz, 1H), 4.85 (d, *J* = 10.8 Hz, 1H), 4.29 – 4.20 (m, 2H), 4.18 – 4.03 (m, 2H), 3.82 (s, 3H), 3.74 (s, 3H), 2.83 (dd, *J* = 13.8, 1.4 Hz, 1H), 2.28 (dd, *J* = 13.8, 11.9 Hz, 1H), 2.22 (s, 3H), 1.25 (t, *J* = 7.1 Hz, 3H), 1.17 (t, *J* = 7.1 Hz, 3H). ^{13}C-NMR (100 MHz, $CDCl_3$): 170.6, 170.3, 169.9, 157.9, 157.2, 148.5, 131.1, 128.4, 127.1, 126.1, 124.7, 119.7, 117.9, 111.7, 109.9, 73.1, 61.9, 61.8, 56.6, 55.5, 51.4, 40.8, 16.4, 14.3, 14.1. HRMS (ESI, Q-TOF) *m/z*: [M + Na]$^+$ Calculated for $C_{25}H_{28}O_9Na$ 495.1631, found 495.1631.

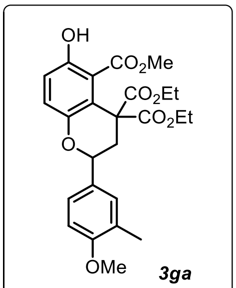

3ga

4,4-Diethyl 5-methyl 2-(benzo[d][1,3]dioxol-5-yl)-6-hydroxychroman-4,4,5tricarboxylate (3ha): 1j (0.1 g, 0.3 mmol), **2a** (0.051 g, 0.3 mmol), **3ha** (0.1 g, 0.21 mmol), Yield: 70%, Nature: White solid, Melting point: 108-110 ºC, R_f: 0.5 (acetone:hexane = 20:80), ^{1}H-NMR (400 MHz, $CDCl_3$): δ 10.72 (s, 1H), 7.10 (d, *J* = 9.2 Hz, 1H), 6.97 (d, *J* = 9.2 Hz, 1H), 6.89 (d, *J* = 1.4 Hz, 1H), 6.84 – 6.78 (m, 2H), 5.96 (s, 2H), 4.87 – 4.84 (m, 1H), 4.29 – 4.21 (m, 2H), 4.16 – 4.07 (m, 2H), 3.74 (s, 3H), 2.82 (dd, *J* = 13.9, 1.7 Hz, 1H), 2.24 (dd, *J* = 13.8, 11.9 Hz, 1H), 1.25 (t, *J* = 7.1 Hz, 3H), 1.17 (t, *J* = 7.1 Hz, 3H). ^{13}C-NMR (100 MHz, $CDCl_3$): 170.6, 170.2, 169.7, 157.2, 148.3, 148.0, 147.7, 133.5, 126.0, 119.8, 119.7, 117.9, 111.7, 108.4, 106.5, 101.3, 73.2, 61.9, 61.8, 56.6, 51.3, 40.9, 14.3, 14.0. HRMS (ESI, Q-TOF) *m/z*: $[M + Na]^+$ Calculated for $C_{24}H_{24}O_{10}Na$ 495.1267, found 495.1267.

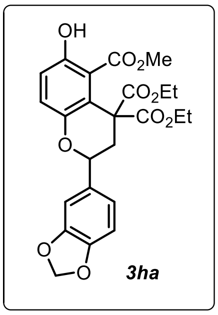

4,4-Diethyl 5-methyl 2-(2,3-dihydrobenzofuran-6-yl)-6-hydroxychroman-4,4,5-tricarboxylate (3ia): 1k (0.1 g, 0.32 mmol), **2a** (0.053 g, 0.32 mmol), **3ia** (0.110 g, 0.23mmol), Yield: 72%, Nature: White solid, Melting point: 124-126 ºC, R_f: 0.5 (acetone:hexane = 20:80), ^{1}H-NMR (400 MHz, $CDCl_3$): δ 10.73 (s, 1H), 7.23 (s, 1H), 7.10 (d, *J* = 9.1 Hz, 2H), 6.96 (d, *J* = 9.2 Hz, 1H), 6.77 (d, *J* = 8.2 Hz, 1H), 4.89 – 4.85 (m, 1H), 4.57 (t, *J* = 8.7 Hz, 2H), 4.29 – 4.20 (m, 2H), 4.15 – 4.04 (m, 2H), 3.74 (s, 3H), 3.20 (t, *J* = 8.7 Hz, 2H), 2.83 (dd, *J* = 13.9, 1.6 Hz, 1H), 2.28 (dd, *J* = 13.8, 11.9 Hz, 1H), 1.25 (t, *J* = 7.1 Hz, 3H), 1.17 (t, *J* = 7.1 Hz, 3H). ^{13}C-NMR (100 MHz, $CDCl_3$): 170.6, 170.3, 169.8, 160.4, 157.2, 148.5, 131.7, 127.6, 126.3, 126.1, 122.8, 119.7, 117.9, 111.7, 109.3, 73.3, 71.5, 61.9, 61.8, 56.6, 51.3, 40.9, 29.7, 14.3, 14.1. HRMS (ESI, Q-TOF) *m/z*: $[M + Na]^+$ Calculated for $C_{25}H_{26}O_9Na$ 493.1475, found 493.1475.

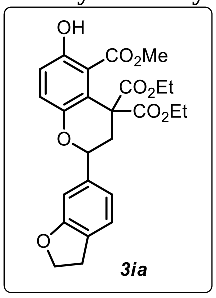

Trimethyl 6-hydroxy-2-mesitylchroman-4,4,5-tricarboxylate (3ja): 1m (0.1 g, 0.36 mmol), **2a** (0.060 g, 0.36 mmol), **3ja** (0.1 g, 0.22 mmol), Yield: 62%, Nature: White solid, Melting point: 208-210 ºC, R_f: 0.5 (acetone:hexane = 20:80), ^{1}H-NMR (400 MHz, $CDCl_3$): δ 10.61 (s, 1H), 7.08 (d, *J* = 9.2 Hz, 1H), 6.98 (d, *J* = 9.2 Hz, 1H), 6.83 (s, 2H), 5.35 – 5.31 (m, 1H), 3.77 (s, 3H), 3.75 (s, 3H), 3.67 (s, 3H), 2.68 (dd, *J* = 14.1, 2.0 Hz, 1H), 2.53 (dd, *J* = 14.0, 12.2 Hz, 1H), 2.30 (s, 6H), 2.24 (s, 3H). ^{13}C-NMR (100 MHz, $CDCl_3$): 170.8, 170.4, 157.0, 148.3, 137.7, 136.1, 131.6, 130.4, 126.0, 120.0, 117.6, 111.9, 71.3, 56.7, 53.0, 52.9, 51.4, 36.9, 20.8, 20.5. HRMS (ESI, Q-TOF) *m/z*: $[M + Na]^+$ Calculated for $C_{24}H_{26}O_8Na$ 465.1525, found 465.1525.

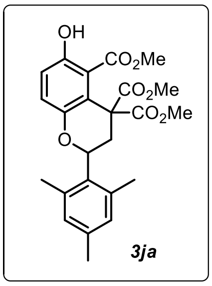

5-Ethyl 4,4-dimethyl 6-hydroxy-2-(4-methoxyphenyl)chroman-4,4,5-tricarboxylate (3ab): 1a (0.1 g, 0.37 mmol), **2b** (0.067 g, 0.37 mmol), **3ab** (0.120 g, 0.27 mmol), Yield: 72%, Nature: White solid, Melting point: 139-141 ºC, R_f: 0.5 (acetone:hexane = 20:80), ^{1}H-NMR (400 MHz, $CDCl_3$): δ 10.82 (s, 1H), 7.30 (d, *J* = 8.7 Hz, 2H), 7.10 (d, *J* = 9.2 Hz, 1H), 6.97 (d, *J* = 9.2 Hz, 1H), 6.90 (d, *J* = 8.7 Hz, 2H), 4.83 (dd, *J* = 11.8, 1.2 Hz, 1H), 4.46 – 4.38 (m, 1H), 4.18 – 4.09 (m, 1H), 3.80 (s, 3H), 3.75 (s, 3H), 3.64 (s, 3H), 2.85 (dd, *J* = 13.8, 1.7 Hz, 1H), 2.28 (dd, *J* =

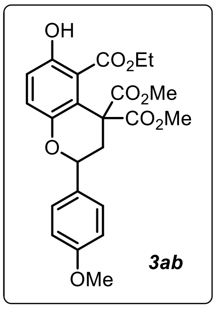

13.7, 11.9 Hz, 1H), 1.29 (t, *J* = 7.1 Hz, 3H). ^{13}C-NMR (100 MHz, $CDCl_3$): 170.9, 170.3, 170.1, 159.8, 157.3, 148.2, 131.5, 127.4, 125.9, 119.9, 117.8, 114.1, 111.9, 73.0, 61.7, 56.6, 55.4, 52.9, 52.8, 41.0, 14.0. HRMS (ESI, Q-TOF) *m/z*: $[M + Na]^+$ Calculated for $C_{23}H_{24}O_9Na$ 467.1318, found 467.1318.

5-Butyl 4,4-dimethyl 6-hydroxy-2-(4-methoxyphenyl)chroman-4,4,5-tricarboxylate (3ac): 1a (0.1 g, 0.37 mmol), **2c** (0.077 g, 0.37 mmol), **3ac** (0.110 g, 0.23 mmol), Yield: 62%, Nature: White solid, Melting point: 134-136 ºC, R_f: 0.5 (acetone:hexane = 20:80), ^{1}H-NMR (400 MHz, $CDCl_3$): δ 10.64 (s, 1H), 7.30 (d, *J* = 8.7 Hz, 2H), 7.10 (d, *J* = 9.2 Hz, 1H), 6.97 (d, *J* = 9.2 Hz, 1H), 6.90 (d, *J* = 8.7 Hz, 2H), 4.83 (d, *J* = 10.8 Hz, 1H), 4.43 – 4.36 (m, 1H), 4.05 – 3.98 (m, 1H), 3.80 (s, 3H), 3.76 (s, 3H), 3.64 (s, 3H), 2.84 (dd, *J* = 13.8, 1.6 Hz, 1H), 2.28 (dd, *J* = 13.7, 12.0 Hz, 1H), 1.71 – 1.60 (m, 2H), 1.38 – 1.28 (m, 2H), 0.94 (t, *J* = 7.4 Hz, 3H). ^{13}C-NMR (100 MHz, $CDCl_3$): 170.8, 170.2, 170.0, 159.8, 157.0, 148.3, 131.5, 127.4, 125.9, 119.9, 117.9, 114.1, 112.0, 73.0, 65.5, 56.0, 55.4, 53.0, 52.8, 41.0, 30.3, 18.9, 13.7. HRMS (ESI, Q-TOF) *m/z*: $[M + Na]^+$ Calculated for $C_{25}H_{29}O_9$ 473.1812, found 473.1808.

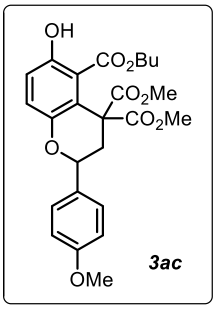

5-Benzyl 4,4-dimethyl 6-hydroxy-2-(4-methoxyphenyl)chroman-4,4,5-tricarboxylate (3ad): 1a (0.1 g, 0.37 mmol), **2d** (0.089 g, 0.37 mmol), **3ad** (0.142 g, 0.28 mmol), **Yield:** 75%, **Nature**: White solid, **Melting point**: 155-158 ºC, **R$_f$:** 0.5 (acetone:hexane = 20:80), ^{1}**H-NMR** (400 MHz, $CDCl_3$): δ 10.71 (s, 1H), 7.44 – 7.26 (m, 7H), 7.10 (d, *J* = 9.1 Hz, 1H), 6.97 (d, *J* = 9.1 Hz, 1H), 6.90 (d, *J* = 8.5 Hz, 2H), 5.50 (d, *J* = 11.6 Hz, 1H), 4.99 (d, *J* = 11.6 Hz, 1H), 4.80 (d, *J* = 11.4 Hz, 1H), 3.80 (s, 3H), 3.52 (s, 3H), 3.38 (s, 3H), 2.91 – 2.75 (m, 1H), 2.33 – 2.23 (m, 1H). ^{13}**C-NMR** (100 MHz, $CDCl_3$): 170.6, 170.2, 169.8, 159.7, 157.3, 148.3, 134.5, 131.5, 130.0, 129.0, 128.7, 127.4, 126.2, 119.9, 117.8, 114.1, 111.8, 73.0, 66.7, 56.6, 55.4, 52.8, 52.7, 41.0. **HRMS (ESI, Q-TOF) *m/z*:** $[M + Na]^+$ Calculated for $C_{28}H_{26}O_9Na$ 529.1475, found 529.1475.

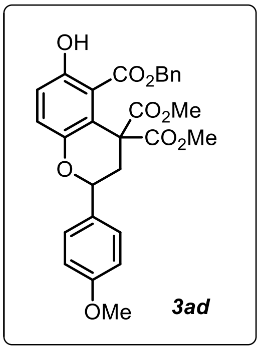

5-Allyl 4,4-dimethyl 6-hydroxy-2-(4-methoxyphenyl)chroman-4,4,5-tricarboxylate (3ae): 1a (0.1 g, 0.37 mmol), **2e** (0.071 g, 0.37 mmol), **3ae** (0.115 g, 0.25 mmol), **Yield:** 68%, **Nature**: White solid, **Melting point**: 128-130 ºC, **R$_f$:** 0.5 (acetone:hexane = 20:80), ^{1}**H-NMR** (400 MHz, $CDCl_3$): δ 10.72 (s, 1H), 7.30 (d, *J* = 8.7 Hz, 2H), 7.11 (d, *J* = 9.2 Hz, 1H), 6.98 (d, *J* = 9.2 Hz, 1H), 6.90 (d, *J* = 8.7 Hz, 2H), 6.01 – 5.90 (m, 1H), 5.38 – 5.28 (m, 2H), 4.85 – 4.79 (m, 2H), 4.58 – 4.51 (m, 1H), 3.80 (s, 3H), 3.72 (s, 3H), 3.63 (s, 3H), 2.84 (dd, *J* = 13.8, 1.8 Hz, 1H), 2.29 (dd, *J* = 13.8, 11.9 Hz, 1H). ^{13}**C-NMR** (100 MHz, $CDCl_3$): 170.8, 170.3, 169.8, 159.8, 157.4, 148.3, 131.5, 131.2, 127.4, 126.2, 120.5, 120.0, 117.8, 114.1, 111.7, 73.0, 66.3, 56.6, 55.4, 53.1, 52.9, 40.9. **HRMS (ESI, Q-TOF) *m/z*:** $[M + Na]^+$ Calculated for $C_{24}H_{24}O_9Na$ 479.1318, found 479.1318.

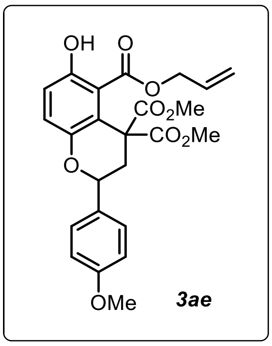

5-(4-bromobenzyl) 4,4-dimethyl 6-hydroxy-2-(4-methoxyphenyl)chroman-4,4,5-tricarboxylate (3af)

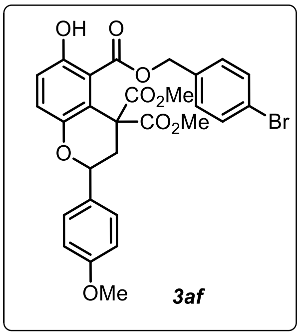

: 1a (0.1 g, 0.37 mmol), **2f** (0.118 g, 0.37 mmol), **3af** (0.16 g, 0.27 mmol), Yield: 72% Nature: White solid, Melting point: 159-161 ºC, R_f: 0.5 (acetone:hexane = 20:80), ^{1}H-NMR (400 MHz, $CDCl_3$): δ 10.62 (s, 1H), 7.50 (d, *J* = 8.4 Hz, 2H), 7.33 – 7.25 (m, 4H), 7.11 (d, *J* = 9.2 Hz, 1H), 6.97 (d, *J* = 9.2 Hz, 1H), 6.90 (d, *J* = 8.7 Hz, 2H), 5.41 (d, *J* = 11.8 Hz, 1H), 4.94 (d, *J* = 11.8 Hz, 1H), 4.81 (d, *J* = 10.8 Hz, 1H), 3.80 (s, 3H), 3.51 (s, 3H), 3.44 (s, 3H), 2.82 (dd, *J* = 13.8, 1.5 Hz, 1H), 2.28 (dd, *J* = 13.7, 11.9 Hz, 1H). ^{13}C-NMR (100 MHz, $CDCl_3$): 170.6, 170.2, 169.8, 159.8, 157.4, 148.4, 133.5, 131.8, 131.7, 131.4, 127.4, 126.3, 123.2, 120.0, 117.7, 114.1, 111.6, 73.0, 65.7, 56.6, 55.4, 52.85, 52.81, 40.9. HRMS (ESI, Q-TOF) *m/z*: $[M + Na]^+$ Calculated for $C_{28}H_{25}O_9BrNa$ 607.0580, found 607.0580.

5-(2-Bromobenzyl) 4,4-dimethyl 6-hydroxy-2-(4-methoxyphenyl)chroman-4,4,5-tricarboxylate

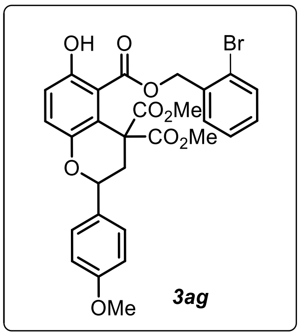

(3ag): 1a (0.1 g, 0.37 mmol), **2g** (0.118 g, 0.37 mmol), **3ag** (0.16 g, 0.22 mmol), Yield: 60% Nature: White solid, Melting point: 160-162 ºC, R_f: 0.5 (acetone:hexane = 20:80), ^{1}H-NMR (400 MHz, $CDCl_3$): δ 10.13 (s, 1H), 7.57 (d, *J* = 7.9 Hz, 1H), 7.36 – 7.25 (m, 4H), 7.20 (d, *J* = 11.5 Hz, 1H), 7.12 (d, *J* = 9.2 Hz, 1H), 6.99 (d, *J* = 9.2 Hz, 1H), 6.89 (d, *J* = 8.6 Hz, 2H), 5.68 (d, *J* = 12.7 Hz, 1H), 5.06 (d, *J* = 12.8 Hz, 1H), 4.82 (d, *J* = 11.2 Hz, 1H), 3.80 (s, 3H), 3.63 (s, 3H), 3.47 (s, 3H), 2.83 (dd, *J* = 13.7, 1.3 Hz, 1H), 2.28 (dd, *J* = 13.6, 12.0 Hz, 1H). ^{13}C-NMR (100 MHz, $CDCl_3$): 170.6, 170.3, 169.0, 159.7, 156.6, 148.5, 134.0, 132.9, 131.5, 130.6, 130.3, 127.7, 127.4, 126.1, 123.5, 120.0, 117.9, 114.1, 112.0, 73.0, 66.2, 56.5, 55.4, 53.0, 52.9, 40.8. HRMS (ESI, Q-TOF) *m/z*: $[M + H]^+$ Calculated for $C_{28}H_{26}O_9Br$ 585.0760, found 585.0766.

5-(4-fluorobenzyl) 4,4-dimethyl 6-hydroxy-2-(4-methoxyphenyl)chroman-4,4,5-tricarboxylate

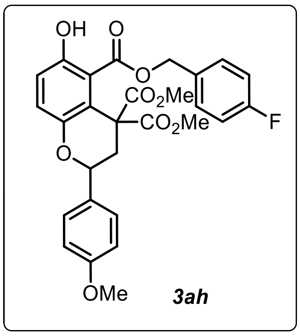

(3ah): 1a (0.1 g, 0.37 mmol), **2h** (0.096 g, 0.37 mmol), **3ah** (0.16 g, 0.244 mmol), Yield: 66% Nature: White solid, Melting point: 149-151 ºC, R_f: 0.5 (acetone:hexane = 20:80), ^{1}H-NMR (400 MHz, $CDCl_3$): δ 10.70 (s, 1H), 7.44 (dd, *J* = 8.6, 5.4 Hz, 2H), 7.28 (d, *J* = 8.8 Hz, 2H), 7.10 (d, *J* = 9.2 Hz, 1H), 7.05 (t, *J* = 8.6 Hz, 2H), 6.97 (d, *J* = 9.2 Hz, 1H), 6.89 (d, *J* = 8.6 Hz, 2H), 5.44 (d, *J* = 11.6 Hz, 1H), 4.96 (d, *J* = 11.6 Hz, 1H), 4.80 (d, *J* = 10.7 Hz, 1H), 3.80 (s, 3H), 3.51 (s, 3H), 3.41 (s, 3H), 2.82 (dd, *J* = 13.8, 1.6 Hz, 1H), 2.27 (dd, *J* = 13.8, 11.8 Hz, 1H). ^{13}C-NMR (100 MHz, $CDCl_3$): 170.6, 170.1, 169.9, 163.1 (d, *J* = 248.3 Hz), 159.8, 157.4, 148.3, 132.29, 132.21, 131.4, 130.4 (d, *J* = 3.2 Hz), 127.4, 126.3, 120.0, 117.7, 115.6 (d, *J* = 21.7 Hz), 114.1, 111.7, 73.0, 65.8, 56.5, 55.4, 52.8, 52.7, 40.9. ^{19}F NMR (376 MHz, $CDCl_3$) δ -112.12. HRMS (ESI, Q-TOF) *m/z*: $[M + Na]^+$ Calculated for $C_{28}H_{26}O_9F$ 525.1561, found 525.1558.

4,4-Dimethyl 5-phenethyl 6-hydroxy-2-(4-methoxyphenyl)chroman-4,4,5-tricarboxylate (3ai): 1a

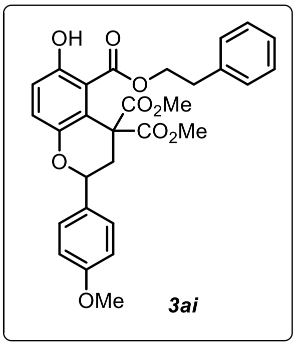

(0.1 g, 0.37 mmol), **2i** (0.094 g, 0.37 mmol), **3ai** (0.145 g, 0.28 mmol), Yield: 76%, Nature: White solid. Melting point: 154-156 ºC R_f: 0.5 (acetone:hexane = 20:80), ^{1}H-NMR (400 MHz, $CDCl_3$): δ 10.42 (s, 1H), 7.34 – 7.28 (m, 4H), 7.26 – 7.22 (m, 3H), 7.12 (d, *J* = 9.2 Hz, 1H), 6.98 (d, *J* = 9.2 Hz, 1H), 6.91 (d, *J* = 8.7 Hz, 2H), 4.86 (dd, *J* = 11.7, 1.2 Hz, 1H), 4.59 – 4.53 (m, 1H), 4.28 – 4.17 (m, 1H), 3.81 (s, 3H), 3.68 (s, 3H), 3.64 (s, 3H), 3.04 – 2.94 (m, 2H), 2.86 (dd, *J* = 13.8, 1.7 Hz, 1H), 2.31 (dd, *J* = 13.8, 11.9 Hz, 1H). ^{13}C-NMR (100 MHz, $CDCl_3$): 170.8, 170.3, 169.8, 159.8, 156.9, 148.4, 136.6, 131.5, 129.0, 128.8, 127.4, 127.0, 126.0, 120.0, 117.9, 114.1, 112.0, 73.0, 65.9, 56.6, 55.4, 52.99, 52.93, 40.9, 34.7. HRMS (ESI, Q-TOF) *m/z*: $[M + Na]^+$ Calculated for $C_{29}H_{28}O_9Na$ 543.1631, found 543.1631.

Trimethyl 6-hydroxy-8-methoxy-2-(4-methoxyphenyl)chroman-4,4,5-tricarboxylate (3aj): 1a (0.1 g,

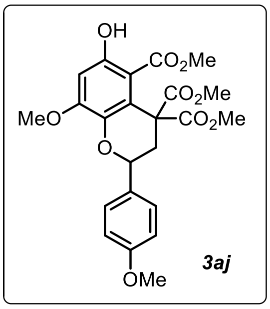

0.37 mmol), **2j** (0.073 g, 0.37 mmol), **3aj** (0.099 g, 0.21 mmol), Yield**:** 57%, Nature: White solid. Melting point: 130-132 ºC. R_f: 0.4 (acetone:hexane = 20:80). ^{1}H-NMR (400 MHz, $CDCl_3$): δ 11.37 (s, 1H), 7.31 (d, *J* = 8.6 Hz, 2H), 6.89 (d, *J* = 8.7 Hz, 2H), 6.51 (s, 1H), 4.84 (d, *J* = 10.6 Hz, 1H), 3.86 (s, 3H), 3.79 (s, 3H), 3.74 (s, 3H), 3.71 (s, 3H), 3.62 (s, 3H), 2.85 (dd, *J* = 13.9, 1.6 Hz, 1H), 2.30 (dd, *J* = 13.8, 11.8 Hz, 1H). ^{13}C-NMR (100 MHz, $CDCl_3$): 170.9, 170.5, 170.2, 159.7, 159.3, 155.3, 139.5, 131.4, 127.5, 118.4, 114.1, 103.0, 100.6, 73.0, 56.7, 56.1, 55.4, 53.0, 52.8, 51.1, 40.9. HRMS (ESI, Q-TOF) *m/z*: $[M + H]^+$ Calculated for $C_{23}H_{25}O_{10}$ 461.1448, found 461.1452.

Trimethyl 6-hydroxy-2-(4-methoxyphenyl)-2*H*-benzo[*h*]chromene-4,4,5(3*H*)-tricarboxylate (3ak):

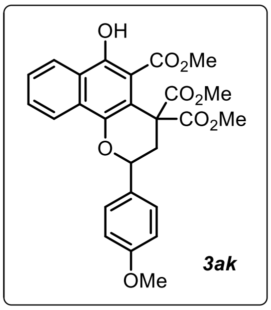

1a (0.1 g, 0.37 mmol), **2k** (0.080 g, 0.37 mmol), **3ak** (0.092 g, 0.191 mmol), Yield: 52% Nature: White solid. Melting point: 144-146 ºC R_f: 0.5 (acetone:hexane = 20:80) ^{1}H-NMR (400 MHz, $CDCl_3$): δ 12.23 (s, 1H), 8.42 (dd, *J* = 7.7, 1.5 Hz, 1H), 8.23 (d, *J* = 7.7 Hz, 1H), 7.65 – 7.55 (m, 2H), 7.41 (d, *J* = 8.7 Hz, 2H), 6.95 (d, *J* = 8.7 Hz, 2H), 5.06 – 5.01 (m, 1H), 3.83 (s, 3H), 3.79 (s, 3H), 3.76 (s, 3H), 3.64 (s, 3H), 2.95 (dd, *J* = 13.7, 1.7 Hz, 1H), 2.38 (dd, *J* = 13.7, 11.9 Hz, 1H). ^{13}C-NMR (100 MHz, $CDCl_3$): 171.5, 171.4, 170.6, 159.7, 157.1, 144.0, 131.9, 129.7, 129.1, 127.4, 127.2, 125.6, 124.0, 122.5, 114.1, 109.5, 104.6, 73.1, 56.6, 55.4, 53.0, 52.8, 51.4, 41.1. HRMS (ESI, Q-TOF) *m/z*: $[M + H]^+$ Calculated for $C_{26}H_{25}O_9$ 481.1499, found 481.1492.

4.4.5 Representative procedure for the synthesis of benzofuran derivatives 4:

A round-bottom flask equipped with magnetic stir bar was charged **1** ((0.1 g, 0.37 mmol), **2** (0.073 g, 0.44 mmol), $In(OTf)_3$ (0.040 g, 20 mol %) and dry DCM (2 ml, 0.2 M) under Nitrogen atmosphere. On completion of the reaction (as monitored by TLC), the reaction mixture was filtered through a small plug of celite and concentrated in rotary evaporator. The crude mixture was further purified by column chromatography on silica gel with acetone/hexane (10:90) as eluent to afford **4**.

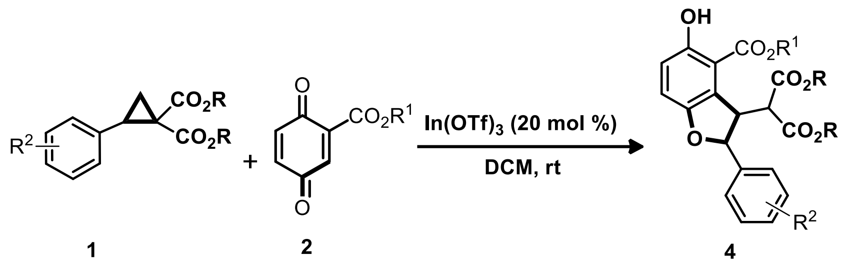

Dimethyl-2-(5-hydroxy-4-(methoxycarbonyl)-2-(4-methoxyphenyl)-2,3-dihydrobenzofuran-3-yl)malonate (4aa):

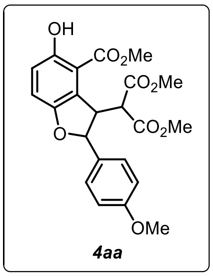

1a (0.1 g, 0.37 mmol), **2a** (0.073 g, 0.44 mmol), **4aa** (0.119 g, 0.28 mmol), Yield: 75% Nature: Viscous liquid, R_f: 0.5 (acetone:hexane = 10:90) ^{1}H-NMR (400 MHz, $CDCl_3$): δ 10.50 (s, 1H), 7.31 (d, *J* = 8.6 Hz, 2H), 7.07 (d, *J* = 8.9 Hz, 1H), 6.89 (d, *J* = 8.9 Hz, 1H), 6.82 (d, *J* = 8.7 Hz, 2H), 5.88 (s, 1H), 4.29 – 4.26 (m, 1H), 3.96 (d, *J* = 4.0 Hz, 1H), 3.87 (s, 3H), 3.78 (s, 3H), 3.75 (s, 3H), 3.55 (s, 3H). ^{13}C-NMR (100 MHz, $CDCl_3$): 169.8, 169.1, 168.3, 159.2, 157.0, 153.2, 133.8, 126.6, 125.1, 119.0, 117.6, 113.9, 109.5, 85.1, 55.3, 54.1, 52.8, 52.6, 52.5, 52.2. HRMS (ESI, Q-TOF) *m/z*: $[M + Na]^+$ Calculated for $C_{22}H_{22}O_9Na$ 453.1162, found 453.1162.

Dimethyl 2-(2-(3,4-dimethoxyphenyl)-5-hydroxy-4-(methoxycarbonyl)-2,3-dihydrobenzofuran-3-yl)malonate (4ba):

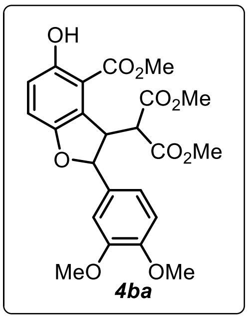

1d (0.1 g, 0.34 mmol), **2f** (0.068 g, 0.41 mmol), **4ba** (0.102 g, 0.22 mmol), Yield: 65% Nature: White solid. Melting point: 150-152 ºC R_f: 0.5 (acetone:hexane = 10:90) ^{1}H-NMR (400 MHz, $CDCl_3$): δ 10.49 (s, 1H), 7.09 (d, *J* = 8.8 Hz, 1H), 7.00 (d, *J* = 1.8 Hz, 1H), 6.93 – 6.88 (m, 2H), 6.77 (d, *J* = 8.3 Hz, 1H), 5.88 (d, *J* = 1.2 Hz, 1H), 4.29 – 4.28 (m, 1H), 3.96 (d, *J* = 3.9 Hz, 1H), 3.88 (s, 3H), 3.83 (s, 3H), 3.82 (s, 3H), 3.78 (s, 3H), 3.56 (s, 3H). ^{13}C-NMR (100 MHz, $CDCl_3$): 169.8, 169.1, 168.3, 157.0, 153.2, 148.9, 148.6, 134.1, 125.2, 119.1, 117.5, 117.3, 110.9, 109.6, 108.8, 85.0, 55.9, 54.1, 52.87, 52.85, 52.7, 52.6, 52.5, 52.2. HRMS (ESI, Q-TOF) *m/z*: $[M + Na]^+$ Calculated for $C_{23}H_{24}O_{10}Na$, 483.1267, found 483.1266.

Dimethyl-2-(2-(4-(benzyloxy)phenyl)-5-hydroxy-4-(methoxycarbonyl)-2,3-dihydrobenzofuran-3-yl)malonate (4ca):

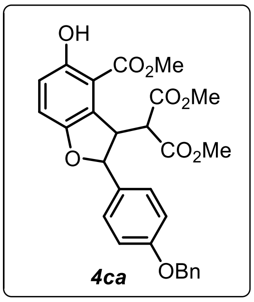

1f (0.1 g, 0.29 mmol), **2a** (0.058 g, 0.35 mmol), **4ca** (0.110 g, 0.22 mmol), Yield: 75% Nature: Viscous liquid. R_f: 0.5 (acetone:hexane = 10:90) ^{1}H-NMR (400 MHz, $CDCl_3$): δ 10.50 (s, 1H), 7.40 – 7.30 (m, 7H), 7.07 (d, *J* = 8.9 Hz, 1H), 6.90 (d, *J* = 8.6 Hz, 3H), 5.88 (d, *J* = 1.4 Hz, 1H), 5.01 (s, 2H), 4.28 – 4.27 (m, 1H), 3.96 (d, *J* = 4.0 Hz, 1H), 3.87 (s, 3H), 3.78 (s, 3H), 3.56 (s, 3H). ^{13}C-NMR (100 MHz, $CDCl_3$): 169.8, 169.1, 168.3, 158.5, 157.1, 153.2, 137.0, 134.0, 128.6, 128.0, 127.5, 126.6, 125.1, 119.1, 117.6, 114.8, 109.5, 85.0, 70.0, 54.1, 52.8, 52.6, 52.5, 52.2. HRMS (ESI, Q-TOF) *m/z*: $[M + Na]^+$ Calculated for $C_{28}H_{26}O_9Na$ 529.1475, found 529.1475.

Diethyl 2-(2-(benzo[*d*][1,3]dioxol-5-yl)-5-hydroxy-4-(methoxycarbonyl)-2,3-dihydrobenzofuran-3-yl)malonate (4da):

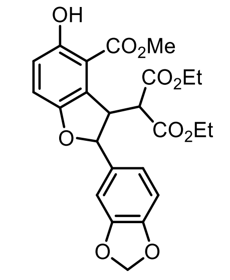

4da

1j (0.1 g, 0.32 mmol), **2a** (0.064 g, 0.39 mmol), **4da** (0.105 g, 0.22 mmol). Yield: 68% Nature: White solid. Melting point: 110-112 ºC R_f: 0.5 (acetone:hexane = 10:90) ^{1}H-NMR (400 MHz, $CDCl_3$): δ 10.51 (s, 1H), 7.05 (d, *J* = 8.9 Hz, 1H), 6.92 – 6.88 (m, 3H), 6.72 (d, *J* = 8.4 Hz, 1H), 5.90 – 5.89 (m, 2H), 5.86 (d, *J* = 1.9 Hz, 1H), 4.29 – 4.20 (m, 1H), 4.05 – 3.99 (m, 2H), 3.91 (d, *J* = 3.8 Hz, 1H), 3.88 (s, 3H), 1.27 (t, *J* = 7.1 Hz, 3H), 1.04 (t, *J* = 7.1 Hz, 3H). ^{13}C-NMR (100 MHz, $CDCl_3$): 169.8, 168.7, 167.8, 157.1, 153.2, 147.8, 147.2, 135.7, 125.3, 119.0, 118.9, 117.6, 109.5, 108.2, 106.0, 101.1, 85.0, 61.8, 61.7, 54.3, 52.5, 52.2, 14.1, 13.8. HRMS (ESI, Q-TOF) *m/z*: $[M + Na]^+$ Calculated for $C_{24}H_{24}O_{10}Na$ 495.1267, found 495.1267.

Diethyl 2-(2-(4-(dimethylamino)phenyl)-5-hydroxy-4-(methoxycarbonyl)-2,3-dihydrobenzofuran-3-yl)malonate (4ea):

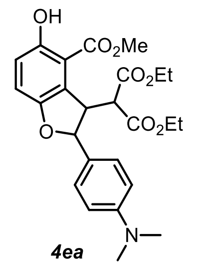

4ea

1l (0.1 g, 0.33 mmol), **2a** (0.064 g, 0.39 mmol), **4ea** (0.110 g, 0.23 mmol) Yield: 70% Nature: Viscous liquid. R_f: 0.5 (acetone:hexane = 10:90) ^{1}H-NMR (400 MHz, $CDCl_3$): δ 10.51 (s, 1H), 7.25 (d, *J* = 8.7 Hz, 2H), 7.04 (d, *J* = 8.8 Hz, 1H), 6.88 (d, *J* = 8.9 Hz, 1H), 6.65 (d, *J* = 9.6 Hz, 2H), 5.87 (d, *J* = 1.9 Hz, 1H), 4.31 – 4.29 (m, 1H), 4.26 – 4.20 (m, 2H), 4.06 – 4.00 (m, 2H), 3.92 (d, *J* = 3.9 Hz, 1H), 3.87 (s, 3H), 2.89 (s, 6H), 1.26 (t, *J* = 7.1 Hz, 3H), 1.05 (t, *J* = 7.1 Hz, 3H). ^{13}C-NMR (100 MHz, $CDCl_3$): 170.0, 168.7, 168.0, 156.9, 153.5, 150.3, 129.5, 126.3, 125.8, 118.7, 117.6, 112.4, 109.6, 85.5, 61.7, 61.6, 54.5, 52.4, 52.0, 40.6, 14.1, 13.8. HRMS (ESI, Q-TOF) *m/z*: $[M + H]^+$ Calculated for $C_{25}H_{30}NO_8$ 472.1971, found 472.1971.

Dimethyl-2-(2-(3-ethoxy-4-methoxyphenyl)-5-hydroxy-4-(methoxycarbonyl)-2,3-dihydrobenzofuran-3-yl)malonate (4fa):

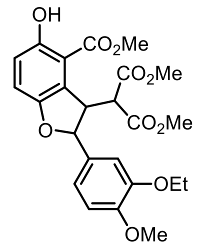

4fa

1g (0.1 g, 0.32 mmol), **2a** (0.063 g, 0.38 mmol), **4fa** (0.106 g, 0.22 mmol). Yield: 68% Nature: White solid Melting point: 124-126 ºC R_f: 0.5 (acetone:hexane = 10:90) ^{1}H-NMR (400 MHz, $CDCl_3$): δ 10.49 (s, 1H), 7.08 (d, *J* = 8.9 Hz, 1H), 6.99 (d, *J* = 2.0 Hz, 1H), 6.90 (d, *J* = 8.7 Hz, 2H), 6.77 (d, *J* = 8.3 Hz, 1H), 5.86 (d, *J* = 1.6 Hz, 1H), 4.29 – 4.27 (m, 1H), 4.08 – 4.02 (m, 2H), 3.96 (d, *J* = 4.0 Hz, 1H), 3.88 (s, 3H), 3.81 (s, 3H), 3.78 (s, 3H), 3.56 (s, 3H), 1.43 (d, *J* = 7.1 Hz, 3H). ^{13}C-NMR (100 MHz, $CDCl_3$): 169.8, 169.1, 168.3, 157.0, 153.2, 148.9, 148.2, 134.1, 125.2, 119.0, 117.5, 117.3, 111.2, 110.2, 109.6, 85.1, 64.3, 55.9, 54.1, 52.8, 52.6, 52.5, 52.2, 14.8. HRMS (ESI, Q-TOF) *m/z*: $[M + Na]^+$ Calculated for $C_{24}H_{26}O_{10}Na$ 497.1424, found 497.1424.

Dimethyl-2-(2-(3-bromo-4-methoxyphenyl)-5-hydroxy-4-(methoxycarbonyl)-2,3-dihydrobenzofuran-3-yl)malonate (4ga):

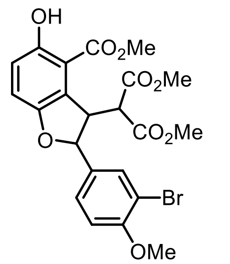

4ga

1h (0.1 g, 0.29 mmol), **2a** (0.058 g, 0.35 mmol), **4ga** (0.092 g, 0.18 mmol). Yield: 62% Nature: White solid. Melting point: 160-162 ºC R_f: 0.5 (acetone:hexane = 10:90) ^{1}H-NMR (400 MHz, $CDCl_3$): δ 10.51 (s, 1H), 7.58 (d, *J* = 2.3 Hz, 1H), 7.32 (dd, *J* = 8.4, 2.0 Hz, 1H), 7.09 (d, *J* = 8.9 Hz, 1H), 6.91 (d, *J* = 8.9 Hz, 1H), 6.82 (d, *J* = 8.6 Hz, 1H), 5.86 (d, *J* = 1.7 Hz, 1H), 4.24 – 4.23 (m, 1H), 3.96 (d, *J* = 4.0 Hz, 1H), 3.89 (s, 3H), 3.84 (s, 3H), 3.80 (s, 3H), 3.55 (s, 3H). ^{13}C-NMR (100 MHz, $CDCl_3$): 169.7, 169.1, 168.2, 157.2, 155.4, 152.9, 135.3, 130.4, 125.6, 124.7, 119.3, 117.7, 111.7, 109.5, 84.1, 56.3, 54.0, 52.9, 52.7, 52.6, 52.2. HRMS (ESI, Q-TOF) *m/z*: $[M + Na]^+$ Calculated for $C_{22}H_{21}O_9BrNa$ 531.0267, found 531.0267.

Diethyl 2-(5-hydroxy-2-(4-methoxy-3-methylphenyl)-4-(methoxycarbonyl)-2,3-dihydrobenzofuran-3-yl)malonate (4ha):

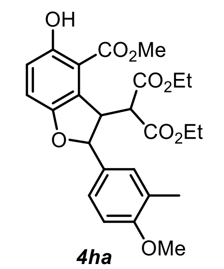

4ha

1i (0.1 g, 0.32 mmol), **2a** (0.063 g, 0.38 mmol), **4ha** (0.112 g, 0.237 mmol). Yield: 74% Nature: Viscous liquid R_f: 0.5 (acetone:hexane = 10:90) ^{1}H-NMR (400 MHz, $CDCl_3$): δ 10.52 (s, 1H), 7.19 – 7.14 (m, 2H), 7.05 (d, *J* = 8.8 Hz, 1H), 6.89 (d, *J* = 8.8 Hz, 1H), 6.73 (d, *J* = 8.3 Hz, 1H), 5.87 (d, *J* = 1.1 Hz, 1H), 4.31 – 4.26 (m, 1H), 4.26 – 4.17 (m, 2H), 4.07 – 4.00 (m, 2H), 3.92 (d, *J* = 3.8 Hz, 1H), 3.88 (s, 3H), 3.77 (s, 3H), 2.16 (s, 3H), 1.27 (t, *J* = 7.1 Hz, 3H), 1.04 (t, *J* = 7.1 Hz, 3H). ^{13}C-NMR (100 MHz, $CDCl_3$): 169.9, 168.7, 167.9, 157.4, 157.0, 153.4, 133.4, 127.7, 126.8, 125.6, 123.9, 118.8, 117.6, 109.7, 109.6, 85.1, 61.8, 61.6, 55.3, 54.4, 52.4, 52.1, 16.4, 14.1, 13.8. HRMS (ESI, Q-TOF) *m/z*: $[M + Na]^+$ Calculated for $C_{25}H_{28}O_9Na$ 495.1631, found 495.1631.

Diethyl 2-(5-hydroxy-4-(methoxycarbonyl)-2,2',3,3'-tetrahydro-[2,5'-bibenzofuran]-3-yl)malonate (4ia):

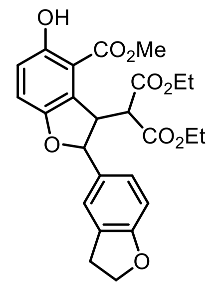

4ia

1k (0.1 g, 0.33 mmol), **2a** (0.065 g, 0.35 mmol), **4ia** (0.115 g, 0.24 mmol) Yield: 72% Nature: White solid Melting point: 104-106 ºC R_f: 0.5 (acetone:hexane = 10:90) ^{1}H-NMR (400 MHz, $CDCl_3$): δ 10.52 (s, 1H), 7.20 (s, 1H), 7.15 (dd, *J* = 8.3, 1.4 Hz, 1H), 7.05 (d, *J* = 8.8 Hz, 1H), 6.89 (d, *J* = 8.8 Hz, 1H), 6.69 (d, *J* = 8.3 Hz, 1H), 5.87 (d, *J* = 1.9 Hz, 1H), 4.51 (t, *J* = 8.7 Hz, 2H), 4.29 – 4.24 (m, 2H), 4.22 – 4.19 (m, 1H), 4.05 – 4.01 (m, 2H), 3.92 (d, *J* = 3.9 Hz, 1H), 3.88 (s, 3H), 3.14 (t, *J* = 8.7 Hz, 2H), 1.26 (t, *J* = 7.1 Hz, 3H), 1.04 (t, *J* = 7.1 Hz, 3H). ^{13}C-NMR (100 MHz, $CDCl_3$): 169.9, 168.8, 167.9, 159.9, 157.0, 153.3, 133.9, 127.3, 125.5, 122.1, 118.9, 117.6, 109.6, 109.1, 85.4, 71.4, 61.8, 61.6, 54.4, 52.4, 52.2, 29.8, 14.1, 13.8. HRMS (ESI, Q-TOF) *m/z*: $[M + Na]^+$ Calculated for $C_{25}H_{26}O_9Na$ 493.1475, found 493.1475.

Dimethyl-2-(4-(ethoxycarbonyl)-5-hydroxy-2-(4-methoxyphenyl)-2,3-dihydrobenzofuran-3-yl) malonate (4ab): **1a** (0.1 g, 0.37 mmol), **2b** (0.081 g, 0.45 mmol), **4ab** (0.125 g, 0.28 mmol). Yield: 75% Nature: White solid. Melting point: 126-128 ºC R_f: 0.5 (acetone:hexane = 10:90) ^{1}H-NMR (400 MHz, $CDCl_3$): δ 10.61 (s, 1H), 7.33 (d, *J* = 8.9 Hz, 2H), 7.06 (d, *J* = 8.8 Hz, 1H), 6.88 (d, *J* = 8.8 Hz, 1H), 6.83 (d, *J* = 8.7 Hz, 2H), 5.91 (d, *J* = 1.1 Hz, 1H), 4.46 – 4.38 (m, 1H), 4.31 – 4.25 (m, 2H), 4.02 (d, *J* = 3.4 Hz, 1H), 3.79 (s, 3H), 3.75 (s, 3H), 3.55 (s, 3H), 1.31 (t, *J* = 7.1 Hz, 3H). ^{13}C-NMR (100 MHz, $CDCl_3$): 169.5, 169.2, 168.3, 159.2, 157.2, 153.1, 133.8, 126.6, 125.3, 119.0, 117.4, 113.9, 109.6, 84.7, 62.0, 55.3, 54.1, 52.8, 52.6, 52.1, 13.7. HRMS (ESI, Q-TOF) *m/z*: $[M + Na]^+$ Calculated for $C_{23}H_{24}O_9Na$ 467.1318, found 467.1318.

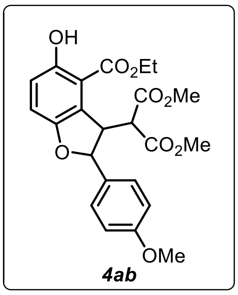

4ab

Dimethyl-2-(4-(butoxycarbonyl)-5-hydroxy-2-(4-methoxyphenyl)-2,3-dihydrobenzofuran-3-yl) malonate (4ac): **1a** (0.1 g, 0.37 mmol), **2c** (0.093 g, 0.45 mmol), **4ac** (0.112 g, 0.238 mmol). Yield: 64% Nature: Viscous liquid R_f: 0.5 (acetone:hexane = 10:90) ^{1}H-NMR (400 MHz, $CDCl_3$): δ 10.62 (s, 1H), 7.34 (d, *J* = 8.6 Hz, 2H), 7.06 (d, *J* = 8.9 Hz, 1H), 6.88 (d, *J* = 8.8 Hz, 1H), 6.83 (d, *J* = 8.8 Hz, 2H), 5.91 (d, *J* = 1.1 Hz, 1H), 4.37 – 4.29 (m, 2H), 4.27 – 4.22 (m, 1H), 4.00 (d, *J* = 3.5 Hz, 1H), 3.79 (s, 3H), 3.76 (s, 3H), 3.54 (s, 3H), 1.69 – 1.63 (m, 2H), 1.38 – 1.32 (m, 2H), 0.91 (t, *J* = 7.4 Hz, 3H). ^{13}C-NMR (100 MHz, $CDCl_3$): 169.6, 169.1, 168.3, 159.2, 157.2, 153.1, 133.7, 126.6, 125.2, 119.0, 117.5, 113.9, 109.7, 84.7, 65.9, 55.3, 54.0, 52.7, 52.6, 52.1, 30.3, 19.3, 13.7. HRMS (ESI, Q-TOF) *m/z*: $[M + H]^+$ Calculated for $C_{25}H_{29}O_9$ 473.1812, found 473.1811.

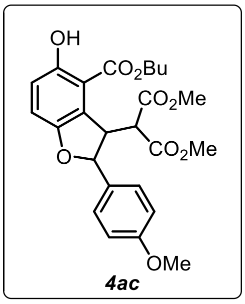

4ac

Dimethyl 2-(4-((benzyloxy)carbonyl)-5-hydroxy-2-(4-methoxyphenyl)-2,3-dihydrobenzofuran-3-yl)malonate (4ad): **1a** (0.1 g, 0.37 mmol), **2d** (0.108 g, 0.45 mmol), **4ad** (0.150 g, 0.296 mmol). Yield: 80% Nature: White solid. Melting point: 150-152 ºC R_f: 0.5 (acetone:hexane = 10:90) ^{1}H-NMR (400 MHz, $CDCl_3$): δ 10.57 (s, 1H), 7.38 – 7.34 (m, 5H), 7.31 (d, *J* = 8.6 Hz, 2H), 7.06 (d, *J* = 8.8 Hz, 1H), 6.88 (d, *J* = 8.8 Hz, 1H), 6.82 (d, *J* = 8.8 Hz, 2H), 5.84 (s, 1H), 5.43 (d, *J* = 11.8 Hz, 1H), 5.15 (d, *J* = 11.8 Hz, 1H), 4.21 – 4.19 (m, 1H), 3.77 (d, *J* = 5.0 Hz, 4H), 3.58 (s, 3H), 3.48 (s, 3H). ^{13}C-NMR (100 MHz, $CDCl_3$): 169.3, 168.6, 168.3, 159.1, 157.3, 153.1, 134.1, 133.8, 129.2, 129.0, 128.9, 126.6, 125.30, 119., 117.7, 113.8, 109.5, 84.6, 68.0, 55.3, 53.7, 52.5, 51.8. HRMS (ESI, Q-TOF) *m/z*: $[M + Na]^+$ Calculated for $C_{28}H_{26}O_9Na$ 529.1475, found 529.1475.

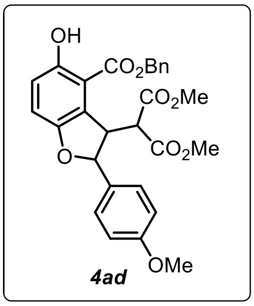

4ad

Dimethyl-2-(4-((allyloxy)carbonyl)-5-hydroxy-2-(4-methoxyphenyl)-2,3-dihydrobenzofuran-3-yl)

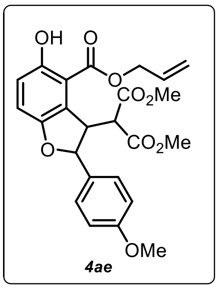

malonate (4ae): 1a (0.1 g, 0.37 mmol), **2e** (0.086 g, 0.45 mmol), **4ae** (0.110 g, 0.24 mmol) Yield: 65% Nature: White solid. Melting point: 156-158 ºC R_f: 0.5 (acetone:hexane = 10:90) ^{1}H-NMR (400 MHz, $CDCl_3$): δ 10.51 (s, 1H), 7.33 (d, *J* = 8.6 Hz, 2H), 7.07 (d, *J* = 8.8 Hz, 1H), 6.89 (d, *J* = 8.8 Hz, 1H), 6.83 (d, *J* = 8.8 Hz, 2H), 6.01 – 5.83 (m, 2H), 5.39 – 5.27 (m, 2H), 4.87 – 4.80 (m, 1H), 4.73 – 4.67 (m, 1H), 4.29 – 4.28 (m, 1H), 3.98 (d, *J* = 3.3 Hz, 1H), 3.78 (s, 3H), 3.76 (s, 3H), 3.53 (s, 3H). ^{13}C-NMR (100 MHz, $CDCl_3$): 169.1, 168.3, 159.2, 157.2, 153.2, 133.8, 130.7, 126.6, 125.4, 121.0, 119.0, 117.6, 113.9, 109.4, 84.7, 66.7, 55.3, 54.0, 52.6, 52.0. HRMS (ESI, Q-TOF) *m/z*: $[M + Na]^+$ Calculated for $C_{24}H_{24}O_9Na$ 479.1318, found 479.1318.

Dimethyl-2-(4-(((4-bromobenzyl)oxy)carbonyl)-5-hydroxy-2-(4-methoxyphenyl)-2,3-dihydrobenzo

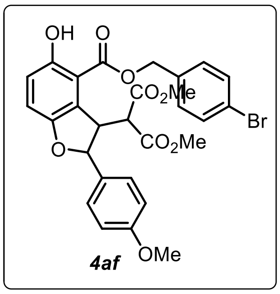

furan-3-yl)malonate (4af): 1a (0.1 g, 0.37 mmol), **2f** (0.144 g, 0.45 mmol), **4af** (0.170 g, 0.29 mmol) Yield: 78% Nature: White solid Melting point: 154-156 ºC R_f: 0.5 (acetone:hexane = 10:90) ^{1}H-NMR (400 MHz, $CDCl_3$): δ 10.50 (s, 1H), 7.48 (s, 2H), 7.30 (d, *J* = 8.7 Hz, 2H), 7.22 (d, *J* = 8.3 Hz, 2H), 7.06 (d, *J* = 8.9 Hz, 1H), 6.89 (d, *J* = 8.9 Hz, 1H), 6.82 (d, *J* = 8.7 Hz, 2H), 5.84 (s, 1H), 5.40 (d, *J* = 11.9 Hz, 1H), 5.07 (d, *J* = 11.9 Hz, 1H), 4.22 – 4.12 (m, 1H), 3.76 (s, 3H), 3.72 (d, *J* = 3.6 Hz, 1H), 3.62 (s, 3H), 3.49 (s, 3H). ^{13}C-NMR (100 MHz, $CDCl_3$): 169.2, 168.6, 168.2, 159.2, 157.4, 153.1, 133.7, 133.1, 132.2, 130.9, 126.6, 125.1, 123.2, 119.1, 117.9, 113.9, 109.3, 84.7, 67.1, 55.3, 53.7, 52.7, 52.6, 51.9. HRMS (ESI, Q-TOF) *m/z*: $[M + H]^+$ Calculated for $C_{28}H_{26}O_9Br$ 585.0760, found 585.0760.

Dimethyl-2-(4-(((2-bromobenzyl)oxy)carbonyl)-5-hydroxy-2-(4-methoxyphenyl)-2,3-dihydrobenzo

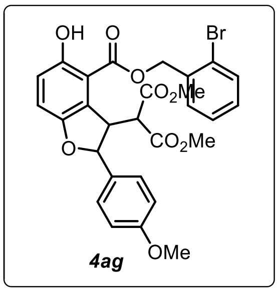

furan-3-yl)malonate (4ag): 1a (0.1 g, 0.37 mmol), **2g** (0.144 g, 0.45 mmol), **4ag** (0.155 g, 0.26 mmol). Yield: 70% Nature: White solid. Melting point: 158-160 ºC R_f: 0.5 (acetone:hexane = 10:90) ^{1}H-NMR (400 MHz, $CDCl_3$): δ 10.54 (s, 1H), 7.59 (dd, *J* = 7.8, 1.2 Hz, 1H), 7.41 (dd, *J* = 7.5, 1.8 Hz, 1H), 7.33 (d, *J* = 8.8 Hz, 3H), 7.27 – 7.24 (m, 1H), 7.06 (d, *J* = 8.8 Hz, 1H), 6.88 (d, *J* = 8.8 Hz, 1H), 6.81 (d, *J* = 8.8 Hz, 2H), 5.85 (s, 1H), 5.47 (d, *J* = 11.9 Hz, 1H), 5.30 (d, *J* = 11.9 Hz, 1H), 4.28 – 4.27 (m, 1H), 3.83 (d, *J* = 3.4 Hz, 1H), 3.76 (s, 3H), 3.57 (s, 3H), 3.48 (s, 3H). ^{13}C-NMR (100 MHz, $CDCl_3$): 169.2, 168.7, 168.4, 159.1, 157.4, 153.0, 133.7, 133.6, 133.3, 132.0, 130.8, 127.8, 126.6, 125.4, 125.0, 118.9, 117.8, 113.8, 109.3, 84.6, 67.5, 55.3, 53.6, 52.6, 51.7. HRMS (ESI, Q-TOF) *m/z*: $[M + H]^+$ Calculated for $C_{28}H_{26}O_9Br$ 585.0760, found 585.0766.

Dimethyl 2-(4-(((4-fluorobenzyl)oxy)carbonyl)-5-hydroxy-2-(4-methoxyphenyl)-2,3-dihydrobenzo

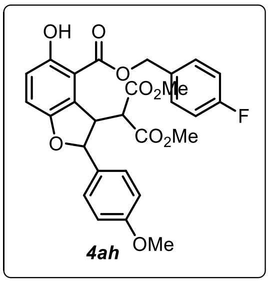

furan-3-yl)malonate (4ah): 1a (0.1 g, 0.37 mmol), **2h** (0.117 g, 0.45 mmol), **4ah** (0.132 g, 0.25 mmol) Yield: 68% Nature: Viscous liquid. R_f: 0.5 (acetone:hexane = 10:90) ^{1}H-NMR (400 MHz, $CDCl_3$): δ 10.53 (s, 1H), 7.36 – 7.27 (m, 4H), 7.04 (dd, *J* = 11.6, 5.0 Hz, 3H), 6.88 (d, *J* = 8.8 Hz, 1H), 6.82 (d, *J* = 8.8 Hz, 2H), 5.83 (d, *J* = 1.1 Hz, 1H), 5.45 – 5.39 (m, 1H), 5.09 (d, *J* = 11.8

Hz, 1H), 4.17 – 4.15 (m, 1H), 3.76 (s, 3H), 3.71 (d, *J* = 3.6 Hz, 1H), 3.61 (s, 3H), 3.48 (s, 3H). ^{13}C-NMR (100 MHz, $CDCl_3$): 169.2, 168.7, 168.2, 163.0 (d, *J* = 248.4 Hz), 159.2, 157.3, 153.1, 133.7, 131.3, 130.1 (d, *J* = 3.1 Hz), 126.6, 125.1, 119.0, 117.8, 116.0 (d, *J* = 21.8 Hz), 113.8, 109.4, 84.7, 67.1, 55.3, 53.7, 52.6, 51.9. ^{19}F NMR (376 MHz, $CDCl_3$) δ -112.00. HRMS (ESI, Q-TOF) *m/z*: $[M + H]^+$ Calculated for $C_{28}H_{26}O_9F$ 525.1561, found 525.1553.

Dimethyl 2-(5-hydroxy-2-(4-methoxyphenyl)-4-(phenethoxycarbonyl)-2,3-dihydrobenzofuran-3-yl)malonate (4ai): **1a** (0.1 g, 0.37 mmol), **2i** (0.115 g, 0.45 mmol), **4ai** (0.155 g, 0.297 mmol) Yield: 80% Nature: White solid Melting point: 109-110 ºC R_f: 0.5 (acetone:hexane = 10:90) ^{1}H-NMR (400 MHz, $CDCl_3$): δ 10.52 (s, 1H), 7.28 (d, *J* = 8.7 Hz, 2H), 7.20 – 7.11 (m, 5H), 7.06 (d, *J* = 8.8 Hz, 1H), 6.88 (d, *J* = 8.8 Hz, 1H), 6.83 (d, *J* = 8.7 Hz, 2H), 5.87 (d, *J* = 1.1 Hz, 1H), 4.58 – 4.52 (m, 2H), 4.25 – 4.23 (m, 1H), 3.95 (d, *J* = 3.8 Hz, 1H), 3.78 (s, 3H), 3.76 (s, 3H), 3.55 (s, 3H), 2.99 (t, *J* = 7.0 Hz, 2H). ^{13}C-NMR (100 MHz, $CDCl_3$): 169.4, 169.0, 168.2, 159.2, 157.2, 153.2, 136.8, 133.7, 128.8, 128.6, 126.9, 126.6, 125.2, 119.0, 117.6, 113.9, 109.5, 84.9, 66.4, 55.3, 54.1, 52.7, 52.6, 51.9, 34.6. HRMS (ESI, Q-TOF) *m/z*: $[M + Na]^+$ Calculated for $C_{29}H_{28}O_9Na$ 543.1631, found 543.1631.

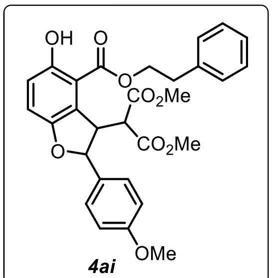

4ai

Dimethyl-2-(5-hydroxy-7-methoxy-4-(methoxycarbonyl)-2-(4-methoxyphenyl)-2,3-dihydrobenzo furan-3-yl)malonate (4aj): **1a** (0.1 g, 0.37 mmol), **2j** (0.088 g, 0.45 mmol), **4aj** (0.095 g, 0.20 mmol) Yield: 54% Nature: White solid. Melting point: 144-146 ºC R_f: 0.5 (acetone:hexane = 10:90) ^{1}H-NMR (400 MHz, $CDCl_3$): δ 10.93 (s, 1H), 7.32 (d, *J* = 8.6 Hz, 2H), 6.82 (d, *J* = 8.7 Hz, 2H), 6.45 (s, 1H), 5.90 (d, *J* = 1.5 Hz, 1H), 4.29 – 4.27 (m, 1H), 3.97 (d, *J* = 4.0 Hz, 1H), 3.91 (s, 3H), 3.83 (s, 3H), 3.76 (s, 3H), 3.75 (s, 3H), 3.60 (s, 3H). ^{13}C-NMR (100 MHz, $CDCl_3$): 169.8, 169.1, 168.1, 159.7, 159.2, 150.8, 142.2, 133.6, 126.5, 125.2, 113.9, 101.4, 100.9, 85.5, 56.1, 55.3, 54.1, 52.7, 52.5, 52.1. HRMS (ESI, Q-TOF) *m/z*: $[M + H]^+$ Calculated for $C_{23}H_{25}O_{10}$ 461.1448, found 461.1441.

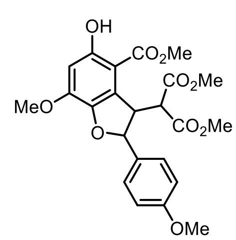

4aj

Dimethyl 2-(5-hydroxy-4-(methoxycarbonyl)-2-(4-methoxyphenyl)-2,3-dihydronaphtho[1,2-b]furan-3-yl)malonate (4ak): **1a** (0.1 g, 0.37 mmol), **2k** (0.097 g, 0.45 mmol), **4ak** (0.103 g, 0.214 mmol) Yield: 58% Nature: White solid. Melting point: 148-150 ºC R_f: 0.5 (acetone:hexane = 10:90) ^{1}H-NMR (400 MHz, $CDCl_3$): δ 11.92 (s, 1H), 8.41 (d, *J* = 8.2 Hz, 1H), 8.04 (d, *J* = 8.2 Hz, 1H), 7.69 – 7.64 (m, 1H), 7.60 – 7.54 (m, 1H), 7.36 (d, *J* = 8.5 Hz, 2H), 6.80 (d, *J* = 8.8 Hz, 2H), 6.04 (d, *J* = 1.6 Hz, 1H), 4.39 – 4.38 (m, 1H), 4.02 (d, *J* = 4.1 Hz, 1H), 3.90 (s, 3H), 3.79 (s, 3H), 3.74 (s, 3H), 3.42 (s, 3H). ^{13}C-NMR (100 MHz, $CDCl_3$): 170.9, 169.3, 168.5, 159.2, 157.2, 148.5, 134.1, 129.8, 126.6, 126.5, 125.6, 124.7, 124.2, 121.7, 113.9, 102.6, 85.0, 55.3, 54.3, 53.2, 52.7, 52.6, 52.4. HRMS (ESI, Q-TOF) *m/z*: $[M + H]^+$ Calculated for $C_{26}H_{25}O_9$ 481.1499, found 481.1467.

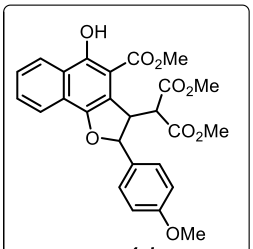

4ak

4.4.6 General procedure for the methylation:[21]

A round-bottom flask equipped with magnetic stir bar was charged 3aa (0.060 g, 0.14 mmol), K2CO3 (0.039 g, 0.28 mmol) and MeI (0.03 g, 0.21 mmol) in DMF (2 ml). On completion (as monitored by TLC), the reaction was quenched with water. The organic layer was washed with water and aqueous layer was extracted with DCM. The combined layer was dried and solvent was removed in vacuo. The crude mixture was further purified by column chromatography on silica gel with ethyl acetate/hexane as eluent to afford 5aa as a white solid.

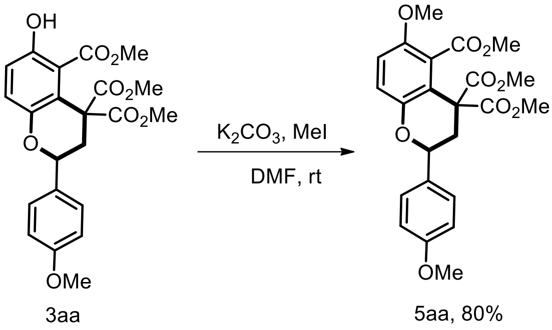

Trimethyl 6-methoxy-2-(4-methoxyphenyl)chroman-4,4,5-tricarboxylate (5aa): 3aa (0.06 g, 0.14 mmol), **5aa** (0.05 g, 0.112 mmol) Yield: 80% Nature: White solid Melting point: 164-166 ºC ^{1}H-NMR (400 MHz, $CDCl_3$): δ 7.35 (d, *J* = 8.6 Hz, 2H), 7.02 (d, *J* = 9.1 Hz, 1H), 6.95 (d, *J* = 9.2 Hz, 1H), 6.91 (d, *J* = 8.8 Hz, 2H), 4.85 (dd, *J* = 11.7, 1.4 Hz, 1H), 3.81 – 3.80 (m, 12H), 3.70 (s, 3H), 2.90 – 2.85 (m, 1H), 2.44 – 2.38 (m, 1H). ^{13}C-NMR (100 MHz, $CDCl_3$): 170.8, 170.0, 167.4, 159.7, 152.0, 149.4, 131.9, 127.4, 123.5, 120.6, 116.5, 114.5, 114.1, 74.0, 57.1, 56.0, 55.4, 53.19, 53.11, 52.2, 39.4. HRMS (ESI, Q-TOF) *m/z*: $[M + Na]^+$ Calculated for $C_{23}H_{24}O_9Na$ 467.1318, found 467.1318.

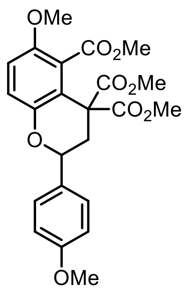

5aa

4.4.6 General procedure for the reduction:

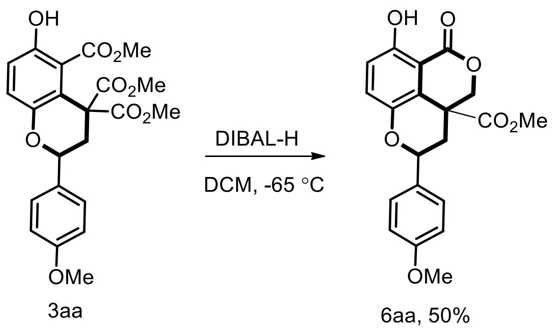

A round-bottom flask equipped with magnetic stir bar was charged **3aa** (0.05 g, 0.12 mmol) in dichloromethane at -65 ºC. After 20 minutes, DIBAL-H (0.36 mmol) was added to the reaction and the reaction was stirred at same temperature for 18 h. On completion, the reaction was quenched with ice and extracted with DCM. Added some 10% H_2SO_4 to the organic layer. Then the organic layer was washed with $NaHCO_3$ and brine. The crude mixture was purified by column chromatography on silica gel with ethyl acetate/hexane as eluent to afford **6aa** as a white solid.

Methyl 7-hydroxy-2-(4-methoxyphenyl)-6-oxo-3,3a,4,6-tetrahydro-2*H*-pyrano[3,4,5-*de*]chromene-3a-carboxylate (6aa):

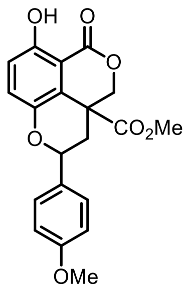

6aa

3aa (0.05 g, 0.12 mmol), **6aa** (0.022 g, 0.06 mmol). Yield: 50% Nature: White solid Melting point: 152-154 ºC ^{1}H-NMR (400 MHz, $CDCl_3$): δ 10.18 (s, 1H), 7.31 (d, *J* = 8.7 Hz, 2H), 7.13 (d, *J* = 9.2 Hz, 1H), 6.95 (d, *J* = 9.2 Hz, 1H), 6.92 (d, *J* = 8.8 Hz, 2H), 4.95 (dd, *J* = 12.1, 2.0 Hz, 1H), 4.81 (d, *J* = 10.7 Hz, 1H), 4.24 (d, *J* = 10.9 Hz, 1H), 3.81 (s, 3H), 3.79 (s, 3H), 2.56 – 2.52 (m, 1H), 1.85 – 1.79 (m, 1H). ^{13}C-NMR (100 MHz, $CDCl_3$): 172.6, 168.5, 159.9, 156.0, 145.0, 131.5, 127.5, 125.8, 119.0, 118.0, 114.2, 106.4, 74.54, 74.52, 55.4, 53.8, 43.5, 34.0. HRMS (ESI, Q-TOF) *m/z*: $[M + H]^+$ Calculated for $C_{20}H_{19}O_7$ 371.1131, found 371.1132.

4.4.7 Procedure for gram scale experiment: A round-bottom flask equipped with magnetic stir bar was charged **1a** (1.0 g, 3.78 mmol), **2a** (0.63 g, 3.78 mmol), $InCl_3$ (0.083 g, 0.378 mmol) and anhydrous DCM (40 mL) under nitrogen atmosphere. The reaction mixture is stirred at room temperature. On completion (as monitored by TLC), the reaction mixture was filtered through celite and concentrated in a rotary evaporator. The resulting crude mixture was then purified on a silica gel column using hexane/acetone as an eluent to isolate **3aa** in 52% overall yield (0.85 g, 1.97 mmol).

4.5 References

1. Taylor, A. P.; Robinson, R. P.; Fobian, Y. M.; Blakemore, D. C.; Jones, L. H.; Fadeyi, O. *Org. Biomol. Chem.* **2016**, *14*, 6611-6637.
2. Zeni, G.; Larock, R. C. *Chem. Rev.*, **2004**, *104*, 2285–2310.
3. Xiu, C. Hua, Z.; Xiao, B. S., Tang, W. J., Zhou, H. P.; Liu, X. H. *Expert Opin Ther Pat*. **2017**, *27*, 1031–1045.
4. Ahmadian, M.; Suh, J. M.; Hah, N.; Liddle, C.; Atkins, A.R.; Downes, M.; Evans, R. M. *Nature Med.* **2013**, *19,* 557–566.
5. Zolezzi, J. M.; Santos, M. J.; Bastias-Candia, S.; Pinto, C.; Godoy, J. A.; Inestrosa, N. C.; Biol *Rev Camb Philos Soc.* **2017**, *92*, 2046–2069.
6. Thevenin, M.; Thoret, S.; Grellier, P.; Dubois, J. *Bioorg. Med. Chem*. **2013**, *21*, 4885-4892.
7. Koca, M.; Kara, H.; Servi, S.; Karatas, F. *Eur. J. Med. Chem*. **2006**, *41*, 664-669.
8. (a) Schneider, T. F.; Kaschel, J.; Werz, D. B. *Angew. Chem. Int. Ed.* **2014**, *53*, 5504 – 5523. (b) Augustin, A.U.; Werz, D.B. *Acc. Chem. Res.* **2021**, *54*, 1528–1541.
9. (a) Ortega, A.; Manzano, R.; Uria, U.; Carrillo, L.; Reyes, E.; Tejero, T.; Merino, P.; Vicario, J. L. *Angew. Chem., Int. Ed*. **2018,** *57*, 8225−8229. (b) Pirenne, V.; Muriel, B.; Waser, J. *Chem. Rev*. **2021**, *121*, 227–263. (c) Xia, L.; Liu, X.; Feng, X. *Angew. Chem., Int. Ed.* **2020**, *133*, 9276-9288. (d) Petzold, M.; Jones, J.G.; Werz, D.B. *Angew. Chem. Int. Ed.* **2019**, *58*, 6225–6229. (e) Racine, S.; de Nanteuil, F.; Serrano, E.; Waser, J. *Angew. Chem., Int. Ed*. **2014**, *53*, 8484-8487.

10. (a) Carson, C. A.; Kerr, M. A. *J. Org. Chem*. **2005**, *70*, 8242-8244. (b) Kreft, A.; Jones, P. G.; Werz, D. B. *Org. Lett.* **2018**, *20*, 2059− 2062. (c) Young, I. S.; Kerr, M. A. *Angew. Chem., Int. Ed.* **2003**, *42*, 3023-3026.
11. (a) Jackson, S. K.; Karadeolian, A.; Driega, A. B.; Kerr, M. A. *J. Am. Chem. Soc.* **2008**, *130*, 4196−4201. (b) Garve, L.K.B.; Petzold, M.; Jones, P. G.; Werz, D. B. *Org. Lett.* **2016**, *18*, 564–567. (c) Das, S.; Chakrabarty, S.; Daniliuc, C.G.; Studer, A. *Org. Lett.* **2016**, *18*, 2784−2787.
12. Chagarovskiy, A. O.; Ivanova, O. A.; Rakhmankulov, E. R.; Budynina, E. M.; Trushkov, I. V.; Melnikov, M. Y. *Adv. Synth. Catal.* **2010**, *352*, 3179 – 3184.
13. (a) Verma, K.; Banerjee, P. *Adv. Synth. Catal*. **2018**, *360*, 3687- 3692. (b) Verma, K.; Banerjee, P. *Adv. Synth. Catal*. **2017**, *359*, 3848-3854.
14. (a) Ghosh, A.; Mandal, S.; Chattaraj, P. K.; Banerjee, P. *Org. Lett.* **2016**, *18*, 4940–4943. (b) Dey, R.; Banerjee, P. *Org. Lett.* **2017**, *19*, 304–307.
15. Zheng, H.; Xu, C.; Wang, Y.; Kang, T.; Liu, X.; Lin, L.; Feng, X. *Chem. Commun*. **2017**, *53*, 6585-6588.
16. Ma, C.; Huang, Y.; Zhao, Y. *ACS Catal.* **2016**, *6*, 6408-6412.
17. Vazquez, J.C.; Davis, J.; Nesterov, V.N.; Wang, H.; Luo, W. *Org. Lett*. **2021**, *23*, 3136−3140.
18. Kaur, N.; Kumar, P.; Dutt, S.; Banerjee, P. *J. Org. Chem*. **2022**, *87*, 7905–7918.
19. Saha, D.; Taily, I. M.; Banerjee, P. *Eur. J. Org. Chem.* **2021,** 5053-5057.
20. (a) Zheng, H.; Xu, C.; Wang, Y.; Kang, T.; Liu, X.; Lin, L.; Feng, X. *Chem. Commun*. **2017**, *53*, 6585-6588. (b) Chen, Y.; Li, G.-X; Peng, A.-Q; Tang, Y; Wang, L. *Org. Lett*. **2022**, *24*, 5525–5529. (c) Xi, C.-C.; Zhao, X.-J; Zhang, K, Zhang, F.-M; Dong, J.-W. Tian, J.-M; Chen, Z.-M; Tu, Y.-Q. *Org. Lett*. **2020**, *22*, 4995−5000.
21. Sun, C.; Ren, C.; Wei, Y.; Qin, B. Zeng, H. *Chem. Commun.*, **2013**, *49*, 5307-5309.

4.6 Mechanistic studies:

(S)-dimethyl 2-(4-methoxyphenyl)cyclopropane-1,1-dicarboxylate (1a):

HPLC analytical spectra

Chiralcel AD-H, Daicel Chemical Industries, Ltd., **Eluent**: Hexane/IPA (90/10); Flow rate: 0.4 ml/min; Detection: UV 226 nm; Enantiomeric mixture: $[\alpha]_D^{20}$: -222.7 (c = 0.59, CH_2Cl_2).

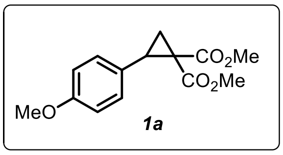

SAMPLE INFORMATION

Sample Name:	p-ome cp rac	Acquired By:	System
Sample Type:	Unknown	Sample Set Name:	pome cp rac
Vial:	1	Acq. Method Set:	Arijit
Injection #:	1	Processing Method:	Navpreet
Injection Volume:	10.00 ul	Channel Name:	226.0nm
Run Time:	30.0 Minutes	Proc. Chnl. Descr.:	2998 PDA 226.0 nm (2998
Date Acquired:	03-Oct-22 11:38:41 PM IST		
Date Processed:	06-Oct-22 12:13:44 PM IST		

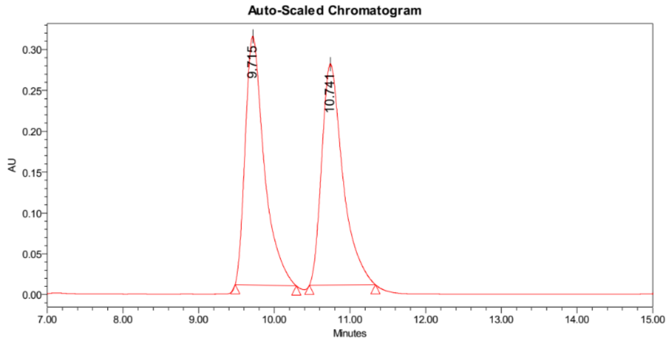

Peak Results

	RT	Area	Height	% Area
1	9.715	5340075	304244	50.29
2	10.741	5277546	270496	49.71

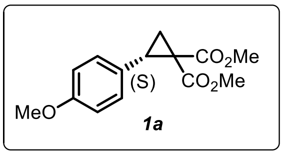

SAMPLE INFORMATION

Sample Name:	p-ome cpN chiral	Acquired By:	System
Sample Type:	Unknown	Sample Set Name:	pome cpN chiral ADH 10% pt4
Vial:	1	Acq. Method Set:	Arijit
Injection #:	1	Processing Method:	Navpreet
Injection Volume:	10.00 ul	Channel Name:	233.2nm
Run Time:	30.0 Minutes	Proc. Chnl. Descr.:	2998 PDA 233.2 nm (2998
Date Acquired:	03-Oct-22 11:59:07 PM IST		
Date Processed:	06-Oct-22 12:12:16 PM IST		

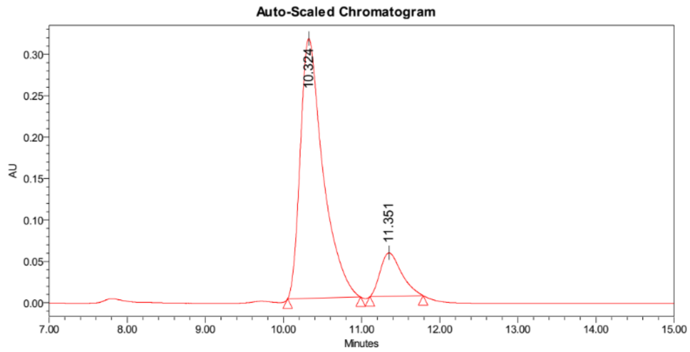

Peak Results

	RT	Area	Height	% Area
1	10.324	6359082	313575	86.50
2	11.351	992757	52484	13.50

3aa: Chiralcel AD-H, Daicel Chemical Industries, Ltd., **Eluent**: Hexane/IPA (95/10); Flow rate: 1.0 ml/min; Detection: UV 226 nm

Product with Racemic Cyclopropane

SAMPLE INFORMATION

Sample Name:	19-03-085	Acquired By:	System
Sample Type:	Unknown	Sample Set Name:	1903085 10% ADH 1 pt
Vial:	1	Acq. Method Set:	Arijit
Injection #:	1	Processing Method:	Navpreet
Injection Volume:	10.00 ul	Channel Name:	218.8nm
Run Time:	30.0 Minutes	Proc. Chnl. Descr.:	2998 PDA 218.8 nm (2998
Date Acquired:	03-Oct-22 10:42:44 PM IST		
Date Processed:	06-Oct-22 12:01:45 PM IST		

Auto-Scaled Chromatogram

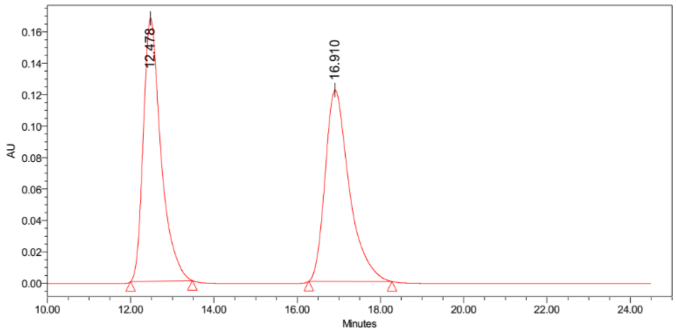

Peak Results

	RT	Area	Height	% Area
1	12.478	4924840	167205	50.15
2	16.910	4894946	121584	49.85

Product with Enantioenriched Cyclopropane

SAMPLE INFORMATION

Sample Name:	19-03-213	Acquired By:	System
Sample Type:	Unknown	Sample Set Name:	1903213 chiral 10% ADH 1 pt
Vial:	1	Acq. Method Set:	Arijit
Injection #:	1	Processing Method:	Navpreet
Injection Volume:	10.00 ul	Channel Name:	218.5nm
Run Time:	30.0 Minutes	Proc. Chnl. Descr.:	2998 PDA 218.5 nm (2998
Date Acquired:	03-Oct-22 10:15:31 PM IST		
Date Processed:	06-Oct-22 11:57:47 AM IST		

Auto-Scaled Chromatogram

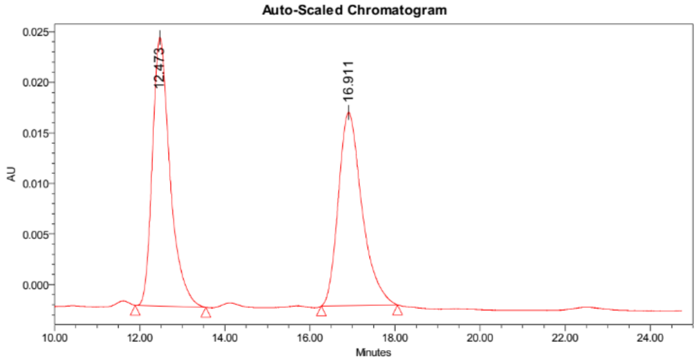

Peak Results

	RT	Area	Height	% Area
1	12.473	765696	26551	50.86
2	16.911	739684	19119	49.14

4.7 NMR spectra of compounds:

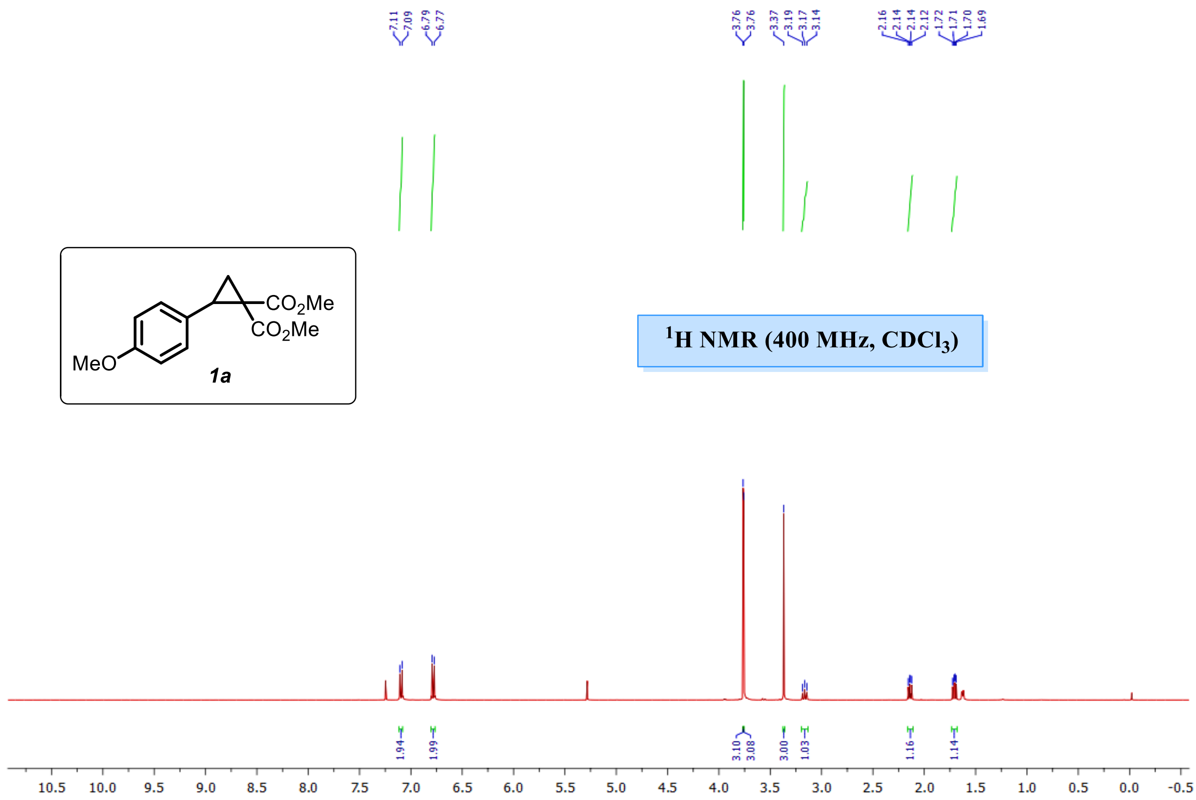

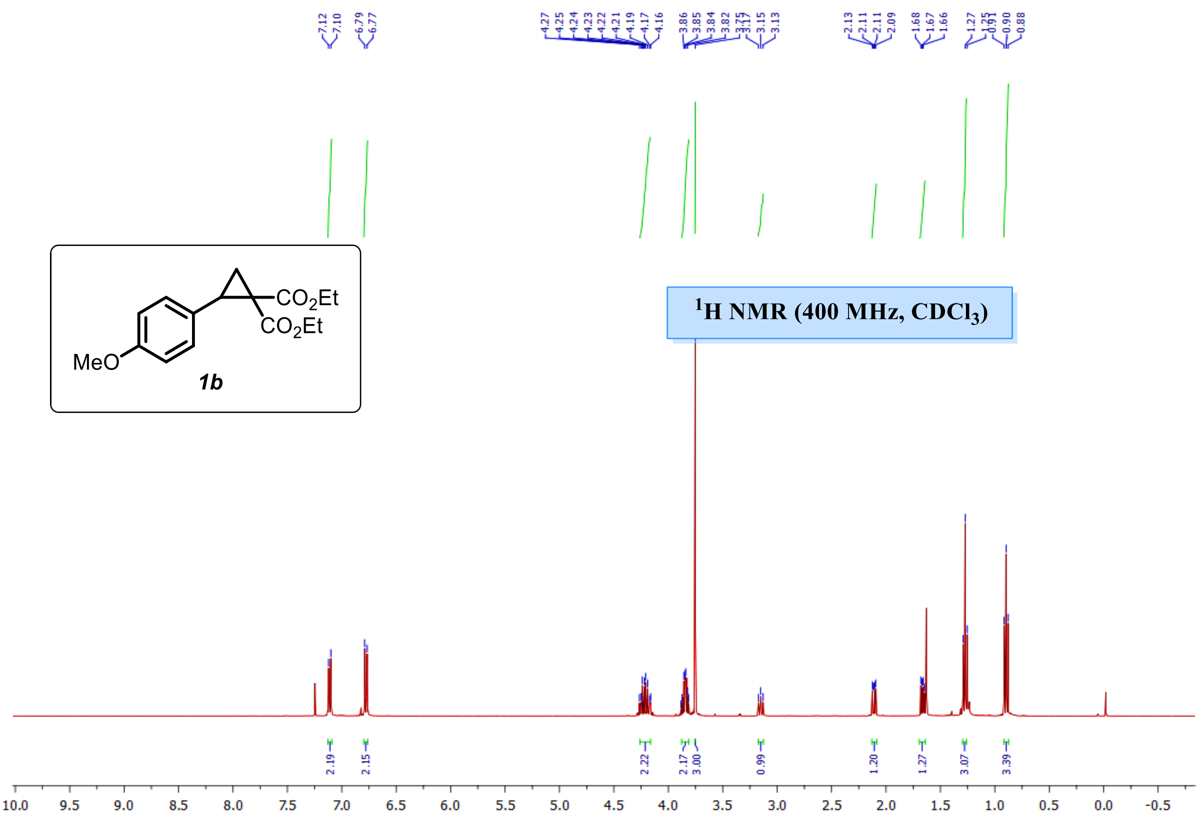

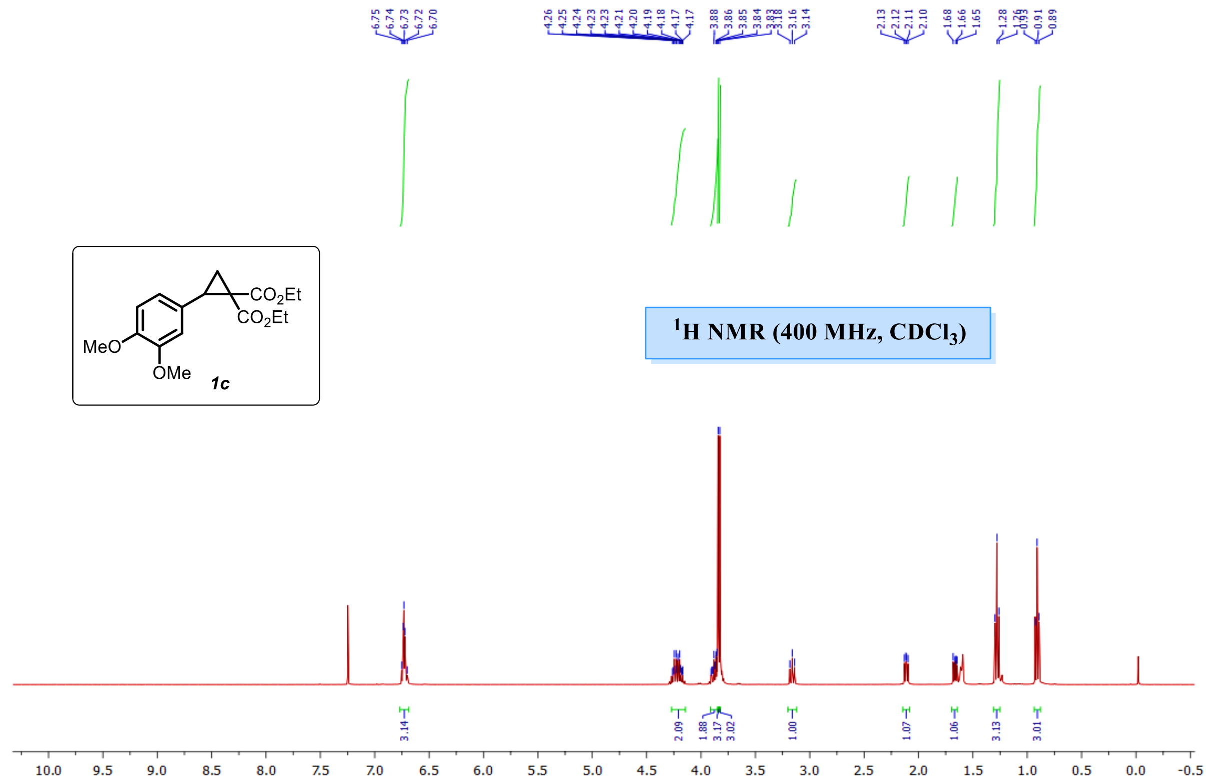

MeO
OMe
CO_2Et
CO_2Et
1c
^{1}H NMR (400 MHz, $CDCl_3$)

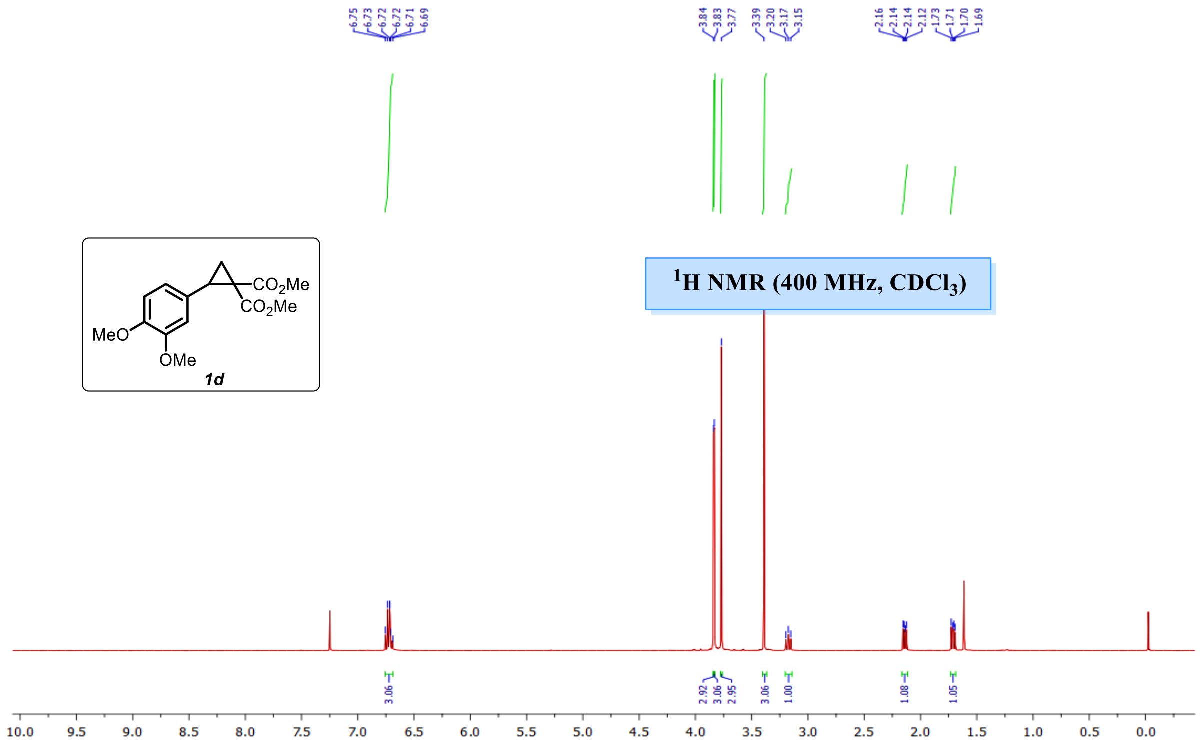

MeO
OMe
CO_2Me
CO_2Me
1d
^{1}H NMR (400 MHz, $CDCl_3$)

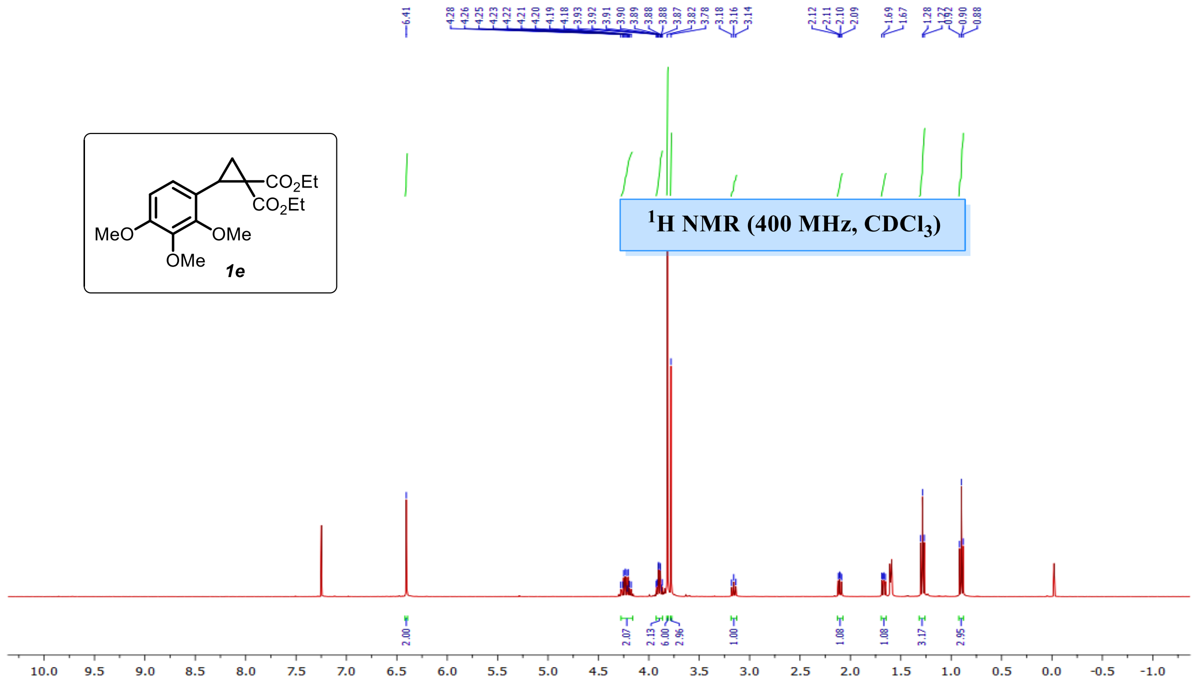
CO2Et
CO2Et
MeO
OMe
OMe
1e
1H NMR (400 MHz, CDCl3)

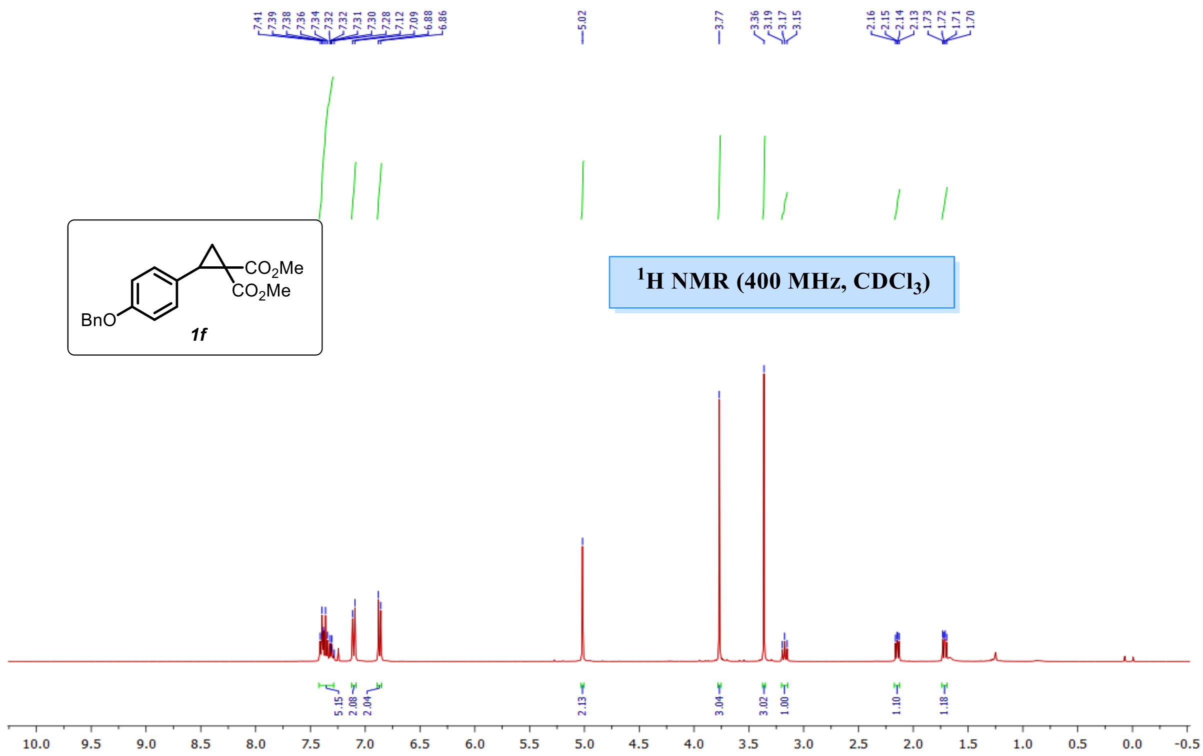
CO2Me
CO2Me
BnO
1f
1H NMR (400 MHz, CDCl3)

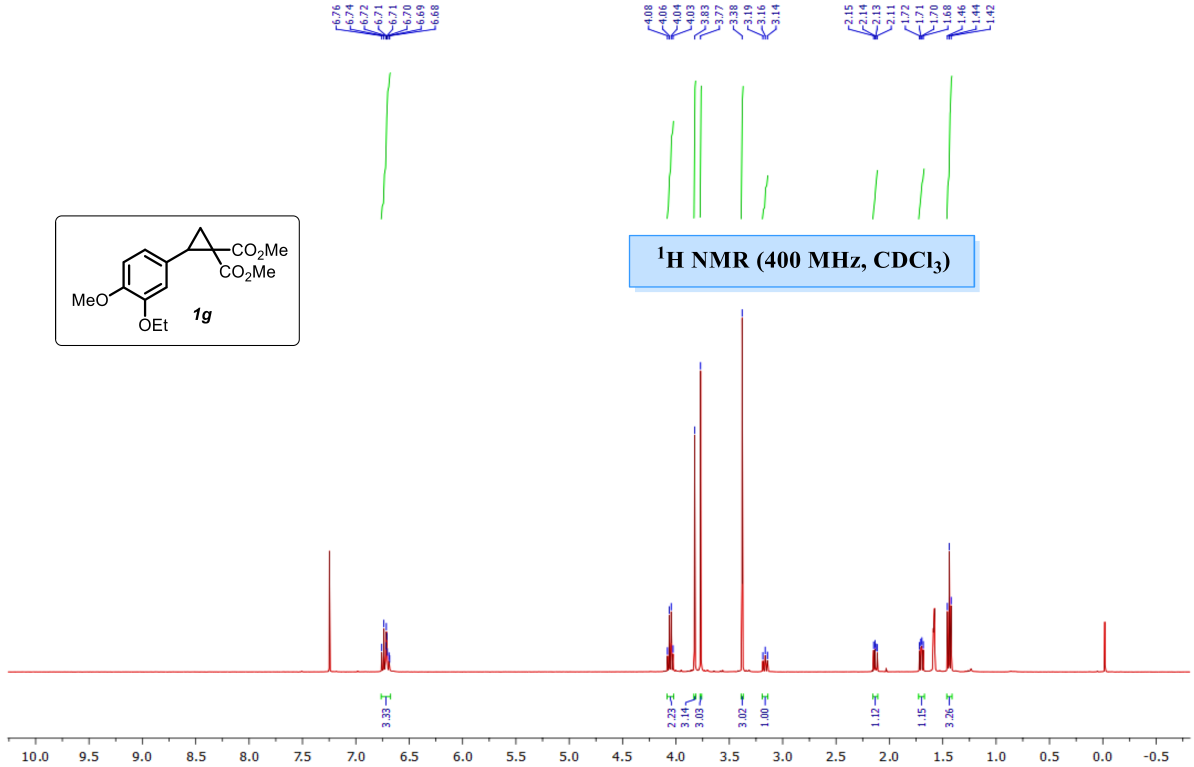
CO2Me
CO2Me
MeO
OEt
1g
1H NMR (400 MHz, CDCl3)

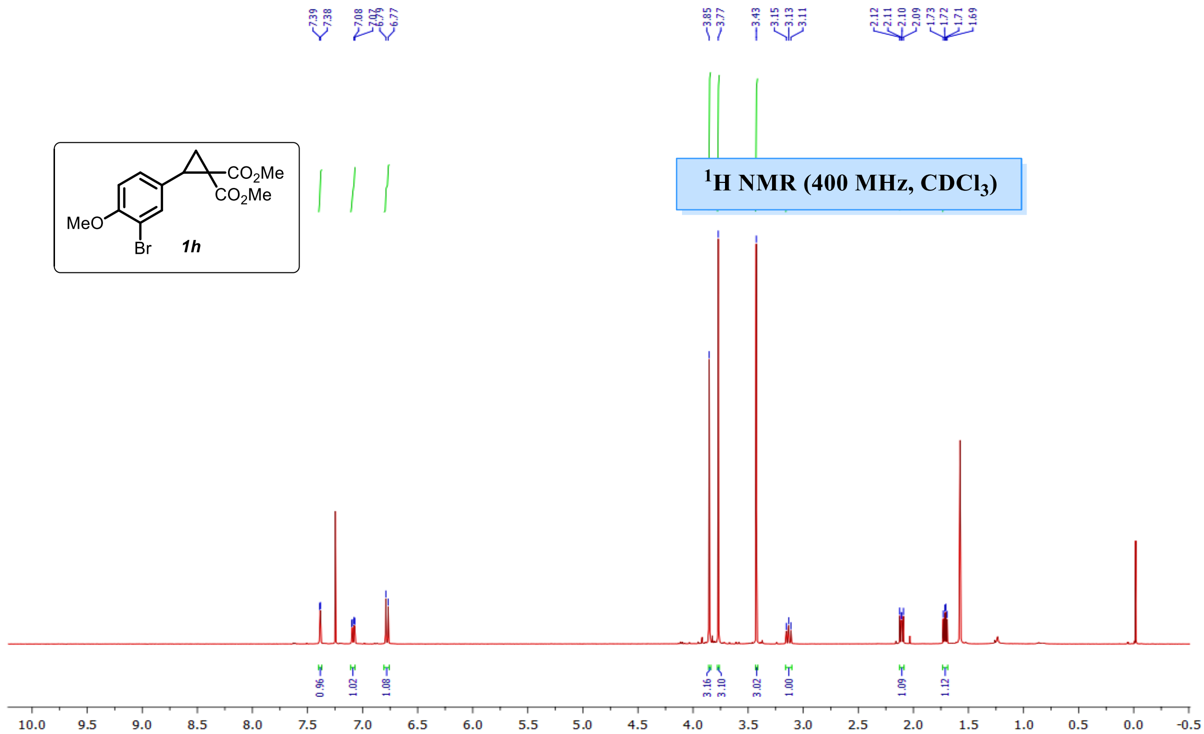
CO2Me
CO2Me
MeO
Br
1h
1H NMR (400 MHz, CDCl3)

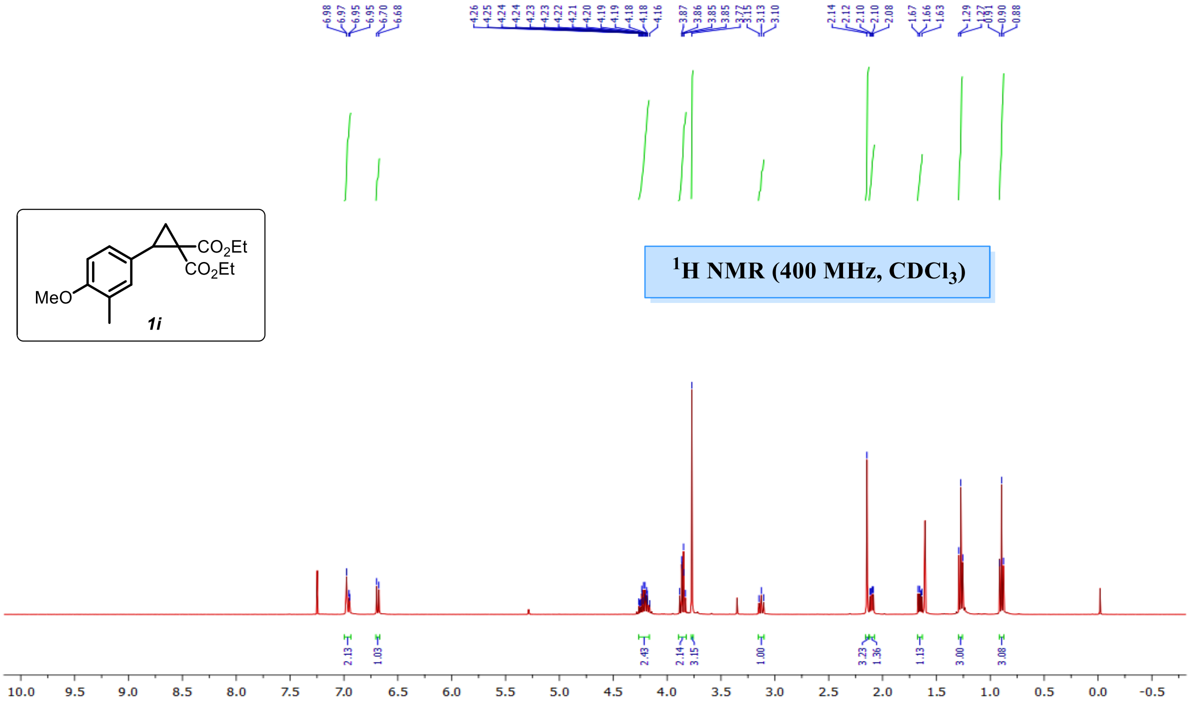
CO2Et
CO2Et
MeO
1i
1H NMR (400 MHz, CDCl3)

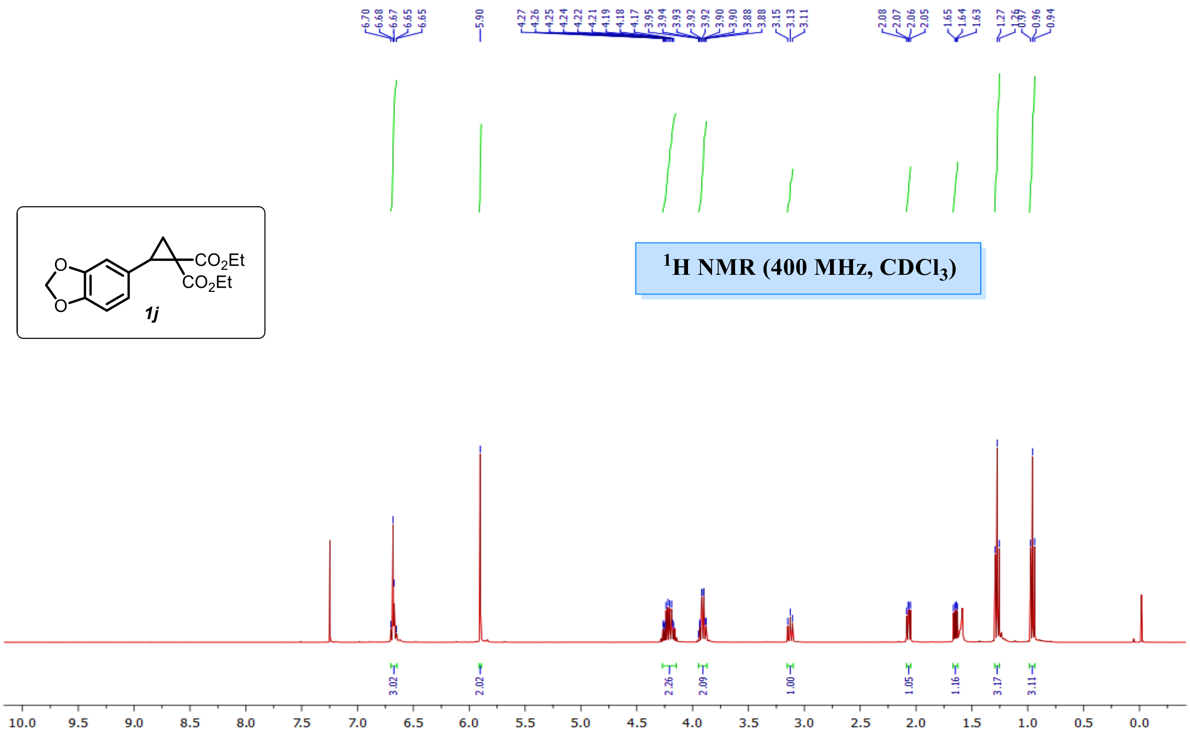
CO2Et
CO2Et
O
O
1j
1H NMR (400 MHz, CDCl3)

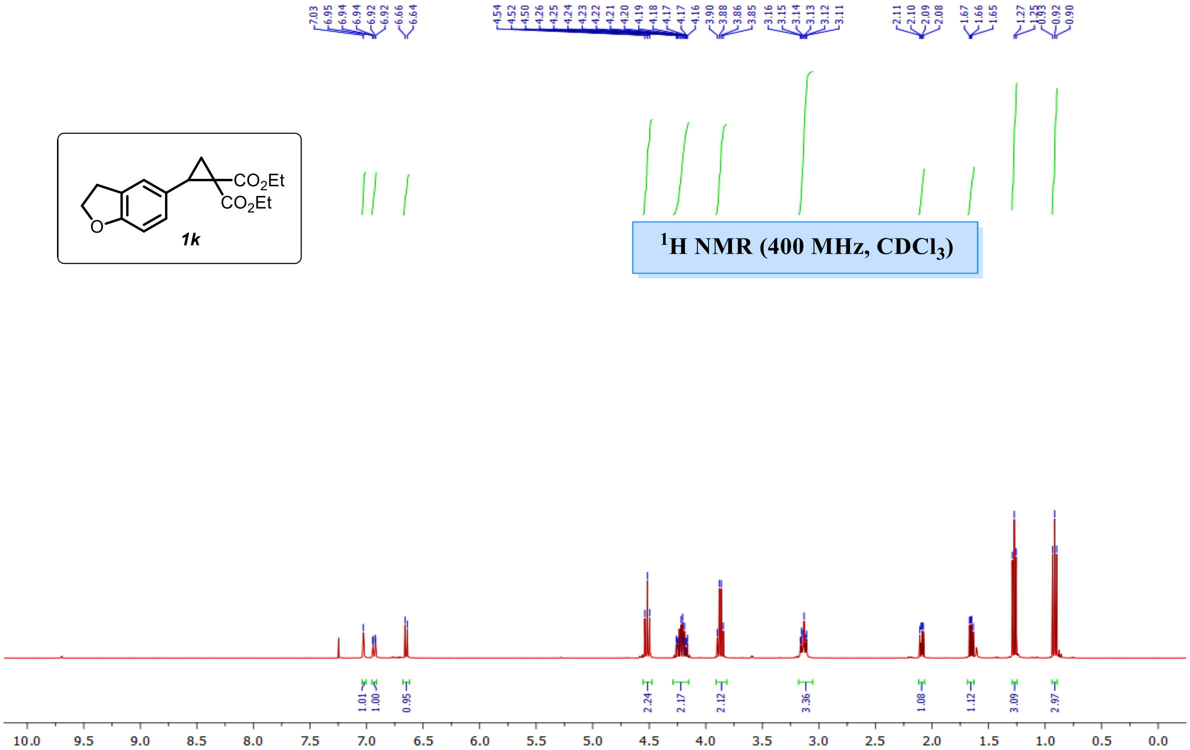
CO2Et
CO2Et
1k
1H NMR (400 MHz, CDCl3)

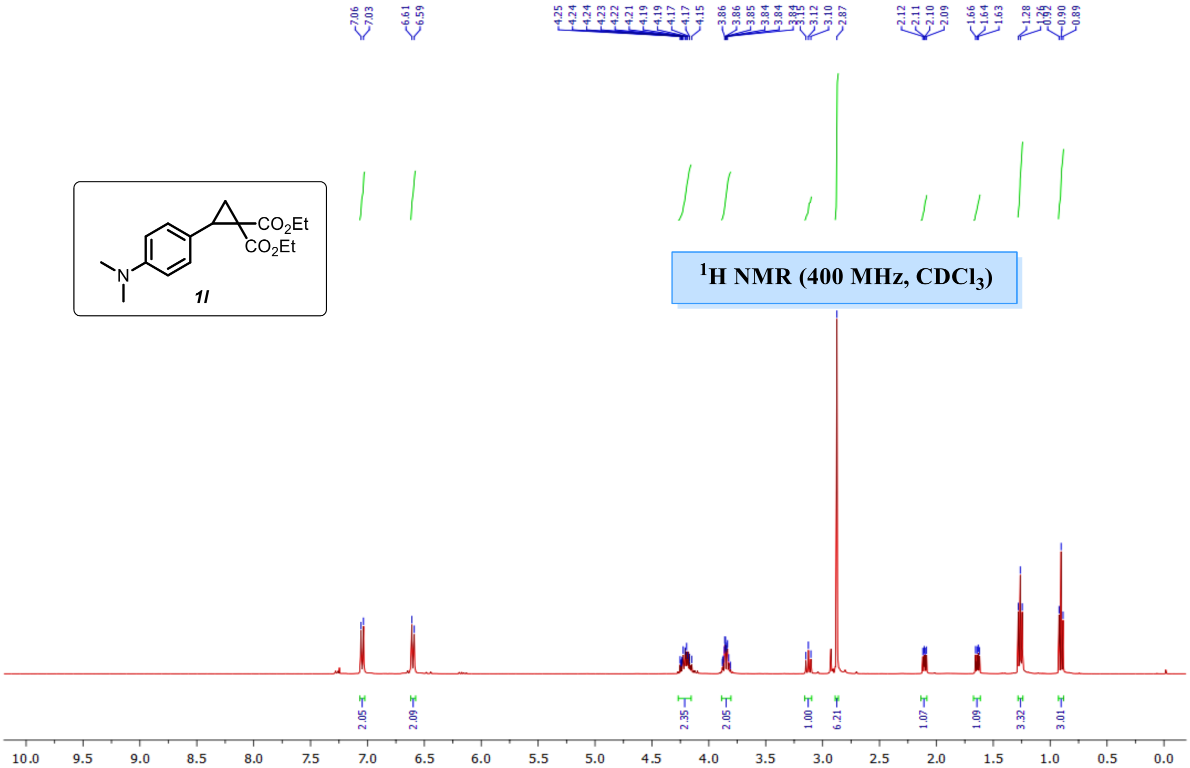
CO2Et
CO2Et
1l
1H NMR (400 MHz, CDCl3)

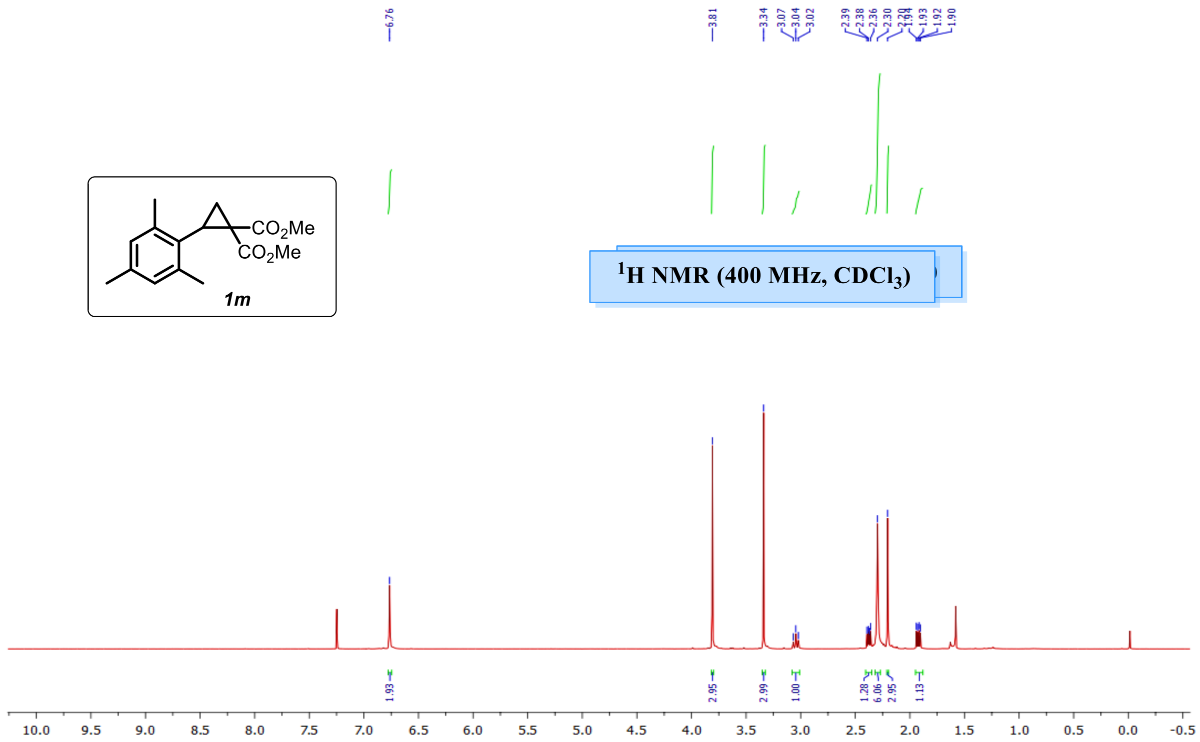
CO2Me
CO2Me
1m
1H NMR (400 MHz, CDCl3)

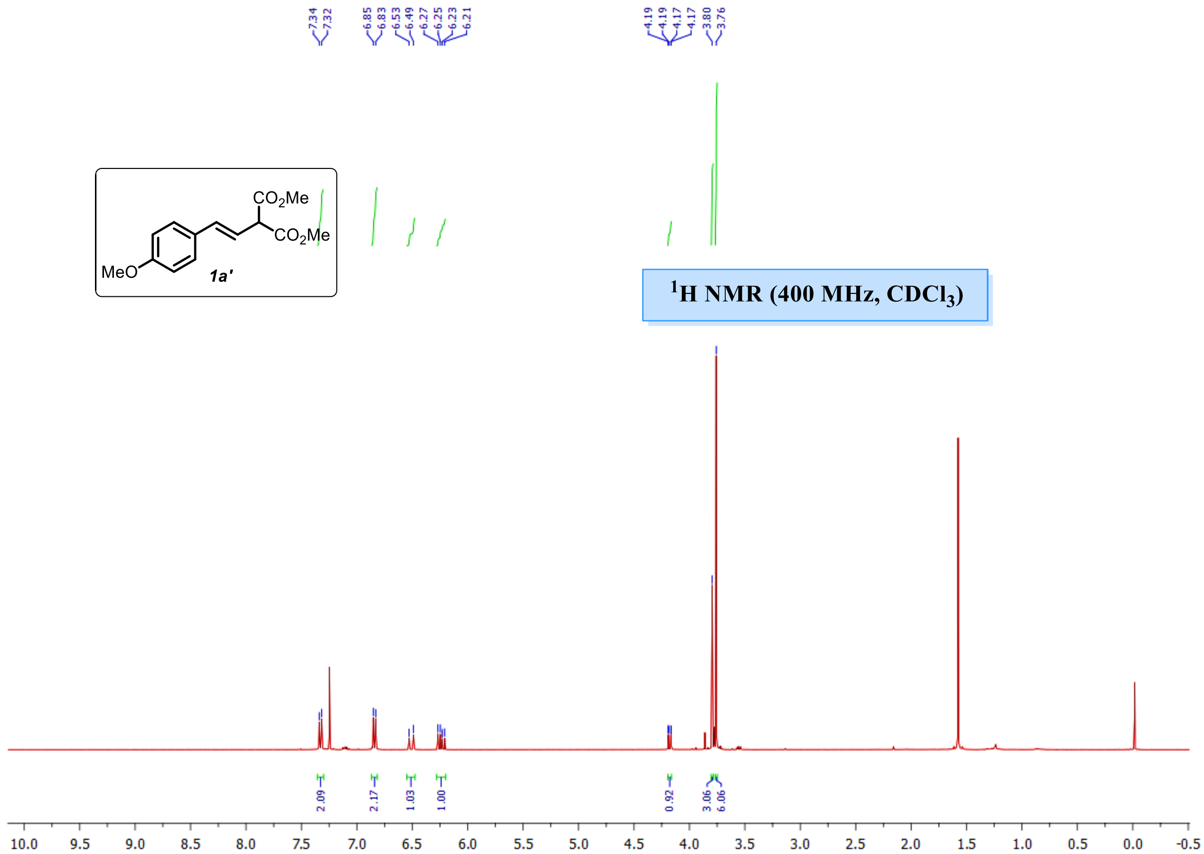
CO2Me
CO2Me
MeO
1a'
1H NMR (400 MHz, CDCl3)

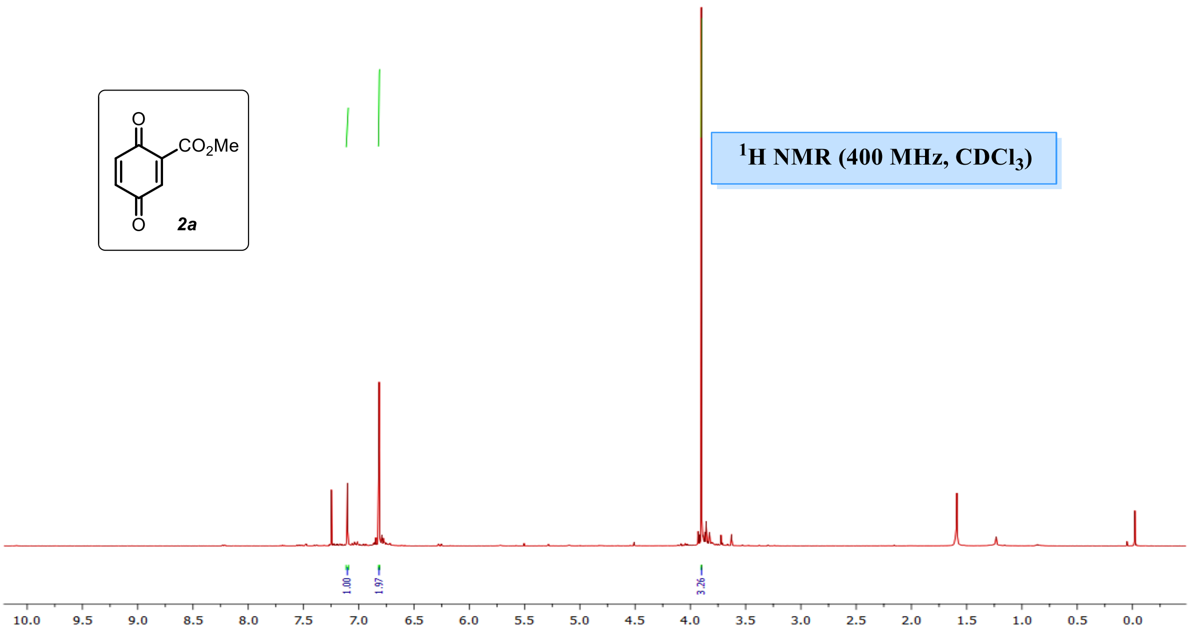
CO_2Me
2a
^1H NMR (400 MHz, $CDCl_3$)
1.00
1.97
3.26
10.0 9.5 9.0 8.5 8.0 7.5 7.0 6.5 6.0 5.5 5.0 4.5 4.0 3.5 3.0 2.5 2.0 1.5 1.0 0.5 0.0

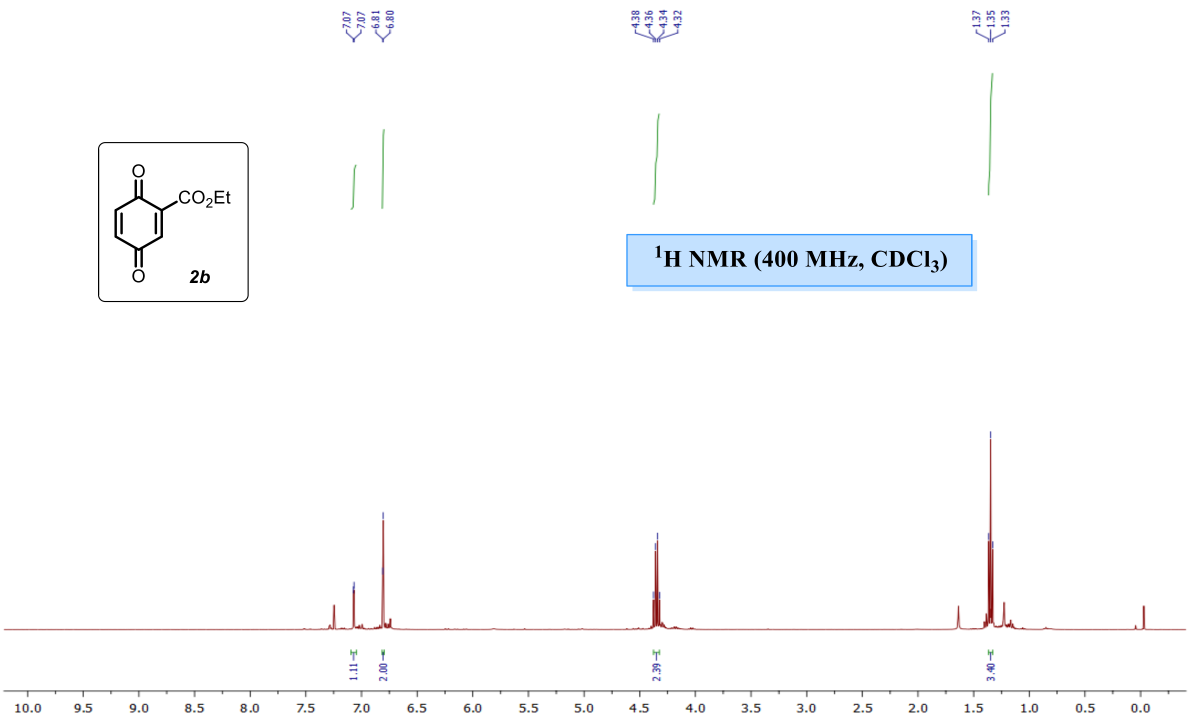
7.07
7.07
6.81
6.80
4.38
4.36
4.34
4.32
1.37
1.35
1.33
CO_2Et
2b
^1H NMR (400 MHz, $CDCl_3$)
1.11
2.00
2.39
3.40
10.0 9.5 9.0 8.5 8.0 7.5 7.0 6.5 6.0 5.5 5.0 4.5 4.0 3.5 3.0 2.5 2.0 1.5 1.0 0.5 0.0

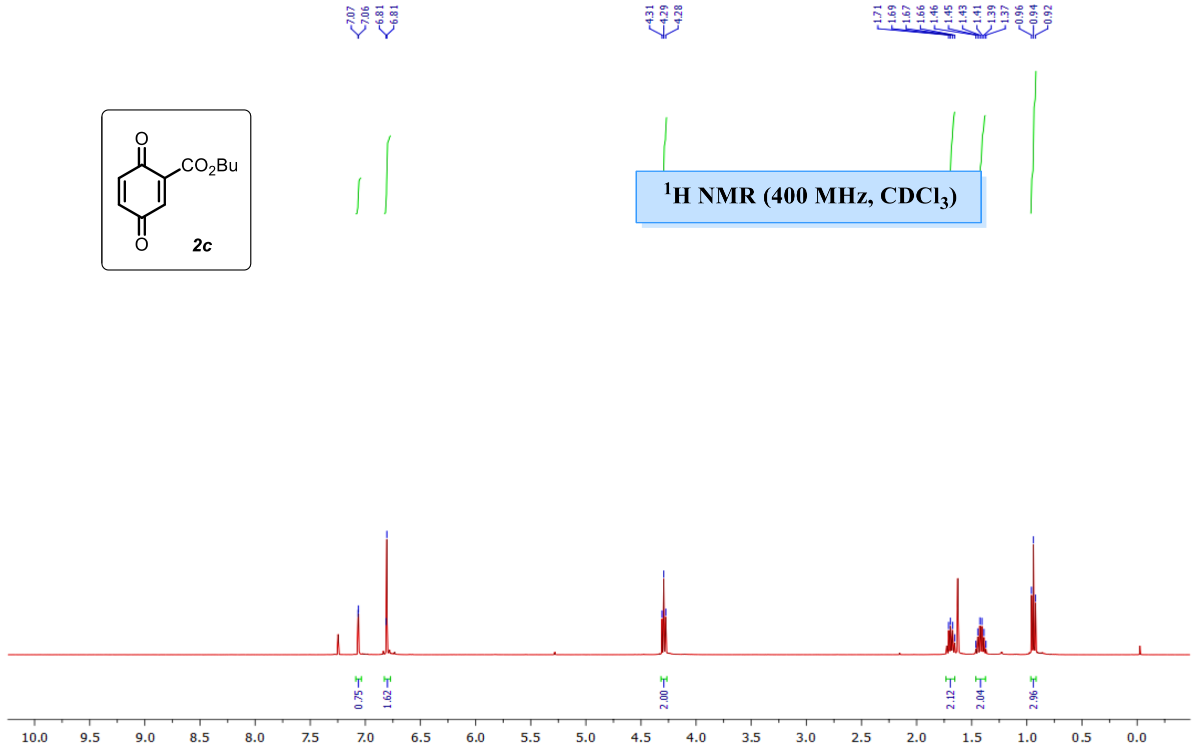
CO2Bu
2c
1H NMR (400 MHz, CDCl3)
7.07
7.06
6.81
6.81
4.31
4.29
4.28
1.71
1.69
1.67
1.66
1.46
1.45
1.43
1.41
1.39
1.37
0.96
0.94
0.92
0.75
1.62
2.00
2.12
2.04
2.96

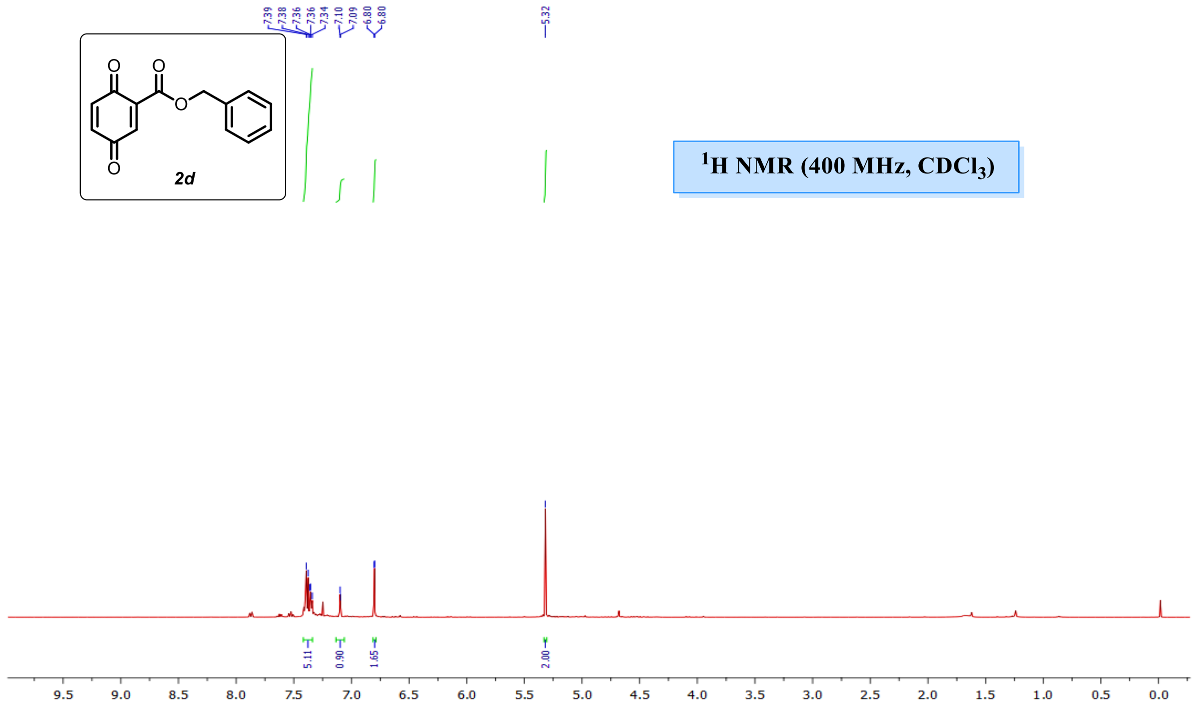
2d
1H NMR (400 MHz, CDCl3)
7.39
7.38
7.36
7.34
7.10
7.09
6.80
6.80
5.32
5.11
0.90
1.65
2.00

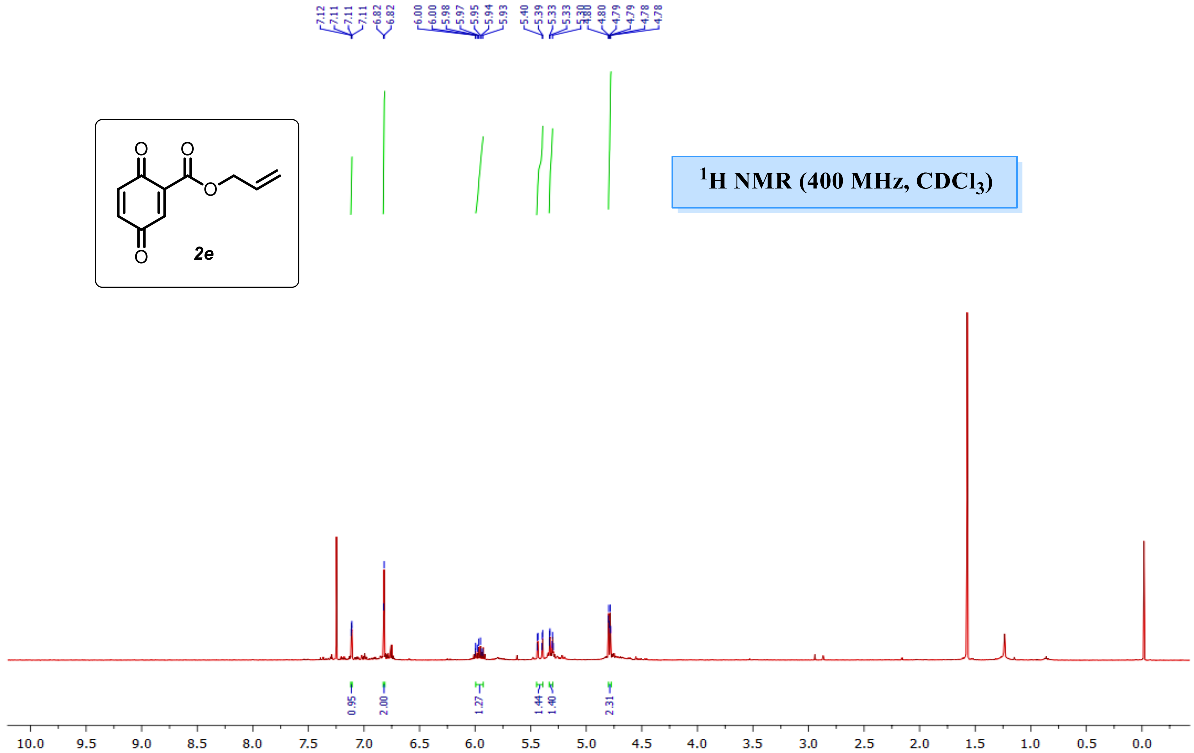
2e
^{1}H NMR (400 MHz, CDCl$_3$)

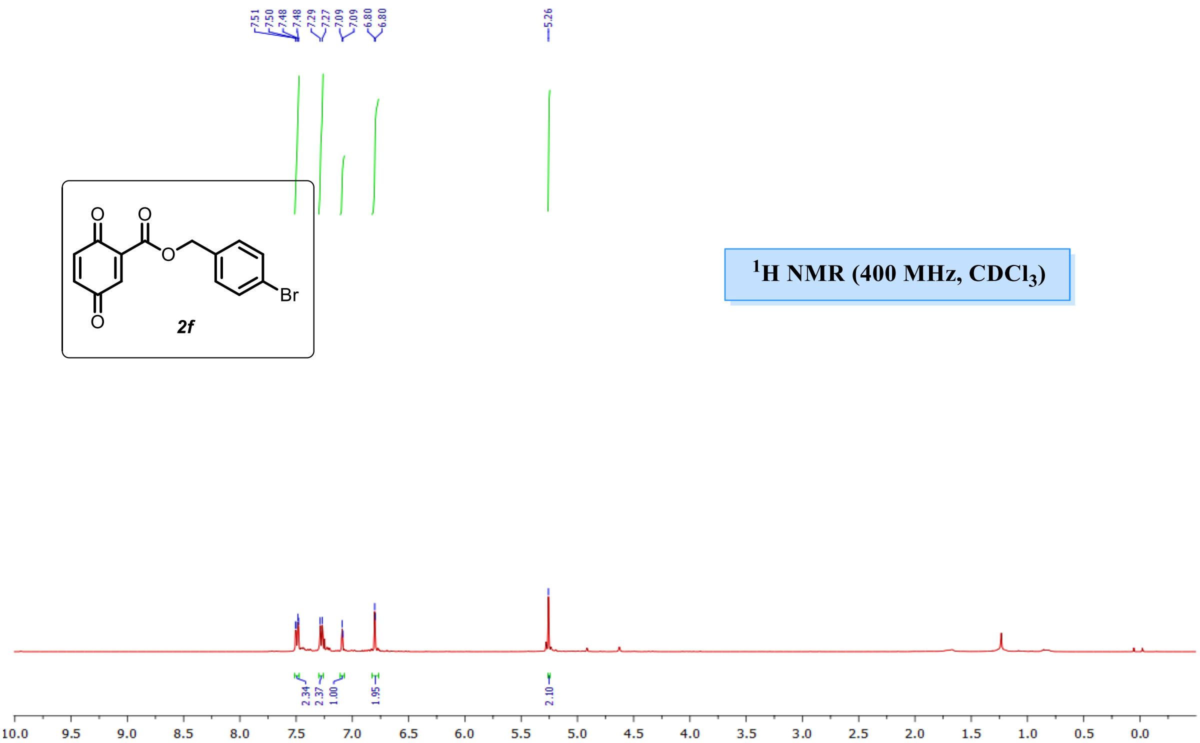
Br
2f
^{1}H NMR (400 MHz, CDCl$_3$)

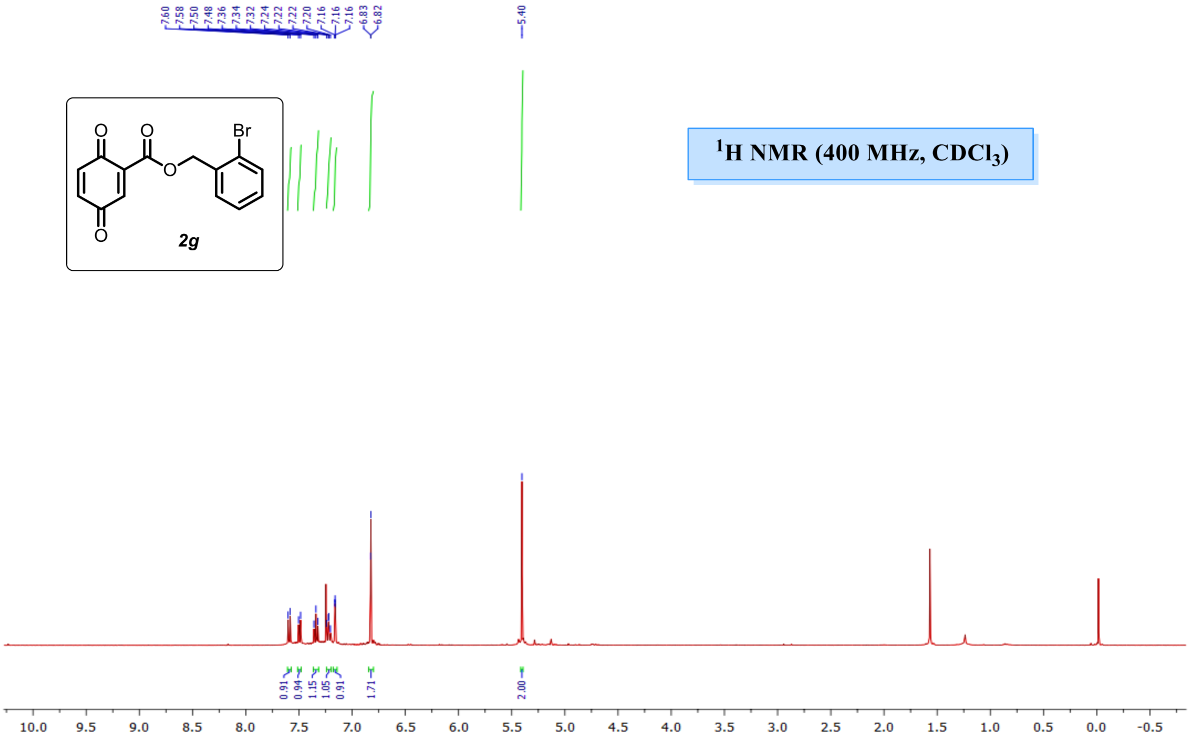

2g
1H NMR (400 MHz, CDCl3)

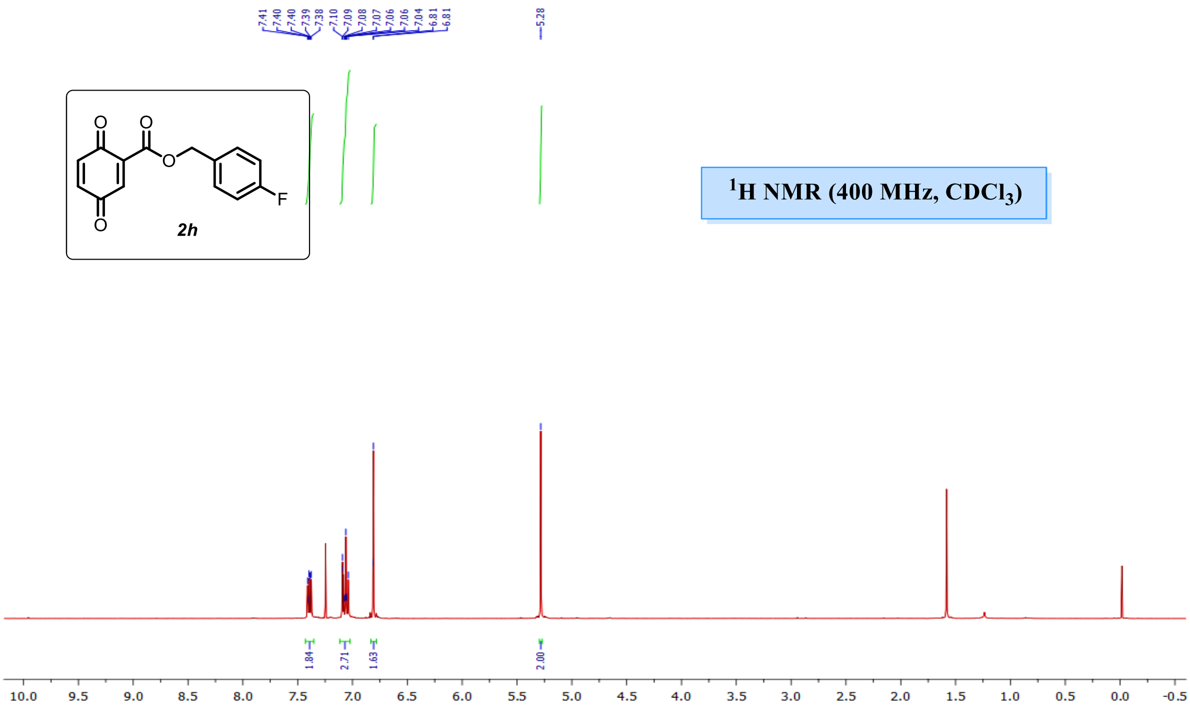

2h
1H NMR (400 MHz, CDCl3)

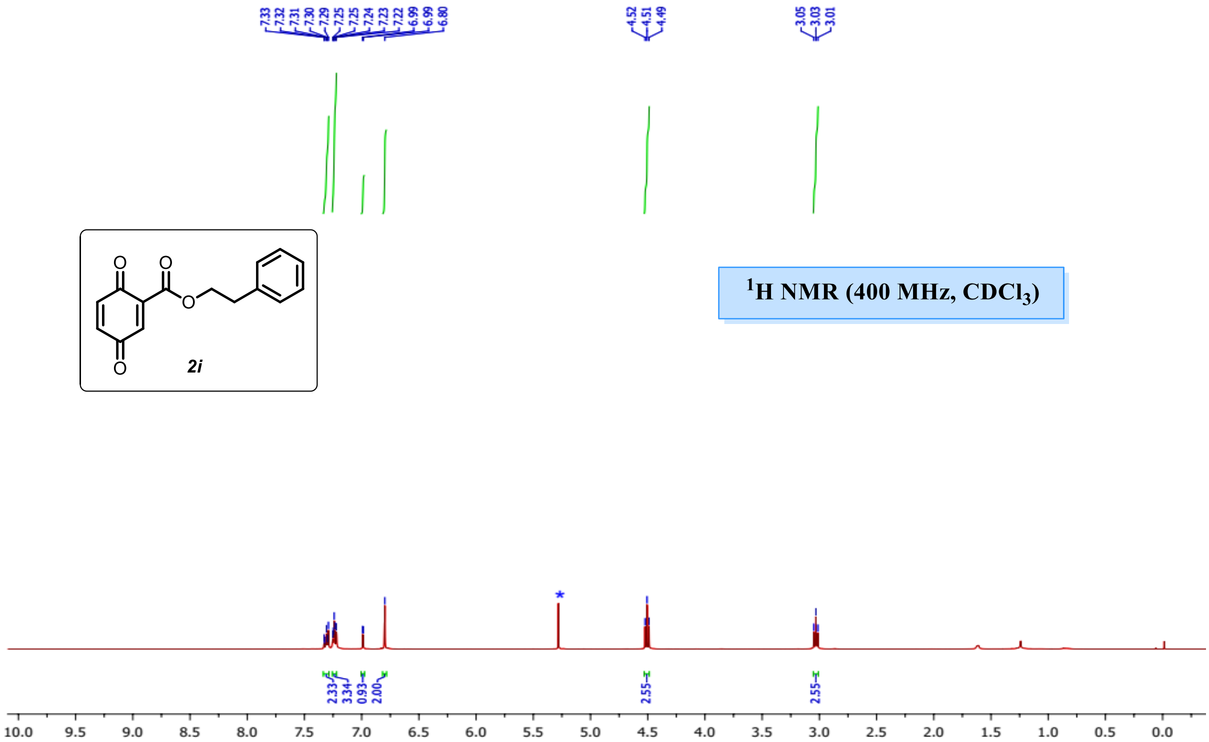
2i
^{1}H NMR (400 MHz, $CDCl_3$)

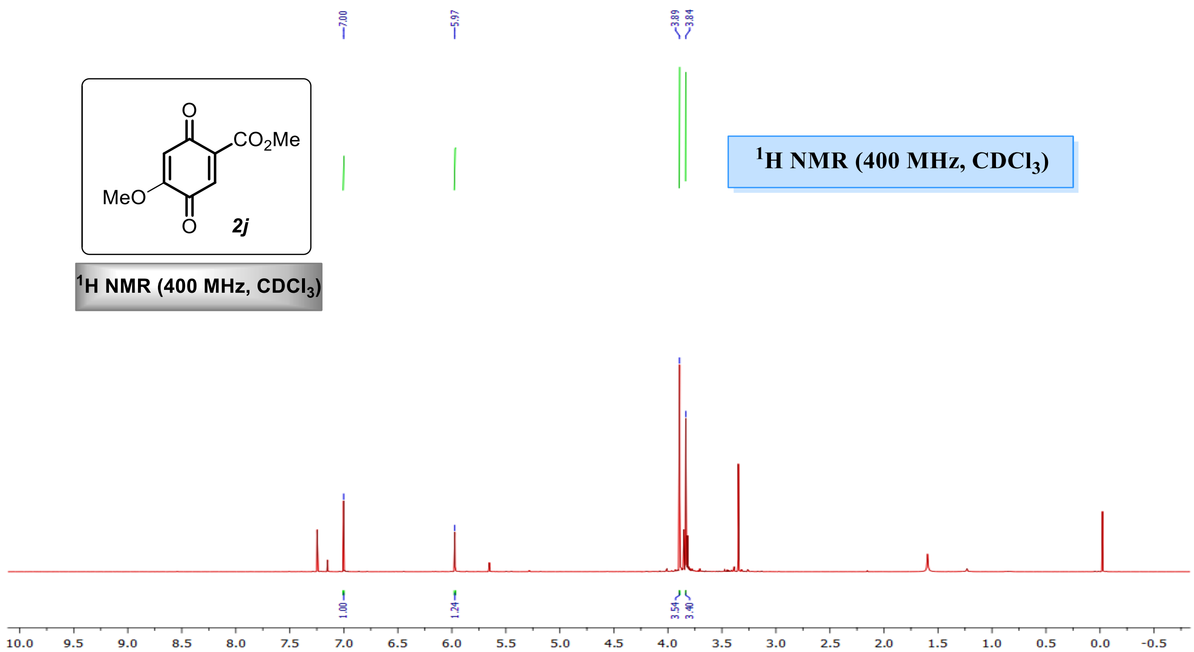
2j
^{1}H NMR (400 MHz, $CDCl_3$)
^{1}H NMR (400 MHz, $CDCl_3$)

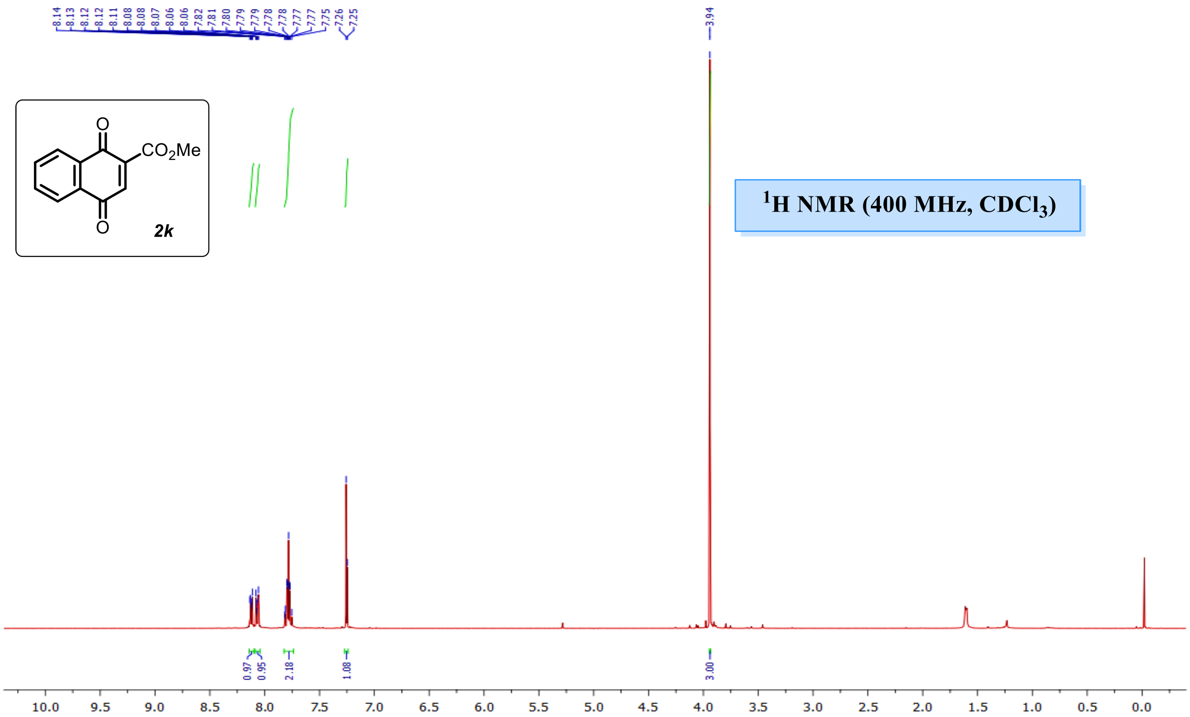
CO2Me
2k
1H NMR (400 MHz, CDCl3)

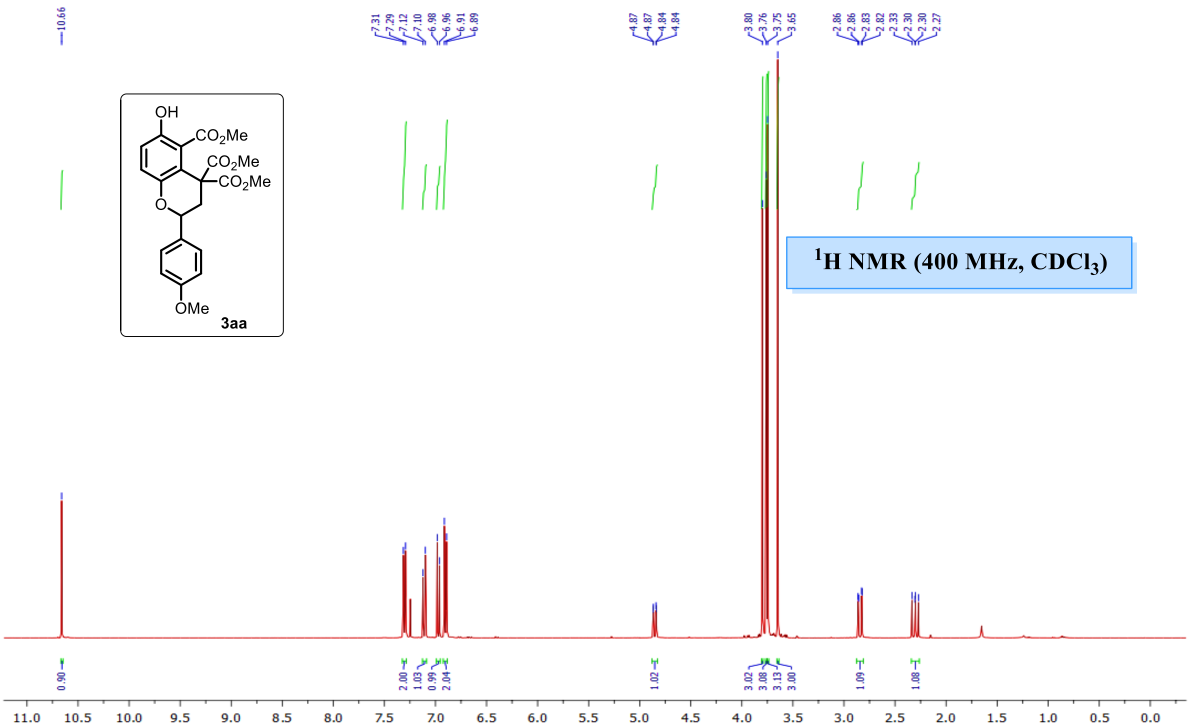
OH
CO2Me
CO2Me
CO2Me
O
OMe
3aa
1H NMR (400 MHz, CDCl3)

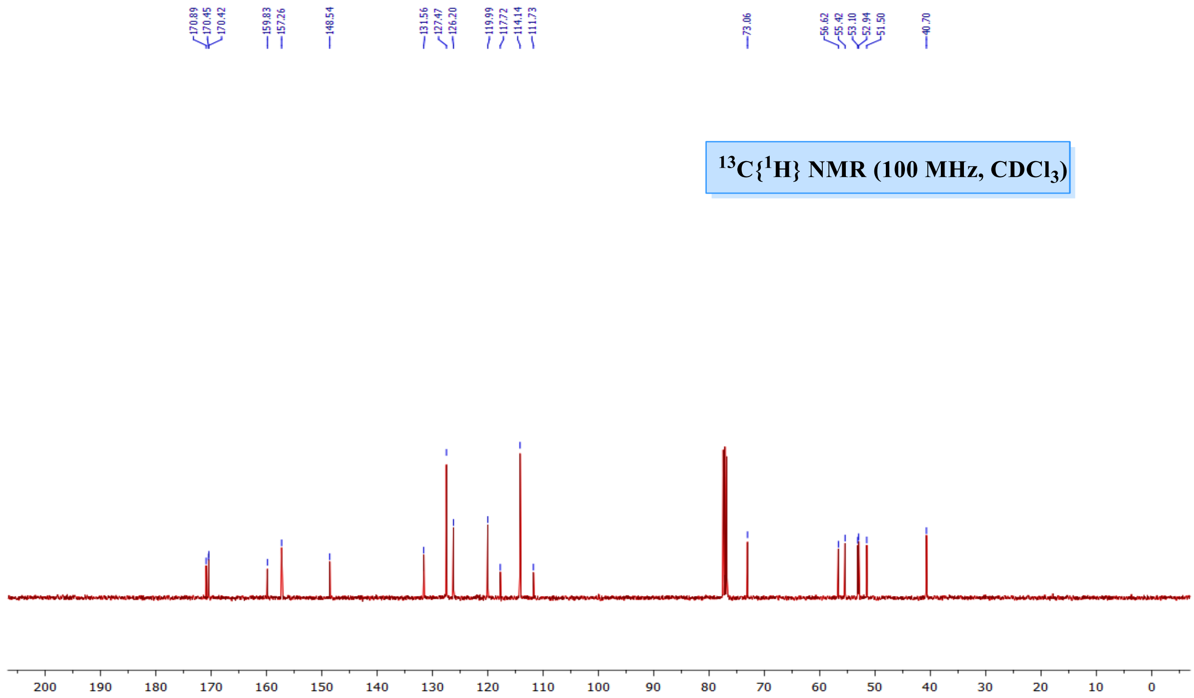
13C{1H} NMR (100 MHz, CDCl3)

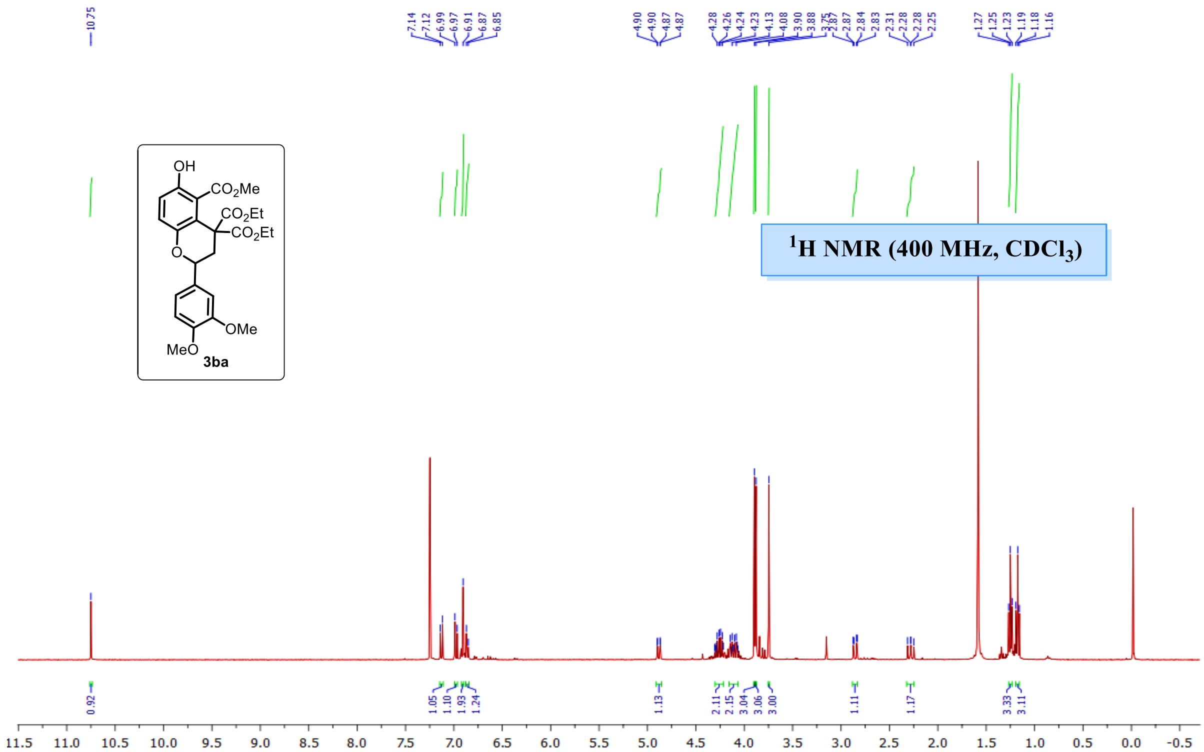
OH
CO2Me
CO2Et
CO2Et
O
OMe
MeO
3ba
1H NMR (400 MHz, CDCl3)

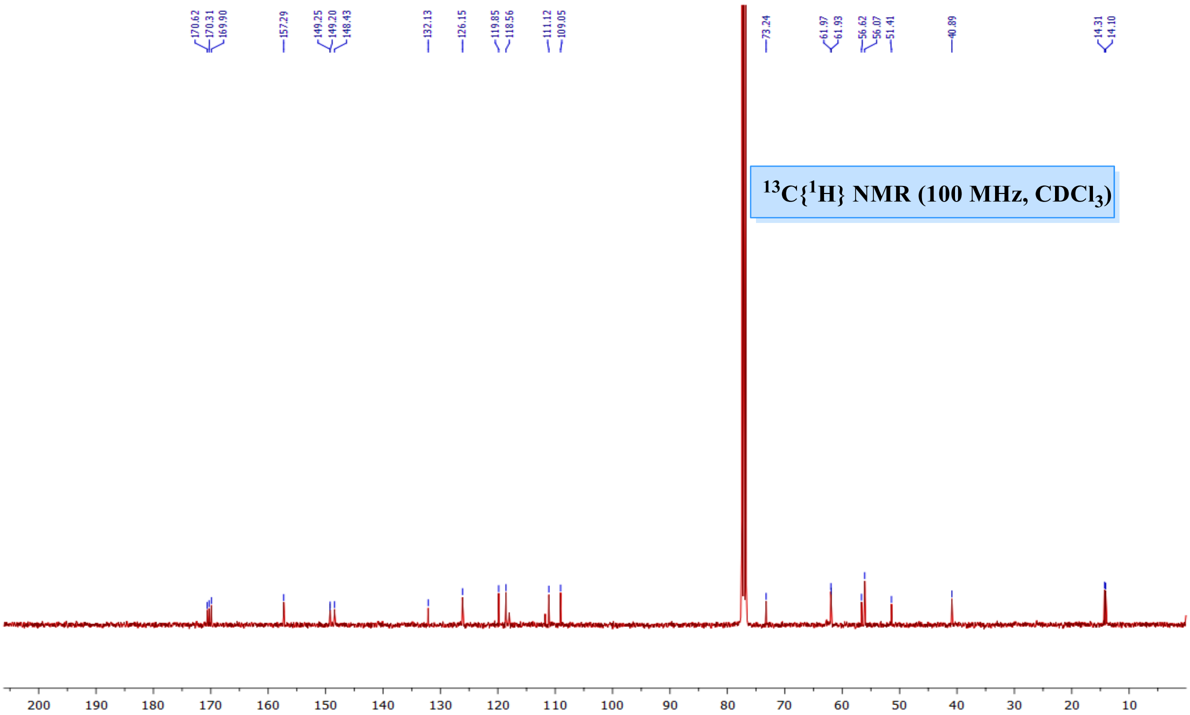
$^{13}C\{^{1}H\}$ NMR (100 MHz, $CDCl_3$)

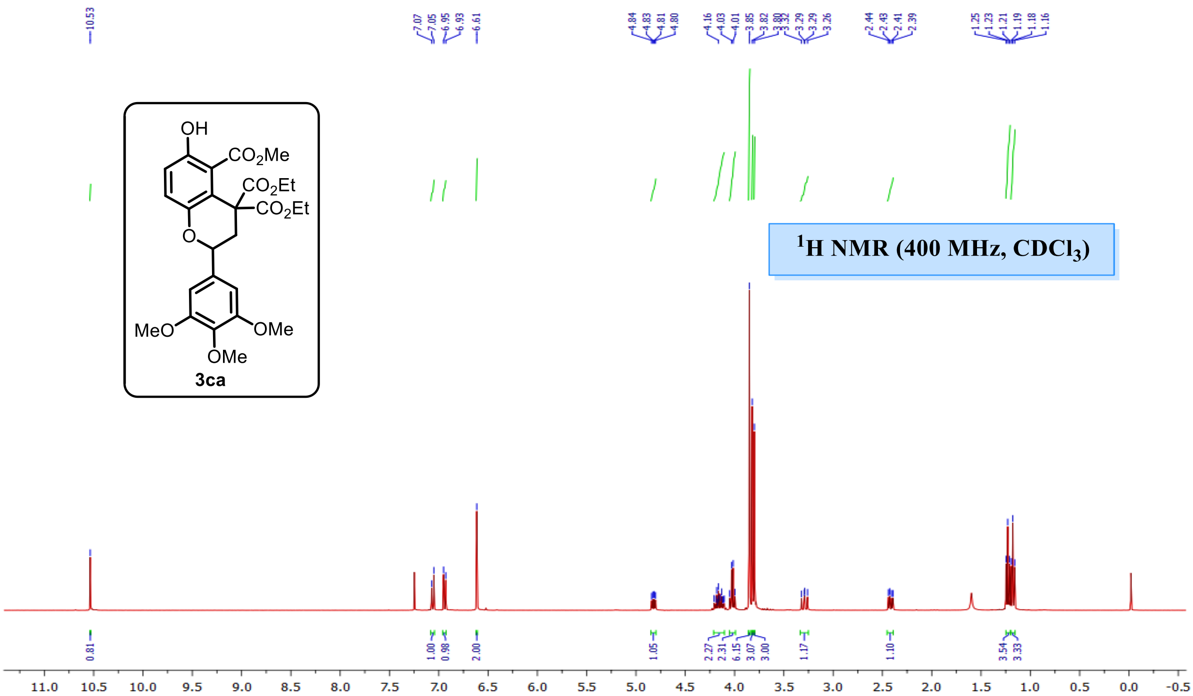
OH
CO_2Me
CO_2Et
CO_2Et
O
MeO
OMe
OMe
3ca
^{1}H NMR (400 MHz, $CDCl_3$)

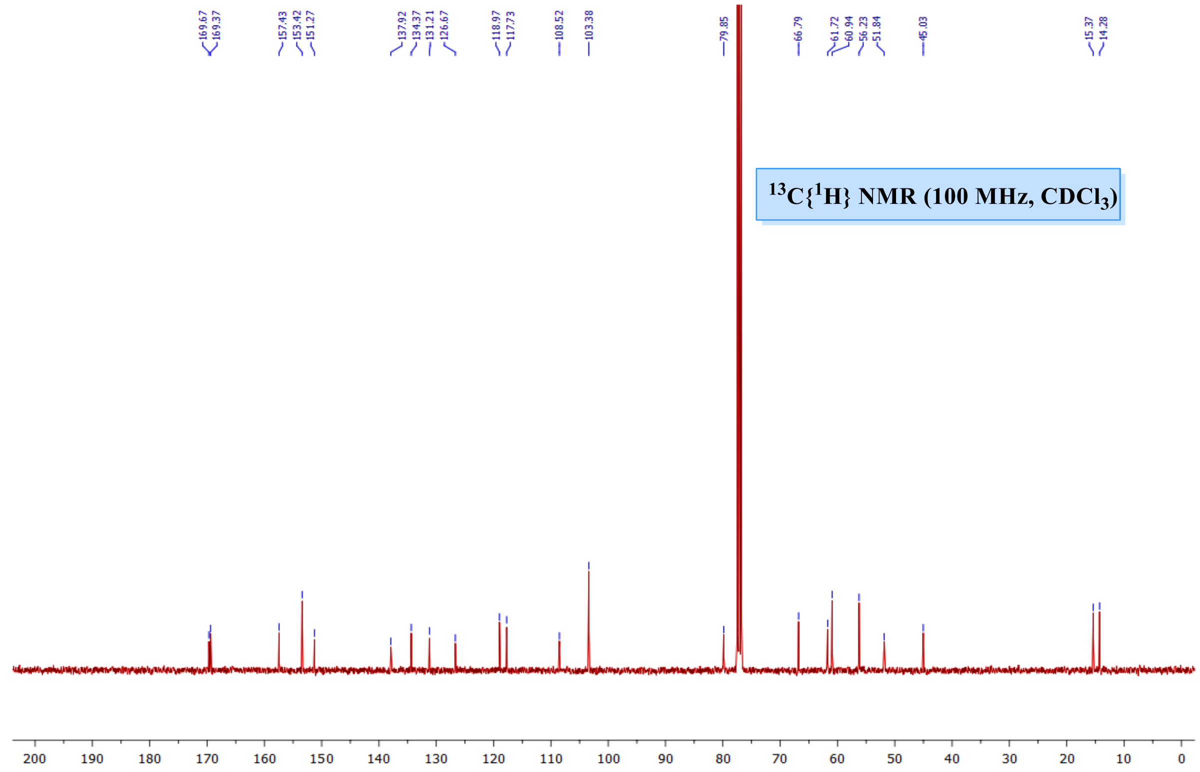
$^{13}C\{^1H\}$ NMR (100 MHz, $CDCl_3$)
169.67 169.37 157.43 153.42 151.27 137.92 134.37 131.21 126.67 118.97 117.73 108.52 103.38 79.85 66.79 61.72 60.94 56.23 51.84 45.03 15.37 14.28
200 190 180 170 160 150 140 130 120 110 100 90 80 70 60 50 40 30 20 10 0

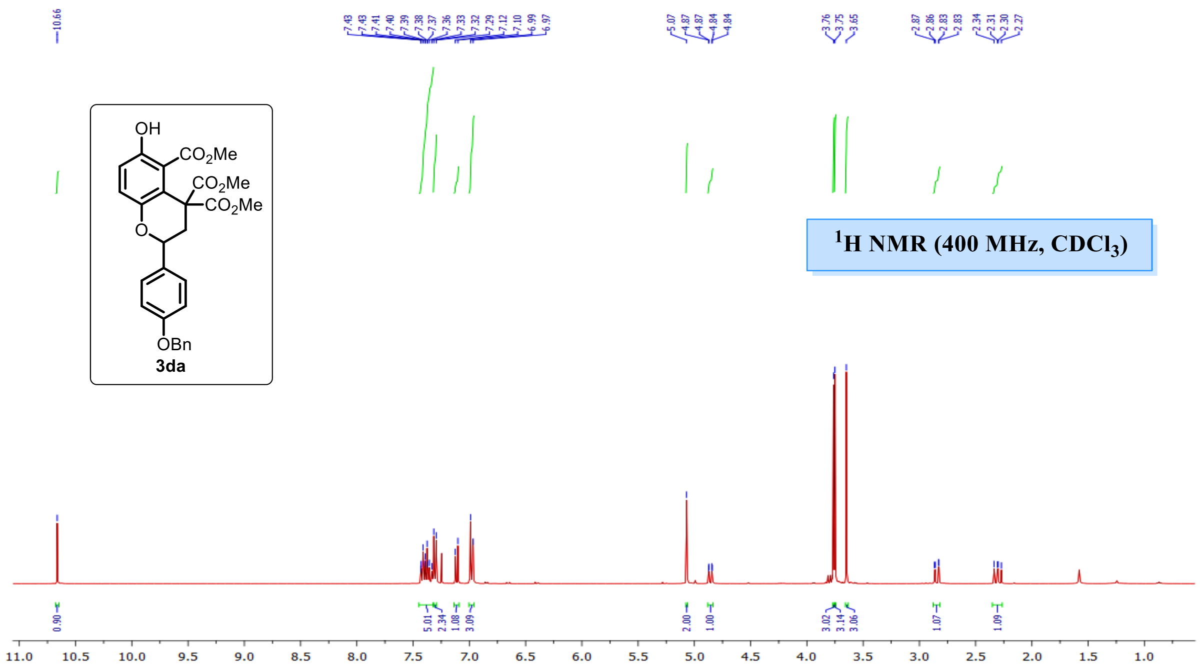
OH
CO_2Me
CO_2Me
CO_2Me
O
OBn
3da
^1H NMR (400 MHz, $CDCl_3$)
11.0 10.5 10.0 9.5 9.0 8.5 8.0 7.5 7.0 6.5 6.0 5.5 5.0 4.5 4.0 3.5 3.0 2.5 2.0 1.5 1.0

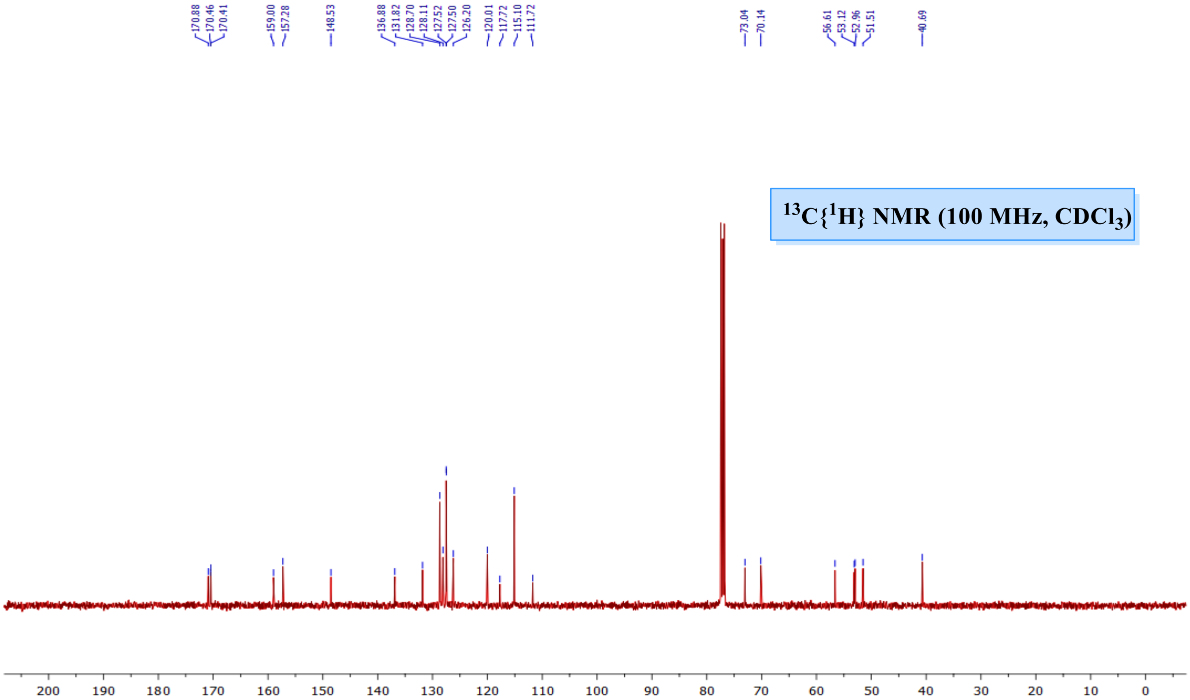

$^{13}C\{^1H\}$ NMR (100 MHz, $CDCl_3$)

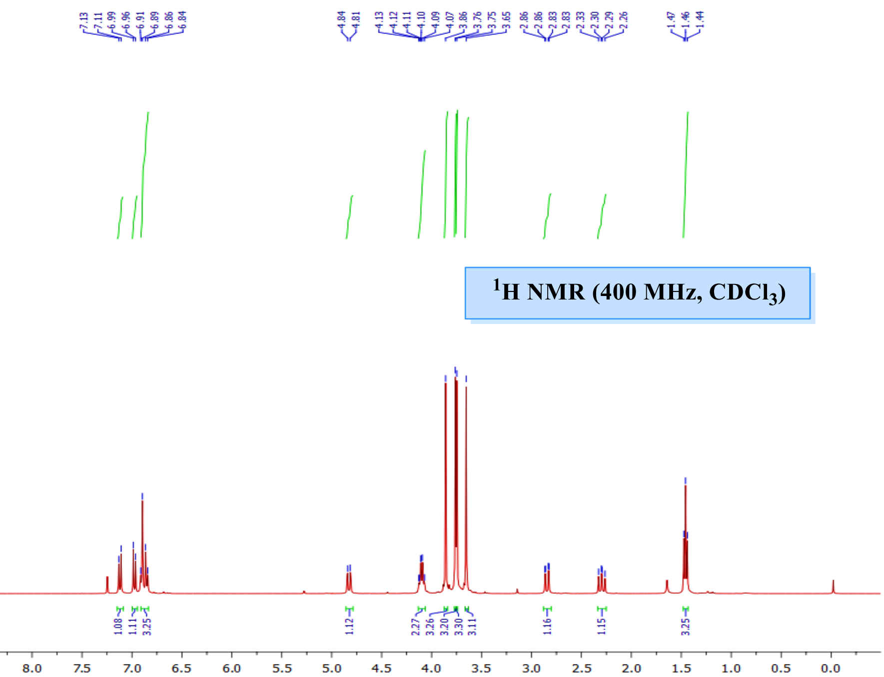

^1H NMR (400 MHz, $CDCl_3$)

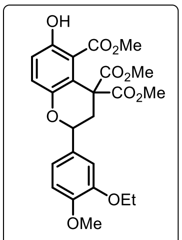

OH
CO_2Me
CO_2Me
CO_2Me
O
OEt
OMe

3ea

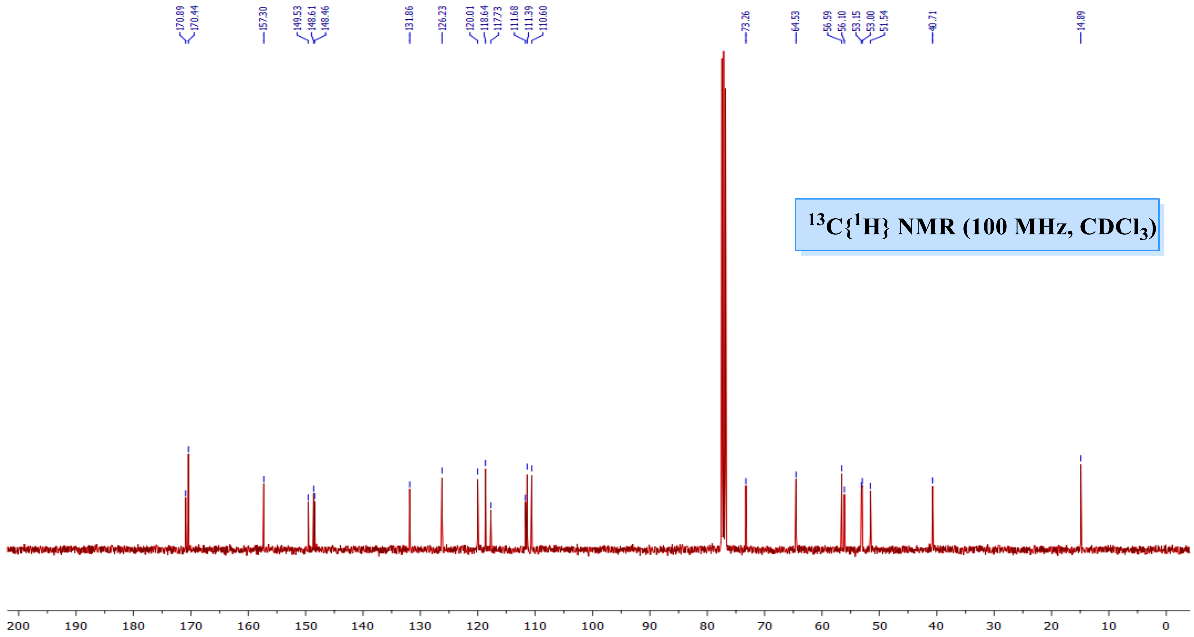
$^{13}C\{^{1}H\}$ NMR (100 MHz, $CDCl_3$)

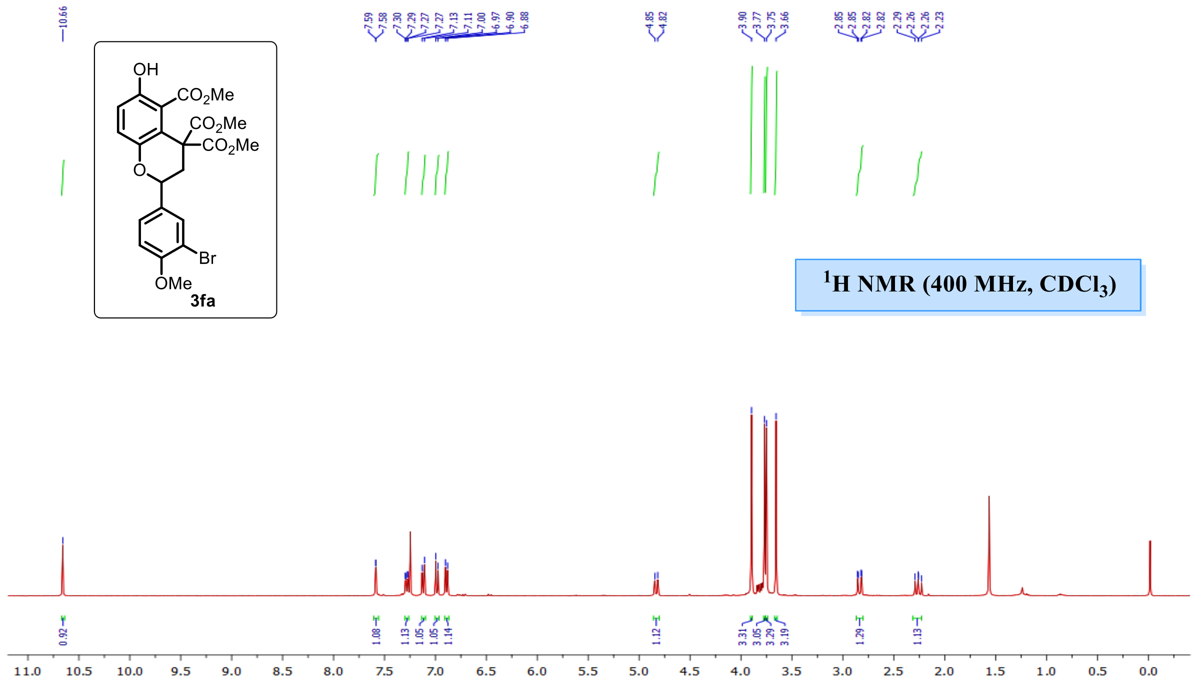
OH
CO_2Me
CO_2Me
CO_2Me
O
Br
OMe
3fa
^{1}H NMR (400 MHz, $CDCl_3$)

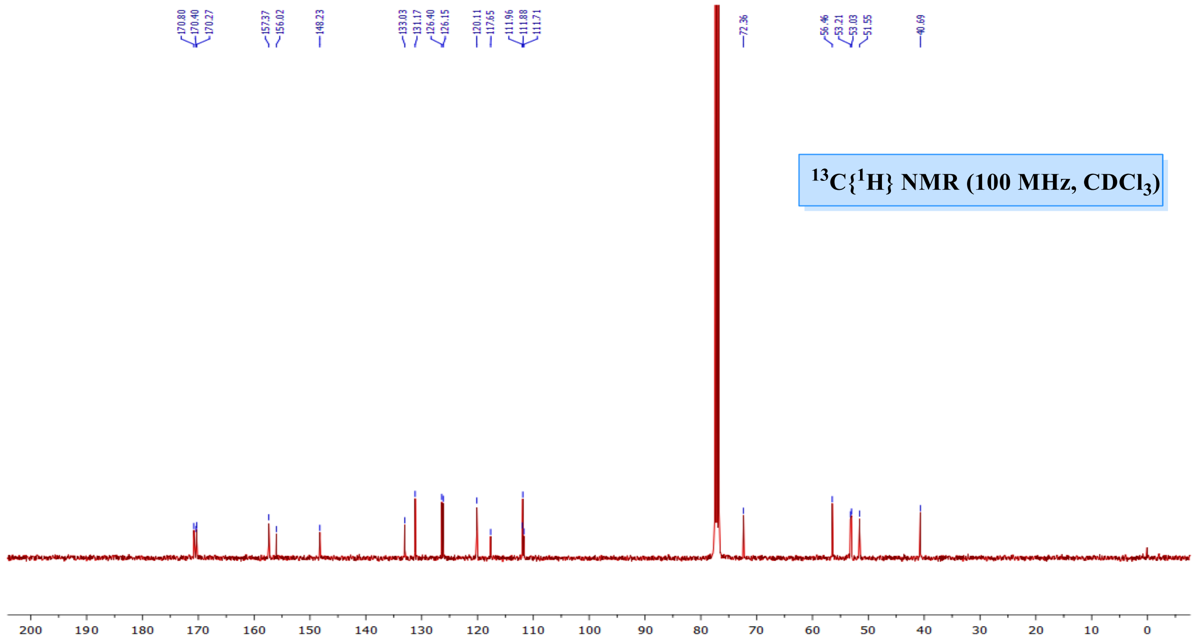
$^{13}C\{^{1}H\}$ NMR (100 MHz, CDCl$_3$)
170.80
170.40
170.27
157.37
156.02
148.23
133.03
131.17
126.40
126.15
120.11
117.65
111.96
111.88
111.71
72.36
56.46
53.21
53.03
51.55
40.69
200
190
180
170
160
150
140
130
120
110
100
90
80
70
60
50
40
30
20
10
0

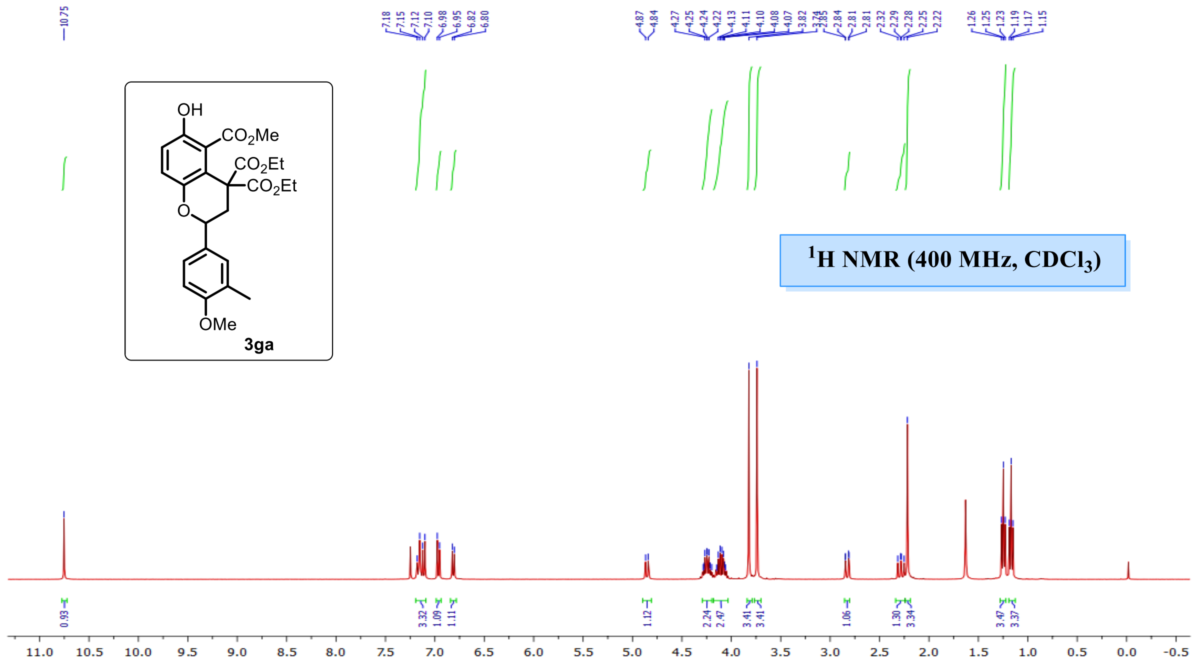
OH
CO2Me
CO2Et
CO2Et
O
OMe
3ga
^{1}H NMR (400 MHz, CDCl$_3$)
10.75
0.93
3.32
1.09
1.11
1.12
2.24
2.47
3.41
3.41
1.06
1.30
3.34
3.47
3.37
11.0
10.5
10.0
9.5
9.0
8.5
8.0
7.5
7.0
6.5
6.0
5.5
5.0
4.5
4.0
3.5
3.0
2.5
2.0
1.5
1.0
0.5
0.0
-0.5

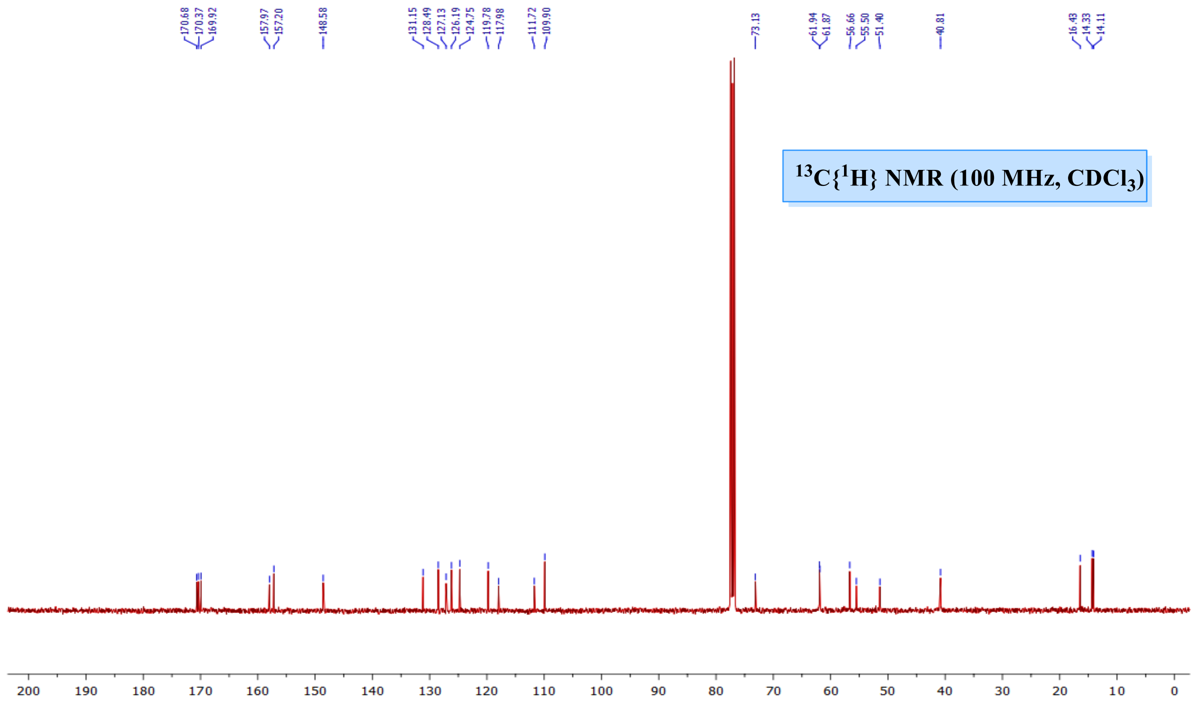
$^{13}C\{^{1}H\}$ NMR (100 MHz, $CDCl_3$)

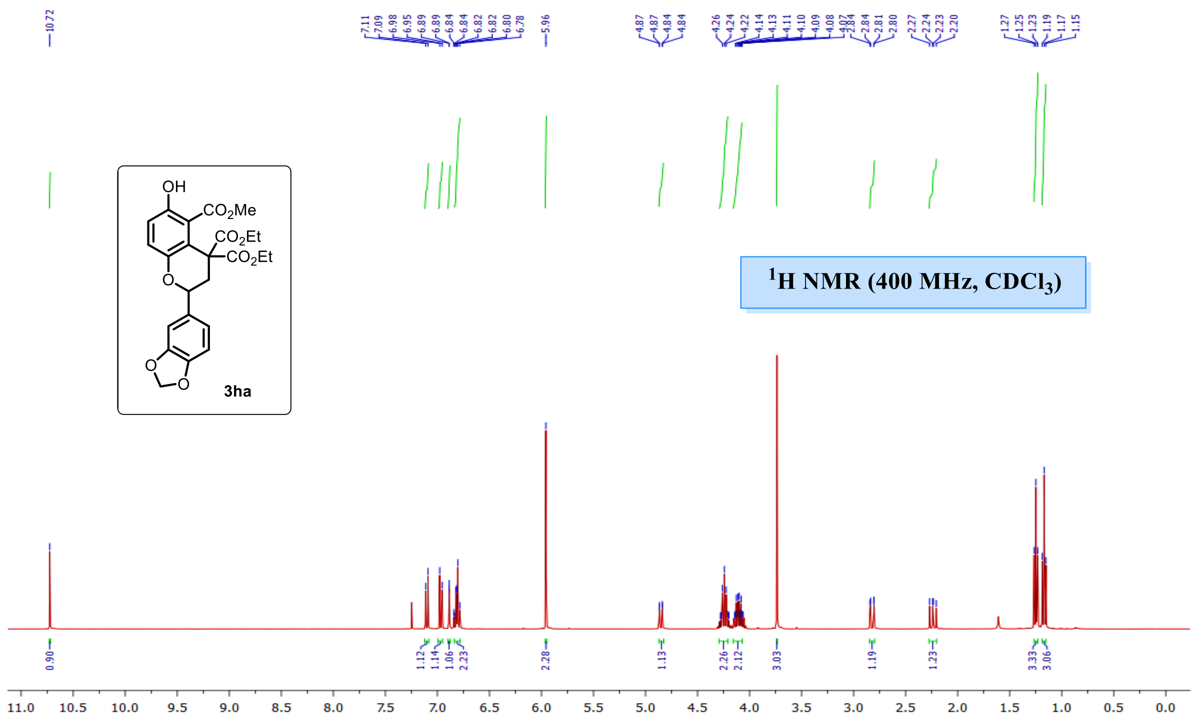
3ha
^{1}H NMR (400 MHz, $CDCl_3$)

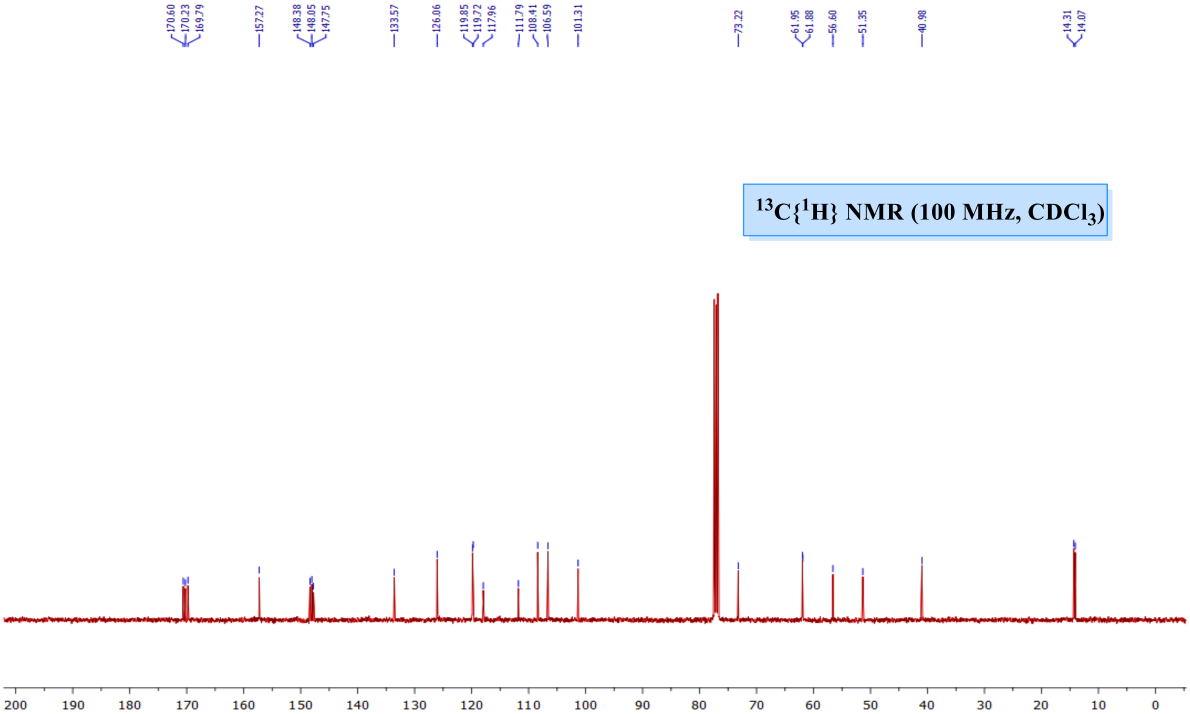
$^{13}C\{^1H\}$ NMR (100 MHz, $CDCl_3$)

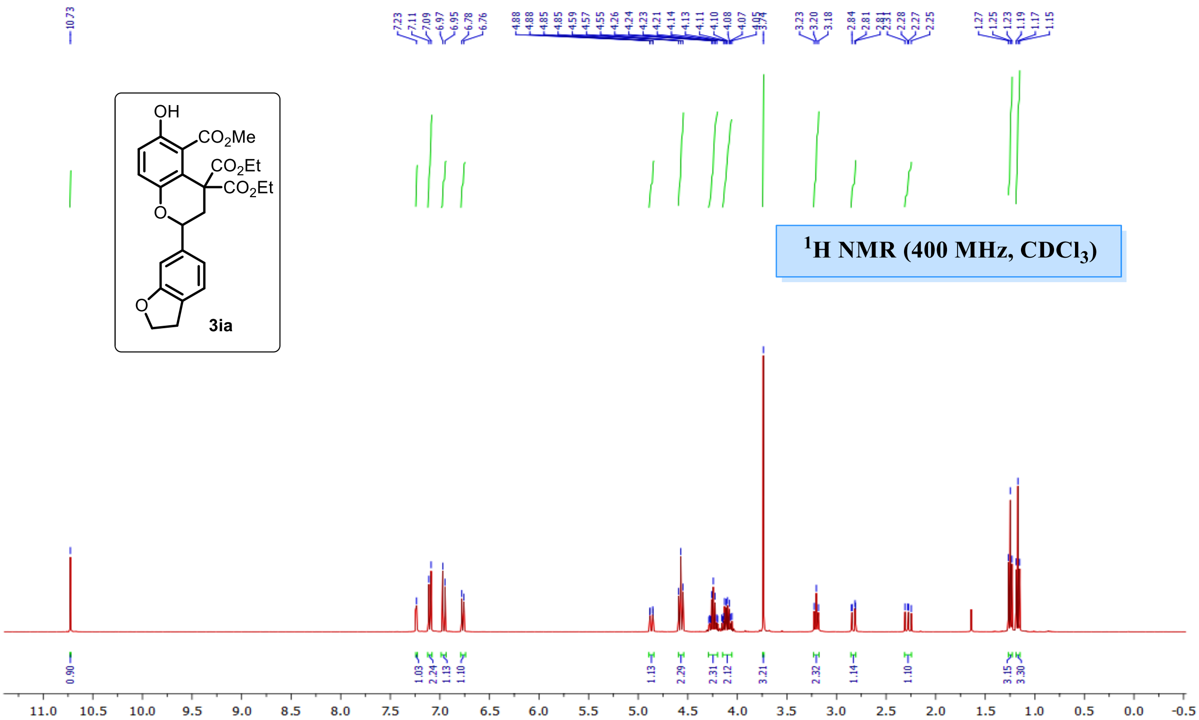
OH
CO_2Me
CO_2Et
CO_2Et
O
O
3ia
^1H NMR (400 MHz, $CDCl_3$)

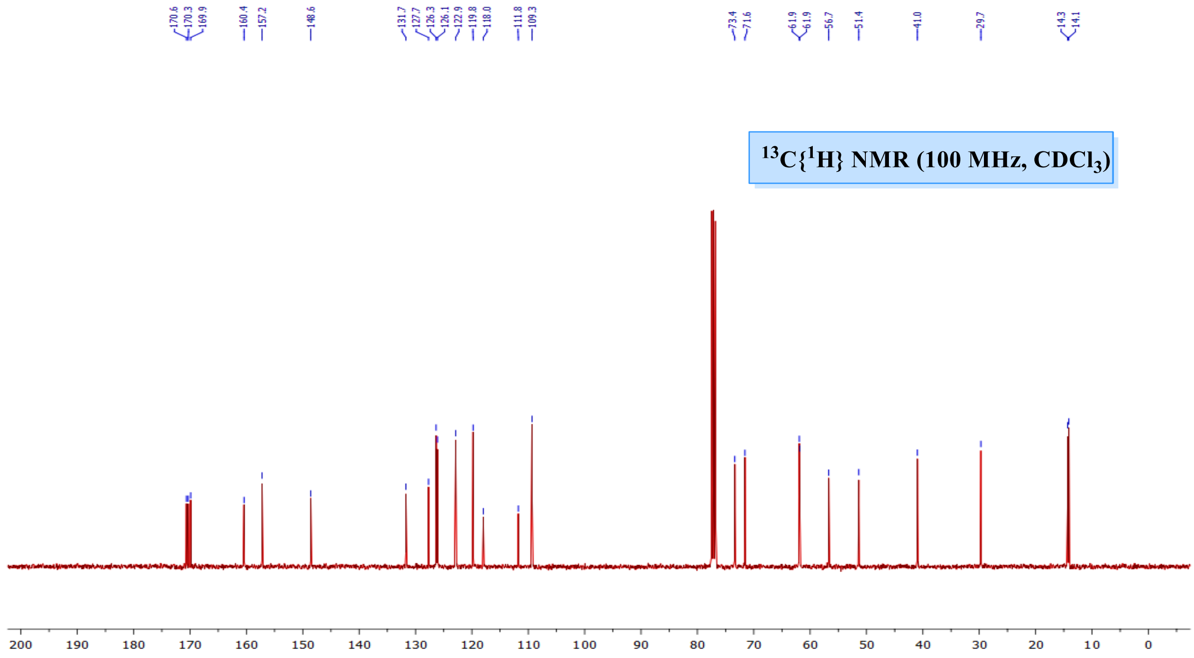
$^{13}C\{^1H\}$ NMR (100 MHz, $CDCl_3$)
170.6 170.3 169.9 160.4 157.2 148.6 131.7 127.7 126.3 126.1 122.9 119.8 118.0 111.8 109.3 73.4 71.6 61.9 61.9 56.7 51.4 41.0 29.7 14.3 14.1
200 190 180 170 160 150 140 130 120 110 100 90 80 70 60 50 40 30 20 10 0

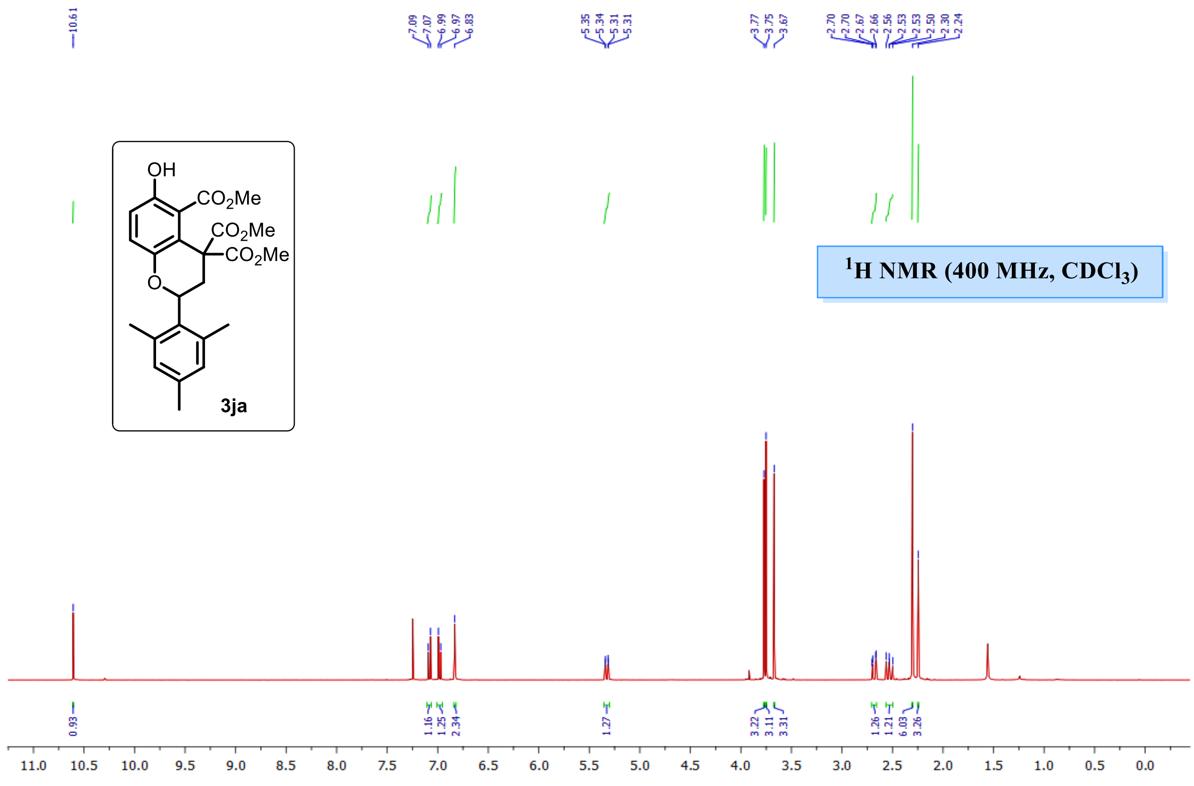
^1H NMR (400 MHz, $CDCl_3$)
OH
CO_2Me
CO_2Me
CO_2Me
O
3ja
10.61 7.09 7.07 6.99 6.97 6.83 5.35 5.34 5.31 5.31 3.77 3.75 3.67 2.70 2.70 2.67 2.66 2.56 2.53 2.53 2.50 2.30 2.24
0.93 1.16 1.25 2.34 1.27 3.22 3.11 3.31 1.26 1.21 6.03 3.26
11.0 10.5 10.0 9.5 9.0 8.5 8.0 7.5 7.0 6.5 6.0 5.5 5.0 4.5 4.0 3.5 3.0 2.5 2.0 1.5 1.0 0.5 0.0

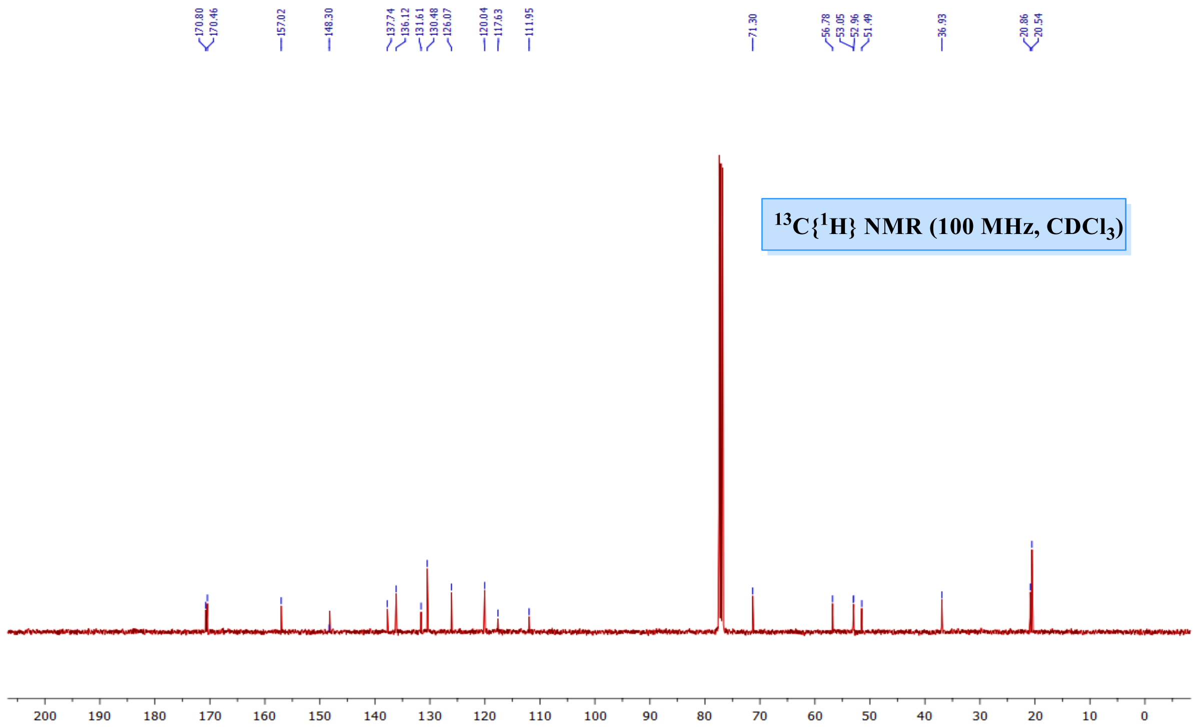
$^{13}C\{^1H\}$ NMR (100 MHz, $CDCl_3$)

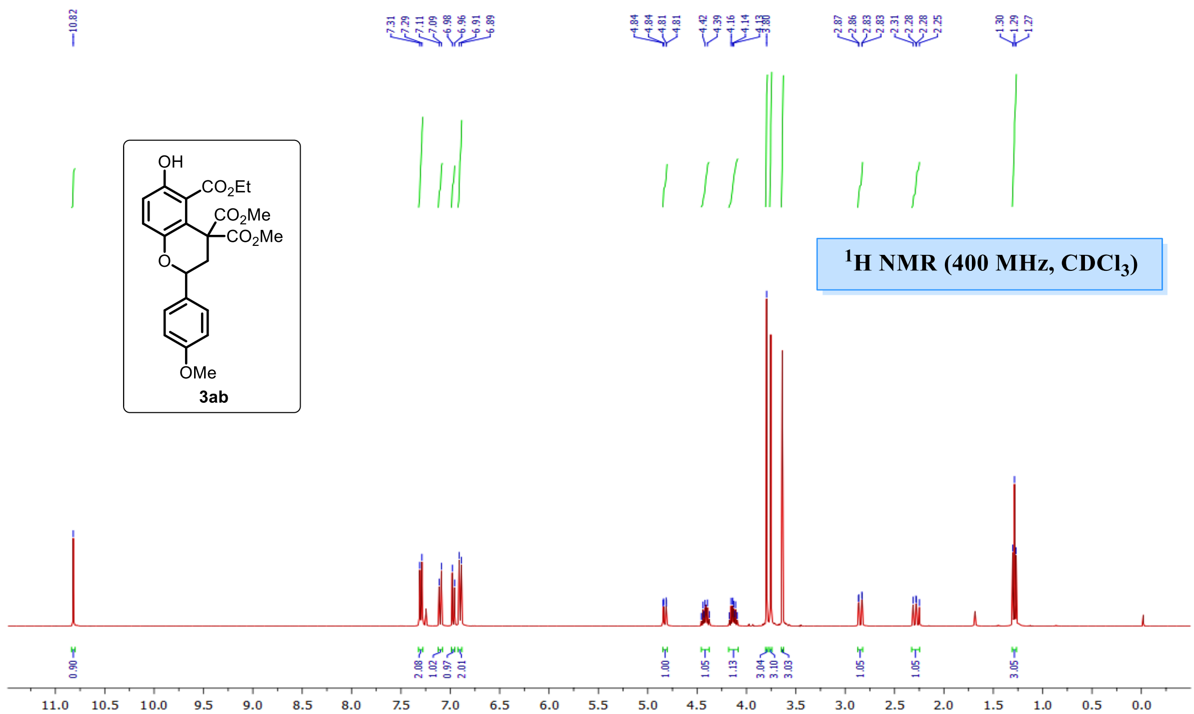
^1H NMR (400 MHz, $CDCl_3$)
3ab

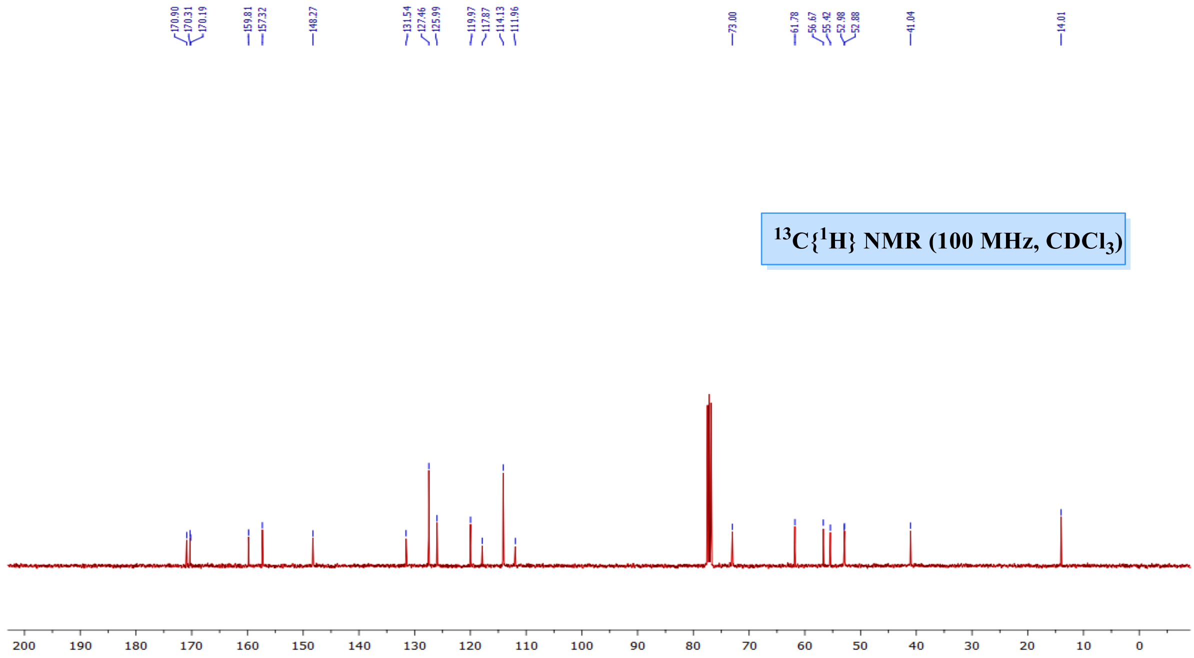
$^{13}C\{^1H\}$ NMR (100 MHz, $CDCl_3$)

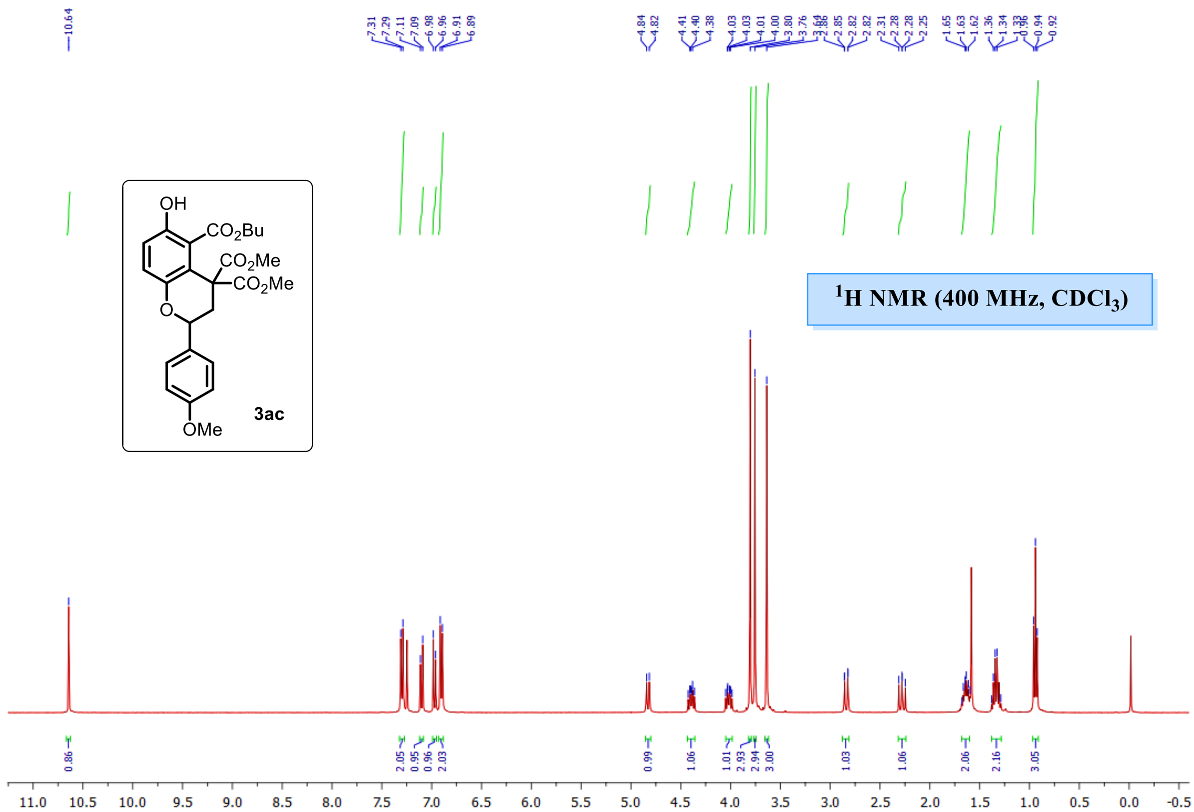
OH
CO_2Bu
CO_2Me
CO_2Me
O
OMe
3ac
^1H NMR (400 MHz, $CDCl_3$)

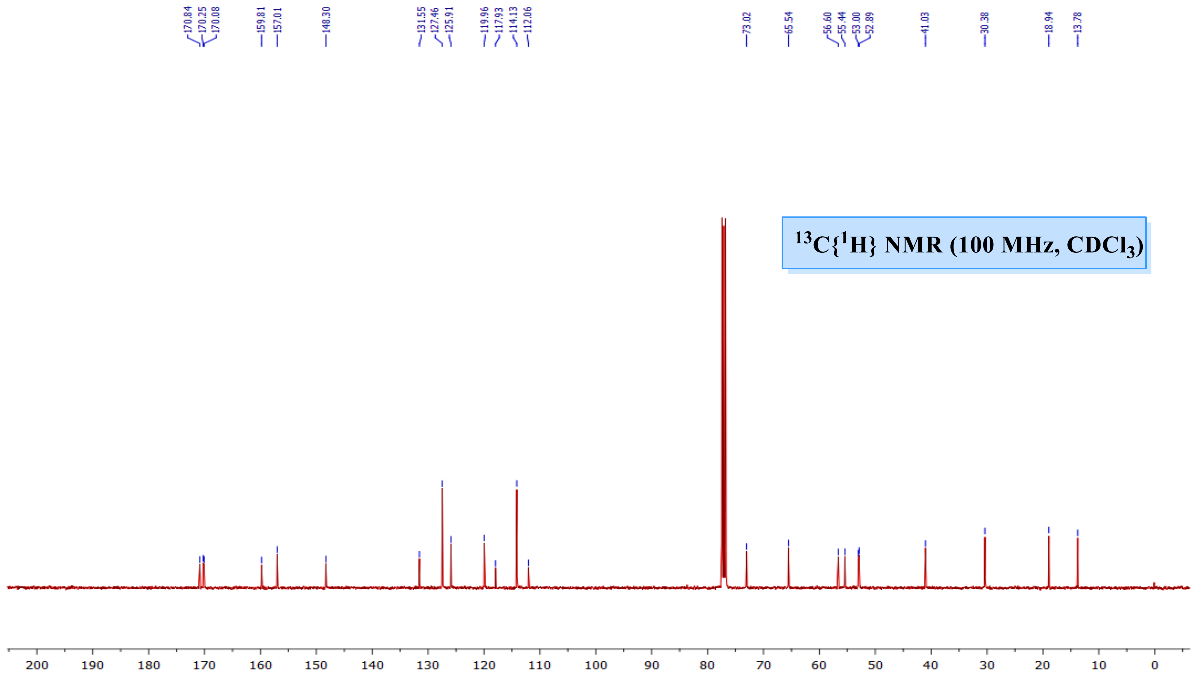

$^{13}C\{^1H\}$ NMR (100 MHz, $CDCl_3$)

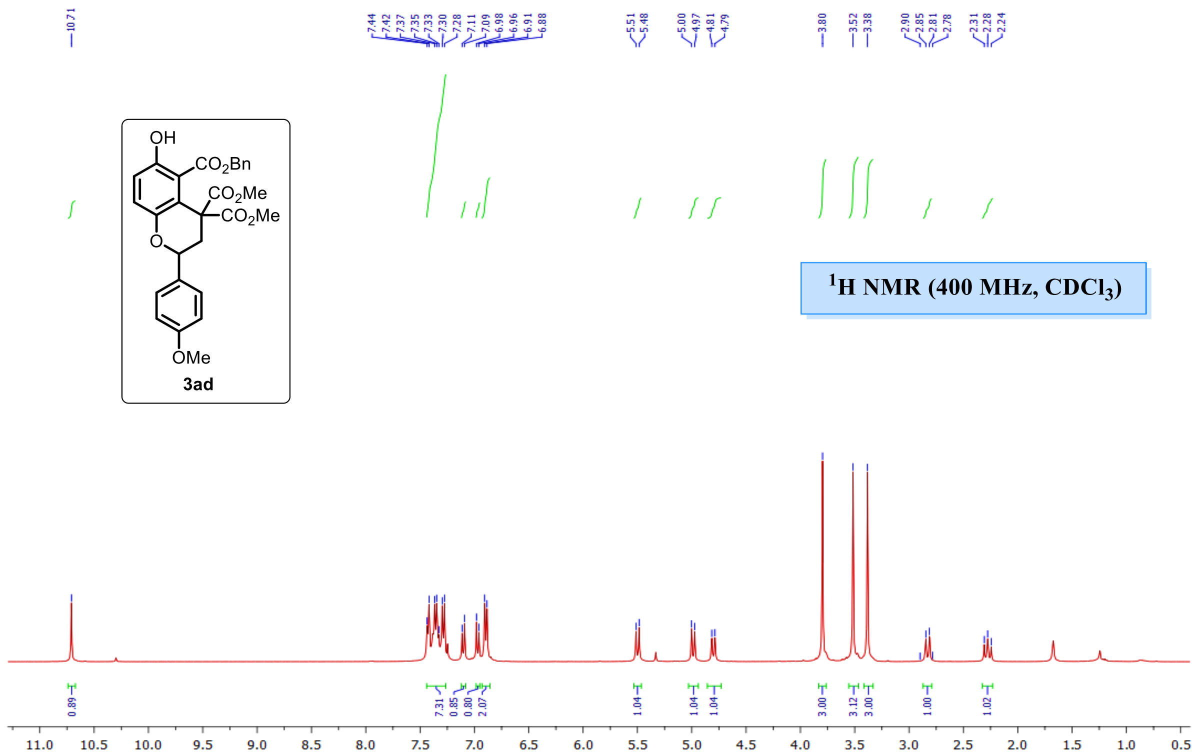

^1H NMR (400 MHz, $CDCl_3$)

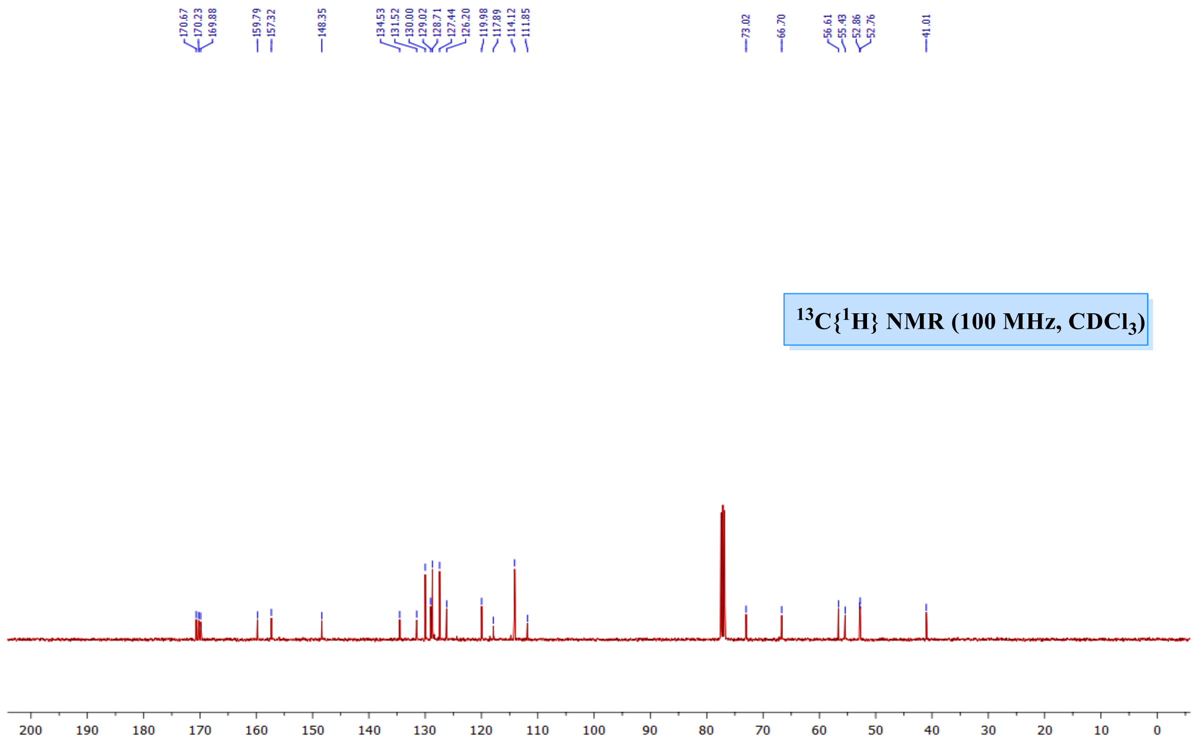
$^{13}C\{^{1}H\}$ NMR (100 MHz, $CDCl_3$)

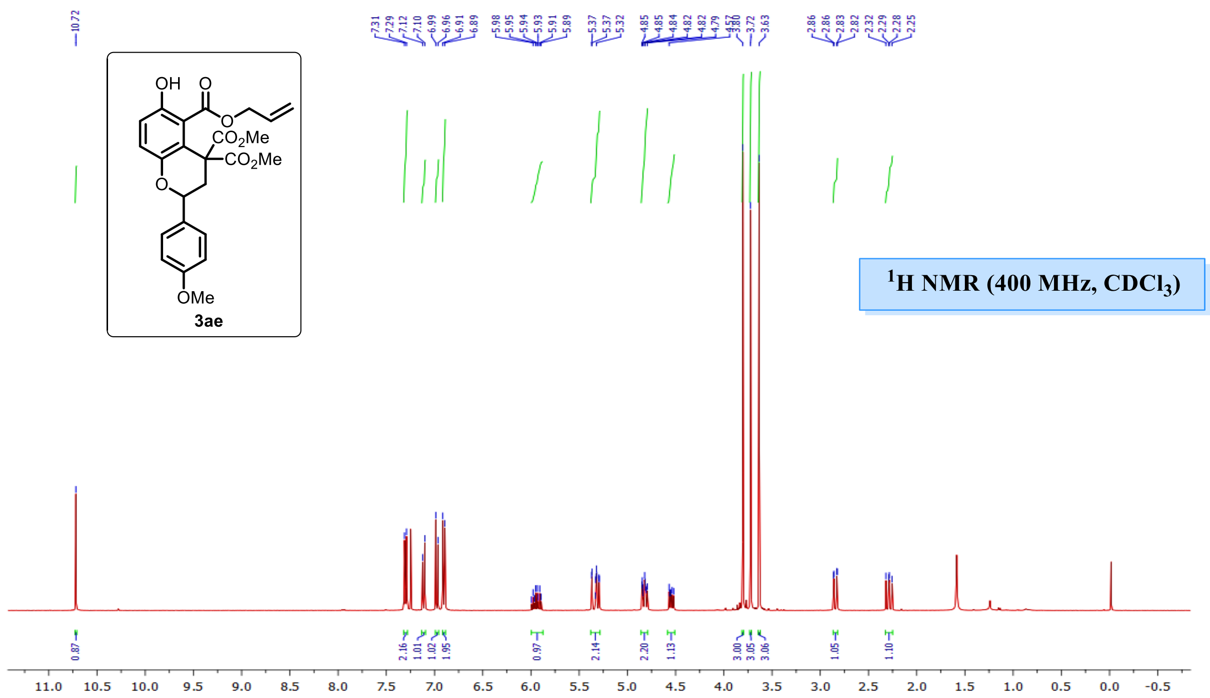
OH
O
O
CO_2Me
CO_2Me
O
OMe
3ae
^{1}H NMR (400 MHz, $CDCl_3$)

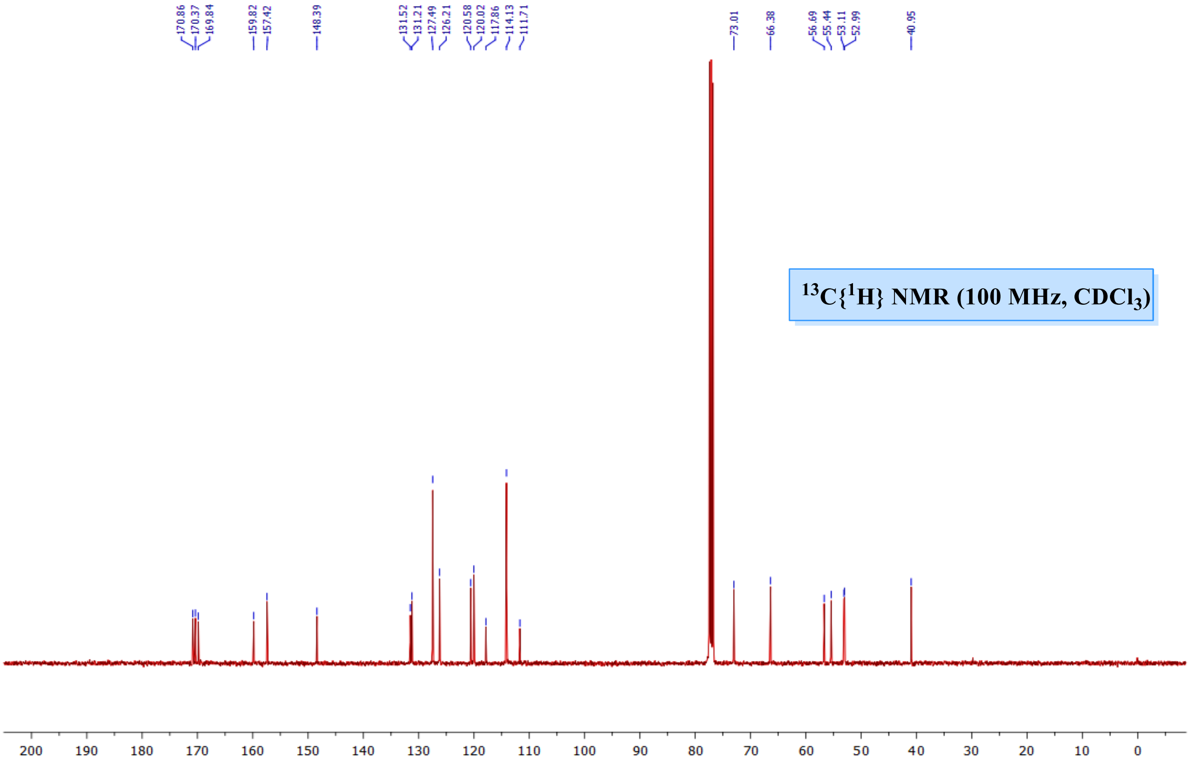
$^{13}C\{^1H\}$ NMR (100 MHz, $CDCl_3$)

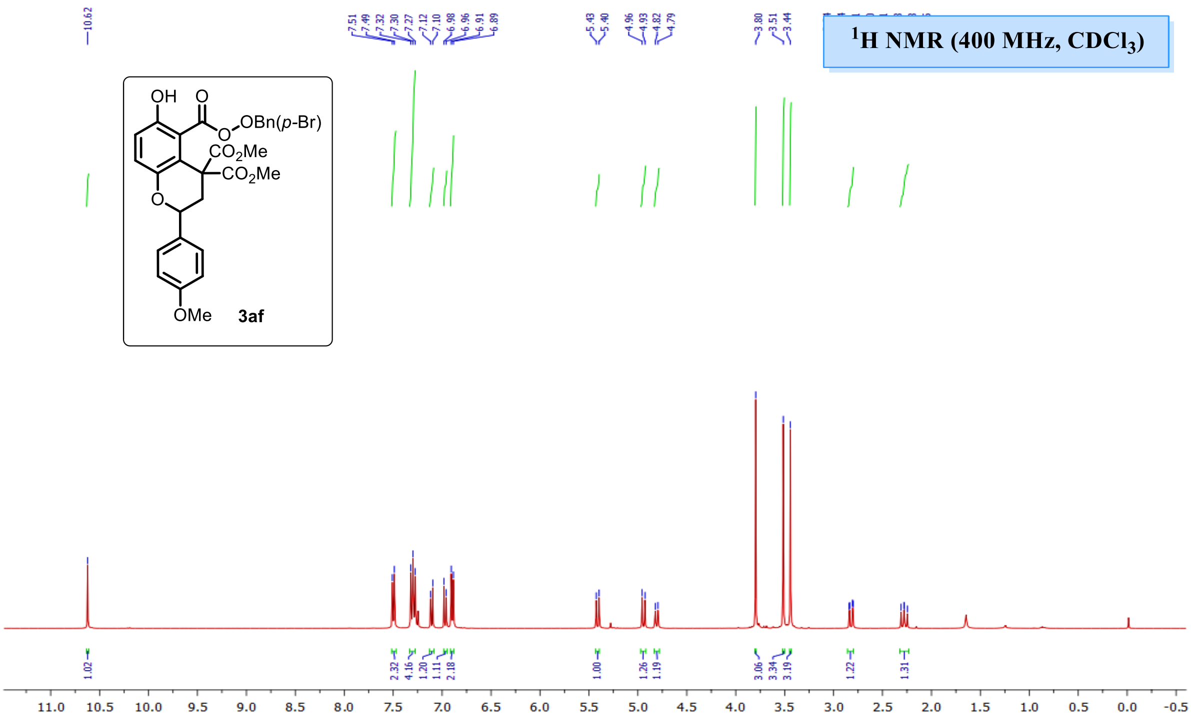
^1H NMR (400 MHz, $CDCl_3$)
OH
O
OBn(*p*-Br)
CO_2Me
CO_2Me
O
OMe
3af

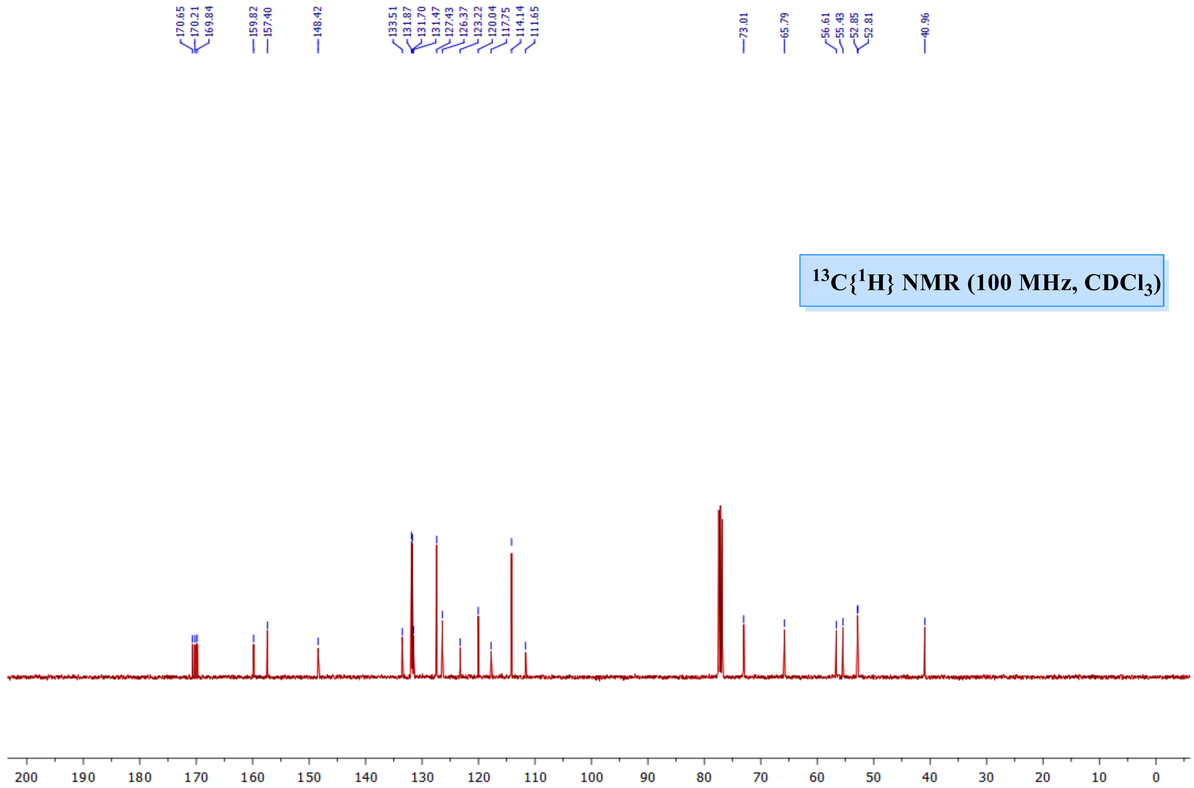
$^{13}C\{^1H\}$ NMR (100 MHz, $CDCl_3$)

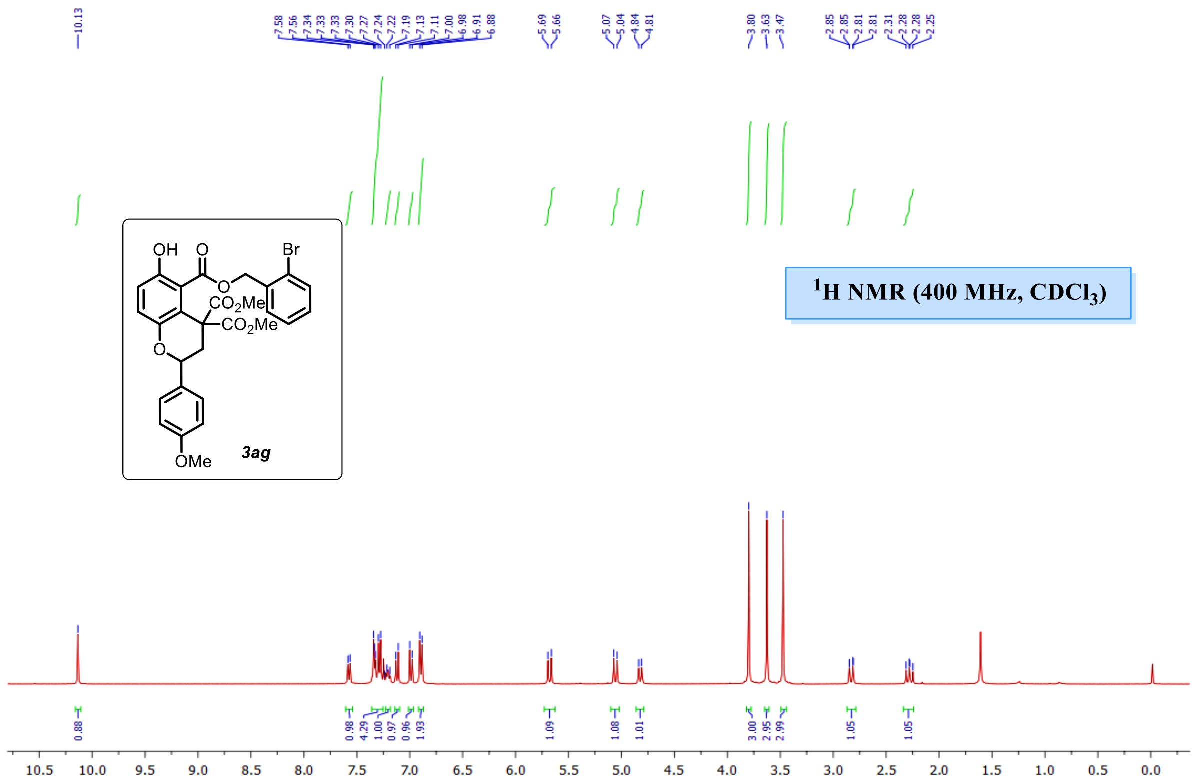
OH
O
Br
CO_2Me
CO_2Me
OMe
3ag
^1H NMR (400 MHz, $CDCl_3$)

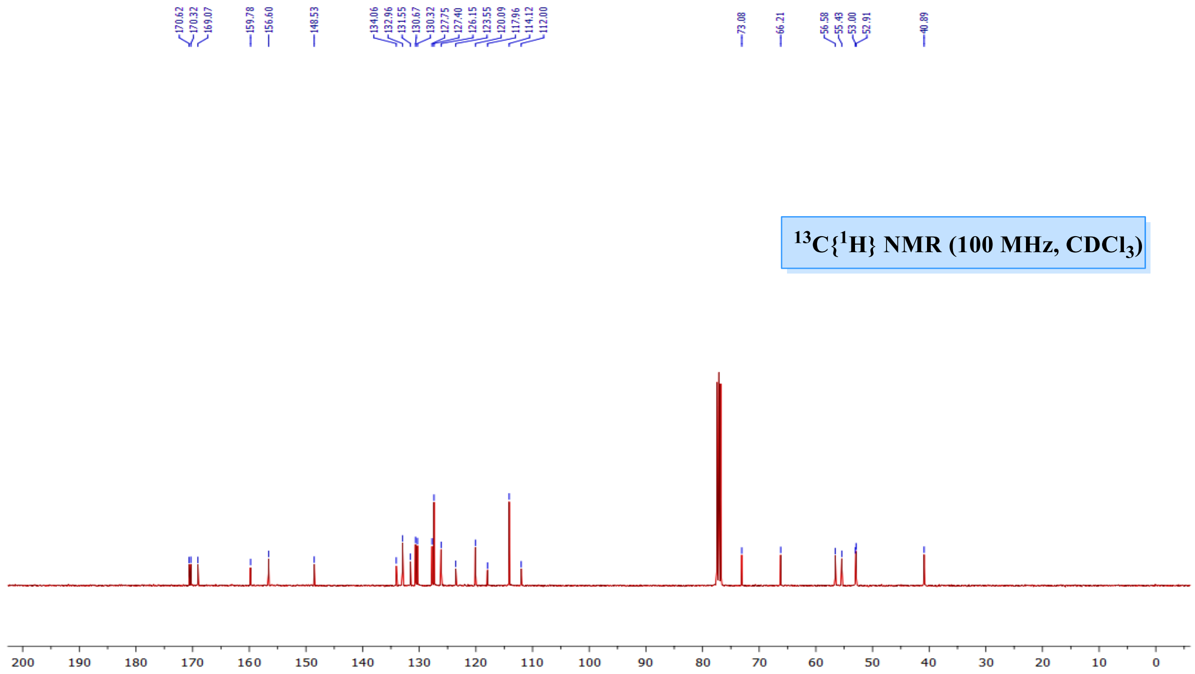
$^{13}C\{^1H\}$ NMR (100 MHz, CDCl$_3$)

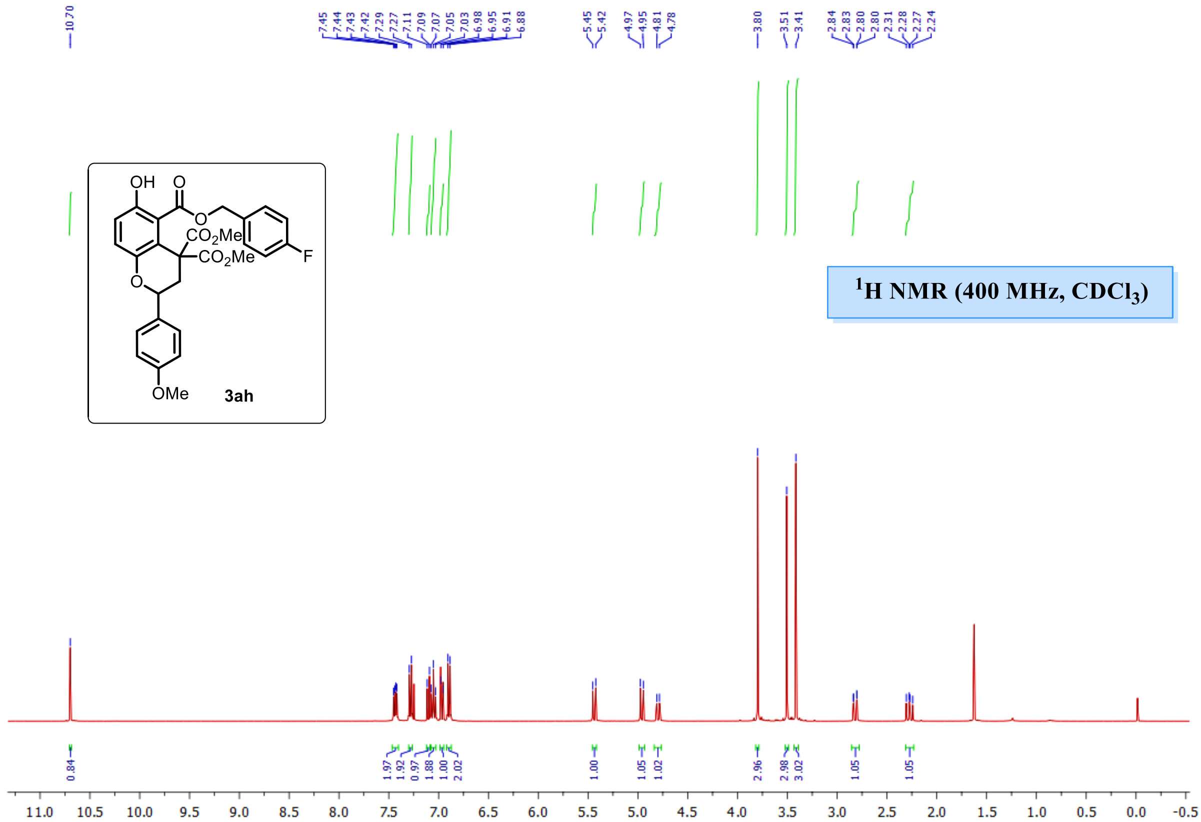
OH
O
O
CO$_2$Me
CO$_2$Me
F
O
OMe
3ah
^1H NMR (400 MHz, CDCl$_3$)

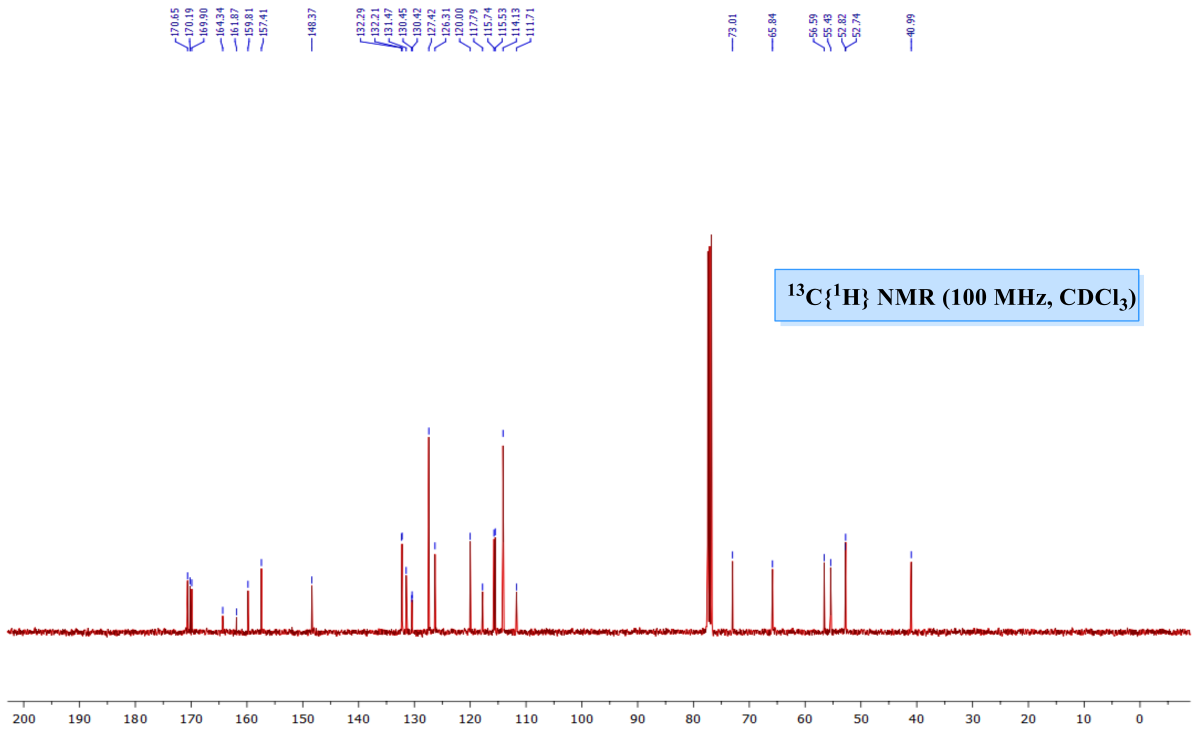
$^{13}C\{^1H\}$ NMR (100 MHz, $CDCl_3$)

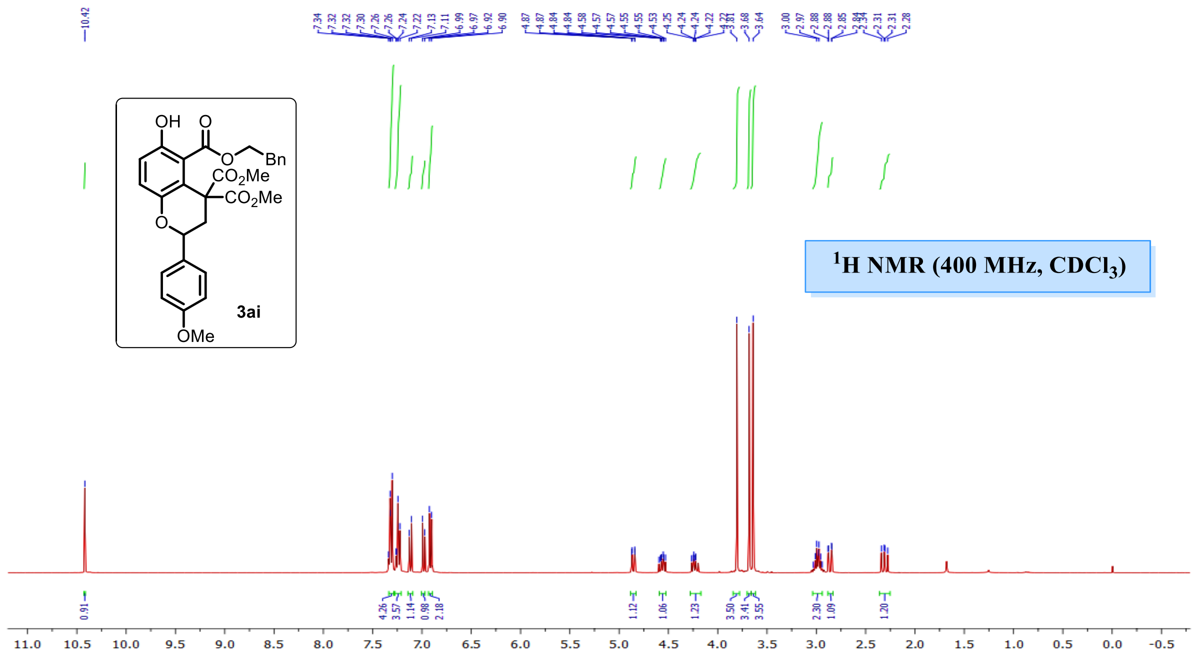
^1H NMR (400 MHz, $CDCl_3$)
3ai

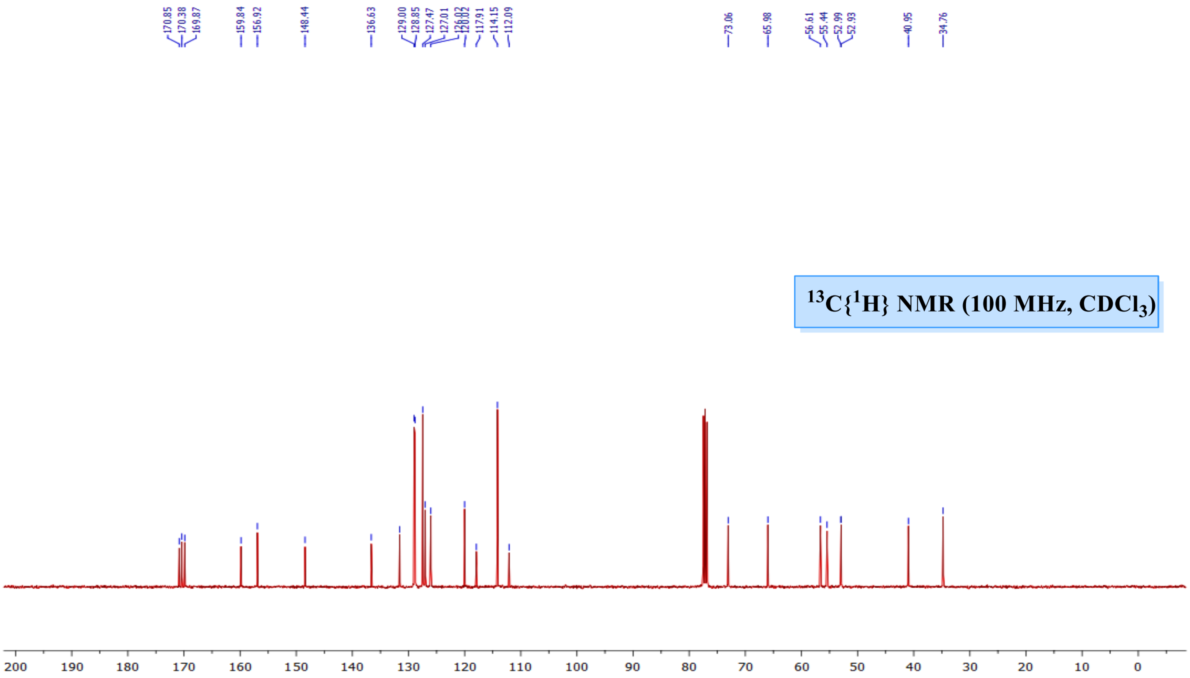
170.85
170.38
169.87
159.84
156.92
148.44
136.63
129.00
128.85
127.47
127.01
126.02
120.02
117.91
114.15
112.09
73.06
65.98
56.61
55.44
52.99
52.93
40.95
34.76
13C{1H} NMR (100 MHz, CDCl3)
200 190 180 170 160 150 140 130 120 110 100 90 80 70 60 50 40 30 20 10 0

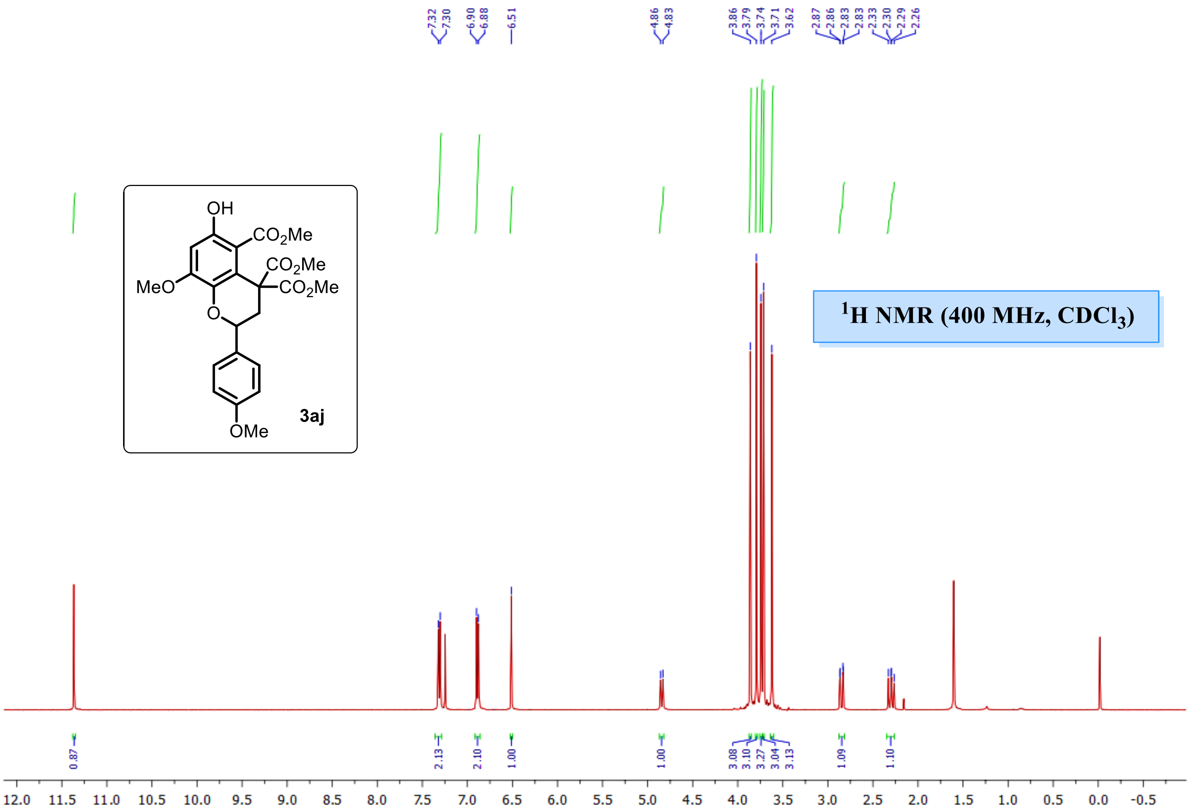
7.32
7.30
6.90
6.88
6.51
4.86
4.83
3.86
3.79
3.74
3.71
3.62
2.87
2.86
2.83
2.83
2.33
2.30
2.29
2.26
OH
CO2Me
CO2Me
CO2Me
MeO
O
OMe
3aj
1H NMR (400 MHz, CDCl3)
0.87
2.13
2.10
1.00
1.00
3.08
3.10
3.27
3.04
3.13
1.09
1.10
12.0 11.5 11.0 10.5 10.0 9.5 9.0 8.5 8.0 7.5 7.0 6.5 6.0 5.5 5.0 4.5 4.0 3.5 3.0 2.5 2.0 1.5 1.0 0.5 0.0 -0.5

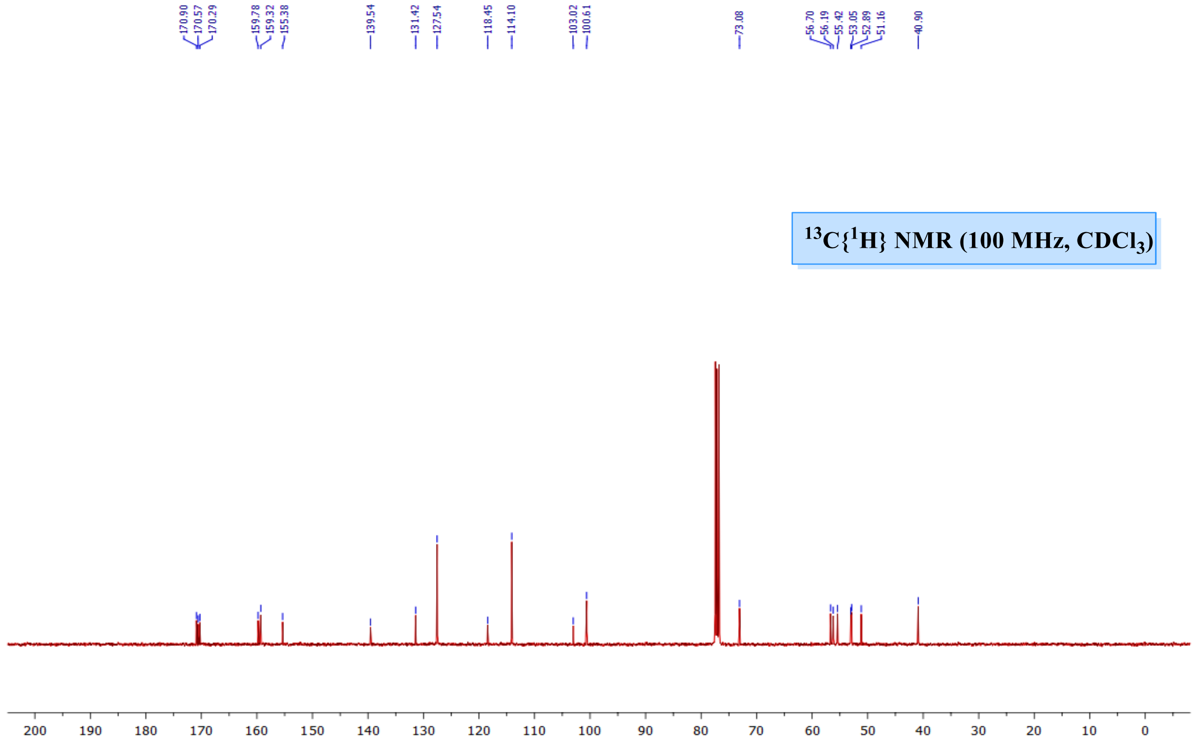
$^{13}C\{^{1}H\}$ NMR (100 MHz, $CDCl_3$)

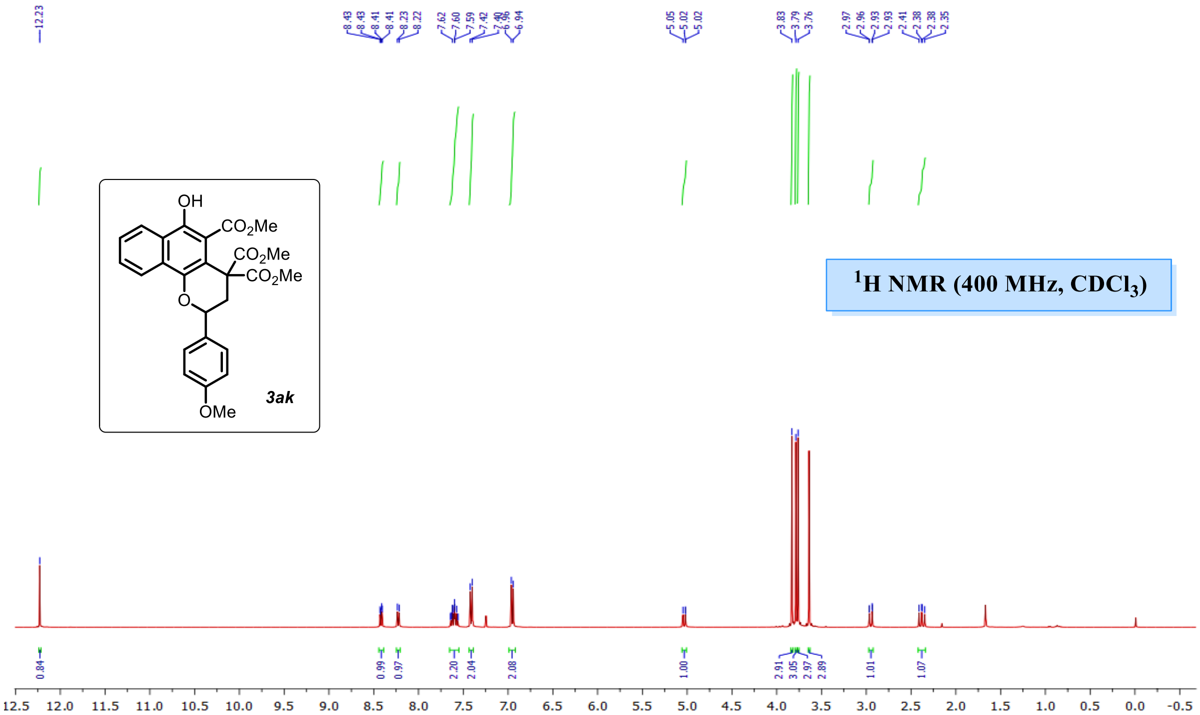
OH
CO_2Me
CO_2Me
CO_2Me
O
OMe
3ak
^{1}H NMR (400 MHz, $CDCl_3$)

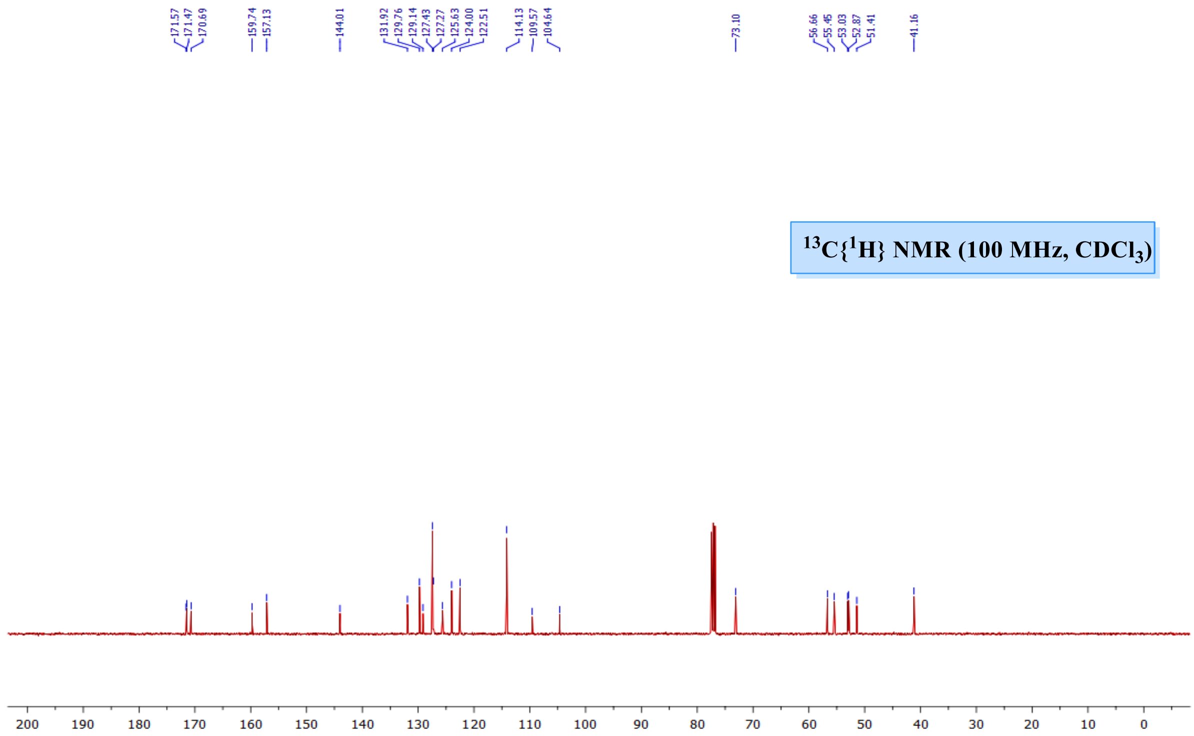
171.57
171.47
170.69
159.74
157.13
144.01
131.92
129.76
129.14
127.43
127.27
125.63
124.00
122.51
114.13
109.57
104.64
73.10
56.66
55.45
53.03
52.87
51.41
41.16
$^{13}C\{^1H\}$ NMR (100 MHz, $CDCl_3$)

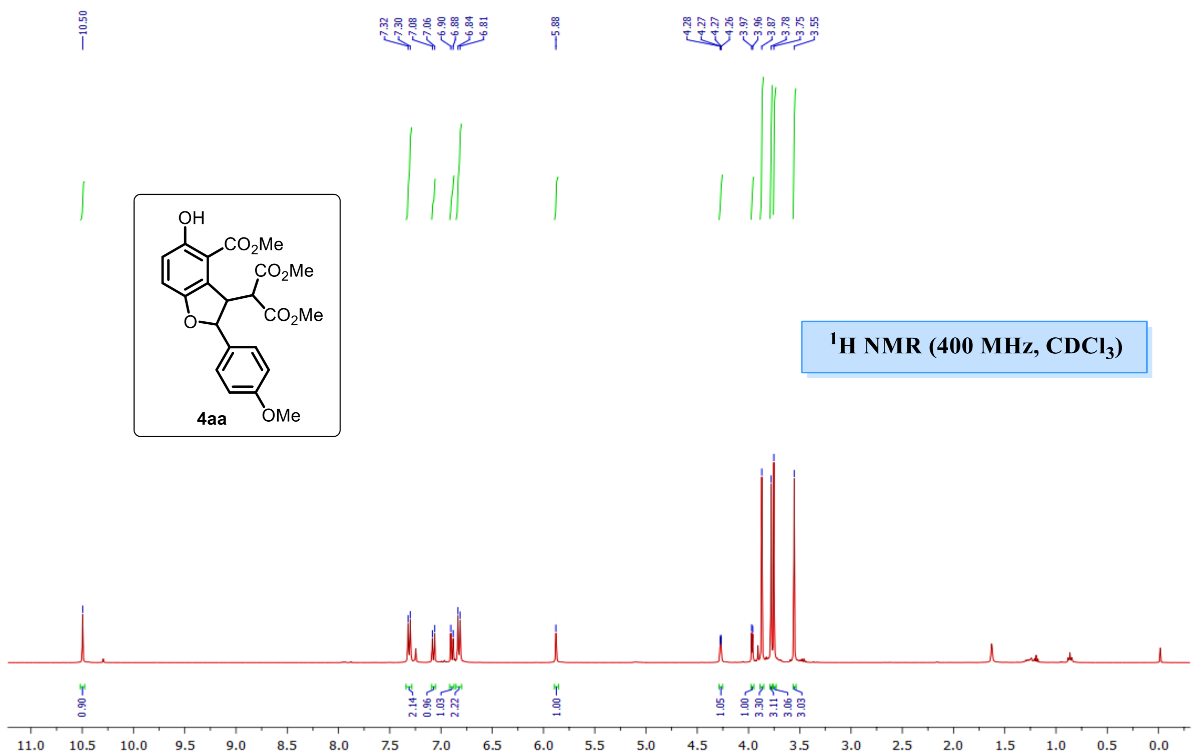
10.50
7.32
7.30
7.08
7.06
6.90
6.88
6.84
6.81
5.88
4.28
4.27
4.27
4.26
3.97
3.96
3.87
3.78
3.75
3.55
^1H NMR (400 MHz, $CDCl_3$)
0.90
2.14
0.96
1.03
2.22
1.00
1.05
1.00
3.30
3.11
3.06
3.03
OH
CO2Me
CO2Me
CO2Me
O
OMe
4aa

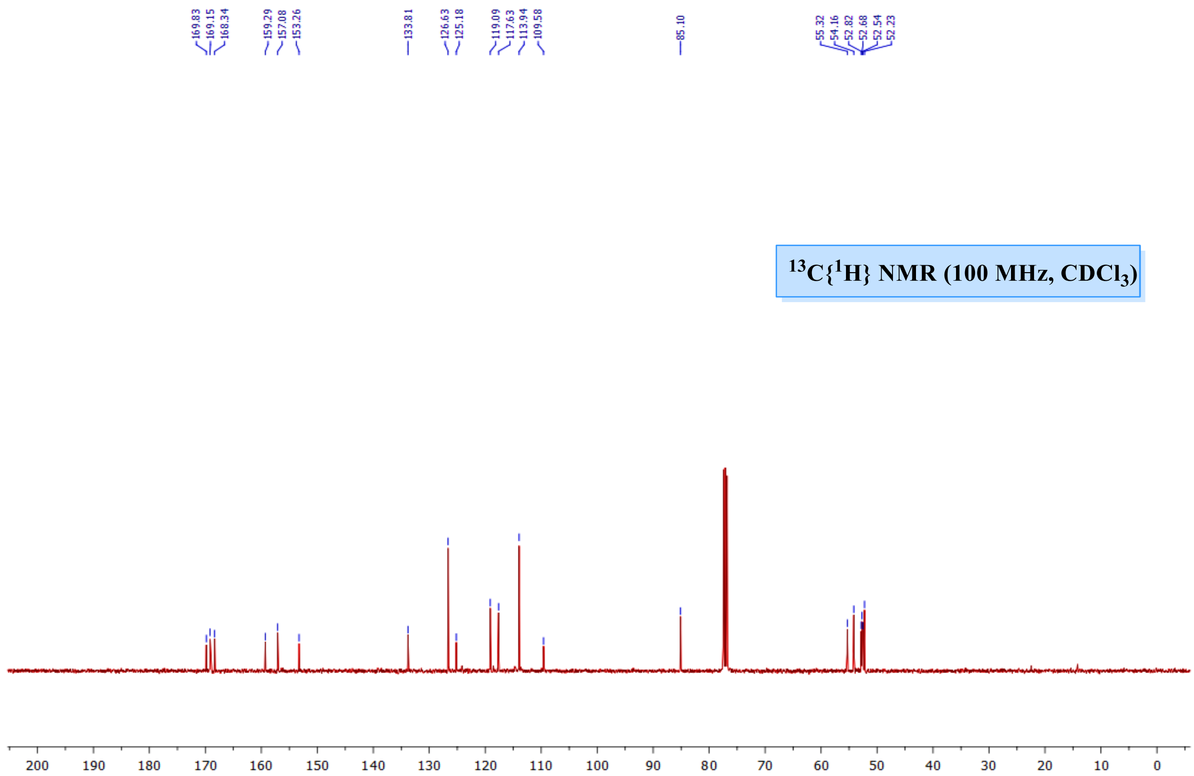
$^{13}C\{^1H\}$ NMR (100 MHz, $CDCl_3$)

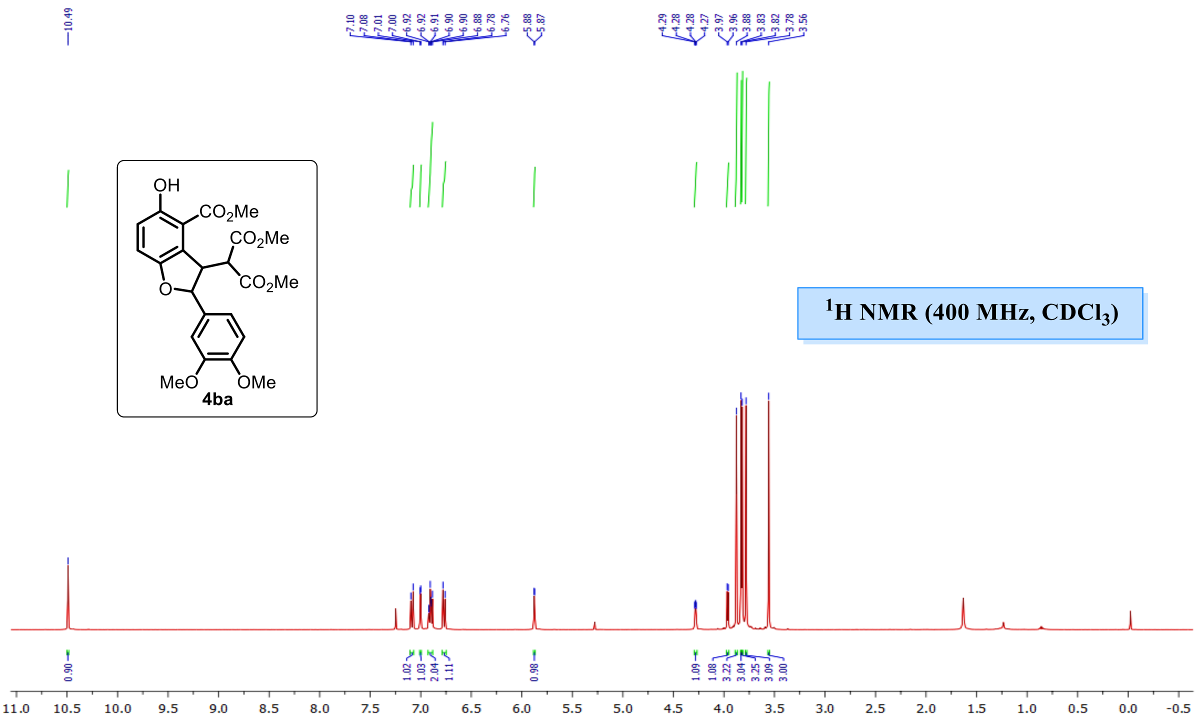
OH
CO_2Me
CO_2Me
CO_2Me
O
MeO
OMe
4ba
^1H NMR (400 MHz, $CDCl_3$)

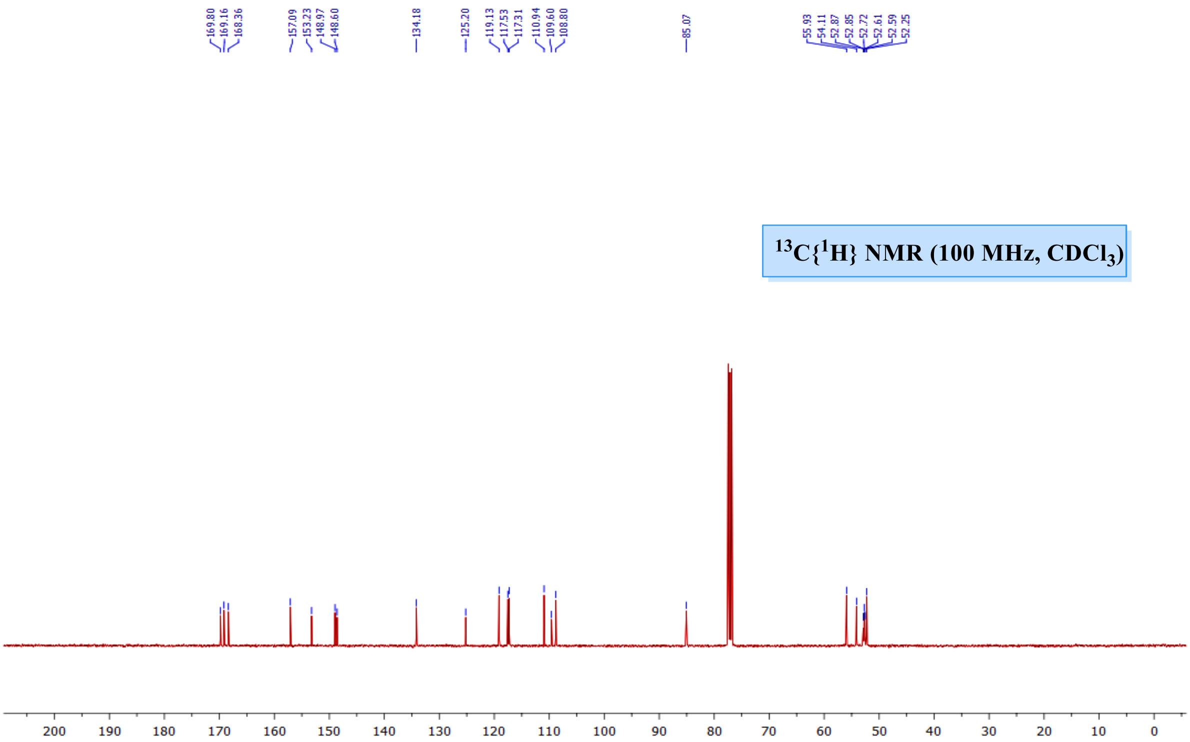
$^{13}C\{^{1}H\}$ NMR (100 MHz, $CDCl_3$)

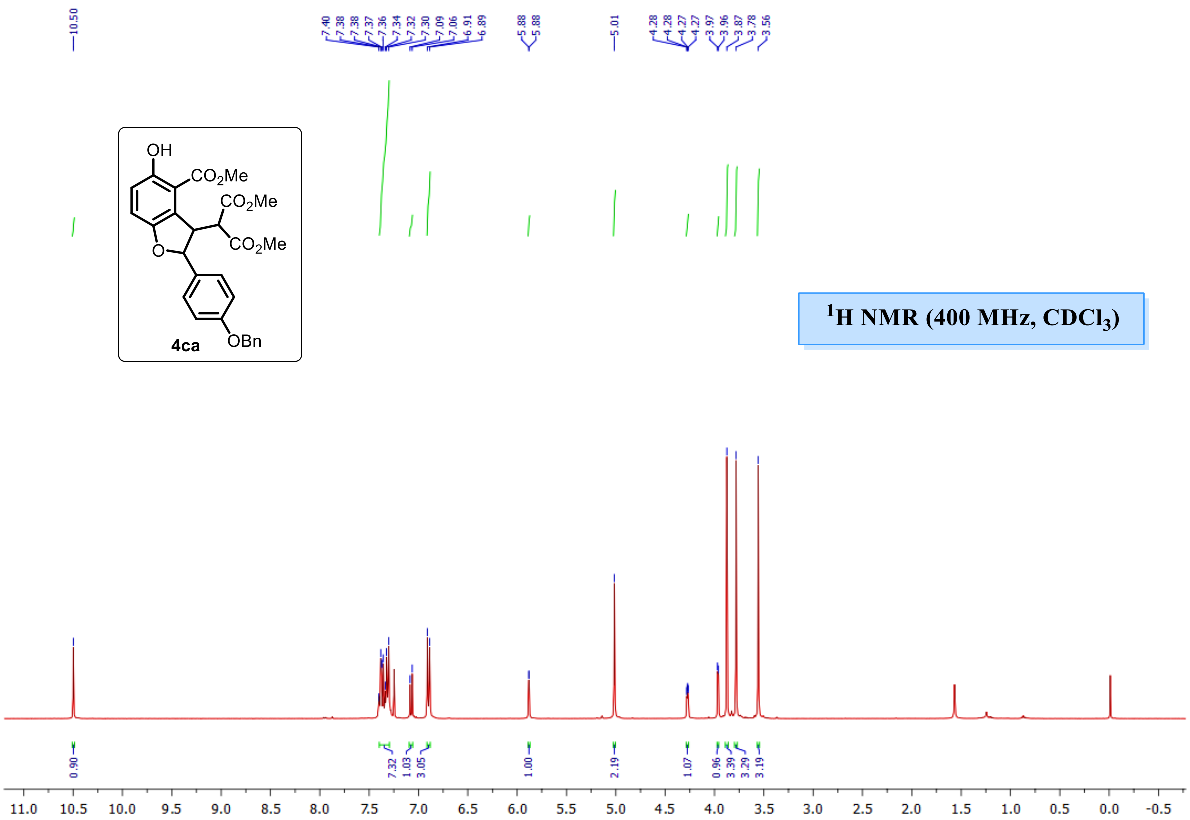
OH
CO_2Me
CO_2Me
CO_2Me
O
OBn
4ca
^{1}H NMR (400 MHz, $CDCl_3$)

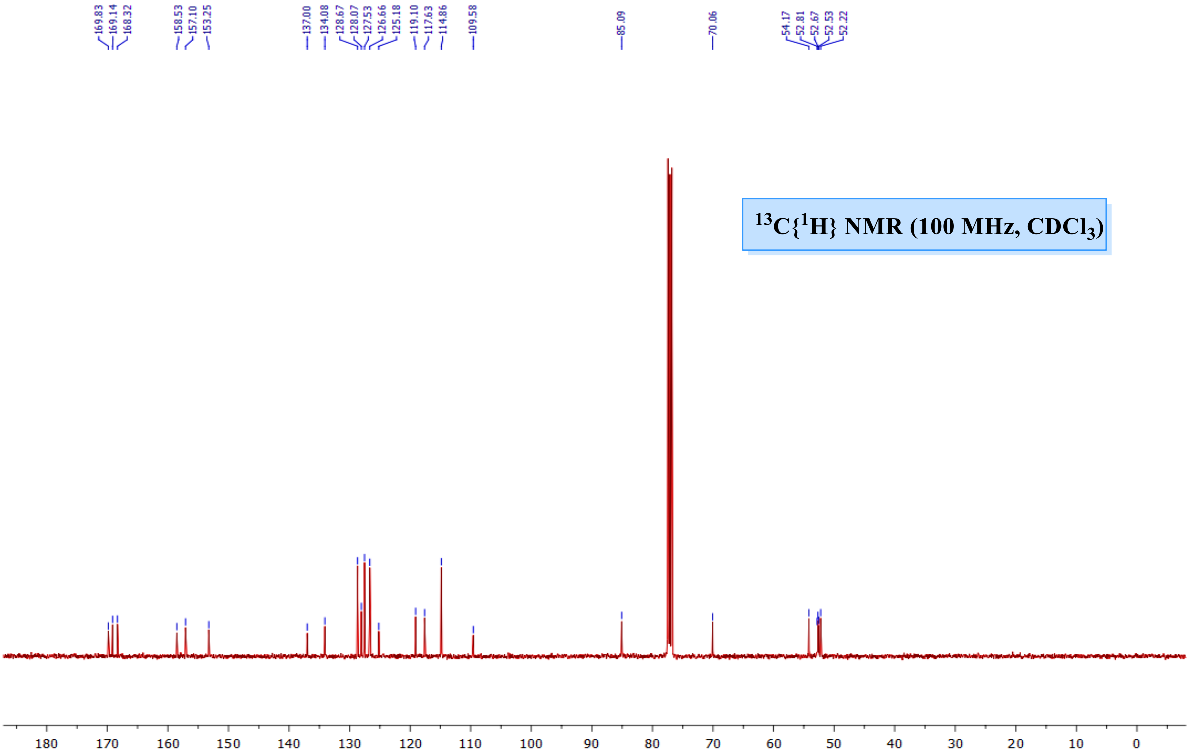
$^{13}C\{^{1}H\}$ NMR (100 MHz, $CDCl_3$)

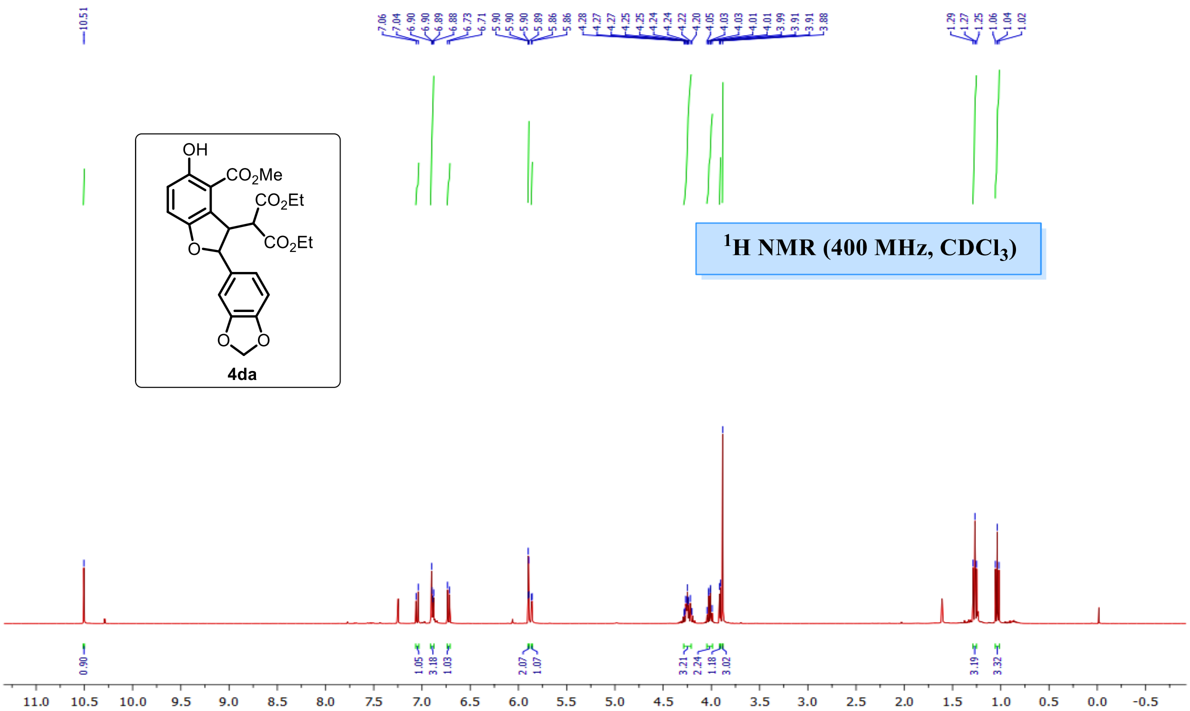
^{1}H NMR (400 MHz, $CDCl_3$)
OH
CO_2Me
CO_2Et
CO_2Et
4da

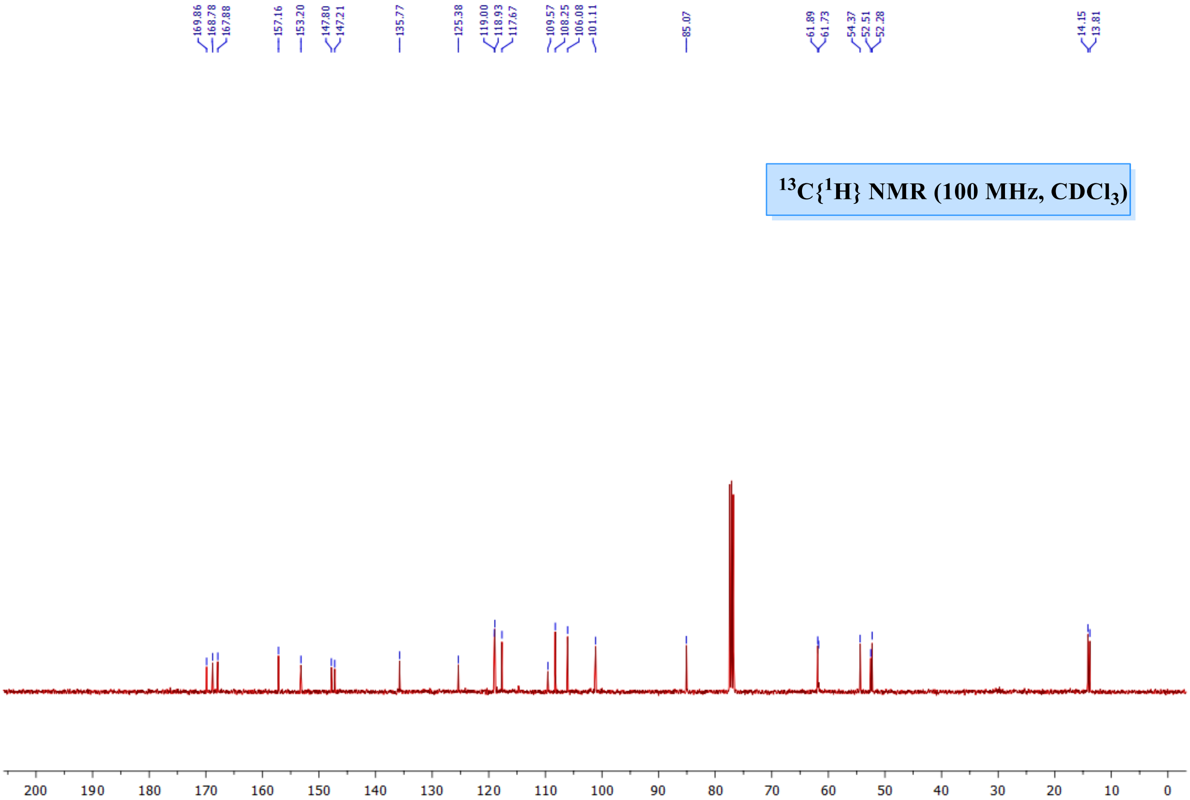
$^{13}C\{^1H\}$ NMR (100 MHz, $CDCl_3$)

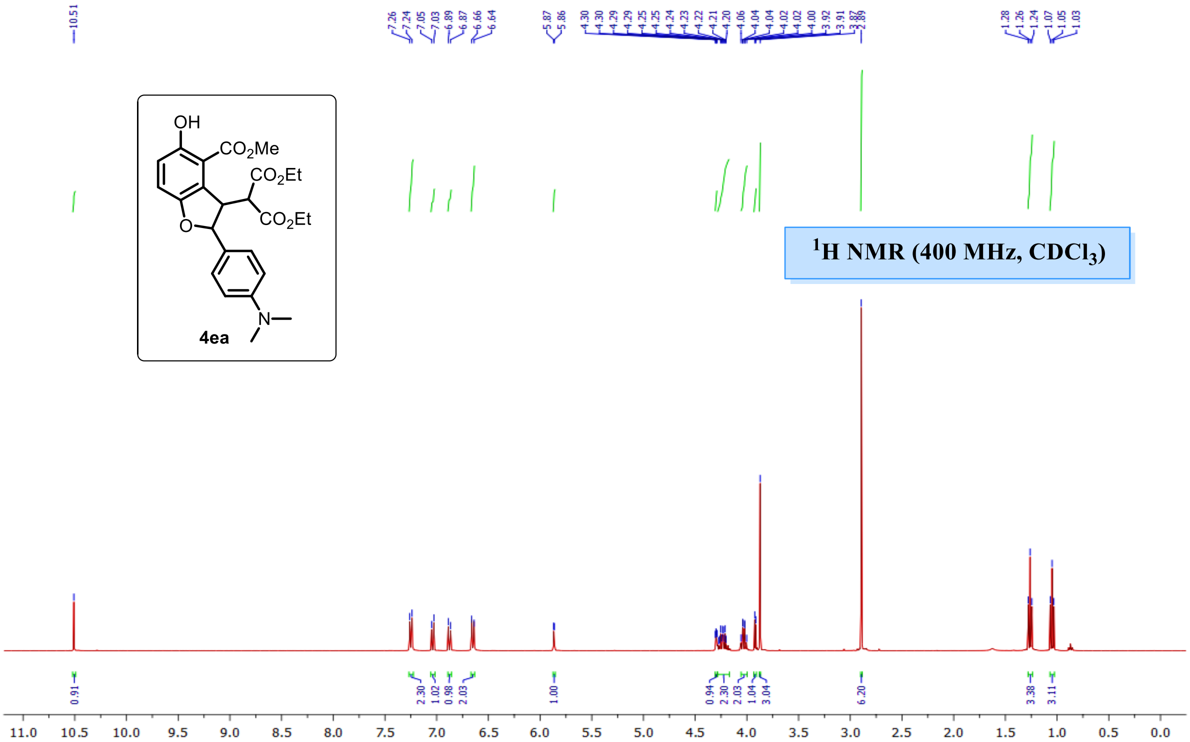
OH
CO_2Me
CO_2Et
CO_2Et
O
N
4ea
^1H NMR (400 MHz, $CDCl_3$)

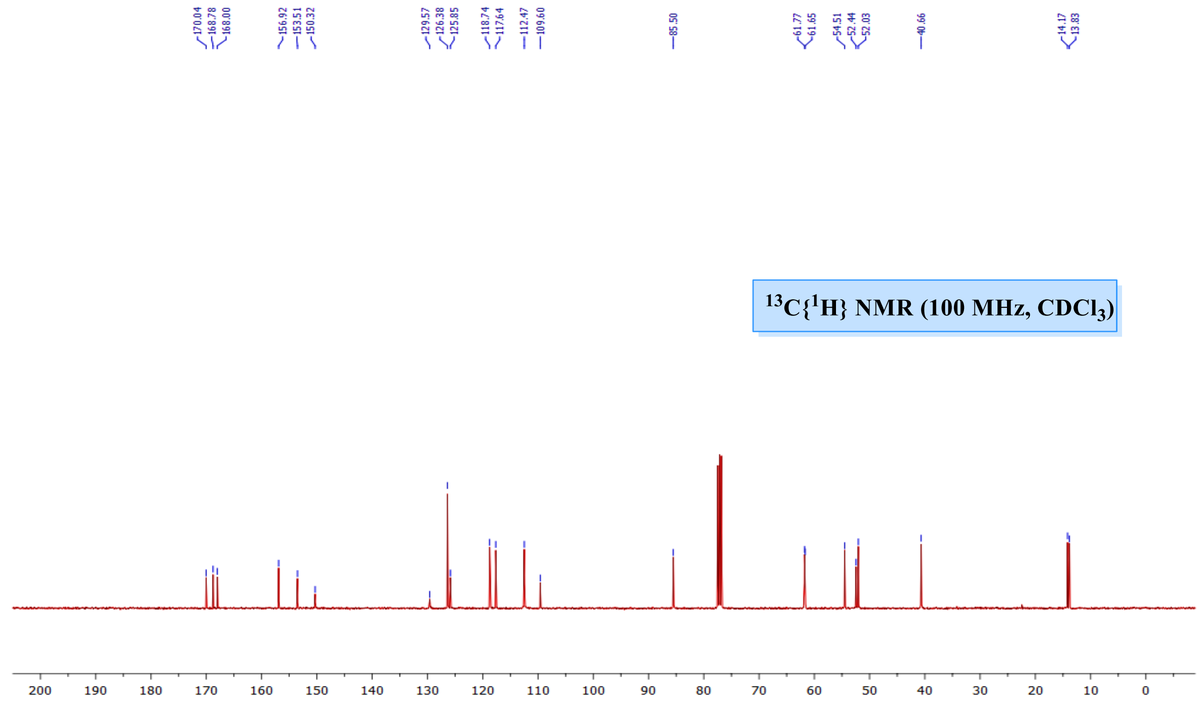
$^{13}C\{^1H\}$ NMR (100 MHz, $CDCl_3$)

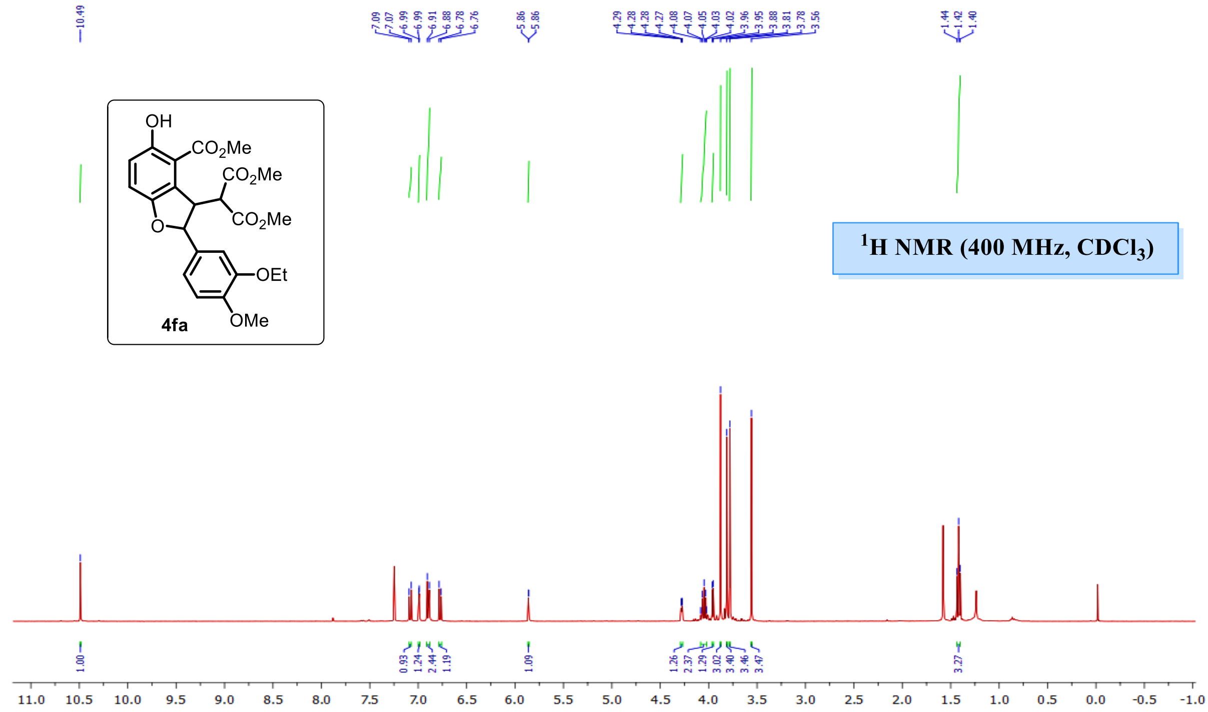
OH
CO2Me
CO2Me
CO2Me
O
OEt
OMe
4fa
^1H NMR (400 MHz, $CDCl_3$)

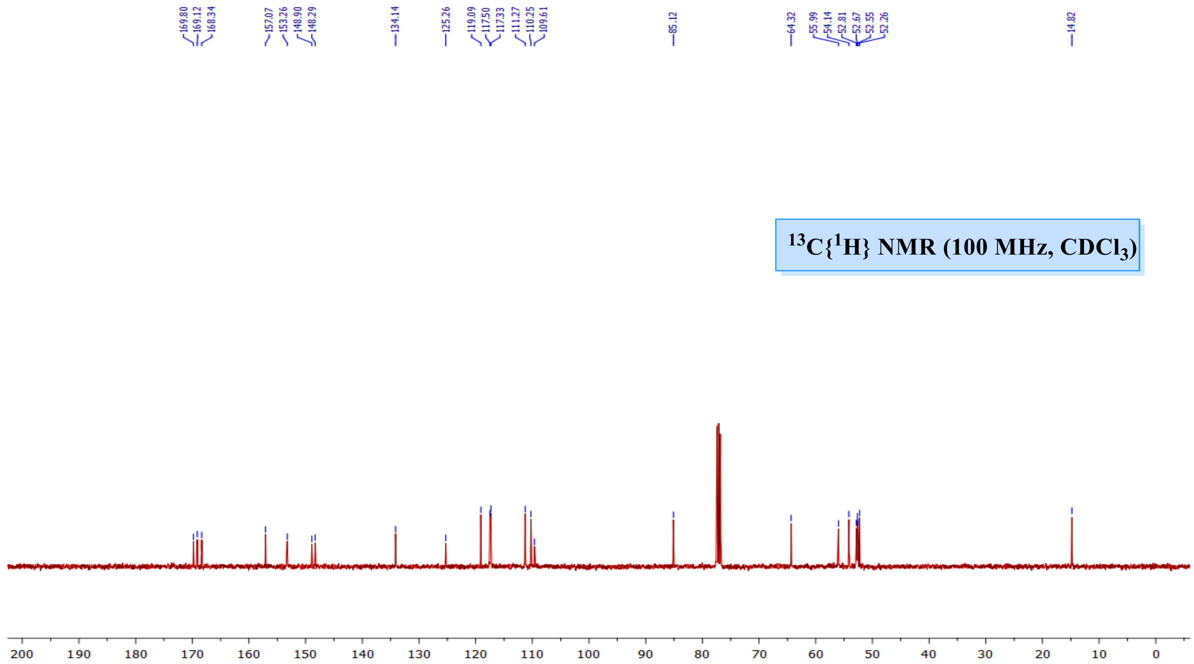
$^{13}C\{^1H\}$ NMR (100 MHz, $CDCl_3$)

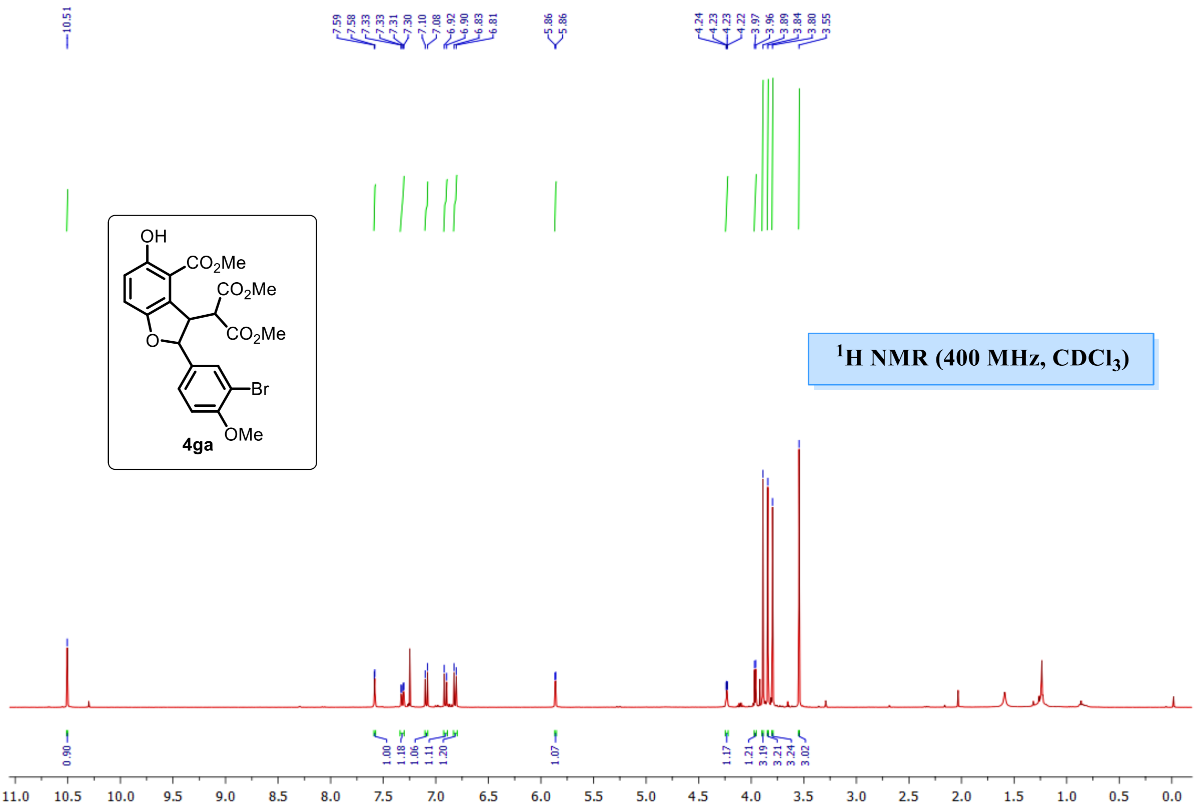
OH
CO_2Me
CO_2Me
CO_2Me
O
Br
OMe
4ga
^1H NMR (400 MHz, $CDCl_3$)

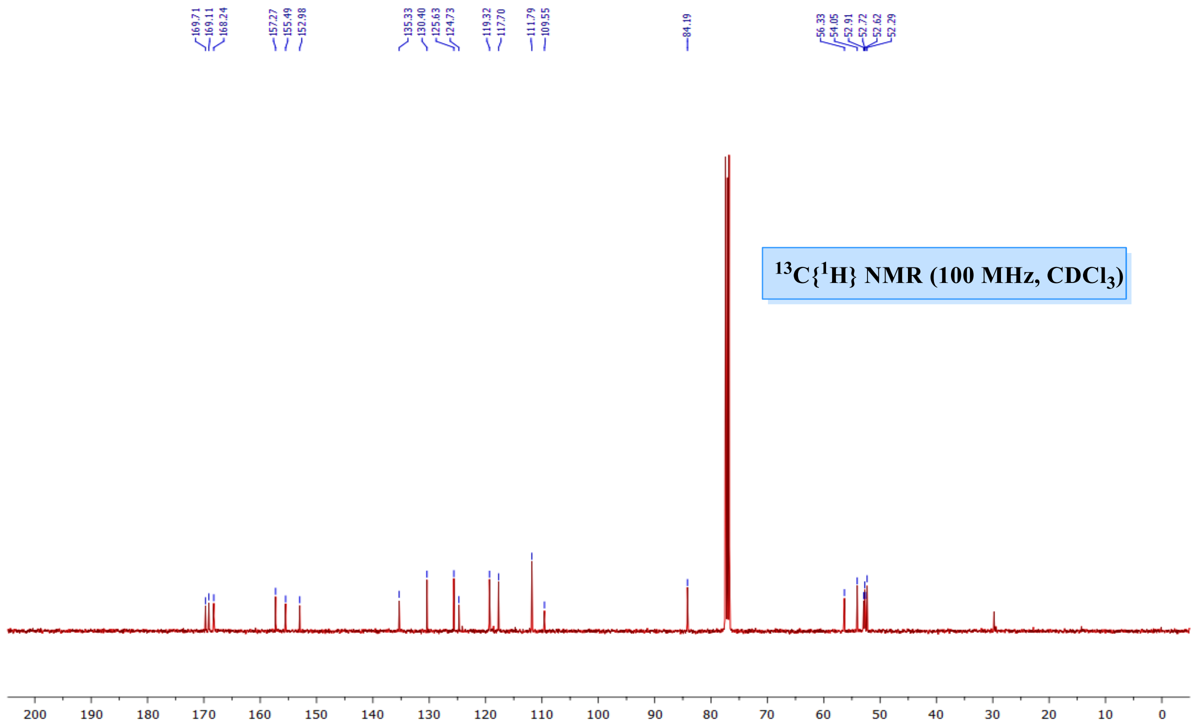
$^{13}C\{^1H\}$ NMR (100 MHz, $CDCl_3$)

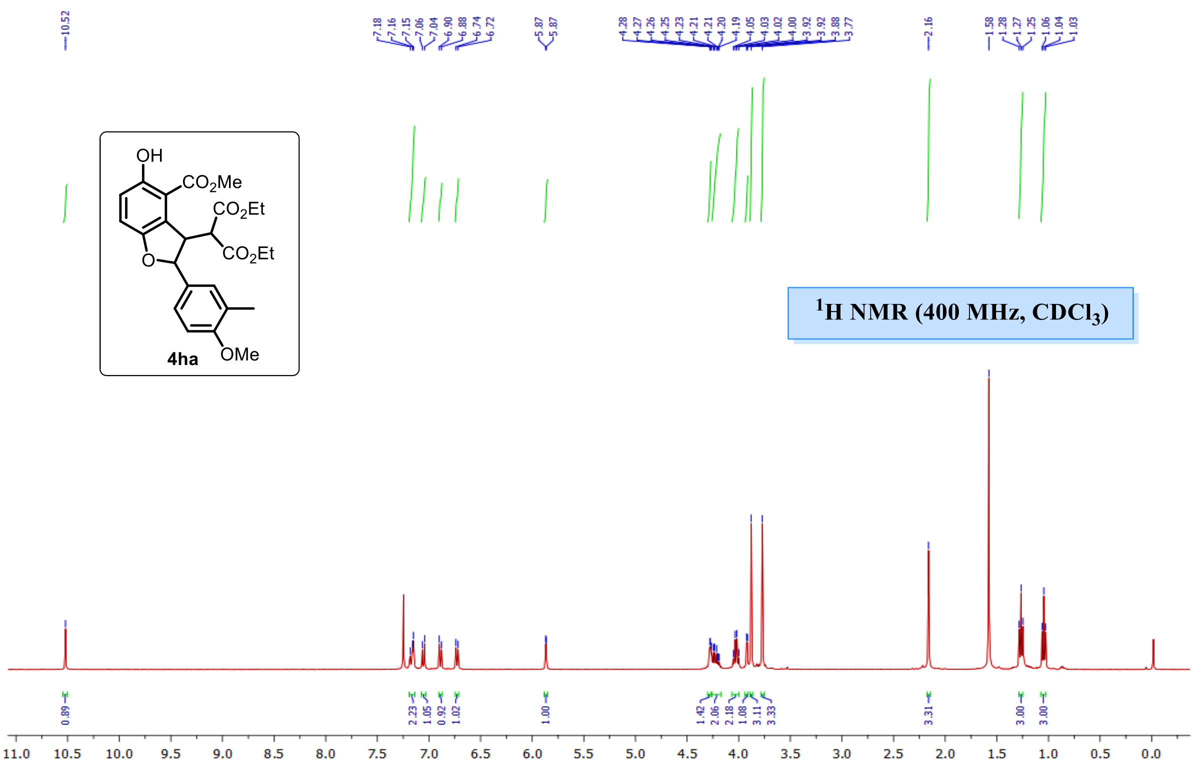
^1H NMR (400 MHz, $CDCl_3$)
4ha

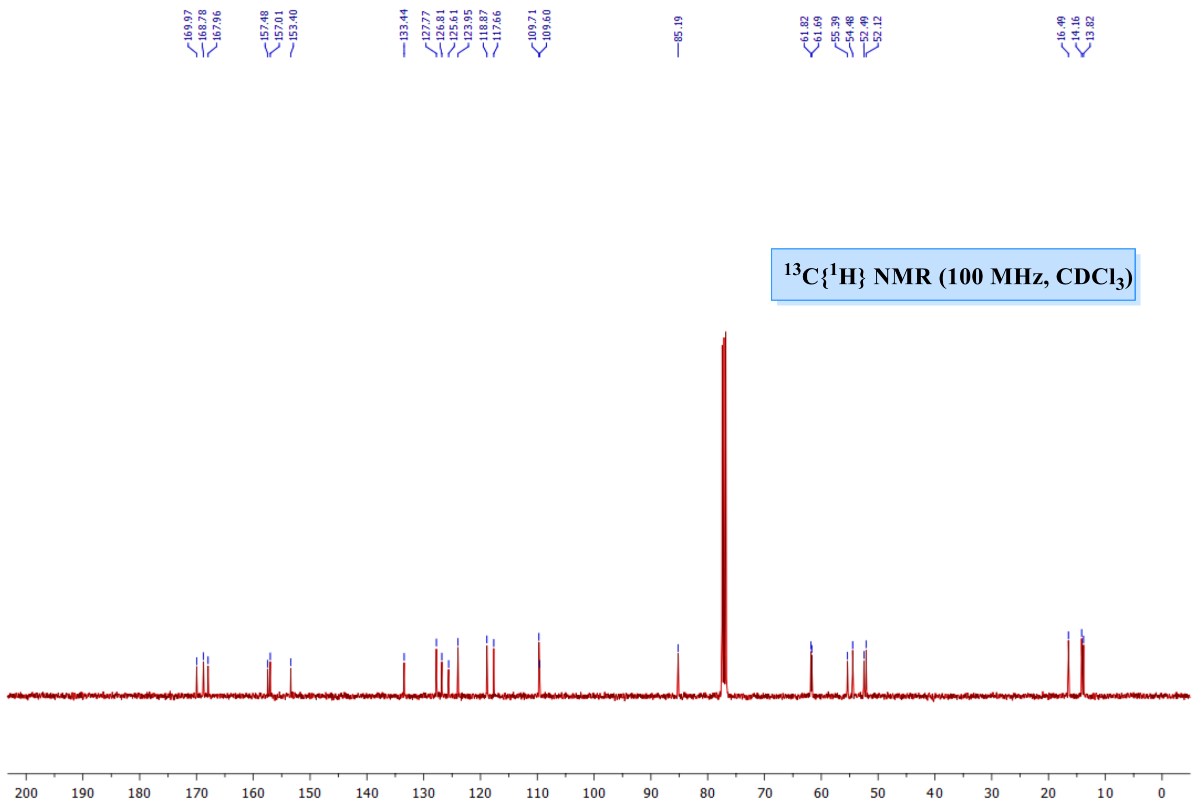
13C{1H} NMR (100 MHz, CDCl3)

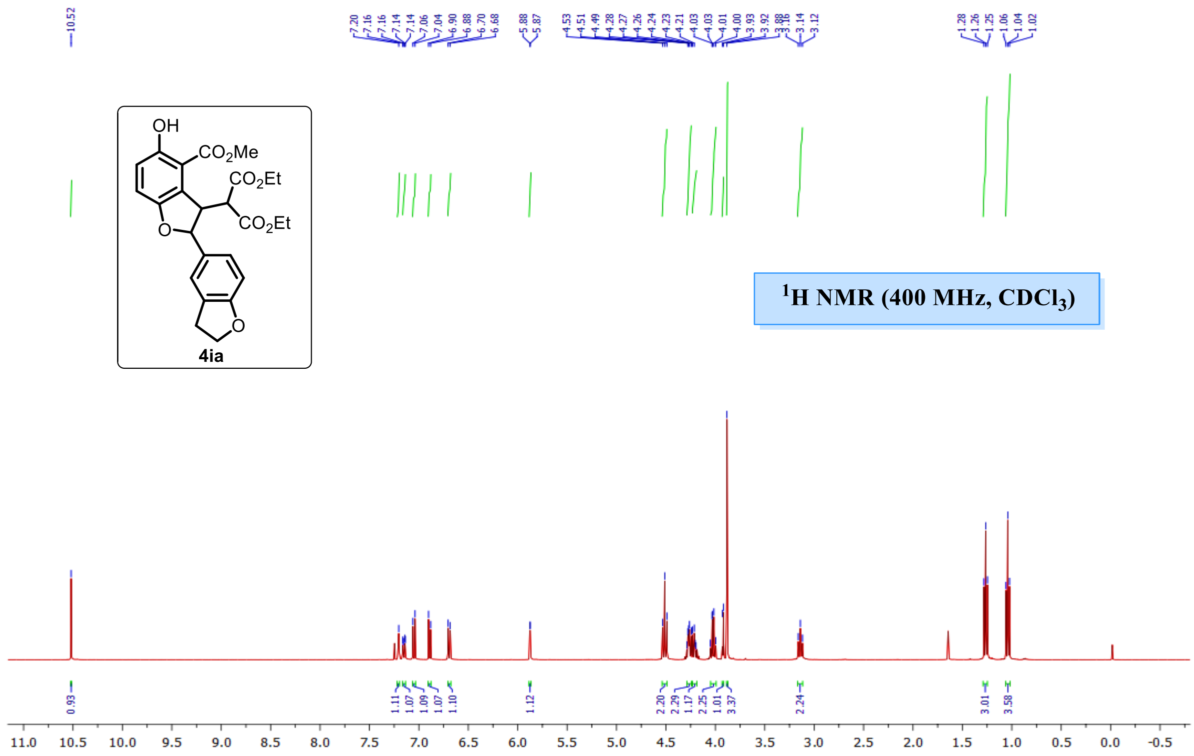
OH
CO2Me
CO2Et
CO2Et
O
O
4ia
1H NMR (400 MHz, CDCl3)

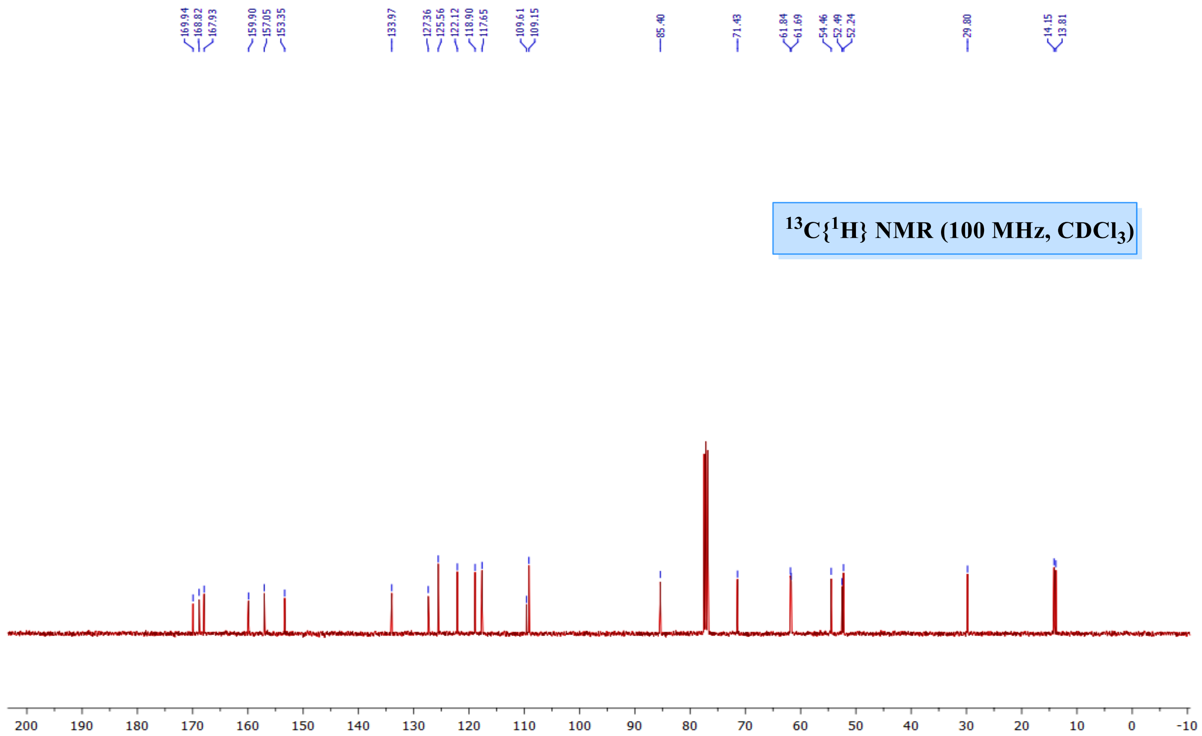
$^{13}C\{^{1}H\}$ NMR (100 MHz, $CDCl_3$)

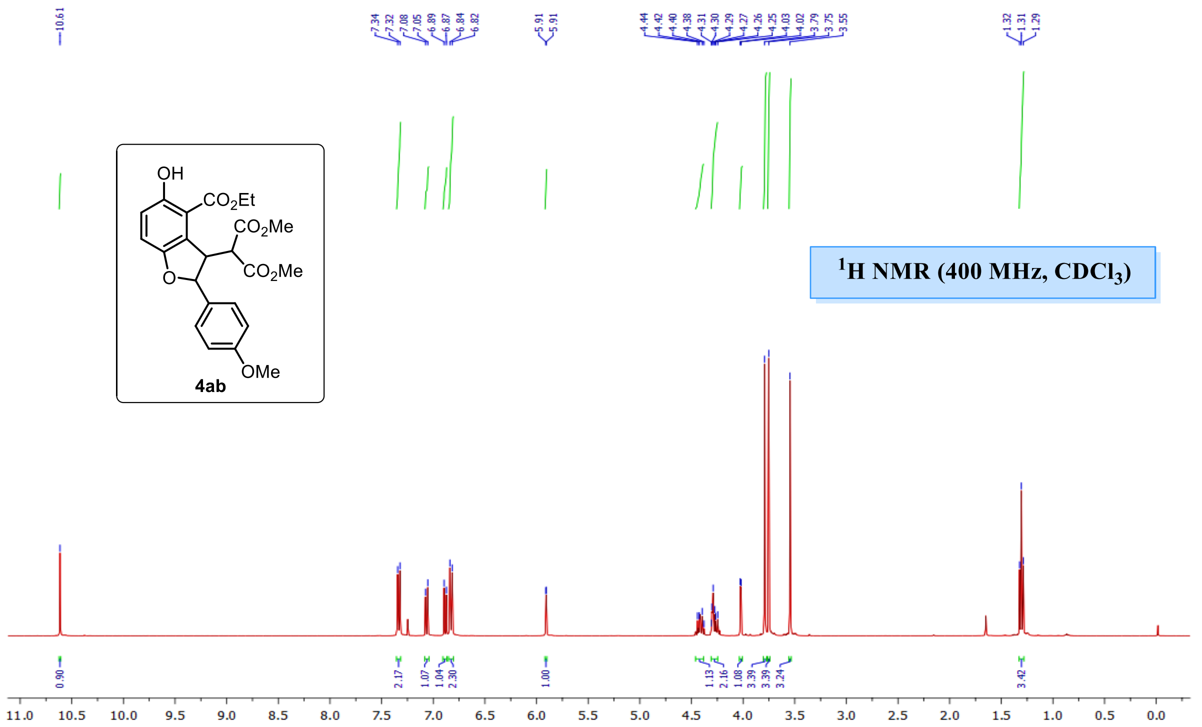
OH
CO_2Et
CO_2Me
CO_2Me
O
OMe
4ab
^{1}H NMR (400 MHz, $CDCl_3$)

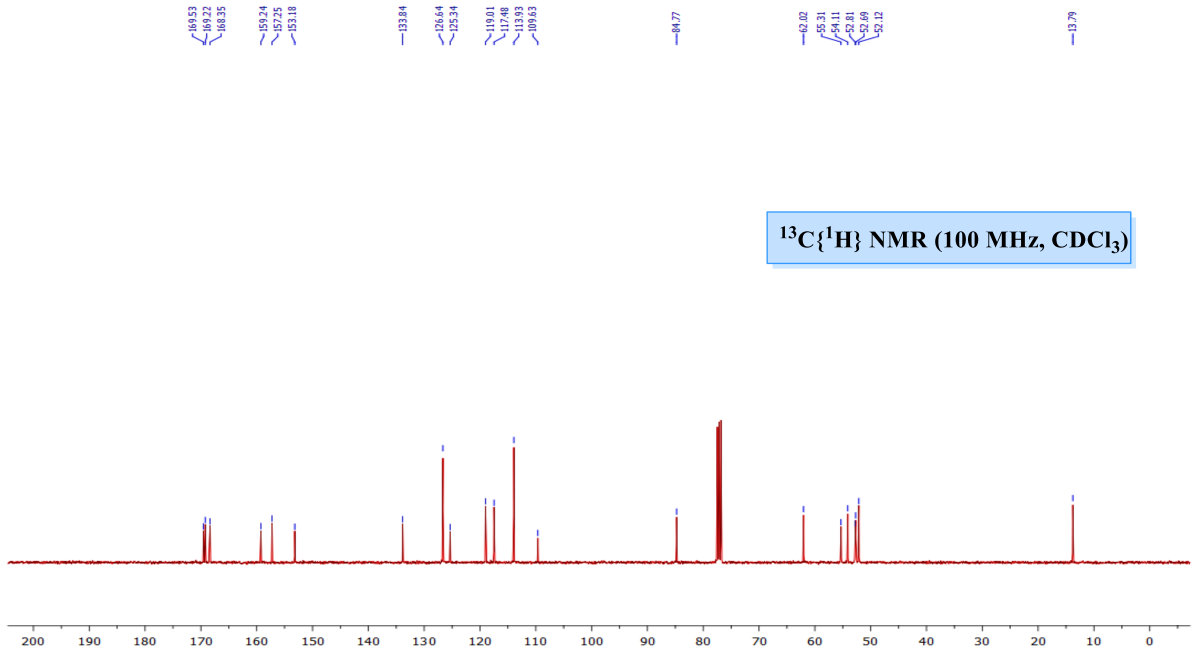
$^{13}C\{^{1}H\}$ NMR (100 MHz, $CDCl_3$)
169.53
169.22
168.35
159.24
157.25
153.18
133.84
126.64
125.34
119.01
117.48
113.93
109.63
84.77
62.02
55.31
54.11
52.81
52.69
52.12
13.79
200 190 180 170 160 150 140 130 120 110 100 90 80 70 60 50 40 30 20 10 0

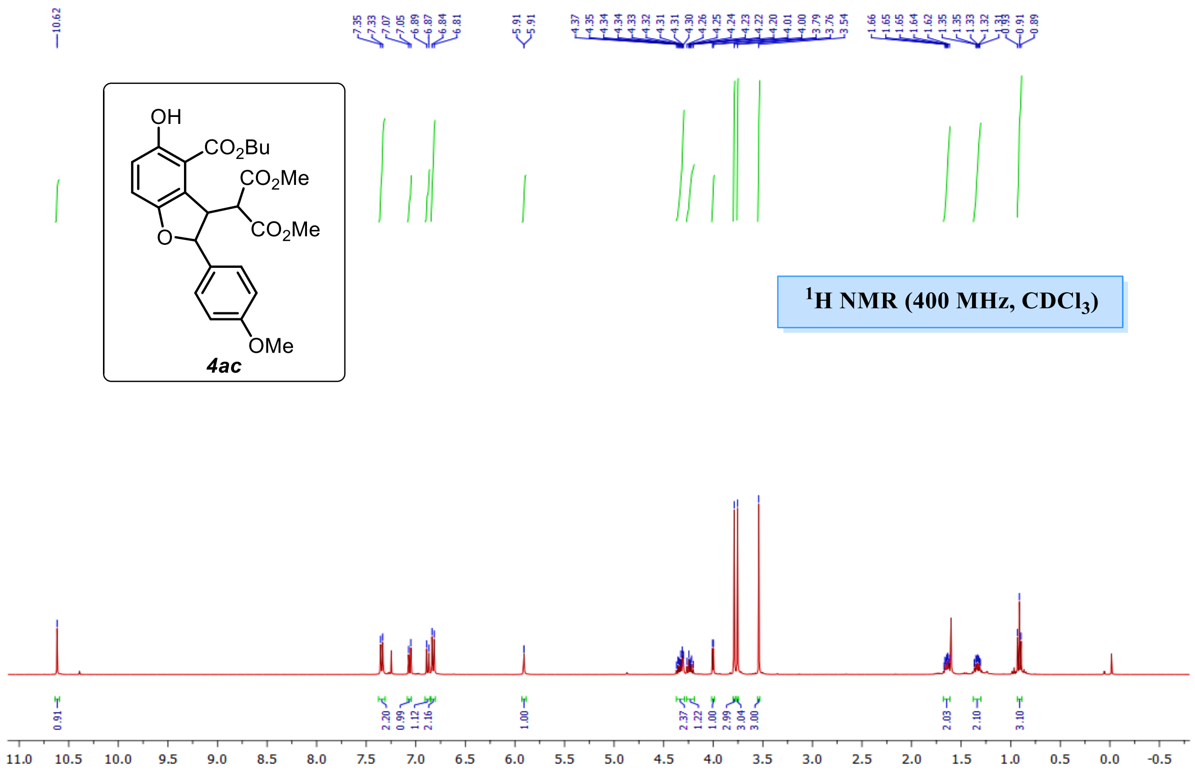
OH
CO_2Bu
CO_2Me
CO_2Me
O
OMe
4ac
^{1}H NMR (400 MHz, $CDCl_3$)
11.0 10.5 10.0 9.5 9.0 8.5 8.0 7.5 7.0 6.5 6.0 5.5 5.0 4.5 4.0 3.5 3.0 2.5 2.0 1.5 1.0 0.5 0.0 -0.5

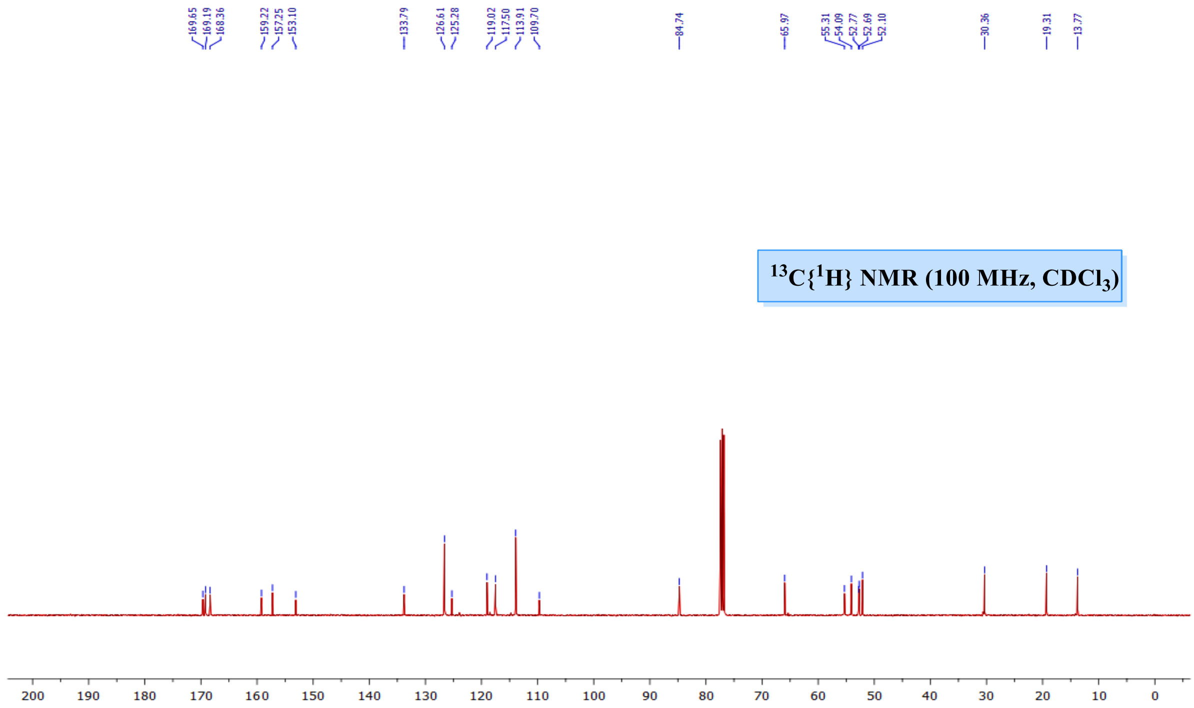
$^{13}C\{^1H\}$ NMR (100 MHz, $CDCl_3$)

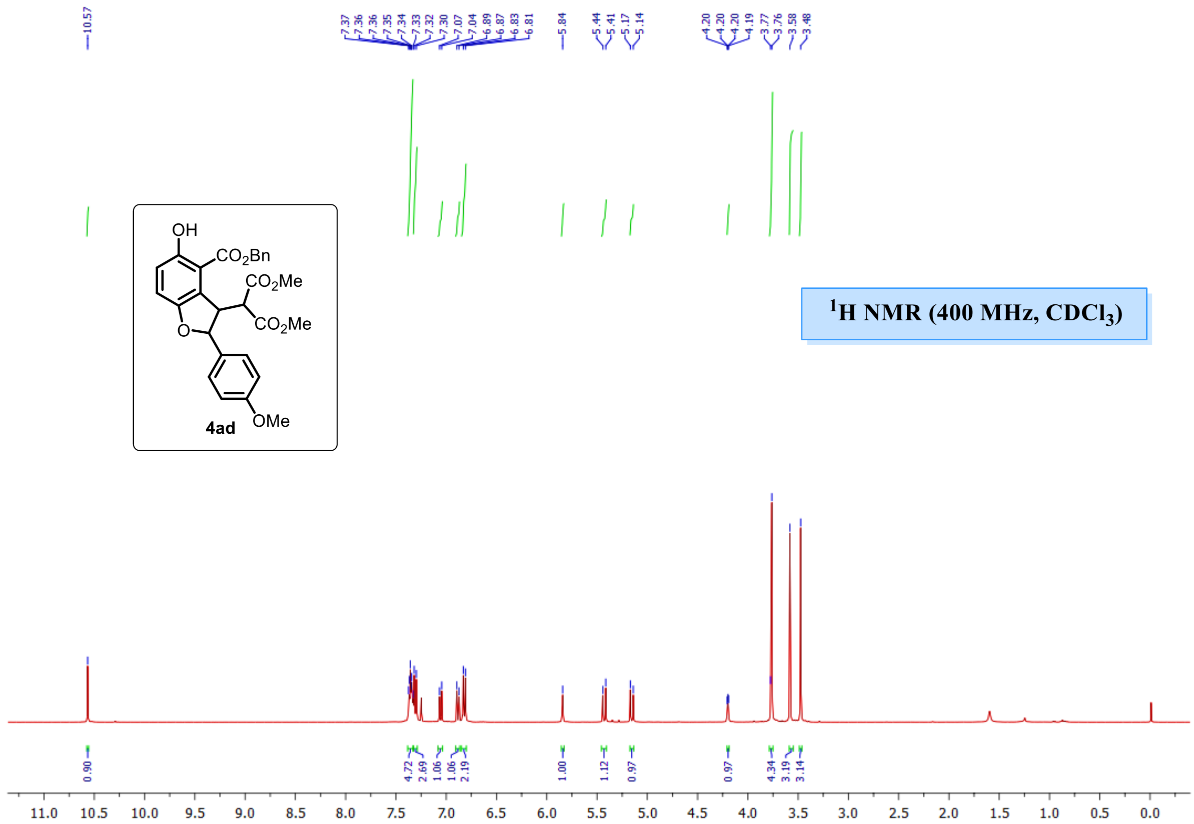
OH
CO_2Bn
CO_2Me
CO_2Me
O
OMe
4ad
^1H NMR (400 MHz, $CDCl_3$)

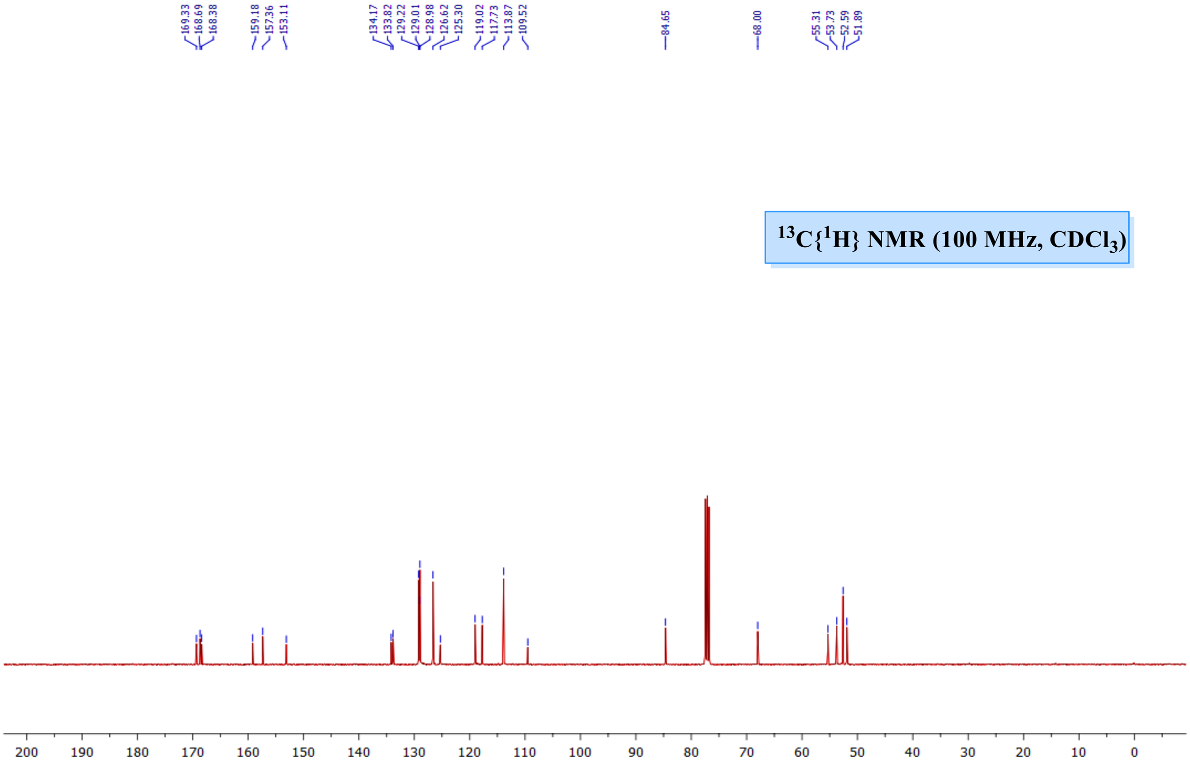
$^{13}C\{^1H\}$ NMR (100 MHz, $CDCl_3$)

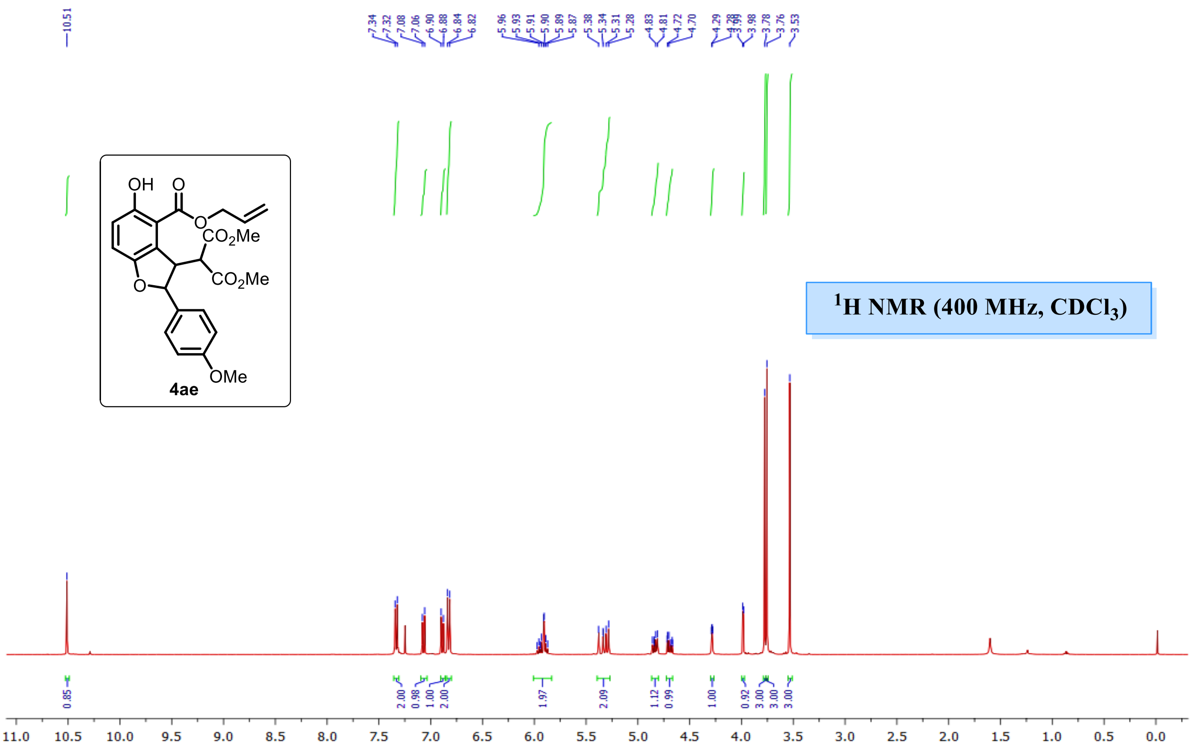
^1H NMR (400 MHz, $CDCl_3$)
4ae

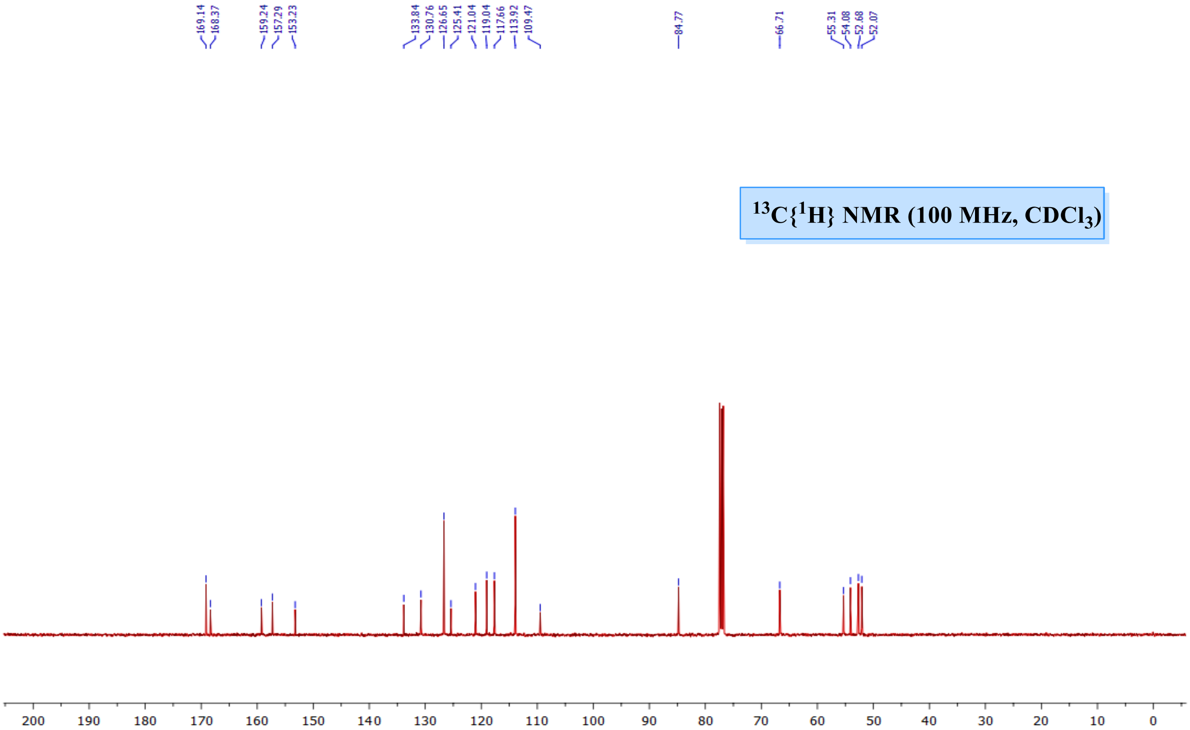
13C{1H} NMR (100 MHz, CDCl3)

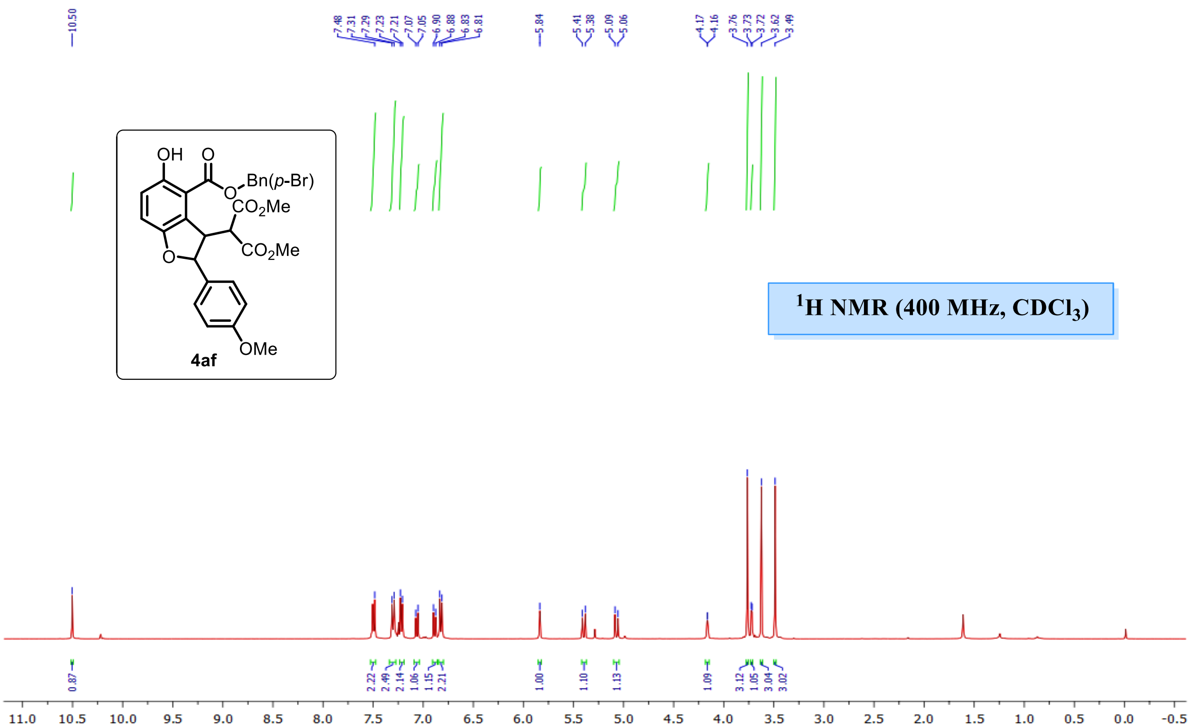
1H NMR (400 MHz, CDCl3)
OH
O
O
Bn(p-Br)
CO2Me
CO2Me
O
OMe
4af

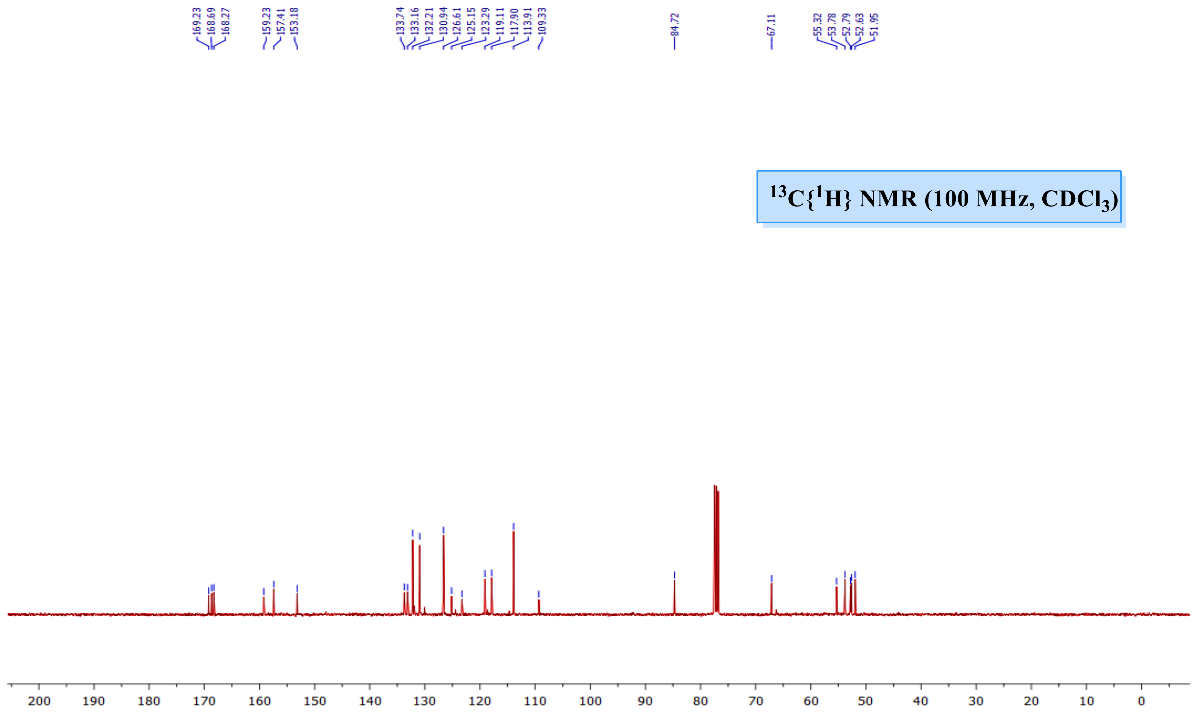

$^{13}C\{^1H\}$ NMR (100 MHz, CDCl$_3$)

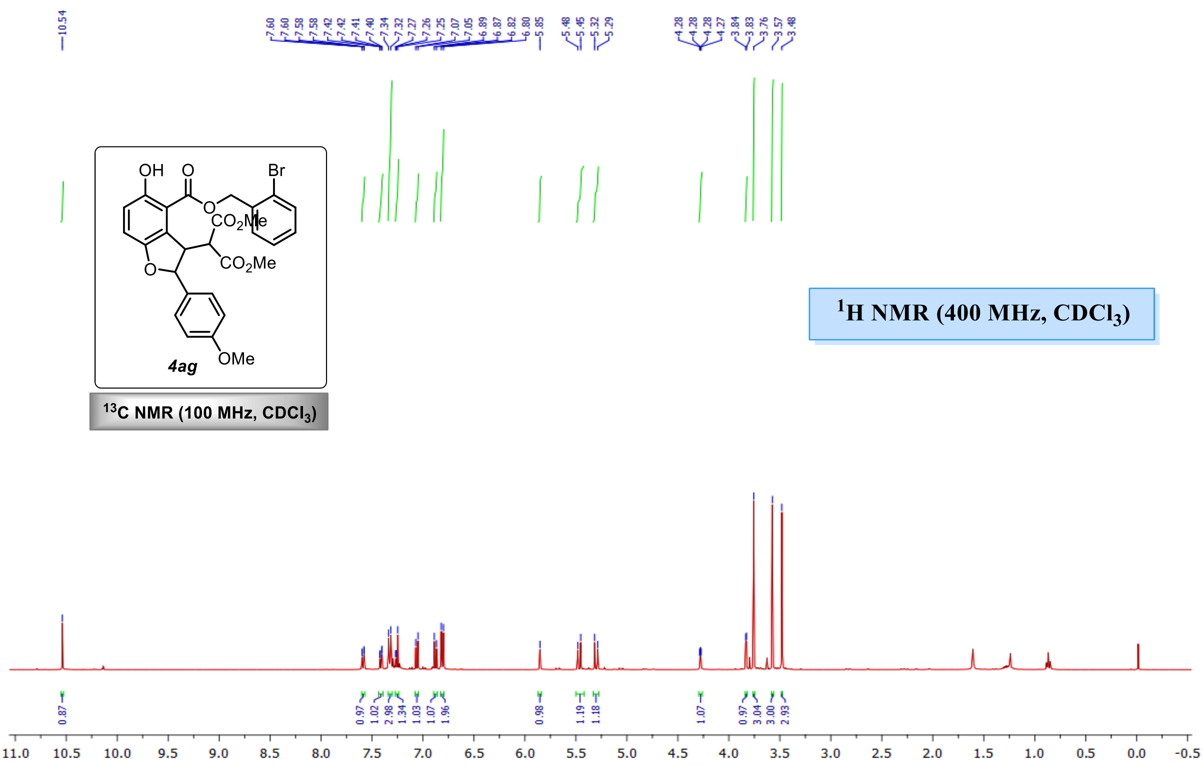

4ag
^{13}C NMR (100 MHz, CDCl$_3$)
^{1}H NMR (400 MHz, CDCl$_3$)

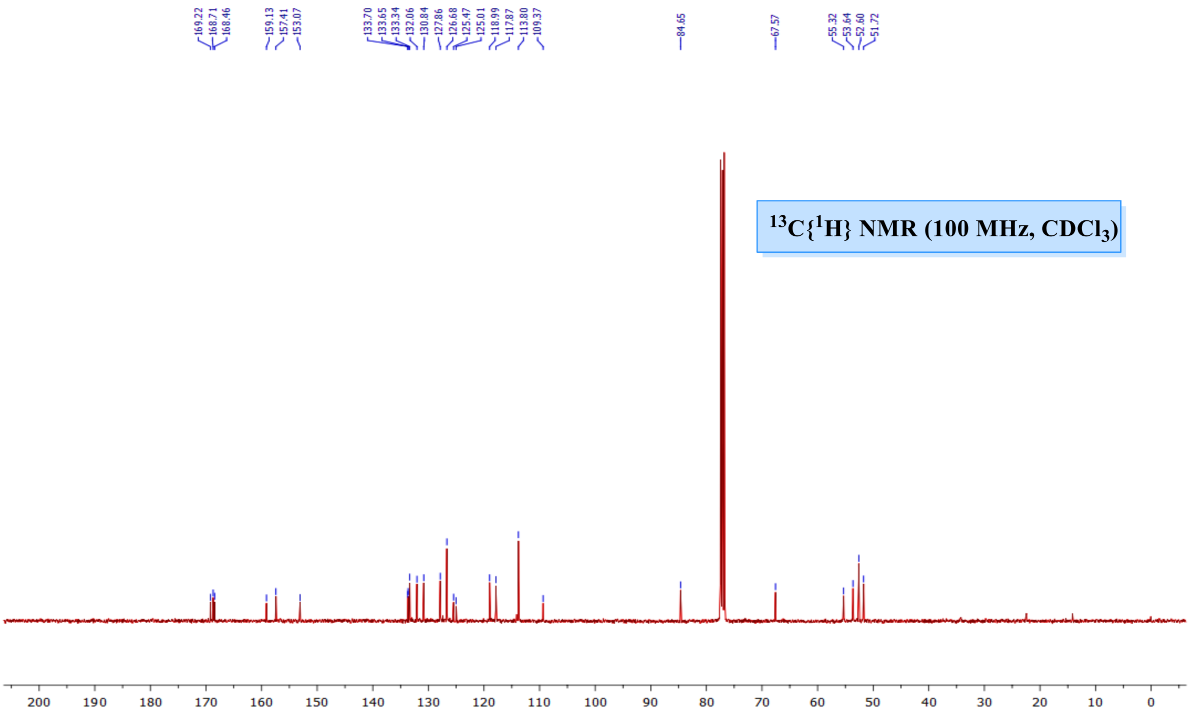
13C{1H} NMR (100 MHz, CDCl3)

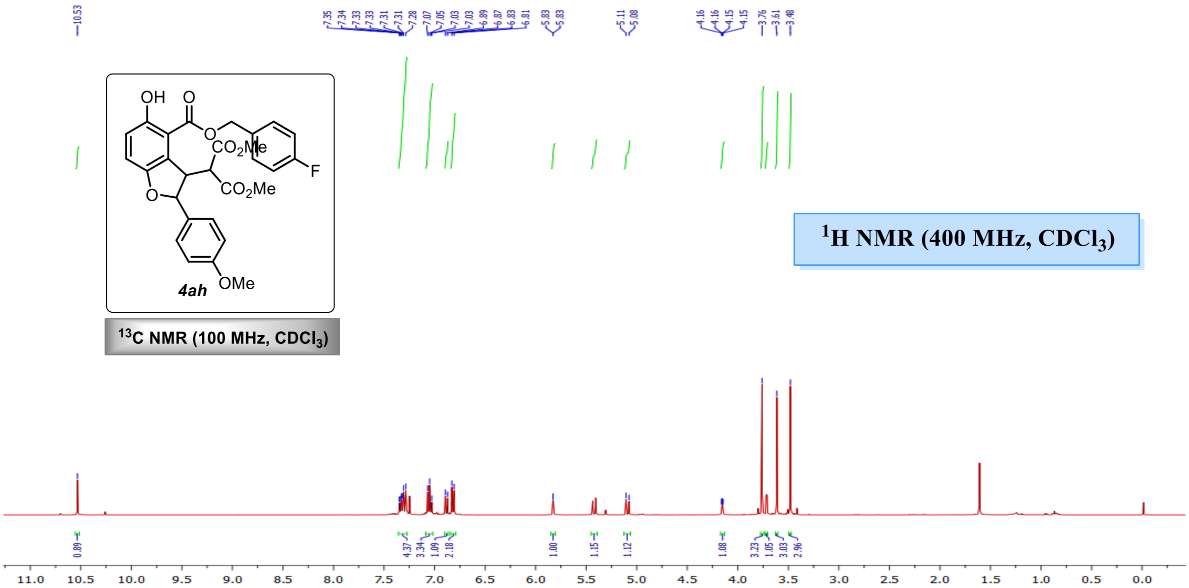
OH
O
O
CO2Me
F
O
CO2Me
OMe
4ah
13C NMR (100 MHz, CDCl3)
1H NMR (400 MHz, CDCl3)

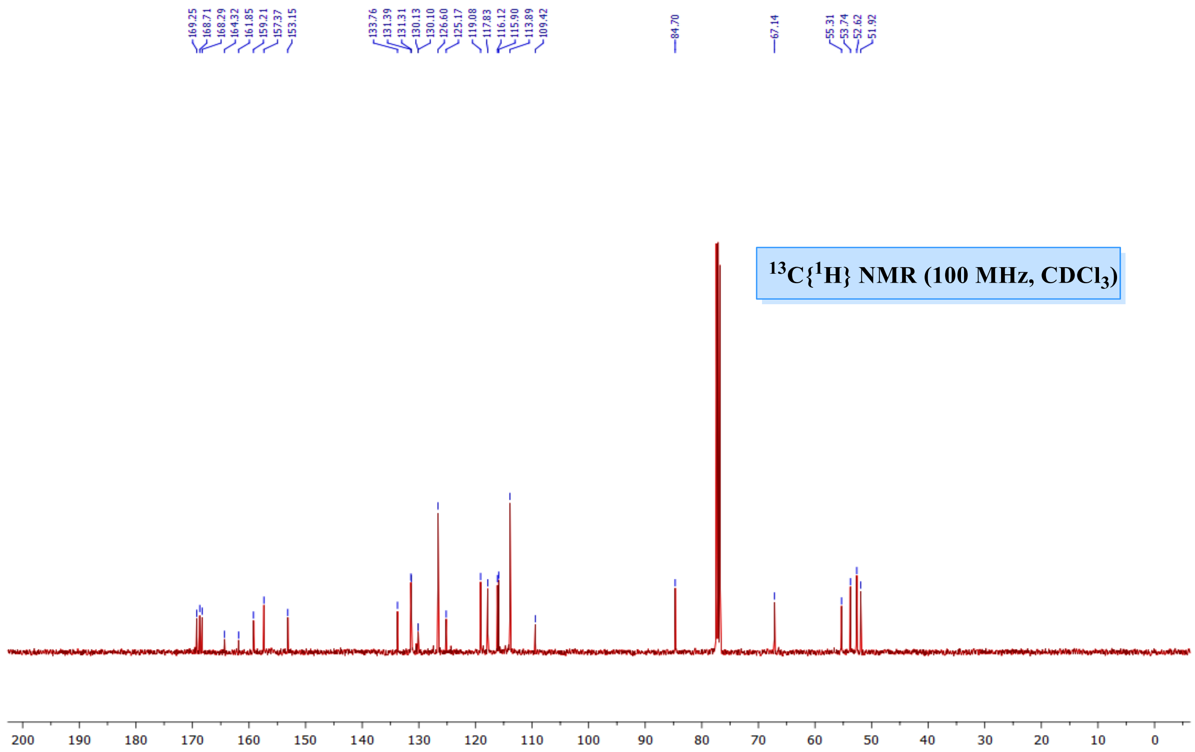
169.25
168.71
168.29
164.32
161.85
159.21
157.37
153.15
133.76
131.39
131.31
130.13
130.10
126.60
125.17
119.08
117.83
116.12
115.90
113.89
109.42
84.70
67.14
55.31
53.74
52.62
51.92
13C{1H} NMR (100 MHz, CDCl3)
200 190 180 170 160 150 140 130 120 110 100 90 80 70 60 50 40 30 20 10 0

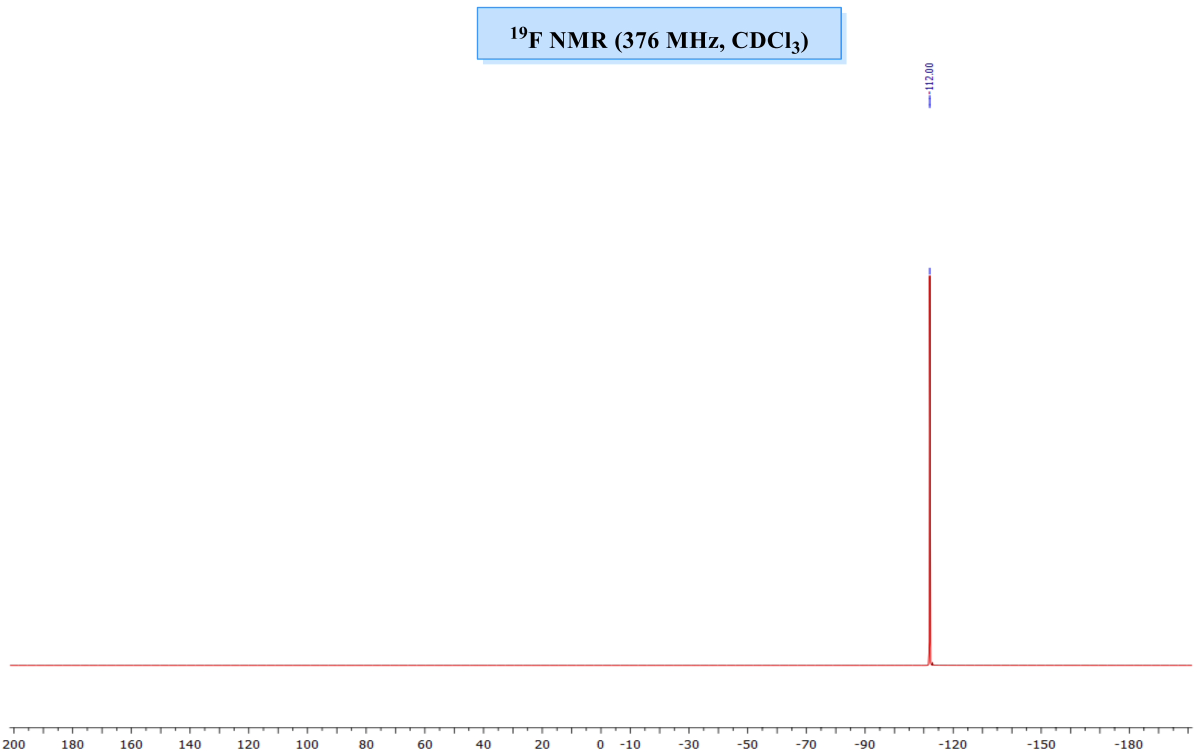
19F NMR (376 MHz, CDCl3)
-112.00
200 180 160 140 120 100 80 60 40 20 0 -10 -30 -50 -70 -90 -120 -150 -180

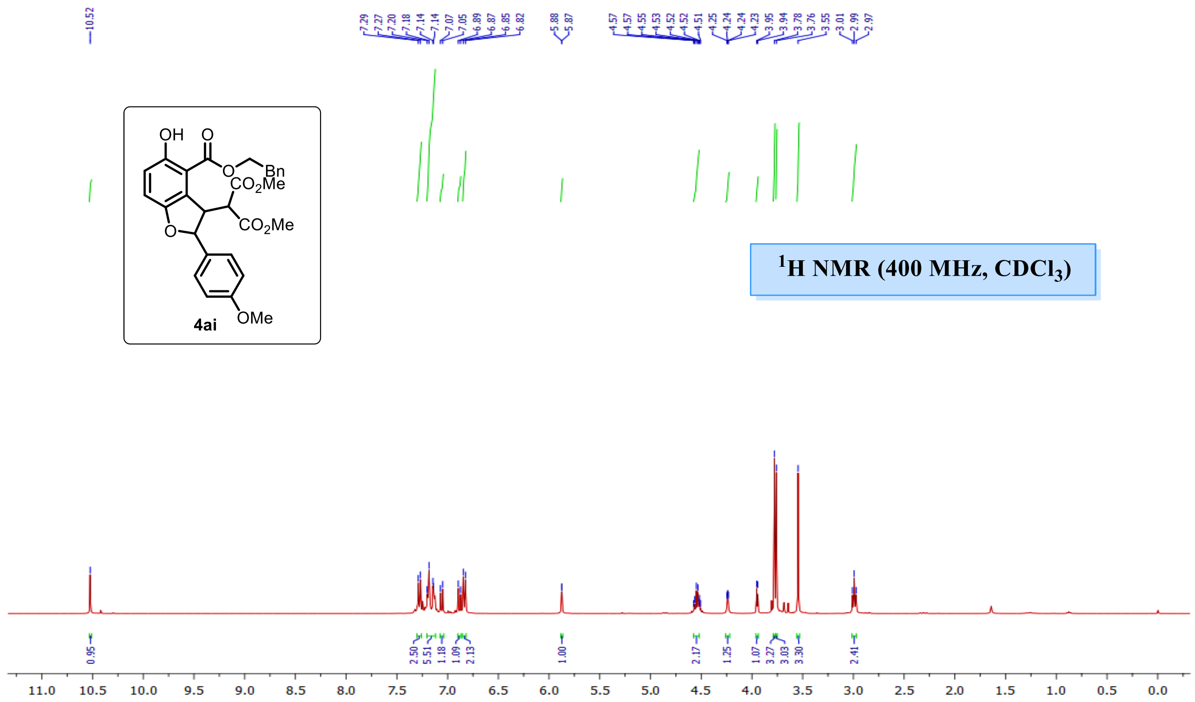
OH
O
O
Bn
CO2Me
CO2Me
O
OMe
4ai
1H NMR (400 MHz, CDCl3)

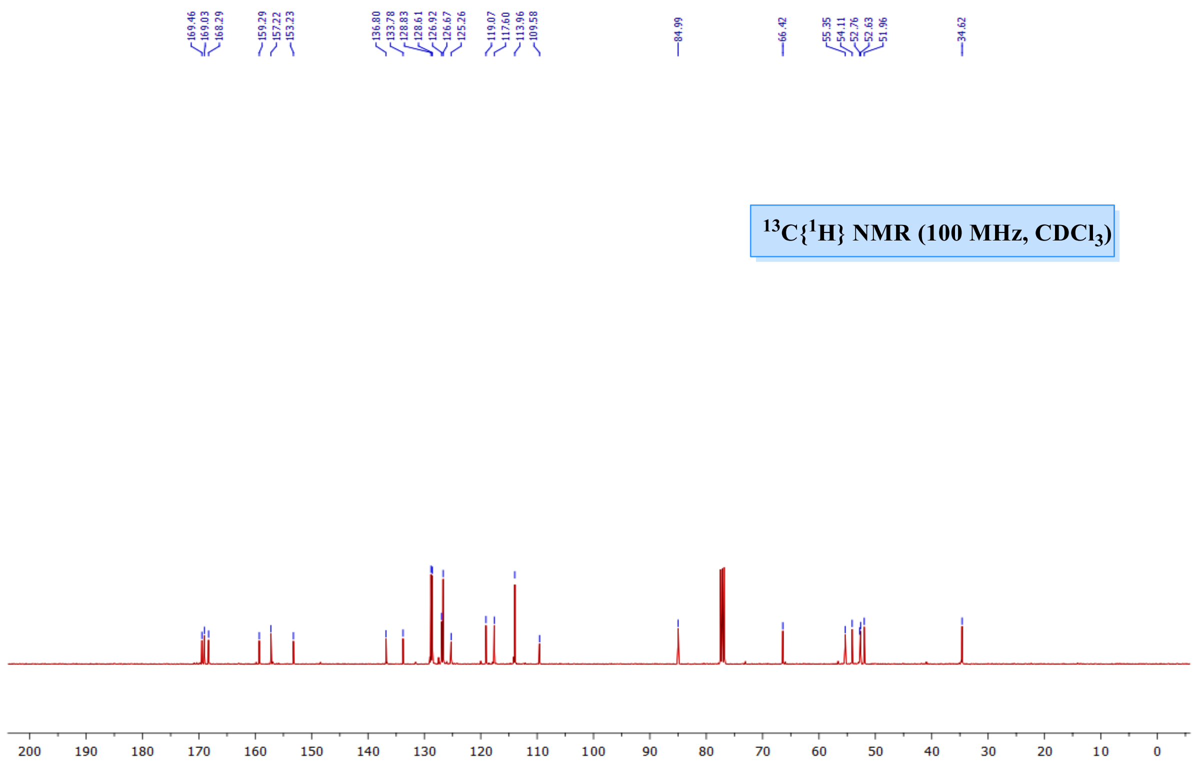
13C{1H} NMR (100 MHz, CDCl3)

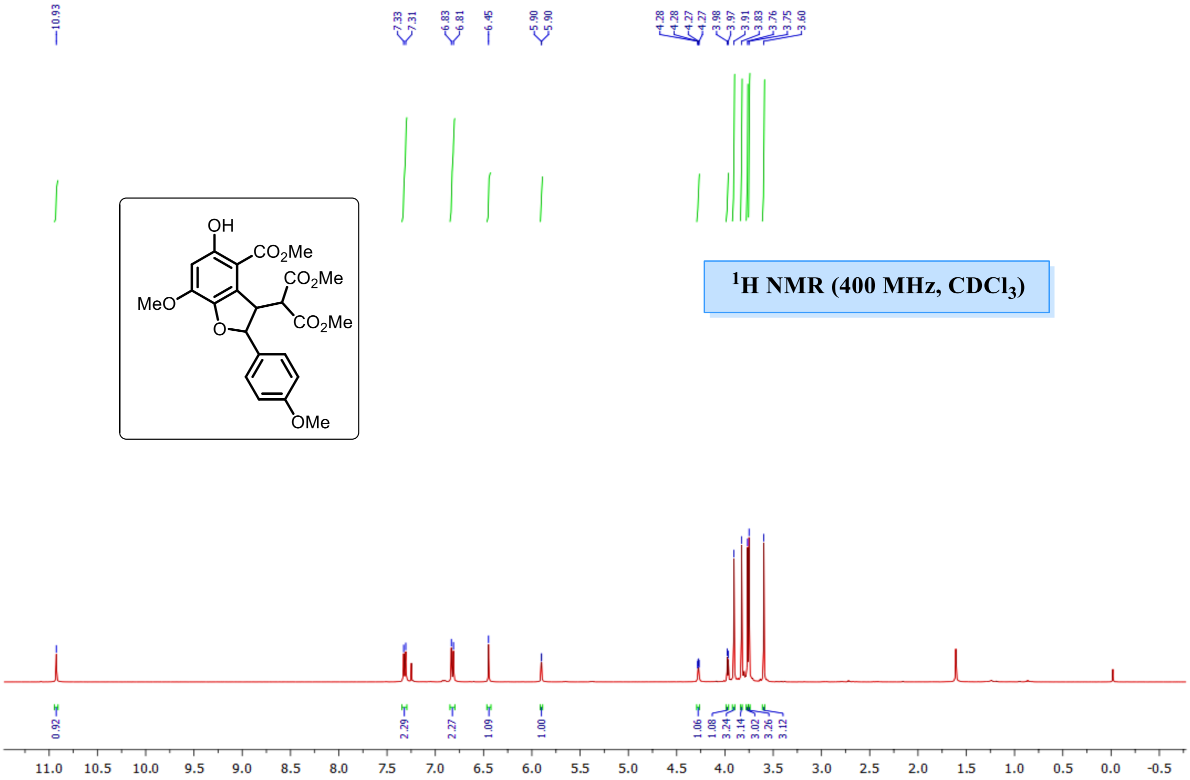
OH
CO2Me
CO2Me
MeO
O
CO2Me
OMe
1H NMR (400 MHz, CDCl3)

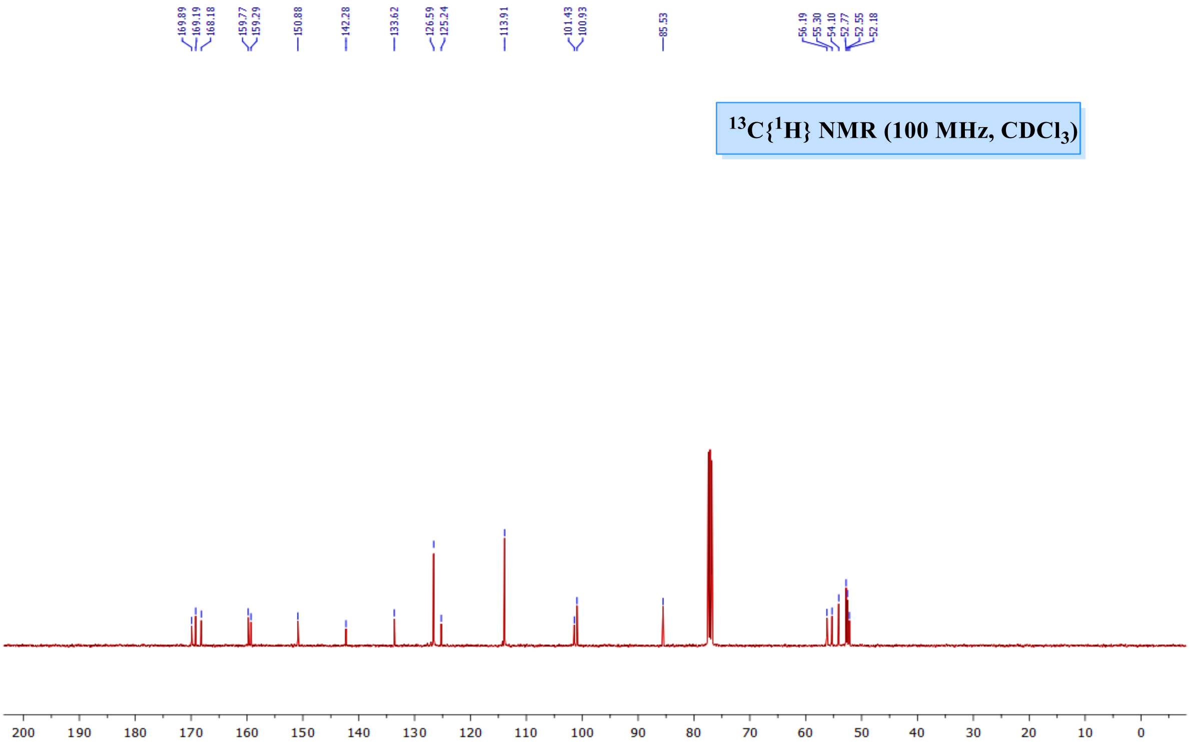
13C{1H} NMR (100 MHz, CDCl3)

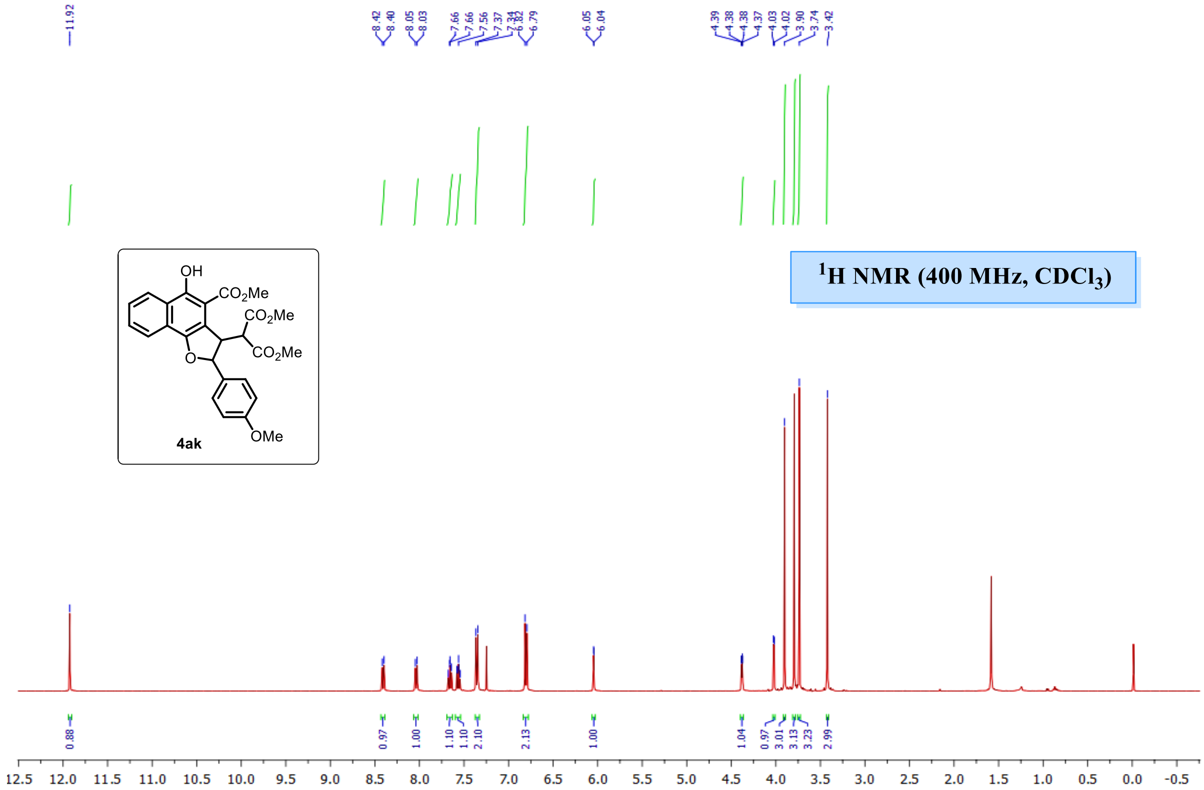

OH
CO2Me
CO2Me
CO2Me
O
OMe
4ak
1H NMR (400 MHz, CDCl3)

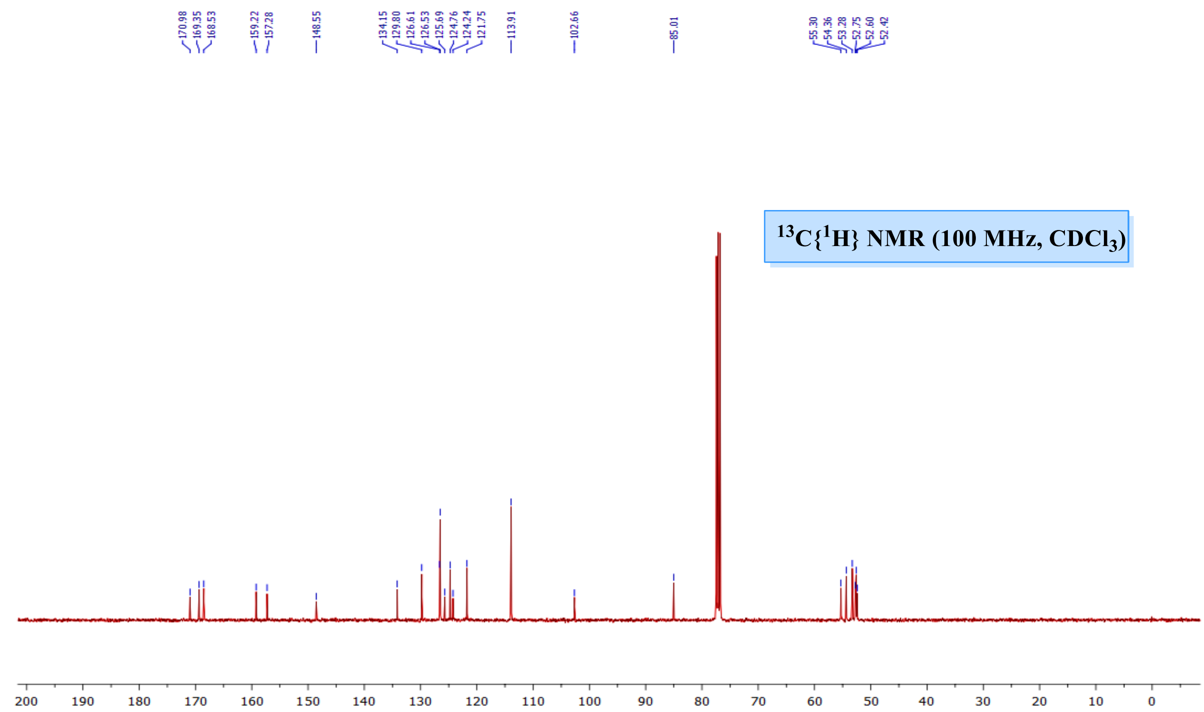

13C{1H} NMR (100 MHz, CDCl3)

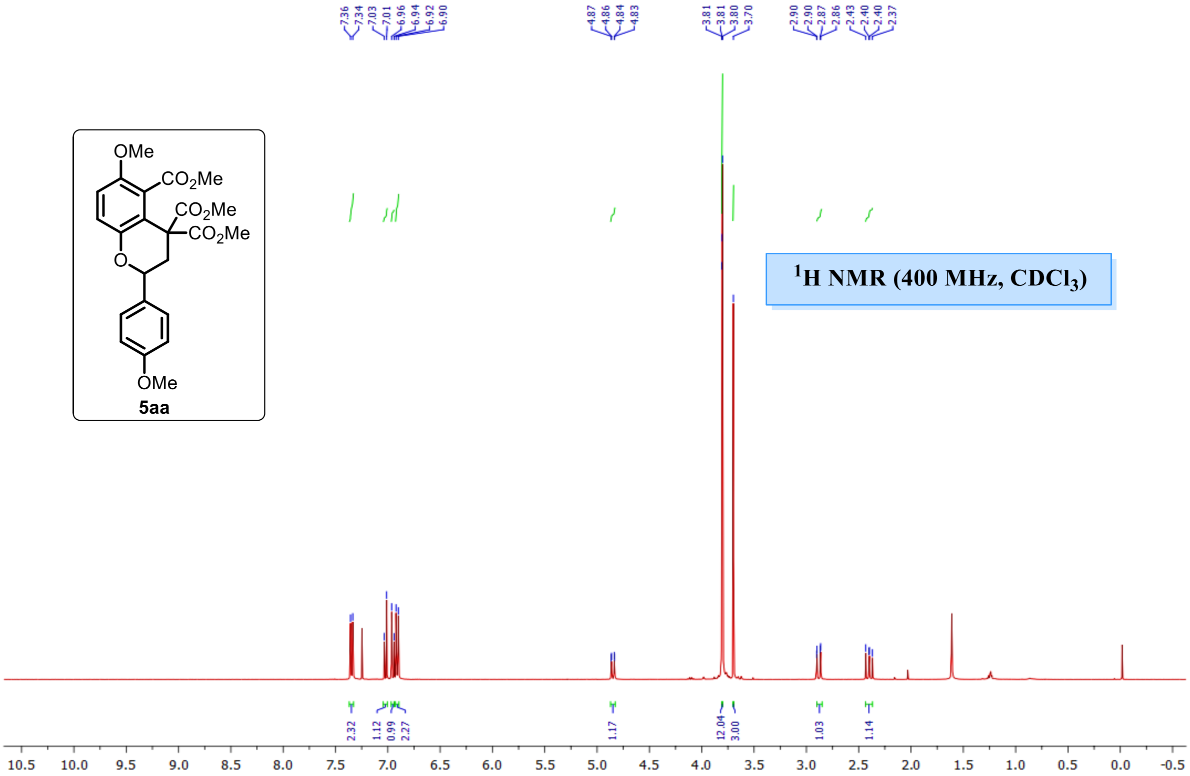
OMe
CO2Me
CO2Me
CO2Me
O
OMe
5aa
1H NMR (400 MHz, CDCl3)

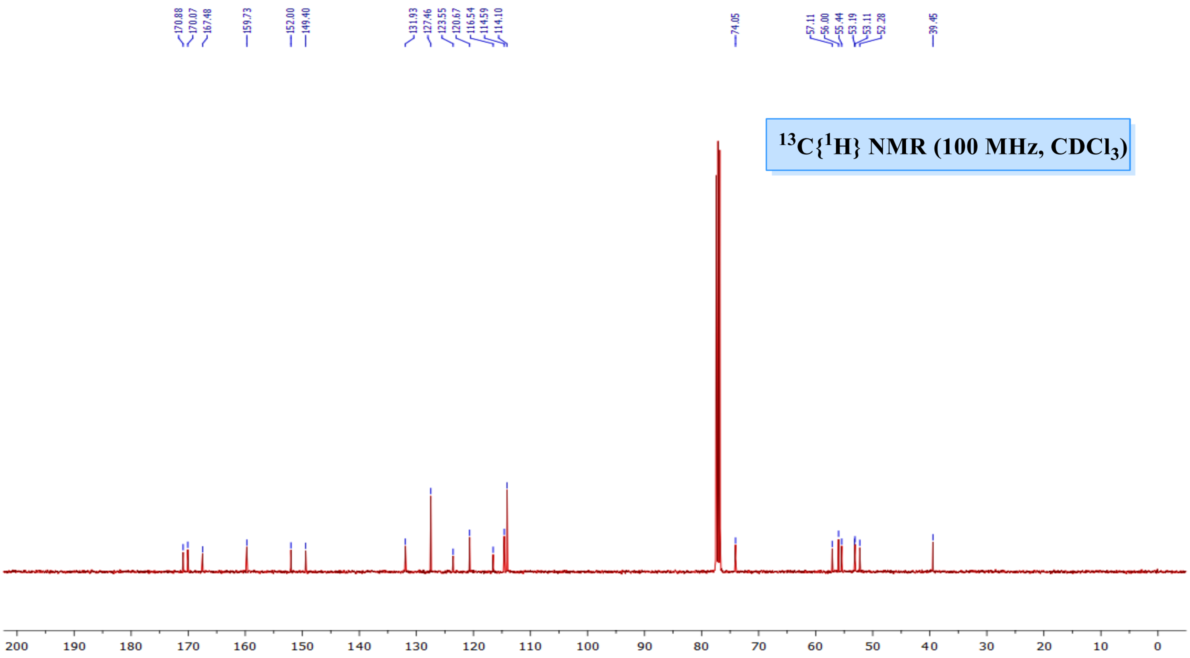
13C{1H} NMR (100 MHz, CDCl3)

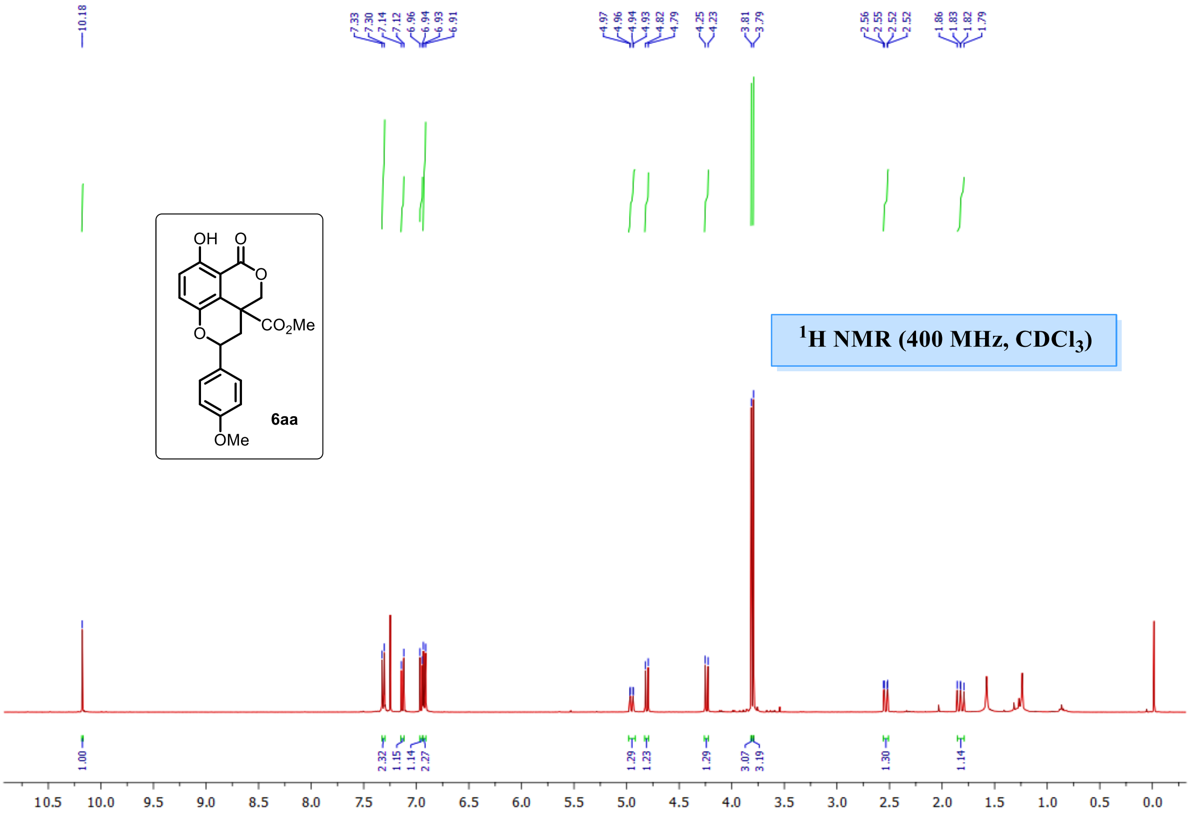
OH
O
O
CO_2Me
O
OMe
6aa
^{1}H NMR (400 MHz, $CDCl_3$)

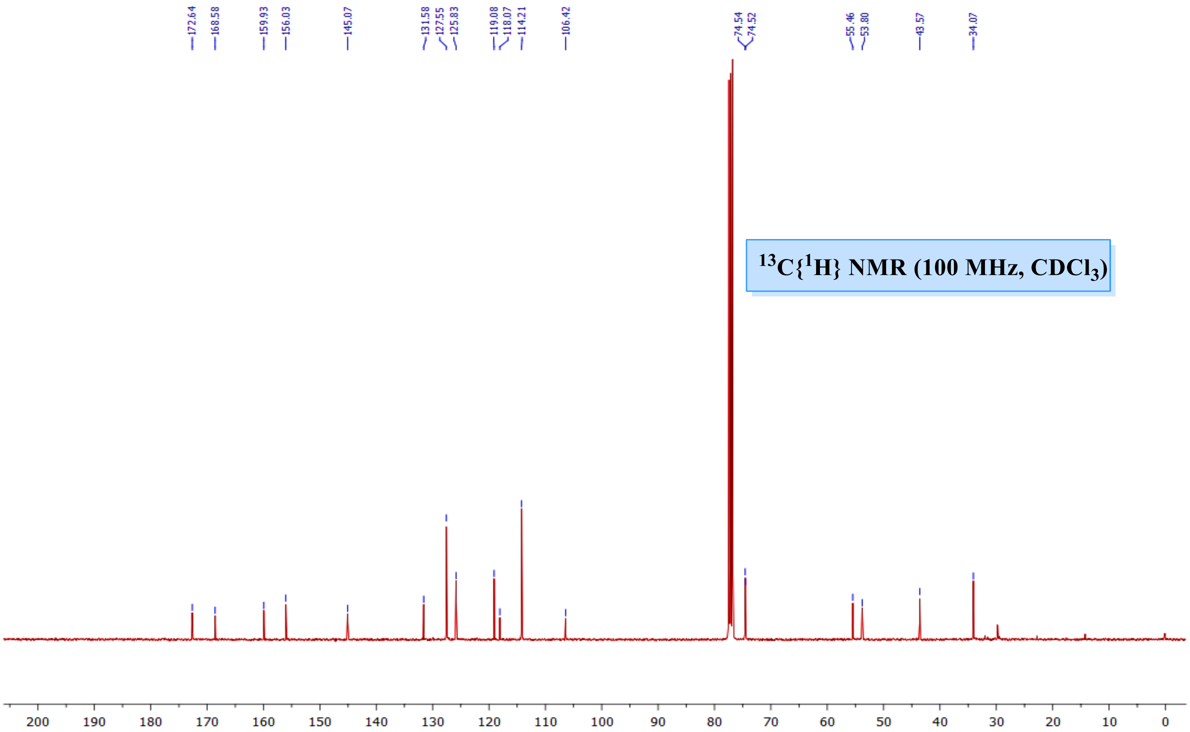
$^{13}C\{^1H\}$ NMR (100 MHz, $CDCl_3$)

Summary and Future Aspects

The work described in this thesis features the diverse strategies for the facile construction of valued nitrogen- and oxygen-containing heterocycles by employing quinone and their analogues along with urea derivatives and strained ring systems as the potential reacting partners. The heterocyclic scaffolds play a vital role in the medicinal chemistry and have wide range of applications in the pharmaceuticals, agrochemicals, food industry etc. The past few years have witnessed great advancements in the construction of heterocyclic scaffolds by using variety of reacting partners. In addition, these achievements have become a source of inspiration to design simple and straightforward approaches for the synthesis of bioactive heterocycles. In this direction, this research work highlights the reactivities of quinone and their analogues with different partner substrate in order to construct new functionalized scaffolds.

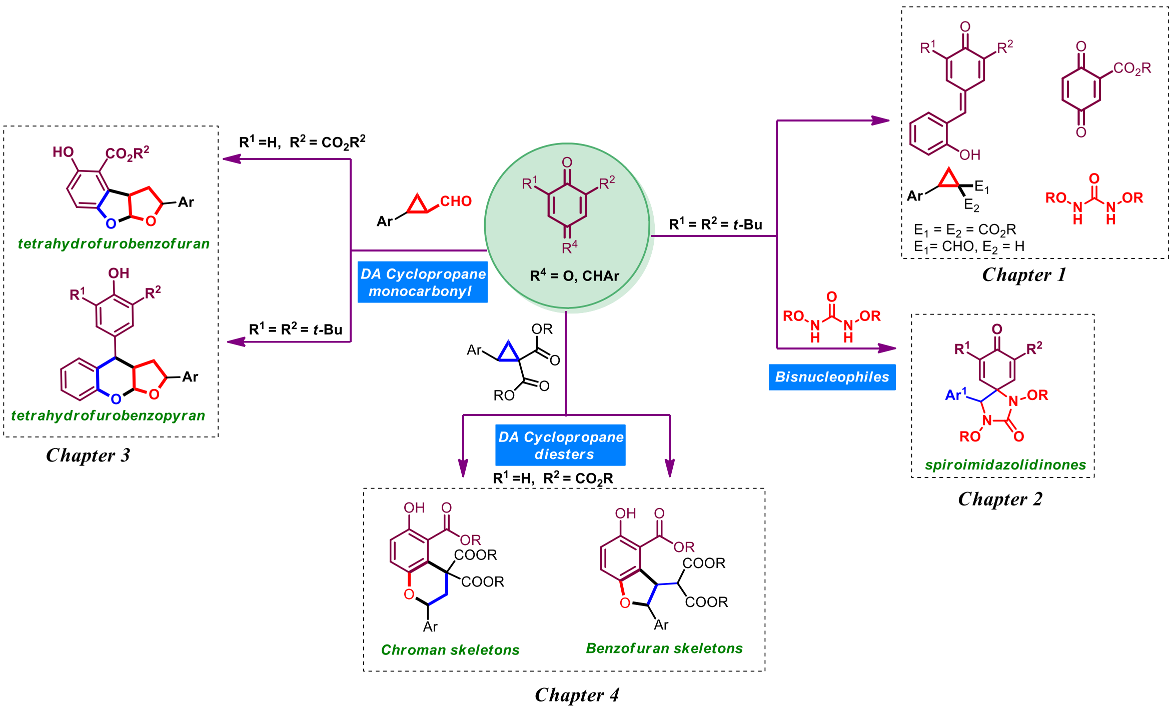

The research work in this thesis is divided into three parts: (a) an efficient and straightforward approach for the spiro-imidazolidinone-cyclohexadienones from *p*-quinone methides (*p*-QMs) and dialkyloxy ureas under mild conditions. (b) Lewis acid catalyzed bicyclization of cyclopropane carbaldehydes with quinone methide and quinone esters to access benzo-fused oxacycles (c) the reactivity of donor-acceptor cyclopropanes in the presence of two different Lewis acids with quinone esters toward the facile synthesis of chroman and benzofuran skeletons.

Chapter 2 describes the reactivities of *p*-QMs and urea derivatives as building blocks towards the construction of spiro-imidazolidinones. The reaction of *p*-quinone methides with urea derivatives in the presence of a base results in the formation of 1,6-conjugate addition product which further on treatment with hypervalent iodine reagent renders the spiro-imidazolidinones. In the follow up chemistry, spiro-imidazolidinone were subjected to debenzylation which afforded the *N*-hydroxy urea ring attached cyclohexadienone and corresponding structures are used for metalloenzyme inhibition activities.

Chapter 3 demonstrates the straightforward one-pot synthesis of tetrahydrofurobenzopyran and tetrahydrofurobenzofuran systems *via* an in-situ ring-expansion of the cyclopropane carbaldehydes followed by a [2+n] cycloaddition with the quinone derivatives. The transformation was compatible with variety of cyclopropane carbaldehydes and quinone methides as well as quinone esters and furnished the product in moderate to good yields. Additionally, the tetrahydrofuranobenzopyran derivative was easily transformed to 3,9a-dihydro-2H-furo[2,3-*b*]chromene, which is also an essential component in many biological scaffolds. Also, the protocol was scalable and provided the product in good yields.

Chapter 4 utilises the dual reactivity of the donor acceptor cyclopropane diesters with quinone esters just by tuning the Lewis acids in order to furnish densely functionalized five- and six-membered oxacycles. The protocol was suitable for variety of cyclopropane and quinone ester derivatives. The control experiments were also performed in order to prove the mechanism. The desired product was also encountered at the gram scale in moderate yields. In order to check the synthetic utility of the protocol, some post-functionalization experiments were also performed.

In future, further exploration of these methodologies to construct nitrogen- and oxygen-heterocycles in the enantioselective manner are some of the opportunities that can be performed. We believe the methodologies displayed in this thesis will prove to be beneficial to the synthetic community in terms of the drug discovery for the future generation.

Appendices

X-ray Diffraction:

For the determination of X-ray crystal structures of 3aa and 4aa, a single-crystal was selected and mounted with paratone oil on a glass fiber using gum. The data was collected at 293K on a CMOS based Bruker D8 Venture PHOTON 100 diffractometer equipped with a INCOATEC micro-focus source with graphite monochromatic Mo Kα radiation (λ = 0.71073 Å) operation at 50 kV and 30 mA. For the integration of diffraction profiles SAINT program[1] was used. Absorption correction was done applying SADABS program.[2] The crystal structure was solved by SIR 92[3] and refined by full matrix least square method using SHELXL-97[4] WinGX system, Ver 1.70.01.[5] All the non-hydrogen atoms in the structure were located the Fourier map and refined anisotropically. The hydrogen atoms were fixed by HFIX in their ideal positions and refined using riding model with isotropic thermal parameters.

Chapter 2

Single crystal X-ray data for compound **4ha**

The CCDC number for the compound **4ha** is CCDC 2038941

Crystal Structure of **4ha**

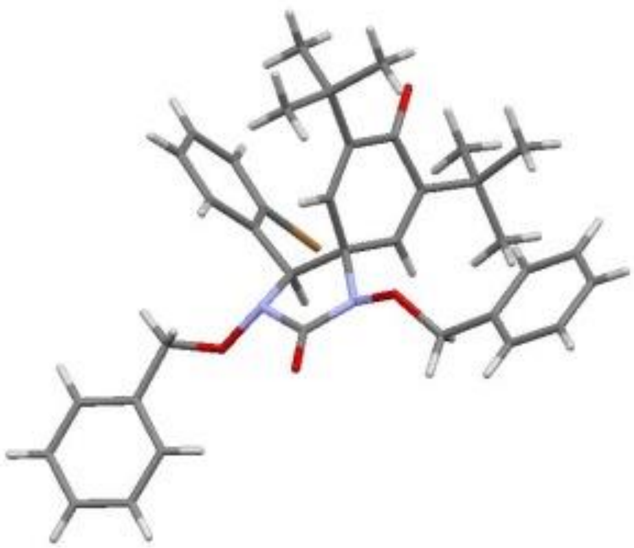

Table 1: Crystal data and structure refinement of 4ha

CCDC No.	CCDC 2038941
Formula	C36 H39 Br N2 O4
Formula weight	643.60
Crystal System	Monoclinic
Space group	P21/c
a, b, c (Å)	9.8031(5) 26.1164(14) 13.0195(7)
α, β, γ (°)	90 101.141(2) 90
V (Å^3)	3270.5(3)
Z	4

Calculated Density (g/cm^3)	1.300, 1.307
Absorption coefficient (mm^{-1})	1.297
F(000)	1344
Crystal Size (mm^3)	0.27 x 0.30 x 0.32
Theta range for data collection:	2.2° to 26.8°
Data set	-12: 12 ; -32: 33 ; -16: 16
Reflection	40034
Independent refl.	[R(int) = 0.063]
data [I > 2σ(I)]	4996
R indices (all data)	R = 0.0416, wR_2 = 0.1046
S	1.01
Min. and Max. Resd. Dens. (e/Å^3)	-0.54 and 0.25

Table 2: Selected bond lengths [Å] of 4ha

Atoms	Bond lengths [Å]	Atoms	Bond lengths [Å]
Br1-C32	1.905(2)	C14-C19	1.495(3)
O1-N1	1.418(2)	C15-C16	1.525(4)
O1 –C5	1.448(3)	C15-C17	1.529(3)
O2-N2	1.411(2)	C15-C18	1.529(3)
O2-C7	1.446(3)	C19-C20	1.497(3)
O3-C6	1.204(2)	C20-C21	1.534(3)
O4-C19	1.217(3)	C20-C25	1.325(3)
N1-C6	1.404(3)	C21-C22	1.538(4)
N1-C26	1.466(2)	C21-C23	1.534(4)
N2-C6	1.374(3)	C21-C24	1.528(3)
N2-C12	1.468(2)	C26-C27	1.500(3)
C1-C2	1.366(4)	C27-C28	1.393(3)
C1-C36	1.358(5)	C27-C32	1.393(3)
C2-C3	1.380(4)	C28-C29	1.372(3)
C3-C4	1.376(3)	C29-C30	1.378(5)
C4-C5	1.497(3)	C30-C31	1.370(5)
C4-C35	1.382(3)	C31-C32	1.388(3)
C7-C8	1.495(3)	C33 –C34	1.379(4)
C8-C9	1.373(3)	C35-C36	1.376(4)
C8-C33	1.373(3)	C1-H1	0.9300
C9-C10	1.384(4)	C2-H39	0.9300

C10-C11	1.360(5)	C3-H3	0.9300
C11-C34	1.357(5)	C5 –H4	0.9700
C12 –C13	1.495(3)	C5-H36	0.9700
C12 –C25	1.491(3)	C7-H30	0.9700
C12-C26	1.585(3)	C7-H35	0.9700
C13-C14	1.328(3)	C9-H32	0.9300
C14-C15	1.532(3)	C10-H33	0.9300
C11-H2	0.9300	C23-H19	0.9600
C13-H5	0.9300	C23-H20	0.9600
C16-H6	0.9600	C24-H21	0.9600
C16-H7	0.9600	C24-H22	0.9600
C16-H8	0.9600	C24-H23	0.9600
C17-H9	0.9600	C25-H24	0.9300
C17-H10	0.9600	C26-H29	0.9800
C17-H11	0.9600	C28-H28	0.9300
C18-H12	0.9600	C29-H25	0.9300
C18-H13	0.9600	C30-H26	0.9300
C18-H14	0.9600	C31-H27	0.9300
C22-H15	0.9600	C33-H34	0.9300
C22-H16	0.9600	C34-H31	0.9300
C22-H17	0.9600	C35-C37	0.9300
C23-H18	0.9600	C36-C38	0.9300

Table 3: Selected bond angles [º] of 4ha

Atoms	Bond angles[º]	Atoms	Bond angles[º]
N1-O1-C5	109.36(14)	C13-C12-C25	113.47(16)
N2-O2-C7	108.49(14)	C13-C12-C26	111.61(15)
O1-N1-C6	112.54(15)	C25-C12-C26	112.11(15)
O1-N1-C26	112.90(14)	C12-C13-C14	124.45(18)
C6-N1-C26	109.25(15)	C13-C14-C15	123.11(18)
O2-N2-C6	117.84(16)	C13-C14-C19	118.04(17)
O2-N2-C12	114.82(14)	C15-C14-C19	118.85(17)
C6-N2-C12	112.50(15)	C14-C15-C16	111.03(19)
C2-C1-C36	119.4(3)	C14-C15-C17	110.05(18)
C1-C2-C3	120.7 (3)	C14-C15-C18	110.14(18)
C2-C3-C4	120.1(2)	C16-C15-C17	108.2(2)

C3-C4-C5	121.4(2)	C16-C15-C18	107.8(2)
C3-C4-C35	118.7(2)	C17-C15-C18	109.62(19)
C5-C4-C35	119.9(2)	O4-C19-C14	120.9(2)
O1-C5-C4	108.61(18)	O4-C19-C20	120.25(19)
O3-C6-N1	126.27 (19)	C14-C19-C20	118.82(17)
O3-C6-N2	128.15(19)	C19-C20-C21	118.83(18)
N1-C6-N2	105.58(16)	C19-C20-C25	118.10(18)
O2-C7-C8	108.75(18)	C21-C20-C25	123.04(19)
C7-C8-C9	120.8(2)	C20-C21-C22	110.03(19)
C7-C8-C33	121.0(2)	C20-C21-C23	110.01(17)
C9-C8-C33	118.1(2)	C20-C21-C24	110.79(18)
C8-C9-C10	121.2(3)	C22-C21-C23	108.1(2)
C9-C10-C11	119.3(3)	C22-C21-C24	109.0(2)
C10-C11-C34	120.6(3)	C23-C21-C24	108.82(19)
N2-C12-C13	111.99(15)	C12-C25-C20	124.51(18)
N2-C12-C25	109.55(16)	N1-C26-C12	99.61(14)
N2-C12-C26	96.97(14)	N1-C26-C27	114.11(16)
C12-C26-C27	113.98(15)	C8-C7-H30	110.00
C26-C27-C28	121.10(18)	C8-C7-H35	110.00
C26-C27-C32	122.00(18)	H30-C7-H35	108.00
C28 –C27-C32	116.79(19)	C8-C9-H32	119.00
C27-C28-C29	122.0(2)	C10-C9-H32	119.00
C28-C29-C30	119.9(3)	C9-C10-H33	120.00
C29-C30-C31	120.0(2)	C11-C10-H33	120.00
C30-C31-C32	119.9(3)	C10-C11-H2	120.00
Br1-C32-C27	121.17(16)	C34-C11-H2	120.00
Br1-C32-C31	117.37(18)	C12-C13-H5	118.00
C27-C32-C31	121.4(2)	C14-C13-H5	118.00
C8-C33-C34	120.9(2)	C15-C16-H6	109.00
C11-C34-C33	119.9(2)	C15-C16-H7	110.00
C4-C35-C36	120.3(3)	C15-C16-H8	109.00
C1-C36-C35	120.8(3)	H6-C16-H8	109.00
C2-C1-H1	120.00	H6-C16-H8	109.00
C36-C1-H1	120.00	H7-C16-H8	109.00
C1-C2-H39	120.00	H7-C16-H8	110.00
C3-C2-H39	120.00	C15-C17-H9	109.00
C2-C3-H3	120.00	C15-C17-H10	109.00
C4 –C3-H3	120.00	C15-C17-H11	109.00

O1-C5-H4	110.00	H9-C17-H10	109.00
O1-C5-H36	110.00	H9-C17-H11	110.00
C4-C5-H4	110.00	H10-C17-H11	110.00
C4-C5-H36	110.00	C15-C18-H12	109.00
H4-C5-H36	108.00	C15-C18-H13	110.00
O2-C7-H30	110.00	C15-C18-H14	109.00
O2-C7-H35	110.00	H12-C18-H13	109.00
H13-C18-H14	109.00	C20-C25-H24	118.00
C21-C22-H15	109.00	N1-C26-H29	110.00
C21-C22-H16	109.00	C12-C26-H29	110.00
C21-C22-H17	109.00	C27-C26-H29	110.00
H15-C22-H16	110.00	C27-C28-H28	119.00
H15-C22-H17	109.00	C29-C28-H28	119.00
H16-C22-H17	110.00	C28-C29-H25	120.00
C21-C23-H18	109.00	C30-C29-H25	120.00
C21-C23-H19	109.00	C29-C30-H26	120.00
C21-C23-H20	109.00	C31-C30-H26	120.00
H18-C23-H19	109.00	C30-C31-H27	120.00
H18-C23-H20	110.00	C32-C31-H27	120.00
H19-C23-H20	110.00	C8-C33-H34	120.00
C21-C24-H21	109.00	C34-C33-H34	120.00
C21-C24-H22	109.00	C11-C34-H31	120.00
C21-C24-H23	109.00	C33-C34-H31	120.00
H21-C24-H22	110.00	C4-C35-H37	120.00
H21-C24-H23	110.00	C36-C35-H37	120.00
H22-C24-H23	109.00	C1-C36-H38	120.00
C12-C25-H24	118.00	C35-C36-H38	120.00

Table 4: Selected hydrogen bonding geometry [Å, º] for a compound 4ha

D--H.. A	D..H	H..A	D..A	D--H..A
C17-- H9..O4	0.9600	2.4500	3.062(3)	121.00
C18-H13..O4	0.9600	2.3200	2.960(3)	123.00
C22-H16..O4	0.9600	2.3500	2.983(3)	122.00
C24-H23..O4	0.9600	2.4400	3.037(3)	120.00
C28-H28..N1	0.9300	2.5600	2.892(3)	101.00

C26-H29..Br1	0.9800	2.7100	3.2037(19)	111.00
C10-H33..O4	0.9300	2.6000	3.518(4)	170.00

Chapter 3

Single crystal X-ray data for compound **3a**

The CCDC number for the compound **3a** is CCDC 2141572

Crystal Structure of **3a**

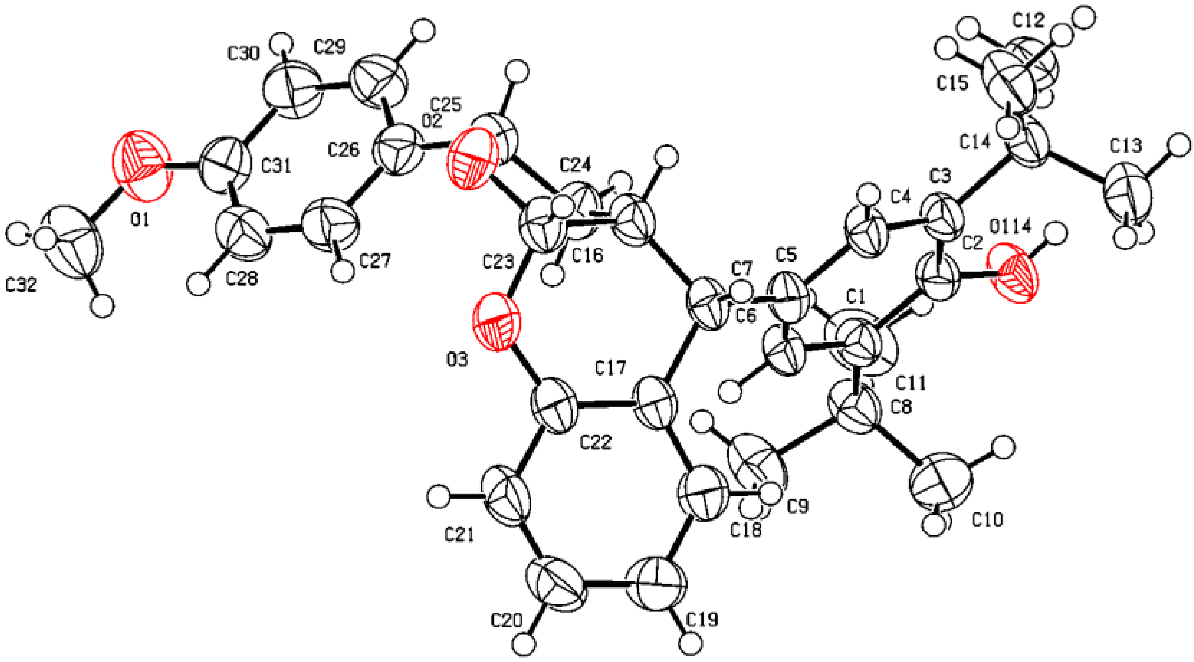

Table 1: Crystal data and structure refinement of 3a

CCDC No.	CCDC 2141572
Formula	C32 H38 N0 O4
Formula weight	486.62
Crystal System	triclinic
Space group	P-1
a, b, c (Å)	10.288(5) 11.320(5) 12.678(5)
α, β, γ (°)	74.825(5) 87.625(5) 70.986(5)
V ($Å^3$)	1345.7(10)
Z	2

Calculated Density (g/cm^3)	1.200, 1.201
Absorption coefficient (mm^{-1})	0.078
F(000)	524
Crystal Size (mm^3)	0.27 x 0.28 x 0.29
Theta range for data collection:	2.6° to 32.8°
Data set	-15: 15; -16: 15; -18: 17
Reflection	30179
Independent refl.	9408 [R(int) = 0.038]
data [I > 2σ(I)]	5153
R indices (all data)	R = 0.0698, wR_2 = 0.2436
S	1.03
Min. and Max. Resd. Dens. (e/Å^3)	-0.23 and 0.41

Table 2: Selected bond lengths [Å] of 3a

Atoms	Bond lengths [Å]	Atoms	Bond lengths [Å]
O1-C31	1.370(3)	C17-C18	1.386(3)
O1-C32	1.409(3)	C18-C19	1.388(3)
O2-C23	1.387(2)	C19-C20	1.386(3)
O2-C25	1.459(2)	C20-C21	1.372(3)
O3-C22	1.380(2)	C21-C22	1.393(3)
O3-C23	1.443(2)	C24-C25	1.529(3)
O114-C2	1.384(2)	C25-C26	1.496(3)
O114-H114	0.8200	C26-C29	1.387(3)
C1-C2	1.411(2)	C26-C27	1.382(3)
C1-C6	1.399(2)	C27-C28	1.390(3)
C1-C8	1.540(2)	C28-C31	1.384(3)
C2-C3	1.404(2)	C29-C30	1.380(3)
C3-C14	1.546(2)	C30-C31	1.380(3)

C3-C4	1.395(2)	C4-H4	0.9300
C4-C5	1.390(2)	C6-H6	0.9300
C5-C6	1.386(2)	C7-H7	0.9800
C5-C7	1.522(2)	C9-H9A	0.9600
C7-C16	1.526(3)	C9-H9B	0.9600
C7-C17	1.515(2)	C9-H9C	0.9600
C8-C10	1.538(3)	C10-H10A	0.9600
C8-C11	1.535(3)	C10-H10B	0.9600
C8-C9	1.533(3)	C10-H10C	0.9600
C12-C14	1.539(3)	C11-H11A	0.9600
C13-C14	1.537(3)	C11-H11B	0.9600
C14-C15	1.536(3)	C11-H11C	0.9600
C16-C23	1.512(2)	C12-H12A	0.9600
C16-C24	1.528(3)	C12-H12B	0.9600
C17-C22	1.397(2)	C12-H12C	0.9600
C13-H13A	0.9600	C23-H23	0.9800
C13-H13B	0.9600	C24-H24A	0.9700
C13-H13C	0.9600	C24-H24B	0.9700
C15-H15A	0.9600	C25-H25	0.9800
C15-H15B	0.9600	C27-H27	0.9300
C15-H15C	0.9600	C28-H28	0.9300
C16-H16	0.9800	C29-H29	0.9300
C18-H18	0.9300	C30-H30	0.9300
C19-H19	0.9300	C32-H32A	0.9600
C20-H20	0.9300	C32-H32B	0.9600
C21-H21	0.9300	C32-H32C	0.9600

Table 3: Selected bond angles [º] of 3a

Atoms	Bond angles[º]	Atoms	Bond angles[º]

C31-O1-C32	118.48(19)	C3-C14-C13	111.20(15)
C23-O2-C25	109.48(14)	C12-C1-C13	111.34(15)
C22-O3-C23	119.58(14)	C12-C14-C15	106.09(16)
C2-O114-H114	109.00	C3-C14-C15	111.38(14)
C2-C1-C8	122.19(14)	C13-C14-C15	106.25(15)
C6-C1-C8	120.81(13)	C7-C16-C24	118.80(14)
C2-C1-C6	116.98(14)	C23-C16-C24	99.44(14)
O114-C2-C3	121.51(13)	C7-C16-C23	114.80(14)
C1-C2-C3	122.72(14)	C7-C17-C18	122.39(15)
O114-C2-C1	115.77(14)	C7-C17-C22	120.15(16)
C2-C3-C14	122.57(13)	C18-C17-C22	117.26(15)
C4-C3-C14	120.79(14)	C17-C18-C19	122.24(17)
C2-C3-C4	116.64(14)	C18-C19-C20	119.1(2)
C3-C4-C5	122.90(15)	C19-C20-C21	120.31(19)
C4-C5-C7	118.18(14)	C20-C21-C22	119.99(18)
C6-C5-C7	123.39(13)	O3-C22-C17	123.82(15)
C4-C5-C6	118.32(14)	O3-C22-C21	115.06(16)
C1-C6-C5	122.30(14)	C17-C22-C21	121.11(18)
C5-C7-C17	116.75(14)	O2-C23-O3	106.14(14)
C16-C7-C17	110.16(13)	O2-C23-C16	106.85(14)
C5-C7-C16	110.26(13)	O3-C23-C16	111.75(15)
C1-C8-C9	111.69(15)	C16-C24-C25	101.72(15)
C1-C8-C11	111.75(17)	O2-C25-C26	110.50(15)
C9-C8-C10	107.20(19)	C24-C25-C26	116.73(16)
C1-C8-C10	109.06(16)	O2-C25-C24	104.67(15)
C10-C8-C11	110.01(18)	C25-C26-C29	119.76(17)
C9-C8-C11	107.02(16)	C27-C26-C29	117.99(18)
C3-C14-C12	110.41(14)	C25-C26-C27	122.25(17)
C26-C27-C28	121.62(19)	C8-C11-H11C	109.00

C27-C28-C31	119.47(19)	H11A-C11-H11B	109.00
C26-C29-C30	120.94(19)	H11A-C11-H11C	110.00
C29-C30-C31	120.58(19)	H11B-C11-H11C	110.00
O1-C31-C30	116.01(18)	C14-C12-H12A	109.00
C28-C31-C30	119.41(18)	C14-C12-H12B	109.00
O1-C31-C28	124.58(18)	C14-C12 -H12C	109.00
C3-C4-H4	119.00	H12A-C12-H12B	109.00
C5-C4-H4	119.00	H12A-C12-H12C	110.00
C1-C6-H6	119.00	H12B-C12-H12C	109.00
C5-C6-H6	119.00	C14-C13-H13A	109.00
C5-C7-H7	106.00	C14-C13-H13B	109.00
C16-C7-H7	106.00	C14-C13-H13C	109.00
C17-C7-H7	106.00	H13A-C13-H13B	109.00
C8-C9-H9A	109.00	H13A-C13-H13C	110.00
C8-C-H9B	109.00	H13B-C13-H13C	109.00
C8-C9-H9C	109.00	C14-C15-H15A	110.00
H9A-C9-H9B	110.00	C14-C15-H15B	109.00
H9A-C9-H9C	109.00	C14-C15-H15C	109.00
H9B-C9-H9C	109.00	H15A-C15-H15B	109.00
C8-C10-H10A	110.00	H15A-C15-H15C	109.00
C8-C10-H10B	110.00	H15B-C15-H15C	109.00
C8-C10-H10C	109.00	C7-C16-H16	108.00
H10A-C10-H10B	110.00	C23-C16-H16	108.00
H10A-C10-H10C	109.00	C24-C16-H16	108.00
H10B-C10-H10C	109.00	C17-C18-H18	119.00
C8-C11-H11A	109.00	C19-C18-H18	119.00
C8-C11-H11B	109.00	C18-C19-H19	120.00
C20-C19-H19	120.00	C26-C25-H25	108.00

C19-C20-H20	120.00	C26-C27-H27	119.00
C21-C20-H20	120.00	C28-C27-H27	119.00
C20-C21-H21	120.00	C27-C28-H28	120.00
C22-C21-H21	120.00	C31-C28-H28	120.00
O2-C23-H23	111.00	C26-C29-H29	120.00
O3-C23-H23	111.00	C30-C29-H29	119.00
C16-C23-H23	111.00	C29-C30-H30	120.00
C16-C24-H24A	111.00	C31-C30-H30	120.00
C16-C24-H24B	111.00	O1-C32-H32A	110.00
C25-C24-H24A	111.00	O1-C32-H32B	109.00
C25-C24-H24B	111.00	O1-C32-H32C	109.00
H24A-C24-H24B	109.00	H32A-C32-H32B	110.00
O2-C25-H25	108.00	H32A-C32-H32C	109.00
C24-C25-H25	108.00	H32B-C32-H32C	109.00

Table 4: Selected hydrogen bonding geometry [Å, º] for a compound 3a

D--H..A	**D..H**	**H..A**	**D..A**	**D--H..A**
O114--H114..O3	0.8200	2.5700	3.160(2)	130.00
C10--H10A..O114	0.9600	2.3900	3.015(3)	122.00
C11--H11A..O114	0.9600	2.2400	2.902(3)	125.00
C12--H12A..O114	0.9600	2.4300	3.081(3)	125.00
C13--H13A..O114	0.9600	2.5300	3.157(3)	123.00
C24--H24B..O1	0.9700	2.5600	3.468(3)	155.00

Single crystal X-ray data for compound **5e**

The CCDC number for the compound **5e** is CCDC 2141574

Crystal Structure of **5e**

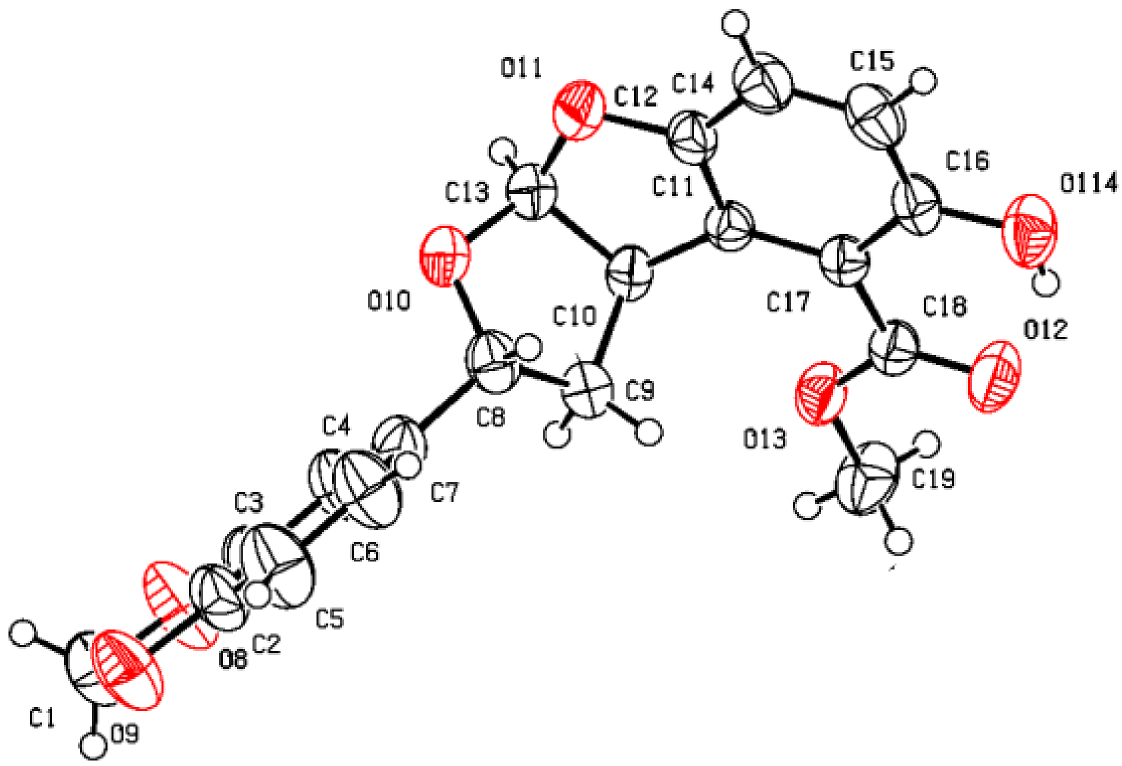

Table 1: Crystal data and structure refinement of 5e

CCDC No.	CCDC 2141574
Formula	C19 H16 O7
Formula weight	356.32
Crystal System	triclinic
Space group	P-1
a, b, c (Å)	10.147(5) 12.472(5) 13.140(5)
α, β, γ (°)	84.334(5) 89.996(5) 86.494(5)
V (Å^3)	1651.7(12)
Z	2
Calculated Density (g/cm^3)	1.430, 1.433
Absorption coefficient (mm^{-1})	0.110
F(000)	744
Crystal Size (mm^3)	0.27 x 0.28 x 0.29
Theta range for data collection:	2.4° to 26.5°

Data set	-12: 12; -15: 15; -16: 16
Reflection	22984
Independent refl.	6805 [R(int) = 0.107]
data [I > 2σ(I)]	3751
R indices (all data)	R = 0.0692, wR_2 = 0.2082
S	1.02
Min. and Max. Resd. Dens. (e/Å^3)	-0.27 and 0.28

Table 2: Selected bond lengths [Å] of 5e

Atoms	Bond lengths [Å]	Atoms	Bond lengths [Å]
O1-C20	1.410(5)	C24-C25	1.403(4)
O1-C21	1.373(4)	C25-C26	1.370(5)
O2-C20	1.409(5)	C25-C27	1.503(4)
O2-C22	1.375(4)	C27-C28	1.525(4)
O3-C27	1.445(3)	C28-C29	1.529(4)
O3-C30	1.388(4)	C29-C30	1.541(4)
O4-C30	1.451(4)	C29-C31	1.507(4)
O4-C32	1.374(3)	C31-C33	1.399(3)
O5-C37	1.220(3)	C31-C32	1.383(4)
O6-C37	1.320(3)	C32-C36	1.376(4)
O6-C38	1.455(4)	C33-C34	1.404(4)
O7-C34	1.361(3)	C33-C37	1.473(4)
O7-H7	0.8200	C34-C35	1.389(4)
O8-C3	1.379(4)	C35-C36	1.383(4)
O8-C1	1.413(5)	O114-C16	1.361(3)
O9-C2	1.376(4)	C20-H20A	0.9700
O9-C1	1.410(5)	C20-H20B	0.9700

O10-C13	1.387(3)	C23-H23	0.9300
O10-C8	1.454(3)	C24-H24	0.9300
O11-C13	1.451(3)	C26-H26	0.9300
O11-C12	1.374(3)	C27-H27	0.9800
O12-C18	1.222(3)	C28-H28A	0.9700
O13-C19	1.449(4)	C28-H28B	0.9700
O13-C18	1.324(3)	C29-H29	0.9800
C21-C24	1.358(5)	C30-H30	0.9800
C21-C22	1.362(5)	C35-H35	0.9300
C22-C23	1.361(5)	C36-H36	0.9300
C23-C26	1.392(5)	C38-H38B	0.9600
C38-H38C	0.9600	C15-C16	1.399(4)
C38-H38A	0.9600	C16-C17	1.404(4)
O114-H114	0.8200	C17-C18	1.468(4)
C2-C5	1.362(5)	C1-H1A	0.9700
C2-C3	1.372(5)	C1-H1B	0.9700
C3-C4	1.353(5)	C4-H4	0.9300
C4-C7	1.398(4)	C5-H5	0.9300
C5-C6	1.394(5)	C6-H6	0.9300
C6-C7	1.375(5)	C8-H8	0.9800
C7-C8	1.495(4)	C9-H9A	0.9700
C8-C9	1.525(4)	C9-H9B	0.9700
C9-C10	1.529(4)	C10-H10	0.9800
C10-C11	1.504(3)	C13-H13	0.9800
C10-C13	1.544(4)	C14-H14	0.9300
C11-C17	1.404(3)	C15-H15	0.9300
C11-C12	1.371(3)	C19-H19A	0.9600
C12-C14	1.379(4)	C19-H19B	0.9600
C14-C15	1.367(4)	C19-H19C	0.9600

Table 3: Selected bond angles [º] of 5e

Atoms	Bond angles[º]	Atoms	Bond angles[º]
C20-O1-C21	106.0(3)	C30-C29-C31	102.6(2)
C20-O2-C22	105.8(3)	C28-C29-C30	103.4(2)
C27 -O3-C30	108.6(2)	C28-C29-C31	115.4(2)
C30-O4-C32	108.1(2)	O3-C30-C29	108.5(3)
C37-O6-C38	116.0(2)	O4-C30-C29	107.3(2)
C34-O7-H7	109.00	O3-C30-O4	110.9(3)
C1-O8-C3	105.9(3)	C29-C31-C33	131.8(2)
C1-O9-C2	105.9(2)	C29-C31-C32	108.2(2)
C8-O10-C13	108.7(2)	C32-C3-C33	120.0(2)
C12-O11-C13	107.91(19)	C31 -C32-C36	122.2(3)
C18-O13-C19	116.4(2)	O4-C32-C36	124.3(3)
O1-C20-O2	108.6(3)	O4-C32-C31	113.6(2)
O1-C21-C24	127.9(3)	C31-C33-C34	117.9(2)
C22-C21-C24	122.5(3)	C31-C33-C37	123.3(2)
O1-C21-C22	109.6(3)	C34-C33-C37	118.8(2)
O2-C22-C23	128.8(3)	C33-C34-C35	120.8(2)
O2C22-C21	109.8(3)	O7-C34-C35	116.4(2)
C21-C22-C23	121.4(3)	O7-C34-C33	122.9(3)
C22-C23-C26	116.8(3)	C34-C35-C36	120.8(3)
C21-C24-C25	117.8(3)	C32-C36-C35	118.3(3)
C26-C25-C27	122.0(3)	O5-C37-O6	122.1(3)
C24-C25-C26	119.0(3)	O6-C37-C33	114.8(2)
C24-C25-C27	119.1(3)	O5-C37-C33	123.1(2)
C23-C26-C25	122.6(3)	O2-C20-H20A	110.00

C25-C27-C28	115.9(3)	O2-C20-H20B	110.00
O3-C27-C25	108.5(2)	O1-C20-H20A	110.00
O3-C27-C28	104.2(2)	O1-C20-H20B	110.00
C27-C2-C29	104.4(2)	H20A-C20-H20B	108.00
C26-C23-H23	122.00	O6-C38-H38C	109.00
C22-C23-H23	122.00	H38A-C38-H38B	109.00
C25-C24-H24	121.00	C16-O114-H114	109.00
C21-C24-H24	121.00	O8-C1-O9	108.6(3)
C23-C26-H26	119.00	O9-C2-C3	109.8(2)
C25-C26-H26	119.00	C3-C2-C5	121.1(3)
C25-C27-H27	109.00	O9-C2-C5	129.1(3)
O3 -C27-H27	109.00	O8-C3-C2	109.3(3)
C2-C27-H27	109.00	O8-C3-C4	128.6(3)
H28A-C28-H28B	109.00	C2-C3-C4	122.2(3)
C27-C28-H28B	111.00	C3-C4-C7	118.5(3)
C27-C28-H28A	111.00	C2-C5-C6	117.0(3)
C29-C28-H28A	111.00	C5-C6-C7	122.6(3)
C29-C28-H28B	111.00	C4-C7-C8	119.9(3)
C28-C29-H29	112.00	C6-C7 -C8	121.5(3)
C30-C29-H29	112.00	C4-C7-C6	118.6(3)
C31-C29-H29	112.00	O10-C8-C7	108.3(2)
O3-C30-H30	110.00	O10-C8-C9	103.3(2)
C29-C30-H30	110.00	C7-C8-C9	116.7(3)
O4-C30-H30	110.00	C8-C9-C10	104.6(2)
C36-C35-H35	120.00	C9-C10-C11	114.4(2)
C34-C35-H35	120.00	C11-C10-C13	102.31(18)
C32-C36-H36	121.00	C9-C10-C13	103.1(2)
C35-C36-H36	121.00	C10 -C11-C12	108.8(2)

H38A-C38-H38C	109.00	C10-C11-C17	131.42(19)
H38B-C38-H38C	109.00	C12-C11-C17	119.8(2)
O6-C38-H38A	109.00	O11-C12 -C11	113.6(2)
O6-C38-H38B	110.00	O11-C12-C14	124.3(2)
C11-C12-C14	122.2(2)	C7-C6-H6	119.00
O10-C13-C10	108.5(2)	O10-C8-H8	109.00
O11-C13-C10	107.3(2)	C7-C8-H8	109.00
O10-C13-O11	111.4(2)	C9-C8-H8	109.00
C12-C14-C15	119.2(3)	C8-C9-H9A	111.00
C14-C15-C16	120.3(3)	C8-C9-H9B	111.00
O114-C16-C15	117.0(2)	C10-C9-H9A	111.00
O114-C16-C17	122.4(3)	C10-C9-H9B	111.00
C15-C16-C17	120.6(2)	H9A-C9-H9B	109.00
C11-C17-C18	123.3(2)	C9-C10-H10	112.00
C16 -C17-C18	118.6(2)	C11-C10-H10	112.00
C11-C17-C16	118.0(2)	C13-C10-H10	112.00
O12-C18-C17	123.7(2)	O10-C13-H13	110.00
O13-C18-C17	114.9(2)	O11-C13-H13	110.00
O12-C18-O13	121.4(3)	C10-C13-H13	110.00
O8-C1-H1A	110.00	C12-C14-H14	120.00
O8-C1-H1B	110.00	C15-C14-H14	120.00
O9-C1-H1A	110.00	C14-C15-H15	120.00
O9-C1-H1B	110.00	C16-C15-H15	120.00
H1A-C1-H1B	108.00	O13-C19-H19A	109.00
C3-C4-H4	121.00	O13-C19-H19B	109.00
C7-C4-H4	121.00	O13-C19-H19C	109.00
C2-C5-H5	121.00	H19A-C19 -H19B	109.00
C6-C5-H5	122.00	H19A -C19-H19C	109.00

C5-C6-H6	119.00	H19B-C19-H19C	109.00

Table 4: Selected hydrogen bonding geometry [Å, º] for a compound 5e

D--H..**A**	**D**..**H**	**H**..**A**	**D**..**A**	**D--H**..**A**
O7--H7..O5	0.8200	1.8700	2.585(3)	146.00
O11--H114..O12	0.8200	1.8600	2.577(3)	146.00
C19--H19A ..O7	0.9600	2.5900	3.446(4)	148.00
C29--H29..O12	0.9800	2.5300	3.117(4)	119.00
C38--H38A..O114	0.9600	2.5700	3.399(4)	145.00

Chapter 4

Single crystal X-ray data for compound **3ba**

The CCDC number for the compound **3ba** is CCDC 2191875

Crystal Structure of **3ba**

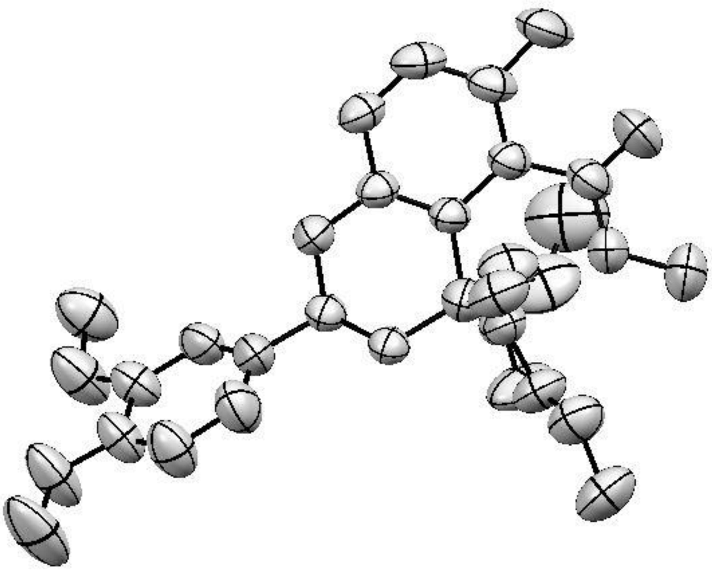

Table 1: Crystal data and structure refinement of 3ba

CCDC No.	CCDC 2191875
Formula	C25 H28 O10
Formula weight	488.47
Crystal System	triclinic
Space group	P-1
a, b, c (Å)	8.6585(12) 10.0906(16) 14.666(2)
α, β, γ (°)	93.219(4) 106.759(4) 97.136(4)
V ($Å^3$)	1211.7(3)
Z	2
Calculated Density (g/cm^3)	1.339
Absorption coefficient (mm^{-1})	0.104
F(000)	516
Crystal Size (mm^3)	0.30 x 0.30 x 0.40
Theta range for data collection:	2.4^o to 25.4^o
Data set	-10: 10; -12: 12; -17: 17
Reflection	17233
Independent refl.	4421 [R(int) = 0.047]
data [I > 2σ(I)]	2743
R indices (all data)	R = 0.0658, wR_2 = 0.1937
S	1.03
Min. and Max. Resd. Dens. (e/$Å^3$)	-0.21 and 0.35

Table 2: Selected bond lengths [Å] of 3ba

Atoms	Bond lengths [Å]	Atoms	Bond lengths [Å]
O1-C1	1.454(4)	C3B-C4	1.528(4)
O1-C2	1.317(4)	C21-C26	1.378(2)

O2A-C5	1.386(4)	C4-C5	1.373(4)
O2A-C6A	1.404(6)	C5-C15	1.396(4)
O2B-C6B	1.487(10)	C6A-C19A	1.497(8)
O2B-C5	1.386(4)	C6A-C7	1.556(7)
O3-C17	1.370(5)	C6B-C19B	1.474(12)
O4-C20	1.191(5)	C6B-C7	1.564(11)
O5-C20	1.312(4)	C7-C12	1.391(5)
O5-C21	1.469(5)	C7-C8	1.349(7)
O6-C23	1.313(5)	C8-C9	1.387(7)
O6-C24	1.470(6)	C9-C10	1.365(5)
O7-C23	1.206(4)	C10-C13	1.391(5)
O8-C14	1.418(5)	C12-C13	1.372(5)
O8-C13	1.372(5)	C15-C16	1.370(5)
O9-C10	1.371(5)	C16-C17	1.379(6)
O9-C11	1.424(6)	C21-C22	1.440(6)
O18-C2	1.215(5)	C24-C25	1.401(10)
O3-H3	0.8200	C1-H1A	0.9600
C2-C3	1.471(5)	C1-H1B	0.9600
C3-C4	1.437(5)	C1-H1C	0.9600
C3-C17	1.392(5)	C6A-H6A	0.9800
C3A-C4	1.528(4)	C6B-H6B	0.9800
C3A-C19A	1.569(7)	C8-H8	0.9300
C3A-C23	1.532(4)	C9-H9	0.9300
C3A-C20	1.542(5)	C11-H11B	0.9600
C3B-C20	1.542(5)	C11-H11C	0.9600
C3B-C23	1.532(4)	C11-H11A	0.9600

Table 3: Selected bond lengths [Å] of 3ba

C12-H12	0.9300	C21-H21A	0.9700
C14-H14A	0.9600	C21-H21B	0.9700
C14-H14B	0.9600	C22-H22A	0.9600
C14-H14C	0.9600	C22-H22B	0.9600
C15-H15	0.9300	C22-H22C	0.9600
C16-H16	0.9300	C24-H24B	0.9700
C19A-H19C	0.9700	C24-H24A	0.9700
C19A-H19D	0.9700	C25-H25A	0.9600
C19B-H19A	0.9700	C25-H25B	0.9600
C19B-H19B	0.9700	C25-H25C	0.9600

Table 3: Selected bond angles [º] of 3ba

Atoms	Bond angles[º]	Atoms	Bond angles[º]
C1-O1-C2	118.6(3)	C3-C4-C3B	122.9(3)
C5-O2A-C6A	114.5(3)	C3A-C4-C5	119.3(3)
C5-O2B-C6B	114.9(4)	C3-C4-C5	117.8(3)
C20-O5-C21	115.4(3)	O2A-C5-C15	113.6(3)
C23-O6-C24	116.2(4)	O2A-C5-C4	124.7(3)
C13-O8-C14	117.6(3)	O2B-C5-C4	124.7(3)
C10-O9-C11	117.9(4)	O2B-C5-C15	113.6(3)
C17-O3-H3	109.00	C4-C5-C15	121.7(3)
O1-C2-O18	120.0(4)	C7-C6A-C19A	108.1(4)
O18-C2-C3	124.0(3)	O2A-C6A-C19A	110.0(5)
O1-C2-C3	116.0(3)	O2A-C6A-C7	106.5(4)
C2-C3-C4	123.9(3)	O2B-C6B-C7	102.1(5)

C4-C3-C17	119.3(3)	C7-C6B-C19B	105.0(7)
C2-C3-C17	116.8(3)	O2B-C6B-C19B	106.8(7)
C4-C3A-C20	107.9(2)	C6A-C7-C8	112.7(4)
C4-C3A-C23	113.9(3)	C6A-C7-C12	129.2(4)
C19A-C3A-C20	115.4(3)	C6B-C7-C8	136.5(4)
C19A-C3A-C23	94.5(3)	C6B-C7-C12	103.3(5)
C20-C3A-C23	115.4(3)	C8-C7-C12	118.0(4)
C4-C3A-C19A	109.4(3)	C7-C8-C9	121.9(4)
C4-C3B-C23	113.9(3)	C8-C9-C10	119.8(4)
C4-C3B-C19B	108.7(4)	O9-C10-C9	124.7(3)
C19B-C3B-C20	86.9(4)	C9-C10-C13	119.5(4)
C19B-C3B-C23	120.7(4)	O9-C10-C13	115.9(3)
C20-C3B-C23	115.4(3)	C7-C12-C13	121.3(4)
C4-C3B-C20	107.9(2)	C10-C13-C12	119.5(3)
C3B-C4-C5	119.3(3)	O8-C13-C12	125.4(3)
C3-C4-C3A	122.9(3)	O8-C13-C10	115.1(3)
C5-C15-C16	120.2(3)	O2B-C6B-H6B	114.00
C15-C16-C17	119.8(3)	C7-C6B-H6B	114.00
O3-C17-C3	122.7(3)	C19B-C6B-H6B	114.00
C3-C17-C16	121.1(3)	C7-C8-H8	119.00
O3-C17-C16	116.2(3)	C9-C8-H8	119.00
C3A-C19A-C6A	108.4(4)	C8-C9-H9	120.00
C3B-C19B-C6B	104.4(7)	C10-C9-H9	120.00
O4-C20-O5	124.2(3)	O9-C11-H11C	109.00
O4-C20-C3A	122.5(3)	H11A -C11-H11B	110.00
O4-C20-C3B	122.5(3)	H11B-C11-H11C	110.00
O5-C20-C3A	113.2(3)	O9-C11-H11B	110.00
O5-C20-C3B	113.2(3)	H11A-C11-H11C	109.00
O5-C21-C22	107.2(3)	O9-C11-H11A	109.00

O6-C23-C3B	112.4(3)	C7-C12-H12	119.00
O6-C23-O7	123.3(3)	C13-C12-H12	119.00
O7-C23-C3A	124.2(4)	O8-C14-H14C	109.00
O7-C23-C3B	124.2(4)	H14A-C14-H14C	109.00
O6-C23-C3A	112.4(3)	H14B-C14-H14C	109.00
O6-C24-C25	109.6(4)	H14A-C14 -H14B	109.00
O1-C1-H1A	109.00	O8-C14-H14A	109.00
O1-C1-H1B	109.00	O8-C14-H14B	110.00
O1-C1-H1C	109.00	C16-C15-H15	120.00
H1A-C1-H1B	110.00	C5-C15-H15	120.00
H1A-C1-H1C	109.00	C15-C16-H16	120.00
H1B-C1-H1C	109.00	C17-C16-H16	120.00
O2A -C6A-H6A	111.00	C3A-C19A-H19D	110.00
C7-C6A-H6A	111.00	H19C-C19A-H19D	108.00
C19A-C6A-H6A	111.00	C6A-C19A-H19C	110.00
C6A-C19A -H19D	110.00	H22A-C22-H22B	109.00
C3A-C19A-H19C	110.00	H22A-C22-H22C	109.00
C3B -C19B-H19A	111.00	H22B -C22-H22C	109.00
C3B-C19B -H19B	111.00	O6 -C24-H24A	110.00
C6B-C19B-H19A	111.00	O6-C24-H24B	110.00
C6B-C19B-H19B	111.00	C25-C24-H24A	110.00
H19A-C19B-H19B	109.00	H24A-C24-H24B	108.00
O5-C21-H21B	110.00	C25 -C24-H24B	110.00
C22-C21-H21A	110.00	C24-C25-H25B	110.00
C22-C21-H21B	110.00	C24-C25-H25C	109.00
H21A-C21-H21B	108.00	C24-C25-H25A	110.00
O5-C21-H21A	110.00	H25A-C25 -H25C	109.00
C21-C22-H22A	109.00	H25B-C25-H25C	109.00
C21-C22-H22B	110.00	H25A-C25-H25B	109.00

C21-C22-H22C	109.00

Table 4: Selected hydrogen bonding geometry [Å, º] for a compound 3ba

D--H..**A**	**D**..**H**	**H**..**A**	**D**..**A**	**D**--**H**..**A**
O3-- H3..O18	0.8200	1.8300	2.540(4)	144.00
C2-- H21B..O18	0.9700	2.5300	3.380(6)	146.00

Single crystal X-ray data for compound **4ba**

The CCDC number for the compound **4ba** is CCDC 2191876

Crystal Structure of **4ba**

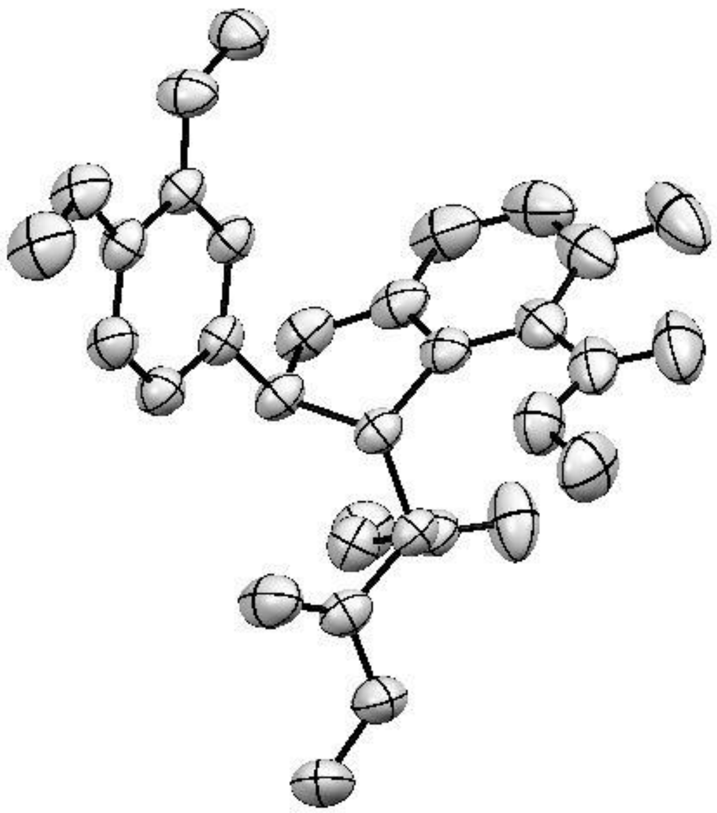

Table 1: Crystal data and structure refinement of 4ba

CCDC No.	CCDC 2191876
Formula	C23 H24 N0 O10
Formula weight	460.42
Crystal System	triclinic
Space group	P-1
a, b, c (Å)	8.822(5) 9.827(5) 12.681(5)
α, β, γ (°)	95.932(5) 93.627(5) 92.454(5)
V ($Å^3$)	1089.9(9)
Z	2
Calculated Density (g/cm^3)	1.400, 1.403
Absorption coefficient (mm^{-1})	0.111
F(000)	484
Crystal Size (mm^3)	0.20 x 0.32 x 0.36
Theta range for data collection:	2.5° to 32.8°
Data set	-13: 13; -14: 14; -19: 19
Reflection	24491
Independent refl.	7700 [R(int) = 0.029]
data [I > 2σ(I)]	4603
R indices (all data)	R = 0.0620, wR_2 = 0.2188
S	1.02
Min. and Max. Resd. Dens. ($e/Å^3$)	-0.31 and 0.36

Table 2: Selected bond lengths [Å] of 4ba

Atoms	Bond lengths [Å]	Atoms	Bond lengths [Å]
O1-C23	1.365(2)	C21-C22	1.394(2)
O1-C28	1.413(2)	C21-C26	1.378(2)
O2-C24	1.369(2)	C22-C23	1.390(2)

O2-C27	1.418(2)	C23-C24	1.406(2)
O3-C16	1.373(2)	C24-C25	1.371(2)
O3-C20	1.451(2)	C25-C26	1.394(2)
O4-C30	1.192(2)	C30-C31	1.518(2)
O5-C29	1.445(2)	C31-C32	1.517(2)
O5-C30	1.331(2)	C14-H14A	0.9600
O6-C32	1.197(2)	C14-H14B	0.9600
O7-C32	1.328(2)	C14-H14C	0.9600
O7-C33	1.440(2)	C17-H17	0.9300
O8-C13	1.223(3)	C18-H18	0.9300
O9-C13	1.323(3)	C19-H19	0.9800
O9-C14	1.449(3)	C20-H20	0.9800
O10-C11	1.359(3)	C22-H22	0.9300
O10-H10	0.8200	C25-H25	0.9300
C11-C12	1.407(3)	C26 -H26	0.9300
C11-C18	1.389(3)	C27-H27A	0.9600
C12-C13	1.477(3)	C27-H27B	0.9600
C12-C15	1.406(2)	C27-H27C	0.9600
C15-C19	1.509(2)	C28 -H28A	0.9600
C15 -C16	1.382(2)	C28-H28B	0.9600
C16-C17	1.390(3)	C28-H28C	0.9600
C17-C18	1.371(3)	C29-H29A	0.9600
C19 -C20	1.560(2)	C29-H29B	0.9600
C20-C21	1.521(2)	C31-H31	0.9800
C33-H33A	0.9600	C33-H33C	0.9600
C33-H33B	0.9600		

Table 3: Selected bond angles [º] of 4ba

Atoms	Bond angles[º]	Atoms	Bond angles[º]
C23-O1-C28	117.97(13)	O3-C20-C21	111.23(12)
C24-O2-C27	116.93(14)	C19-C20-C21	110.57(12)
C16-O3-C20	106.81(12)	C20-C21-C26	118.62(13)
C29-O5-C30	116.05(13)	C22-C21-C26	119.42(14)
C32-O7-C33	116.51(13)	C20-C21-C22	121.87(14)
C13-O9-C14	116.49(16)	C21-C22-C23	120.82(14)
C11-O10-H10	109.00	O1-C23-C22	125.36(14)
O10-C11-C18	116.66(17)	O1-C2-C24	115.49(13)
C12-C11-C18	120.7(2)	C22-C23-C24	119.14(13)
O10-C11-C12	122.69(19)	O2-C24-C25	124.85(15)
C11-C12-C15	117.63(16)	C23-C24-C25	119.58(14)
C13-C12-C15	123.54(17)	O2-C24-C23	115.57(13)
C11-C12-C13	118.79(18)	C24-C25-C26	121.00(16)
O8-C13-C12	123.3(2)	C21-C26-C25	119.99(15)
O9-C13-C12	114.26(16)	O4-C30-O5	123.16(15)
O8-C13-O9	122.5(2)	O4-C30-C31	124.79(15)
C12-C15-C16	120.01(15)	O5-C30-C31	112.00(12)
C16-C15-C19	107.21(14)	C19-C31-C32	111.21(12)
C12-C15-C19	132.57(14)	C30-C31-C32	112.90(12)
O3-C16-C15	113.83(14)	C19-C31-C30	112.02(12)
C15-C16-C17	122.09(18)	O6-C32-C31	125.41(14)
O3-C16-C17	124.08(17)	O7-C32-C31	111.10(13)
C16-C17-C18	117.99(19)	O6-C32-O7	123.49(15)
C11-C18-C17	121.56(17)	O9-C14-H14A	109.00
C15-C19-C20	100.76(11)	O9-C14-H14B	109.00
C15-C19-C31	111.05(11)	O9-C14-H14C	109.00

C20-C19-C31	115.32(12)	H14A-C14-H14B	109.00
O3-C20-C19	105.39(11)	H14A-C14-H14C	109.00
H14B-C14-H14C	109.00	H27B-C27-H27C	110.00
C16-C17-H17	121.00	O1-C28-H28A	109.00
C18-C17-H17	121.00	O1-C28-H28B	109.00
C11-C18-H18	119.00	O1-C28-H28C	109.00
C17-C18-H18	119.00	H28A-C28-H28B	109.00
C15-C19-H19	110.00	H28A-C28-H28C	109.00
C20-C19-H19	110.00	H28B-C28-H28C	110.00
C31-C19-H19	110.00	O5-C29-H29A	109.00
O3-C20-H20	110.00	O5-C29-H29B	109.00
C19-C20-H20	110.00	O5-C29-H29C	109.00
C21-C20-H20	110.00	H29A-C29-H29B	109.00
C21-C22-H22	120.00	H29A-C29-H29C	110.00
C23-C22-H22	120.00	H29B-C29-H29C	109.00
C24-C25-H25	119.00	C19-C31-H31	107.00
C26-C25-H25	120.00	C30-C31-H31	107.00
C21-C26-H26	120.00	C32-C31-H31	107.00
C25-C26-H26	120.00	O7-C33-H33A	109.00
O2-C27-H27A	109.00	O7-C33-H33B	109.00
O2-C27-H27B	109.00	O7-C33-H33C	110.00
O2-C27-H27C	109.00	H33A-C33-H33B	109.00
H27A-C27-H27B	109.00	H33A-C33-H33C	109.00
H27A-C27-H27C	109.00	H33B-C33-H33C	110.00

Table 4: Selected hydrogen bonding geometry [Å, º] for a compound 4ba

D--H..**A**	**D**..**H**	**H**..**A**	**D**..**A**	**D--H**..**A**
O10 -- H10 ..O8	0.8200	1.8800	2.599(3)	146.00

C19 -- H19 ..O9	0.9800	2.4100	2.855(2)	107.00
C20 -- H20 .. O6	0.9800	2.5300	3.035(3)	112.00
C22--H22 ..O3	0.9300	2.5400	2.852(2)	100.00
C27-- H27A ..O10	0.9600	2.4700	3.382(3)	159.00

References:

1. Bruker, SAINT V7.68A, Bruker AXS Inc., Madison (WI, USA) 2005. SI-160
2. Sheldrick, G. M. SADABS 2008/2, Göttingen 2008.
3. Altomare, A.; Cascarano, G.; Giacovazzo, C.; Guagliardi, A. J. Appl. Cryst. 1993, 26, 343.
4. Sheldrick, G. M. SHELXL-97, Program for Crystal Structure Solution and Refinement, University of Göttingen, Göttingen, Germany 1997.
5. Farrugia, L. J. J. Appl. Cryst. 1999, 32, 837.

Bio-Data

Name: Navpreet Kaur

Date of Birth: 03 February, 1996

Educational Qualification:

- **2016**: Bachelor of Science from A. S. College Khanna, Panjab University, India.
- **2018**: Masters of Science (Chemistry) from MCM DAV College Chandigarh, Panjab University, India.

Achievements and Awards:

- Qualified **Central Universities Common Entrance Test (PUCET)** in 2016.
- Qualified **Graduate Aptitude Test for Engineering (GATE)** in 2018.